

Multigenerational Effects of Abnormal Folate Metabolism on Embryo Growth and Development

Katerina Menelaou



This thesis is submitted for the degree of
Doctor of Philosophy

Newnham College
University of Cambridge

June 2019

Declaration

This thesis is the result of my own work and includes nothing which is the outcome of work done in collaboration except as declared in the Preface and specified in the text.

It is not substantially the same as any that I have submitted, or, is being concurrently submitted for a degree or diploma or other qualification at the University of Cambridge or any other University or similar institution except as declared in the Preface and specified in the text. I further state that no substantial part of my thesis has already been submitted, or, is being concurrently submitted for any such degree, diploma or other qualification at the University of Cambridge or any other University or similar institution except as declared in the Preface and specified in the text.

It does not exceed the prescribed word limit for the relevant Degree Committee.

Multigenerational Effects of Abnormal Folate Metabolism on Embryo Growth and Development

Katerina Menelaou

It has been known for decades that maternal folate deficiency impairs fetal development. However, the molecular mechanism of folate metabolism remains unclear. To explore this, we study a mouse model of abnormal folate metabolism whereby the gene *Mtrr* was mutated causing a knockdown effect. MTRR is a key enzyme required for the progression of folate and methionine metabolism, which are important for DNA synthesis and cellular methylation. The *Mtrr^{gt}* mutation disrupts folate metabolism, alters global and locus-specific DNA methylation, and causes a wide spectrum of developmental phenotypes including growth defects and congenital malformations. Remarkably, the *Mtrr^{gt}* mouse line is a model of transgenerational epigenetic inheritance since the congenital malformations persist at least up to four wildtype generations after an *Mtrr^{+/gt}* maternal grandparent. In contrast, the growth phenotypes only appear until the F2 generation and have been attributed to an atypical uterine environment in the wildtype F1 generation as determined by a blastocyst transfer experiment. This thesis aims to examine how the *Mtrr^{gt}* mutation influences uterine biology and fetoplacental growth. First, the effects of intrinsic and parental *Mtrr* deficiency on uterine structure and function at estrus and decidualisation at gestational day (GD) 6.5 were determined. We found that a paternal *Mtrr^{gt}* allele was sufficient to alter the cellular structure of the uterine epithelium and outer myometrium at estrus. Furthermore, decidualisation was abnormal at GD6.5 based on mRNA expression analysis of key decidual markers. Next, to determine how an atypical uterine environment caused by the *Mtrr^{gt}* mutation might influence fetoplacental growth, an unbiased transcriptome analysis of placentas at embryonic day (E)10.5 with specific growth phenotypes and from specific *Mtrr^{gt}* pedigrees was completed. The *Mtrr^{gt/gt}* mutation altered the placental transcriptome in a phenotype-specific manner. Genes involved in embryo growth and placental transport were differentially expressed between *Mtrr^{gt/gt}* and C57Bl/6 placentas. This result suggests that intrinsic *Mtrr* deficiency affects the placental transcriptome and potentially fetal growth. However, transcriptomes of C57Bl/6 placentas and placentas of wildtype conceptuses derived from an *Mtrr^{+/gt}* maternal grandfather were similar. This suggests that the F1 uterine phenotype caused by abnormal folate metabolism in F0 does not affect the placental transcriptome of the F2 generation at E10.5. Simultaneously, RNA-seq was performed on F2 *Mtrr^{+/+}* placentas after blastocyst transfer to determine whether programming effects of the F1 maternal environment become apparent in the F2 offspring after a normal uterine environment was provided. While fetal growth enhancement in transferred F2 conceptuses was more frequent in these litters, only six genes were upregulated in placentas of transferred growth enhanced, but not phenotypically normal F2 *Mtrr^{+/+}* compared to transferred C57Bl/6 conceptuses. One remarkable finding was that the blastocyst transfer procedure affected placental gene expression and development, indicating a potential influence of blastocyst transfer, as part of assisted reproductive technology procedures in humans, on fetoplacental growth. Overall,

these results indicate that while the *Mtrr^{gt}* mutation in mice is sufficient to impair the uterine structure and function in their wildtype daughters, this does not substantially alter the placental transcriptome of their wildtype grandprogeny. However, *Mtrr* deficiency in the placenta cells themselves alters the transcriptome. In summary, abnormal folate metabolism caused by the *Mtrr^{gt}* mutation affects the uterine environment, which potentially affects placental development. Normal folate metabolism is required to establish a normal maternal-fetal interface. If disrupted, the effects persist for multiple generations.

Dedication

Στους γονείς μου, Μενέλαο και Έλενα,
και την αδερφή μου, Άντρεα,
για την αγάπη, τη συμπαράσταση και τη στήριξή τους.

Acknowledgements

I am grateful to my supervisor, Dr. Erica Watson, who gave me the opportunity to work in her lab, believed in me, and advised me during this journey. Also, my co-supervisor Prof. William Colledge, for all his advice, support and discussions during my PhD.

A big thank you to the people in the CTR, especially Maria, who has been an awesome friend and has supported me throughout, Jorge, and Stephen. To Nuala and Emma, for their kindness and support. To Simon, for sharing his expertise with me. To Colleen Geary-Joo from the University of Calgary for performing the embryo transfer experiments. To Gina, for performing the bisulfite pyrosequencing and helping me with the mouse breeding at the beginning of my PhD, and to Russell, Malwina and Xiaohui for analysing my RNA-sequencing data.

I am deeply thankful to Newnham College and Leventis Foundation for their financial support.

My time in Cambridge wouldn't be the same without the people in Newnham, who made it feel like home. Especially the girls in Whitstead, the girls in W3, and the tutors, especially Dr. Kate Fleet, who were there for me throughout my PhD.

Last but not least, I would like to thank my family: my parents and my sister for supporting me throughout my PhD, writing this thesis, and my life in general.

Table of contents

Declaration form	II
Abstract	III
Dedication	V
Acknowledgements	VI
Table of contents	VII
List of tables	XI
List of figures	XII
List of abbreviations	XIV

Chapter 1: Introduction

1.1 Fetal growth restriction (FGR)	2
1.1.1 Definition of FGR	2
1.1.2 Aetiology of FGR	3
1.1.3 Examples of causes of FGR in humans and mice	3
1.1.4 Long-term effects of FGR	4
1.1.5 Further studies are required on the causes of FGR	6
1.2 The mouse reproductive tract	7
1.2.1 The non-pregnant mouse uterus and oviducts	7
1.2.2 The estrous cycle in mice	8
1.2.2.1 Estrous cycle vs menstrual cycle	8
1.2.2.2 Hormonal regulation of the estrous cycle	10
1.2.2.3 Changes in the ovaries	12
1.2.2.4 Changes in the uterus	13
1.2.2.5 Abnormal cyclicity and infertility	15
1.2.3 From estrous cycle to pregnancy in mice	17
1.2.3.1 The estrous cycle after mating and maintenance of corpus luteum and progesterone	17
1.2.3.2 Changes in the uterus after fertilisation	18
1.2.3.3 Decidualisation after implantation	19
1.2.3.4 Gene expression during estrous cycle affects decidualisation	21
1.2.3.5 Factors that regulate decidualisation	22
1.2.3.6 Factors that regulate angiogenesis	24
1.2.4 Endometrial causes of FGR	24
1.3 Mouse placenta development and function	26
1.3.1 Structure and function of the mature mouse placenta	27
1.3.2 Mouse placenta development	28
1.3.3 Maternal components of the mouse placenta	29
1.3.4 Poor placenta development and function can lead to FGR	31
1.4 Folate metabolism and reproductive health	33
1.4.1 Role of folate in uterine health and pregnancy in humans and mice	34
1.4.2 Bioavailability and metabolism of folate	36
1.4.3 The molecular function of folate	37
1.4.4 Folate transport and metabolism-related mutations in mice and humans that affect development and uterine health	42
1.4.5 Folate supplementation, uterine health, and pregnancy in humans and mice	43

1.4.6	What is missing from the field?	45
1.5	Multigenerational effects of folate metabolism.....	45
1.5.1	Maternal effects of folate metabolism.....	45
1.5.2	<i>Mtrr^{gt}</i> mouse model of abnormal folate metabolism.....	47
1.5.2.1	FGR in the <i>Mtrr^{gt}</i> mouse model.....	47
1.5.2.2	Epigenetic instability in the <i>Mtrr^{gt}</i> mouse model	51
1.5.2.3	The growth phenotypes in F2 generation are due to an atypical uterine environment of the F1 females	52
1.6	Hypothesis and Aims	52

Chapter 2: Methods

2.1	Ethical approval.....	55
2.2	Mouse pedigrees and diet.....	55
2.3	Blastocyst transfer	56
2.3.1	Collecting blastocysts	56
2.3.2	Oviduct transfer	56
2.3.3	Dissection of transferred conceptuses.....	57
2.4	Genotyping	57
2.5	Phenotypic analysis of developmental phenotypes at E10.5.....	58
2.6	Uterine tissue collection and processing	59
2.6.1	Estrus stage (non-pregnant) uteri	59
2.6.2	Uteri during early pregnancy (GD6.5).....	60
2.6.3	Tissue processing	60
2.7	H&E staining and immunohistochemistry	60
2.8	RNA extraction and DNase treatment.....	61
2.9	DNA/RNA extraction.....	62
2.10	RNA-sequencing	62
2.11	RNA-sequencing data analysis.....	62
2.12	Gene ontology analysis.....	63
2.13	RT-qPCR analysis of gene expression	64
2.13.1	Primer design	64
2.13.2	Reverse transcription	64
2.13.3	Real time qPCR.....	64
2.14	Bisulfite pyrosequencing	65
2.15	Statistical analysis.....	65

Chapter 3: The effects of abnormal folate metabolism on the uterus during estrus

3.1	Introduction	73
3.2	Results	75
3.2.1	Estrous cycle duration is unaffected by an intrinsic or paternal <i>Mtrr^{gt}</i> allele....	75
3.2.2	Analysis of expression of <i>Mtrr</i> mRNA and protein in the estrus-staged uterus	77
3.2.3	Analysis of folate-related proteins in <i>Mtrr</i> uteri at estrus.....	80
3.2.4	Decreased mRNA expression of DNA methylation machinery enzymes in uteri at estrus from <i>Mtrr</i> pedigrees.....	81

3.2.5	Intrinsic and parental <i>Mtrr</i> ^{gt} allele causes abnormal uterine morphology at estrus	82
3.2.6	Cell density in outer myometrium is increased by parental <i>Mtrr</i> deficiency	87
3.2.7	Analysis of genetic markers of uterine cells in the <i>Mtrr</i> ^{gt} mouse line	94
3.2.8	Altered cell polarity in uterine lumen epithelium of <i>Mtrr</i> mice at estrus	96
3.2.9	Decreased levels of progesterone receptor mRNA and protein in the <i>Mtrr</i> uteri	99
3.3	Discussion	101

Chapter 4: The effects of abnormal folate metabolism on decidualisation

4.1	Introduction	107
4.2	Results	108
4.2.1	The <i>Mtrr</i> ^{gt} mutation does not affect the litter size at GD6.5	108
4.2.2	Abnormal folate metabolism does not affect implantation site weight at GD6.5	110
4.2.3	Analysis of MTRR gene and protein expression in decidua at GD6.5	110
4.2.4	Abnormal folate metabolism in males potentially affects the decidualisation reaction of their wildtype daughters at GD6.5	112
4.2.5	Analysis of decidual marker expression in implantation sites at GD6.5	115
4.2.6	Analysis of growth restriction at E6.5	118
4.3	Discussion	119

Chapter 5: The effects of intrinsic abnormal folate metabolism on the placental transcriptome at E10.5

5.1	Introduction	124
5.2	Results	124
5.2.1	RNA quality control	125
5.2.2	Quality control of RNA sequencing data	126
5.2.3	Sample RNA largely clusters based on their experimental group	127
5.2.4	The <i>Mtrr</i> ^{gt/gt} placentas are transcriptionally variable	128
5.2.5	Improving the stringency of the <i>Mtrr</i> ^{gt/gt} RNA-sequencing dataset	135
5.2.6	The DEGs in the <i>Mtrr</i> locus	143
5.2.7	Gene ontology analysis of the DEGs	143
5.2.8	DEGs that are involved in placental function and embryo growth	146
5.2.9	Altered CpG methylation as a predicted mechanism for gene misexpression in <i>Mtrr</i> ^{gt/gt} placentas	149
5.2.10	Predicted changes in histone modifications as a mechanism for placental gene misexpression	153
5.2.11	Analysis of the placental transcriptome in F2 <i>Mtrr</i> ^{+/+} conceptuses at E10.5	154
5.3	Discussion	156

Chapter 6: The effects of blastocyst transfer on the placental transcriptome at E10.5

6.1	Introduction	162
6.2	Results	164
6.2.1	Maternal grandpaternal abnormal folate metabolism affects the placental transcriptome in a growth phenotype-dependent manner	164
6.2.2	Blastocyst transfer leads to possible increase in placental efficiency at E10.5	166
6.2.3	Transferred conceptuses have a different placental transcriptome than non-transferred	177
6.2.4	Comparison of DEGs between placentas of non-transferred and transferred conceptuses at E10.5	183
6.2.5	DEGs caused by the embryo transfer protocol	184
6.2.5.1	All major placental cell types are represented by DEGs in transferred C57Bl/6 placentas	185
6.2.5.2	DEG are involved in placental development and function	186
6.2.5.3	Dysregulation of DNA methylation by blastocyst transfer is unlikely to be the primary mechanism of transcriptional disruption	191
6.2.5.4	Some DEGs cluster in the genome implying common transcriptional regulation	196
6.2.6	DEGs as a result of developmental programming of F2 <i>Mtrr</i> ^{+/+} conceptuses	199
6.2.6.1	F2 <i>Mtrr</i> ^{+/+} conceptuses respond differently to the blastocyst transfer into a BDF1 uterus at E3.0 compared to C57Bl/6 conceptuses	199
6.2.6.2	Genes involved in transport are misexpressed after transfer of blastocysts into the recipient uterine environment	203
6.2.6.3	The uterine environment of the recipient female might cause changes in epigenetic regulation of gene expression	204
6.2.6.4	The abnormal uterine environment affects genes implicated in growth, placental phenotypes, and/or embryonic lethality at midgestation	206
6.3	Discussion	208

Chapter 7: Discussion and future directions

7.1	Summary	217
7.2	Developmental programming in the <i>Mtrr</i> ^{gt} model	218
7.2.1	Abnormal uterine morphology and function in <i>Mtrr</i> ^{gt/gt} and F1 <i>Mtrr</i> ^{+/+} mice	219
7.2.2	Abnormal placental transcriptome in <i>Mtrr</i> ^{gt/gt} and F2 <i>Mtrr</i> ^{+/+} mice	222
7.2.3	Associations between abnormal uterine and placental phenotypes	224
7.2.4	The blastocyst transfer process affects fetoplacental growth, suggesting ART might affect the adult health of ART-born children	226
7.3	Sexual dimorphism in the <i>Mtrr</i> ^{gt} model	228
7.4	<i>MTRR</i> polymorphisms in the human population	229
7.5	Further analysis of placental phenotype and function in the <i>Mtrr</i> ^{gt} model	230
7.6	Future directions	232
	Bibliography	233
	Appendix A	316
	Appendix B	324

B1.1 Introduction	324
B1.2 Methods.....	326
B1.3 Results	326
B1.4 Discussion	328
Appendix C	331

List of tables

1.1 Changes in mouse reproductive organs during the estrous cycle.	14
1.2 Phenotypic frequencies in litters from <i>Mtrr</i> ^{+/<i>gt</i>} intercrosses compared to C57Bl/6 crosses.	49
1.3 Phenotypic frequencies caused by <i>Mtrr</i> ^{+/<i>gt</i>} maternal grandmothers of grandfathers at E10.5 compared to C57Bl/6 controls.	50
2.1 Primer sequences used for RT-qPCR for analysis of gene expression.....	66
2.2 Bisulfide pyrosequencing primers.	71
5.1 The number of misexpressed placental genes at E10.5.	129
5.2 Number of DEGs per <i>Mtrr</i> genotype and phenotype.....	133
5.3 Number of DEGs in <i>Mtrr</i> ^{<i>gt/gt</i>} placentas at E10.5 per <i>Mtrr</i> genotype and phenotype.....	140
5.4 DEGs with transport function in phenotypically normal <i>Mtrr</i> ^{<i>gt/gt</i>} placentas at E10.5.....	144
5.5 DEGs with transport function in growth restricted <i>Mtrr</i> ^{<i>gt/gt</i>} placentas at E10.5.	145
5.6 DEGs in phenotypically normal <i>Mtrr</i> ^{<i>gt/gt</i>} placentas related to placental function.....	147
5.7 DEGs in placentas of growth restricted <i>Mtrr</i> ^{<i>gt/gt</i>} related to placental phenotypes.	148
5.8 DEGs in <i>Mtrr</i> ^{<i>gt/gt</i>} placentas with known regulation by DNA methylation.....	151
6.1 Chromosomal location and placental expression of DEGs.....	166
6.2 Relationship between C57Bl/6 embryos transferred at E3.5 into recipient female and embryonic phenotype at E10.5.	169
6.3 Relationship between F2 <i>Mtrr</i> ^{+/<i>+</i>} embryos transferred at E3.5 into recipient female and embryonic phenotype at E10.5.	170
6.4 Phenotypic comparison of C57Bl/6 control conceptuses and C57Bl/6 transfer conceptuses at E10.5.	171
6.5 Phenotypic comparison of non-transferred F2 <i>Mtrr</i> ^{+/<i>+</i>} conceptuses and transferred <i>Mtrr</i> ^{+/<i>+</i>} conceptuses at E10.5.	175
6.6 Number of DEGs in transferred placentas per genotype and phenotype.....	180
6.7 DEGs implicated in growth, placental phenotypes, and/or embryonic lethality at midgestation.	188
6.8 DEGs encoding proteins with transporter activity.....	189
6.9 DEG with known regulation by DNA methylation	193
6.10 DEGs with transport activity in placentas of transferred F2 <i>Mtrr</i> ^{+/<i>+</i>} conceptuses.	204
6.11 Genes whose expression is epigenetically regulated by DNA methylation and were differentially expressed in F2 <i>Mtrr</i> ^{+/<i>+</i>} but not C57Bl/6 conceptuses at E10.5 after blastocyst transfer.	205
6.12 DEGs implicated in growth, placental phenotypes, and/or embryonic lethality at midgestation in placentas of transferred F2 <i>Mtrr</i> ^{+/<i>+</i>} conceptuses.....	208

List of figures

1.1 Schematic cross section of the sexually mature mouse uterus.	7
1.2 The levels of hypothalamic, pituitary, and ovarian hormones during the estrous cycle....	11
1.3 Schematic of an implantation site at E6.5.....	21
1.4 Mouse placenta development.....	28
1.5 Folate and methionine metabolism.	37
2.1 Schematic diagrams of robust genetic pedigrees established to address the role of abnormal folate metabolism on uterine and placental structure and function.	57
2.2 Cells of vaginal smears at each stage of the estrous cycle in adult mice.....	59
3.1 The <i>Mtrr</i> ^{gt} mutation does not affect estrous cyclicity.....	76
3.2 <i>Mtrr</i> transcript and MTRR protein expression in the mouse uterus at estrus.....	79
3.3 Analysis of folate-related and DNA methylation machinery gene expression in the mouse uterus at estrus.....	81
3.4 Histological analysis of <i>Mtrr</i> uteri at estrus.....	84
3.5 Histological analysis of F1 <i>Mtrr</i> uteri at estrus.	86
3.6 Decreased cell density in the outer myometrium of <i>Mtrr</i> uteri at estrus.	88
3.7 Analysis of cell proliferation and apoptosis in the uterine tissue of littermate females from <i>Mtrr</i> ^{+gt} intercrosses at estrus.	91
3.8 Analysis of cell proliferation and apoptosis in the uterine tissue of F1 females at estrus.	93
3.9 Marker expression in the uterine tissues of <i>Mtrr</i> mice at estrus.....	96
3.10 Misexpression of pan-cadherin protein in the uterus of <i>Mtrr</i> mice at estrus.	98
3.11 Expression of progesterone receptor in <i>Mtrr</i> uteri at estrus.	100
4.1 Litter statistics of GD6.5 dissections after <i>Mtrr</i> females were mated with C57Bl/6 males.	109
4.2 <i>Mtrr</i> transcript and protein expression in whole implantation sites at GD6.5.....	112
4.3 Analysis of decidual morphology in implantation sites at E6.5.	114
4.4 Relative mRNA expression of decidualisation markers in GD6.5 implantation sites....	117
4.5 Analysis of growth restriction at E6.5.	119
5.1 RNA sample quality control.	125
5.2 RNA sequencing data quality control.	126
5.3 PCA plot of sequenced placenta samples.	128
5.4 Degree of differential gene expression in <i>Mtrr</i> ^{gt/gt} placentas at E10.5 depends on growth phenotype.....	130
5.5 Validation of RNA-sequencing data by RT-qPCR analysis.....	131
5.6 Data quality control for the second round of RNA sequencing.....	133
5.7 Bioinformatic analysis of data from the second RNA sequencing experiment.	134
5.8 Principal component analysis plots used to exclude outliers.....	137
5.9 Bioinformatic analysis of the RNA sequencing data from placentas of C57Bl/6, and phenotypically normal (PN) and growth restricted (GR) <i>Mtrr</i> ^{gt/gt} conceptuses.....	138
5.10 Validation by RT-qPCR analysis of downregulated genes identified by RNA- sequencing.....	141
5.11 Validation by RT-qPCR analysis of up-regulated genes identified by RNA-sequencing.	142
5.12 Gene expression correlation between the RNA-sequencing data and the qPCR results.	142
5.13 The percentage of DEGs in <i>Mtrr</i> ^{gt/gt} placentas that were associated with CpG repeats.	149
5.14 Frequency of histone modifications associated with genes that were misexpressed in <i>Mtrr</i> ^{gt/gt} placentas.....	154

5.15 Bioinformatic analysis of the RNA sequencing data from placentas of C57Bl/6 and F2 <i>Mtrr</i> ^{+/+} conceptuses.....	156
6.1 Bioinformatic analysis of the RNA sequencing data from C57Bl/6, and placentas of F2 <i>Mtrr</i> ^{+/+} conceptuses after blastocyst transfer.	165
6.2 Blastocyst transfer results in small placentas with a potential for increased efficiency at E10.5.	172
6.3 Blastocyst transfer into the normal BDF1 environment results in bigger embryos and placentas with a potential for increased efficiency at E10.5.....	176
6.4 Bioinformatic analysis of the RNA sequencing data to compare placental transcriptome of non-transferred and transferred conceptuses.	178
6.5 Validation of RNA-sequencing data by RT-qPCR analysis of downregulated genes.....	181
6.6 Validation of RNA-sequencing data by RT-qPCR analysis of upregulated and non-differentially expressed genes.....	182
6.7 Gene expression correlation between the RNA-sequencing data and the qPCR results.	183
6.8 Comparisons between the DEGs of controls and transferred conceptuses.....	184
6.9 Spatial analysis of differentially expressed genes identified in placentas of transferred conceptuses.	186
6.10 Functional analysis of differentially expressed genes identified in placentas of transferred conceptuses.	187
6.11 Unlikely that blastocyst transfer directly alters placental gene expression via CpG methylation.	195
6.12 Clustering of differentially expressed genes in the genome suggests shared regulatory regions.....	198
6.13 Gene ontology analysis of the DEGs in transferred C57Bl/6 but not F2 <i>Mtrr</i> ^{+/+} placentas.....	200
6.14 Gene ontology analysis of the DEGs in transferred F2 <i>Mtrr</i> ^{+/+} placentas.	202

List of abbreviations

AP	anterior posterior
ART	assisted reproductive technologies
BDF1	F1 resulting from crossing C57BL/6J (B6) female and DBA/2J (D2) male
BSA	bovine serum albumin
DD	developmentally delayed
DEG	differentially expressed gene
DV	dorsal ventral
E	embryonic day
E2	estradiol
EPC	ectoplacental cone
ES	embryonic stem cell
ExE	extraembryonic ectoderm
FC	fold change
FEV	fetal endothelial vascular cells
FGR	fetal growth restriction
FSH	follicle stimulating hormone
GD	gestational day
GE	growth enhanced
GR	growth restricted
GnRH	gonadotrophin-releasing hormone
gt	gene trap
ICM	inner cell mass
ICSI	intracytoplasmic sperm injection
IGF1	insulin-like growth factor 1
IRS	insulin receptor substrate
IVF	<i>in vitro</i> fertilisation
LH	luteinising hormone
MA	log-intensity ratio (M), log-intensity average (A)
MTRR	methionine synthase reductase
NTD	neural tube defects
P4	progesterone
PC	principal component
PCA	principal component analysis
PCOS	polycystic ovary syndrome
PDZ	primary decidual zone
PN	phenotypically normal
PBS	phosphate-buffered saline
qPCR	quantitative polymerase chain reaction
RIN	RNA integrity number
S-AdoMet	S-adenosylmethionine
SAR	spiral artery remodelling
SD	severe defects
SDZ	secondary decidual zone
SpT	spongiotrophoblast
TB	trophoblast
TE	trophectoderm
TGC	trophoblast giant cell

THF	tetrahydrofolate
TS	trophoblast stem cell
uNK	uterine natural killer cell

Chapter 1: Introduction

1.1 Fetal growth restriction (FGR)

1.1.1 Definition of FGR

Fetal growth restriction (FGR) is defined as the failure of the fetus to reach its full growth potential, as predetermined by its genome (Figueras & Gardosi 2011; Gardosi et al. 1992). Embryo growth is determined by measuring the crown-rump length using ultrasound. FGR affects 10-15% of human pregnancies (Suhag & Berghella 2013). According to the World Health Organisation (Kiserud et al. 2017), FGR is strongly associated with perinatal morbidity, including perinatal asphyxia, hypothermia, and hypoglycaemia. FGR can also lead to mortality in 50% of pre-term fetuses, and 20% of full-term fetuses (Gardosi et al. 2013). Full term FGR fetuses are at a higher risk of developing cardiovascular diseases (Menendez-Castro, Rascher & Hartner 2018), and metabolic syndrome (Ma & Hardy 2012; Neitzke, Harder & Plagemann 2011; Valsamakis et al. 2006), and having abnormal neural development (Baschat 2014; Demicheva & Crispi 2014; Sehgal, Crispi & Boode 2017) in adult life.

There are two types of FGR (Sharma, Shastri & Sharma 2016). Symmetrical FGR is early-onset and it is usually caused by a genetic disorder, or an infection intrinsic to the fetus. All of the fetal organs, including the brain are equally affected, and the fetal weight, length, and head circumference are reduced. Asymmetrical FGR is late-onset and may be caused by various factors, including utero-placental insufficiency, maternal undernutrition, hypoxia, stress, or advanced maternal age. It is characterised by unaffected brain growth, at the expense of the rest of the fetal organs (Sharma, Shastri & Sharma 2016). In this case, there is decreased fetal weight, but normal fetal length (Krishna & Bhalerao 2011). Fetuses with symmetrical FGR have a higher incidence of brain dysfunction and neurodevelopmental impairment than those with asymmetrical FGR (Hartkopf et al. 2018). The 70-80% of FGR cases are asymmetrical, while the rest (20-30%) are symmetrical. Fetuses with asymmetrical FGR have better prognosis than those with symmetrical FGR (Sharma, Shastri & Sharma 2016), as they are able to catch-up on growth postnatally (Wollmann 1998), and the brain is unaffected, therefore they have a decreased risk of neurodevelopmental impairment.

1.1.2 Aetiology of FGR

The aetiology of growth restriction was discovered using animal models (Haugaard & Bauer 2001; Morrison 2008), but also from examination of human placentas from pregnancies complicated with FGR (Redline & Pappin 1995; Roberts & Post 2008; Scifres & Nelson 2009). In FGR, fetal growth is impaired by maternal, fetal, and/or placental factors (Grivell, Dodd & Robinson 2009). Factors arising from the mother and her environment include nutrition (Ceesay et al. 1997; Christian 2003; Haider & Bhutta 2017; Kramer & Kakuma 2003), congenital uterine anomalies (Chan et al. 2011), age (Joseph et al. 2005), fertility treatment (Schieve et al. 2007), smoking (Andres & Day 2000), or medical conditions during pregnancy, such as hypertension (Brown et al. 2000). Fetal factors include chromosomal disorders (Reisman 1970) and twin pregnancies (Fox et al. 2011). Finally, fetal growth is dependent on a functional placenta. The placenta is responsible for delivery of oxygen and nutrients to the fetus, as well as removal of waste products such as carbon dioxide and urea (Gude et al. 2004). FGR is associated with abnormalities in embryo implantation and placental development. The most common cause of FGR is small placental size or abnormal vascular development of either the trophoblast or the decidua, leading to uteroplacental insufficiency (Barry, Rozance & Anthony 2008; Grivell, Dodd & Robinson 2009; Roberts & Post 2008). This will be further discussed in Sections 1.2.4 and 1.3.4. Altogether, these studies show that the cause of FGR lies in maternal, fetal, and/or placental factors.

1.1.3 Examples of causes of FGR in humans and mice

FGR is a multifactorial condition, and is associated, amongst others, with maternal malnutrition, and placental hormone signalling. For instance, from October 1944 until May 1945, Amsterdam experienced a famine, due to decreased food shipments from farm towns, widely known as the Dutch famine (Banning 1946). Pregnant women were consuming low-nutritional status food, leading to decreased birthweight of *in utero* exposed infants (Lumey 1992). Additionally, placentas from pregnancies complicated with FGR have increased insulin-like growth factor 1 (IGF-1) receptor expression and impaired insulin receptor substrate 2 (IRS-2) signalling (Laviola et al. 2005), highlighting the significance of placental hormone signalling on embryo growth.

To better understand the causes of FGR in humans, mice are often used as models. This is because mice are small in size, easy to maintain, and inexpensive to house. Additionally, their

genomes are similar enough to humans, and can be easily manipulated (Emes et al. 2003; Swanson & David 2015). Their gestation lasts around 21 days, which reduces the time and expenses (Swanson & David 2015). Examples of FGR in mice include *Erk3*^{-/-} mice born from *Erk3*^{+/-} intercrosses. ERK3 (extracellular signal-regulated kinase 3) is a protein kinase that is important for the regulation of cell growth and differentiation. *Erk3*^{-/-} mice die between postnatal days 2-5, mainly from severe respiratory distress (Klinger et al. 2009). Respiratory distress is a severe consequence of FGR (Rosenberg 2008), and severe reduction of visceral organ growth. *Erk3*^{-/-} and *Erk3*^{+/-} had decreased birthweight compared to their *Erk3*^{+/+} littermates, suggesting the loss of a single *Erk*⁺ allele in mice causes growth restriction (Klinger et al. 2009). In addition, *eNOS*^{-/-} mice had reduced fetal weight and abdominal circumference compared to *eNOS*^{+/+}, due to decreased placental system A transport and placenta hypoxia at E17.5 characterised by increased superoxide levels. Endothelial nitric oxide synthase (eNOS) is required for the synthesis of the cellular signalling molecule nitric oxide, which regulates vasodilation. This suggests that the growth restriction observed in this model is due to uteroplacental hypoxia (Kusinski et al. 2012). Finally, unilateral ovariectomy in mice leads to production of a litter of 13 pups in one uterine horn. This results in decreased placental blood flow among the fetuses, leading to FGR in the middle fetuses (Coe et al. 2008). Altogether, these studies provide examples of causes of FGR in mice and highlight the significance of using mouse models to study FGR in the human population.

1.1.4 Long-term effects of FGR

Exposure of fetuses to adverse intrauterine conditions that cause FGR, has long-term effects on the adult health, particularly affecting the cardiovascular, renal, and metabolic function (Demicheva & Crispi 2014; Sharma, Shastri & Sharma 2016). The Developmental Origins of Health and Disease hypothesis (DOHaD) was first described in 1990 (Barker et al. 1990), and highlights the potential effects of exposure to an abnormal uterine environment on development and health later in life. Epidemiological studies have shown that an individual who is exposed to different environmental cues as an embryo is more susceptible to develop diseases later in life (Hanson & Gluckman 2014; Jirtle & Skinner 2007). Under adverse intrauterine conditions, such as intrauterine malnutrition due to maternal malnutrition or obesity, the placenta is able to adapt its function to ensure optimal fetal growth (Tarrade et al. 2015). The “Thrifty Hypothesis”, proposed in 1992 (Hales & Barker 2001, 2013) suggests

that the fetus compensates for maternal nutritional deficiency, or nutrient deprivation by altering its tissue sensitivity, physiology and metabolism. For instance, maternal undernutrition leads to metabolic changes, blood flow redistribution, and alteration of the fetal and placental hormone production, in order to ensure optimal embryo growth (Fowden 1995; Osmond & Barker 2000). More specifically, in asymmetrical FGR, it assures optimal growth of the brain, which is a key organ, at the expense of organs such as the pancreas, leading to abnormal pancreatic function later in life. Impaired function of the pancreatic β -cells in the islets of Langerhans, predispose the individual to type II diabetes (Hales & Barker 2001). The fetus expects that the postnatal environment will be similar to the intrauterine one, therefore these adaptations made in fetal life, will ensure optimal health in the postnatal life. However, this is not the case, when there is different nutrient supply in the postnatal environment, compared to the intrauterine environment. The process by which these adaptations happen is called fetal programming. Exposure in the suboptimal intrauterine environment leads to growth restriction and low birth weight, and ultimately catch-up growth during postnatal life (Gicquel, El-Osta & Le Bouc 2008). Low birth weight has been associated with hypertension, glucose intolerance, insulin resistance, hyperlipidaemia, obesity, and reproductive disorders in the adult life (Barker et al. 1990, 1993; Barker 1997; Hales & Barker 2013). Adults who were *in utero* exposed to the Dutch famine developed metabolic syndrome and cardiovascular disease (Ravelli et al. 1999; de Rooij et al. 2006). Men who were exposed *in utero* to the famine, developed hypertension related to a large placental surface due to large placental breadth and a round-shaped surface, suggesting hypertension was due to compensatory expansion of the placental surface. In contrast, the relationship between placental size and hypertension was similar in females exposed *in utero* to the Dutch famine, and those who were not (van Abeelen et al. 2011). Additionally, peri-adolescent children who were born small for gestational age have higher systolic blood pressure and lower glomerular filtration rate, which indicate systolic hypertension and renal dysfunction, respectively (Chan et al. 2010). In addition, these children had higher augmentation index and higher insulin serum levels two hours after glucose load, suggesting arterial stiffness and abnormal metabolism, respectively (Chan et al. 2010). FGR caused by exposure to a hypoxic (11.5% O₂) environment during GD15.0-GD21.0 leads to increased cardiac susceptibility of rats to ischaemia/reperfusion injury, and a mismatch between glycolysis and glucose oxidation in the myocardium, leading to proton accumulation, suggesting decreased cardiac efficiency during reperfusion (Rueda-Clausen et al. 2011). FGR babies can experience catch-up growth, especially if they have asymmetrical FGR (Crume et

al. 2014). These children have normal body mass index at one year of age. However, in adolescence, they have higher waist circumference, higher insulin levels, insulin resistance, and lower adiponectin levels, indicating metabolic dysfunction (Crume et al. 2014). Type II diabetes mellitus is another metabolic long-term effect of FGR, associated with insulin resistance (Simmons, Templeton & Gertz 2001; Vuguin et al. 2004) and abnormal pancreatic islet development and β -cell function (Boehmer, Limesand & Rozance 2017). Altogether, these studies show the long-term effects of FGR originating from exposure to an abnormal uterine environment, supporting the theory of fetal programming.

The long-term effects of FGR have also been demonstrated in mice. For instance, litters born to mothers fed a low-protein diet during pregnancy had lower mean birth weight than controls. However, male offspring had normal weight at 8 weeks of age, but were obese at 32 weeks of age, exhibiting increased adiposity and glucose intolerance. In contrast, female offspring were growth restricted from birth until at least 32 weeks of age, showing a sex-specific effect of dietary protein restriction in the growth of offspring (Bhasin et al. 2009). When pregnant females lacking the low-density lipoprotein receptor (*Ldlr*) were fed a high fat diet to develop hypercholesterolemia, their offspring also developed FGR characterised by decreased birth weight, and decreased weight and length at 90 days of age compared to *Ldlr*^{-/-} females fed a normal diet. The progeny of high fat-diet *Ldlr*^{-/-} females also had decreased gonadal fat pad weight to body weight ratio, and bigger atherosclerotic lesions than the progeny of normal-diet *Ldlr*^{-/-} females (Bhasin et al. 2009). In the studies that assess the long-term effects of either low-protein diet or *Ldlr* deficiency, the mothers had also decreased circulating amino acid levels, possibly resulting in reduced fetal amino acid levels, leading to abnormal metabolic programming of the fetus (Bhasin et al. 2009). Altogether, these studies show the long-term effects of FGR in mice.

1.1.5 Further studies are required on the causes of FGR

Early diagnosis and prevention of FGR can prevent the long-term effects in adulthood, and in future generations. Current guidelines to prevent FGR include discouraging smoking during pregnancy and encouraging an optimal maternal nutrition before and during pregnancy, and administration of low-dose aspirin (McCowan, Figueras & Anderson 2018). Smoking during pregnancy can cause chronic gestational hypoxia (Longo 1976), which accelerates ovarian aging and lowers ovarian reserve in the *in utero*-exposed rats (Aiken et al. 2019). However,

little is known about the effects of maternal malnutrition, such as vitamin deficiencies, on the uterine environment and placental health. Ultimately, abnormal uterine and placental development or function can affect fetal growth. More research is required to assess the specific mechanisms of maternal malnutrition, for instance vitamin deficiencies, on FGR.

1.2 The mouse reproductive tract

In the previous section we discussed the aetiology and long-term effects of FGR. However, to further understand how the uterine environment prevents the embryo from reaching its full growth potential during development, we need to look at the uterine structure and function both during the estrous cycle, and during pregnancy.

1.2.1 The non-pregnant mouse uterus and oviducts

The female mouse has a duplex uterus, consisting of two uterine horns (Figure 1.1A). These are long, tubular structures, each of them terminating cranially to the oviduct. The oviducts are 1.8cm long, narrow tubular structures, and at the end of each there is an ovary (Rendi et al. 2012). Caudally, the uterine horns connect to the cervix (Figure 1.1A). The cervix is duplex, as there are two cervical canals, one for each uterine horn, and therefore conceptuses are not able to move between the uterine horns (Pang et al. 2014).

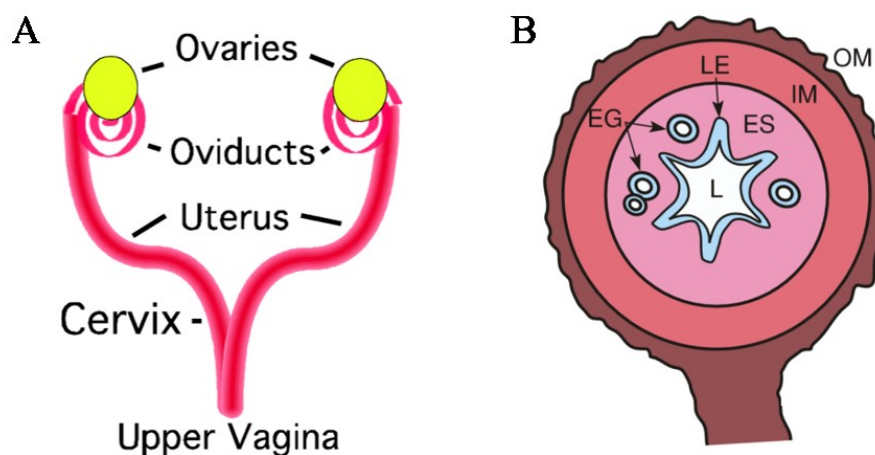


Figure 1.1 Schematic cross section of the sexually mature mouse uterus.

(A) Overview of the female mouse reproductive tract. (B) The sexually mature mouse uterus. OM: outer myometrium, IM: inner myometrium, ES: endometrial stroma, LE: lumen epithelium, L: lumen, EG: endometrial glands. Reproduced from Teixeira, Rueda and Pru, (2008).

The uterus is composed of two layers of myometrial tissue, the outer myometrium and the inner myometrium (Figure 1.1B), which are composed of longitudinal and circular myometrial cells, respectively (Brody & Cunha 1989). The endometrial stroma contains stromal cells, luminal epithelium, and endometrial glands. The glands are formed by post-natal day 15, when the uterus reaches its mature sexual stage (Teixeira, Rueda & Pru 2008). The endometrial glands are surrounded by the glandular epithelial cells (Figure 1.1B). The uterus contains a lumen, surrounded by luminal epithelial cells (Figure 1.1B; Teixeira, Rueda and Pru, 2008). On the other hand, the oviducts can be split up into five parts: the intramuscular portion, that is located in the uterine wall; the isthmus, which is the narrowest part; the ampulla, which is the central region of the tube; the infundibulum, which is the open, funnel-shaped part that is close to the ovary; and finally, the fimbriated end. The fimbriated end contains finger-like structures that help movement of the ovulated oocyte into the oviducts during estrus (Rendi et al. 2012). The appearance of the uterine structures changes over the course of the estrous cycle (Pang et al. 2014), as will be described in the next section.

1.2.2 The estrous cycle in mice

The uterus is essential for mammalian reproduction. A functioning uterus is important for the fertility and health of women, but also for the health of their offspring (Spencer et al. 2005). Abnormal uterine development during fetal life can lead to infertility, or affect embryonic development of future generations (Spencer et al. 2005). Postnatally, the mouse uterus undergoes two developmental processes, both of which are driven by steroid hormones produced by the ovary. The first developmental process occurs in the absence of conception and is known as the estrous cycle (Green 1966). The second developmental process occurs during pregnancy and is known as decidualisation.

1.2.2.1 Estrous cycle vs menstrual cycle

The estrous cycle in mice is the equivalent of the menstrual cycle in humans. The main functions of the estrous and menstrual cycles are the maturation and release of oocytes from the ovaries and the establishment and maintenance of the endometrial lining necessary for embryo implantation (Sato, Nasu & Tsuchitani 2016). Female mice reach sexual maturity at 5 weeks of age (Silver 1995). Proper function of the hypothalamic-pituitary-ovarian axis is

essential for normal reproductive function in both mice and humans. The menstrual cycle occurs in humans and non-human, anthropoid primates, such as monkeys, and apes, and lasts for an average of 28 days. The estrous cycle occurs in non-primates, such as rodents, dogs, and cows (Sato, Nasu & Tsuchitani 2016). The duration of the estrous cycle varies between species. For example, it lasts for 18-24 days in cattle, and an average of five days in mice. The short duration of the estrous cycle in mice, makes them a good model to study the hypothalamic-pituitary-ovarian axis function, and the changes in the uterus that occur during the cycle (Caligioni 2009). In humans, the menstrual cycle consists of two phases (Hawkins & Matzuk 2008). The proliferative phase is characterised by an increase in serum estrogen concentration leading to rapid proliferation of the endometrium. Levels of follicle stimulating hormone (FSH) also increase, leading to ovarian follicle maturation. Ovulation, which is the release of the mature oocyte into the oviduct occurs on day 14 of the cycle, following the luteinising hormone (LH) surge (Hawkins & Matzuk 2008). The ruptured follicle transforms into a progesterone-producing corpus luteum. The next phase of the menstrual cycle, the secretory phase, is characterised by increased progesterone and estrogen, that stimulate further proliferation of the endometrium, so that it can accept the potential blastocyst. If no implantation occurs, the new cycle starts with menses, which is the discharge of the endometrial lining from the uterus, and lasts for five days. On day six, the proliferative phase is repeated (Hawkins & Matzuk 2008).

In contrast to the menstrual cycle, the estrous cycle in mice consists of four phases: proestrus, estrus, metestrus, and diestrus (Caligioni, 2009; Figure 1.2) and lasts on average five days, unless it is interrupted by pregnancy. The four stages of the estrous cycle in mice can be determined by vaginal smears, as the combination of cell types present in the vaginal epithelium at each stage is unique (Caligioni 2009; Gonzalez 2016). Mice are poly-estrous mammals, since if embryo implantation does not occur, a new estrous cycle is initiated. The estrous cycle was first studied in 1922 (Allen 1922). The effects of FSH, LH, estrogen, and progesterone, are similar in mice and humans, and will be further explained in the next sections. In mice, ovulation occurs during the estrus stage. If implantation does not occur, the endometrium is reabsorbed, instead of discharged, and this is the main disadvantage of the use of mice to study women's reproductive health. The first rodent species known to menstruate, the spiny mouse, was discovered in 2016 (Bellofiore et al. 2016), and therefore can be used in the future instead of the commonly used laboratory mouse to assess the mechanisms of endometrial shedding and proliferation.

1.2.2.2 Hormonal regulation of the estrous cycle

The periodicity of the estrous cycle is dependent on the hypothalamic-pituitary-ovarian axis and on a cascade of events originating from gonadotrophin releasing hormone (GnRH) neurons (Miller & Takahashi 2014). GnRH is released in a pulsatile manner (Tsutsumi & Webster 2009) from GnRH neurons in the hypothalamus (Figure 1.2). GnRH binds the GnRH receptors in the anterior pituitary gland to stimulate secretion of the gonadotropic hormones FSH and LH (Rispoli & Nett 2005). FSH binds to its receptors on the granulosa cells of the developing follicles (George, Dille & Heckert 2011) and stimulates maturation of the ovarian follicle (Rimon-Dahari et al. 2016). LH binds to its receptors on theca cells of the pre-ovulatory follicles (Zhang et al. 2001) and stimulates ovulation (Miller & Takahashi 2014). The developing and matured follicles in the ovary produce estradiol (E2), while the ruptured follicles, known as corpus lutea, produce progesterone (P4).

On the afternoon of the preovulatory proestrus stage, which lasts around 13 hours (Table 1.1), the hypothalamic GnRH pulsatile frequency and expression of GnRH receptors in the anterior pituitary increase (Miller and Takahashi, 2014; Figure 1.2). This leads to an increased production of FSH, stimulating ovarian follicle maturation (Rimon-Dahari et al. 2016). As oocyte maturation occurs in proestrus, E2 levels increase, providing a positive feedback loop for more GnRH release from the hypothalamus (Herbison 2008) and subsequently more FSH and LH release from the anterior pituitary. As E2 levels peak, the LH surge occurs, and mice enter the estrus stage (Czieselsky et al. 2016). The LH surge induces ovulation. High E2 levels prevent dopamine secretion by the hypothalamus (Cramer, Parker & Porter 1979), which in turn increases prolactin secretion by the anterior pituitary (Ben-Jonathan & Hnasko 2001). After ovulation, E2 production decreases. The ruptured follicles are transformed into corpus lutea (Bachelot & Binart 2005). P4 produced by the corpus lutea provides a negative feedback signal for GnRH secretion, therefore inhibiting further GnRH secretion by the hypothalamus. Prolactin, which is induced by mating, is required for maintenance of the corpus luteum (Stocco 2012). Maintenance of the corpus luteum causes further reduction in E2 and further increase of P4, therefore inhibiting GnRH secretion by the hypothalamus (Bashour & Wray 2012). This suppresses further E2 production, releasing dopamine from suppression. Metestrus is the stage following estrus. Dopamine levels increase in metestrus, due to decreased E2 production. Increased dopamine levels suppress prolactin (Ben-Jonathan & Hnasko 2001) leading to regression of the corpus luteum (Port et al. 2000) and a decrease in P4 production. As a result, GnRH is released from inhibition by P4. The females enter

diestrus while an increase of hypothalamic GnRH stimulates FSH and LH secretion, initiating the development of further follicles, and therefore preparing them for maturation during the following cycles (Wood et al. 2007). The follicle-derived E2 provides a positive feedback signal for GnRH secretion and the females re-enter the proestrus stage. Overall, the hypothalamic-pituitary-ovarian axis regulates a cascade of events that are essential for the periodicity of the estrous cycle, and therefore female fertility. These hormonal changes result in the maturation and release of oocytes, and the preparation and maintenance of the endometrium for blastocyst implantation and pregnancy.

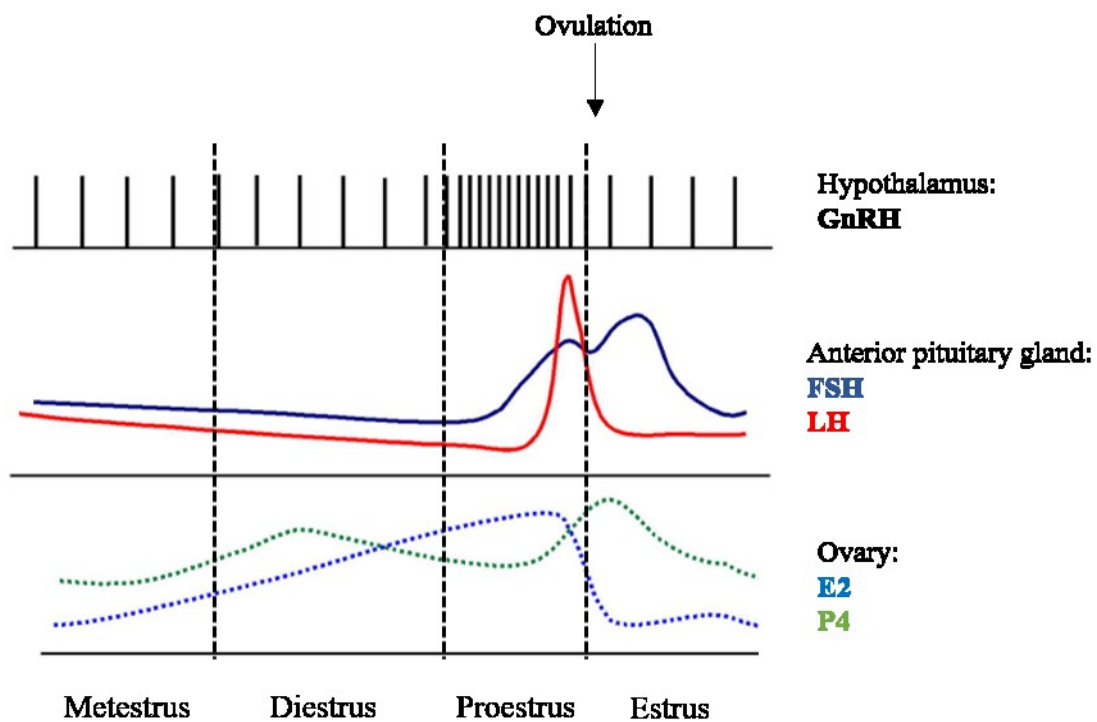


Figure 1.2 The levels of hypothalamic, pituitary, and ovarian hormones during the estrous cycle.

Modified from Miller and Takahashi (2014).

1.2.2.3 Changes in the ovaries

The hormonal changes during the estrous cycle guide the events taking place in the ovary, which include follicle development and maturation, and ovulation. The female mouse, as other mammalian species like humans and dogs, is born with a predetermined number of oocytes. By 5 weeks of age, when mice reach their sexual maturity (Buckland et al. 1981), each ovary has 10,000 oocytes (Nagy, Vintersten & Behringer 2003). FSH binds to FSH receptors on granulosa cells of the developing follicles, leading to gradual development and maturation of the oocytes, a process known as folliculogenesis (Rimon-Dahari et al. 2016). Follicle development occurs mostly during diestrus. Primordial follicles, which contain the primary oocytes, mature into primary follicles. Oocytes are arrested at prophase I of the first meiotic division at this stage. During proestrus, when GnRH and therefore FSH increase further, the follicles mature. The primary follicles mature into preantral (early Graafian) follicles. Completion of meiosis I occurs in response to further increase in FSH leading to the formation of the antral, also known as Graafian follicles, ready for ovulation. The secondary oocyte then arrests in metaphase of meiosis II, which will resume after fertilisation. E2 produced by the preantral and antral follicles provides a positive feedback signal, inducing more GnRH secretion, and subsequently more FSH secretion to induce follicle maturation (Green, 1966; Figure 1.2). E2 secretion peaks at the Graafian follicle stage (100-200pg/ml blood), causing a peak in GnRH production through a positive feedback loop (Figure 1.2). A peak in GnRH secretion induces the LH surge, leading to the rupture of the Graafian follicle and the release of the mature oocyte (ovulation; Amleh and Dean, 2002).

Mice are spontaneous ovulators, and ovulation occurs in estrus (Table 1.1; Green, 1966). During ovulation, 6-16 oocytes are released into the oviduct. The ruptured follicles transform into progesterone-producing corpus lutea (Rimon-Dahari et al. 2016). The oocytes are fertile for 8-12 hours after ovulation in the mouse reproductive tract and the peak fertility rate is achieved in the morning of the estrus stage, which lasts around 15 hours (Table 1.1). In metestrus, the corpus lutea regress, leading to decreased P4 levels, which then cause an increase in GnRH and subsequently FSH secretion, to induce development of new follicles. The events taking place in the ovary, are therefore regulated by hypothalamic, pituitary, and ovarian hormones, in a cyclical manner.

1.2.2.4 Changes in the uterus

The ovarian hormones E2 and P4 influence the preparation of the endometrium for blastocyst implantation. The endometrium proliferates, and the endometrial cells and blood vessels reach maximum proliferation capacity in diestrus (Green 1966), as a result of increasing E2 levels produced by the developing follicles. In diestrus the uterus appears thin and elongated (Bachelot & Binart 2005) and the uterine lumen is collapsed (Wood et al. 2007). Next, E2 produced by the developing follicles in proestrus induces further proliferation of the endometrium, therefore increases the uterine width. The endometrium is undulating, with projections of endometrial tissue into the lumen (Bertolin & Murphy 2014; Wood et al. 2007). The epithelial cells undergo active mitosis, and there are few leukocytes present. Increased E2 levels in proestrus also reduce endometrial stromal cell apoptosis (Wood et al. 2007). During estrus, the E2 levels drop, therefore endometrial proliferation stops. In proestrus and estrus, the uterus is thick and swollen, due to increased secretions by the endometrial glands. Endometrial stroma cell proliferation is correlated with increasing E2 levels during proestrus and estrus. At estrus, there is increased extracellular fluid throughout the endometrium, which starts decreasing in late estrus. Additionally, P4 levels increase, due to the formation of the corpus luteum, inducing the secretory activity of the oviducts and the endometrium to nurture the ovulated oocyte (Green 1966; Miller & Takahashi 2014; Wood et al. 2007). P4 is required for the preparation of the endometrium for pregnancy, and its maintenance during gestation (Bachelot & Binart 2005). Finally, during metestrus, a decrease in P4 and low levels of E2 lead to resorption of the endometrium (Caligioni 2009). The endometrial oedema decreases significantly, while stromal cell apoptosis peaks, resulting in a thinner endometrium. Overall, the remodelling of the endometrium during the estrous cycle, that aims to prepare it for blastocyst implantation and maintenance of pregnancy, is guided by the ovarian hormones, produced in a regulated manner, as a response to the pituitary hormones FSH and LH.

Ovarian hormone levels also influence other uterine structures, such as endometrial glands and luminal epithelia. Proliferation of the glandular epithelium peaks at proestrus and metestrus. It negatively correlates with E2 levels, but it is independent of P4 levels. Increased E2 levels in proestrus reduce the frequency of luminal and glandular epithelial cell apoptosis (Wood et al. 2007). Although E2 negatively correlates with proliferation of glandular epithelia cells, it positively correlates with proliferation of stromal cells. On the other hand, apoptosis of luminal epithelial cells and stromal cells peaks at metestrus and it is inversely

Table 1.1 Changes in mouse reproductive organs during the estrous cycle.

Estrous cycle stage	Proestrus	Estrus	Metestrus	Diestrus
Duration (hrs)	13	15	13	56
Vaginal smear	N±C	C	L±C±N	L
Hormone levels	Increased GnRH pulsatility am: Increased E2 pm: LH surge Low P4	am: Elevated E2 pm: Drop in E2 Very low LH and FSH Increase in P4 Decreased GnRH pulsatility	Low E2 Very low LH and FSH Low P4	Initial increase of GnRH, FSH, LH, and E2
Vaginal epithelium	Many cell layers, active mitoses, increasing cornification of the granulosa cell layer, the 4-5 outer layers consist of nucleated cells.	The outer nucleated cell layer is lost. The outer layer now contains cornified cells. There are 12 layers of nucleated cells underneath. Decreased mitosis.	The cornified layer is delaminated. Few layers of nucleated cells. Many leukocytes appear in the outer layers.	Few layers of nucleated cells. Many leukocytes appear in the outer layers. Growth starts at the end of diestrus.
Uterus	E2 causes proliferation of the endometrium. Hyperaemia and distension. Active mitoses in the epithelium. Few leukocytes.	Increase in P4 induces the secretory activity of the oviducts and endometrium. Maximum distension and mitotic activity. No leukocytes.	Decreased distension. Epithelial penetration by leukocytes. Decrease in P4 causes degeneration of the epithelium.	Anemic uterus. Uterine walls collapse. Some uterine gland secretions. Epithelium contains many leukocytes. Initial endometrial proliferation after E2 secretion.
Ovary and oviduct	Follicle maturation. Large and distended follicles. Few mitoses in the germinal epithelium and follicle cells.	Ovulation. Distension of the upper part of the oviduct. Active mitoses of the germinal epithelium and follicle cells.	Regression of corpora lutea. Oocytes present in the oviduct. Few mitoses in the germinal epithelium and follicle cells.	Rapid growth of follicle at the end of diestrus.

N: nucleated epithelial cells, C: cornified squamous epithelial cells, L: leukocytes, E2: estradiol, LH: luteinising hormone, FSH: follicle stimulating hormone, am: morning, pm: evening. Table modified from (Green 1966).

correlated with E2 levels. P4 levels are inversely correlated with stromal cell apoptosis only (Wood et al. 2007). The luminal epithelium appears rough and uneven at metestrus, and smooth in the other stages of the estrous cycle (Wood et al. 2007). This might be a result of increased apoptosis of luminal epithelial cells in metestrus. Little is known about the morphology of the cells in the different uterine structures, such as myometrium, or lumen epithelium. However, E2 and P4 levels do not influence the myometrial thickness (Wood et al. 2007). Overall, the ovarian hormone levels during the estrous cycle affect not only the structure of the endometrium, but also the glandular and luminal epithelia. These changes aim to create a receptive environment following ovulation and prepare the uterus for blastocyst implantation.

1.2.2.5 Abnormal cyclicity and infertility

Abnormal estrous or menstrual cycles are associated with infertility. Anovulatory disorders caused by hypothalamic-pituitary-ovarian axis dysfunction are a leading cause of infertility (Mikhael, Punjala-Patel & Gavrilova-Jordan 2019). These disorders are classified into three groups, by the World Health Organisation. Group I, which accounts for 10% of ovulation disorders, involves hypogonadotropic hypogonadism resulting from hypothalamic failure. In this case, the ovaries are functionally competent, but there is no GnRH and subsequently no FSH or LH produced, therefore the ovaries fail to function (Jindal & Jindal 2015). Group II, which accounts for 85% of ovulation disorders, involves the polycystic ovary syndrome (PCOS), and abnormal body mass index, resulting from dysfunction of the hypothalamic-pituitary-ovarian axis. PCOS is characterised by excess androgen production by the ovaries or the adrenal glands. Additionally, it causes anovulation due to arrested follicular development, increasing the risk of infertility (Macut 2009). Group III involves ovarian failure, leading to oocyte depletion, resulting from premature ovarian insufficiency caused by genetic or iatrogenic factors (Mikhael, Punjala-Patel & Gavrilova-Jordan 2019). Additionally, E2 and P4 produced during the menstrual cycle are essential for endometrial proliferation and induction of endometrial receptivity following ovulation, respectively (Paulson 2011). For instance, abnormal expression of endometrial E2 or P4 receptors during the menstrual cycle can lead to decreased proliferation and receptivity of the endometrium, and ultimately implantation failure (Fung et al. 2018; Garcia et al. 1988; Lessey et al. 1988). Moreover, E2 upregulates endometrial Mucin 1 (*Muc1*) expression in mice, while P4 antagonises the action of E2. *Muc1* expression is reduced during the window in implantation and its loss is

considered a prerequisite for a receptive endometrium (Dharmaraj, Gendler & Carson 2009). A polymorphism in the variable number tandem repeat of *MUC1* resulted in a protein with significantly less O-glycosylation sites, which might possibly be associated with implantation failure (Horne et al. 2001). Therefore, the regulation of *MUC1* expression by P4 is essential for endometrial receptivity. Abnormal cyclicality and abnormal production of E2 and P4 can therefore impair endometrial receptivity, leading to implantation failure (Hashimoto et al. 2017). Altogether, these data show that abnormal function of either the hypothalamus, the pituitary, or the ovaries, can lead to anovulation or abnormal endometrial receptivity, and therefore infertility.

Like humans, abnormal function of the hypothalamic-pituitary-ovarian axis can cause anovulation, abnormal folliculogenesis, and infertility in animals. In female mice, testicular orphan receptor 4 (TR4) induces LH receptor gene expression. *Tr4^{-/-}* mice have prolonged diestrus stages, smaller ovaries, fewer corpora lutea, intensive granulosa cell apoptosis, and impaired folliculogenesis (Chen et al. 2008). Although not assessed, it was hypothesised that reduced LH receptor expression on theca cells leads to reduced E2 and P4 levels (Chen et al. 2008). Additionally, deficiency of Complement-3 (*C3*) in mice, which is important for immune responses, leads to an extended estrous cycle and higher resorption rates at E14.5, as a result of decreased spongiotrophoblast and labyrinth areas of the placenta (Chow et al. 2009). Similarly, in horses, anovulation leads to infertility (McCue & Act 1998). It occurs because of insufficient pituitary FSH and LH, leading to inadequate development and maturation of the follicles, or insufficient E2 production from the follicles, not able to trigger the LH surge to induce ovulation. The anovulatory follicles persist in the ovaries and result in abnormal estrus behaviour and prolonged inter-ovulatory intervals. Bitches undergo an anestrus 2-10-month period where the reproductive tract undergoes uterine regeneration and endocrine preparation, before entering the next estrus phase. Shortened anestrus leads to shorter interestrus interval, resulting in difficulties in breeding (Wanke, Loza & Rebuelto 2006). Prolonged estrus in bitches leads to prolonged exposure of the ovaries to estrogen, leading to ovarian cysts and ovarian tumors (Blendinger 2007). Additionally, hormonal changes during the estrous cycle regulate *Muc1* expression. *Muc1* levels peak at proestrus and estrus in response to E2 (Braga & Gendler 1993). *Muc1* levels decrease in metestrus and diestrus, and the authors suggests that this might be in response to P4 (Braga & Gendler 1993). *Muc1* is important for endometrial receptivity, and decreased *MUC1* is a marker of endometrial receptivity in women with recurrent implantation failure (Wu et al. 2018).

Therefore, abnormal cyclicity and abnormal changes in hormone levels during estrus can impair *Muc1* expression, leading to decreased endometrial receptivity and ultimately implantation failure. Altogether, these studies show how abnormal cyclicity impairs fertility, by affecting either ovulation, or endometrial receptivity.

1.2.3 From estrous cycle to pregnancy in mice

Mating of mice usually occurs in the early morning of the estrus stage, when the females are more likely to be receptive to males (Byers et al. 2012). Copulation is identified by the presence of a copulatory plug the next morning, which is considered to be embryonic day (E) 0.5. The formation of the copulatory plug prevents the female from mating with other males, but it does not guarantee pregnancy (Sutter et al. 2015). During a successful mating, the sperm travels through the uterus to the ampulla part of the oviducts, where fertilisation occurs (Deb, Reese & Paria 2006). The fertilised eggs are released from meiotic arrest, completing the second meiotic division (MacLennan et al. 2015), forming the zygote. The zygote undergoes mitotic divisions, to reach the cleavage stages to form the morula, and ultimately, the blastocyst, by E3.5 (Li, Zheng & Dean 2010).

1.2.3.1 The estrous cycle after mating and maintenance of corpus luteum and progesterone

After mating at the estrus stage, the ruptured follicle is transformed into the corpus luteum (see Section 1.2.2) and the estrous cycle is interrupted. Cervical stimulation during mating inhibits dopamine secretion, therefore increasing pituitary prolactin levels (Poletini et al. 2010). Prolactin is released in a pulsatile manner (Helena et al. 2009). In rodents, prolactin is essential for the maintenance of the corpus luteum for the first 8-9 days of pregnancy, until the placenta takes over P4 production (Bachelot & Binart 2007; Risk & Gibori 2001; Stocco 2012). Maintenance of the corpus luteum results in high P4 levels, which inhibit GnRH secretion by the hypothalamus. Low levels of GnRH and E2 prevent the development of further follicles and maintain low FSH and LH levels. These hormonal changes block further follicle development, ovulation and cyclicity, so that pregnancy can be maintained. After E8.5 mouse placental lactogens 1 and 2 produced by the trophoblast giant cells to maintain the corpus luteum (Malassiné, Frenzo & Evain-Brion 2003). The corpus luteum is not affected by a hypophysectomy (removal of the hypophysis) after E10.5, since it is maintained

by placental lactogens. If sterile copulation occurs, i.e. mating with a vasectomised male and therefore fertilisation does not occur, the mice enter a pseudopregnant state, where the metestrus stage is prolonged by 10-13 days. The corpus luteum in mice is responsible for P4 secretion throughout gestation (Risk & Gibori 2001). From E7.5 the corpus luteum starts increasing its size, reaching its maximal diameter on E12.5 (Greenwald & Rothchild 1968). The P4 produced by the corpus luteum is therefore key for blocking estrous cyclicity and initiating a successful pregnancy.

1.2.3.2 Changes in the uterus after fertilisation

Embryo implantation and development depend upon the different cell types present in the uterus that undergo dynamic changes at the peri-implantation and post-implantation stages (Jeong et al. 2010). The formation of the corpus luteum and the peak in P4 and E2 lead to optimal uterine receptivity between E3.5 and E4.5 (Wang & Dey 2006). This is mediated by MUC1, which is expressed by the apical surface of the uterine epithelial cells (Surveyor et al. 1995). High levels of MUC1 prevents embryo implantation, and therefore its loss contributes to the acquirement of a receptive uterine state (Surveyor et al. 1995). E2 stimulates *Muc1* expression, while P4 antagonises the stimulatory effects of E2 on *Muc1* expression (Surveyor et al. 1995). A successful pregnancy relies on the interaction between the implanting blastocyst and the receptive endometrium (Aplin & Ruane 2017). At the peri-implantation period, the apical plasma membrane of the uterine epithelial cells flatten, by losing their microvilli (Cha et al. 2014). The blastocysts are only able to attach when the apical surface of the cells is flattened (Murphy 2004). The uterine horns elongate before and during implantation (Finn 1968). This is important because embryo spacing in the uterine horns relies on the simultaneous elongation of the outer myometrial layer and contraction of the inner myometrial layer (Chen et al. 2011; Yoshinaga 2013). Endometrial stroma oedema is observed due to reabsorption of the intraluminal uterine fluid, leading to closure of the uterine lumen (Huet-Hudson & Dey 1990). This facilitates interactions between the uterine epithelium and the blastocyst, necessary for implantation (Chen et al. 2013). Studies in human *in vitro* fertilisation have highlighted the importance of synchronising blastocyst development with the endometrial environment, to prevent implantation failure (Valdes, Schutt & Simon 2017). If implantation occurs beyond the window of implantation, there is increased risk of spontaneous abortion (Wilcox, Baird & Weinberg 1999), or peri-implantation pregnancy loss (Norwitz, Schust & Fisher 2001). Uterine gland secretions are

also important for successful implantation. For instance, leukemia inhibitory factor (LIF), which is expressed by the uterine glands, is essential for embryo implantation (Stewart et al. 1992). Implantation failure was observed in *Lif*^{-/-} females. However, the blastocysts of *Lif*^{-/-} females that were transferred to a wildtype pseudopregnant female could implant and develop to term (Stewart et al. 1992). Other mice lacking functional uterine glands show defects in blastocyst implantation, which could be a result of the absence of LIF (Dunlap et al. 2011; Filant & Spencer 2013; Jeong et al. 2010). In mice, embryo implantation consists of three steps: (a) apposition, where the mural trophoblast cells of the blastocyst contact the epithelial cells at the antimesometrial side of the uterus, which is the side opposite the mesometrial blood vessels (Daikoku et al. 2011), (b) attachment, where the trophoblast cells of the blastocyst attach to the receptive endometrium, and (c) invasion, where the trophoblast cells cross the endometrial epithelial basement membrane to reach the endometrial stroma (Dey et al. 2004; Ruane et al. 2017). At E5.5, the lumen epithelial cells that are near the blastocyst undergo apoptosis (Filant & Spencer 2014; Joswig et al. 2003). Altogether, these studies show the changes that happen in the uterus after fertilisation and are essential for embryo implantation and development. However, one of the most important uterine changes is the process of decidualisation, which will be discussed next.

1.2.3.3 Decidualisation after implantation

The interaction of the implanting embryo with the uterine luminal epithelium stimulates decidualisation (Favaro, Abrahamsohn & Zorn 2014). Decidualisation is required for successful blastocyst implantation (Lee & Demayo 2004) and involves morphogenetic, biochemical, and vascular changes in the pregnant uterus, that are driven by activation of E2 and P4 receptors. More specifically, decidualisation involves: (a) transdifferentiation of endometrial stromal cells into decidual cells, (b) extracellular matrix remodelling of the endometrial stroma, (c) production of molecules important for maternal-fetal interactions, (d) maternal angiogenesis essential for nutrient supply to the embryo, and (e) influx of uterine natural killer (uNK) cells with immunoregulatory and vasculogenetic roles (Favaro, Abrahamsohn & Zorn 2014). This process is therefore essential to provide an optimal intrauterine environment for embryo development.

As a transient tissue, the murine decidua begins to form at E4.5 from the antimesometrial pole and it only occurs in the implantation sites (Lim & Wang 2010). The decidual cells

undergo extensive proliferation and differentiation between E4.5 and E7.5 and become polyploid (Sroga, Ma & Das 2012). It is speculated that the cells' polyploid status ensures that they have a limited lifespan (Das 2009), although the mechanism is unknown. The limited lifespan of the decidual cells, however, is essential for decidual regression. Failure of decidual regression can lead to reduced trophoblast invasion and abnormal labyrinth development (Lague et al. 2010). Decidualised stromal cells produce growth factors and cytokines to support growth of the developing embryo (Ramathal et al., 2010).

Decidualisation leads to the formation of a thicker endometrial wall (Fraser et al. 2015). During decidualisation, increased endometrial vascular permeability necessary for nutrient supply to the embryo is also prominent.

The decidual cells at the antimesometrial pole form the avascular and epithelioid primary decidual zone (PDZ; Figure 1.3). The stromal cells proximal to the PDZ proliferate, undergo subsequent apoptosis, and disappear by E7.5. At E6.5, the trophoctoderm-derived ectoplacental cone penetrates the mesometrial decidua, which is enriched with maternal blood vessels (Lim & Wang 2010). The stromal cells next to the PDZ continue to proliferate and differentiate into polyploid decidual cells to form the secondary decidual zone (SDZ; Figure 1.3), which is fully developed by E6.5 (F. Gao et al. 2015; Tan et al. 2002). The SDZ contains polyploid decidual cells that are found in lateral and antimesometrial decidual zones. Mitochondrial activity is critical for the development of decidual cell polyploidy. Polyploid cells express genes associated with mitochondrial function, as shown by microarray analysis of polyploid and non-polyploid decidual cells and inhibition of mitochondrial activity attenuates decidual cell polyploidy (Ma et al. 2011). In contrast, a non-polyploid decidual zone forms after proliferation and differentiation of mesometrial stromal cells by E7.5 (F. Gao et al. 2015). The cells in the SDZ eventually also undergo apoptosis, a process known as decidual regression, allowing the implantation chamber to enlarge and support growth of the developing embryo (Tan et al. 2002). Inadequate decidual regression due to decreased apoptosis can lead to an abnormally thick decidual layer, obstructing trophoblast invasion, and therefore placentation (Lague et al. 2010).

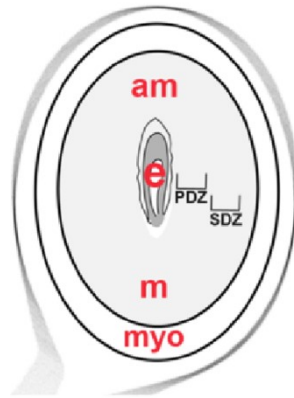


Figure 1.3 Schematic of an implantation site at E6.5.

am: antimesometrial region, m: mesometrial region, myo: myometrium, PDZ: primary decidual zone, SDZ: secondary decidual zone; Reproduced from Douglas et al. (2014).

1.2.3.4 Gene expression during estrous cycle affects decidualisation

Estrous cyclicity is regulated by the hypothalamic-pituitary-ovarian axis. However, the molecular mechanisms, such as transcription factors that regulate the events that take place during the cycle, are not well understood. The estrous cycle is driven by gene regulatory networks, and genes are specifically expressed at each stage of the cycle (Lee et al. 2005; Tan et al. 2003; Yip et al. 2013). Transcriptome analysis revealed that the Wntless-related integration site (WNT) signalling pathway was activated in estrus compared to proestrus (Yip et al. 2013). WNT signalling is important for proper decidualisation (Sonderregger, Pollheimer & Knöfler 2010). Additionally, proteinases and protease inhibitors, that regulate the uterine extracellular architecture, are differentially expressed between proestrus and estrus. For instance, *Serpine2* is upregulated in estrus (Yip et al. 2013), is expressed by the luminal and glandular epithelial cells and is involved in uterine tissue remodelling (Chern et al. 2010). The Hedgehog pathway is also activated in estrus compared to proestrus, as genes involved such as *Smo*, *Bmp4*, *Bmp6*, *Wnt2* and *Wnt7a* were upregulated during estrus (Yip et al. 2013). The hedgehog pathway is activated in response to P4 signalling in luminal and glandular epithelial cells (Simon et al. 2009), and is essential for implantation (Harman et al. 2011). Overall, these data suggest that molecular events that occur in parallel with E2 action on endometrial proliferation, ensure that the endometrium expresses the receptors and molecules necessary to accept the blastocyst and maintain a successful pregnancy.

1.2.3.5 Factors that regulate decidualisation

Extracellular matrix remodelling is essential during decidualisation. Differentiation of endometrial stroma cells into decidual cells, intense cell growth, and formation of intercellular junctions lead to decreased extracellular spaces in the endometrium (Favaro, Abrahamsohn & Zorn 2014). As a result, remodelling of the endometrial extracellular matrix occurs (Abrahamsohn & Zorn 1993). During extracellular matrix remodelling, collagen fibres become thicker. Collagen types I, III, and V have specific expression patterns. Collagen I is expressed in the non-decidualised endometrial stroma of the inter-implantation sites. Collagens III and V are found in the basement membrane of the uterine glands of the inter-implantation sites and they appear in the decidua after E6.5 (Favaro, Abrahamsohn & Zorn 2014). Extracellular matrix remodelling is also essential for further placenta development and will be discussed in Section 1.3.3.

Decidualisation is regulated by transcription factors (Lim & Wang 2010). During normal decidualisation, *Hoxa10* and *Cyclin-D3* regulate *FoxM1* transcription and nuclear translocation, respectively. FOXM1 is a transcription factor that is essential for mitosis in the mesometrial decidual zone, leading to formation of diploid cells (Gao et al. 2015). FOXM1 also causes endoreduplication of the cells in the lateral and anti-mesometrial secondary decidual zone, leading to polyploid cell formation. Loss of uterine *FoxM1* leads to arrest of the cell cycle prior to mitosis by downregulation of the mitotic regulators *Ccnb1*, *Cdc25b*, and *Cenpf* (Gao et al. 2015). This leads to increased formation of polyploid cells leading to increased secondary decidual zone, and decreased numbers of diploid cells leading to smaller mesometrial area. Changes in regional decidualisation, for instance in the size of the different decidual areas, impairs pregnancy progression, and leads to pregnancy loss during decidualisation (Gao et al. 2015). Therefore, proper regulation of *FoxM1* leads to proper regional decidualisation, and ultimately proper embryo growth. Additionally, *Prl8a2* is expressed in the anti-mesometrial decidua of mouse and rat (Orwig, Dai, et al. 1997; Orwig, Ishimura, et al. 1997; Orwig, Rasmussen & Soares 1997; Rasmussen et al. 1996, 1997; Roby et al. 1993) and inhibits activation of endometrial stress pathways in decidual cells (Alam, Konno & Soares 2015). *Bmp2* is also used as a marker of decidualisation. Conditional ablation of *Bmp2* in the uterus does not affect implantation, but the uterine stroma fails to differentiate into decidual cells, therefore decidualisation fails (Lee et al. 2007). Treatment of E4.5 pregnant uteri with progesterone receptor (PR) antagonist led to significant downregulation of *Bmp2* at E5.5, suggesting *Bmp2* is a downstream target of PR signalling

(Li et al. 2007). In addition, stromal cell differentiation was induced in a primary culture of undifferentiated stromal cells derived from pregnant mice after addition of recombinant *Bmp2* (Li et al. 2007). Addition of BMP2-specific siRNA in the cell culture prevented the differentiation process. *Wnt4* is a downstream target of BMP2 signalling. Addition of BMP2 in the cell culture led to an increase in WNT4 expression and induced stromal cell differentiation (Li et al. 2007), suggesting that BMP2 and WNT4 mediate P4-induced stromal cell differentiation. NR2F2 is a transcription factor whose role in implantation and decidualisation is well established (Wetendorf & DeMayo 2012). NR2F2 is highly expressed in uterine stroma cells and it is known to activate *Bmp2* transcription (Kurihara et al. 2007). *Nr2f2*^{+/-} females display reduced fecundity, abnormal estrous cyclicity, delayed puberty, reduced decidualisation as indicated by wet weights of the uterine horns, and postnatal growth retardation compared to wildtype littermates (Takamoto et al. 2005). *Ihh* is also found downstream of PGR and activates *Nr2f2*. Conditional ablation of *Ihh* in PGR-positive uterine cells leads to attachment failure. In addition, when the uterine horns of these *Ihh*^{-/-} females were traumatized by a needle scratch in order to induce artificial decidualisation, they failed to undergo decidualisation (Lee et al. 2006). HOXA10, another transcription factor, is highly expressed in the decidualising uterine stroma cells (Das 2010) and it regulates the responsiveness of uterine stromal cells to P4 during implantation and decidualisation (Lim et al. 1999). *Hoxa10* mutant females exhibit failure of implantation and resorption of embryos in the early postimplantation period (Benson et al. 1996). HAND2 is another transcription factor that is regulated by P4 during decidualisation (Okada et al. 2014). *Hand2* is expressed by the endometrial stromal cells prior to implantation, but it peaks in the uterus during decidualisation and its expression is regulated by P4 (Huyen & Bany 2011). SiRNA-mediated reduction of *Hand2* mRNA leads to defective decidualisation and decreased expression of decidual markers (Huyen & Bany 2011). Pharmacological inhibition of *Notch1* led to impaired artificial induction of decidualisation, as indicated by a decreased uterine wet weight ratio of the decidual horn to the control horn in mice with pharmacological intervention compared to controls (Afshar et al. 2011). Altogether, these studies show that activation of *Pgr* and its downstream targets, such as *Bmp2*, *Nr2f2*, and *Wnt4* is essential for stromal cell decidualisation.

1.2.3.6 Factors that regulate angiogenesis

Uterine angiogenesis also occurs in the pregnant uterus during decidualisation. Angiogenesis involves the formation of new blood vessels from pre-existing ones to facilitate perfusion of the implantation site by the maternal blood (Adamson et al. 2002). Decidual cells are important for maternal blood vessel formation in the uterus (Fraser et al. 2015). For instance, decidual NK cells control vessel stability by inducing expression of the adhesion molecule *Icam1* in the endothelial cells (Fraser et al. 2015). The angiogenic factor VEGF and its receptors, VEGFR1 and VEGFR2, encoded by *Flt-1* and *Flk-1*, respectively, expressed by uterine endothelial cells are required for uterine angiogenesis (Matsumoto et al. 2002). Mice administered with a FLT1 blocking antibody during the pre-implantation and peri-implantation period showed decreased decidual vascular density. However, embryo implantation and pregnancy progression were not affected (Douglas et al. 2014). In addition, cyclooxygenases are the key enzymes for prostaglandin biosynthesis. Prostaglandins regulate angiogenesis during implantation and decidualisation (Finetti et al. 2008; Lim, Gupta, et al. 1999). For instance, *Cox2*^{-/-} mice exhibited impaired implantation and attenuation of uterine angiogenesis due to defective VEGF signalling (Matsumoto et al. 2002). Transfer of the embryos in a P4-treated *Cox2*^{-/-} pseudopregnant recipient led to embryo attachment, but abnormal decidualisation was characterised by decreased vascular permeability. Aberrant expression of PECAM-1, which is expressed early during vascular development, was observed in *Cox2*^{-/-} recipients resulting in reduced mesometrial decidual area. Finally, cell-cell communications are important for decidual cell function, such as production of angiogenic factors, as determined by conditional mutants of the gap junction protein Connexin 43 (*Cx43*; Laws et al. 2008).

1.2.4 Endometrial causes of FGR

Fetuses developing in a structurally abnormal uterus develop deformations (Miller, Dunn & Smith 1979), although there is little evidence linking abnormal uterine development and structure to FGR. There is also little evidence linking the estrous cycle to FGR. For instance, P4 and E2 levels affect collagen. Collagen type-IV is found on the basement membrane of luminal and glandular epithelial cells. At estrus, collagen type-IV is lost from the luminal cells but it is at similar levels in glandular cells compared to other stages of the cycle. P4 and E2 levels inversely correlate with the degradation of collagen type-IV from the basement

membrane of luminal and glandular epithelia cells, respectively (Wood et al. 2007). Although not shown, it has been suggested that inefficient degradation of collagen type-IV in response to P4 and E2 can lead to occlusion of blood vessels and possibly interfere with vascularisation (Rahima & Soderwall 1977). In turn, abnormal uteroplacental vascularisation can lead to FGR (Noguchi et al. 2009). The little evidence linking the estrous cycle to FGR could be because disruption of the estrous cycle can impair the preparation of the uterus for implantation, and therefore lead to implantation defects. However, there is some evidence that links endometrial function to FGR. As mentioned in the previous section, abnormal gene expression during the estrous cycle can affect uterine decidualisation during early pregnancy. Disrupted decidualisation can impair the blood flow and oxygen and nutrient transport to the developing fetus, leading to abnormal embryo growth (Wang & Dey 2006). For example, delayed implantation occurred as a result of maternal deletion of the homeobox gene *Msx1*, lysophosphatidic acid receptor 3 (*Lpar3*), prostaglandin synthase 2 (*Ptgs2*), or phospholipase A2 (*Pla2g4a*), leading to defective post-implantation development and retarded fetoplacental growth (Daikoku et al. 2011; Song et al. 2002; Ye et al. 2005). Similarly, disruption of decidualisation due to deletion of genes involved in decidualisation, such as *Bmpr2*, results in FGR at E9.5-E10.5 due to defective decidual cell proliferation, impaired decidual vascularisation, and ultimately abnormal nutrient transport (Nagashima et al. 2013). Decidual cell apoptosis is essential for trophoblast invasion. Deletion of *Pten* from the myometrial and stromal/decidual cells resulted in decreased apoptosis and subsequent decreased decidual regression. As a result, the decidual layer was abnormally thick, leading to defective trophoblast invasion and delayed spiral artery remodelling (SAR; see Section 1.3). This was frequently associated with FGR, possibly due to decreased nutrient supply to the embryo (Lague et al. 2010). Similarly, *Mmp9* deficiency led to abnormal trophoblast differentiation and invasion and ultimately FGR in mice (Plaks et al. 2013). Additionally, CX43, which is encoded by *Gjal*, is expressed in the decidual cells and is required for the transdifferentiation of stromal cells into decidual cells, and for angiogenesis. A dominant mutation of *Gjal* in the mother leads to abnormal decidual angiogenesis and increased expression of angiogenic factors, such as *Vegfa*, *Flt1*, *Kdr*, and *Fgf2*. This resulted in disorganised and dilated maternal blood spaces in the decidua, and ultimately decreased surface area available for exchange of nutrients, gas and waste products. As a result, the fetal weight at E17.5 was reduced, indicating FGR (Winterhager et al. 2013). A uterine *Nodal* knockout in the mothers led to malformation of the decidual basalis and abnormal placentation, characterised by larger decidual zone at E8.5, increased TGC expansion at E10.5, FGR at E15.5-E16.5, and fetal loss

by E17.5 (Park et al. 2012). Additionally, uterine *Lk5* knockout in the mothers led to fewer and smaller implantation sites, uterine haemorrhage, unclosed uterine lumen, and shallow trophoblast invasion at GD8.5. At E9.5, the antimesometrial decidual area appeared thicker, possibly limiting fetal growth. At E10.5, the labyrinth layer was smaller, the TGC were expanded, and FGR was observed (Peng et al. 2015). Moreover, maternal floor infarction and massive chronic intervillitis are pathological diagnoses involving excessive fibrin deposition and are associated with FGR. In both cases, mononuclear or giant cells from the maternal circulation infiltrate the villi, leading to villous vascular occlusion, therefore preventing proper vascular development and function (Roberts & Post 2008). Tissues from pregnancies complicated with fetal growth restriction are characterised by defective myometrial SAR, including decreased muscle disruption, increased number of extravillous-cytotrophoblast surrounding the decidual and myometrial vessels and less fibrinoid deposition in the decidual myometrial vessels (Lyall, Robson & Bulmer 2013). Finally, fetal thrombotic vasculopathy characterised by fetal vascular obstructive lesions cause villous infarction and leads to FGR (Roberts & Post 2008). Altogether, these studies show that abnormal endometrial function, such as abnormal endometrial gene expression and abnormal decidualisation and angiogenesis can cause FGR.

1.3 Mouse placenta development and function

The placenta is a highly specialised organ. It is responsible not only for anchoring the developing embryo on the maternal endometrium, therefore preventing its rejection by the maternal immune system, but also for the transport of nutrients, gases, and waste products between the maternal and fetal circulations. The placenta functions to support embryo growth and development (Cross, Simmons & Watson 2003). In the previous section we talked about the maternal tissues of the mouse placenta and discussed the endometrial causes of FGR. However, the placenta is a chimeric organ, consisting of both maternal and fetal tissues. Therefore, in this section we will give an overview of placental development and discuss the interactions between the maternal and fetal components of the placenta. Additionally, we will discuss how the fetal tissues of the placenta can contribute to FGR.

1.3.1 Structure and function of the mature mouse placenta

The mouse is a good model organism to study placentation in humans. The invasive and endocrine trophoblast is called the extravillous cytotrophoblast in humans, which is analogous to the trophoblast giant cells and glycogen trophoblast cells in mice (Silva & Serakides 2016). In both species, the trophoblast is invasive and non-proliferative, with mononuclear polyploid cells. In addition, the transport and barrier trophoblast, known as chorionic villi and labyrinth in humans and mice respectively, is haemochorial, since the chorion is in direct contact with the maternal blood. Both the chorionic villi in humans, and the labyrinth in mice, have a syncytiotrophoblast layer that is formed by cell fusion. Syncytiotrophoblast cells are therefore polyploid in both species (Cross et al. 2003).

The mature mouse placenta (E14.5) is divided into histologically distinct areas: the maternal decidua, that derives from the proliferation and differentiation of endometrial stroma cells, the junctional zone, and the labyrinth (Figure 1.4; John 2013; Watson & Cross 2005). The maternal decidua contains the spiral artery-associated TGCs, that derive from the ectoplacental cone. The maternal decidua is in direct contact with a layer of parietal trophoblast giant cells (p-TGCs). P-TGCs derive from the ectoplacental cone and surround the lacunae, which are large lakes of blood that lead to the uterine veins (Rai & Cross 2014).

The next compartment of the placenta is the junctional zone, which contains four ectoplacental cone (EPC)-derived cell types: the spongiotrophoblast cells, the glycogen cells, the canal TGCs, and the channel TGCs. The spongiotrophoblast cells have an endocrine function and secrete the placental prolactins and pregnancy-specific glycoproteins. These proteins are essential for protecting the developing fetus from being attacked by the maternal immune system, and to remodel the blood vessels of the placenta and the maternal decidua (Kammerer & Zimmermann 2010; Wu et al. 2008). The glycogen trophoblast cells store glycogen, that is catabolised to glucose upon activation of glucagon receptors (Coan, Conroy & Burton 2006). The glucose is then released into the maternal bloodstream, and then transported to the fetus through glucose transporters (Hay 2006). Glycogen trophoblast cell number increases from E12.5 to E16.5 by 80-fold, while it decreases by E18.5 (Coan, Conroy & Burton 2006). The maternal blood travels through pipe-like structures formed by canal TGCs to the bottom of the labyrinth, while the deoxygenated blood is removed from the labyrinth by channel TGCs that form small channels (Rai & Cross 2014).

Finally, the labyrinth is the area of the placenta where maternal and fetal circulations come into close proximity to exchange nutrients, gases, and waste products. The labyrinth contains fetal endothelial cells derived from the allantois, as well as trophoblast cells derived from the chorion, which include two types of syncytiotrophoblast cells (SynT-I and SynT-II), and sinusoidal TGCs (sTGC; Maltepe, Bakardjiev & Fisher 2010; Simmons & Cross 2005). The sTGCs are in direct contact with the maternal blood. The SynT-I cells are found between the sTGCs and the SynT-II, while the SynT-II cells are the ones closest to the fetal endothelial cells. These three types of trophoblast cells form a trilaminar structure. The efficiency of nutrient and gas exchange largely depends on the thickness of this trilaminar structure, as well as the density of transporter proteins, and degree of branching (Sandovici et al. 2012).

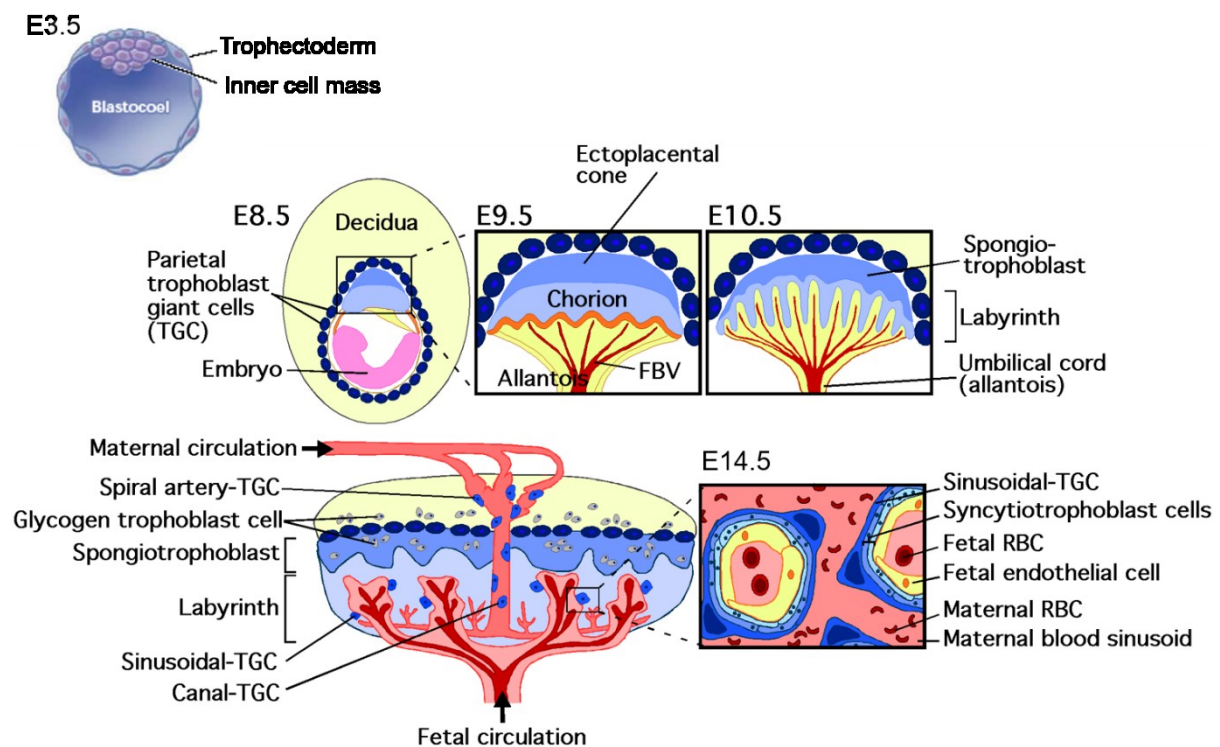


Figure 1.4 Mouse placenta development.

The development of the trophoblast lineage begins at E3.5. The chorioallantoic attachment is established by E8.5, and the mature placenta is formed by E14.5. Image by Erica D. Watson.

1.3.2 Mouse placenta development

The extraembryonic lineages in mice are established at E3.5, when the first differentiation step occurs to create the blastocyst (Cross, Werb & Fisher 1994). The blastocyst consists of a fluid-filled cavity, called the blastocoele, a compacted inner cell mass (ICM) composed of irregular, non-polarised cells, and an outer cell layer, called the trophectoderm (Figure 1.4).

The trophoctoderm which is in direct contact with the ICM is called the polar trophoctoderm, while the part of it that is on the opposite side, is called the mural trophoctoderm. The trophoctoderm is formed of polarised epithelial cells with apical microvilli (Cross, Werb & Fisher 1994).

During embryo implantation (E4.5) the mural trophoctoderm differentiates into primary trophoblast giant cells, which are analogous to the extravillous cytotrophoblast cells in humans (Rossant & Cross 2001). These are polyploid cells, since they undergo endoreduplication, by replicating their genome, without undergoing cell division. The polar trophoctoderm gives rise to the extraembryonic ectoderm (ExE) and the EPC (Rossant & Cross 2001). The ExE contributes to the chorion, that will form the labyrinth, while the EPC differentiates into the secondary parietal and the spiral artery TGCs, and cells forming the junctional zone, including spongiotrophoblast, glycogen cells, canal TGCs, and channel TGCs. (Tunster et al. 2016). The ICM, on the other hand, gives rise to extraembryonic mesoderm that differentiates into the chorionic mesoderm and allantois. Chorioallantoic attachment occurs at E8.5 (Figure 1.4) and is essential for labyrinth formation. At E9.0, branching morphogenesis initiates, which aims to form dense villi across the chorion, at the chorioallantoic interface. Villi are the structures responsible for the exchange of nutrient, gas, and waste products between the maternal and fetal circulations (Cross, Simmons & Watson 2003). Branching morphogenesis causes the labyrinth layer to expand (Cross et al. 2006). By E10.5, angiogenesis takes place in the chorionic villi (Rossant & Cross 2001). The primary villi undergo a second round of branching and elongation, forming the mature labyrinth by E14.5. Simultaneously, the trophoblast cells undergo differentiation to form the sTGC, SynT-I, and SynT-II, which separate the fetal capillaries from the maternal blood sinuses (Simmons & Cross 2005). Ultimately, the mature placenta is formed at E14.5.

1.3.3 Maternal components of the mouse placenta

As mentioned in Sections 1.2.3 and 1.3.1, the mouse uterus undergoes decidualisation during early pregnancy, and the decidua is one of the maternal components of the mature mouse placenta. The spiral arteries are the other main maternal component of the placenta. The spiral arteries are lined by endothelial cells and converge into the maternal canals. The maternal canals are lined by canal TGCs. Exchange of nutrient, gas, and waste products between the fetus and the mother occurs in the maternal sinusoids in the labyrinth, which are

lined by sinusoidal TGCs (Rennie et al. 2014). During SAR, the invading trophoblast cells induce apoptosis of the endothelial cells, and ultimately replace them in the spiral arteries (Ashton et al. 2005). Spiral arteries remodel between E6.5-E7.5 and undergo outward hypertrophic SAR, when their lumen widens, and their muscular wall thickens between E7.5 and E10.5. During E8.5-E9.5, they undergo outward hypotrophic SAR when their lumen widens, but the muscular wall gets thinner (Charalambous, Elia & Georgiades 2012; Osol & Mandala 2009). This remodelling of the spiral arteries leads to the formation of dilated, inelastic tubes with decreased vascular resistance, that lack maternal vasomotor control. SAR is essential for establishing normal maternal blood flow and therefore normal embryo growth.

Interactions between the maternal and fetal components of the placenta are essential for normal placentation. For example, trophoblast invasion is a prominent feature of placenta development (Anin, Vince & Quenby 2004) and occurs in two waves. The first wave of invasion is endovascular and perivascular and occurs during implantation and early placentation. The trophoblast cells penetrate the mesometrium and replace the vascular endothelial cells in the spiral arteries, a process known as SAR. Vascular remodelling precedes trophoblast invasion, and SAR is reduced in the absence of trophoblasts (Whitley & Cartwright 2010). These trophoblast cells express TGC markers, such as *Plf1*. The second wave of invasion, the interstitial invasion, occurs after E13.5. *Tpbpa*⁺ glycogen trophoblast cells invade the decidua basalis (Adamson et al. 2002; Cross et al. 2002; Silva & Serakides 2016). Successful trophoblast invasion requires degradation of the extracellular matrix and expression of adhesion molecules by the trophoblasts. The trophoblast secretes proteases that break down the decidual tissue to make space for the developing embryo (Aplin 2000). Metalloproteinases MMP2, MMP9, and MMP14 are highly expressed by the trophoblast cells at the fetal-maternal interface and are involved in the degradation of extracellular matrix (Lala & Graham 1990). Degradation of the extracellular matrix is required for successful trophoblast invasion into the decidua (Favaro, Abrahamsohn & Zorn 2014). However, expression of metalloproteinases ceases in the decidua. Instead, tissue inhibitor metalloproteinase (TIMP) 3 is expressed by decidual cells to prevent excessive extracellular matrix degradation and excessive trophoblast invasion (Moore & Crocker 2012). Alterations in decidual extracellular matrix remodelling have been associated with impaired decidualisation (White, Robb & Salamonsen 2004). Extensive or inadequate trophoblast invasion leads to maladaptation of uteroplacental arteries and ultimately altered uteroplacental blood flow, which is associated with FGR. Lactogen is also secreted by the

trophoblast and found in the maternal circulation (Aplin 2000). Altogether, these studies show the importance of the interactions between the maternal and fetal components of the placenta for normal placentation.

1.3.4 Poor placenta development and function can lead to FGR

The main function of the placenta is the exchange of nutrients, gases, and waste products between the maternal and fetal circulations (Watson & Cross 2005). Abnormal development and function of the placental labyrinth, such as abnormal development of the blood vessels necessary for this exchange, or abnormal transport across the maternal-fetal interface, can limit the nutrients that are being delivered to the developing fetus, leading to FGR (Scifres & Nelson 2009). In addition, the adaptive changes of the spiral arteries that happen during pregnancy ensure adequate blood supply to the developing fetus. Ablation of *Tpbpa*-positive cells, which would normally differentiate into the invasive trophoblast, impairs trophoblast invasion of the spiral arteries, leading to defective SAR (Hu & Cross 2011). Defective remodelling of the spiral arteries results in decreased uteroplacental blood flow, increased vascular resistance, and a subsequent decrease of blood flow to the placenta, causing impaired nutrient and oxygen transport to the embryo, which prevents aerobic fetal growth (Krishna & Bhalerao 2011; Swanson & David 2015). These features are often indicators of pre-eclampsia (Granger et al. 2002). Doppler ultrasound is a non-invasive method used to assess blood flow in uteroplacental circulation (Campbell et al. 1983), by measuring the resistance index and pulsatility index of the uterine arteries as indicators of impedance. High resistance and pulsatility indices are associated with FGR (Dugoff et al. 2005; van den Elzen et al. 1995; Harrington et al. 1997; Khanduri et al. 2017; Martin et al. 2001).

Junctional zone defects that affect vascularisation can also cause FGR. For instance, a hypomorphic mutation of *Ascl2* or a targeted ablation of *Hrtal* lead to a smaller junctional zone with fewer spongiotrophoblast and glycogen cells, and FGR at E15.5 and E14.5, respectively (Hasan et al. 2015; Oh-McGinnis, Bogutz & Lefebvre 2011). Overexpression of *Ascl2* also leads to a smaller junctional zone with reduced spongiotrophoblast numbers, but with more glycogen cells that mislocalise in the labyrinth (Tunster et al. 2016). Targeted ablation of *Esx1* in embryonic stem cells leads to enlarged junctional zone with excessive numbers of glycogen cells and mislocalisation of spongiotrophoblast cells in the labyrinth. In addition, abnormal branching of the fetal blood vessels in the labyrinth was observed. These

placental defects were associated with FGR between E16.5 and E18.5 (Li & Behringer 1998). *Phlda2* overexpression or targeted ablation led to smaller junctional zone with fewer glycogen cells, or enlarged junctional zone with increased glycogen cell numbers, respectively. Both overexpression and targeted ablation of *Phlda2* led to FGR at E16.5 and E18.5, respectively (Tunster, Creeth & John 2016; Tunster, Tycko & John 2010). Altogether, these studies show that abnormalities in the development and function of the junctional zone can cause FGR.

Labyrinth defects can also cause FGR. Deletion of a labyrinthine trophoblast-specific transcript of *Igf2* (P0) led to placental growth restriction by E11.5. Mutant fetuses exhibited growth restriction after E15.5 and had decreased birth weight. This was a result of decreased passive permeability of the placenta, with a compensatory increase of active amino acid transport at the initial stages of pregnancy. During late pregnancy, compensation fails resulting in FGR (Constância et al. 2002; Sibley et al. 2004). Additionally, *Pkba*^{-/-} mice exhibit FGR at E14.5 and have hypotrophic placentas with decreased vascular branching and decreased labyrinth area covered by blood vessels (Yang et al. 2003). *Egfl7*^{-/-} conceptuses have reduced placental weights and develop fetal growth restriction, as a result of reduced fetal blood space in the labyrinth and reduced chorioallantoic branching morphogenesis. Genes involved in branching morphogenesis such as *Gcm1*, *Syna*, and *Synb* were also downregulated in *Egfl7*^{-/-} placentas in E8.5 and E9.5 (Lacko et al. 2017). Moreover, genetic ablation of *Plk2* or *Rgcc* results in small labyrinth and defective angiogenesis, leading to FGR in E14.5-E18.5 or E16.5, respectively (Cui, Guo & Chen 2013; Ma, Charron & Erikson 2003). Finally, ablation of *Synb* leads to abnormal vascularisation of the labyrinth, enlarged maternal blood spaces with extremely thin walls, and FGR at E18.5 (Dupressoir et al. 2011). Placental overexpression of genes can also impair labyrinth development. For instance, overexpression of *Flt1* causes altered trophoblast differentiation, small labyrinth, and loss of glycogen cells. In addition, decreased expression of fatty acid and cholesterol transporters CD36 and ABCA1, respectively, was observed. As a result, fetal weight was reduced at E18.5 (Kuhnel et al. 2017). Embryos overexpressing *Pgf* in T cells exhibited reduced angiogenesis of the placenta, causing placenta detachment from the uterus and pregnancy loss. However, when this defect was not severe enough to lead to pregnancy loss, the newborn litters were growth restricted (Kang et al. 2014). Altogether, these studies show that misexpression of genes involved in the development of the different placental structures can lead to abnormal placental morphology and function, ultimately causing FGR.

Abnormal placental development leading to abnormal expression and distribution of transporters, and prevention of direct contact of maternal and fetal blood (Brett et al. 2014) causes abnormal placental transport function, inadequate nutrient delivery to the embryo, and ultimately it impairs embryo growth and development (Bell & Ehrhardt 2002; Brett et al. 2014; Desoye, Gauster & Wadsack 2011; Winterhager & Gellhaus 2017). Placental growth factor (PIGF), VEGF receptor, and kinase insert domain receptor were reduced in placentas from pregnancies complicated with FGR, in contrast to normal, or preeclamptic pregnancies (Alahakoon et al. 2018). Reduced expression of these angiogenic factors, might be the cause of loss of vasculature and villous architecture in the human placentas (Alahakoon et al. 2018). Altogether, these studies show that FGR can be caused by abnormal placenta development leading to inadequate blood flow to the embryo, or inadequate nutrient transport through defective transport systems.

1.4 Folate metabolism and reproductive health

In the previous sections we discussed how the maternal and fetal components of the placenta can affect fetal growth. Next, in this thesis we will focus on folate metabolism and the effects of abnormal folate metabolism on embryo growth and development.

Abnormal folate metabolism has been associated with a variety of diseases, including cancer, Down's syndrome (Bagley & Selhub 1998; James et al. 1999; Wang et al. 2008), neural tube defects (NTD), vascular diseases (reviewed by (Nazki, Sameer & Ganaie 2014)), and depression (Miller 2008). A clinical indicator of folate deficiency in humans is hyperhomocysteinemia (Blom & Smulders 2011). Hyperhomocysteinemia is caused by a decreased rate of conversion of homocysteine into methionine (see Section 1.4.2) and is a risk factor for cardiovascular diseases (Verhaar, Stroes & Rabelink 2002). Folate deficiency impairs the immune function, as it leads to decreased T-cell proliferation, cell cycle arrest in the S phase due to nucleotide imbalance, apoptosis and misincorporation of uracil into DNA (Courtemanche et al. 2004). Culture of primary human CD8⁺ T-lymphocytes in media that contained folate, thymidine or a nucleoside mixture, led to restored nucleotide and cell imbalances (Courtemanche et al. 2004). Hypomethylated DNA isolated from livers of methyl-deficient rats was shown to be more sensitive to DNA double strand breaks, especially in the tumour suppressor p53 gene (Pogribny et al. 1995), possibly leading to cancer development. All these diseases are seemingly unrelated. The molecular mechanism

of folate metabolism is not well understood, which is particularly surprising, given that we have known the importance of folate metabolism in health for decades.

1.4.1 Role of folate in uterine health and pregnancy in humans and mice

Hyperhomocysteinemia is an indicator of folate deficiency in humans (Blom & Smulders 2011). Ovarian follicular fluid levels reflect systemic homocysteine levels (Ebisch et al. 2006). High follicular fluid homocysteine levels are associated with endometriosis and decreased embryo quality on day 3 in *in vitro* fertilisation (IVF) cycles (Ebisch et al. 2006). Low levels of homocysteine in the follicular fluid are associated with better oocyte quality, and folate supplementation increases the percentage of mature oocytes (Szymanski & Kazdepka-Zieminska 2003). Rhesus monkeys have been used as models to study the role of folate deficiency on the function of the reproductive system. Folate-restricted diet led to the presence of atretic and cystic ovarian follicles lacking granulosa cells in the ovaries. As a result, these monkeys had low pre-ovulatory E2, and low mid-luteal P4 levels and experienced irregular menstrual cycles (Mohanty & Das 1982). Therefore, folate is important for oocyte development and regular menstrual cycles, by maintaining normal hormone levels. However, little is known about the role of folate on the uterine structure and function in mice.

Folate has also a role in embryo and placenta development. For instance, if hyperhomocysteinemia, which is a clinical indicator of folate deficiency, occurs in the third trimester of human pregnancy, it predicts low birth weight (Takimoto et al. 2007), increased risk of hypertensive illness, and premature delivery (Lindblad et al. 2005), while in the second trimester does not increase the risk of FGR (Hogg et al. 2000). In addition, abnormal maternal and fetal plasma folate, vitamin B12, and homocysteine concentrations increase the risk of placenta abruption (Ray & Laskin 1999) and are associated with decreased placenta weight and birth weight, and increased risk of adverse pregnancy outcomes, such as pre-eclampsia, small for gestational age babies (Bergen et al. 2012), and FGR (Jiang, Cao & Chen 2016; Lindblad et al. 2005; Muthayya et al. 2006; Sram et al. 2005). Placenta dysfunction, such as increased trophoblast proliferation and apoptosis, abnormal placental hormone levels, and reduced amino acid transport, has also been associated with abnormal microRNA expression in pregnant women with low folate status (Baker et al. 2017). Target genes of the misexpressed microRNAs include *Myc*, *Vegfa*, *Cdkn1c*, and *Tp53*, all of which have altered expression in pregnancies complicated with FGR (Heazell et al. 2011;

Novakovic et al. 2006; Rajaraman et al. 2010; Roh et al. 2005; Whitehead et al. 2013). Altogether, these studies show that abnormal levels of folate and homocysteine affect placenta development and function, and ultimately lead to impaired embryo growth. However, the molecular mechanism by which folate is important for embryo development, is not well understood.

Additionally, nutritional folate deficiency inhibits placental mammalian target of rapamycin (mTOR) signalling pathway. mTOR is a serine/threonine kinase. It is activated by oxygen, ATP, glucose, amino acids, insulin, and growth factor signalling, and regulates protein translation (Bar-Peled & Sabatini 2014; Chen et al. 2011; Ito, Ruegg & Takeda 2018; Miniaci et al. 2015). Therefore, it controls cell growth and proliferation (Mori et al. 2014). mTOR also regulates placental amino acid transport activity (Roos et al. 2009). Folate deficiency in primary human trophoblast cells inhibits mTOR signalling, suggesting a link between folate levels and placental nutrient transport with potential consequence in fetal growth in humans (Rosario, Powell & Jansson 2017). Finally, maternal exposure to folic acid antagonists, such as drugs used to treat epilepsy and mood disorders (Lambie & Johnson 1985), increased the risk of pre-eclampsia, placenta abruption, fetal growth restriction, and fetal death (Wen, Zhou, et al. 2008). Folic acid antagonists bind to the folic acid receptors and prevent their activation by folate. These studies show how molecular pathways downstream of folate are disrupted by folate deficiency or exposure to folic acid antagonists, and ultimately affect pregnancy.

To better understand the effects of nutritional folate deficiency in humans, mouse models of folate deficiency are used. For instance, folate deficiency inhibits mTOR signalling not only in primary human trophoblast cells (Rosario, Powell & Jansson 2017), but also in mice, leading to decreased trophoblast plasma membrane amino acid transporter activity and growth restriction (Rosario et al. 2017). Additionally, mice fed a folate-deficient diet had poor reproductive outcomes when mated with control males. Specifically, increased resorption rates at GD12.5-15.5 and GD14.5 and decreased fetal weights and developmental delay at GD17.5 were observed (Burgoon et al. 2002). Folate-deficiency also caused reduced number of implantation sites and hypermethylation of decidualisation-specific genes *Nr1h3* and *Nr5a1* (Geng et al. 2015), and abnormal decidual angiogenesis (Li et al. 2015). The latter causes uteroplacental insufficiency, leading to abnormal fetal growth (Krishna & Bhalerao 2011; Swanson & David 2015). Altogether, these studies show that folate deficiency in mice affects implantation and decidualisation and leads to FGR.

1.4.2 Bioavailability and metabolism of folate

Folate is a member of the vitamin B family (Mahmood 2014). In contrast to plants, mammals cannot synthesise folate *de novo* (Basset et al. 2002). An excellent source of naturally-occurring folate are green leafy vegetables, beans, and dark green vegetables such as broccoli (Chan, Bailey & O'Connor 2013). During pregnancy, folate is transported from the mother to the fetus through the folate receptors on the placenta. Folate is absorbed in the small intestine (Milman 2012) and is biochemically inactive. It exists either as a monoglutamate, or as a polyglutamate, which hydrolyses into monoglutamate in the intestinal mucosa prior to transport. It is hydrophilic, and enters the cells either via folate-carriers, or receptors. Folate carriers include reduced folate carrier 1 (RFC1), also known as SLC19A1, and the proton-coupled folate receptors (PCFT), also known as SLC46A1. Alternatively, folate enters the cells via endocytosis, via folate receptors expressed by the apical membrane of the small intestine, such as folate receptors (FOLR), also known as folate binding protein (Zhao, Matherly & Goldman 2009). Once absorbed, folate is delivered to the liver, where it is stored. Folate is also stored in red blood cells and kidney cells. Folate is reduced to its main circulating form, 5-methyltetrahydrofolate (Smulders et al. 2006; Visentin et al. 2014), through biochemical reactions (Figure 1.5).

Folate metabolism is important for DNA synthesis, amino acid synthesis, and the release of methyl groups for cellular methylation (Locasale 2013). Folate is converted into dihydrofolate, which is then converted into tetrahydrofolate (THF) by dihydrofolate reductase (DHFR). THF is then reversibly converted to 5,10-methylene THF by MTHFD. *Mthfd* codes for a protein with three enzymatic activities: methylenetetrahydrofolate dehydrogenase, methenyltetrahydrofolate cyclohydrolase and formate-tetrahydrofolate ligase (Neagos et al. 2010). This protein converts 5,10-methylene-THF into THF, creating two intermediate products: 5,10-methenyl-THF and 10-formyl-THF (Neagos et al. 2010). Next, 5,10-methylene THF is irreversibly converted into 5-methyl-THF, which is the main form of circulating folate, by methylene tetrahydrofolate reductase (MTHFR; Figure 1.5; Ghandour et al. 2004; Hart et al. 2002). Methionine synthase reductase (MTRR) is a key enzyme for the progression of folate or methionine cycles, as it is essential for the activation of methionine synthase (MS) through the reductive methylation of its vitamin B12 cofactor (Kazuhiro Yamada et al. 2006) and links the folate and methionine metabolisms (Mahmood 2014; Shane & Stokstad 1985). 5-methyl-THF acts as a methyl donor for homocysteine methylation, a reaction that is catalysed by MS. Transfer of a methyl group from 5-methyl-

THF to homocysteine leads to formation of methionine and THF. Methionine is then converted to S-adenosylmethionine (S-AdoMet), by methionine adenosyltransferase. S-AdoMet is an important methyl donor for methylation of DNA, RNA, histones and other cellular components (Ghandour et al. 2002; Jacob et al. 1998; Locasale 2013). Methyltransferases transfer methyl groups from S-AdoMet to cellular substrates, producing S-adenosyl-homocysteine (AdoHcy), which is then converted into homocysteine by S-adenosyl-homocysteine hydrolase. Abnormal folate metabolism or folate deficiency are usually associated with hyperhomocysteinemia due to the decreased rate of conversion of homocysteine into methionine, decreased availability of methyl groups for cellular methylation due to decreased S-AdoMet levels, and a methyl-trap due to the decreased rate of methyl group donation from 5-methyl-THF to homocysteine (Bailey et al. 2015; Blom & Smulders 2011; Cuskelly et al. 2001; Padmanabhan et al. 2013).

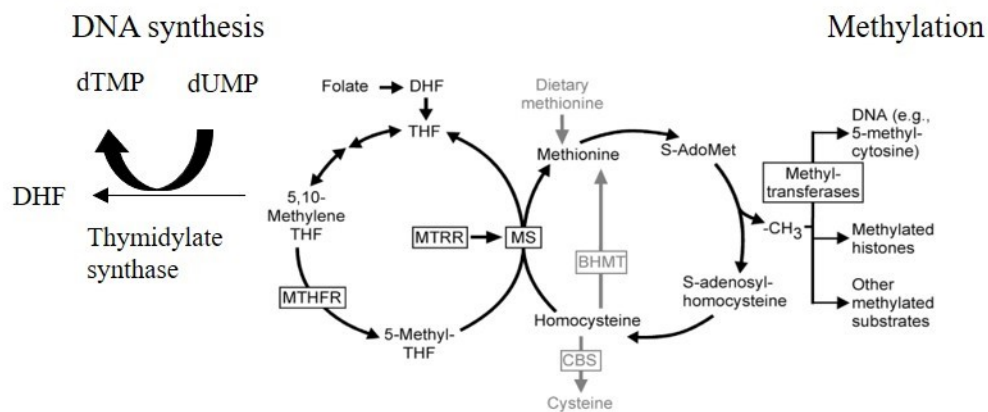


Figure 1.5 Folate and methionine metabolism.

The folate metabolism is required for release of methyl groups for cellular methylation, for the production of dTMP, essential for DNA synthesis, and for amino acid synthesis. dTMP: deoxythymidine monophosphate, dUMP: deoxyuridine monophosphate, DHF: dihydrofolate, THF: tetrahydrofolate, MTHFR: methylenetetrahydrofolate reductase, MTRR: methionine synthase reductase, MS: methionine synthase, CBS: cystathionine beta synthase, BHMT: Betaine—homocysteine S-methyltransferase

1.4.3 The molecular function of folate

Folate metabolism is required for DNA replication, amino acid synthesis, and the release of methyl groups necessary for cellular methylation (Figure 1.5). Folate metabolism leads to production of dTMP, and therefore is required for DNA synthesis. Abnormal folate

metabolism prevents the formation of dTMP from dUMP. Decreased levels of dTMP cause misincorporation of dUMP, as an alternative to dTMP in the DNA. DNA that contains dUMP is prone to mutations. dUMP misincorporation activates the DNA repair mechanisms, causes DNA breaks, and decreases DNA stability (Blount et al. 1997; Reidy 1988; Wickramasinghe & Fida 1993). Genetic instability and accumulation of mutations trigger the cell-cycle checkpoints resulting in proliferation arrest, or cell death. However, if the checkpoints are defective due to mutations, uncontrolled cell proliferation occurs (Khanna & Jackson 2001), ultimately leading to cancer (Duthie & Hawdon 1998; Melnyk et al. 1999). Additionally, DNA is synthesised *de novo* during the S-phase of the cell cycle. Nucleotide demand for DNA synthesis is therefore increased during cell proliferation. As a result, abnormal DNA synthesis can affect cell proliferation (Crider et al. 2012). Abnormal cell proliferation might lead to cancer, or abnormal cell differentiation, leading to impaired organ development and function (Copp, Brook & Roberts 1988). Increased cell proliferation that requires extensive DNA replication occurs during embryo development, therefore the developing embryos are particularly sensitive to folate levels.

Folate metabolism is also important for the synthesis of amino acids methionine, homocysteine, and cysteine. Methionine is an essential amino acid and therefore should be obtained from diet, although it is synthesised in the one-carbon cycle. On the other hand, homocysteine and cysteine are non-essential amino acids. Homocysteine derives from the metabolism of dietary methionine. Cystathionine- β -synthase catalyses the condensation of homocysteine and serine to form cystathionine. Then, cystathionine- γ -lyase is required for the hydrolysis of cystathionine to form cysteine, α -ketobutyrate, and ammonia.

Additionally, folate metabolism results in the production of S-AdoMet, which acts as a methyl donor necessary for cellular methylation. Disruption of the folate cycle can result in decreased availability of methyl groups and therefore disruption of cellular methylation. Abnormal methylation of DNA and histones affects gene expression, a process known as epigenetic regulation (Jones & Takai 2001). Folate deficiency or abnormal folate metabolism causes global DNA hypomethylation (Davis & Uthus 2003; James et al. 2003; Piyathilake et al. 2000; Smith et al. 1995; Wang et al. 2012; Wasson et al. 2006), but also locus-specific dysregulation of DNA methylation, including DNA hypermethylation and hypomethylation (Charles, Johnson & Belshaw 2012; Jhaveri, Wagner & Trepel 2001; Padmanabhan et al. 2013). For instance, periconceptional folate dietary restriction in sheep caused locus-specific DNA hypomethylation and hypermethylation in the offspring (Sinclair et al. 2007).

Abnormal folate metabolism due to a gene-trap mutation in the *Mtrr* gene (*Mtrr^{gt}*) caused global DNA hypomethylation in livers of adult *Mtrr^{gt/gt}* mice compared to C57Bl/6 controls (Padmanabhan et al. 2013). Global DNA hypomethylation and locus-specific dysregulation of DNA methylation associated with changes in gene expression were also observed in E10.5 placentas but not embryos of phenotypically normal and growth restricted *Mtrr^{gt/gt}* conceptuses (Padmanabhan et al. 2013). Folate deficiency is also associated with histone methylation. Histone demethylase LSD1 is a folate-binding protein (Luka et al. 2011). Histone modifications were measured by mass spectrometry in livers of mice fed a folate deficient diet. Increased levels of methylated lysine 4 of histone 3 were observed in folate deficient mice. It is speculated that increased histone methylation is due to decreased LSD1 activity, as a result of folate deficiency (Garcia et al. 2016). Folate metabolism has therefore a role on DNA and histone methylation. Embryo development is regulated by epigenetic mechanisms (Gabory, Attig & Junien 2011; Gicquel, El-Osta & Le Bouc 2008; Shi & Wu 2009) and epigenetic reprogramming (Hajkova 2011) occurs during embryo development. As a result, embryo development is particularly sensitive to changes in folate availability. Altogether, the folate cycle is important for synthesis of amino acids, synthesis of dTMP important for DNA replication, and release of methyl groups, important for methylation of cellular substances.

The mechanisms by which folate affects specifically placental development and function remain unknown. Possible mechanisms include epigenetic regulation of placental development, regulation of trophoblast invasion, placental vascularisation, or placental transport activity. Placental development is regulated by epigenetic modifications (Fowden et al. 2011; Tunster, Jensen & John 2013). For instance, mice lacking the maternally expressed *Phlda2* gene have placental overgrowth characterised by expansion of the spongiotrophoblast (Frank et al. 2002). Additionally, a two-fold increase in the expression of the imprinted *Phlda2* gene decreases the junctional zone area and increases the glycogen stores. This is accompanied by FGR at E16.5 (Tunster, Tycko & John 2010). It is possible that the decreased availability of methyl groups caused by abnormal folate metabolism or folate deficiency, alter the methylation and expression of the imprinted genes in the placenta. Imprinted genes have a role in placenta development (Fowden et al. 2006; Fowden et al. 2011), therefore their misexpression can impair placentation. Folate regulates trophoblast invasion and placental development in humans. Culture of placental explants in folate media increased extravillous trophoblast invasion, leading to increased secretion of MMP2, MMP3,

and MMP9 in a folate concentration-dependent manner (Williams et al. 2011). These metalloproteinases are required to remodel the extracellular matrix during trophoblast invasion (Cohen, Meisser & Bischof 2006). Balanced cell proliferation and apoptosis is essential for trophoblast invasion and normal placentation (Naicker et al. 2013) and folic acid affects these processes *in vitro* in a concentration-dependent manner (Williams et al. 2011). Culture of cytotrophoblast cells in folate-free medium increased cell apoptosis (Steeegers-Theunissen et al. 2000) and decreased placental system A amino acid transport function, by possibly regulating post-translational modifications of nutrient transporters (Baker 2015). Folic acid also increased the placental vascular density *in vitro* (Williams et al. 2011). Folate deficiency led to decreased cell viability and impaired invasion of the HT8-8/SVneo human extravillous trophoblast cell line, while folate supplementation increased its proliferation. Folate supplementation also reduced cellular viability of the villous trophoblast BeWo cell line (Ahmed et al. 2016). Altogether, these studies show that abnormal folate metabolism or folate deficiency affect trophoblast function, while folate supplementation rescues some of the effects.

Folate deficiency also affects the decidualisation reaction, therefore impairing embryonic development. The mechanism by which folate affects the decidualisation reaction and therefore embryo development is still not well understood, however it is suggested that dysregulation of DNA methylation and associated changes in gene expression may play a role. The effects of folate deficiency and DNA methyltransferases (*Dnmt*) deficiencies on development are similar. DNMTs methylate cytosine to form 5-methylcytosine. DNMT1 is the maintenance DNA methyltransferase that adds methyl groups in CpG sites during mitosis (Estève et al. 2006). *Dnmt1* knockout causes abnormal embryonic development and embryonic lethality in mice, therefore *Dnmt1* is essential for viability (Li, Bestor & Jaenisch 1992). *Dnmt1p* and *Dnmt1o* are sex-specific isoforms of *Dnmt1*, expressed in male germ cells and oocytes, respectively. Loss of *Dnmt1o* leads to abnormal imprinting during early development, and embryonic lethality in mice (Howell et al. 2001). *Dnmt2* is required for the methylation of transfer RNA molecules (Goll et al. 2006). *De novo* methylation is catalysed by DNMT3a and DNMT3b, and their cofactor DNMT3L. *Dnmt3a*^{-/-} causes postnatal lethality associated with growth restriction in mice. *Dnmt3b*^{-/-} mouse embryos suffer from more severe FGR and also neural tube defects (NTD), therefore die *in utero* (Okano et al. 1999). Maternal *Dnmt3l* deficiency also causes NTD (Hata et al. 2002). Its loss also causes abnormal placenta development, such as failure of chorioallantoic attachment, absent labyrinth, and decreased

spongiotrophoblast layer. These abnormalities result from abnormal establishment of maternal imprints in the placenta (Arima et al. 2006). Altogether, these data highlight the similar effects of folate deficiency and DNMT deficiencies on embryonic development, suggesting that dysregulation of DNA methylation and the associated changes in gene expression can be a mechanism by which folate deficiency affects embryo development.

DNMT1 and DNMT3A regulate DNA methylation in the mouse uterus. At GD3.5, DNMT1 is expressed by the luminal and glandular epithelial and stromal cells. DNMT3A shows similar, but weaker and sporadic expression. At GD6.5, DNMT1 is expressed by the mesometrial and antimesometrial decidua (Gao et al. 2012), and as before, DNMT3A shows similar, but weaker expression. In the uterus between the implantation sites at GD6.5, DNMT1 expression is limited in the luminal and glandular epithelium and stroma cells (Gao et al. 2012). Intraperitoneal injections of 5-aza-dC to inhibit DNA methylation were performed either at pre-implantation (days 3 and 4), post-implantation (days 5-7), or peri-implantation (days 3-7) period. Injections during the pre-implantation period did not affect the number of implantation sites, but reduced stromal cell proliferation at GD3.5 and GD4.5, without affecting *Esr1* or *Pgr* mRNA expression, compared to the controls. This suggests that embryo implantation is not affected by inhibition of DNA methylation. However, post-implantation and peri-implantation inhibition of DNA methylation caused a reduction in implantation site weight at GD7.5, without affecting the number of implantation sites. Defective decidualisation, abnormal expression of stromal cell differentiation and endothelial cell proliferation markers, and an increase in the number of degenerated embryos were also observed, the latter suggesting inhibition of uterine DNA methylation leads to pregnancy loss. Inhibition of DNA methylation also affected deciduoma development and aberrant gene methylation (Gao et al. 2012). DNA methylation is therefore essential for the decidualisation process and possibly embryo development.

Hyperhomocysteinemia is a clinical indicator of folate deficiency in humans and is thought to be responsible for many folate deficiency-related disorders. For instance, low plasma folate and hyperhomocysteinemia increase the risk of coronary artery diseases, such as stable and unstable angina pectoris, and myocardial infarction (Ma et al. 2017) and other vascular diseases (Blom & Smulders 2011; Boushey et al. 1995; Graham et al. 1997; Lanska 2010; Li et al. 2016; McNulty et al. 2008; Ward 2001). Low methionine levels caused by folate deficiency cause fat accumulation in the liver, leading to impaired liver function (da Silva et al. 2014), impaired creatinine production in piglets (Robinson et al. 2016), and impaired

collagen formation important for skin and connective tissue formation in mice (Ables et al. 2012). Hyperhomocysteinemia is toxic for the cells and has been associated with neurodegeneration (Currò et al. 2014). Folate food fortification programmes in the USA and folic supplementation decreases the risk of cardiovascular diseases and stroke (Antoniades et al. 2009; Li et al. 2016). Altogether, these studies highlight the consequences of folate deficiency-associated hyperhomocysteinemia on vascular health.

1.4.4 Folate transport and metabolism-related mutations in mice and humans that affect development and uterine health

The effects of folate in mouse and human health can be studied through mutations of genes that disrupt folate metabolism. Mutations in human genes have been associated with adverse developmental outcomes. Studies have shown that mutations of genes involved in folate transport and metabolism, such as *RFC1*, *MTHFD1*, *MTHFR*, and *MTRR* are linked to NTD in humans (Brody et al. 2002; Jiang et al. 2014; De Marco et al. 2006; Relton et al. 2004; Relton et al. 2004). Abnormal folate metabolism in humans caused by mutations in genes involved in folate metabolism such as *MS*, *TS*, and *MTHFD1* is associated with recurrent pregnancy loss (Kim et al. 2013; Parle-McDermott et al. 2005). In addition, a mutation in the maternal or fetal *MTR* gene (A2756G) was associated with uteroplacental insufficiency, which was defined as preeclampsia, intrauterine growth restriction, placenta abruption, and gestational hypertension. Folate supplementation rescued the effects only of maternal *MTR* deficiency (Furness et al. 2008). Maternal *MTHFD1* polymorphism (G1958A) was associated with FGR (Furness et al. 2008).

However, the studies of the effects of folate metabolism in humans are limited, since we cannot manipulate the human genome. Therefore, the mouse is used as a model to assess the effects of abnormal folate metabolism on embryo development. Homozygous mutation of the folate carrier *Rfc1* is embryonic lethal. Maternal folic acid supplementation during pregnancy prolongs the survival of the *Rfc1*^{-/-} embryos until midgestation or E18.5, in a dose-dependent manner. However, *Rfc1*^{-/-} embryos that survive until midgestation are developmentally delayed, and exhibit failed chorioallantoic attachment and congenital malformations compared to their *Rfc1*^{+/+} littermates. *Rfc1*^{-/-} embryos that survive until E18.5 have congenital malformations (Waes et al. 2008). *Folbp1*^{-/-} embryos derived from *Folbp1*^{+/-} intercrosses exhibit developmental delay at E8.5 and E9.5, with decreased somite numbers, and have an

open neural tube at E9.5. They eventually die *in utero* before neural tube closure (Piedrahita et al. 1999). Mouse models used to study the role of folate in development and uterine and placental function showed that folate plays an important role in placentation (Ahmed et al. 2016; Pickell et al. 2009; Steegers-Theunissen et al. 2000; Williams et al. 2011). For example, loss of RFC1 in mice leads to placental defects, such as failure of chorioallantoic fusion (Waes et al. 2008). Moreover, *Mthfr*^{+/+} and *Mthfr*^{+/-} females were fed either a control, or a folate-deficient diet and mated with *Mthfr*^{+/-} males (Pickell et al. 2009). At E10.5, embryonic lethality was increased in the folate-deficient mice compared to those fed a normal diet in both genotypic groups, while developmental delay, decreased embryonic weight, and decreased embryonic crown-rump length were caused by either maternal *Mthfr* or folate deficiencies (Pickell et al. 2009). Dietary folate deficiency alone caused decreased placenta weight, decreased total placental area, and decreased trophoblast invasion. Also, small and disorganised placental layers with fewer primary giant cells, and fewer spongiotrophoblast cells between the giant cell layer and the labyrinth were observed by cell-marker staining, and compacted labyrinth layer (Pickell et al. 2009). However, this study is flawed, since they used *Mthfr*^{+/-} males, instead of control males, and therefore the results could be due to a paternal effect. In addition, targeted disruption of *Ms* in mice causes hyperhomocysteinemia and fetal lethality (Swanson, Liu & Baker 2001), while a gene-trap mutation in the *Mtrr* gene causes increased resorption, growth restriction, developmental delay, congenital heart defects, and cardiovascular malfunction in the progeny (Deng et al. 2008). Altogether, these studies show that mutations in genes involved in folate transport and metabolism cause developmental phenotypes in mice.

1.4.5 Folate supplementation, uterine health, and pregnancy in humans and mice

Folate is a water-soluble, naturally-occurring vitamin, while folic acid is the synthetic form used for dietary supplementation (Elkin & Higham 2000). In 1991, the Centers for Disease Control and Prevention (CDC) highlighted the importance of folate in pregnancy, by recommending folic acid supplementation, typically 4000µg/day (CDC 1991) for women whose previous pregnancies were affected by NTD. NTD is a group of congenital malformations caused by abnormal formation of neural tube (Detrait et al. 2005). It was suggested that women should take supplements during the periconceptual period and in early pregnancy. In 1992, U.S Public Health Service recommended folic acid supplementation of

400µg/day to all women who are at an age of having children (MMWR 1992). These recommendations were reinforced by the Institute of Medicine recommendations in 1998 (IoM 1998) and the U.S. Preventive Services Task Force in 2009 (Task 2009). Folic acid supplementation can be achieved by either taking vitamin supplements, or by consuming products made with folic acid-fortified flour. The initial recommendation was based on evidence that folate supplementation can prevent NTD (Czeizel & Dudas 1992; MRC 1991).

Folic acid supplementation improves uterine health. Periconceptual folic acid supplementation increases folate and decreases homocysteine levels in the ovarian follicular fluid, with the latter having a correlation with the follicle diameter. Follicle diameter is an indicator of oocyte maturation (Boxmeer et al. 2008). Dietary folate supplementation improved human reproductive health by increasing P4 levels during the luteal phase of the menstrual cycle in premenopausal women and decreasing anovulation rates (Gaskins et al. 2012).

Folic acid supplementation and addition of folic acid in flour, a process known as folic acid fortification, does not prevent only NTD (Bailey, Rampersaud & Kauwell 2003; Morris et al. 2016; MRC 1991). In the early 1900s, it was found that folic acid supplementation cures megaloblastic anaemia in pregnant women (Hoffbrand 2001; Mitchell, Snell & Williams 1941). It also decreased the risk of preeclampsia (Wen, Chen, et al. 2008), which is known to be associated with increased risk of FGR (Odegard et al. 2000). Folic acid and vitamin B6 supplementation of women with hyperhomocysteinemia and a history of pregnancy complicated with FGR led to normal homocysteine levels, while it decreased the risk of FGR in future pregnancies (Leeda et al. 1998).

The benefits of folic acid supplementation on embryo development have also been studied in rodents. Administration of 25mg/kg/day or 50mg/kg/day of folic acid in *Rfc1^{+/-}* female mice prolonged the survival of *Rfc1^{-/-}* embryos, which otherwise would die early post-implantation, until E9.5 or E18.5, respectively (Waes et al. 2008). Folic acid supplementation in rats during pregnancy prevented the protein restriction diet-associated elevated systolic blood pressure and reduced endothelial nitric oxide synthase mRNA levels in offspring (Torrens et al. 2006). Overall, folic acid supplementation is beneficial for embryo growth and prevents adverse pregnancy outcomes.

1.4.6 What is missing from the field?

Folate deficiency and abnormal folate metabolism have important implications on embryo growth and development. Therefore, normal folate levels and metabolism are essential for a successful and healthy pregnancy. However, little is known about the effects of folate deficiency or abnormal folate deficiency on the uterine structure and function during the receptive estrus stage, and therefore further studies are required to address this.

1.5 Multigenerational effects of folate metabolism on development

In the previous section we discussed the role of folate in uterine health. Previously, we also talked about the endometrial causes of FGR, as well as how poor placental development and function can cause FGR. In this section, we will discuss the effects of an abnormal uterine environment caused by abnormal folate metabolism on embryo growth and development.

1.5.1 Maternal effects of folate metabolism on development

Folate deficiency or abnormal folate metabolism in the mother can affect embryo development. Studies have shown an effect of folate deficiency on the peri-implantation uterine structure and function, as well as on the decidualisation reaction in mice, although the mechanism by which folate affects uterine function and therefore embryo development is not well understood. For instance, implantation sites at E4.5 derived from folate-deficient female mice showed decreased methylation and downregulation of estrogen receptor (*Esr1*) expression (Gao et al. 2012b). As the receptor of the ovarian hormone estrogen, *Esr1* plays a role in the progression of the estrous cycle and endometrium proliferation (Wood et al. 2007). Misexpression of *Esr1*, can therefore impair embryo implantation. In contrast to the methylation levels of *Esr1*, the methylation status of *Pgr* and E-cadherin (*Cdh1*) was not affected by folate deficiency in the mother. As the receptor of the ovarian hormone P4, *Pgr* is essential for the maintenance of pregnancy (Wetendorf et al. 2017). *Cdh1* is essential for endometrial differentiation and gland development (Reardon et al. 2012). Therefore, since folate deficiency does not affect *Pgr* and *Cdh1* methylation and embryo implantation occurs normally in mice, the folate deficiency-induced abnormalities in embryo growth and development are possibly due to events taking place after implantation (Gao et al. 2012b).

Maternal folate deficiency also impairs decidualisation. When decidualisation was artificially induced by intraluminal infusion of sesame oil, the deciduoma (tissue after induced decidualisation) in the folate-deficient mice was inelastic and softer compared to the control, as determined by assessment of the uterine gross anatomy, and expressed decreased levels of the decidualisation marker *Bmp2*. Folate deficiency also restrained decidualisation of endometrial stem cells *in vitro* (Geng et al. 2015). Finally, folate deficiency alters the DNA methylation patterns of genes related to decidualisation. For instance, higher CpG methylation levels were identified in the promoter region and the CpG islands in the decidual tissues of folate-deficient females compared to controls. Increased methylation levels were associated with downregulation of expression of decidualisation-related genes, such as *Nr5a1*, and *Nr1h3*. Folate deficiency therefore alters decidualisation in the pregnant folate-deficient females (Geng et al. 2015).

Folate is important for decidual angiogenesis, a process necessary to support embryo development (Winterhager et al. 2013). Folate deficiency in female mice mated with control males lead to restrained decidual angiogenesis, accompanied by abnormal vascular density and enlarged and elongated vascular sinus in implantation sites at E5.5, E6.5, and E7.5 (Li et al. 2015). Implantation sites also showed decreases in *Vegfa*, *Vegfr2*, *Plgf*, *Pgr*, and *Esr1* mRNA and protein expression. Pregnant females also had reduced serum P4, E2, LH, and prolactin (Li et al. 2015). Possible mechanisms for impaired angiogenesis could include the vasculotoxic effects of folate deficiency-induced hyperhomocysteinemia, and the hormonal imbalance, although further studies are required to solve this.

Folate deficiency impairs the decidual regression process. Implantation sites from folate-deficient mice at E6.5 and E7.5 have decreased *Bax/Bcl2* mRNA and protein ratios. These genes are important to initiate the apoptotic process in the decidualised mesometrium (Dai, Moulton & Ogle 2000). In addition, folate-deficient mice do not exhibit a change in mitochondrial transmembrane potential, which is observed in control mice, suggesting that the decidual cell apoptosis is inhibited via the mitochondrial apoptosis pathway in folate-deficient mice (Liao et al. 2015).

Although not directly assessed, it is hypothesised that *MTHFR* mutation in combination with low folate intake can lead to hyperhomocysteinemia-associated decidual vasculopathy in humans (Kramer et al. 2001). Decidual vasculopathy is an incomplete or abnormal remodelling of the spiral arteries, leading in tissue necrosis (Stevens et al. 2012). It can cause

pre-eclampsia, FGR, or preterm birth (Kramer et al. 2001; Stevens et al. 2012). However, more studies in humans are required to assess the effects of folate deficiency and abnormal folate metabolism on the decidual reaction. Altogether, these studies highlight that folate deficiency impairs decidualisation, and might have a detrimental effect on embryo growth and development, although the exact mechanism remains unclear.

1.5.2 *Mtrr^{gt}* mouse model of abnormal folate metabolism

To assess the effects of abnormal folate metabolism on embryo growth and development, the *Mtrr^{gt}* mouse model was generated. The *Mtrr^{gt}* mutation is hypomorphic, as *Mtrr^{+/+}* transcript and methionine synthase activity was found in liver, kidney, brain, and heart of *Mtrr^{gt/gt}* mice tissues, although these levels were significantly decreased compared to *Mtrr^{+/+}* mice (Elmore et al. 2007). Complete loss of *Mtrr* activity causes embryonic lethality, however the hypomorphic *Mtrr^{gt}* mutation leads to viable *Mtrr^{gt/gt}* mice (Elmore et al. 2007).

The *Mtrr^{gt}* mutation leads to altered metabolic phenotype. *Mtrr^{gt/gt}* mice had significantly higher plasma homocysteine levels compared to *Mtrr^{+/gt}* and *Mtrr^{+/+}* mice (Elmore et al. 2007; Padmanabhan et al. 2013), which correlate with previous studies showing that folate deficiency is associated with hyperhomocysteinemia (Bailey et al. 2015; Blom & Smulders 2011; Cuskelly et al. 2001). Inversely, the levels of plasma methionine were significantly decreased in the *Mtrr^{gt/gt}* compared to the *Mtrr^{+/+}* (Elmore et al. 2007). The levels of AdoMet and AdoHcy were significantly increased and reduced, respectively, in *Mtrr^{gt/gt}* livers compared to *Mtrr^{+/+}*, confirming a metabolic derangement caused by the *Mtrr^{gt}* mutation (Elmore et al. 2007).

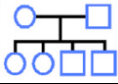
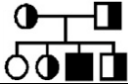
1.5.2.1 FGR in the *Mtrr^{gt}* mouse model

Mtrr^{gt/gt} embryos derived from *Mtrr^{gt/gt}* parents have a wide spectrum of developmental phenotypes at midgestation (E10.5). These include growth defects, such as growth restriction and developmental delay, and congenital abnormalities, such as NTD (open neural tube in the cranial or spinal cord regions), heart defects (pericardial oedema, reversed heart looping and enlarged hearts), and abnormal placental development (eccentric chorioallantoic attachment and haemorrhage; Padmanabhan et al. 2013). C57Bl/6 mice were used as controls, since the *Mtrr^{gt}* mouse line was created in a C57Bl/6 genetic background (Elmore et al. 2007). This

suggests the abnormal folate metabolism due to the *Mtrr^{gt}* mutation affects embryo development by midgestation.

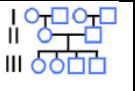
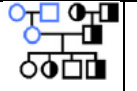
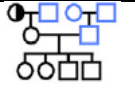
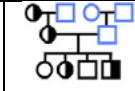
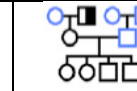
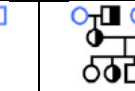
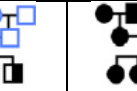
Interestingly, *Mtrr^{+/+}*, *Mtrr^{+/gt}*, and *Mtrr^{gt/gt}* progeny of *Mtrr^{+/gt}* intercrosses displayed similar developmental defects to the *Mtrr^{gt/gt}* mice derived from *Mtrr^{gt/gt}* parents. All the embryonic phenotypes were similarly affected, suggesting a parental *Mtrr^{gt}* allele might be sufficient to cause the developmental defects (Table 1.2). However, litters derived from a C57Bl/6 mother and a *Mtrr^{+/gt}* father were phenotypically normal, suggesting the developmental phenotypes are observed only through the maternal lineage (Table 1.3; Padmanabhan et al. 2013). *Mtrr^{+/+}* conceptuses (F2) derived from a *Mtrr^{+/+}* mother (F1), and a *Mtrr^{+/gt}* maternal grandparent (F0) had similar developmental phenotypes to those observed in *Mtrr^{+/+}*, *Mtrr^{+/gt}*, and *Mtrr^{gt/gt}* progeny of *Mtrr^{+/gt}* intercrosses, and in *Mtrr^{gt/gt}* mice derived from *Mtrr^{gt/gt}* parents. Additionally, growth enhancement was observed in F2 *Mtrr^{+/+}* embryos at E10.5. Notably, the developmental phenotypes were observed in a higher frequency in the *Mtrr^{gt/gt}* conceptuses compared to the F2 *Mtrr^{+/+}* conceptuses at E10.5 (Table 1.3; Padmanabhan et al. 2013). Developmental delay or significant frequencies of growth restriction at E10.5 did not persist past F2 generation. In contrast, the congenital abnormalities persisted in the *Mtrr^{+/+}* conceptuses from generations F2, F3, and F4 derived from an *Mtrr^{+/gt}* maternal ancestor (Padmanabhan et al. 2013). This is important, since it suggests that the *Mtrr^{gt}* model is a model of transgenerational epigenetic inheritance. However, the mechanism by which epigenetic factors are transmitted through the germline leading to congenital abnormalities, is still unknown. An embryo transfer experiment showed that the growth phenotypes but not the congenital malformations were due to an atypical uterine environment of the F1 generation (Padmanabhan et al. 2013).

Table 1.2 Phenotypic frequencies in litters from *Mtrr*^{+/*gt*} intercrosses compared to C57Bl/6 crosses.

			Phenotypic frequencies arising from <i>Mtrr</i> ^{+/<i>gt</i>} intercrosses			
	C57Bl/6 (93)	All (155)	<i>Mtrr</i> ^{+/+} (36)	<i>Mtrr</i> ^{+/<i>gt</i>} (77)	<i>Mtrr</i> ^{gt/<i>gt</i>} (37)	Not available (5)
Embryonic genotype (N)						
Normal stage	8.9±0.4 (95.7%)	5.1±0.7** (55.5%)	19/36 (52.8%)	44/77 (57.1%)	23/37 (62.2%)	-
Developmental delay	0.0	1.8±0.6* (20.0%)	10/36 (27.8%)	14/77 (18.2%)	7/37 (18.9%)	-
Severe abnormalities	0.0	1.2±0.3*** (12.9%)	6/36 (16.7%)	8/77 (10.4%)	5/37 (13.5%)	1/5 (20.0%)
Resorption	0.4±0.2 (4.3%)	1.1±0.3 (11.6%)	1/36 (2.8%)	11/77 (14.3%)	2/37 (5.4%)	4/5 (80.0%)
Total	9.3±.03 (100%)	9.1±0.6 (100%)	36/36 (100%)	77/77 (100%)	37/37 (100%)	5/5 (100%)

Data are presented as average number of conceptuses per litter ± SEM followed by the percentage of total conceptuses in brackets. Table adapted from Padmanabhan et al. (2013).

Table 1.3 Phenotypic frequencies caused by *Mtrr*^{+/-gt} maternal grandmothers of grandfathers at E10.5 compared to C57Bl/6 controls.

								
No. of maternal grandmothers ^a , maternal grandfathers ^b , or fathers ^c		3 ^{a,b}	3 ^c	7 ^a	7 ^a	3 ^b	4 ^b	7 ^a , 3 ^b
No. of litters (No. of conceptuses)		10 (93)	10 (94)	10 (83)	14 (129)	10 (89)	10 (87)	21 (176)
Average conceptuses/litter		9.3±0.3	9.4±0.3	8.2±0.9	9.2±0.4	8.9±0.5	8.7±0.3	8.4±0.06
Normal developmental stage	Normal	8.5±5 (91.4%)	8.1±0.5 (86.2%)	3.2±1.0*** (39.0%)	5.9±0.7* (64.3%)	4.2±0.9*** (47.2%)	3.9±0.9*** (44.8%)	2.7±0.8*** (32.4%)
	Growth Enhanced	0.0	0.1±0.1 (1.1%)	0.2±0.2 (2.4%)	0.0	0.7±0.3* (7.9%)	0.5±0.2 (3.5%)	0.0
	Growth Restricted	0.4±0.2 (4.3%)	0.7±0.6 (7.4%)	1.8±0.8 (22.0%)	1.0±0.5 (10.9%)	2.0±0.8 (22.5%)	1.7±0.6* (21.8%)	1.2±0.5 (14.8%)
Developmental delay		0.0	0.0	0.7±0.3* (8.5%)	0.6±0.3* (7.0%)	0.6±0.3 (6.7%)	1.1±0.5* (12.6%)	1.9±0.5** (22.2%)
Severe abnormalities		0.0	0.1±0.1 (1.1)	1.4±0.3*** (17.1%)	1.1±0.3** (11.6%)	1.0±0.2*** (12.4%)	0.8±0.3* (9.2%)	1.3±0.2*** (15.9%)
Resorptions		0.4±0.4 (4.3%)	0.4±0.2 (4.3%)	0.9±0.4 (11.0%)	0.6±0.1 (6.2%)	0.3±0.2 (3.4%)	0.7±0.3 (8.0%)	1.2±0.4 (14.2%)

Data are presented as number of conceptuses per litter with a specific phenotype and average number of phenotypically affected conceptuses per litter ± SEM followed by the percentage of total conceptuses in brackets. Table adapted from Padmanabhan et al. (2013).

1.5.2.2 Epigenetic instability in the *Mtrr*^{gt} mouse model

The *Mtrr*^{gt} mutation causes epigenetic instability in adult tissues and placentas at E10.5, suggesting a possible mechanism for the developmental phenotypes (Padmanabhan et al. 2013). Disruption of the folate cycle inhibits the transmission of methyl groups that are required by cellular methylation, such as methylation of DNA, RNA, and histones (Locasale 2013). Global DNA hypomethylation was observed in non-pregnant uteri and livers of adult *Mtrr*^{+/^{gt}} and *Mtrr*^{+/⁺} mice, and livers of *Mtrr*^{gt/^{gt}} mice compared to C57Bl/6 controls. Global DNA methylation of adult *Mtrr*^{gt/^{gt}} uteri was trending downwards but did not reach significance. Interestingly, global DNA methylation in the brains remained unaltered (Padmanabhan et al. 2013), suggesting a sparing effect to protect brain development. Dysregulation of DNA methylation in the nonpregnant uteri could be associated with the observed developmental phenotypes. Global DNA hypomethylation was also observed in placentas at E10.5 but not embryos of normal and growth restricted *Mtrr*^{gt/^{gt}} and F2 *Mtrr*^{+/⁺} conceptuses, suggesting the placentas are more prone to epigenetic instability than the embryos in the *Mtrr*^{gt} model (Padmanabhan et al. 2013). Dysregulation of locus-specific DNA methylation was also observed in placentas at E10.5, characterised by both DNA hypermethylation and DNA hypomethylation (Padmanabhan et al. 2013). The degree of CpG methylation change correlated to the severity of phenotype, indicating epigenetic instability in the *Mtrr*^{gt} model. Changes in expression of genes involved in placental growth were associated with DNA methylation changes. The overall hypermethylation in the differentially methylated region of the genes was associated with downregulation of gene expression (Padmanabhan et al. 2013). It was hypothesised that DNA methylation dysregulation precedes any changes in gene expression because DNA methylation changes were not always associated with gene expression changes (Padmanabhan et al. 2013). The mechanism behind locus-specific hypermethylation in models of global DNA hypomethylation, remains unknown (Cho et al. 2010; Deng et al. 2006; Padmanabhan et al. 2013). In summary, the *Mtrr*^{gt} mutation causes abnormal folate metabolism and limited availability of methyl groups necessary for DNA methylation. This leads to global DNA hypomethylation and locus-specific dysregulation of DNA methylation in E10.5 placentas, causing misexpression of genes that are necessary for normal placental development, and developmental phenotypes (Padmanabhan et al. 2013).

1.5.2.3 The growth phenotypes in F2 generation are due to an atypical uterine environment of the F1 females

As highlighted earlier, the *Mtrr^{gt}* model is a model of transgenerational epigenetic inheritance, and the growth phenotypes do not persist past the F2 generation, suggesting they are associated with an abnormal uterine environment of the F1 generation. However, the mechanism is unknown. It is therefore possible that the mechanism of inheritance of the developmental phenotypes involves either inheritance of an epigenetic factor via the germline, or the uterine environment is implicated. In order to identify the mechanism, and assess the possibility that the maternal environment is responsible for the phenotypes, a blastocyst transfer experiment was performed (Padmanabhan et al. 2013). Briefly, an *Mtrr^{+/+}* female (F1) derived from one *Mtrr^{+/gt}* parent (F0) was mated with a C57Bl/6 male. At E3.0, prior to embryo implantation, the *Mtrr^{+/+}* grandprogeny (F2) was transferred into a control E2.5 pseudopregnant B6D2F1 female, who has not been previously exposed to the *Mtrr^{gt}* mutation. The embryos were dissected at E10.5 and scored for phenotypes. This developmental stage was selected since previous dissections were performed also at midgestation. C57Bl/6 embryos were also transferred and used as controls. This experiment revealed two distinct epigenetic mechanisms in the *Mtrr^{gt}* model: a) The growth defects were rescued after transfer of the embryos in a normal uterine environment, suggesting these are due to an atypical uterine environment of F1 *Mtrr^{+/+}* females, and b) the congenital abnormalities persisted even after blastocyst transfer, suggesting these are due to inheritance of epimutations through the germline (Padmanabhan et al. 2013). Remarkably, an increased frequency of growth enhancement was observed in the transferred embryos derived from an either maternal *Mtrr^{+/gt}* grandparent (Padmanabhan et al. 2013). The mechanism by which the uterine environment of F1 *Mtrr^{+/+}* females metabolically programmes the growth of their embryos during the first three days of development, is still unknown. It is possible that abnormal folate metabolism in either parent affects the uterine development and function, decidualisation, placentation, and placental function in their wildtype daughters, leading to growth defects in their wildtype grandprogeny.

1.6 Hypothesis and Aims

Despite the number of studies in the literature showing an effect of folate deficiency and abnormal folate metabolism on embryo growth and development, little is known about the mechanism by which folate leads to growth defects and congenital abnormalities. The

blastocyst transfer experiment revealed that the growth phenotypes in F2 *Mtrr*^{+/+} conceptuses are due to an atypical uterine environment of F1 *Mtrr*^{+/+} females. In this thesis, I used specific genetic pedigrees of the *Mtrr*^{gt} mouse model to examine the effects of abnormal folate metabolism on uterine development and fetoplacental growth.

We hypothesise that the *Mtrr* deficiency affects the uterine structure and function at estrus, impairs the decidualisation reaction during pregnancy, and alters the placental transcriptome at midgestation, ultimately causing FGR. To test these hypotheses, specific aims were addressed, including:

- a. To assess the effects of intrinsic and paternal *Mtrr* deficiency on the uterine structure and function of *Mtrr*^{gt/gt} and F1 *Mtrr*^{+/+} females (Chapter 3).
- b. To assess the effects of intrinsic and paternal *Mtrr* deficiency on decidualisation at GD6.5 (Chapter 4).
- c. Global DNA hypomethylation was observed in placentas, but not embryos at E10.5. Therefore, to assess the effects of intrinsic and maternal grandpaternal *Mtrr* deficiency on the placental transcriptome, we performed an unbiased RNA-sequencing experiment where we sequenced RNA from placentas of *Mtrr*^{gt/gt} and F2 *Mtrr*^{+/+} conceptuses with growth phenotypes. C57Bl/6 placentas were used as control (Chapter 5).
- d. The RNA-sequencing experiment revealed that the blastocyst transfer experiment alone was sufficient to affect the placental transcriptome. Assisted reproductive technology (ART) in humans can have a big impact on the placental transcriptome of the mother, therefore possibly affecting their offspring's embryonic development and adult health. To assess the effects of blastocyst transfer on the placental transcriptome at E10.5, we compared the transcriptomes of non-transferred and transferred C57Bl/6 placentas, and the transcriptomes of non-transferred and transferred F2 *Mtrr*^{+/+} placentas (Chapter 6).

Chapter 2: Methods

2.1 Ethical approval

All experiments were performed according to the UK Government Home Office licensing procedures. This research was regulated under the Animals (Scientific Procedures) Act 1986 Amendment Regulations 2012 following ethical review by the University of Cambridge Animal Welfare and Ethical Review Body (AWERB). The blastocyst transfer experiments were performed also in accordance with the Canadian Council on Animal Care and the University of Calgary Committee on Animal Care (protocol number M06109).

2.2 Mouse pedigrees and diet

The *Mtrr*^{gt} mouse line was originally generated as previously described (Elmore et al. 2007; Padmanabhan et al. 2013). Briefly, the *Mtrr* gene-trap (gt) vector was randomly inserted into 129/P2 embryonic stem (ES) cells. The ES cells were injected into C57Bl/6 blastocysts and then implanted into pseudopregnant females. The resulting males were tested for germline transmission of the *Mtrr*^{gt} allele. Mice with germline transmission were backcrossed for eight generations into the C57Bl/6 genetic background (Elmore et al. 2007; Padmanabhan et al. 2013). Therefore, C57Bl/6 mice (The Jackson Laboratory, Bar Harbor, USA) were used in all experiments as controls. C57Bl/6 mice were bred in house and maintained in separate cages from the *Mtrr*^{gt} mouse line (Figure 2.1A). The following genetic pedigrees were used to determine the effects of abnormal folate metabolism on embryo growth and development (Figure 2.1). *Mtrr*^{+ /gt} intercrosses generated *Mtrr*^{+ /+}, *Mtrr*^{+ /gt}, and *Mtrr*^{gt /gt} offspring (Figure 2.1B). *Mtrr*^{gt /gt} mice were derived by mating *Mtrr*^{gt /gt} females with *Mtrr*^{gt /gt} males (Figure 2.1C). The *Mtrr*^{+ /gt} paternal pedigree derived by mating an *Mtrr*^{+ /gt} male with a C57Bl/6 female to generate *Mtrr*^{+ /+} and *Mtrr*^{+ /gt} offspring (Figure 2.1D). The *Mtrr*^{+ /gt} maternal grandfather pedigree (Figure 2.1E) involved mating an *Mtrr*^{+ /gt} male (F0) and a C57Bl/6 female (F0). Their *Mtrr*^{+ /+} daughters (F1) were mated with C57Bl/6 males to generate the F2 *Mtrr*^{+ /+} mice. Mice were fed a normal breeding diet (Rodent no.3 breeding chow, Special Diet Services, Essex, UK) *ad libitum* from weaning onwards. Details of the dietary components can be found in Padmanabhan *et al.* (2013).

2.3 Blastocyst transfer

The blastocyst transfer experiments were previously performed by Colleen Geary-Joo (University of Calgary) and Dr. Erica Watson as described in detail (Padmanabhan et al. 2013). No hormones were used.

2.3.1 Collecting blastocysts

Pregnant females were euthanised by cervical dislocation followed by decapitation. The abdominal cavity was opened, and a cut was made between the ovary and the oviduct. The uterus was also cut close to the oviduct. The oviduct and the attached segment of the uterus were transferred in M2 medium (Sigma-Aldrich, Gillingham, UK). The blastocysts were flushed from the oviducts and uteri of F1 *Mtrr*^{+/+} females using a flushing needle and 0.1ml of M2 medium. C57Bl/6 blastocysts were also flushed and used as a control. The flushed blastocysts were cultured in KSOM media (Millipore, Etobicoke, ON, Canada) microdrops covered in mineral oil (Millipore, Etobicoke, ON, Canada) at 37°C for no more than 30 minutes. This unavoidable culture period allowed for the surgical preparation of the recipient female.

2.3.2 Oviduct transfer

The blastocysts were transferred into B6D2F1 females (F1 hybrid females from C57Bl/6 x DBA/2 mating) 2.5 days after mating them with vasectomized C57Bl/6 males (i.e., gestational day [GD] 2.5 equivalent; Ueda et al. 2003). B6D2F1 mice have 50% genetic similarity to C57Bl/6 mice and were used because C57Bl/6 females are notoriously poor recipients for blastocyst transfer. Noon of the day that the copulatory plug was detected was considered embryonic (E) day 0.5. Pseudopregnant B6D2F1 females were weighed and anaesthetised by intraperitoneal injection. The flushed blastocysts were transferred into M2 media at room temperature. The transfer pipette was loaded with M2 media, then a small air bubble, then M2 media, and then a second small air bubble. The blastocysts were then loaded in the transfer pipette, followed by another air bubble. A small incision was made on the recipient's female skin and the reproductive organs were exposed. Using the stereomicroscope, the infundibulum and the ampulla were located, and the loaded transfer pipette was inserted into the oviduct opening. The blastocysts were then transferred to the ampulla. The procedure was repeated for both oviducts. Blastocysts were transferred regardless of appearance and litters were never pooled (Figure 2.1G). C57Bl/6 embryos were

transferred into B6D2F1 recipients as a control (Figure 2.1F). The B6D2F1 females were then sutured and allowed to recover from the injected anaesthetic.

2.3.3 Dissection of transferred conceptuses

Transferred litters were dissected at E10.5, the timing of which corresponded to the staging of the recipient pseudopregnant females. Embryos and placentas from transferred conceptuses were dissected, scored for phenotypes, photographed, and stored at -80°C .

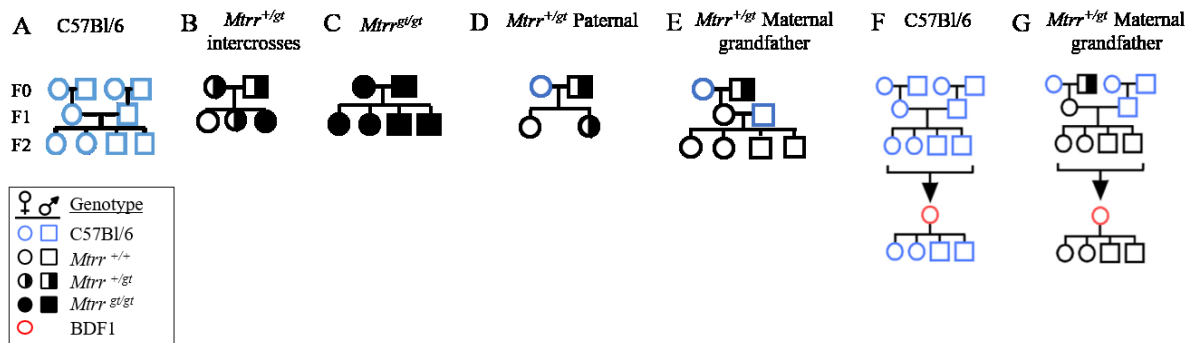


Figure 2.1 Schematic diagrams of robust genetic pedigrees established to address the role of abnormal folate metabolism on uterine and placental structure and function. (A) C57Bl/6 control pedigree (B) $Mtrr^{+/gt}$ intercrosses (C) The $Mtrr^{gt/gt}$ pedigree (D) The $Mtrr^{+/gt}$ paternal pedigree (E) The $Mtrr^{+/gt}$ maternal grandfather pedigree was derived by mating a $Mtrr^{+/gt}$ male (F0) and a C57Bl/6 female. Then, their $Mtrr^{+/+}$ (F1) daughter was mated with a C57Bl/6 male (F1) to get the $Mtrr^{+/+}$ F2 mice. (F-G) Pedigrees illustrating a blastocyst transfer experiment that was previously performed (Padmanabhan et al. 2013) including those in which F2 blastocysts that were transferred into the oviducts of control BDF1 pseudopregnant females at GD2.5. Conceptuses were allowed to develop until E10.5 when they were dissected and scored for phenotypes. (F) Control transfer experiment whereby C57Bl/6 blastocysts were transferred into the recipient female. (G) Blastocyst transfer experiment whereby F2 $Mtrr^{+/+}$ blastocysts derived from an $Mtrr^{+/gt}$ maternal grandfather were transferred into the recipient female. Circle: female, square: male, blue outline: C57Bl/6, white-filled symbols with black outline: $Mtrr^{+/+}$, semi-filled symbols: $Mtrr^{+/gt}$, black-filled symbols: $Mtrr^{gt/gt}$, red outline: BDF1.

2.4 Genotyping

DNA samples were obtained from yolk sacs or ear notches for PCR genotyping. *Mtrr* genotypes were confirmed using a three-primer PCR reaction (a: GAGATTGGGTCCCTCTTCCAC, b: CGACTTCCGGAGCGGATCTC, c: GCTGCGCTTCTGAATCCACAG), as previously described (Padmanabhan et al. 2013). Sex genotypes were determined using primers against *Ube1* (F:

TGGTCTGGACCCAAACGCTGTCCACA, *Ube1* R:
GGCAGCAGCCATCACATAATCCAGATG) or *Rmb31* (F:
CACCTTAAGAACAAGCCAATACA, *Rmb31* R: GGCTTGTCTGAAAACATTTGG) as
previously described (Chuma & Nakatsuji 2001; Tunster 2017).

2.5 Phenotypic analysis of developmental phenotypes at E10.5

Noon of the day that the vaginal plug was detected was considered E0.5. Pregnant mice were euthanised by cervical dislocation followed by decapitation at GD 10.5. Dissections were performed in 1x phosphate buffered saline (PBS). Each conceptus was individually scored for phenotypes as previously described (Padmanabhan et al. 2013, 2017; see below). Growth defects and congenital abnormalities were assessed. The conceptuses were photographed using a Zeiss SteReo Discovery V8 microscope with an AxioCam MRc5 camera and AxioVision 4.7.2 software (Carl Zeiss) before weighing and snap-freezing in liquid nitrogen for molecular analysis.

Growth defects: Crown-rump lengths of the embryos were determined using the AxioVision 4.7.2 software. Embryos with a crown-rump length that was less than or greater than two standard deviations from mean C57Bl/6 crown-rump length were considered growth restricted or growth enhanced, respectively. Embryonic somite staging was determined according to e-Mouse Atlas Project (<http://www.emouseatlas.org>) whereby 30-39 somite pairs were considered the normal range for E10.5. Embryos with less than 30 somite pairs were considered developmentally delayed. Embryos with growth defects, were otherwise phenotypically normal, i.e. did not display one or more congenital malformations (Padmanabhan et al. 2013, 2017).

Severely affected conceptuses: The gross morphology of extraembryonic (yolk sac, chorioallantoic placenta, and amnion) and embryonic tissues were assessed. Congenital abnormalities included placental defects (e.g. placenta hemorrhage, off-centered chorioallantoic attachment), and embryonic defects (e.g. open neural tube, pericardial edema, reversed cardiac looping). Implantation sites with two or more embryos (i.e. twinning) were also considered severely affected (Padmanabhan et al. 2013, 2017).

2.6 Uterine tissue collection and processing

2.6.1 Estrus stage (non-pregnant) uteri

The estrous cycle of post-pubertal female mice was monitored by examining vaginal smears as previously described (Caligioni 2009; McLean et al. 2012) so that uteri could be collected during the estrus stage. Vaginal cells were obtained by dipping the plug check tool into 1x PBS and inserting its tip into the vaginal opening of a manually restrained mouse. The vaginal smear was spread on a glass slide. Cells from each vaginal smear were stained for 5 minutes with 50% Giemsa stain (48900, Fluka Chemika) and microscopically examined. Estrus stage is characterised by predominantly cornified epithelial cells (Figure 2.2B). This differs from the smears of mice in proestrus stage, which include mostly nucleated epithelial and some cornified epithelial cells (Figure 2.2A). During metestrus, some nucleated epithelial cells are present, as well as many leukocytes (Figure 2.2C), while in diestrus there are only leukocytes (Figure 2.2D; McLean et al. 2012). Females who went through three consecutive normal cycles (i.e., the proestrus was followed by the estrous; Caligioni 2009) were euthanised at noon of the day that the vaginal smears determined the presence of cornified epithelial cells indicating estrous stage. The uterus was removed, weighed, and dissected in 1x PBS. One of the uterine horns was cut into three pieces using a sterile scalpel, snap frozen and stored at -80°C for molecular analysis. The other uterine horn was cut into three pieces and fixed overnight in 10% natural-buffered formalin (HT501128, Sigma-Aldrich) at 4°C for histological processing.

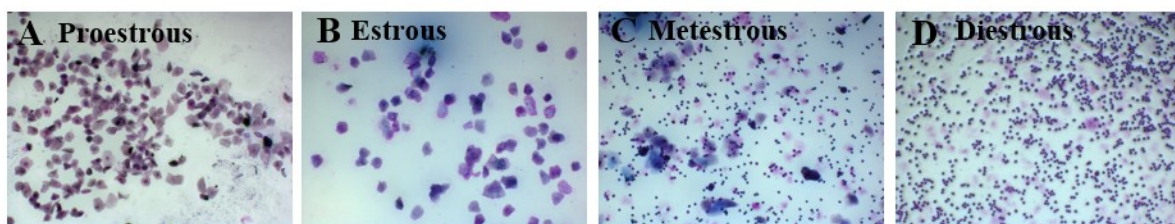


Figure 2.2 Cells of vaginal smears at each stage of the estrous cycle in adult mice.

(A) Proestrus stage, where nucleated epithelial and cornified squamous epithelial cells are present. (B) Estrus stage, where the majority of the cells are cornified squamous epithelia. (C) Metestrus stage, where some nucleated epithelial and cornified squamous epithelial cells are present, and a large leukocyte population is present. (D) Diestrus stage, where only leukocytes are present.

2.6.2 Uteri during early pregnancy (GD6.5)

Noon of the day that the vaginal plug was detected was considered GD0.5. The pregnant females were euthanised at GD6.5 and the uteri were removed. The number of implantation sites in each uterine horn was noted. The uterus was cut between each implantation site, which were then weighed. Then, half of the implantation sites were snap frozen in liquid nitrogen for molecular analysis and half of the implantation sites were processed for histology. Implantation sites from each uterine horn were represented in each experiment.

2.6.3 Tissue processing

The formalin-fixed tissue was washed three times in 1x PBS for 20 minutes and dehydrated in ascending concentrations of ethanol. The uterine tissues were stored in 100% ethanol at 4°C until all the samples were collected and then washed twice in HistoClear (HS202, National Diagnostics). The tissue was embedded in paraffin using standard procedures. The tissue was sectioned to 5µm sections using a manual microtome (RM2235, Leica).

2.7 H&E staining and immunohistochemistry

Tissue sections were deparaffinized in xylene (IS8126, Thermo Fisher) and rehydrated in descending concentrations of ethanol. For hematoxylin and eosin (H&E) staining, standard staining procedures were used. For immunohistochemistry, endogenous peroxidase activity was quenched using 3% hydrogen peroxide (H/1750/15, Fisher Scientific). Antigen retrieval was performed by addition of trypsin (T7168-20TAB, Sigma Aldrich) for 10 minutes at room temperature. The sections were washed with 1x PBST (1xPBS with 20% Tween20) and blocked with 5% serum (D9663 Sigma Aldrich) in 1% bovine serum albumin (BSA; A4503, Sigma Aldrich) in PBS for one hour. Tissue was incubated overnight at 4°C using the following primary antibody dilutions in 5% serum, 1%BSA in 1x PBST: 1:100, rabbit anti-Ki67 (ab15580, Abcam), 1:50, rabbit anti-caspase 3 (#9661, Cell Signalling Technologies), 1:100, rabbit anti-progesterone receptor (ab63605, Abcam), 1:100, rabbit anti-pan cadherin (ab16505, Abcam), or 1:100 rabbit anti-MTRR (26994-1-AP, Proteintech Europe, Manchester, UK). The sections were washed in 1x PBST. Tissue was incubated for 1 hour at room temperature in donkey anti-rabbit (ab6802-1, Abcam) secondary antibody diluted 1:300 in 5% serum, 1%BSA in 1x PBST. The immunoreactive signals were developed using a DAB

substrate kit (ab64238, Abcam). Slides were coverslip mounted using DPX mountant (360294, VWR). A Zeiss AxioImager A1 light microscope, Zeiss AxioCam MRc5 camera and AxioVision 4.7.1 acquisition software (Carl Zeiss) were used to obtain micrographs. Alternatively, the slides were scanned using NanoZoomer (Hamamatsu Photonics, UK) and the NDP Scan 2.5 software. Images were analysed using ImageJ software (Schneider, Rasband & Eliceiri 2012) and the ImageJ cell counter plugin. The histological analyses were performed blind to the treatment group.

2.8 RNA extraction and DNase treatment

RNA was extracted from tissues using the Trizol method. Briefly, 1ml TRI Reagent (T9424, Sigma Aldrich) was added to the tissue in a Matrix D tube (6913-100, MP Biomedicals). The tissue samples were homogenised using the MagNa Lyser (Roche) homogenizer. The placenta samples were homogenised at 6000x speed for 20 seconds. The uterine tissues were cut into 2-3 pieces each and homogenised at 6500x for 25-30 seconds, four times with intervening rests on ice for 1 minute. The implantation sites at GD6.5 were homogenised at 6000x for 30 seconds, four times with a 20 second rest in ice in between. Samples were left to stand for 5 minutes at room temperature and then transferred to Eppendorf tubes with 200µl chloroform. Each sample was shaken vigorously for 15 seconds and left to stand at room temperature for 15 minutes before being centrifuged at 12,000g for 15 minutes at 4°C. The colourless upper phase that contains RNA was transferred in a fresh tube with 500µl isopropanol. Samples were centrifuged at 12,000g for 10 minutes at 4°C. The pellet was air-dried, resuspended in 400 µl of ice-cold diethyl pyrocarbonate-treated water and 400µl of 4 M lithium chloride. RNA was allowed to precipitate overnight at -20°C and then centrifuged at 20,000g for 30 minutes at 4°C. The pellet was washed in 500µl of 75% ethanol, centrifuged at 20,000g for 10 minutes at 4°C, air-dried and resuspended in 55µl of DEPC-treated water. The quality and concentration of the extracted RNA were determined by NanoDrop and its integrity was determined in an RNA gel. RNA was stored at -80°C. The extracted RNA was treated with DNase I (M0303S, New England Biolabs) and EDTA (R1021, Thermo Scientific) according to the manufacturer's instructions. The DNase-treated RNA was re-purified by performing LiCl precipitation, as described above.

2.9 DNA/RNA extraction

In order to extract both DNA and RNA from the same sample simultaneously, whole placentas at E10.5 were homogenized using lysing matrix D beads (MP Biomedicals, Carlsbad, CA, USA). Total RNA and genomic DNA were purified using the AllPrep DNA/RNA kit (QIAGEN, Manchester, UK) according to manufacturer's instructions. All RNA extracts were treated with DNaseI, as previously described.

2.10 RNA-sequencing

RNA quality control, library preparation and sequencing were performed at the Cambridge Genomic Services, Department of Pathology, University of Cambridge as follows. The concentration of the samples was determined using UV absorption at 260nm with a spectrophotometer plate reader, the SpectroStar (BMG Labtech). The purity of the RNA was determined by the 260/280 and 260/230 ratios using the SpectroStar. The integrity was determined by the RNA Integrity Number (RIN), which was generated by the Agilent TapeStation Bioanalyzer. The sample libraries were prepared using the TruSeq stranded mRNA Library Preparation kit (RS-122-2101, Illumina), according to the manufacturer's instructions. Quantitative RT-qPCR was performed to quantify the libraries (SY-930-1010, Illumina) according to the manufacturers' instructions. The quality of each RNA library was determined by the RIN, which was generated by the Agilent TapeStation Bioanalyzer. Each RNA sample was barcoded individually using adaptor sequences, and the samples were pooled together for sequencing. Each sequencing run was performed in the NextSeq500 sequencer (SY-415-9001DOC, Illumina) using the high output, 75 cycle kit, according to manufacturers' instructions. A 1% PhiX library was prepared and used as a sequencing/calibration control. Sequencing was performed to reach an average of 20 million reads per sample, using 75bp single end reads.

2.11 RNA-sequencing data analysis

Bioinformatic analysis of the raw RNA-sequencing data was performed by Dr. Russell Hamilton, Dr. Malwina Prater, and Dr. Xiaohui Zhao. Quality control of Fastq files was performed using FastQC and fastq_screen. Sequences were trimmed with Trim Galore!, and aligned to GRCm38 mouse genome using STAR aligner (Dobin et al. 2013; Dobin & Gingeras 2015). Alignments were processed using custom ClusterFlow (v0.5dev) pipelines

and assessed using MultiQC (0.9.dev0; Ewels, Lundin & Max 2016). Gene quantification was determined with HTSeq-Counts (v0.6.1p1). Additional quality control was performed with rRNA and mtRNA counts script, feature counts (v 1.5.0-p2) and qualimap (v2.2). Principal component analysis and MA plots were created in R Studio. Differential gene expression was performed with DESeq2 package (v1.16.1, R v3.4.0). Read counts were normalised on the estimated size factors. Heat maps were generated with 'pheatmap' R package. The Venn diagrams were created with InteractiVenn (Heberle et al. 2015). The UpSetR tables were created with the UpSetR package (Conway, Lex & Gehlenborg 2017). The cnet plot was created using the ReactomePA R package.

2.12 Gene ontology analysis

Gene ontology was performed using DAVID (Huang, Lempicki & Sherman 2009; Huang, Sherman & Lempicki 2009) and Enrichr (Chen et al. 2013; Kuleshov et al. 2016). Analysis of placental expression of genes was determined using online databases. The databases included the Mouse Encode Project (<http://www.mouseencode.org/>; Davis et al. 2018; Dunham et al. 2012; Yue et al. 2014) and the Mouse Cell Atlas (<http://bis.zju.edu.cn/MCA/>; Han et al. 2018), which assess general RNA expression in C57Bl/6 placentas at term (E19.0) via transcriptome analyses, and the Human Protein Atlas (<https://www.proteinatlas.org/>; Uhlen et al. 2015), which assesses homolog protein expression in human placentas at term via immunohistochemistry. The list of 50 random genes was generated using the Random Gene Set Generator (www.molbiotools.com). Data were also obtained from Deciphering the Mechanisms of Developmental Disorders (<https://dmdd.org.uk>), which is a programme funded by the Wellcome Trust (www.wellcome.ac.uk) with support from the Francis Crick Institute (www.crick.ac.uk) and is licensed under a Creative Commons Attribution license (<https://creativecommons.org/licenses/by/4.0/legalcode>). Other online databases used include the Mouse Genome Informatics (<http://www.informatics.jax.org/>; Bult et al. 2019), the Mouse ENCODE Consortium 2012 (Stamatoyannopoulos et al. 2012), and the UCSC Genome Browser (<http://genome.ucsc.edu/>) using mm9 mouse genome (Haeussler et al. 2019; Kent et al. 2002).

2.13 RT-qPCR analysis of gene expression

2.13.1 Primer design

The gene accession numbers according to RefSeq (NR or NM) were found using the Universal Probe Library of Roche Life Science (https://lifescience.roche.com/en_gb/brands/universal-probe-library.html). Unless otherwise stated, the primers were designed using the NCBI primer design tool (Ye et al. 2012). Primer pairs were designed with a maximum amplicon size of 150 bp and an optimal melting temperature of 60°C (Ye et al. 2012). Primers were optimised according to Real-time PCR Application Guide (BioRad). For primer sequences, refer to Table 2.1.

2.13.2 Reverse transcription

The DNase-treated RNA was incubated with random hexamer primers (S0142, Thermo Scientific) at 65°C for 5 minutes and then in ice for at least 2 minutes. Primed RNA was reverse transcribed using RevertAid H Minus Reverse Transcriptase (EP0452, Thermo Scientific), RiboLock RNase inhibitor (EO0382, Thermo Scientific), and dNTPs (11969064001, Roche) according to the manufacturer's instructions. The synthesized cDNA was stored at -20°C. For long term storage, cDNA was stored at -80°C.

2.13.3 Real time qPCR

Real-time qPCR amplification was performed to assess relative mRNA levels using SYBR Green (RT-SY2X-03+WOUN, Eurogentec) on Opticon 2 system (MJ Research). All primers listed below were optimised with the following protocol. The enzyme was activated at 95°C for 10 minutes and the cDNA was amplified for 40 cycles under the following conditions: denaturation at 95°C for 30 seconds, annealing at 60°C for 30 seconds, and extension at 72°C for 45 seconds. cDNA was diluted 1:5 to a final concentration of 5 ng/μl and 1 μl was used per reaction. Transcript levels were normalised to *Hprt* or *Polr2a* (Solano et al. 2016). mRNA levels of the housekeeping gene were similar between groups. RNA levels were analysed using the $\Delta\Delta C_t$ method (Livak & Schmittgen 2001). cDNA levels in C57Bl/6 tissues were normalised to 1. Experiments were conducted with technical duplicates or triplicates and at least four biological replicates.

2.14 Bisulfite pyrosequencing

Bisulfite pyrosequencing was performed by Dr. Gina Blake. Genomic DNA was bisulfite-converted using the one-step method of the Imprint DNA Modification Kit (MOD50, Sigma), according to manufacturer's instructions. Non-template controls were used to ensure absence of contamination. Pyrosequencing was used to quantify methylation at individual CpG sites, as previously described (Tost & Gut 2007). Pyrosequencing primers were designed using PyroMark Assay Design Software 2.0 (Qiagen). A PCR reaction was performed using 50ng of bisulfite-converted DNA as a template, together with 0.2 μ M of each biotinylated primer and 0.25 units of HotStarTaq DNA polymerase (QIAGEN). Refer to Table 2.2 for primer sequences. During PCR the DNA was amplified for 40 cycles under the following conditions: denaturation at 95°C for 30 seconds, annealing at the annealing temperature (Table 2.2) for 30 seconds, and extension at 72°C for 45 seconds. PCR products were purified using Strepavidin Sepharose High Performance columns (Sigma Aldrich) and hybridised to the sequencing primer using a PyroMark Q96 Vacuum Prep Workstation (Qiagen). The mean CpG methylation was calculated using at least four biological replicates and two technical replicates.

2.15 Statistical analysis

Statistical analyses were performed using GraphPad Prism 6 software. Histology, immunohistochemistry, and RT-qPCR data of gene expression in the uteri were analysed using one-way ANOVA with Kruskal-Wallis correction where appropriate, since four groups were compared. The post-hoc Tukey's test for multiple comparisons was used to determine which means differ from the rest. Two-way ANOVA with post-hoc Sidak's test for multiple comparisons was used to compare the mean differences between transferred and non-transferred conceptuses in a sex-dependent manner. RT-qPCR data of placental gene expression and bisulfite pyrosequencing were analysed using Mann-Whitney test, or independent t-test with Welch correction where appropriate, since two groups were compared. P values less than 0.05 were considered statistically significant. The nbinomTest was used in R to calculate the p-value and p-adjusted value of differentially expressed genes (DEGs).

Table 2.1 Primer sequences used for RT-qPCR for analysis of gene expression.

Gene	Forward primer*	Reverse primer	Conc.	Reference
<i>2610020C07Rik</i>	GGAAGTTTTCTGACACATGCACA	CAAGCCAAGATTGACCCCCT	100nM	-
<i>Acta2</i>	GTCCCAGACATCAGGGAGTAA	TCGGATACTTCAGCGTCAGGA	100nM	-
<i>Adamdec1</i>	GAGGGCTTGAGAACAACCAGA	GCCCCAGAAGATGCTTGGT	150nM	-
<i>Aldh3a1</i>	TCCTGCTCGAGATCTTCTCTTAC	GGAGGTGCCACATGACTTTAGG	200nM	(Nishiyama et al. 2015)
<i>Ang2</i>	GAAAGGAAGCCCTTATGGACGA	ATCTGAACCCTTTAGAGGCTCG	200nM	-
<i>Ankra2</i>	GGCATCTGTCTTATTTAAAGCTGAG	CGTTTCCCCTGTGCTTGTTG	100nM	-
<i>Anxa8</i>	ACTCACCTGATGAGAGTGTTCCG	AAGTAGCTGTGGACGTTCCG	200nM	-
<i>Atp2b2</i>	AGTCGAGGAGACAGAGCTGA	CTGGCATCTACATGGTCGGG	100nM	-
<i>Bmp2</i>	CCTGAAGCAGAGACCCACCC	CTGGAAGTTCCTCCACGGCT	200nM	(Woods et al. 2017)
<i>Cadps</i>	CCCCATCTCACAATTTTACGC	TCAAAGAGGGAAGCGTGGTC	150nM	-
<i>Calcoco2</i>	GGCTGCTGTTCTTGACTT	TCAGTGAGGGTGTAATAGCACAT	100nM	-
<i>Ccl1</i>	GACATTCGGCGGTTGCTCTA	GTAAGCATGCTCTTGCTGTCAAC	200nM	-
<i>Cdh1</i>	AACCCAAGGCACGTATCAGGG	ACTGCTGGTCAGGATCGTTG	100nM	-
<i>Ceacam14</i>	GAGCTTGGAACAGCACGAGA	TTAAAAGGGAGACTGTGAGCAGGA	200nM	-
<i>Clca3a1</i>	ACCCCGAGGCAGAGTCTTT	CACATTGGTGCCAGTGATCC	200nM	-
<i>Cldn10</i>	GGGCTGCTCTTTCATCGG	GTAGCCCATTCTGGGTGTCT	200nM	-
<i>Cldn11</i>	TCCCCACCTGCCGAAAAATG	ACGTAGCCTGGAAGGATGAGG	200nM	-
<i>Crybg3</i>	CCAATTGGAACCACTCGGGA	GGTCAGGTCGGCACATTCTT	200nM	-
<i>Ctla4</i>	CCATGCCCGGATTCTGACTT	GGACTTCTTTTCTTTAGCATCTTG	200nM	-
<i>Ctsm</i>	TTGGAAAGCTGTGCAGTGGA	GCATGGCCAGGAAGATAGCA	150nM	-
<i>Ctsq</i>	GGGTTTGCTGACATGACTGA	CCAAGTGCACGTTTCCAGAG	200nM	-
<i>Dazl</i>	CTAGGCAGCCACCTCACGTA	GAAGTTGTGGCAGACATGATGG	200nM	-
<i>Dhtkd1</i>	GTACCCTGCAGCTGTGTCAA	TCTTTGCTTCAGCAGGGCAT	50nM	-
<i>Dnmt1</i>	CCTAGTTCGGTGGCTACGAGGAGAA	TCTCTCTCCTCTGCAGCCGACTCA	150nM	(Kowluru, Shan & Mishra 2016)

<i>Dnmt3a</i>	CCGCCTCTTCTTTGAGTTCTAC	AGATGTCCCTCTTGTCACCTAACG	100nM	(Ding et al. 2012)
<i>Dnmt3b</i>	TTCAGTGACCAGTCCTCAGACACGAA	TCAGAAGGCTGGAGACCTCCCTCTT	100nM	(Anier et al. 2010)
<i>Dusp4</i>	GCCTGCTTAAAGGTGGCTATG	GCCAGGGCCTTGGTTTTAGA	200nM	-
<i>E130309F12Rik (Plppr1)</i>	CTCCCACGCAAGCGGAAT	CAGAAACTGTCCAGGCTTTGG	100nM	-
<i>EpCam</i>	TTGCTCCAAACTGGCGTCTA	TCGTACAGCCCATCGTTGTT	200nM	-
<i>Esr1</i>	CACCAGATCCAAGGGAA	CGGCGTTGAACTCGTAG	200nM	(Li et al. 2017)
<i>Fbp2</i>	ACAGAAAGACCACGGAGGATG	TGTCCTGTGGAAAGAGCGAC	150nM	-
<i>Folr1</i>	GGCCCTGAGGACAATTTACA	TCGGGGAACACTCATAGAGG	200nM	(Kooistra, Trasler & Baltz 2013)
<i>Foxa2</i>	CGGCCAGCGAGTTAAAGTATG	TTGCTCACGGAAGAGTAGCC	200nM	-
<i>G530011O06Rik</i>	TTTAGGCACAGGCATCGGAA	AGCATTTTCGGTGAAGCAGGA	150nM	-
<i>Gapdh</i>	CATGGCCTTCCGTGTTCTT	GCGGCACGTCAGATCCA	200nM	(Gillich et al. 2012)
<i>Gbp2b</i>	TCCCTTAAACTTCAGGAACAGGA	GATCGAGGTGGAGGCATGTT	100nM	-
<i>Gm773</i>	TGGAAACTTAAGCCTGCATTTGT	TGCTGTAAGTGTAGAGTGTGCT	150nM	-
<i>Gm773</i>	TGGAAACTTAAGCCTGCATTTGT	TGCTGTAAGTGTAGAGTGTGCT	150nM	-
<i>Hand2</i>	CACCAGCTACATCGCCTACC	TCTCATTCAGCTCTTTCTTCTCT	150nM	-
<i>Hhip11</i>	GCTGCACATGGGGTCATCTA	CGGATGAACTTTTCCTTGGGC	200nM	-
<i>Hoxa10</i>	CACAGGCCACTTCGTGTTCTT	TTGTCCGCAGCATCGTAGAG	200nM	-
<i>Hprt</i>	CAGGCCAGACTTTGTTGGAT	TTGCGCTCATCTTAGGCTTT	200nM	(Rameix-Welti et al. 2014)
<i>Hsd3b6</i>	CCAGGGAGCAATTCTTCAACCT	TGACAGCTGCAGTGTGGATA	200nM	-
<i>Il33</i>	AACTCCAAGATTTCCCCGGC	TTATGGTGAGGCCAGAACGG	200nM	-
<i>Jchain</i>	AGCGACCATTCTTGCTGACA	TGTTCAAAGGGACAACAATTCGG	200nM	-
<i>Klk9</i>	GCTGGCCTCTTCTACCTCAC	GACCCACAGGTACGGCTTTC	150nM	-
<i>Klra7</i>	CTCTCCAATGAGTGTAAGTGCAA	AGCTTTGGGGGACCAGAGTA	100nM	-

<i>Klra8</i>	TTCTTCTTGGAGCCTCTTAGGG	AAAATATGTCCTGTGTCTCCACC	200nM	-
<i>Klrb1c</i>	GAGTGTCTTAGTGCGAGTCTTAGT	TTGTGGGCACTCTAAATTAAGTAA	200nM	-
<i>Med12</i>	TCCCCTACTGCTGCGATACT	GAGCCAATCTCCGGGTACAG	200nM	-
<i>Mndal</i>	AAGTGGAGGGGAGTGGACAA	TTGGTGACCTTGATCTTGACGA	150nM	-
<i>Mthfr</i>	AGCTTGAAGCCACCTGGACTGTAT	AGACTAGCGTTGCTGGGTTTCAGA	100nM	(Uthus & Brown-Borg 2006)
<i>Mtrr (WT)</i>	CCTTCAGGAGAATGGCTACG	GGACCAGATGTCCTGCAGAT	150nM	-
<i>Mtrr (WT+gt)</i>	GGTTTTCCGCAGATCTTCAC	CTGTGTCAGGTGGGTCTCCT	150nM	(Padmanabhan et al. 2013)
<i>Myocd</i>	CCAACACCTTGCCAGTTATC	GGAGCTTGTGCTGCCAAAG	200nM	-
<i>Myot</i>	CCCCCTCTGAGCTAAGGAAAC	GGTTCAGCAAGTCAGAAGC	150nM	-
<i>Ndufa4l2</i>	TAAAAAGACACCCTGGGCTCAT	TGGGTTGTTCTTTCTGTCCCA	200nM	-
<i>Nell1</i>	ACCTAAATCGCACTTGCCCA	TGACCAAGTCTCGTCTCTGC	200nM	-
<i>Nkg7</i>	CATGGCTTTTTCTGCAGCTCTC	GCCTAGGTAGAAGGACCAGGA	150nM	-
<i>Noct</i>	GCGTCCCCGAACAGTGAGTT	AGGATCGATGGGCTCCAGAT	150nM	-
<i>Nr2f2</i>	GCCAGTACTGCCGCCTCAA	CAAACGCCCCGTGGGTAGGC	200nM	(Woods et al. 2017)
<i>Pgr</i>	GCCTATAACCGATCTCCCTG	TTCCCTATGAGTGGCTTCTAC	200nM	(Li et al. 2017)
<i>Pianp</i>	CACCAGGCATGCAGTAAAGG	GAGCAGGTGGTAATACGGACA	100nM	-
<i>Pilrb1</i>	GAGTCTGACCAAGCCCAGTA	TTGAGTGCTTGGGTACGTT	150nM	-
<i>Polr2a</i>	GAGTCCAGAACGAGTGCATGA	ACAGGCAACACTGTGACAATC	100nM	(Rakoczy et al. 2017)
<i>Polr2a</i>	GAGTCCAGAACGAGTGCATGA	ACAGGCAACACTGTGACAATC	100nM	(Rakoczy et al. 2017)
<i>Ppef1</i>	CTAAGAAAGTGATAAAAGCCGCGT	CATTTGGCCTTGCTCGTCAG	150nM	-
<i>Prl3d1</i>	CATTCCTGCGGAGCCTGAAA	GGAGCCTACATTGTGGTGGGA	200nM	-
<i>Prl3d1</i>	GGAGCCTACATTGTGGTGGGA	CATTCCTGCGGAGCCTGAAA	200nM	-
<i>Prl7a2</i>	ACTGCGCAAGACATATACAGTCA	AATTGTGGCAGCAGGTGAGA	200nM	-
<i>PscA</i>	CTGCATCCAGGTGCTGCT	GCGCGATGTAAAGCAACTGT	200nM	-

<i>Psg25</i>	GCAGGAGCTGAAGGTCTTTTCA	TAGGTTAAGATGGAGGCTGTGA	200nM	-
<i>Psg27</i>	GGTTGACACCTCCCTTTCCC	GGCTTGTGGATCTTTTGGCAG	200nM	-
<i>Ptafr</i>	TGAGCTCCTCCTACAGGCAT	TCGGAAAGAGCGTGTATCGAA	200nM	-
<i>Ptgdr</i>	CCTGCCTTTAATTTATCGTGCGT	GATGAAGATCCAGGGGTCCAC	200nM	-
<i>Rem1</i>	GCTGGGAGGTGTGTACGAG	AGTACACGATGACGTAGGCG	200nM	-
<i>Rfc1</i>	GGGTGTGCTACGTGACCTTT	ACGGAACTGATCACGGACTT	100nM	(Kooistra, Trasler & Baltz 2013)
<i>Rgs1</i>	ATCGGCCAAGTCCAAAGACAT	TTTTGACCTGTCTGGTTGGC	150nM	-
<i>Rmrp</i>	AAGTCACTGTTAGCCCGCC	TGAGAATGAGCCCCGTGTG	200nM	-
<i>RNase2a</i>	AGACTGGGAAACATGGGTCTGG	ATGCTGGATGTCAAACCACCG	200nM	-
<i>Rpph1</i>	CTGGGAAGGTCTGAGACTTGG	CCAGTCTGCCAAGCGTA	200nM	-
<i>Serf2</i>	CATGACCCGCGGTAACCAG	CTGCATGATCTCCGAGTCCC	200nM	-
<i>Sfrp5</i>	TTCCCCCTGGACAACGACCT	CGCTGTGCTCCATCTCACACT	200nM	(Woods et al. 2017)
<i>Slc2a2</i>	TCCCTTGGTTCATGGTTGCT	AGGAAGTCCGCAATGTACTGG	200nM	-
<i>Slit3</i>	CTCAAGACGCTGATGTTGCG	GGCAGTTGCAGTTGAAAGGG	200nM	-
<i>Star</i>	AGCTCTCTGCTTGGTTCTCAA	TCCAGCCTTCCTGGTTGTTG	200nM	-
<i>Stim1</i>	AGGAGATTGTGTCGCCCTTG	GGGTCAAATCCCTCTGAGATCC	200nM	-
<i>Tet1</i>	ACACAGTGGTGCTAATGCAG	AGCATGAACGGGAGAATCGG	200nM	(Stryjewska et al. 2017)
<i>Tet2</i>	ACCTGGCTACTGTCATTGCTCC	TGCAGTGACTCCTGAGAATGGC	50nM	-
<i>Tet3</i>	AGGCAGCTAAGCACCTCAG	GGCCCCGTAAGATGACACAG	50nM	(Hwang et al. 2016)
<i>Tex13b</i>	AGATAGAACGCAAGGAGGCG	GGTGGCAAATCTTGCGTGTA	100nM	-
<i>Tmem55a</i>	ATTCTGTGGATGGAAGTGGAGG	GATGGTGACATACGCACAGC	50nM	-
<i>Tmprss11bnl</i>	GATGCTGGAGAACAACCCAGA	TCCCACAGCGGTTGTTGATAA	200nM	-
<i>Tmprss11e</i>	TGTTGGAGGGACACCAGTAGA	TGGATGGGTCCTTGTGTGTTT	200nM	-
<i>Tpbpa</i>	ACTGGAGTGCCAGCACAGC	GCAGTTCAGCATCCAAGTGGC	200nM	(Cambuli et al. 2014)

<i>Tpbpb</i>	GAAGTGCAAGAGCAGAAGGATA	GCTGACCAAAGAAGACTCTCAA	200nM	-
<i>Tspan8</i>	AGTCGGAGTTCAAGTGCTGT	GGGTAAACGGAACTCCCCTG	200nM	-
<i>Ugt2b34</i>	AGGATGACTTTCATGGAGAGGG	GAGTGTCGTGGGTCTTCCTAAT	200nM	-
<i>Vimentin</i>	AACTGCACGATGAAGAGATCCA	GCCACGCTTTCATACTGCTG	200nM	-
<i>Wif1</i>	CCCGATGTATGAACGGTGGT	GGTGGTTGAGCAGTTTGCTTT	150nM	-
<i>Zkscan3</i>	CTGCGTTCGCGGTCTTTTAC	GCAGAGTGTGAGTCCAAGGT	200nM	-

*All primers are listed in the 5' to 3' orientation.

Table 2.2 Bisulfite pyrosequencing primers.

Location	Forward primer*	Reverse primer	Sequencing primer	Ta (°C)	Reference
<i>Prl3d1</i> promoter: set a	[biotin]- TTAGATTATATGGGGGATA TG TAGTATG	TCCTTAAAAATTATTAACATCCTCTTTA CA	ACATCCTCTTTAC ATTTAAC	56	-
set b	TGTGTTAAATGTAAAGAG GATGTTAATAAT	[biotin]-ACCAAAC TATACCTAAACCCA	AATGTTGTTTATT AATAGATATTGA	56	-
set c	TTGGAGTAAATGTATATTG TGAGATGT	[biotin]- ACAACAACAATTACATTCCTACTAT	AAATAAGTATTT TATTAAGTAATA G	56	-
set d	ATTGTTGTTGTTGGTGTTA AGT	[biotin]- CCAAAAACAAAAACATTACTTACAAAT T	TGTTATGGTGTTT ATTGAAG	56	-
<i>Rasgrfl</i> DMR	GGGAAGATTATTAGTTGG GGAGGTG	[biotin]- CAACAAAAACCAAATATCAATCCTAA C	ATTAGAGTTAAA TATAAAGAATGG	54	(Padmanabhan et al. 2013)

*All primers are listed in the 5' to 3' orientation.

Chapter 3: The effects of abnormal folate metabolism on the uterus during estrus

This chapter includes experiments that have been performed in collaboration. Dr. J. Rakoczy performed the immunohistochemical staining for MTRR expression on estrus-staged uteri and GD8.5 implantation sites.

3.1 Introduction

The importance of folate has been well examined during pregnancy. However, the effects of abnormal folate metabolism on the structure and function of the non-pregnant uterus is not well established. Profound changes were observed in the reproductive organs of folate-deficient rhesus monkeys compared to controls (Mohanty & Das 1982). For instance, more atresic and cystic ovarian follicles lacking granulosa cells were observed in the ovaries of folate-deficient monkeys. This impaired the ovarian hormone secretion, leading to irregular menstrual cycles and decreased serum E2 and P4 levels. Folate deficiency also caused abnormal proliferation and maturation, megaloblastosis and multinucleation in the cervico-vaginal epithelium. Finally, decreased cell proliferation of the luminal epithelium of the uterus was observed in folate-deficient monkeys (Mohanty & Das 1982). In addition, folate supplementation did not affect the uterine horn weight of gilts, but information is not available for uterine histology (Matte, Girard & Tremblay 1993). The effects of folate supplementation and folate receptor 4 (*Folr4*) mutation on gene expression in the periconceptional mouse uterus were assessed via microarray (Salbaum, Kruger & Kappen 2013). In the wildtype mice, folic acid supplementation led to increased expression of genes involved in lipid metabolism, and decreased expression of genes involved in vasculature development. Folic acid supplementation in the mice lacking *Folr4* had more profound effects on gene expression, and it affected the immune system, mitochondrial, and ribosomal function. Folic acid supplementation of *Folr4*^{-/-} mice also increased histone methylation patterns, compared to non-supplemented *Folr4*^{-/-} mice, suggesting a mechanism for differential gene expression. This suggested that periconceptional supplementation with folic acid alters the uterine transcriptome (Salbaum, Kruger & Kappen 2013). No data are available for humans.

Mouse reproductive success depends on estrous cyclicity, which is regulated by hypothalamic GnRH, pituitary LH and FSH, and ovarian E2 and P4 hormones. As mentioned in Section 1.2.2, the estrous cycle lasts around five days and has four stages: proestrus, when oocyte maturation occurs; estrus, when ovulation occurs; metestrus, when the mature oocytes move through the oviducts into the uterus; and diestrus, when the unfertilised oocytes are eliminated (Table 1.1). The maturing follicles produce E2, and therefore E2 peaks at proestrus, when follicles reach the mature Graafian follicle stage. A peak in E2 induces the LH surge (Green 1966). E2 also induces epithelial and stromal cell proliferation in the uterus, therefore the uterus mitotic activity and uterine width peak at morning of the estrus stage

(Martin & Finn 1968; Tibbetts et al. 1998; Wood et al. 2007). Proestrus and estrus stages are characterised by increased endometrial gland secretions, leading to uterine distention (Green 1966). The E2-producing ruptured follicle transforms into a P4-producing corpus luteum, and the female enters the metestrus stage, followed by diestrus. P4 secretion increases and binds to the progesterone receptor on the luminal and glandular epithelium of the uterus. Once the receptor is activated, a signalling cascade results that is important for preparing the uterus for potential implantation of blastocysts, for the secretory transformation of the uterine glands, and maintenance of pregnancy (Riesewijk 2003).

The *Mtrr^{gt/gt}* mutation causes growth defects including growth restriction and developmental delay in mice. Furthermore, these growth defects in addition to growth enhancement were observed in the wildtype grandprogeny (F2) of *Mtrr^{+gt}* mice (F0; Padmanabhan et al. 2013). Through a blastocyst transfer experiment, the Watson lab previously determined that these growth defects were associated with an abnormal uterine environment of the F1 *Mtrr^{+/+}* females (Padmanabhan et al. 2013), though the details of this abnormality remain unknown. The *Mtrr^{gt}* mutation leads to global DNA hypomethylation in adult tissues, including the non-pregnant *Mtrr^{+/+}* uteri, and increased plasma total homocysteine levels in the *Mtrr^{gt/gt}* mice (Elmore et al. 2007; Padmanabhan et al. 2013), which may contribute to an atypical maternal environment. The mechanism by which the *Mtrr^{gt}* allele in mice causes an atypical uterine environment in their wildtype daughters that gives rise to growth defects in their wildtype grandprogeny at midgestation is still unknown, but epigenetic mechanisms are possibly implicated. The aim of this chapter is to assess the effects of *Mtrr^{gt}* mutation on the uterine structure and function during estrus. Here, we hypothesise that the *Mtrr^{gt}* mutation affects the uterine structure and function at estrus, possibly leading to abnormal decidualisation during pregnancy and ultimately FGR. To test this, hypothesis we assessed the intrinsic effect of the *Mtrr^{gt}* mutation by assessing *Mtrr^{+gt}* and *Mtrr^{gt/gt}* females, and the parental effect of *Mtrr^{gt}* mutation by assessing *Mtrr^{+/+}* females derived from either an *Mtrr^{+gt}* father or *Mtrr^{+gt}* parents. This will explore the characteristics of an atypical uterine environment as a cause for offspring growth phenotypes.

3.2 Results

3.2.1 Estrous cycle duration is unaffected by an intrinsic or paternal *Mtrr^{gt}* allele

To examine the effects of abnormal folate metabolism on estrous cyclicity, we assessed the estrous cycles of *Mtrr^{+/+}*, *Mtrr^{+/gt}* and *Mtrr^{gt/gt}* post-pubertal female mice littermates derived from *Mtrr^{+/gt}* intercrosses (Figure 2.1B) compared to C57Bl/6 control females (Figure 2.1A). We also assessed the paternal effect of *Mtrr^{gt}* allele by assessing *Mtrr^{+/+}* and *Mtrr^{+/gt}* females derived from an *Mtrr^{+/gt}* father and C57Bl/6 mother (Figure 2.1D). Four mice were assessed per genotypic group. For each female, the estrous cycle was monitored daily for at least three cycles. This was done by generating vaginal smears at the same time each day. The cycling females were euthanised during the estrus stage, and uterine tissue was collected for histological and molecular analyses. The age of the females at the time of dissection averaged between 11-19 weeks.

First, we assessed the length of the entire estrous cycle in days. One estrous cycle was determined as the days between two estrus stages with at least one intervening day in proestrus stage (i.e., estrus, proestrus, estrus; Caligioni 2009). No differences between C57Bl/6 (4.3 ± 0.6 days; mean \pm SEM), *Mtrr^{+/+}* (3.6 ± 0.5 days), *Mtrr^{+/gt}* (4.1 ± 0.9 days) or *Mtrr^{gt/gt}* (4.3 ± 0.6 days, $p=0.4$) females were observed (Figure 3.1A). Next, we determined the length of each stage including proestrus, estrus and metestrus/diestrus stages in each genotypic group. Again, the duration of each stage in *Mtrr^{+/+}*, *Mtrr^{+/gt}* and *Mtrr^{gt/gt}* females was similar to controls (Figure 3.1B-D). Furthermore, no difference in estrous cycle length was observed in F1 *Mtrr^{+/+}* females (4.4 ± 0.8 days) or F1 *Mtrr^{+/gt}* females (3.9 ± 0.5 days) compared to C57Bl/6 controls (4.2 ± 0.2 days, $p=0.4$; Figure 3.1E). The duration of each stage of the estrous cycle was also similar in F1 *Mtrr^{+/+}* and F1 *Mtrr^{+/gt}* females compared to C57Bl/6 females (Figure 3.1F-H). Therefore, neither an intrinsic nor a parental *Mtrr^{gt}* allele affects the duration of the estrous cycle in mice.

Next, uterine tissue was collected for histological and molecular analyses. First, one uterine horn from each mouse was weighed after dissection. No difference ($p=0.1$) in uterine weight was determined between C57Bl/6 (0.020 ± 0.008 g), *Mtrr^{+/+}* (0.04 ± 0.02 g), *Mtrr^{+/gt}* (0.030 ± 0.004 g) or *Mtrr^{gt/gt}* (0.030 ± 0.007 g; Figure 3.1I). Furthermore, no difference ($p=0.2$) in the average uterine horn weight was observed in F1 *Mtrr^{+/+}* females (0.020 ± 0.006 g) and F1

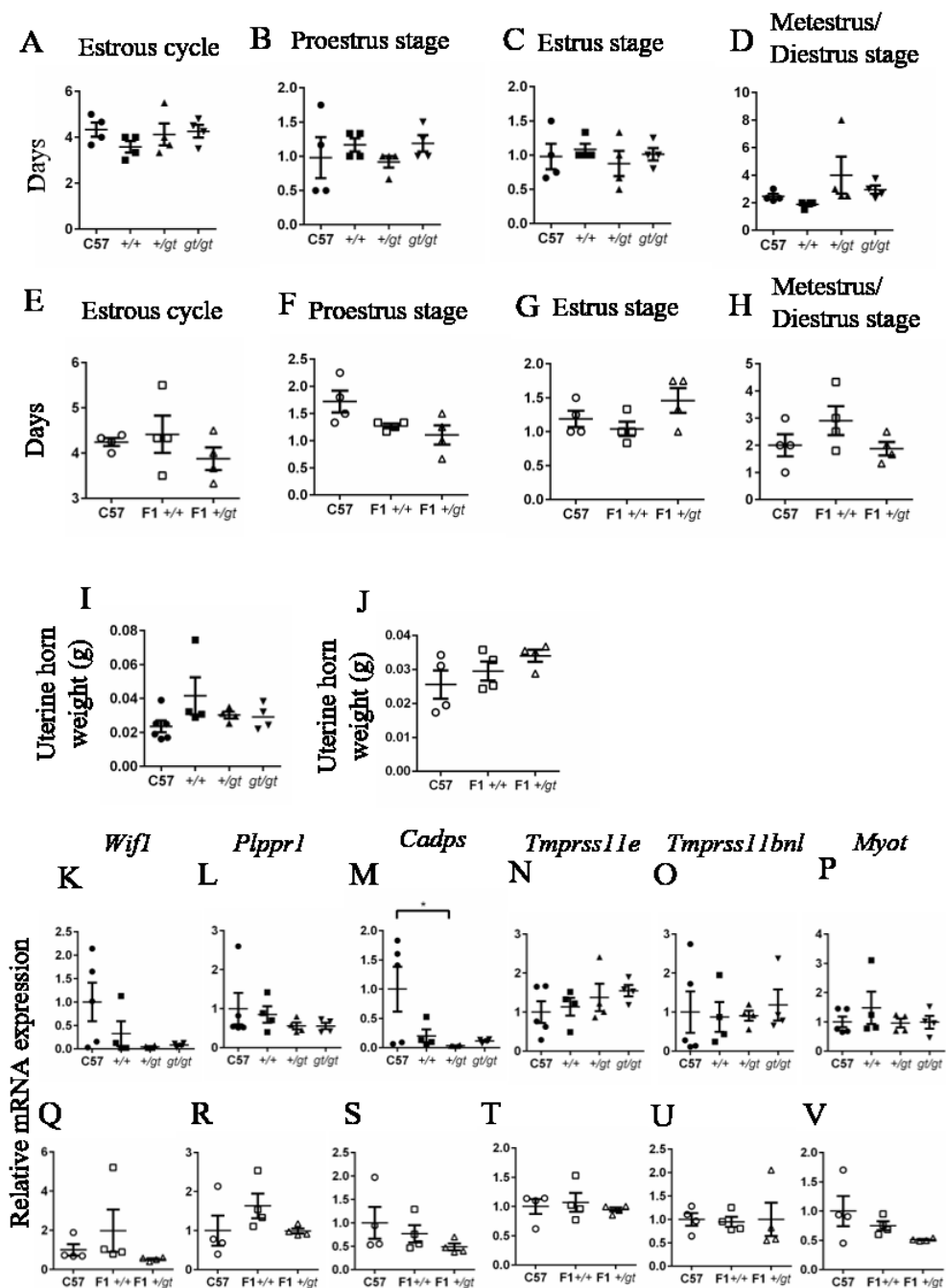


Figure 3.1 The *Mtrr^{gt}* mutation does not affect estrous cyclicity.

(A-H) Graphs depicting (A, E) the average duration of the whole estrous cycle, (B, F) the average duration of the proestrus stage, (C, G) the average duration of the estrus stage, and (D, H) the average duration of the metestrus/diestrus stages combined. Data are presented in mean ± SEM. (I-J) Graphs representing the average uterine horn weight per genotype. Data are presented in mean ± SEM. n=4-5 females per genotype. (K-V) Analysis of (K-M, Q-S) estrus stage-specific and (N-O, T-V) proestrus stage-specific gene expression in estrus stage uterine horns. n=4-5 females per genotype. *Hprt* was used as a housekeeping gene. Data are presented as fold change compared to C57Bl/6 controls (normalised to 1). Statistical analysis: one-way ANOVA, *p<0.05.

Mtrr^{+/*gt*} females (0.030 ± 0.004 g) compared to C57Bl/6 controls (0.030 ± 0.008 g; Figure 3.1J). One limitation of this analysis, is that we did not take into account the body weight to calculate the uterus:body weight ratio. Next, we determined whether genes that are normally expressed in either estrus stage or proestrus stage uteri were altered in estrus stage uteri from each pedigree via RT-qPCR analysis. Under normal conditions, the genes *Wif1*, *Plppr1*, and *Cadps* are highly expressed in estrus and lowly expressed in proestrus (Yip et al., 2013). We observed that *Wif1* and *Plppr1* mRNA expression was not statistically different between all *Mtrr* uterine groups compared to the C57Bl/6 controls (Figure 3.1K-L, Q-R), however *Cadps* mRNA expression was decreased (p=0.033) in the *Mtrr*^{+/*gt*} uteri compared to C57Bl/6 (Figure 3.1M). mRNA expression of all three genes was quite variable in some C57Bl/6 control uteri (Figure 3.1K-M), which might explain the lack of significance. Why expression levels were so variable in the controls is unclear, though it is possible that gene expression fluctuates even within the estrus stage. Increasing the sample size for each experimental group will make this result more robust. The expression of estrus-specific genes was similar in the F1 *Mtrr*^{+/*+*} and F1 *Mtrr*^{+/*gt*} compared to C57Bl/6 females (Figure 3.1Q-S). The expression of three proestrus-specific genes *Tmprss11e*, *Trmpss11bnl*, and *Myot* (Yip et al., 2013) was also similar in estrus-staged uteri from *Mtrr* and C57Bl/6 females (Figure 3.1N-P, T-V). Altogether, these data suggest that *Mtrr*^{*gt*} mutation does not affect estrous cyclicity and that the hypothalamic-pituitary-ovarian axis is likely functioning properly.

3.2.2 Analysis of expression of *Mtrr* mRNA and protein in the estrus-staged uterus

The Watson lab previously showed that the *Mtrr*^{*gt*} allele is a knockdown mutation since *Mtrr*^{*gt/gt*} mice express wildtype *Mtrr* transcript (Elmore et al. 2007; Padmanabhan et al. 2013). However, the degree of *Mtrr* knockdown varies between tissue types (Elmore et al. 2007; Padmanabhan et al. 2013). Therefore, to confirm the level of wildtype *Mtrr* transcript expression in the uteri of *Mtrr*^{+/*+*}, *Mtrr*^{+/*gt*} and *Mtrr*^{*gt/gt*} female littermates compared to C57Bl/6 females, RT-qPCR analysis was performed. Wildtype *Mtrr* transcript was detected using primers that anneal downstream of the gene-trap insertion site in the *Mtrr* locus. As expected, there was no difference in wildtype *Mtrr* transcript levels between the *Mtrr*^{+/*+*} and the C57Bl/6 uteri (Figure 3.2A). This result suggests that a paramutation effect (Hollick 2016) is not present in *Mtrr*^{+/*+*} uteri, confirming what was previously shown by Padmanabhan *et al.* (2013). Furthermore, the expression of the *Mtrr* wildtype transcript was

decreased to 43.0% and 13.1% of control levels in *Mtrr*^{+/*gt*} and *Mtrr*^{*gt/gt*} uteri, respectively ($p < 0.0001$; Figure 3.2A), a result consistent with *Mtrr* genetic knockdown and previous observations (Padmanabhan et al. 2013). Next, we determined whether “total *Mtrr*” transcript levels, which contain both wildtype and mutant transcripts, were altered by the gene-trap insertion. Total *Mtrr* mRNA levels were determined using RT-qPCR primers that anneal upstream of the gene-trap insertion and can be used to indicate whether a mutant cell attempts to up-regulate *Mtrr* transcription in response to low MTRR protein expression. There was no difference in the expression of total *Mtrr* in *Mtrr*^{+/*+*}, *Mtrr*^{+/*gt*} and *Mtrr*^{*gt/gt*} uteri compared to the controls (Figure 3.2B). This result suggests that the *Mtrr*^{+/*gt*} or *Mtrr*^{*gt/gt*} uterine cells do not compensate for MTRR deficiency at a transcriptional level.

A similar analysis was performed on the uteri of F1 *Mtrr*^{+/*+*} and F1 *Mtrr*^{+/*gt*} females derived from an *Mtrr*^{+/*gt*} father and a C57Bl/6 mother. The average *Mtrr* wildtype transcript levels in F1 *Mtrr*^{+/*+*} uteri (60.0% of control levels) and F1 *Mtrr*^{+/*gt*} uteri (29.0% of control levels; $p = 0.005$) were much lower than expected (100% and ~50-60% of control transcript levels, respectively; Figure 3.2C). While total *Mtrr* mRNA expression in F1 *Mtrr*^{+/*+*} uterine tissue was similar to controls, expression in F1 *Mtrr*^{+/*gt*} uteri was 55% of control levels, which is much lower than expected ($p = 0.03$; Figure 3.2D). Although it is unclear why F1 *Mtrr*^{+/*gt*} uteri have reduced total *Mtrr* transcript expression, it is possible that *Mtrr* transcripts might be degraded due to a paramutation effect. This is interesting given that this result was specific to a paternal effect of *Mtrr* deficiency and not apparent in *Mtrr*^{+/*+*} females derived from *Mtrr*^{+/*gt*} intercrosses.

To explore this finding further, we sought to confirm the *Mtrr*^{*gt*} genotype of the F1 uterine samples used in this analysis. A conventional PCR reaction was performed using a three-primer reaction to determine the presence or absence of the gene-trap (Padmanabhan et al. 2013) in DNA collected from ear notches of the females in question. On the electrophoresis gel, the PCR product at 272 bp indicated a wildtype allele and the band at 383 bp indicated a mutant allele (lanes 13-15, Figure 3.2E). Indeed, the DNA samples from the C57Bl/6 and F1 *Mtrr*^{+/*+*} females displayed a single wildtype band at 272 bp on the DNA gel (lanes 1-4 and 5-8 respectively, Figure 3.2E). As expected, DNA from F1 *Mtrr*^{+/*gt*} females revealed two bands, a wildtype and mutant allele (lanes 9-12, Figure 3.2E). Therefore, the genotypes of the F1 mice used in this analysis were confirmed. It remains unclear as to why *Mtrr* transcript levels are lower F1 *Mtrr*^{+/*gt*} uteri.

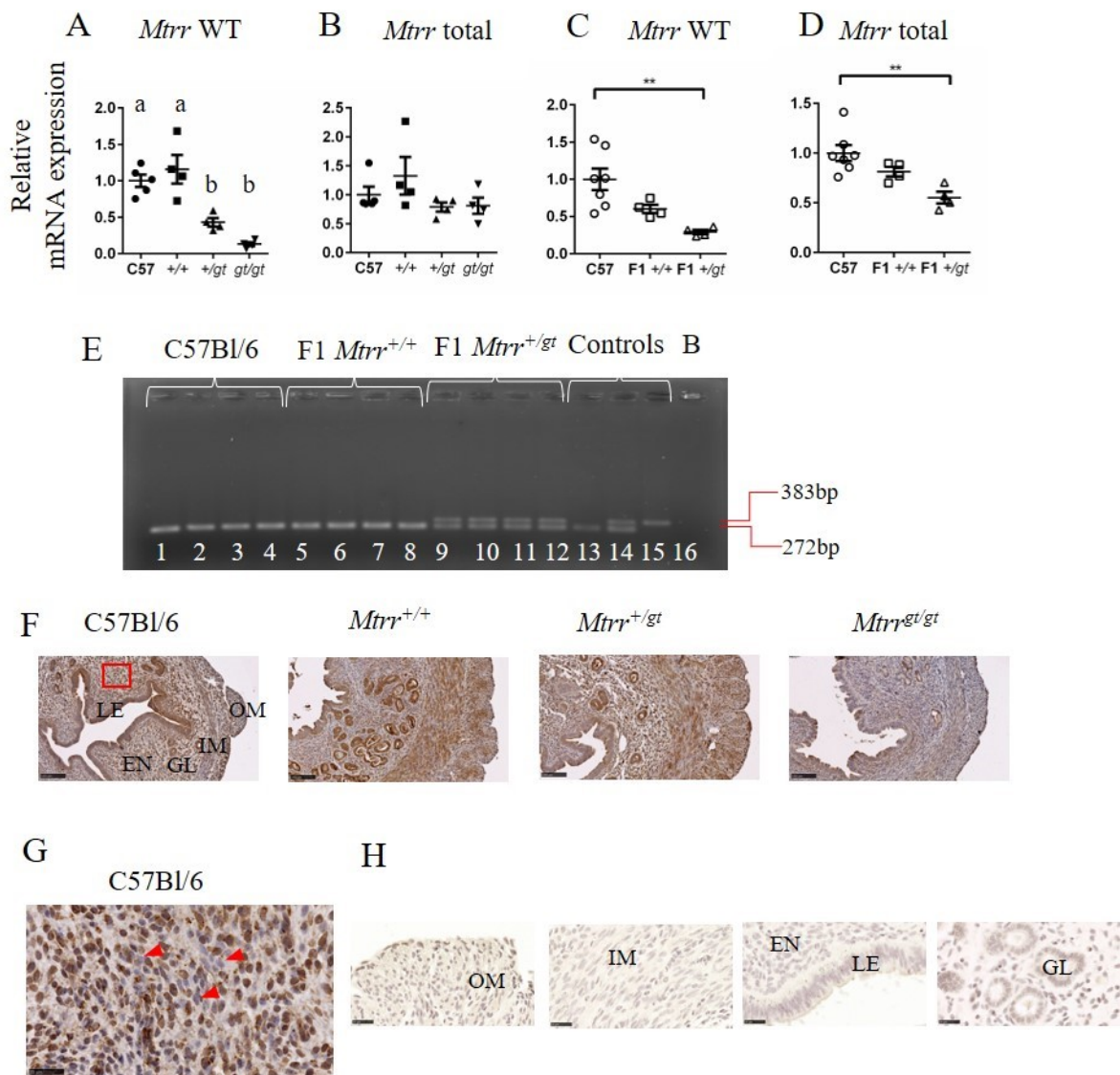


Figure 3.2 *Mtrr* transcript and MTRR protein expression in the mouse uterus at estrus. (A-D) Graphs showing relative *Mtrr* mRNA expression. n=4-7 uteri per genotype. Data are presented as mean \pm SEM. Statistical test: One way ANOVA, a p<0.05 when compared to b, **p<0.01. (E) Electrophoresis gel showing DNA bands at 272 bp (*Mtrr* wildtype transcript) and 383 bp (*Mtrr* gene-trapped transcript) to verify the *Mtrr* genotypes of F1 females assessed. Samples 1-4: C57Bl/6 females, 5-8: F1 *Mtrr*^{+/+} females, 9-12: F1 *Mtrr*^{+ /gt} females, 13: *Mtrr*^{+/+} DNA, 14: *Mtrr*^{+ /gt} DNA, 15: *Mtrr*^{gt/gt} DNA, 16: No template control. (F-G) Representative uterine sections from C57Bl/6, *Mtrr*^{+/+}, *Mtrr*^{+ /gt} and *Mtrr*^{gt/gt} females at estrus that were stained with an MTRR antibody (brown). DNA, purple. Boxed region in panel (F) represents higher magnification of the endometrium shown in panel (G). Red arrows in panel (G) indicate cells with no MTRR expression. (H) No primary antibody controls. Scale bars: (F) 100 μ m, (G) 25 μ m, (H) 15 μ m. LE: lumen epithelium, GL: glands, EN: endometrium, IM: inner myometrium, OM: outer myometrium.

Next, MTRR protein levels were assessed in the uterine tissues at estrus using histological methods to determine cellular localization of MTRR expression in C57Bl/6 uterus, and to determine whether MTRR protein expression correlates with *Mtrr* mRNA expression. Immunohistochemistry was performed (in collaboration with Dr J. Rakoczy) on histological sections of C57Bl/6, *Mtrr*^{+/+}, *Mtrr*^{+/*gt*}, and *Mtrr*^{*gt/gt*} uteri at estrus using an antibody against MTRR. Within C57Bl/6 uterine tissue, MTRR protein expression was detected in all the uterine structures, including outer and inner myometrial layers, endometrium, glandular epithelium, and lumen epithelium (Figure 3.2F, H). However, there were some stromal cells within the endometrium with undetectable MTRR expression (Figure 3.2G). Nuclear and cytoplasmic staining was apparent in all uterine cell types (Figure 3.2F). Qualitatively, MTRR protein levels in the *Mtrr*^{+/*gt*} uterine sections were slightly less than those in the C57Bl/6 and *Mtrr*^{+/+} uteri (Figure 3.2F). There was also a clear decrease in MTRR protein levels in the *Mtrr*^{*gt/gt*} uterine tissues compared to C57Bl/6 controls (Figure 3.2F). Overall, these data indicate that MTRR protein expression is widely expressed within the uterus at estrus and is substantially decreased but still detectable in *Mtrr*^{*gt/gt*} tissue.

3.2.3 Analysis of folate-related proteins in *Mtrr* uteri at estrus

Next, we determined whether gene expression of folate receptors, carriers, or enzymes was altered in *Mtrr*^{+/*gt*} and *Mtrr*^{*gt/gt*} uterine tissues as a compensatory mechanism to *Mtrr* deficiency. We assessed the mRNA expression of genes that encode for folate transporters *Folr1* and *Rfc1*, and folate metabolic enzyme, *Mthfr* in C57Bl/6, *Mtrr*^{+/+}, *Mtrr*^{+/*gt*} and *Mtrr*^{*gt/gt*} uteri and F1 *Mtrr*^{+/+} and F1 *Mtrr*^{+/*gt*} uteri via RT-qPCR analysis. No difference in mRNA expression was apparent in all *Mtrr* genotypes compared to C57Bl/6 controls (Figure 3.3A, B). The exception was the expression of *Rfc1* mRNA, which was decreased in the F1 *Mtrr*^{+/*gt*} uteri (48% of C57Bl/6 expression, p=0.048; Figure 3.3B). While *Rfc1* mRNA expression displayed a downward trend in F1 *Mtrr*^{+/+} females compared to the C57Bl/6, the result was not statistically significant (Figure 3.3B). It is unclear why F1 *Mtrr*^{+/*gt*} females derived from an *Mtrr*^{+/*gt*} father and not *Mtrr*^{+/*gt*} females derived from *Mtrr*^{+/*gt*} parents show changes in *Rfc1* mRNA expression, but it is possible that a maternal *Mtrr*^{*gt*} allele is required to compensate for changes in *Rfc1* mRNA caused by the paternal *Mtrr*^{*gt*} allele. A future experiment should include assessment of protein expression of these key folate factors to determine whether uterine cells compensate for *Mtrr* deficiency at a translational level.

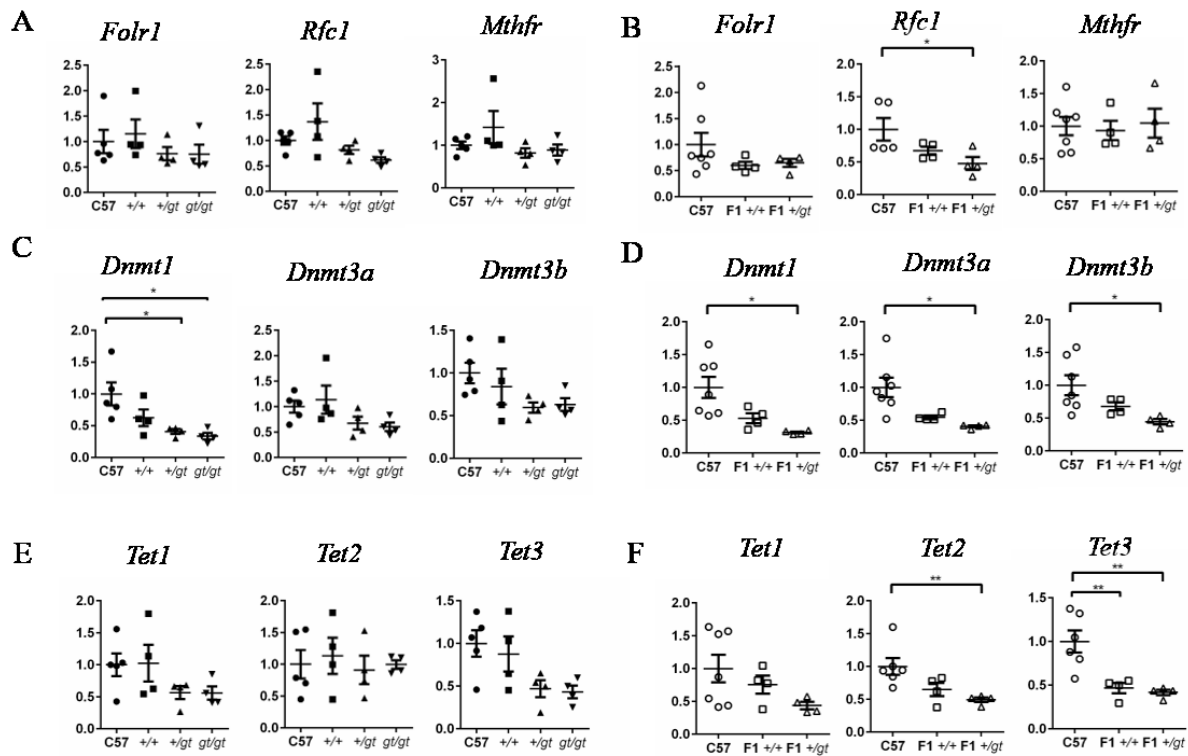


Figure 3.3 Analysis of folate-related and DNA methylation machinery gene expression in the mouse uterus at estrus.

Relative mRNA expression of (A-B) folate related genes including *Folr1*, *Rfc1*, and *Mthfr* and (C-F) DNA methylation machinery genes including (C-D) *Dnmt1*, *Dnmt3a*, *Dnmt3b*, and (E-F) *Tet1*, *Tet2*, and *Tet3* in uteri at estrus stage from the following genotypes: (A, C, E) C57Bl/6, *Mtrr*^{+/+}, *Mtrr*^{+/gt}, *Mtrr*^{gt/gt}, (B, D, F) C57Bl/6, F1 *Mtrr*^{+/+}, and F1 *Mtrr*^{+/gt}. *Hprt* was used as a housekeeping gene, n=4-7 females per genotype. Data are presented as mean ± SEM and as a fold change compared to C57Bl/6 controls (normalised to 1). Statistical test: One-way ANOVA, *p<0.05, **p<0.01.

3.2.4 Decreased mRNA expression of DNA methylation machinery enzymes in uteri at estrus from *Mtrr* pedigrees

It was previously shown that global DNA hypomethylation occurs in the uteri of *Mtrr*^{+/+}, *Mtrr*^{+/gt}, and *Mtrr*^{gt/gt} mice (Padmanabhan et al. 2013). How changes in methyl group availability affect the expression of the DNA methylation machinery enzymes has not yet been determined in the *Mtrr*^{gt} model. Therefore, we examined the mRNA expression of DNA methyltransferase (*Dnmt*) genes including *Dnmt1*, *Dnmt3a*, and *Dnmt3b* and genes that encode for ten-eleven-translocase (*Tet*) enzymes involved in the demethylation of DNA including *Tet1*, *Tet2*, and *Tet3* in C57Bl/6, *Mtrr*^{+/+}, *Mtrr*^{+/gt}, *Mtrr*^{gt/gt}, F1 *Mtrr*^{+/+} and F1 *Mtrr*^{+/gt} uterine tissues at estrus.

While there was no difference in *Dnmt3a* or *Dnmt3b* mRNA expression between C57Bl/6, *Mtrr*^{+/+}, *Mtrr*^{+/*gt*} and *Mtrr*^{*gt/gt*} uteri, *Dnmt1* mRNA expression was decreased in the *Mtrr*^{+/*gt*} and *Mtrr*^{*gt/gt*} uteri (p=0.01), but not *Mtrr*^{+/+} uteri compared to C57Bl/6 controls (Figure 3.3C). Our data suggest that there might be an intrinsic effect of the *Mtrr*^{*gt*} mutation on *Dnmt1* mRNA expression. Similarly, *Dnmt1* mRNA expression was not altered in F1 *Mtrr*^{+/+} uteri and was decreased in the F1 *Mtrr*^{+/*gt*} uteri (p=0.01; Figure 3.3D). However, in contrast to *Mtrr*^{+/*gt*} females from *Mtrr*^{+/*gt*} intercrosses, *Dnmt3a* (p=0.009) and *Dnmt3b* (p=0.028) mRNA expression in the F1 *Mtrr*^{+/*gt*} uteri was reduced compared to the C57Bl/6 uteri (Figure 3.3E). DNMT protein expression levels should be determined to better understand the functional implications of this finding.

In contrast to *Dnmt* expression, *Tet1*, *Tet2*, and *Tet3* mRNA expression remained unaltered in *Mtrr*^{+/+}, *Mtrr*^{+/*gt*} and *Mtrr*^{*gt/gt*} uteri (Figure 3.3E). Interestingly, variation in the expression of these genes was observed mainly in the C57Bl/6 and *Mtrr*^{+/+} uteri. Although there was a decreasing trend in *Tet1* mRNA levels in the F1 *Mtrr*^{+/+} and F1 *Mtrr*^{+/*gt*} uteri, the result was not statistically significant (Figure 3.3F). In contrast, *Tet2* mRNA was decreased in the F1 *Mtrr*^{+/*gt*} uteri (p=0.017), and *Tet3* mRNA was decreased in both the F1 *Mtrr*^{+/+} and F1 *Mtrr*^{+/*gt*} uteri (p=0.0023) compared to C57Bl/6 (Figure 3.3F). Altogether, these data suggest that the expression of DNA methylation machinery was most dysregulated in the F1 *Mtrr*^{+/*gt*} uteri. It is unclear why F1 *Mtrr*^{+/*gt*} females derived from an *Mtrr*^{+/*gt*} father and not *Mtrr*^{+/*gt*} females derived from *Mtrr*^{+/*gt*} parents show changes in DNA methylation machinery enzyme expression, but this result is consistent with the expression of *Rfc1* mRNA.

3.2.5 Intrinsic and parental *Mtrr*^{*gt*} allele causes abnormal uterine morphology at estrus

To determine whether an intrinsic or parental *Mtrr*^{*gt*} allele(s) affects the uterine morphology at estrus, we performed H&E staining on histological sections of *Mtrr*^{+/+}, *Mtrr*^{+/*gt*} and *Mtrr*^{*gt/gt*} uteri and compared them to C57Bl/6 control uteri (n = 4 females per group). First, the thickness of the uterine myometrium was assessed. Overall, only *Mtrr*^{+/*gt*} females had a total myometrium thickness that was larger than controls (p=0.017; Figure 3.4A-B). Although myometrial thickness of *Mtrr*^{*gt/gt*} uteri was also increased, the difference was not significant (Figure 3.4A-B). Total myometrial thickness in *Mtrr*^{+/+} was similar to C57Bl/6

(Figure 3.4). When the myometrium was broken down into inner and outer myometrium as determined by the presence of circular and longitudinal myometrial cells respectively (Brody & Cunha 1989), the outer myometrium was observed to be thicker in *Mtrr*^{+/+}, *Mtrr*^{+/*gt*} and *Mtrr*^{*gt/gt*} uteri (p=0.0094) compared to C57Bl/6 controls (Figure 3.4A-B). On the other hand, the inner myometrium was thicker only in the *Mtrr*^{+/+} females (p=0.025; Figure 3.4A-B). Next, we observed that the overall thickness of the endometrial layer of each *Mtrr* genotypic group was on average similar to C57Bl/6 controls (Figure 3.4A, C). Additionally, the number and diameter of endometrial glands over the long and short axes was not affected by *Mtrr* deficiency (Figure 3.4A, D-F). The whole uterus diameter was not different in any of the *Mtrr* genotypes (Figure 3.4G). Thicker myometrium and normal whole uterus diameter in the *Mtrr*^{+/+}, *Mtrr*^{+/*gt*} and *Mtrr*^{*gt/gt*} uteri could suggest differences in the lumen size, although we found that the percentage of lumen area to the whole uterus area is similar between C57Bl/6, *Mtrr*^{+/+}, and *Mtrr*^{*gt/gt*} uteri, but higher in the *Mtrr*^{+/*gt*} uteri (p=0.0004, Figure 3.4H). Increasing the sample size would improve the statistical power and give us more reliable results. Remarkably, we observed that the luminal epithelium was highly invaginated in the uteri of *Mtrr*^{+/+}, *Mtrr*^{+/*gt*} and *Mtrr*^{*gt/gt*} females (Figure 3.4A). This was in contrast to the smooth luminal epithelium in the C57Bl/6 control uteri (Figure 3.4A). Since an abnormal uterine phenotype was observed in *Mtrr*^{+/+} females, these data suggest that the parental *Mtrr*^{*gt*} allele is an important factor controlling gross uterine morphology.

Next, to determine whether paternal *Mtrr* deficiency was sufficient to affect uterine structure at estrus, we performed a similar analysis on histological sections of F1 *Mtrr*^{+/+} and F1 *Mtrr*^{+/*gt*} uteri derived from an *Mtrr*^{+/*gt*} father and a C57Bl/6 mother (Figure 2.1D) and compared them to C57Bl/6 control uteri (n = 4 females per group). Overall, F1 *Mtrr*^{+/+} and F1 *Mtrr*^{+/*gt*} females had a total myometrium thickness that was larger than controls (p=0.01; Figure 3.5A-B). When the myometrium was broken down into inner and outer myometrium, the outer myometrium was observed to be thicker in F1 *Mtrr*^{+/+} and F1 *Mtrr*^{+/*gt*} uteri (p=0.038) compared to C57Bl/6 controls (Figure 3.5A-B), which were similar to the increased myometrial thickness observed in the uteri of females derived from *Mtrr*^{+/*gt*} intercrosses (Figure 3.4B). On the other hand, the inner myometrium was

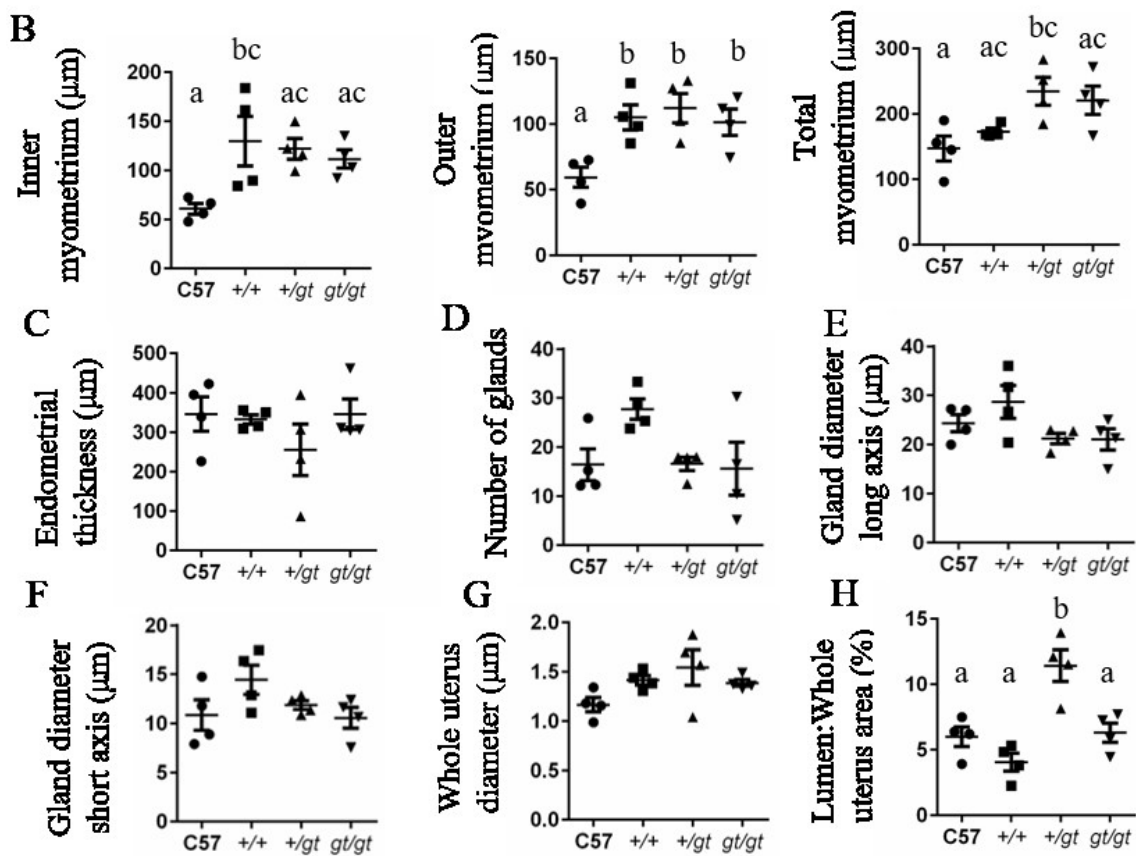
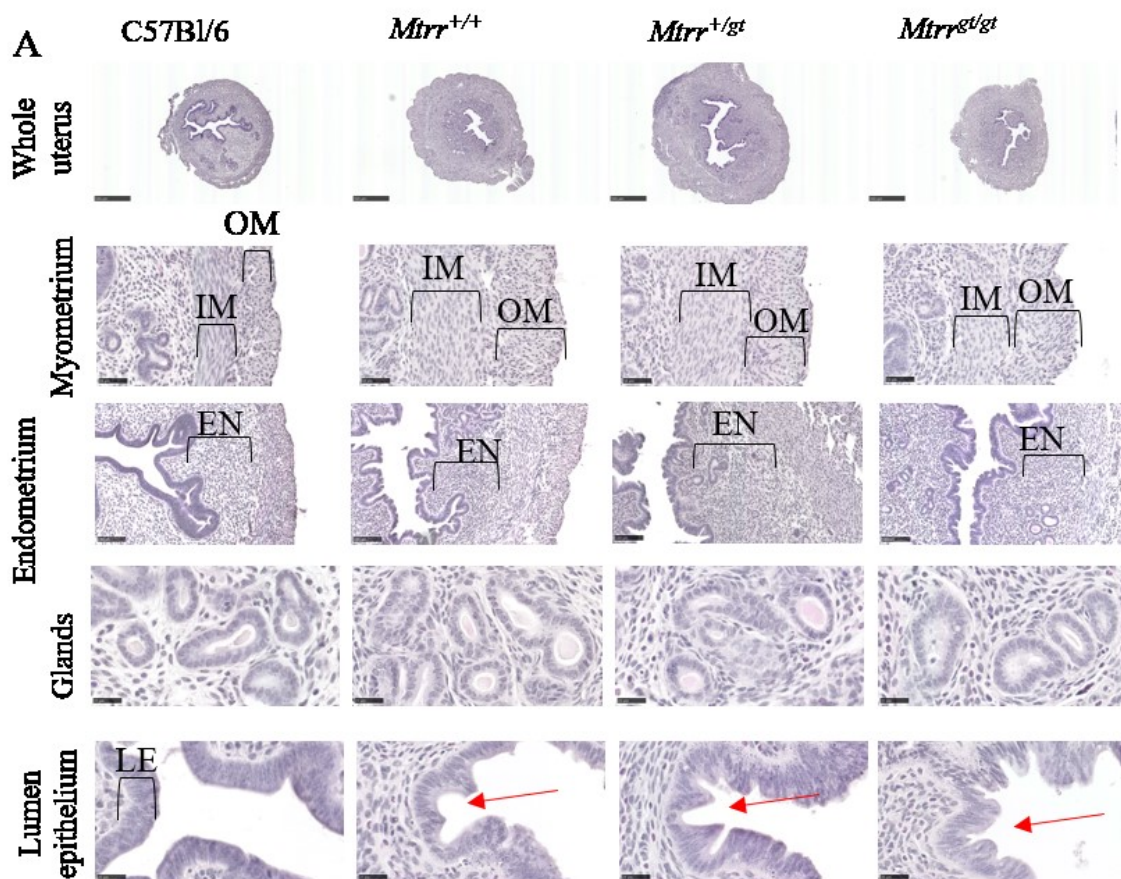


Figure 3.4 Histological analysis of *Mtrr* uteri at estrus.

(A) Representative histological sections of uteri from C57Bl/6, *Mtrr*^{+/+}, *Mtrr*^{+/*gt*} and *Mtrr*^{*gt/gt*} females. Blue, nuclei; pink, cytoplasm. EN, endometrium; LE, lumen epithelium; IM, inner myometrium; OM, outer myometrium. Scale bars: whole uterus, 500 μ m; endometrium, 100 μ m; myometrium, 50 μ m; glands and lumen, 25 μ m. Red arrow shows invagination in the lumen epithelium. (B-E) Graphs quantifying (B) myometrium thickness, (C) endometrium thickness, (D) number of glands, (E-F) gland diameters along the (E) short axis and the (F) long axis, (G) whole uterus diameter, (H) percentage of lumen:uterus area. Data presented as mean \pm SEM. n=4 females per genotype, One-way ANOVA. a $p < 0.05$ when compared to b and c; b $p < 0.05$ when compared to a and c; c $p < 0.05$ when compared to a and b.

unchanged (Figure 3.5A-B). Next, we observed that the overall thickness of the endometrial layer of F1 *Mtrr*^{+/+} and F1 *Mtrr*^{+/*gt*} uteri was on average similar to C57Bl/6 controls (Figure 3.5A, C) and the number and diameter of endometrial glands were unaffected (Figure 3.5A, D-E). Furthermore, the lumen epithelium was highly invaginated in F1 *Mtrr*^{+/+} and F1 *Mtrr*^{+/*gt*} uteri (Figure 3.5A), which was in contrast to the smooth luminal epithelium in the C57Bl/6 control uteri, and similar to the invaginations observed in the uteri of females derived from *Mtrr*^{+/*gt*} intercrosses (Figure 3.4A). The whole uterus diameter or the lumen:uterus area were not different in each case (Figure 3.5F-G), even though the myometrium was thicker in the uteri of F1 *Mtrr*^{+/+} and F1 *Mtrr*^{+/*gt*} females. Since we observed some variability in the quantification of the lumen:uterus area, increasing the sample size could give us more reliable results. Altogether, these data suggest that the paternal *Mtrr*^{*gt*} allele is an important factor controlling gross uterine morphology since F1 *Mtrr*^{+/+} uteri were affected in a similar manner to F1 *Mtrr*^{+/*gt*} uteri. Since these uteri show similar phenotypes to females derived from *Mtrr*^{+/*gt*} intercrosses, it will be important to explore a maternal *Mtrr*^{+/*gt*} effect to determine whether *Mtrr* deficiency in a single parent is sufficient to affect the uterine morphology of their daughters, or if only a paternal *Mtrr*^{*gt*} allele is required.

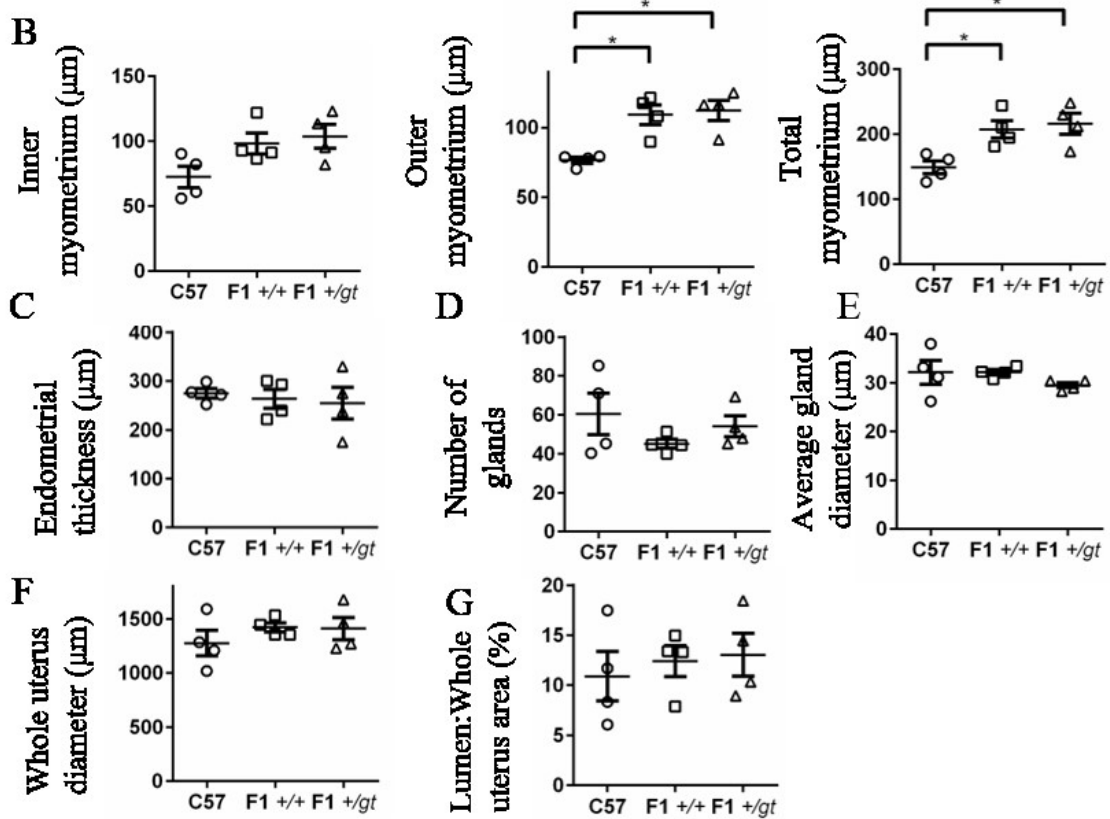
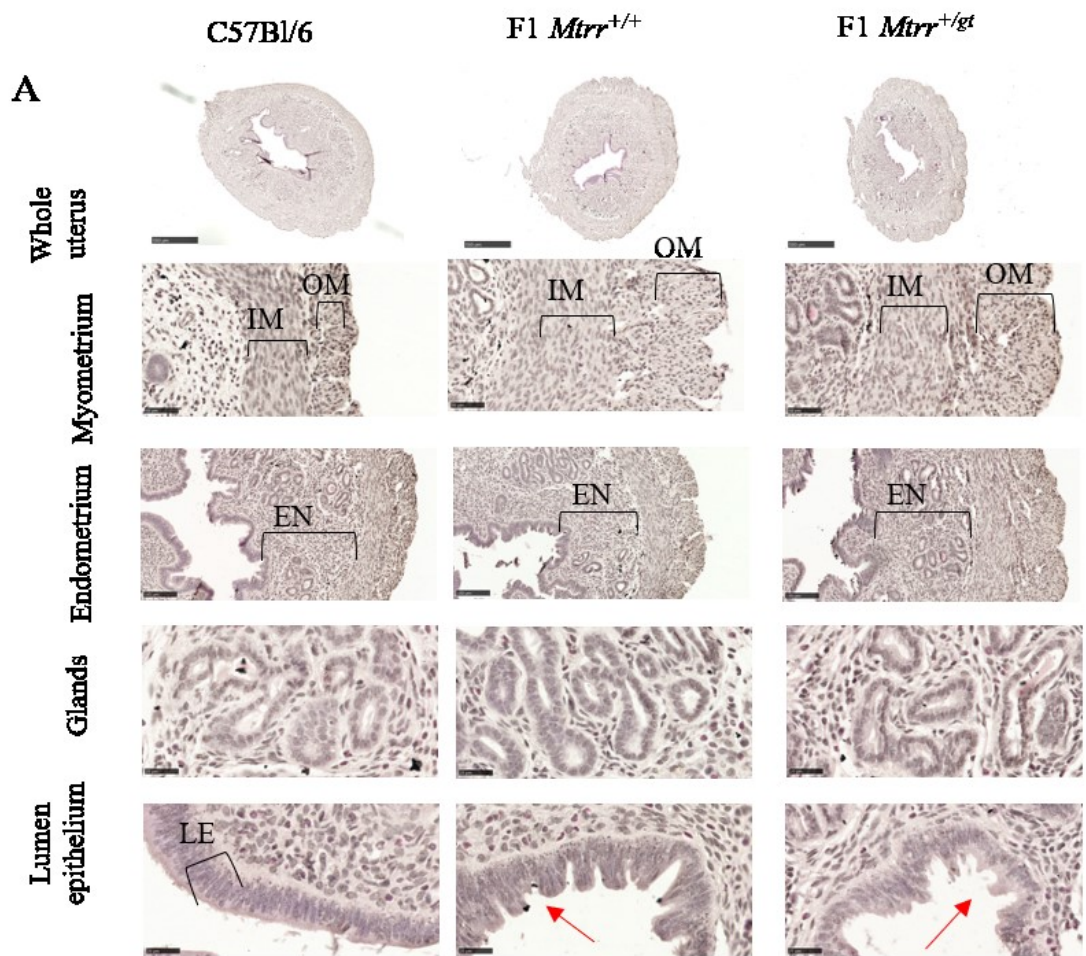


Figure 3.5 Histological analysis of F1 *Mtrr* uteri at estrus.

(A) Representative histological sections of uteri from C57Bl/6, F1 *Mtrr*^{+/+} and F1 *Mtrr*^{+/*gt*} females. Scale bars: whole uterus, 500 μ m; endometrium, 100 μ m; myometrium, 50 μ m; glands and lumen, 25 μ m. Red arrow shows invagination in the lumen epithelium. LE, lumen epithelium; IM, inner myometrium; OM, outer myometrium; EN, endometrium. (B-E) Graphs quantifying (B) myometrium thickness, (C) endometrium thickness, (D) gland number, (E) gland diameter, (F) whole uterus diameter, (H) percentage of lumen:uterus area. Data presented as mean \pm SEM. n=4 females per genotype. Statistical test: One-way ANOVA *p<0.05.

3.2.6 Cell density in outer myometrium is increased by parental *Mtrr* deficiency

The increased outer myometrial thickness observed in all *Mtrr* genotypes might be attributed to: a) increased cell size, and/or b) increased cell number caused by increased cell proliferation or decreased apoptosis. First, we analysed *Mtrr*^{+/+}, *Mtrr*^{+/*gt*} and *Mtrr*^{*gt/gt*}, and F1 *Mtrr*^{+/+} and F1 *Mtrr*^{+/*gt*} uteri at estrus by counting the number of cells in specified areas to determine cell density. For this analysis, we assessed the uterine samples that were stained with H&E using ImageJ. When analysing all genotypes, there was no difference in the cell density in the endometrium or the inner myometrium compared to C57Bl/6 controls (Figure 3.6A, C-D, F-G). However, the density of the cells in the outer myometrium was lower in all the *Mtrr* genotypes (p<0.019) compared to C57Bl/6 controls. More specifically, the cell density in the outer myometrium of *Mtrr*^{+/+}, *Mtrr*^{+/*gt*} and *Mtrr*^{*gt/gt*}, F1 *Mtrr*^{+/+} and F1 *Mtrr*^{+/*gt*} uteri was 68.1%, 59.5%, 58.9%, 60.1%, and 63.6%, respectively of the cell density in the C57Bl/6 controls (Figure 3.6A, B, E). The cell nuclei in *Mtrr*^{*gt/gt*} appear bigger than those in C57Bl/6, *Mtrr*^{+/+} and *Mtrr*^{+/*gt*} uteri (Figure 3.6A). This result suggests that increased cell size and possibly an increase in the extracellular matrix space might be responsible for increased outer myometrial thickness in the *Mtrr*^{*gt*} mouse model and that paternal *Mtrr* deficiency is sufficient to cause this phenotype.

Next, we investigated whether changes in cell proliferation and/or cell apoptosis were associated with increased myometrial thickness. The uterine sections were immunostained with antibodies against Ki67 and Caspase3 protein to assess cell proliferation and cell apoptosis, respectively. No primary antibody controls are shown in Figure 3.2G and Figure 3.8A. Cells positive for Ki67 or Caspase3 were quantified in the endometrium and the inner

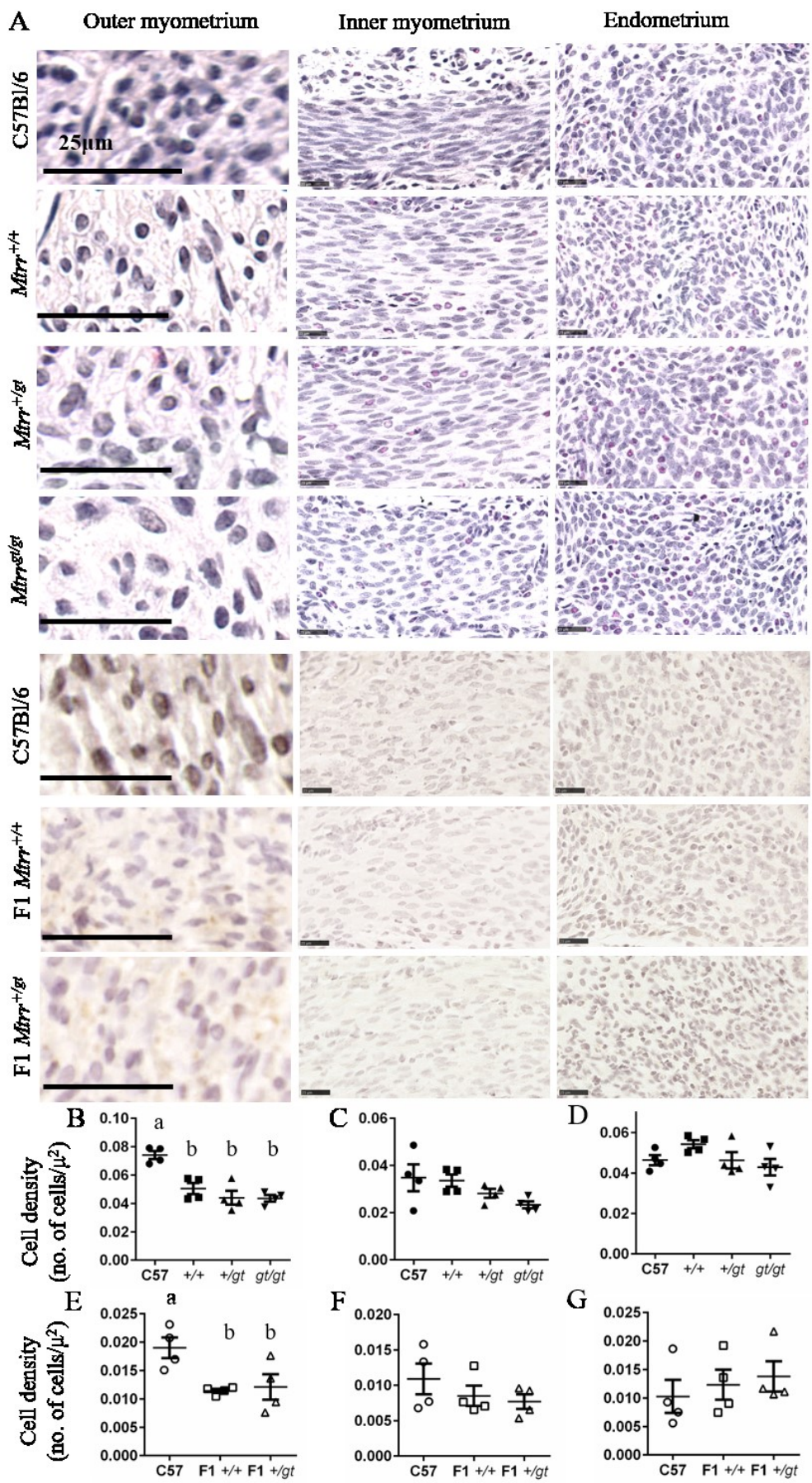


Figure 3.6 Decreased cell density in the outer myometrium of *Mtrr* uteri at estrus.

(A) Representative images of uterine histological sections from C57Bl/6, *Mtrr*^{+/+}, *Mtrr*^{+/*gt*}, *Mtrr*^{*gt/gt*}, F1 *Mtrr*^{+/+} and F1 *Mtrr*^{+/*gt*} females at estrus stained with hemotoxylin (blue). Outer myometrium, inner myometrium, and endometrium are shown. Scale bars: 25 μ m. (B-G) Graphs depicting cell density in the outer myometrium (B, E), inner myometrium (C, F), and endometrium (D, G) in (B-D) *Mtrr*^{+/+}, *Mtrr*^{+/*gt*} and *Mtrr*^{*gt/gt*} uteri and (E-G) F1 *Mtrr*^{+/+} and F1 *Mtrr*^{+/*gt*} uteri compared to C57Bl/6 controls. Data are presented as mean \pm SEM. n=4 females per genotype. Statistical test: One-way ANOVA, a p<0.05 when compared to b.

and outer myometrial layers. Interestingly, there was an increased number of Ki67⁺ cells in the endometrium of *Mtrr*^{+/*gt*} and *Mtrr*^{*gt/gt*} females (p=0.0079) compared to C57Bl/6 controls (Figure 3.7A-B). This occurred even though the endometrial thickness was not different (Figure 3.4A, C). There was also an upward trend of Ki67⁺ cells in *Mtrr*^{+/+} endometrium, though the difference did not reach statistical significance (Figure 3.7B). In contrast, the number of Ki67⁺ cells in the inner and outer myometrial layers of *Mtrr*^{+/+}, *Mtrr*^{+/*gt*} and *Mtrr*^{*gt/gt*} uteri was unaffected compared to controls (Figure 3.7A-B) indicating cell proliferation was not likely responsible for a thicker outer myometrial layer. Interestingly, we were not able to quantify the Ki67⁺ staining in the luminal or glandular epithelium of any uterine group assessed, since in all the genotypes we observed staining of the apical surface of all the glandular epithelial and luminal epithelial cells (Figure 3.8A).

Additionally, there were no differences in the percentage of Ki67⁺ cells in all uterine structures assessed between C57Bl/6, F1 *Mtrr*^{+/+} and F1 *Mtrr*^{+/*gt*} uteri (Figure 3.8A-B). Staining in Figure 3.8A is better than in Figure 3.7A, since the brown nuclei are more visible. Therefore, immunostaining of *Mtrr*^{+/+}, *Mtrr*^{+/*gt*} and *Mtrr*^{*gt/gt*} uteri with Ki67 antibody should be repeated for more reliable results. Altogether, these data suggest that cell proliferation occurs at a normal rate in these uteri and is an unlikely cause for the increase in outer myometrial layer thickness.

The number of Caspase3⁺ cells was also similar throughout the uteri of *Mtrr*^{+/+}, *Mtrr*^{+/*gt*} and *Mtrr*^{*gt/gt*} females compared to the C57Bl/6 controls (Figure 3.7C-D). No primary antibody controls are shown in Figure 3.2G for each uterine structure. Furthermore, the percentage of Caspase3⁺ cells in the endometrium, uterine epithelial layer, and glandular cells was similar in F1 *Mtrr*^{+/+}, F1 *Mtrr*^{+/*gt*} and C57Bl/6 uteri (Figure 3.8C-D). While Caspase3 expression was undetectable in the inner myometrial layer, a decrease in the percentage of Caspase3⁺ cells was apparent in the outer myometrium only within F1 *Mtrr*^{+/+} uteri compared to

C57Bl/6 ($p=0.02$; Figure 3.8C-D). A high degree of variation within each genotype was observed in these graphs (Figure 3.7D). To alleviate this variation, more females should be assessed. This result in F1 $Mtrr^{+/+}$ uteri correlates with the decreased cell density in the outer myometrium, but contradicts the increased myometrial thickness. Overall, these data indicate that increased myometrial thickness is caused by paternal $Mtrr$ deficiency since females derived from $Mtrr^{+/gt}$ intercrosses or from $Mtrr^{+/gt}$ fathers displayed this phenotype regardless of the presence of an intrinsic $Mtrr^{gt}$ allele. Increased myometrial thickness is likely associated with increased cell size at the exclusion of changes in cell proliferation and cell apoptosis in all genotypes except F1 $Mtrr^{+/+}$ uteri, which are characterised by decreased cell apoptosis in the outer myometrium.

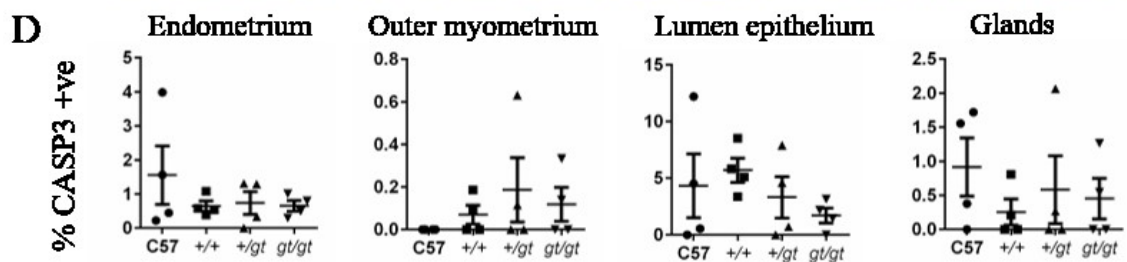
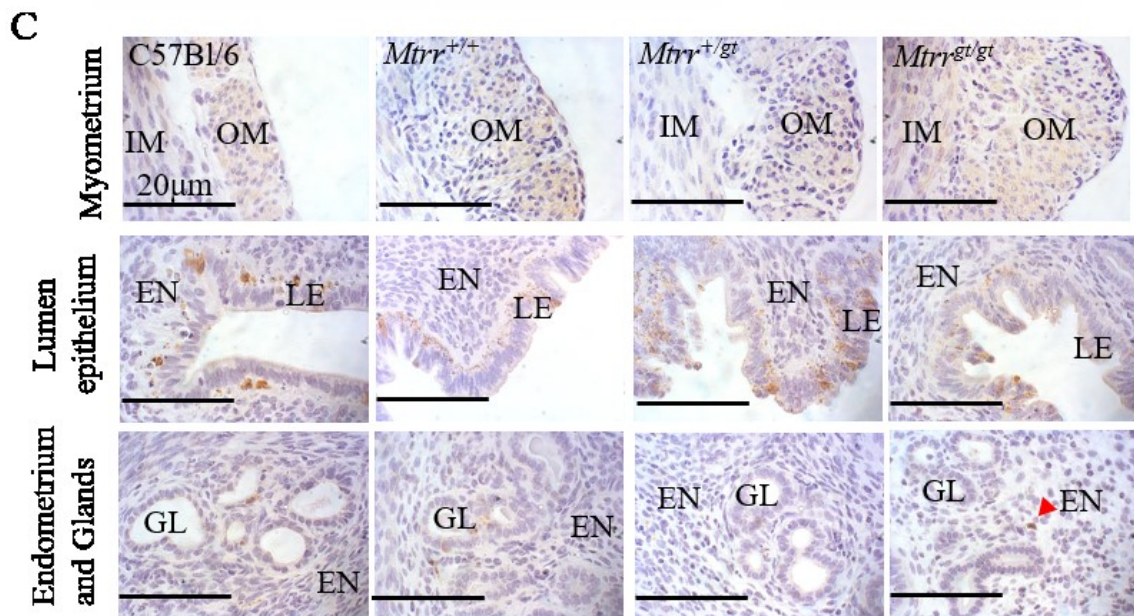
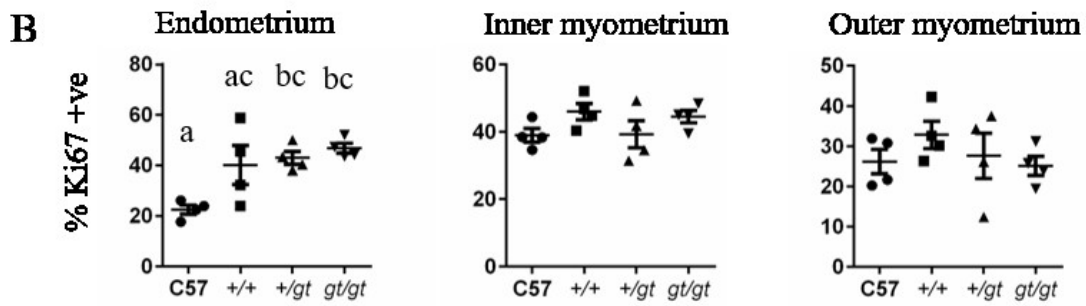
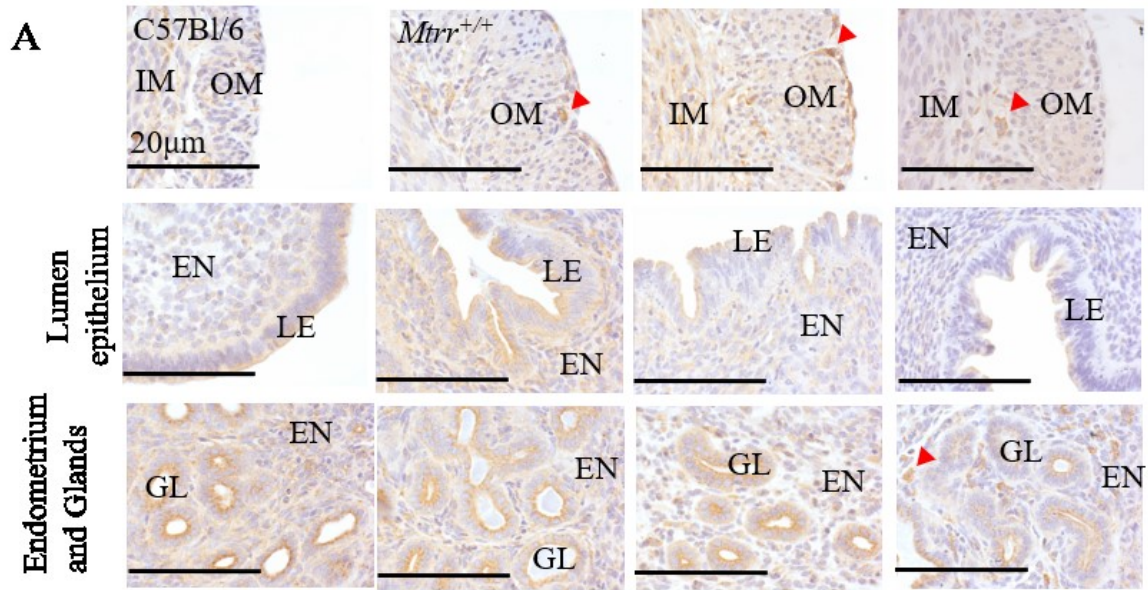


Figure 3.7 Analysis of cell proliferation and apoptosis in the uterine tissue of littermate females from *Mtrr*^{+/*gt*} intercrosses at estrus.

(A) Representative uterine histological sections stained with anti-Ki67 (brown) to assess cell proliferation in the myometrium and endometrium of uteri from C57Bl/6, *Mtrr*^{+/*+*}, *Mtrr*^{+/*gt*}, and *Mtrr*^{*gt*/*gt*} females. Scale bars: 20 μ m. Sections were counterstained with hematoxylin (blue). (B) Quantification of the percentage of Ki67⁺ cells out of the total number of cells counted in a defined area of the endometrium, inner myometrium, and outer myometrium of C57Bl/6, *Mtrr*^{+/*+*}, *Mtrr*^{+/*gt*}, and *Mtrr*^{*gt*/*gt*} uteri at estrus. Data are presented as mean \pm sem. N=4 females per genotype assessed. (C) Representative uterine histological sections stained with anti-CASP3 (brown) to assess apoptosis in the myometrium and endometrium of uteri from C57Bl/6, *Mtrr*^{+/*+*}, *Mtrr*^{+/*gt*}, and *Mtrr*^{*gt*/*gt*} females. Scale bars: 20 μ m. Sections were counterstained with hematoxylin (blue). (D) Quantification of the percentage of CASP3⁺ cells out of the total number of cells counted in a defined area of endometrium, outer myometrium, lumen epithelium, and glands of C57Bl/6, *Mtrr*^{+/*+*}, *Mtrr*^{+/*gt*}, and *Mtrr*^{*gt*/*gt*} uteri at estrus. LE, lumen epithelium; IM, inner myometrium; OM, outer myometrium; EN, endometrium; GL, glands. Red arrows point at positively stained cells. Data are presented as mean \pm sem. Statistical test: One-way ANOVA. a p <0.05 when compared to b and c; b p <0.05 when compared to a and c; c p <0.05 when compared to a and b.

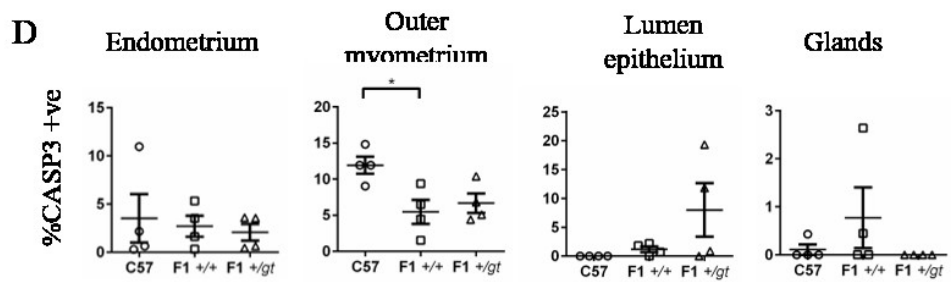
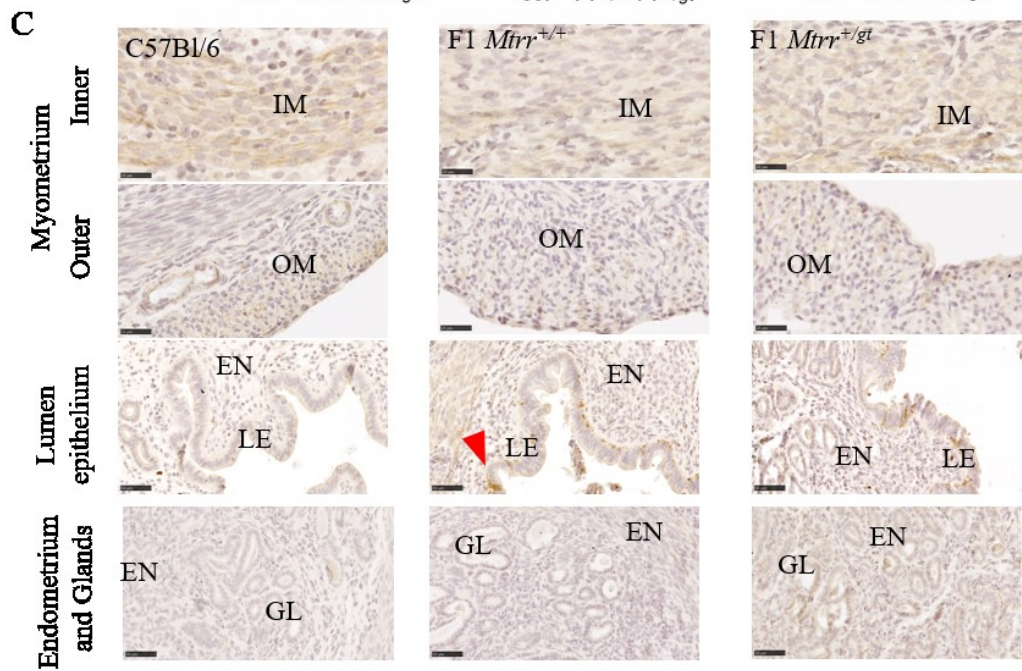
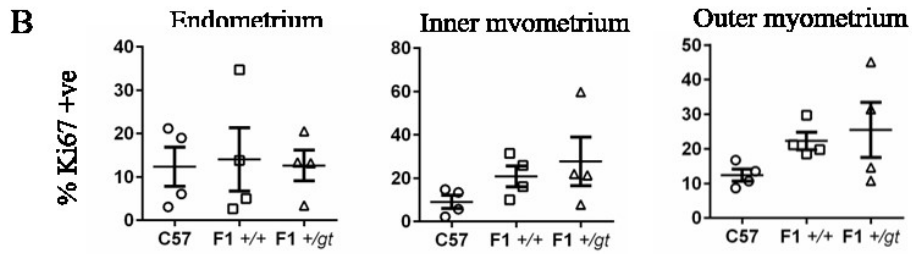
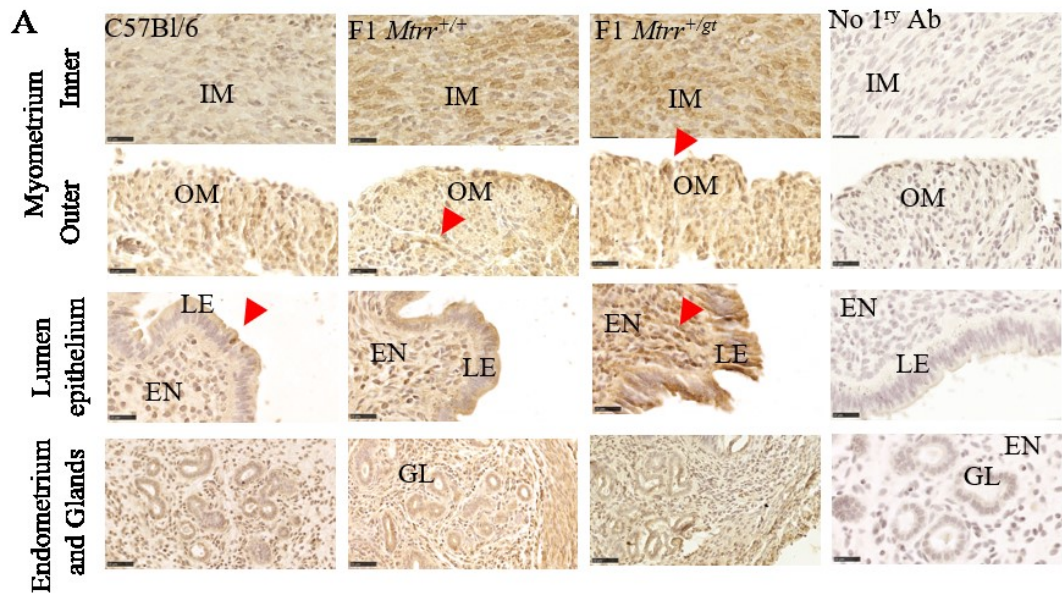


Figure 3.8 Analysis of cell proliferation and apoptosis in the uterine tissue of F1 females at estrus.

(A) Representative uterine sections stained with anti-Ki67 (brown) to assess cell proliferation in the myometrium and endometrium of C57Bl/6, F1 *Mtrr*^{+/+} and F1 *Mtrr*^{+/*gt*} uteri at estrus. Scale bars: 20 μ m. Sections were counterstained with hemotoxylin (blue). (B) Quantification of the percentage of Ki67⁺ cells out of the total number of cells counted in a defined area in endometrium, inner myometrium, and outer myometrium of C57Bl/6, F1 *Mtrr*^{+/+} and F1 *Mtrr*^{+/*gt*} uteri. Data are presented as mean \pm sem. N=4 females per genotype assessed. (C) Representative uterine sections stained with anti-CASP3 to assess cell apoptosis in the myometrium and endometrium of C57Bl/6, F1 *Mtrr*^{+/+} and F1 *Mtrr*^{+/*gt*} uteri at estrus. Scale bars: 20 μ m. Sections were counterstained with hemotoxylin (blue). (D) Quantification of the percentage of CASP3⁺ cells out of the total number of cells counted in a defined area in endometrium, outer myometrium, lumen epithelium, and glands of C57Bl/6, F1 *Mtrr*^{+/+} and F1 *Mtrr*^{+/*gt*} uteri. LE, lumen epithelium; IM, inner myometrium; OM, outer myometrium; EN, endometrium; GL, glands. Red arrows point at positively stained cells. Data are presented as mean \pm SEM. Statistical test: One-way ANOVA, *p<0.05.

3.2.7 Analysis of genetic markers of uterine cells in the *Mtrr*^{gt} mouse line

Given that there is increased outer myometrial thickness associated with decreased cell density in the uteri of *Mtrr*^{+/+}, *Mtrr*^{+/*gt*} and *Mtrr*^{gt/*gt*}, and F1 *Mtrr*^{+/+} and F1 *Mtrr*^{+/*gt*} females at estrus, we wanted to assess the molecular character of the myometrial cells. To do this, we assessed the expression of known uterine smooth muscle cell marker genes *Myocd* and *Acta2* via qPCR. *Myocd* and *Acta2* are genes expressed by uterine smooth muscle cells (Gao, Bayless & Li 2014). *Myocd* is an E2-responsive gene (Kararigas, Nguyen & Jarry 2014) and encodes for a transcription factor necessary for differentiation of the smooth muscle cell lineage (Wang et al. 2003). *Myocd* is also a critical regulator of smooth muscle gene expression during postnatal development (Wang et al. 2003). Analysis of *Myocd* mRNA expression in C57Bl/6, *Mtrr*^{+/+}, *Mtrr*^{+/*gt*} and *Mtrr*^{gt/*gt*} uteri revealed a difference (p=0.03), although multiple comparison analysis revealed no significance. However, *Myocd* expression was reduced in *Mtrr*^{+/*gt*} and *Mtrr*^{gt/*gt*} uteri compared to C57Bl/6 controls (Figure 3.9A), and *Myocd* mRNA expression was reduced in F1 *Mtrr*^{+/*gt*} uteri compared to controls (p=0.016, Figure 3.9F). F1 *Mtrr*^{+/+} females showed decreased levels of *Myocd* expression compared to controls, though this effect was not statistically significant (Figure 3.9F). *Acta2* encodes for the major component of the contractile muscle (Perrin & Ervasti 2010). *Acta2* mRNA expression was unaltered in *Mtrr*^{+/+}, *Mtrr*^{+/*gt*} and *Mtrr*^{gt/*gt*}, and F1 *Mtrr*^{+/+} and F1 *Mtrr*^{+/*gt*}

uteri compared to controls ($p=0.068$; Figure 3.9B, G) and could suggest normal number of myometrial cells. Altogether, these data suggest that an intrinsic and, possibly paternal, *Mtrr^{gt}* allele might affect the differentiation of the stem/progenitor myometrial cells that are present in the adult myometrium (Szotek et al. 2007), and thus contributing to the outer myometrial phenotype. To increase the robustness of this data, more uterine samples should be assessed.

Next, we wanted to determine whether gene expression in other key uterine cell types was affected by the *Mtrr^{gt}* mutation. By RT-qPCR, we assessed the expression of *Epcam*, *Vim*, and *Foxa2* mRNA in the uteri of *Mtrr^{+/+}*, *Mtrr^{+/gt}* and *Mtrr^{gt/gt}*, and F1 *Mtrr^{+/+}* and F1 *Mtrr^{+/gt}* uteri compared to controls. *Epcam* encodes for a cell adhesion molecule that is expressed by the lumen epithelial cells (Deane et al. 2016). The gene *Vim* encodes for the intermediate filament vimentin and is a marker of uterine stromal cells within the endometrial layer (Clercq, Hennes & Vriens 2017). *Foxa2* mRNA expression is important for uterine gland development and continues to be expressed within the glands during estrus (Chang et al. 2018; Kelleher et al. 2017). Overall, the mRNA expression of all these uterine markers assessed was not different in the uteri of *Mtrr^{+/+}*, *Mtrr^{+/gt}* and *Mtrr^{gt/gt}* females compared to the controls (Figure 3.9C-E). There was also no difference in the mRNA expression of the uterine markers assessed in the uteri of F1 *Mtrr^{+/+}* and *Mtrr^{+/gt}* females compared to the controls (Figure 3.9H-J). Based on the marker genes selected, these data confirm our histological evidence that the endometrium and glands are normal in *Mtrr* uteri at estrus. The uterine lumen epithelium will be assessed further below.

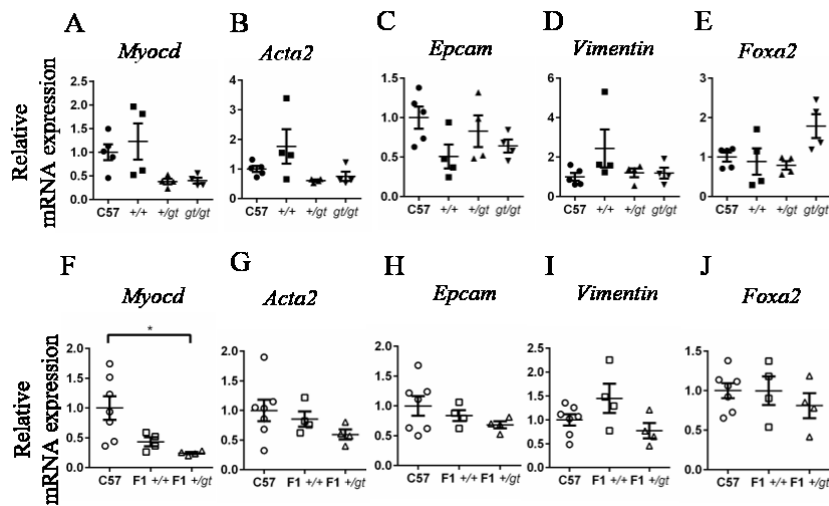


Figure 3.9 Marker expression in the uterine tissues of *Mtrr* mice at estrus.

Relative mRNA expression of marker genes specific to myometrium (*Myocd* and *Acta2*), lumen epithelium (*Epcam*), stromal cells (*Vimentin*), and uterine glands (*Foxa2*) in (A-E) *Mtrr*^{+/+}, *Mtrr*^{+/gt}, and *Mtrr*^{gt/gt} uteri at estrus and (F-J) F1 *Mtrr*^{+/+} and F1 *Mtrr*^{+/gt} uteri at estrus compared to C57Bl/6 controls. Transcript levels were normalised to *Hprt* RNA levels. Data are presented as fold change compared to C57Bl/6 controls (normalised to 1) and as the mean ± SEM. n=4-6 females per genotype assessed. Statistical test: One-way ANOVA *p<0.05.

3.2.8 Altered cell polarity in uterine lumen epithelium of *Mtrr* mice at estrus

To further characterise the hyper-invagination phenotype of the luminal epithelium of *Mtrr*^{+/+}, *Mtrr*^{+/gt}, *Mtrr*^{gt/gt}, F1 *Mtrr*^{+/+}, and F1 *Mtrr*^{+/gt} uteri, we assessed higher magnification images of histological sections. The epithelial cells of the C57Bl/6 uteri appeared in a monolayer of polarised epithelium whereas in the *Mtrr* genotypes, the luminal epithelium was disorganised and, in some cases, 3-4 cells thick (Figure 3.10A, C). A schematic image was generated whereby the cell nuclei in the lumen epithelium were outlined to better show the disruption in cell organisation in the *Mtrr* uteri compared to the C57Bl/6 controls (Figure 3.10A, C). Since the epithelial cells appeared disorganised, we immunostained uterine sections with a pan-cadherin antibody to mark cell-cell adhesion junctions that are important for establishing epithelial cell polarity (Desai et al. 2009; Reardon et al. 2012). Instead of appearing at the lateral and apical cell membranes of the uterine epithelium as in C57Bl/6 uteri (Figure 3.10A), pan-cadherin expression was decreased, localised cytoplasmically and largely undetectable at the basolateral membranes of the luminal cells of *Mtrr*^{+/+}, *Mtrr*^{+/gt} and *Mtrr*^{gt/gt} uterine sections (Figure 3.10A) and F1 *Mtrr*^{+/+} and F1 *Mtrr*^{+/gt} uterine sections

(Figure 3.10C). Control sections stained only with the secondary antibody are shown in Figure 3.8A. A similar decrease in pan-cadherin expression was also apparent in the glandular epithelium of *Mtrr*^{+/*gt*} and *Mtrr*^{*gt*/*gt*} uterine sections (Figure 3.10A) and F1 *Mtrr*^{+/*gt*} uterine sections (Figure 3.10C) compared to controls suggesting that cell polarity of glandular epithelium might also be affected by the *Mtrr*^{*gt*} mutation. Next, to determine whether *Mtrr*^{*gt*} mutation affects the transcription of the gene encoding for E-cadherin, we analysed *Cdh1* mRNA expression levels using qPCR in uteri at estrus. E-cadherin protein is an important component of adherens junctions and necessary for the establishment of cell polarity (Desai et al. 2009). Although variation was observed in the C57Bl/6 and *Mtrr*^{+/*+*} uteri, mean *Cdh1* mRNA expression was unaltered in all the *Mtrr* genotypes (Figures 3.10B, D). This result correlates with *Epcam* mRNA levels, which were unaltered (Figure 3.9C, H), and suggests that the transcription of cell adhesion molecules is not altered by *Mtrr* deficiency. Normal *Cdh1* mRNA expression and decreased pan-cadherin protein staining suggests that either the protein is not translated at normal levels or cannot be properly localised to the cell membrane to establish cell-cell junctions and cell polarity.

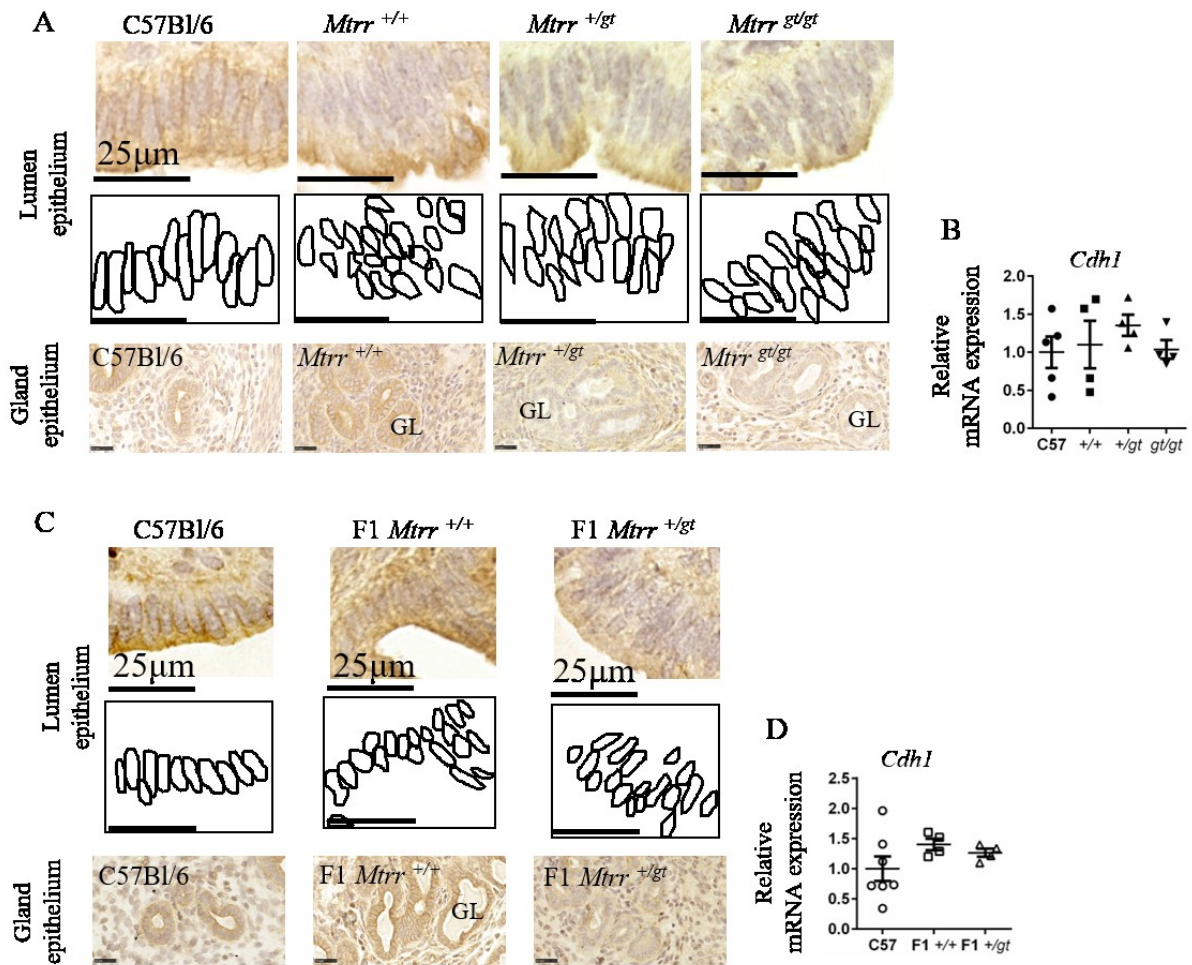


Figure 3.10 Misexpression of pan-cadherin protein in the uterus of *Mtrr* mice at estrus.

(A, C) Representative uterine sections of females derived from (A) *Mtrr*^{+/gt} intercrosses or (C) F1 females derived from an *Mtrr*^{+/gt} father and a C57Bl/6 mother that were immunostained with an antibody against pan-Cadherin (brown). The lumen epithelium and glandular epithelium are shown. Scale bars: 25 μ m.; Sections were counterstained with hematoxylin (blue). Under each image of the lumen epithelium, a schematic drawing was produced to highlight the nuclear organization (black outline). (B, D) Relative mRNA expression of *Cdh1* in the uteri of C57Bl/6, *Mtrr*^{+/+}, *Mtrr*^{+/gt}, *Mtrr*^{gt/gt}, F1 *Mtrr*^{+/+} and F1 *Mtrr*^{+/gt} females at estrus. Transcript levels were normalised to *Hprt* RNA levels. n=4-7 for female per genotype assessed. Data are presented as fold change compared to C57Bl/6 controls (normalised to 1) and as mean \pm SEM. Statistical test: One-way ANOVA.

3.2.9 Decreased levels of progesterone receptor mRNA and protein in the *Mtrr* uteri

To explore whether disrupted cell polarity affects the function of the uterine lumen, we assessed progesterone receptor (*Pgr*) and estrogen receptor (*Esr1*) expression via RT-qPCR and immunohistochemistry in *Mtrr*^{+/+}, *Mtrr*^{+/*gt*}, *Mtrr*^{*gt/gt*}, F1 *Mtrr*^{+/+}, and F1 *Mtrr*^{+/*gt*} uteri compared to C57Bl/6 controls at estrus. The expression of *Esr1* mRNA was within the normal range in the uteri of all the *Mtrr* genotypes at estrus compared to the controls (Figure 3.11A, D). On the other hand, while a downwards trend was observed in *Mtrr*^{+/+} and *Mtrr*^{+/*gt*} uteri at estrus, *Pgr* mRNA expression was decreased in the *Mtrr*^{*gt/gt*} uteri at estrus compared to the controls (p=0.035; Figure 3.11C). *Pgr* mRNA expression was also statistically reduced in the F1 *Mtrr*^{+/+} and F1 *Mtrr*^{+/*gt*} uteri compared to the controls (p=0.01; Figure 3.11F). The decreased expression of *Pgr* mRNA was confirmed at the protein level using immunohistochemistry on histological sections (Figure 3.11B, E). Control sections with no primary antibody are shown in Figure 3.8A. Correspondingly, decreased expression intensity of the PGR protein in the glandular and luminal epithelia was apparent in *Mtrr*^{+/*gt*} and *Mtrr*^{*gt/gt*} uteri and similarly in the F1 *Mtrr*^{+/+} and F1 *Mtrr*^{+/*gt*} uteri compared to controls (Figure 3.11B, E). The PGR antibody staining in the C57Bl/6 and *Mtrr*^{+/+} tissues appeared to be similar (Figure 3.11B). The decrease in *Pgr* mRNA and protein expression in uteri at the estrus stage suggests that the epithelial cells have not differentiated and/or organised well enough to establish proper polarity to express progesterone receptors and initiate progesterone signalling.

Overall, these data suggest that altered luminal polarity caused by an intrinsic or paternal *Mtrr*^{*gt*} allele might alter P4 signalling and, ultimately, uterine function including embryo receptivity.

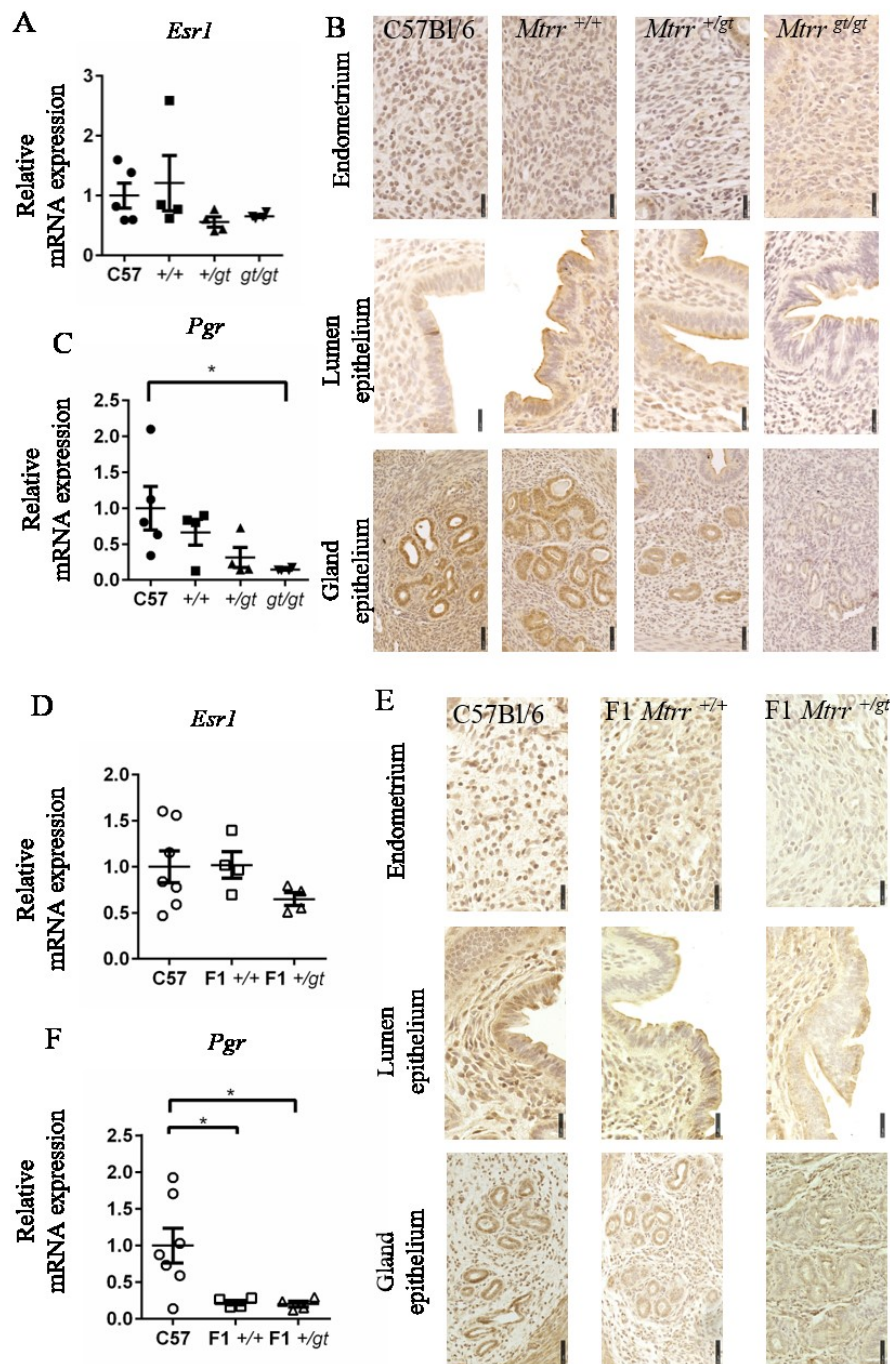


Figure 3.11 Expression of progesterone receptor in *Mtrr* uteri at estrus.

(A, C-D, F) Relative mRNA expression of (A, D) *Esr1*, (C, F) *Pgr* in females derived from (A, C) *Mtrr*^{+/*gt*} intercrosses or (D, F) F1 females derived from an *Mtrr*^{+/*gt*} father compared to C57Bl/6 controls. Transcript levels were normalised to *Hprt* RNA levels. n=4-7 females per genotype assessed. Data are presented as mean ± SEM and as fold change compared to C57Bl/6 controls (normalised to 1). (B, E) Representative uterine sections of females derived from (B) *Mtrr*^{+/*gt*} intercrosses or (E) F1 females derived from an *Mtrr*^{+/*gt*} father. Sections were immunostained with anti-PGR (brown) and counterstained with hemotoxylin (blue). Scale bars: 25µm. Statistical test: One-way ANOVA. *p<0.05.

3.3 Discussion

Here, we first assessed the effects of intrinsic and paternal *Mtrr*^{gt} mutation on uterine structure and function in non-pregnant females at estrus. We found that the paternal *Mtrr*^{gt} mutation appears to be important for initiating uterine phenotypes including thicker outer myometrium due to increased cell size and decreased apoptosis, and abnormal cell polarity in the epithelium lining the uterine lumen. The latter result was associated with improper presentation of PGR on the uterine lumen epithelium. PGR expression was also decreased in the uterine gland epithelium. Estrous cyclicity was normal indicating that the function of the hypothalamic-pituitary-ovarian axis was likely unaltered by a paternal or intrinsic *Mtrr*^{gt} mutation. Overall, this uterine phenotype caused by paternal *Mtrr* deficiency might prevent or delay normal blastocyst implantation or predict abnormal decidualisation during pregnancy.

While the estrous cycle was determined to occur normally in the females of all *Mtrr*^{gt} genotypes and pedigrees assessed, one drawback of our methodology was that the metestrus and diestrus stages were grouped together. This is because we determined estrous cyclicity by proestrus followed by estrus (Caligioni 2009) and did not initially pay attention to the other stages individually. The vaginal smears were stained with Giemsa stain but were not fixed, and therefore retrospectively reassessing the smears to identify the duration of metestrus and diestrus stages separately is not possible. Even though we observed normal estrous cyclicity, if we were to repeat this experiment, we would identify these stages separately. Furthermore, collection of uterine tissues at the proestrus, metestrus, and diestrus stages, would help us to identify the intrinsic and paternal effects of the *Mtrr*^{gt} mutation on the uterine morphology in different estrus stages, and identify possible further discrepancies in the uterine cell differentiation in the *Mtrr* mouse model.

Surprisingly, wildtype and total *Mtrr* transcripts were unexpectedly low in F1 *Mtrr*^{+/+} and F1 *Mtrr*^{+/^{gt}} uteri at estrus compared to C57Bl/6 controls. A similar effect was not observed in *Mtrr*^{+/+}, *Mtrr*^{+/^{gt}} and *Mtrr*^{gt/^{gt}} uteri in females derived from *Mtrr*^{+/^{gt}} intercrosses. This result indicates that paternal *Mtrr* deficiency might alter the expression of the *Mtrr* locus, even at the wildtype allele. Since the *Mtrr*^{gt} mutation causes global hypomethylation of the cell, alterations in epigenetic regulation (e.g., DNA methylation or histone methylation) might occur at the *Mtrr* locus (among other loci) to suppress *Mtrr* gene expression. Indeed, mRNA expression of genes encoding for the DNA methylation machinery (e.g., *Dnmt1*, *Dnmt3a*, *Dnmt3b*, *Tet2*, *Tet3*) was decreased in the F1 *Mtrr*^{+/^{gt}} females, which might further disrupt

DNA methylation patterns. However, this epigenetic effect would need to be inherited by F1 *Mtrr*^{+/+} females and the mechanism for inheritance of DNA methylation marks, if it exists, is not well understood. Our data also suggest a potential paramutation effect similar than observed in the *kit* mutant (Pilu 2011). In this case, the paramutagenic mutant allele (*Kit*^{tm1Af}) affected the transcription of the wildtype allele in heterozygous mice by causing the degradation of wildtype transcripts, leading to mice with white tails. When these heterozygous mice were crossed with wildtype mice with coloured tails, all the progeny, even the wildtype, had white tails. This suggests that the wildtype paramutated allele gained paramutagenic activity and reduced the expression of the other wildtype allele in *Kit*^{+/+} mice (Pilu 2011). The Watson lab previously showed that a direct paramutation effect was unlikely since F2 generation wildtype placentas and embryos from an *Mtrr*^{+/*gt*} maternal grandparent showed normal levels of wildtype *Mtrr* transcript (Padmanabhan et al. 2013). However, this finding may not carry over to F1 *Mtrr*^{+/+} uterine tissue. This experiment should be repeated in new F1 *Mtrr*^{+/+} and F1 *Mtrr*^{+/*gt*} uterine samples at estrus to rule out a paramutation effect.

The uterine tissue morphology of estrus stage females derived from an *Mtrr*^{+/*gt*} father was characterised by a highly invaginated and apolar luminal epithelium and increased thickness of the outer myometrial layer that was associated with decreased apoptosis and decreased cell density. The invaginations observed in the *Mtrr* lumen epithelium at estrus resemble those observed in control uteri at metestrus (Wood et al. 2007). This suggests that the morphological changes in the luminal epithelium of the *Mtrr* uteri over the course of the estrous cycle occur quicker than expected. To further assess this, histological analysis of *Mtrr* uteri from different stages of the estrous cycle is required. In addition, since the morphological changes in the uterus are driven by the ovarian hormones E2 and P4, assessment of plasma E2 and P4 at different stages of the estrous cycle is required. To further assess whether cell and nuclear size in the outer myometrium are related to a thicker outer myometrial layer, we could stain the histological sections with a cell membrane marker, such as anti-CD44 (Kennel et al. 1993) or CellMask stains that target the plasma membrane, which would allow us to visualise the cell boundaries and measure its size using software, such as ImageJ. An alternative hypothesis is that inappropriate cell adhesion may prevent normal myometrial structure causing the cells to appear larger. Further analysis is required.

Constitutive activation of transforming growth factor beta receptor 1 (*Tgfb β 1*) in the mouse uterus leads to increased myometrial thickness (Gao et al. 2015). *Tgfb β 1* is expressed in the myometrium (Gao, Li & Li 2014) and is required for myometrial development during the

early postnatal uterine development (Gao, Bayless & Li 2014). Analysis of *Tgfbr1* mRNA expression would assess whether the increased myometrial thickness observed in our model is due to abnormal early postnatal uterine development.

The uterine lumen epithelium of *Mtrr* females appeared abnormal. Specifically, we observed defects in the apicobasal polarity based on the mislocalisation of pan-cadherin antibody expression, and also defects in planar cell polarity based on the observation that the cells are not organised in a monolayer as in C57Bl/6, but in layers that are 2-3 cells thick. Apicobasal polarity refers to the different function of the apical and basal cell membranes. The apical membrane has a secretory function, expresses channels and transporters, and faces the lumen. The basal cell membrane contains mostly proteins involved in interactions with the extracellular matrix (Marcinkevicius, Fernandez-Gonzalez & Zallen 2009). This is different from planar cell polarity, which refers to how cells orientate within the plane of the epithelial tissue (Devenport 2014). The pan-cadherin antibody binds to all members of the cadherin superfamily including classical cadherins (such as E-cadherin, N-cadherin, P-cadherin), protocadherins, seven-pass transmembrane cadherins and desmosomal cadherins (Angst, Marcozzi & Magee 2001; Harmon, Desai & Green 2009; Nollet, Kools & Van Roy 2000). To confirm a polarity phenotype, analysis of the expression and cellular localisation of specific cadherins should take place as well as other proteins in adherent junction complexes that help generate a polarised cell layer. E-cadherin protein is expressed in the uterine epithelial cells also during early pregnancy, with higher expression at the apical membrane of the endometrium in the peri-implantation sites, compared to the inter-implantation sites (Jha et al. 2006). mRNA expression of *Cdh1*, which encodes for E-cadherin, was unchanged in the F1 uteri. Even if E-cadherin protein expression is normal, it is possible that its localisation is altered to prevent the establishment of cell polarity and abnormal organisation of the lumen epithelium cell layer. *Cdh1* is important for uterine development and function. A conditional ablation of *Cdh1* (*Cdh1^{d/d}*) in the neonatal mouse uterus induced abnormal epithelial proliferation, excessive apoptosis, and abnormal stromal differentiation, with no apparent effects on the myometrium (Reardon et al. 2012). In addition, *Cdh1^{d/d}* altered the expression of *Wnt* and *Hox* genes, that are involved in uterine development. *Cdh1^{d/d}* mice had decreased expression of epithelial *Wnt* genes, *Wnt* receptors, and epithelial and stromal *Hox* genes, and were infertile due to defects in implantation and decidualisation (Reardon et al. 2012). Abnormal decidualisation can lead to FGR (see Section 1.2.4), which is one of the phenotypes observed in the *Mtrrst* model (Padmanabhan et al. 2013). This suggests that

abnormal expression of CDH1 in the *Mtrr* mice can impair uterine function during pregnancy.

Reduced expression of cadherins causes the cell junctions to loosen and reduces apicobasal polarity, which prevents the establishment of proper signalling pathways (Gradilla et al. 2018). The decrease in *Pgr* mRNA and PGR protein expression at the estrus stage uteri of *Mtrr* females indicates that P4 signalling might be disrupted. However, it is unclear whether this is attributed to poor organisation of the uterine luminal cells or whether defective P4 signalling has affected cellular organisation. After ovulation, P4 is produced by the corpus luteum and is essential to prepare the endometrium for implantation and maintenance of pregnancy (Goyeneche et al. 2003; Wang & Dey 2006; Wetendorf & DeMayo 2014). *Pgr*^{-/-} females exhibit uterine epithelial hyperplasia and inflammation but display a normal endometrium and myometrium (Lydon et al. 1995; Mulac-Jericevic & Conneely 2004) suggesting that the increased myometrial thickness observed in the uteri of *Mtrr* females is independent of the decreased PGR expression. As a mitogen, P4 induces uterine stromal cell proliferation (Clarke & Sutherland 1990; Rider 2002). Exogenous administration of P4 also prolongs the window of receptivity up to day 6 (Song, Han & Lim 2007) suggesting that poor P4 signalling might reduce the blastocyst implantation window or prevent it from occurring. However, in the *Mtrr* model we observe normal litter sizes, suggesting that implantation is not altered (Padmanabhan et al. 2013). Further experiments are required to explore P4 signalling in the *Mtrr* model, such as assessing the mRNA and protein expression of P4 signalling target genes in the mouse uterus, such as *Areg*, *Wnt4*, *Bmp2*, *Ihh*, and *Hoxa10*. Stromal *Esr1* activation has been shown to suppress expression of *Pgr* mRNA in the uterine epithelium (Mehta et al. 2016). However, in our *Mtrr* model, *Esr1* mRNA was similarly expressed to the C57Bl/6 when the whole uterus was considered. These results might suggest that suppression of *Pgr* mRNA and protein expression is independent of the *Esr1*. Despite this, E2 levels might be increased in *Mtrr* females and causing increased estrogen signalling through the estrogen receptor. Ovariectomised mice treated with a high dose (24.0 g/kg) of the herb ginseng, which has an estrogenic effect, had increased lumen epithelial thickness including multiple cell layers (Xu et al. 2014), a phenotype similar to the *Mtrr* uteri. To examine this hypothesis, an ELISA experiment should be performed to measure blood estrogen levels in *Mtrr* females during proestrus and estrus.

Abnormal cell polarity in *Mtrr* uteri might alter cell-cell signalling and subsequent uterine function, such as decidualisation or receptivity to blastocysts. The effects of folate deficiency on blastocyst implantation are disputed since some studies find normal litter sizes at GD4.5 (Gao et al. 2012b) and others find abnormal litter sizes after GD5.5 (Geng et al. 2015). The *Mtrr^{gt}* model shows normal litter sizes at GD6.5 (see Chapter 4) and up to GD10.5 (Padmanabhan et al. 2013), which supports the hypothesis that blastocysts implant at a normal frequency in mothers carrying one or two *Mtrr^{gt}* alleles or had a father who was a carrier. Even though the frequency of blastocyst implantation was normal in the *Mtrr* model based on litter sizes at GD6.5, it is possible that there are implantation defects. We have observed the occurrence of twinning of wildtype conceptuses derived from an *Mtrr* mutant maternal grandparent, or from *Mtrr^{gt/gt}* intercrosses (Padmanabhan et al. 2013). These conceptuses, which share an implantation site, are not identical given that they are different sexes, based on PCR genotyping of yolk sac tissue (E. Watson, unpublished). The cause is unclear; however, it is possible that improper signalling from the uterus to the embryo affects embryo spacing. It is unclear whether poor spacing is due to abnormalities in the blastocyst or uterine lining. Alternatively, the uterus might display late blastocyst receptivity to cause developmental delay or growth restriction in the embryo. More analysis is required to assess possible dysregulation of the window of implantation, by looking at the expression of receptivity markers such as *Muc1*, *Lif*, and *Itgβ3* at the peri-implantation stage uterus (E3.5; Raheem 2018). *Muc1* is an anti-adhesive expressed by the lumen epithelium. Increased levels of *Muc1* prevent embryo attachment (Surveyor et al. 1995). *Lif* is secreted by the endometrial gland and stromal cells and binds its receptor on the luminal epithelium (Cullinan et al. 1996; Raheem 2018; Song & Lim 2006; Xu et al. 2012). *Lif1* signals embryo implantation via an autocrine/paracrine manner (Cullinan et al. 1996). *Itgβ3* is an adhesive molecule expressed both by the endometrium and the blastocyst (Raheem 2018). Altogether, these studies could suggest that either of these factors might be dysregulated in the *Mtrr^{gt}* model, causing altered blastocyst spacing or delayed implantation.

Overall, we showed that paternal abnormal folate metabolism alters uterine structure and function, in particular the cell polarity in the uterine lumen and the expression of progesterone receptor. Therefore, it will be important to assess how this affects decidualisation of the uterus and embryo implantation and growth.

Chapter 4: The effects of abnormal folate metabolism on decidualisation

This chapter includes experiments that have been performed in collaboration, as indicated. Staining of GD8.5 implantation sites with MTRR antibody was performed by Dr. Rakoczy.

4.1 Introduction

Decidualisation, the differentiation of endometrial stromal cells into epithelioid cells, starts at GD4.5 at the antimesometrial zone. Differentiation of the stromal cells close to the primary decidual zone occurs by GD5.5, while the secondary decidual zone is fully developed by GD6.5 (Lim & Wang 2010; Figure 1.3). Growth factors and cytokines secreted by the decidualised cells are essential for embryo growth (Fraser et al. 2015; Lim & Wang 2010; Ramathal et al. 2010). In humans, the decidualised cells provide nutrients for the embryo until the placenta matures fully, regulate trophoblast invasion, sense and distinguish between high- and low-quality embryos, modulate the maternal immune system so it does not attack the semi-allogenic embryo, and provide the embryo with access to maternal vasculature (Cha, Sun & Dey 2012; Gellersen & Brosens 2014).

Nutritional folate deficiency might affect the decidualisation process, since implantation sites of folate-deficient females showed hypomethylation and downregulation of *Esr1* (Gao et al. 2012a), hypermethylation of decidualisation-specific genes *Nrlh3* and *Nr5a1*, stunted decidual bulges (Geng et al. 2015) and abnormal decidual angiogenesis in mice (Li et al. 2015).

Abnormal decidual vascularisation causes uteroplacental insufficiency, therefore impairing nutrient and oxygen transport, leading to abnormal fetal growth (Krishna & Bhalerao 2011; Swanson & David 2015). However, it is unknown whether abnormal folate metabolism has the same effects on decidualisation as nutritional folate deficiency. More specifically, the role of the *Mtrr^{gt}* mutation in this process is unknown.

In Chapter 3, we showed that structure and gene expression in the *Mtrr* uteri at estrus is altered. More specifically, uteri of *Mtrr* females have altered lumen epithelial organisation and polarity, and increased outer myometrial thickness. Progesterone signalling may be altered as indicated by low PGR expression in the uterine epithelial cells. In addition, we have observed the occurrence of twinning of conceptuses derived from either *Mtrr^{gt/gt}* intercrosses, or an *Mtrr^{+/gt}* maternal grandparent (Padmanabhan et al. 2013). Twinning is when two or more blastocysts implant into the uterus in close proximity so that their implantation sites merge into one single site. Approximately 5% and 25% of all severely affected conceptuses from *Mtrr^{gt/gt}* and F1 *Mtrr^{+/+}* females, respectively, share an implantation site (Padmanabhan et al. 2013, 2017). While the cause is unclear, it is possible that the uteri of these females are unable to regulate blastocyst spacing at implantation or that the blastocysts, themselves, are unable to signal to one another to optimise spacing.

Altogether, these data might suggest that blastocyst receptivity and/or decidualisation potential might be affected by the *Mtrr^{gt}* mutation compared to control uteri. We therefore hypothesise that the *Mtrr^{gt}* mutation affects decidualisation, which consequently impairs embryonic growth. To explore this further, we assessed the effects of intrinsic and paternal *Mtrr^{gt}* mutation on frequency of implantation, litter sizes, and decidualisation at GD6.5.

4.2 Results

4.2.1 The *Mtrr^{gt}* mutation does not affect the litter size at GD6.5

To assess the effects of the *Mtrr^{gt}* mutation on the frequency of blastocyst implantation, we mated C57Bl/6 males with *Mtrr^{+/+}*, *Mtrr^{+/gt}*, and *Mtrr^{gt/gt}* females derived from *Mtrr^{+/gt}* intercrosses and with F1 *Mtrr^{+/+}* and F1 *Mtrr^{+/gt}* females derived from *Mtrr^{+/gt}* fathers to assess the effects of intrinsic and paternal *Mtrr* deficiency on the litter size at GD6.5. This stage was chosen because it allowed for easy analysis of implantation sites a short time after implantation occurs (at GD4.5). C57Bl/6 implantation sites at GD6.5 were used as controls. Four litters were assessed per genotypic group. Mating with C57Bl/6 males was performed to eliminate any potential paternally-inherited effects of the *Mtrr^{gt}* mutation on the decidual reaction as caused by the fetal genotype, sperm, or seminal fluid. All the vaginal plugs detected at GD0.5 resulted in pregnancies regardless of the female genotype suggesting the fertility is unlikely to be compromised by intrinsic or paternal *Mtrr^{gt}* mutation. At GD6.5, we compared the overall litter sizes and found that compared to C57Bl/6 controls (8.5 ± 0.6 implantation sites/litter), all *Mtrr* females displayed normal litter sizes (Figure 4.1A-C). However, *Mtrr^{gt/gt}* (7.8 ± 1.7 implantation sites/litter) and *Mtrr^{+/gt}* (10.3 ± 1.0 implantation sites/litter) females were different from each other ($p=0.04$). To increase the robustness of this result, sample sizes should be increased. Overall, the result indicated that implantation occurred at a normal rate regardless of the presence of the *Mtrr^{gt}* allele in the mother. These data are supported by the observation of normal litter sizes at GD10.5 in litters from *Mtrr^{gt/gt}* intercrosses (Padmanabhan et al. 2013).

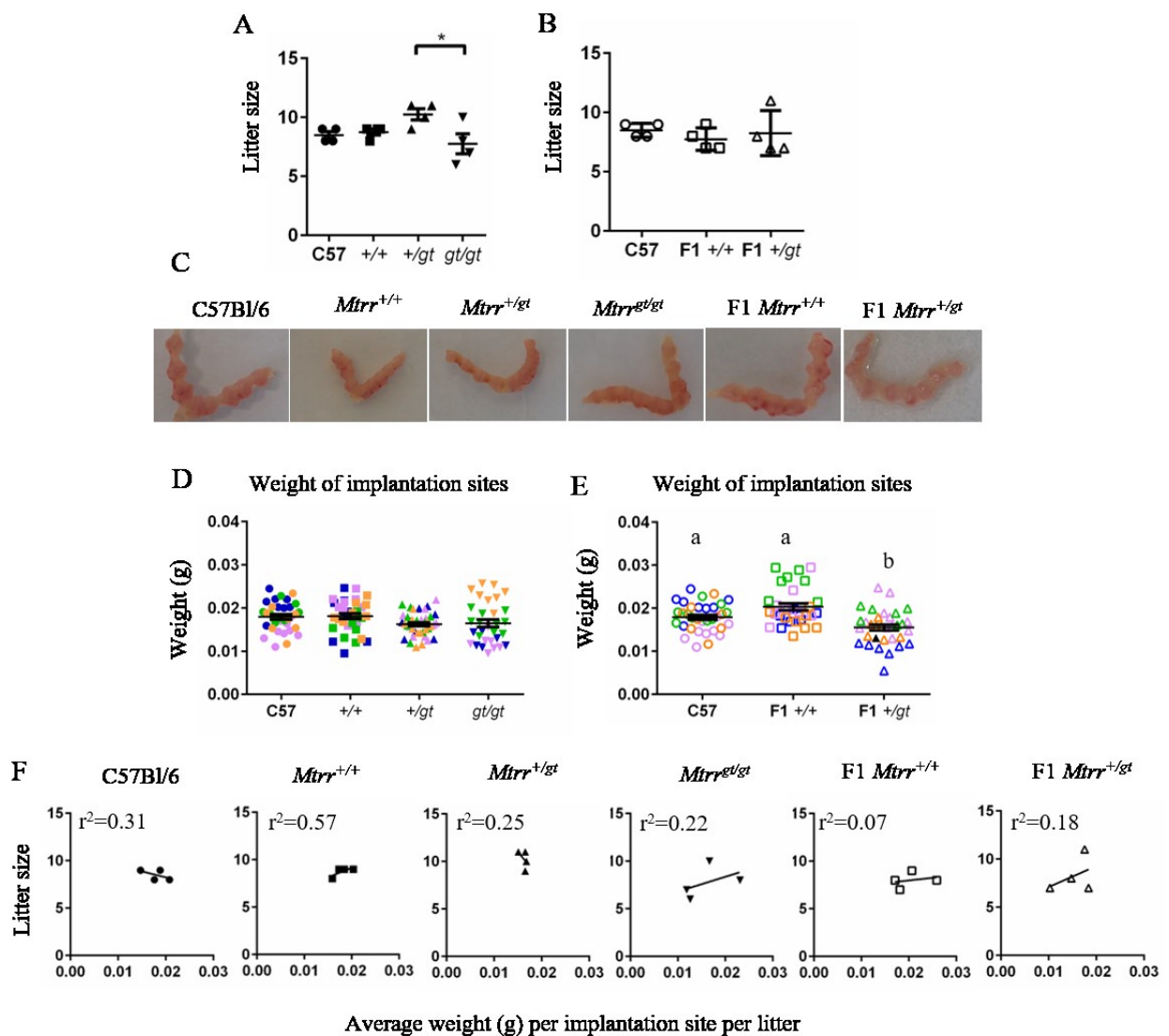


Figure 4.1 Litter statistics of GD6.5 dissections after *Mtrr* females were mated with C57Bl/6 males.

(A-B) Graphs showing litter size at GD6.5 in (A) females derived from *Mtrr*^{+/gt} intercrosses and (B) females derived from an *Mtrr*^{+/gt} father compared to C57Bl/6 control matings. Data are presented as mean \pm SEM. n=4 litters per female genotype. Statistical test: One-way ANOVA *p<0.05. (C) Representative images of pregnant uteri at GD6.5 from each mating. (D-E) Graphs depicting the weight of implantation sites derived from the indicated maternal genotype. n=4 litters per maternal genotype. Implantation sites from the same litter are colour matched. Data are presented as mean \pm SEM. Statistical test: One-way ANOVA, a p<0.05 when compared to b. (F) Graphs comparing the average weight of implantation sites/litter to litter size. n=4 litters per adult female genotype.

4.2.2 Abnormal folate metabolism does not affect implantation site weight at GD6.5

To explore whether the decidualisation reaction occurred normally, the weight of individual implantation sites at GD6.5 was assessed per *Mtrr* maternal genotype. At GD6.5, implantation sites are largely composed of maternal decidua. The fetoplacental component is very small at this stage and contributes little to the overall weight. Uteri were dissected at GD6.5 and scissors were used to cut between and close to each implantation site before weighing. No differences in average implantation site weight were detected between litters from *Mtrr*^{+/+}, *Mtrr*^{+/*gt*}, and *Mtrr*^{*gt/gt*} females compared to C57Bl/6 control litters (Figure 4.1D). However, the average weight of implantation sites from F1 *Mtrr*^{+/*gt*} females was less than those from F1 *Mtrr*^{+/+} females or C57Bl/6 females (p=0.0001; Figure 4.1E). This result is difficult to resolve since the litters of *Mtrr*^{+/*gt*} females from *Mtrr*^{+/*gt*} intercrosses did not show a similar effect. It suggests a maternal *Mtrr*^{*gt*} allele in the F0 generation might have a protective effect on decidualisation of their *Mtrr*^{+/*gt*} daughter's uterus. The different phenotype between F1 *Mtrr*^{+/+} and F1 *Mtrr*^{+/*gt*} could be due to an additive effect of a paternal *Mtrr*^{*gt*} allele and intrinsic *Mtrr*^{*gt*} allele. The decrease in implantation site weight might be a result of abnormal decidualisation due to defects in progesterone signalling. *Pgr* expression will be assessed later. To determine whether litter size impacted the weight of each implantation site, we performed a linear regression analysis (Figure 4.1F). We found that there was no correlation between litter size and average implantation site weight within any of the *Mtrr* maternal genotypic groups at GD6.5. This suggests that even in case of intrinsic or parental abnormal folate metabolism, the litter size does not affect the implantation site weight at GD6.5.

4.2.3 Analysis of MTRR gene and protein expression in decidua at GD6.5

Similar to Chapter 3, we assessed wildtype and total *Mtrr* transcript expression in whole implantation sites at GD6.5 collected from matings of C57Bl/6 males with C57Bl/6, *Mtrr*^{+/+}, *Mtrr*^{+/*gt*}, *Mtrr*^{*gt/gt*}, F1 *Mtrr*^{+/+} or F1 *Mtrr*^{+/*gt*} females. The analysis was completed via RT-qPCR. In matings of C57Bl/6 males with *Mtrr*^{+/*gt*} females, we were unable to determine the genotype of the resulting offspring at GD6.5 (i.e., *Mtrr*^{+/+} or *Mtrr*^{+/*gt*}). However, since the majority of each implantation site is composed of maternal decidua and uterus at this stage, the *Mtrr* genotypic contribution by the conceptus is unlikely to affect the result. Wildtype

Mtrr transcript expression in the decidua of *Mtrr*^{+/+}, *Mtrr*^{+/*gt*}, or *Mtrr*^{*gt/gt*} females was as expected (Figure 4.2A), since implantation sites of *Mtrr*^{+/+} females displayed wildtype *Mtrr* transcript levels that were 98% of C57Bl/6 levels whereas the implantation sites of *Mtrr*^{+/*gt*} and *Mtrr*^{*gt/gt*} females showed an appropriate reduction of expression (62.0% and 6.0% of control levels, respectively; Figure 4.2A). The expression of the *Mtrr* wildtype transcript was similar between implantation sites of F1 *Mtrr*^{+/+} and C57Bl/6 females and was decreased as expected to 62.0% of C57Bl/6 levels in the implantation sites of F1 *Mtrr*^{+/*gt*} females (Figure 4.2C). Also, as expected, there was no difference in total *Mtrr* transcript expression in implantation sites at GD6.5 between any of maternal genotype groups tested (Figure 4.2B, D).

To determine the spatial pattern of MTRR protein expression in the decidua, immunohistochemistry on implantation sites from C57Bl/6 intercrosses at GD8.5 was performed (in collaboration with J. Rakoczy), since implantation sites at GD6.5 were not available at the time of this analysis. We observed widespread decidual expression of MTRR protein in the regressing primary decidual zone, the decidua basalis, and the lateral decidua (Figure 4.2E-G). The secondary decidual zone showed a distinct staining pattern for MTRR protein, whereby expression was restricted to the cells on the outer edge (Figure 4.2E, G). There was also widespread MTRR expression in fetally-derived tissue including the trophoblast giant cell layer, ectoplacental cone, chorion, yolk sac and embryo. In the future, immunohistochemistry for the MTRR protein should be performed in C57Bl/6 implantation sites at GD6.5 to determine whether decidual expression pattern is consistent over time.

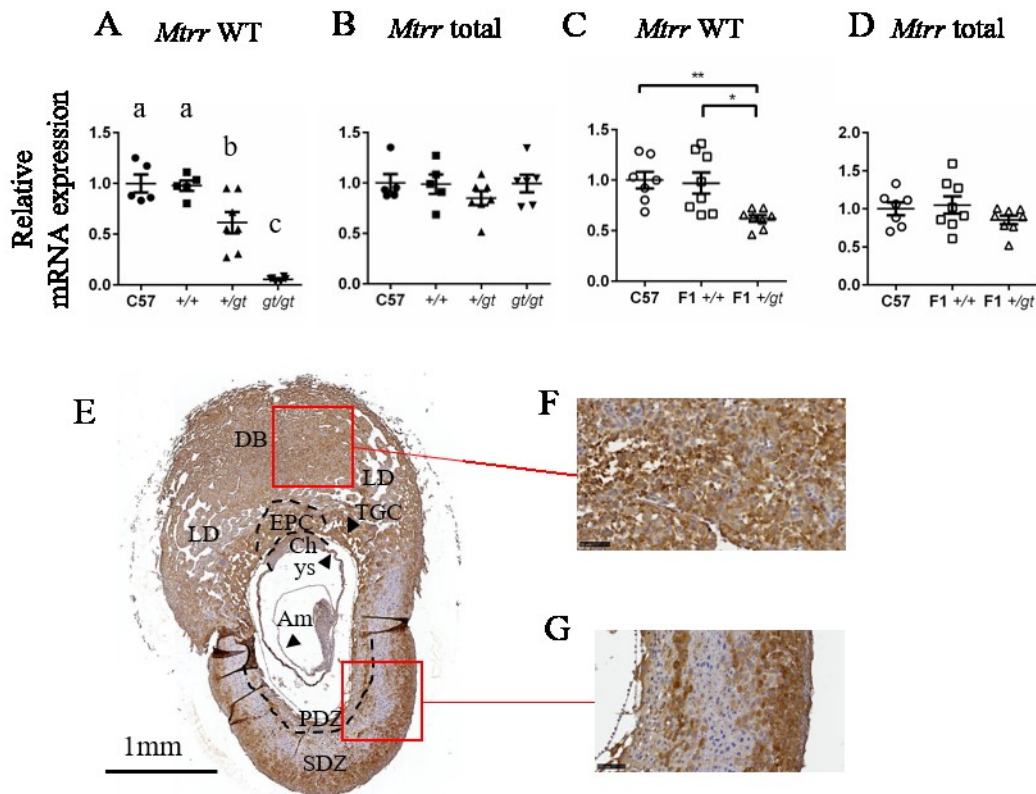


Figure 4.2 *Mtrr* transcript and protein expression in whole implantation sites at GD6.5. (A-D) Relative mRNA expression of (A, C) wildtype *Mtrr* transcript and (B, D) total *Mtrr* transcript in implantation sites of females derived from *Mtrr*^{+/*gt*} intercrosses (A-B) or from a *Mtrr*^{+/*gt*} father (C-D). Data are presented as mean ± SEM. N=5-8 per genotype. Statistical test: One-way ANOVA **p*<0.05, ***p*<0.01. (E-G) Representative sections of a C57Bl/6 implantation site at GD8.5 stained with anti-MTRR (brown) and counterstained with hematoxylin (blue). Scale bars: (E) 1mm, (F) 50µm, (G) 100µm. Am: amnion, ys: yolk sac, DB: decidua basalis, LD: lateral decidua, myo: myometrium, TGC: trophoblast giant cells, Ch: chorion, EPC: ectoplacental cone, PDZ: primary decidual zone (dotted line), SDZ: secondary decidual zone.

4.2.4 Abnormal folate metabolism in males potentially affects the decidualisation reaction of their wildtype daughters at GD6.5

To test whether intrinsic *Mtrr* deficiency affects regional decidualisation after implantation, implantation sites (including surrounding uterus) of C57Bl/6, *Mtrr*^{+/*+*}, *Mtrr*^{+/*gt*}, or *Mtrr*^{*gt*/*gt*} females mated with C57Bl/6 males were dissected at GD6.5, and either embedded in paraffin for histological analysis or frozen for molecular analysis. Histological sections of implantations sites at GD6.5 were stained with H&E to assess gross morphology. First, decidual thickness in the antimesometrial and mesometrial regions and on the left and right

sides of the conceptus were measured. Three histological sections per each implantation site were assessed and 1-2 implantation sites from at least four litters were assessed per maternal genotype. All experiments were done without taking into account the fetal genotype. We did not observe any difference in the antimesometrial or mesometrial distances, or the left and right decidual zones in implantation sites of *Mtrr*^{+/+}, *Mtrr*^{+/*gt*}, or *Mtrr*^{*gt/gt*} females compared to C57Bl/6 controls (Figure 4.3A-B). Regional decidualisation was also assessed in implantation sites at GD6.5 of F1 *Mtrr*^{+/+} and F1 *Mtrr*^{+/*gt*} females derived from an *Mtrr*^{+/*gt*} father. We observed an increase in the antimesometrial (p=0.04) and mesometrial (p=0.03) distances in implantation sites at GD6.5 from F1 *Mtrr*^{+/+} females compared to C57Bl/6 females (Figure 4.3A, C). No differences were apparent when measuring decidual zones on the left or right of the conceptus (Figure 4.3A, C). Next, we assessed cell density in the lateral decidua. While there was no difference in decidual cell density in implantation sites from *Mtrr*^{+/+}, *Mtrr*^{+/*gt*}, or *Mtrr*^{*gt/gt*} females compared to controls (p=0.1; Figure 4.3D-E), there was a decrease in cell density in the implantation sites of F1 *Mtrr*^{+/+} and F1 *Mtrr*^{+/*gt*} females compared to C57Bl/6 (p=0.017; Figure 4.3D, F). The latter result suggests that the decidual cells are bigger in response to the *Mtrr*^{*gt*} allele in the F0 males. The cell density in the antimesometrial and mesometrial areas should also be assessed in the future. Furthermore, it will be important to examine the cell types that make up the decidua, such as uNK cells, macrophages, cytotoxic T cells, dendritic cells, and innate lymphoid cells via immunohistochemistry to see whether any cell population is altered in the *Mtrr* females. Overall, these data show that there may be a decidua phenotype in implantation sites in litters of F1 *Mtrr*^{+/+} and F1 *Mtrr*^{+/*gt*} females.

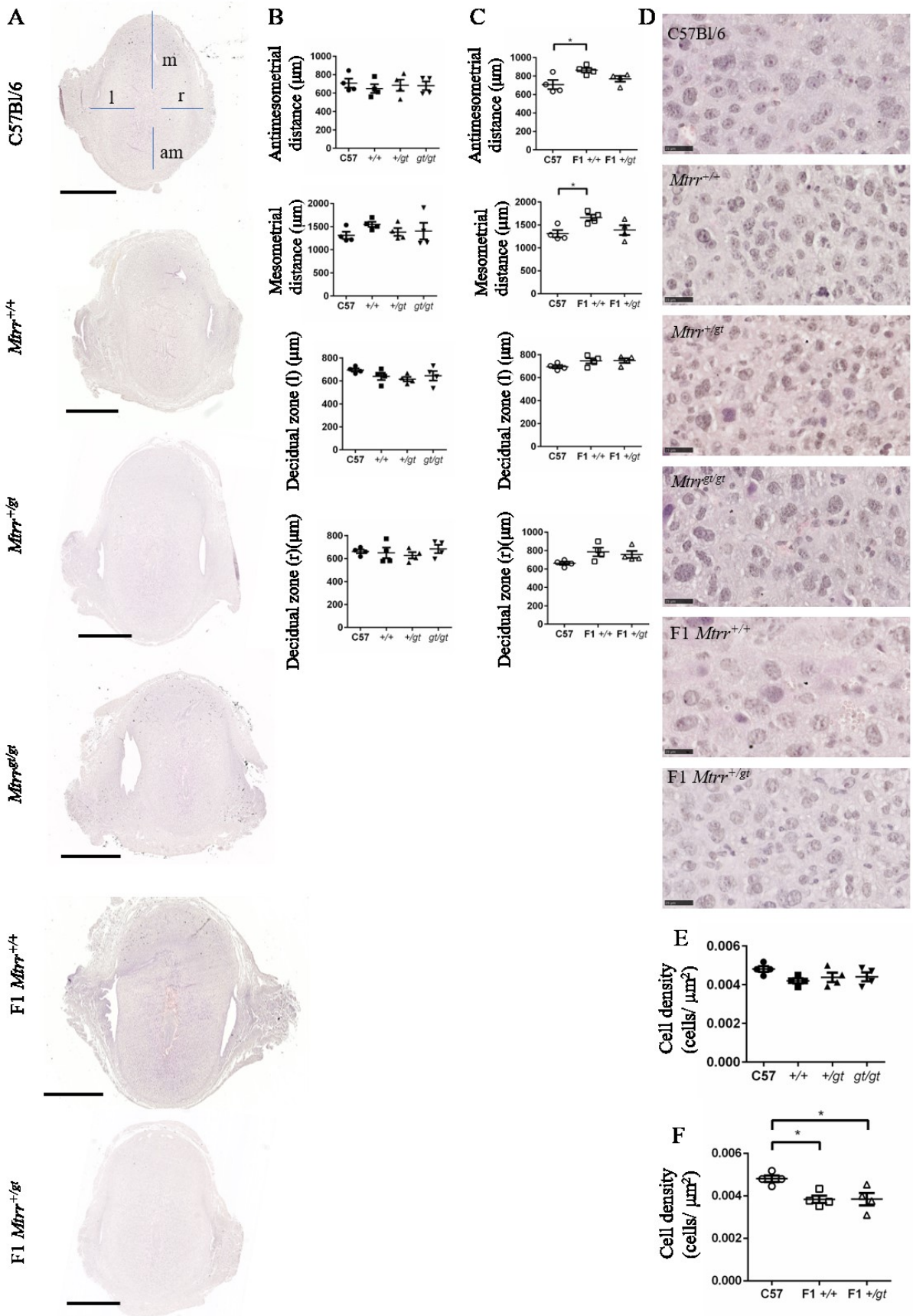


Figure 4.3 Analysis of decidual morphology in implantation sites at E6.5.

(A) Representative histological sections of implantation sites at E6.5 stained with H&E. Conceptuses from litters of C57Bl/6, *Mtrr*^{+/+}, *Mtrr*^{+/*gt*} and *Mtrr*^{gt/*gt*} females are shown. Also, conceptuses from F1 *Mtrr*^{+/+} and F1 *Mtrr*^{+/*gt*} females derived from an *Mtrr*^{+/*gt*} male are shown. All females were mated with C57Bl/6 male. The genotype of the conceptus was not taken into account. Scale bar: 1 mm. m: mesometrial decidua, am: anti-mesometrial decidua, r: right decidual zone, l: left decidual zone. (B-C) Quantification of the distances of each decidual region as denoted in the top panel in (A). Implantation sites of litters from females from (B) *Mtrr*^{+/*gt*} intercrosses or (C) an *Mtrr*^{+/*gt*} father were assessed. Data are presented as mean ± SEM. Two implantation sites were assessed per litter. N=4 litters per adult female genotype. (D) Representative images of lateral decidua stained with H&E. Maternal genotype shown. Scale bars: 50 µm. (E-F) Quantification of cell density in the lateral decidua of implantation sites whose mothers are derived (E) from *Mtrr*^{+/*gt*} intercrosses or (F) from an *Mtrr*^{+/*gt*} male. Data are presented as mean ± SEM. n=4 implantation sites per maternal genotype. Statistical analysis: One-way ANOVA, *p<0.05.

4.2.5 Analysis of decidual marker expression in implantation sites at GD6.5

The process of decidualisation is dependent on progesterone receptor signalling (Large & DeMayo 2012). Since we have previously observed a decrease in progesterone receptor protein expression in the *Mtrr*^{+/+}, *Mtrr*^{+/*gt*}, or *Mtrr*^{gt/*gt*} uteri at estrus, we wanted to determine whether a similar finding occurred at GD6.5 with the potential to affect decidualisation during pregnancy. We assessed *Pgr* mRNA expression via RT-PCR in whole implantation sites at GD6.5 derived from mating C57Bl/6 males with C57Bl/6, *Mtrr*^{+/+}, *Mtrr*^{+/*gt*}, *Mtrr*^{gt/*gt*}, F1 *Mtrr*^{+/+}, or F1 *Mtrr*^{+/*gt*} females. There was a decrease in *Pgr* mRNA expression in implantation sites of *Mtrr*^{+/*gt*} and *Mtrr*^{gt/*gt*} females compared to implantation sites of C57Bl/6 females (p=0.0002; Figure 4.4A). No change in *Pgr* mRNA expression was observed in *Mtrr*^{+/+} females compared to the C57Bl/6 (Figure 4.4A). Furthermore, a decrease in *Pgr* mRNA expression was observed in implantation sites of F1 *Mtrr*^{+/*gt*} females compared to C57Bl/6 females (p=0.003; Figure 4.4B). No change in *Pgr* mRNA expression was observed in F1 *Mtrr*^{+/+} females (Figure 4.4B). Altogether, these data suggest that intrinsic but not paternal abnormal folate metabolism affects *Pgr* mRNA expression at GD6.5. PGR protein expression in implantation sites at GD6.5 should be assessed in the future.

To further assess molecular differences in the decidua of implantation sites at GD6.5 caused by the maternal *Mtrr* genotype, we assessed the expression of genes important for

decidualisation (e.g., *Hoxa10*, *Hand2*, *Nrf2f*, *Bmp2*, *Sfrp5* and *Cdh1*) via qPCR analysis. HOXA10 is a regulator of progesterone responsiveness of uterine stromal cells, and therefore important during implantation and decidualisation (Lim, Ma, et al. 1999). *Hand2* is also a gene that is regulated by progesterone during decidualisation (Okada et al. 2014). However, *Hoxa10* and *Hand2* mRNA expression did not change in implantation sites at GD6.5 derived from *Mtrr*^{+/+}, *Mtrr*^{+/*gt*}, or *Mtrr*^{*gt/gt*} females (Figure 4.4C, D). These data are inconsistent with *Pgr* mRNA expression levels in *Mtrr*^{+/*gt*} and *Mtrr*^{*gt/gt*} implantation sites (Figure 4.4A), although PGR protein levels should be assessed to address this inconsistency. Interestingly, *Hoxa10* mRNA expression was decreased in the implantation sites of F1 *Mtrr*^{+/*gt*} mothers compared to those from either C57Bl/6 or F1 *Mtrr*^{+/+} females (p=0.0005; Figure 4.4I), a similar trend to *Pgr* mRNA expression in similar implantation sites (Figure 4.4B). *Hand2* expression was only slightly decreased in F1 *Mtrr*^{+/*gt*} implantation sites but the result was not statistically significant (Figure 4.4J). The inconsistency of *Hoxa10* and *Hand2* expression in implantation sites at GD6.5 from *Mtrr*^{+/*gt*} females derived from either two *Mtrr*^{+/*gt*} parents or only an *Mtrr*^{+/*gt*} father needs to be resolved.

NR2F2 is a transcription factor that is highly expressed in uterine stroma cells and is important for decidualisation (Kurihara et al. 2007). It is known to activate *Bmp2* transcription (Wetendorf & DeMayo 2012). We observed a decrease in *Nr2f2* and *Bmp2* mRNA expression specifically in implantation sites from *Mtrr*^{+/*gt*} and *Mtrr*^{*gt/gt*} females compared to C57Bl/6 controls (p=0.0012; Figure 4.4E-F). *Bmp2* mRNA was lower in implantation sites from *Mtrr*^{+/+} females than controls (Figure 4.4F) even though *Nr2f2* expression did not change (Figure 4.4E). These data suggest that only an intrinsic *Mtrr*^{*gt*} allele is sufficient to affect *Nr2f2* expression and that another transcription factor beyond NR2F2 might regulate *Bmp2* during decidualisation. In support of this finding, normal levels of *Nr2f2* mRNA were found in implantation sites from F1 *Mtrr*^{+/+} and F1 *Mtrr*^{+/*gt*} females (Figure 4.4K) despite decreased *Bmp2* mRNA levels (Figure 4.4L). SFRP5 is an inhibitor of WNT signalling (Bovolenta et al. 2008; Stuckenholtz et al. 2013) and is involved in stromal cell differentiation and decidualisation (Li et al. 2007). Expression of *Sfrp5* mRNA was within the normal range in all of the *Mtrr* implantation sites assessed compared to the controls (Figure 4.4G, M). Lastly, CDH1, also known as E-cadherin, is a protein important for decidualisation (Reardon et al. 2012). While *Cdh1* mRNA expression was unaltered in all *Mtrr* uteri during estrus (Chapter 3), we observed a decrease in *Cdh1* mRNA expression at GD6.5 only in *Mtrr*^{+/*gt*} and *Mtrr*^{*gt/gt*} uteri compared to the C57Bl/6 controls (p=0.03; Figure

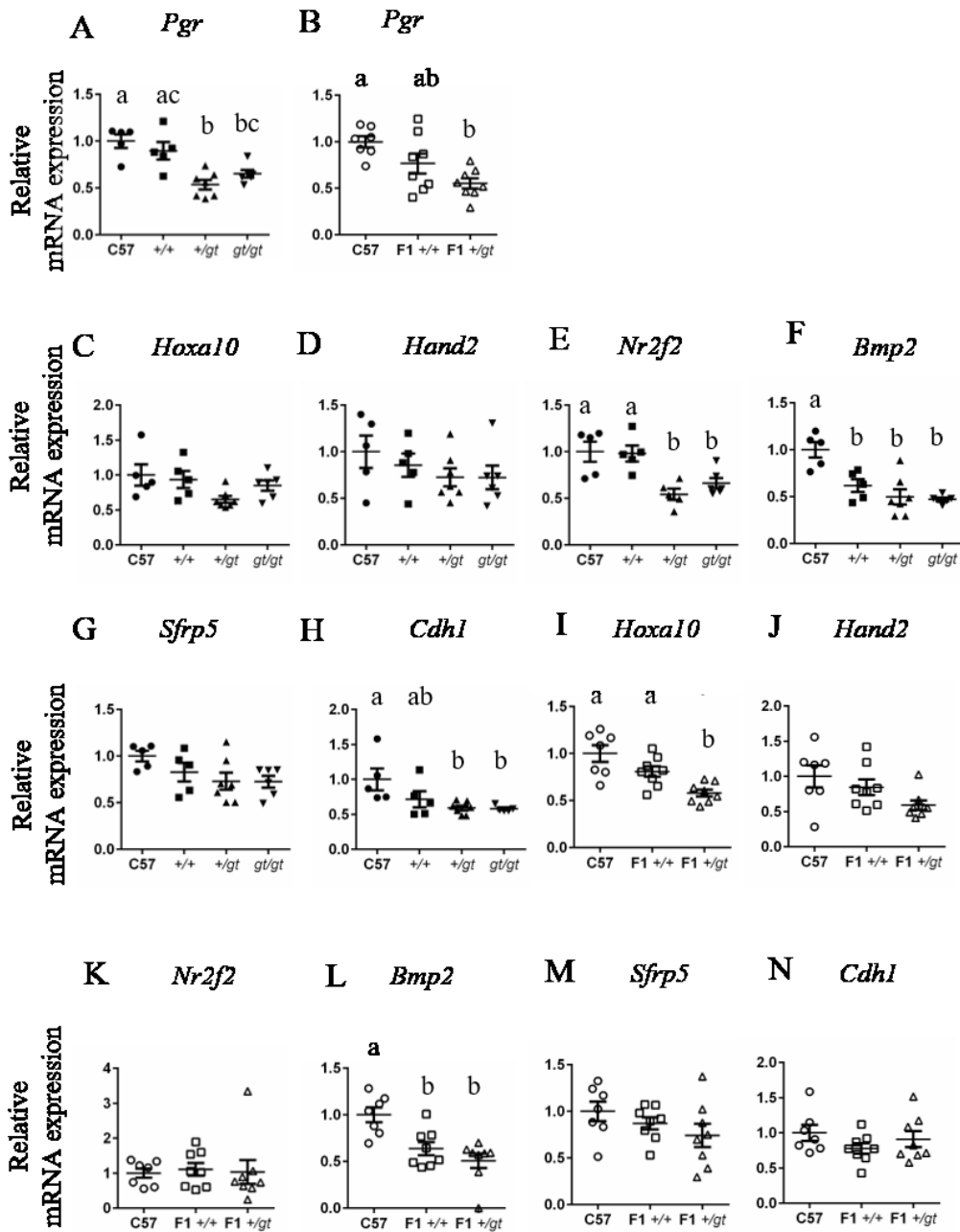


Figure 4.4 Relative mRNA expression of decidualisation markers in GD6.5 implantation sites.

Graphs depicting relative mRNA expression of genes involved in decidualisation in implantation sites from mothers derived from either (A, C-H) *Mtrr*^{+/-gt} intercrosses or (B, I-N) from an *Mtrr*^{+/-gt} father. *Polr2a* mRNA was used as a housekeeping gene. n=5-7 implantation sites from each adult female genotype. Data are presented as fold change compared to C57Bl/6 controls (normalised to 1). Statistical test: One-way ANOVA, a p<0.05 when compared to b and c; b p<0.05 when compared to a and c; c p<0.05 when compared to a and b.

4.4H). A downward trend in *Cdh1* mRNA expression was also observed in *Mtrr*^{+/+} uteri at GD6.5, though this did not reach statistical significance compared to C57Bl/6 uteri (Figure 4.4N). *Cdh1* mRNA expression was similar in C57Bl/6, F1 *Mtrr*^{+/+} and F1 *Mtrr*^{+/*gt*} females at GD6.5, suggesting a combined effect of a maternal and an intrinsic *Mtrr*^{*gt*} allele to disrupt its expression.

In summary, even though histological sections did not show gross alterations in decidualisation at GD6.5, gene expression of decidualisation markers were disrupted by one or more intrinsic *Mtrr*^{*gt*} allele. While *Pgr* mRNA expression is altered, this effect on decidualisation may in part be independent of progesterone signalling, since we observe normal *Pgr* mRNA expression, but abnormal expression of *Bmp2* mRNA in *Mtrr*^{+/+} and F1 *Mtrr*^{+/+} females. For instance, BMP2 is a downstream mediator of *Egfr* signalling and ablation of *Egfr* in mice results in defects in decidualisation (Large et al. 2014), and this is independent of *Pgr* signalling. The misexpression of some, but not all, decidual markers suggests that specific pathways important for proper decidualisation might be affected (e.g., BMP2 signalling).

4.2.6 Analysis of growth restriction at E6.5

Defective decidualisation is known to cause growth restriction (Plaisier 2011). We previously observed growth defects in embryos at E10.5 from the *Mtrr*^{*gt*} mouse line that were shown to be associated with the uterine environment (Padmanabhan et al. 2013). While a specific uterine defect has not yet been identified, we wanted to determine whether the growth restriction phenotype in conceptuses associated with intrinsic or paternal *Mtrr*^{*gt*} mutation appeared as early as E6.5. To do this, we assessed conceptuses in histological sections of implantation sites at GD6.5 obtained from mating C57Bl/6 males with *Mtrr*^{+/+}, *Mtrr*^{+/*gt*}, and *Mtrr*^{*gt*/*gt*} females derived from *Mtrr*^{+/*gt*} intercrosses or with F1 *Mtrr*^{+/+} and F1 *Mtrr*^{+/*gt*} females derived from *Mtrr*^{+/*gt*} fathers. The anterior-posterior (AP) and dorsal-ventral (DV) axis of each conceptus (n=1-2 conceptuses per litter, n=4 litters per genotype) was measured and the average lengths per litter were determined (Figure 4.5A, B). No differences in AP and DV axis lengths of the conceptuses were observed in the conceptuses derived from *Mtrr*^{+/+}, *Mtrr*^{+/*gt*}, or *Mtrr*^{*gt*/*gt*} (Figure 4.5A), or from F1 *Mtrr*^{+/+} and F1 *Mtrr*^{+/*gt*} mothers compared to C57Bl/6 implantation sites (Figure 4.5B). Of note, the genotype of the conceptus was not

taken into account in the litters derived from *Mtrr*^{+/*gt*} females (e.g., *Mtrr*^{+/*+*} and *Mtrr*^{+/*gt*} conceptuses result from these matings). Therefore, the size of implantation sites and conceptuses were largely unaffected by grandpaternal or maternal *Mtrr* genotype at E6.5. Overall, these data suggest that fetal growth restriction occurs after E6.5. Furthermore, other physiological differences in factors that comprise the ‘maternal environment’ might be disrupted by the *Mtrr*^{*gt*} mutation to cause the growth defects in their offspring. For instance, folate has been associated with thyroid stimulating hormone (Lippi et al. 2008). Specifically, folic acid supplementation in adolescent rats led to suppression of thyroid hormone function (Sittig et al. 2012). Clinical hypothyroidism has been associated with FGR (Tong et al. 2016).

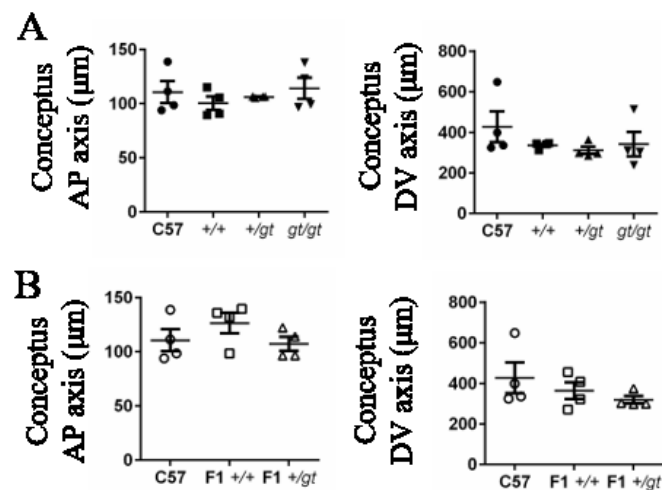


Figure 4.5 Analysis of growth restriction at E6.5.

(A-B) Graphs depicting the average lengths of the conceptuses in implantation sites of females derived from (A) *Mtrr*^{+/*gt*} intercrosses or (B) *Mtrr*^{+/*gt*} fathers. AP: anterior-posterior axis, DV: dorsal-ventral axis. Data are presented as mean ± SEM. n=4 implantation sites per maternal genotype. Statistical analysis: One-way ANOVA.

4.3 Discussion

We assessed the effects of intrinsic and paternal abnormal folate metabolism on gross decidual structure and expression of decidual markers at GD6.5. We did not observe any structural defects in the decidua, however the expression of some decidual markers was disrupted by an intrinsic or parental *Mtrr*^{*gt*} mutation. This suggests that decidualisation could be affected after GD6.5.

Our study revealed that there is a decrease in *Pgr* mRNA in implantation sites of *Mtrr* females with one or two *Mtrr^{gt}* alleles. Progesterone and its receptor regulate decidualisation by the activation of cascade reactions (Kurihara et al. 2007; Large & DeMayo 2012). Progesterone induces stromal cell differentiation (Li et al. 2007). Activation of PGR in the uterine epithelium induces activation of *Ihh*, which in turn activates *Nr2f2* in the uterine stroma. *Nr2f2* mRNA was decreased in females derived from *Mtrr^{+gt}* intercrosses with at least one *Mtrr^{gt}* allele, which correlates with *Pgr* mRNA levels. Interestingly, even though *Pgr* mRNA was decreased in F1 *Mtrr^{+gt}* females, *Nr2f2* levels were normal, suggesting a compensatory mechanism that restores *Nr2f2* expression in females with an *Mtrr^{+gt}* father only. *Nr2f2* activation leads to upregulation of *Bmp2* and possibly *Hand2* (Li et al. 2007; Okada et al. 2014). We observed decreased expression of *Bmp2* and normal expression of *Hand2* in all the *Mtrr* females assessed. This suggests that the *Bmp2*, but not *Hand2* signalling pathway is affected by abnormal *Pgr* mRNA expression. Interestingly though, wildtype females from both pedigrees had normal *Pgr* mRNA but decreased *Bmp2* mRNA expression, suggesting dysregulation of *Bmp2* expression by other factors, such as *Egfr* (Large et al. 2014) is possible. Analysis of PGR and BMP2 protein levels is required. PGR activation in the uterine stroma also activates *Hoxa10* expression (Kurihara et al. 2007; Large & DeMayo 2012). *Hoxa10* regulates progesterone responsiveness of uterine stromal cells, and therefore is important during implantation and decidualisation (Lim, Ma, et al. 1999). *Hoxa10* mRNA expression was normal in all *Mtrr* females assessed, except F1 *Mtrr^{+gt}* females, compared to C57Bl/6 controls, suggesting an alternative mechanism of *Hoxa10* mRNA expression, independent of PGR signalling. In the case of F1 *Mtrr^{+gt}* decidua at GD6.5, decreased *Hoxa10* mRNA expression might suggest that uterine stromal cells are less responsive to progesterone thus impairing decidualisation. In addition, *Hoxa10* expression is known to be regulated by methylation (Wu et al. 2005). We observed global DNA hypomethylation in the adult non-pregnant uteri in *Mtrr^{+gt}* and *Mtrr^{gt/gt}* females (Padmanabhan et al. 2013), suggesting that altered DNA methylation levels of *Hoxa10* promoter might alter gene expression. It is therefore possible that *Hoxa10* is hypomethylated also in the pregnant uteri and decidual tissues. However, others showed that dietary folate deficiency did not affect *Hoxa10* promoter methylation or mRNA expression levels in endometrial tissues of pseudopregnant mice (Long et al. 2012).

Whether there is a link between *Pgr* mRNA and *Cdh1* mRNA levels remains unclear, although some suggest that progesterone can induce the expression of *Cdh1* during embryo

implantation (Jha et al. 2006). Additionally, neither *Pgr* nor *Cdh1* mRNA expression at GD4.5 has been affected by a folate-deficient diet (Gao et al. 2012b). We observed decreased *Cdh1* mRNA expression in *Mtrr*^{+/*gt*} and *Mtrr*^{gt/*gt*} females at GD6.5, which correlates with *Pgr* mRNA levels. However, we did not observe decreased *Cdh1* expression in F1 *Mtrr*^{+/*gt*} females, even though *Pgr* mRNA levels were decreased. Decreased expression of *Cdh1* mRNA in *Mtrr*^{+/*gt*} and *Mtrr*^{gt/*gt*} uteri can prevent the establishment of proper signalling pathways in the uterus (Gradilla et al. 2018).

Folate deficiency was previously shown to decrease apoptosis of decidual cells at GD6.5, at the time of decidual regression initiation (Liao et al. 2015). This supports our finding of increased decidual size in the implantation sites of F1 *Mtrr*^{+/*+*} conceptuses at GD6.5, although analysis of apoptosis by immunohistochemistry using anti-Caspase 3 antibody is required. Further analysis is required to determine the distinct populations of cells in the maternal decidua and relate the decrease in cell density to their function. Staining the implantation sites with PAS and DBA (Chen et al. 2012) will determine the uterine natural killer (uNK) cell population. Uterine NK cells regulate SAR and trophoblast invasion, therefore have a role in placental function (Gaynor & Colucci 2017; Soares et al. 2014). The spiral arteries are high-resistance, low-flow vessels, and they are remodelled into low-resistance, high-flow during SAR. During this process, uNK cells induce vascular smooth muscle cells apoptosis or migration, leading to decreased vessel contractility, and prime the vessel for remodelling (Cartwright et al. 2010). Failure to transform the spiral arteries leads to reduced capability of meeting the nutritional demands of the developing fetus, leading to FGR (Lyall, Robson & Bulmer 2013). In addition, flow cytometry could be performed to assess all the decidual cell populations, including uNK cells, macrophages, cytotoxic T cells, dendritic cells, *Ptprc*⁺ (CD45⁺), and innate lymphoid cells (Mori et al. 2016). SAR is dependent on uNK cells (Gaynor & Colucci 2017), therefore abnormal uterine cell populations might affect this process, ultimately causing FGR.

Bmp2 mRNA expression, which is required for decidualisation, was reduced in uterine tissues at day 8 of pseudopregnancy in mice fed a folate-deficient diet where decidualisation was artificially induced, by intraluminal infusion of sesame oil, compared to normal-fed mice (Geng et al. 2015). Accordingly, a downregulation of *Bmp2* mRNA expression was observed in implantation sites of all the *Mtrr* females compared to C57Bl/6. *Bmp2* regulates the transformation of the endometrial stromal cells into epithelioid decidual cells (Lee et al.

2007), therefore decreased *Bmp2* expression in the *Mtrr* uteri could indicate abnormal transformation of endometrial stromal cells. Abnormal transformation of stromal cells leads to impaired formation of the decidua tissue, and ultimately altered transfer of nutrients to the fetus causing FGR. However, in the *Mtrr^{gt}* model we did not observe any gross morphological abnormalities in the decidua tissue, suggesting that *Bmp2* likely affects the decidualisation reaction after GD6.5.

Overall, we showed here that intrinsic and paternal abnormal folate metabolism affect the decidualisation reaction at the molecular level. Whether only one or both parents have abnormal folate metabolism is important, since a maternal *Mtrr^{gt}* allele seems to have a protective effect on *Hoxa10* expression, while a paternal *Mtrr^{gt}* allele seems to have a protective effect on *Cdh1* and *Nr2f2* mRNA expression. One parental *Mtrr^{gt}* allele is sufficient to alter *Bmp2* expression, while an intrinsic *Mtrr^{gt}* allele is sufficient to alter *Pgr* expression. It is possible, that even though embryo growth was normal at E6.5, the growth defects observed in the *Mtrr* model at E10.5 are due to abnormal decidualisation reaction as early as GD6.5.

Chapter 5: The effects of intrinsic abnormal folate metabolism on the placental transcriptome at E10.5

The RNA sequencing was performed by the Cambridge Genomic Services, Department of Pathology. The bioinformatic analysis of the RNA sequencing was performed by Dr. Malwina Prater, Dr. Xiaohui Zhao, and Dr. Russell Hamilton.

5.1 Introduction

We previously showed that the growth phenotypes observed in the F2 *Mtrr*^{+/+} conceptuses derived from an *Mtrr*^{+/gt} maternal grandparent are due to the abnormal uterine environment of their *Mtrr*^{+/+} mothers (Padmanabhan et al. 2013). Furthermore, global DNA hypomethylation and dysregulation of locus-specific DNA methylation were observed in placentas of *Mtrr*^{gt/gt} and F2 *Mtrr*^{+/+} conceptuses at E10.5 (Padmanabhan et al. 2013). These changes were associated with gene misexpression. Interestingly, altered DNA methylation was only observed in placentas and not in the associated embryos, suggesting a placenta-specific effect (Padmanabhan et al. 2013). Therefore, we wanted to determine the extent to which the *Mtrr*^{gt} mutation alters the placental transcriptome in the *Mtrr*^{gt/gt} conceptuses and in the F2 *Mtrr*^{+/+} grandprogeny derived from an *Mtrr*^{+/gt} maternal grandfather. Furthermore, we aimed to determine whether providing a new uterine environment to the F2 *Mtrr*^{+/+} generation by way of an embryo transfer experiment, normalises the placental transcriptome at E10.5.

5.2 Results

To examine the effects of intrinsic and ancestral abnormal folate metabolism on the placental transcriptome, RNA from placentas at E10.5 was sequenced. We also considered whether conceptuses with growth phenotypes caused by the *Mtrr*^{gt} mutation had an altered placental transcriptome. To assess the effects of intrinsic abnormal folate metabolism on placental transcriptome, we extracted RNA from placental samples of phenotypically normal and growth restricted *Mtrr*^{gt/gt} conceptuses (Figure 2.1C). To assess the effects of maternal grandpaternal *Mtrr*^{gt} mutation on placental gene expression of their wildtype grandprogeny, RNA from placentas of phenotypically normal and growth enhanced F2 *Mtrr*^{+/+} conceptuses derived from an *Mtrr*^{+/+} mother and an *Mtrr*^{+/gt} maternal grandfather was analysed (Figure 2.1E). In both experiments, RNA from normal C57Bl/6 placentas at E10.5 was used as a control. Finally, to understand whether transcriptional changes caused by ancestral *Mtrr* deficiency could be normalised, we assessed the placental transcriptome of phenotypically normal and growth enhanced F2 *Mtrr*^{+/+} conceptuses at E10.5 derived from an *Mtrr*^{+/gt} maternal grandfather that were transferred into the uterus of a normal recipient female at E3.0 (Padmanabhan et al. 2013; Figure 2.1G). The placentas of normal C57Bl/6 transferred conceptuses were used as control in this experiment (Figure 2.1F). All placentas analysed

were from male conceptuses to avoid any discrepancies in the transcriptome that might be due to sexual dimorphism (Clifton 2010; Gallou-Kabani et al. 2010).

5.2.1 RNA quality control

RNA was isolated from placental samples of male conceptuses at E10.5 of the pedigrees and growth phenotypes mentioned above and sequenced (initially n=4 placentas per category, 32 samples in total). First, the integrity and overall quality of total RNA was performed by running the samples on an RNA gel (Figure 5.1A). Ribosomal RNA, which represents more than 80% of total RNA and is comprised of the 28S and 18S subunits, is represented by two bands on the RNA gel, and suggests good overall quality of the samples. The sample quality was excellent, with sample absorbance peaks around 260 nm (Figure 5.1B) and a minimum RNA integrity number of 8.2 (Figure 5.1C). A minimum RNA integrity number of 8.0 is considered sufficient and suitable for RNA sequencing. The RNA library preparation and sequencing were performed by the Cambridge Genomic Services, as described in Section 2.10.

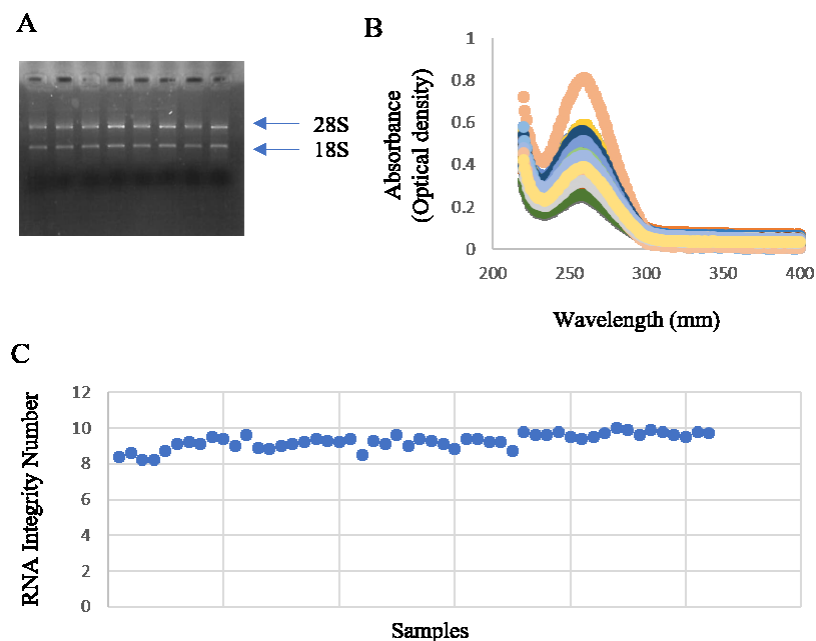


Figure 5.1 RNA sample quality control.

(A) A representative RNA gel, showing the 18S and 28S rRNA bands. (B) Absorbance spectrum of the RNA samples, showing a peak at 260nm. (C) RNA Integrity number (RIN) of all RNA samples sequenced.

5.2.2 Quality control of RNA sequencing data

Before bioinformatics analysis of the RNA sequencing data, we performed a data quality control analysis using MultiQC (Ewels, Lundin & Max 2016; Figure 5.2). First, a FastQ Screen was performed to align the sequences to known genomes. In all samples, at least 85% of the sequences were aligned to the mouse genome, as expected. Less than 15% were aligned to multiple genomes, and the rest gave no hits (Figure 5.2A) suggesting a successful sequencing run. Next, the genomic origin of the sequenced reads was determined. Around 65% of the reads were aligned to exonic sequences, 10% to intronic, and 25% to intergenic regions (Figure 5.2B). The presence of intronic sequences in the samples might be a result of unspliced mRNA. The Phred Score, which is a measure of the probability that a given base is called incorrectly by the sequencer and therefore, estimates the sequencing quality, was calculated. The Phred Score per base and read counts was above 30, suggesting that the individual sequence reads and mean sequencing were of good quality (Figure 5.2C-D). The percentage of the GC content per sequence was calculated and showed mean %GC content between 40% and 60%, which is the optimal GC content (Figure 5.2E). Finally, the base N content, which is the percentage of cases in which the sequencer was unable to call a base correctly, and therefore assigned an N base, was calculated to be less than 0.5%, suggesting sufficient confidence in more than 99.5% of the bases (Figure 5.2F). Therefore, the RNA sequencing data was of good quality, and we were confident to proceed to bioinformatic analysis.

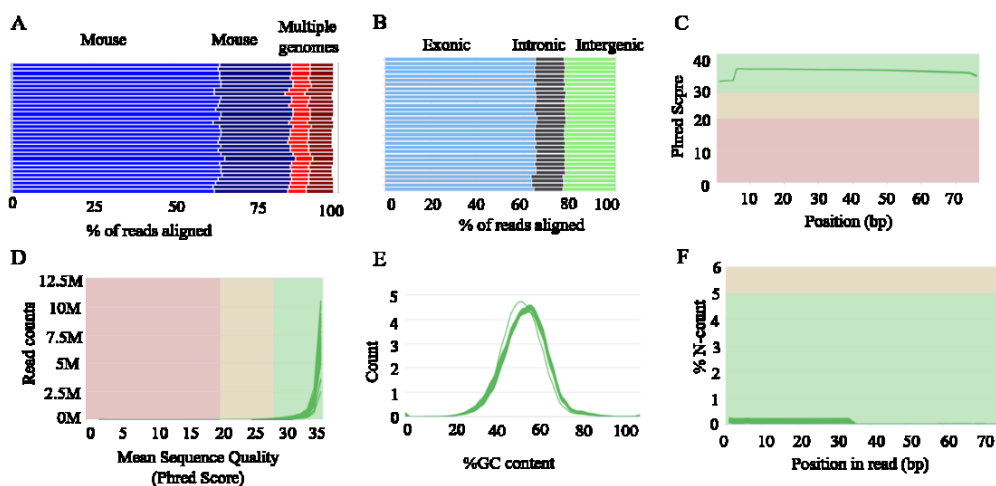


Figure 5.2 RNA sequencing data quality control.

(A) Percentage of the RNA sequencing reads aligned to mouse and other genomes. (B) Percentage of reads aligned to exonic, intronic, and intergenic regions. (C) Phred score along

the RNA sequencing read (which is approximately 75bp long). (D) Phred score per read counts. (E) Percentage of the GC content in each read. (F) Percentage of an unknown base along the sequence read.

5.2.3 Sample RNA largely clusters based on their experimental group

To understand whether the samples clustered together based on their transcriptomes, we created a Principal Component Analysis (PCA) plot based on the 500 most variably expressed genes. The first principal component (PC1), which is on the x-axis, is the direction at which the samples show the highest variation, while the second principal component (PC2), which is on the y-axis, is the direction at which the samples show the second highest variation (Ringnér 2008). We observed that the blastocyst transfer experiment is the factor that caused the highest variation in gene expression. Placentas from non-transferred conceptuses clustered on the left-hand side of the PCA plot, while the placentas from transferred conceptuses clustered on the right-hand side (Figure 5.3). Therefore, the variation in the PC1 represents the blastocyst transfer process. In addition, we observed that the RNA samples clustered by growth phenotype. For instance, placentas of growth enhanced conceptuses clustered at the bottom of the PCA plot, both in the transferred and non-transferred groups. The phenotypically normal conceptuses clustered in the middle of the plot, except for three *Mtrr^{gt/gt}* placentas (black arrows in Figure 5.3) that clustered closer to the placentas of growth restricted *Mtrr^{gt/gt}* conceptuses than to the phenotypically normal C57Bl/6 or F2 *Mtrr^{+/+}* non-transferred conceptuses. However, the placentas of growth restricted *Mtrr^{gt/gt}* conceptuses cluster on the top of the PCA plot (Figure 5.3). One phenotypically normal F2 *Mtrr^{+/+}* transferred sample was an exception, since it clustered with the growth enhanced placentas (turquoise arrow in Figure 5.3). When considering the transferred samples, PC2 represents the growth phenotype.

The remainder of this chapter will focus on the analysis of *Mtrr^{gt/gt}* placentas. Further analyses of the F2 *Mtrr^{+/+}* placentas is presented and discussed in Chapter 6. We also identified that the embryo transfer procedure itself alters the placental transcriptome. Analysis of these data is also presented in Chapter 6.

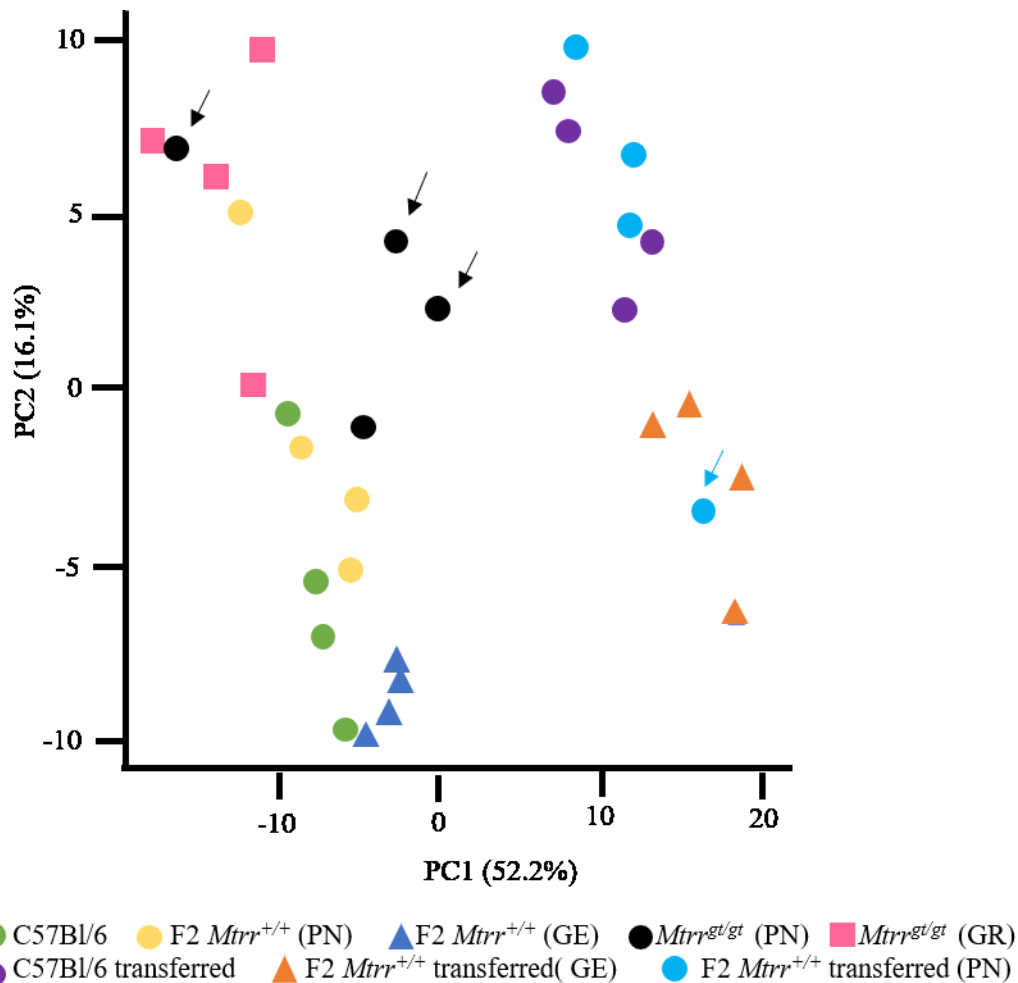


Figure 5.3 PCA plot of sequenced placenta samples.

Principal component analysis (PCA) based on the 500 most variable genes showing the clustering of whole male placentas according to their transcriptome. Green circle: C57Bl/6, yellow circle: F2 *Mtrr*^{+/+} (PN), blue triangle: F2 *Mtrr*^{+/+} (GE), black circle: *Mtrr*^{gt/gt} (PN), pink square: *Mtrr*^{gt/gt} (GR), purple circle: C57Bl/6 transferred, orange triangle: F2 *Mtrr*^{+/+} transferred (GE), blue circle: F2 *Mtrr*^{+/+} transferred (PN). Black arrows indicate the *Mtrr*^{gt/gt} samples that are variable, turquoise arrow indicates the outlier *Mtrr*^{+/+} placenta.

5.2.4 The *Mtrr*^{gt/gt} placentas are transcriptionally variable

Our analysis initially focused on *Mtrr*^{gt/gt} placentas. The cut-off p-value to consider a gene as differentially expressed was $p < 0.05$. Additionally, we set the cut-off fold change to two ($\log_2\text{foldchange}=1$; Table 5.1) to eliminate the genes that were differentially expressed with less than two folds in *Mtrr*^{gt/gt} placentas. This is because the higher the fold change, the more likely it is that the differential expression is of biological significance. MA plots, a heatmap, and lists of differentially expressed genes (DEGs) were created (Figure 5.4). The MA plot

plots the log-intensity ratios (M) versus the log-intensity averages (A). The x-axis shows the normalised read counts, while the y-axis shows the log₂fold-change. We identified only 10 DEGs (i.e., four down-regulated genes, six up-regulated genes) in the placentas of phenotypically normal *Mtrr^{gt/gt}* conceptuses compared to the C57Bl/6 control placentas (Figure 5.4A, Table 5.1). *Mtrr^{gt/gt}* placentas from growth restricted conceptuses were appreciably more affected. We identified 38 DEGs (i.e. six downregulated genes, thirty-two upregulated genes) in the placentas of growth restricted *Mtrr^{gt/gt}* conceptuses compared to the C57Bl/6 placentas (Figure 5.4B, Table 5.1). When the transcriptomes of placentas of phenotypically normal and growth restricted *Mtrr^{gt/gt}* conceptuses were compared, 20 DEGs were identified (i.e. four downregulated genes, 16 upregulated genes (Figure 5.4C, Table 5.1). Together, these data suggest that as the phenotype of *Mtrr^{gt/gt}* conceptuses becomes worse, their transcriptome is altered to a greater degree. However, fewer DEGs were identified than expected.

A heatmap representing fold change of gene expression shows that two *Mtrr^{gt/gt}* placentas have a higher fold change of expression of four genes: *Psca*, *Ang2*, *Adamdec1*, and *Ftl2-ps* compared to the other placentas (Figure 5.4D). These *Mtrr^{gt/gt}* placentas represent those that did not cluster with the others in the PCA plot (black arrows, Figure 5.3). In addition, there is no clear clustering of the samples based on their phenotype (dendrogram on left hand side, Figure 5.4D).

Table 5.1 The number of misexpressed placental genes at E10.5.

Comparison	C57Bl/6 Vs <i>Mtrr^{gt/gt}</i> (PN)		C57Bl/6 Vs <i>Mtrr^{gt/gt}</i> (GR)		<i>Mtrr^{gt/gt}</i> (PN) Vs <i>Mtrr^{gt/gt}</i> (GR)	
	Down in <i>Mtrr^{gt/gt}</i> (PN)	Up in <i>Mtrr^{gt/gt}</i> (PN)	Down in <i>Mtrr^{gt/gt}</i> (GR)	Up in <i>Mtrr^{gt/gt}</i> (GR)	Down in <i>Mtrr^{gt/gt}</i> (GR)	Up in <i>Mtrr^{gt/gt}</i> (GR)
1.5<fc<2	72	165	147	320	37	124
fc>2	4	6	6	32	4	16

PN: phenotypically normal, GR: growth restricted, FC: fold-change

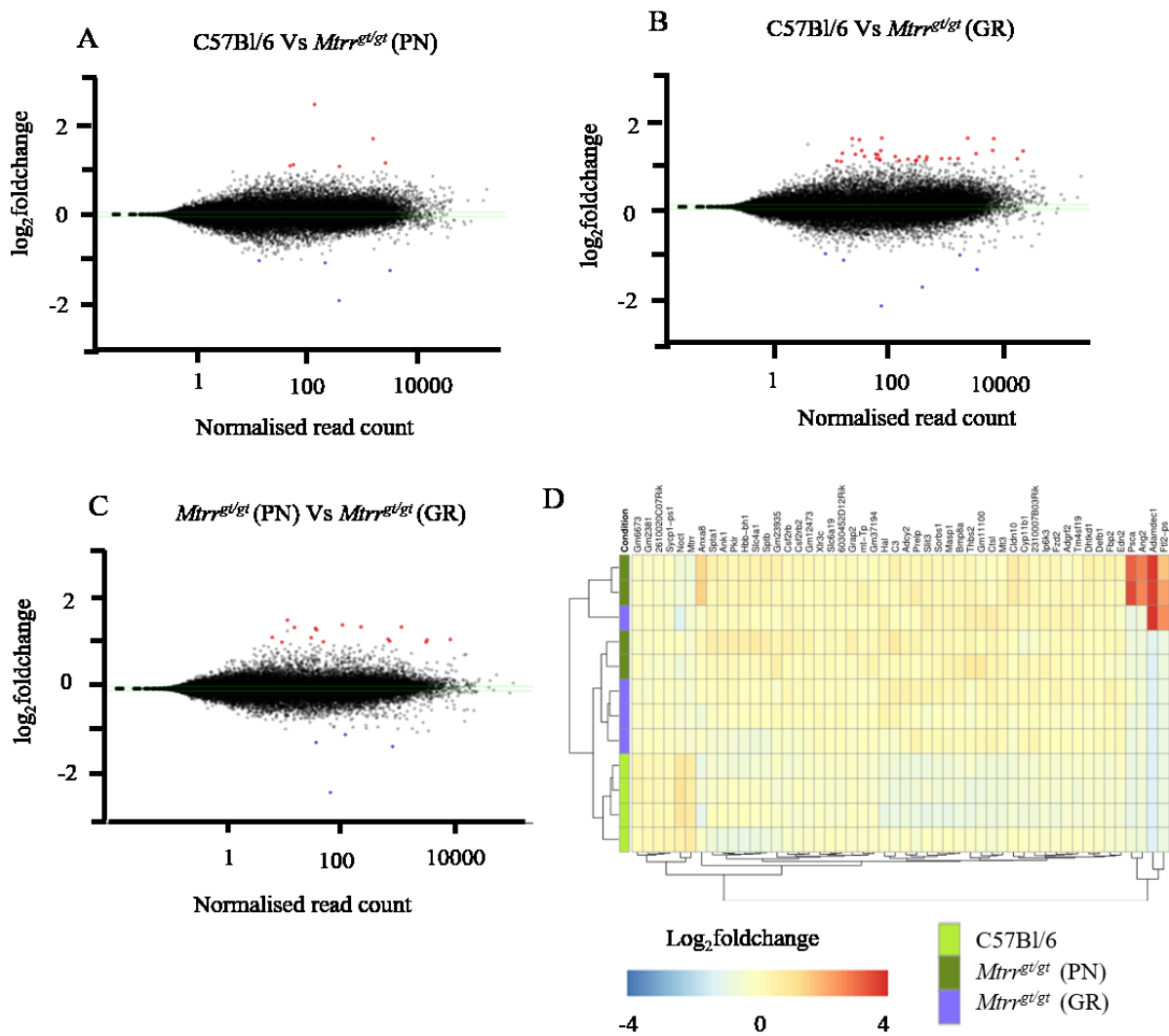


Figure 5.4 Degree of differential gene expression in *Mtrr^{g/gt}* placentas at E10.5 depends on growth phenotype.

(A-C) MA plots showing differential gene expression between (A) placentas of C57Bl/6 and phenotypically normal *Mtrr^{g/gt}* conceptuses, (B) placentas of C57Bl/6 and growth restricted *Mtrr^{g/gt}* conceptuses and (C) placentas of phenotypically normal and growth restricted *Mtrr^{g/gt}* conceptuses (D) Heatmap showing the 50 most variable genes in phenotypically normal (PN, dark green) and growth restricted (GR, purple) *Mtrr^{g/gt}* placentas compared to C57Bl/6 (light green) placentas at E10.5. Each column represents one gene. Each row represents an individual placenta. Degree of gene expression change: red, up-regulated; blue, down-regulated; yellow, no change.

To validate the RNA sequencing experiment via RT-qPCR, we used placentas from phenotypically normal *Mtrr^{g/gt}* conceptuses and compared them to the C57Bl/6 controls. For each group, we used up to four placentas that were sequenced, in addition to up to eight new

placentas (Figure 5.5). Ten genes with at least 1.5-fold change in expression were validated. Considering that only C57Bl/6 and phenotypically normal *Mtrr*^{gt/gt} samples were available for validation, and only ten genes were differentially expressed between them, we chose to also validate genes with at least 1.5-fold change, due to unavailability of specific primers for some of the genes with a 2-fold change. While all four downregulated genes in *Mtrr*^{gt/gt} placentas validated (Figure 5.5A), none of the upregulated genes validated (Figure 5.5B). *Polr2a* was used as a reference gene, since its expression was shown to remain constant in the placenta throughout gestation (Solano et al. 2016). As expected, *Mtrr* gene expression was reduced in all *Mtrr*^{gt/gt} placentas compared to C57Bl/6. Interestingly, *Slit3* mRNA was downregulated in *Mtrr*^{gt/gt} placentas, which contradicts the RNA sequencing data (p=0.02; Figure 5.5B). This might be due to the large variability in *Slit3* mRNA expression in the C57Bl/6 placentas that underwent RNA-sequencing (Figure 5.5B). Furthermore, the expression of *Anxa8* and *Psca* mRNA was higher in two of the sequenced *Mtrr*^{gt/gt} samples as determined by RNA-sequencing (Figure 5.4D) and RT-qPCR analysis (Figure 5.5B). Since the total validation success was only 40%, and we observed a high degree of variability in gene expression in the sequenced samples, this suggested to us that more samples should be sequenced.

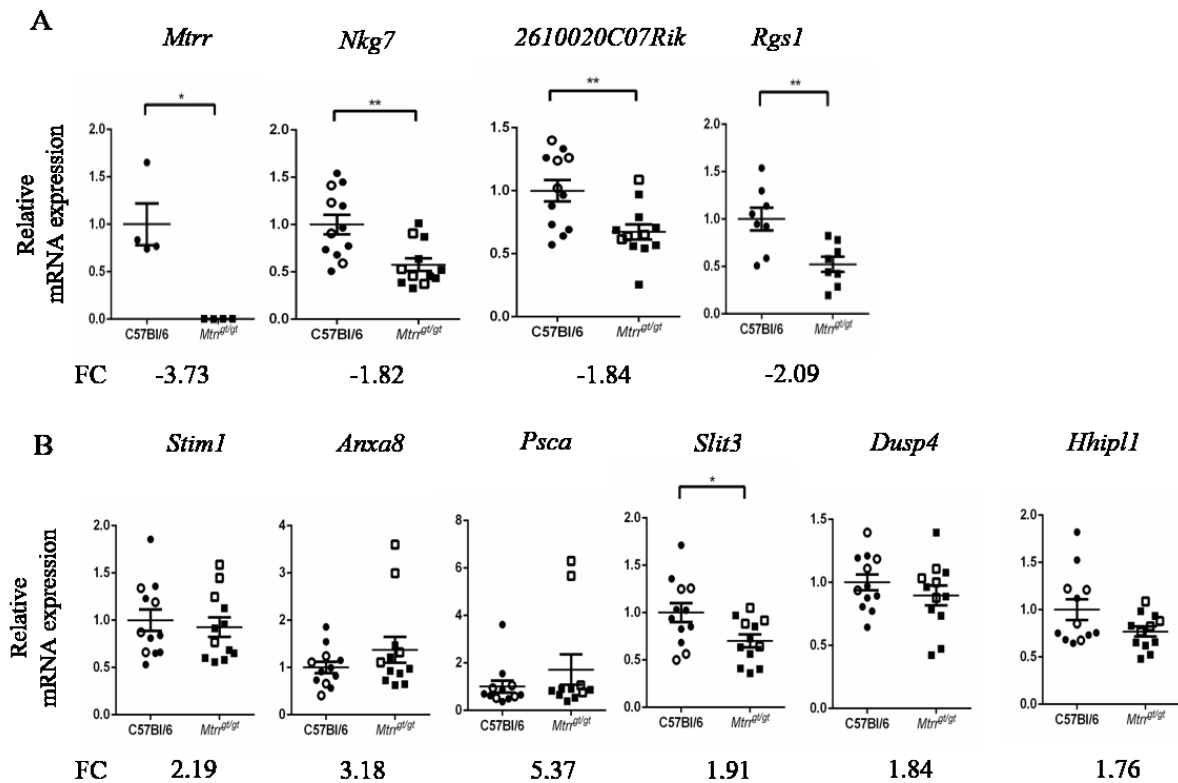


Figure 5.5 Validation of RNA-sequencing data by RT-qPCR analysis.

Graphs show transcripts that were (A) downregulated and (B) upregulated in the placentas of phenotypically normal *Mtrr^{gt/gt}* conceptuses (squares) compared to the C57Bl/6 (circles). Sequenced (hollow shapes) and non-sequenced (full shapes) samples were used. Data are presented as fold change compared to controls (normalised to 1). N=4-12 placental samples per genotype. The number below each graph represents the fold change (FC) observed in the RNA-sequencing experiment. Unpaired t tests with Welch correction or Mann-Whitney tests, where appropriate, were performed to independently compare *Mtrr^{gt/gt}* placentas to control placentas. *P<0.05, **P<0.01.

Therefore, the RNA sequencing experiment was repeated to increase the sample size.

Placentas from phenotypically normal conceptuses (N=10 placentas) and growth restricted *Mtrr^{gt/gt}* conceptuses (N=3 placentas) were considered. Considering that the abnormal uterine environment causes growth phenotypes (Padmanabhan et al. 2013), we have sequenced samples from thirteen different *Mtrr^{gt/gt}* litters, representing thirteen different maternal environments. An additional four C57Bl/6 placentas were also sequenced. To correct for batch effects between sequencing runs, one placental sample per genotype and phenotype group was re-sequenced.

After sequencing the new libraries, the data were combined with the sequencing data of the first experiment, giving us a total of eight C57Bl/6 placentas, fourteen placentas from phenotypically normal *Mtrr^{gt/gt}* conceptuses, and seven placentas from growth restricted *Mtrr^{gt/gt}* conceptuses. Data quality control showed that the data were of good quality (Figure 5.6). Batch effects corrections were performed and a PCA plot was created excluding only one C57Bl/6 outlier (not shown; Figure 5.7A). When more placental samples were included, phenotypic clustering of *Mtrr^{gt/gt}* placentas did not occur. However, both *Mtrr^{gt/gt}* placental groups tended to cluster separately from C57Bl/6, with a few exceptions (Figure 5.7A). Initially, without excluding any samples, MA plots, heatmaps, and the lists of DEG were created. As before, the cut-off fold change for differential expression was two ($\log_2\text{foldchange}=1$). Table 5.2 shows the number of DEGs per *Mtrr* genotype and phenotype.

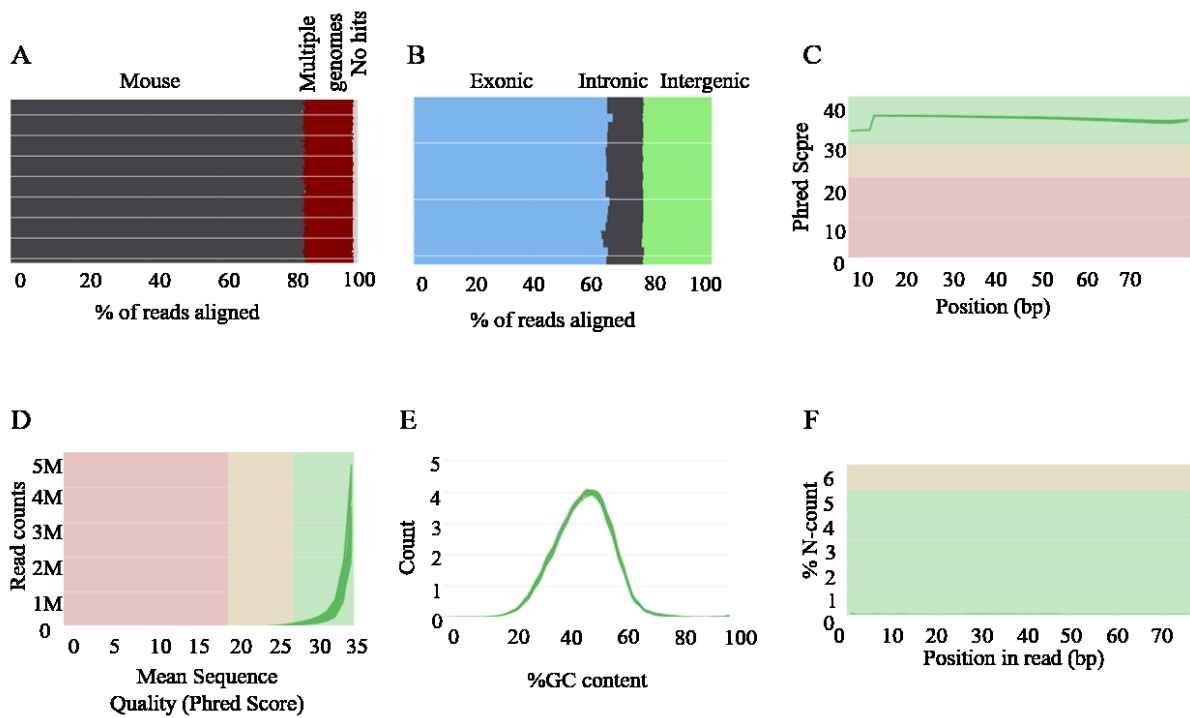


Figure 5.6 Data quality control for the second round of RNA sequencing.

(A) Percentage of the RNA sequencing reads aligned to mouse and other genomes. (B) Percentage of reads aligned to exonic, intronic, and intergenic regions. (C) Phred score along the RNA sequencing read. (D) Phred score per read counts. (E) Percentage of the GC content in each read. (F) Percentage of an unknown base along the sequence read.

Table 5.2 Number of DEGs per *Mtrr* genotype and phenotype.

Comparison	C57Bl/6 vs <i>Mtrr^{gt/gt}</i> (PN)		C57Bl/6 vs <i>Mtrr^{gt/gt}</i> (GR)		<i>Mtrr^{gt/gt}</i> (PN) vs <i>Mtrr^{gt/gt}</i> (GR)	
	Down in <i>Mtrr^{gt/gt}</i> (PN)	Up in <i>Mtrr^{gt/gt}</i> (PN)	Down in <i>Mtrr^{gt/gt}</i> (GR)	Up in <i>Mtrr^{gt/gt}</i> (GR)	Down in <i>Mtrr^{gt/gt}</i> (GR)	Up in <i>Mtrr^{gt/gt}</i> (GR)
2<fc<4	15	22	53	38	1	0
4<fc<11	6	3	24	3	0	0
Total	21	25	77	41	1	0

PN: phenotypically normal, GR: growth restricted, FC: fold-change

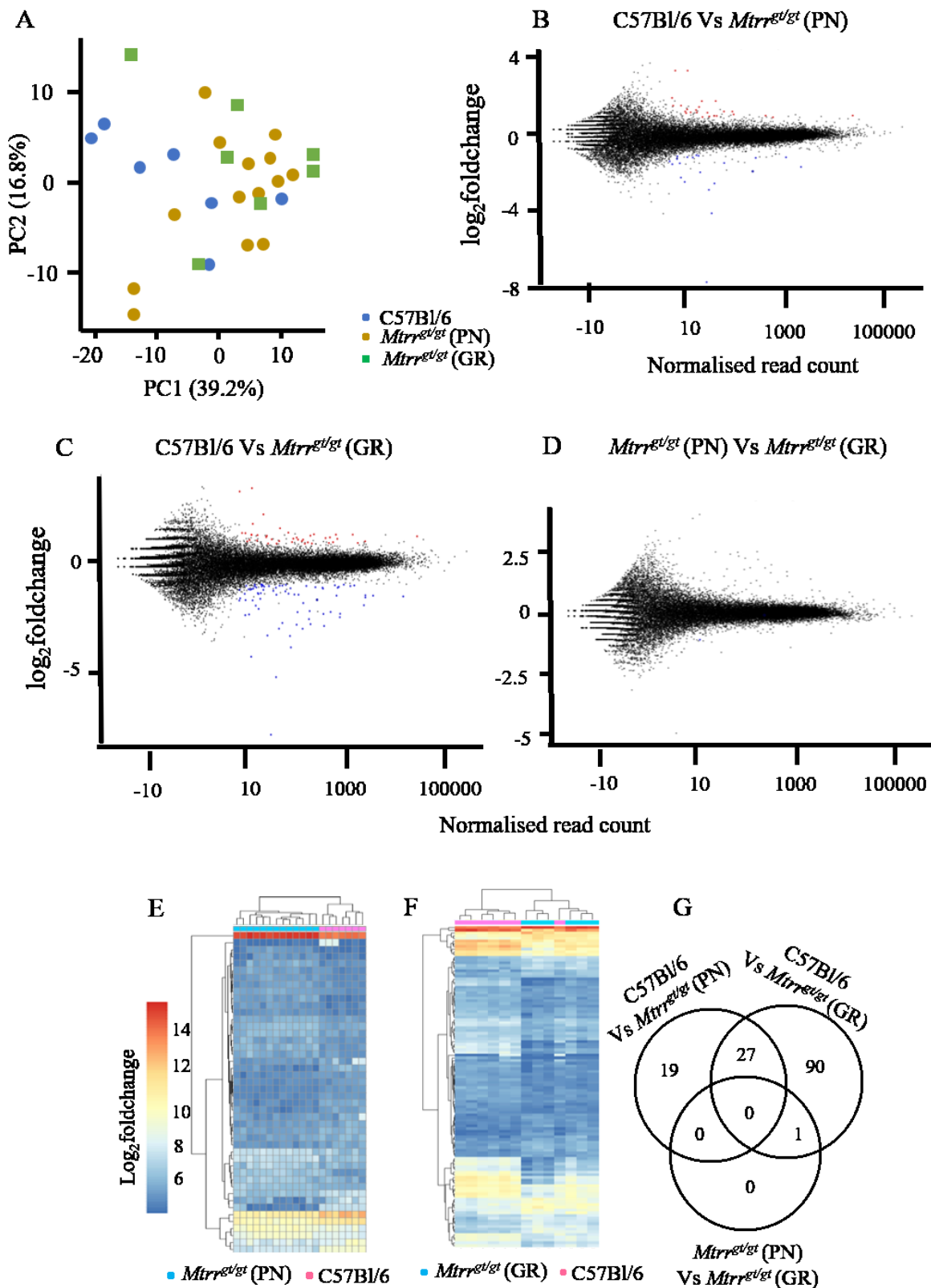


Figure 5.7 Bioinformatic analysis of data from the second RNA sequencing experiment. (A) PCA plot based on the 500 most variable genes in the C57Bl/6 and *Mtrr^{g1/g1}* samples. Blue circles: C57Bl/6 placentas; green squares: growth restricted (GR) *Mtrr^{g1/g1}* placentas; gold

circles: phenotypically normal (PN) *Mtrr^{gt/gt}* placentas. (B-D) MA plots showing differential gene expression between placentas of (B) C57Bl/6 and phenotypically normal *Mtrr^{gt/gt}* conceptuses, (C) C57Bl/6 and growth restricted *Mtrr^{gt/gt}* conceptuses and (D) phenotypically normal and growth restricted *Mtrr^{gt/gt}* conceptuses. (E-F) Heatmaps showing differential gene expression between placentas of (E) C57Bl/6 and phenotypically normal *Mtrr^{gt/gt}* conceptuses, and (F) C57Bl/6 and growth restricted *Mtrr^{gt/gt}* conceptuses. Each column represents an individual placenta. Each row represents one gene. (G) Venn diagram comparing the DEG numbers between the three comparisons.

In the dendrogram above each heatmap, a separation in clustering between the C57Bl/6 controls and *Mtrr^{gt/gt}* placentas was largely observed (Figure 5.7E-F). No heatmap was created to compare the placental transcriptome of phenotypically normal and growth restricted *Mtrr^{gt/gt}* conceptuses, since only one gene was differentially expressed between the two groups. Interestingly, we identified 27 genes (*Eps811*, *Slc5a4b*, *Dlx4*, *Fbp2*, *Ctsl*, *Adcy2*, *Noct*, *St8sia2*, *Iqcm*, *Mt3*, *Heph11*, *Cdc14b*, *Mtrr*, *Gbp2b*, *Vat11*, *Ube2ql1*, *Cbx7*, *Xlr3c*, *Khdc1a*, *Fbp1*, *Zfp429*, *Zfp456*, *Gm6673*, *Gm10251*, *Gm16907*, *Gm9522*, and *Gm43305*) that were similarly differentially expressed between C57Bl/6 and *Mtrr^{gt/gt}* placentas regardless of phenotype (Figure 5.7G). Altogether, these data suggest that the placental transcriptomes of phenotypically normal and growth restricted *Mtrr^{gt/gt}* conceptuses are similar.

5.2.5 Improving the stringency of the *Mtrr^{gt/gt}* RNA-sequencing dataset

Given that a few DEGs were identified when comparing the placental transcriptomes of phenotypically normal and growth restricted *Mtrr^{gt/gt}* conceptuses, we assessed the PCA plots more closely. Using statistical methods (Conesa et al. 2016), we decided to exclude any potential outliers in order to obtain a more stringent dataset. First, a PCA plot was created using all of the samples sequenced (Figure 5.8A). Within this PCA plot, there was a clear C57Bl/6 outlier which was excluded from future analysis (blue dot in red circle; Figure 5.8A). This sample was removed to avoid skewing the data. Further PCA plots were generated revealing seven *Mtrr^{gt/gt}* outliers and an additional C57Bl/6 outlier (Figure 5.8B-C), which were excluded from the final data. Another PCA plot was created using the remaining samples (Figure 5.8B). Here, we observed that the placenta from the growth restricted *Mtrr^{gt/gt}* conceptus shown as an orange dot in red circle clusters with the placentas of phenotypically normal conceptuses of the same pedigree. Even though the embryo is

characterised as growth restricted based on its crown-rump length, its placental weight was 0.0645g, which was higher than the average placental weight of the phenotypically normal ($0.04\pm 0.008\text{g}$) or the rest growth restricted conceptuses ($0.04\pm 0.001\text{g}$). This could suggest that the placenta is trying to compensate for the restricted growth of the embryo. Additionally, the phenotypically normal *Mtrr^{gt/gt}* sample shown as a purple dot in red circle clusters with the placentas of growth restricted conceptuses from the same pedigree. There were not any different features in this animal. However, these two samples were excluded from further analysis, to prevent skewing of the results. Another PCA plot was created (Figure 5.8C), showing that the placental sample from the growth restricted *Mtrr^{gt/gt}* conceptus shown as an orange dot in red circle clusters with the phenotypically normal samples. Even though the placenta and embryo weights, as well as the embryo:placenta weight ratio was similar to the other samples of this phenotypic group, this sample was excluded from further analysis. The three phenotypically normal *Mtrr^{gt/gt}* samples shown as purple dots in red circles were also outliers, based on their position on the PCA plot. Two of these samples were the same outliers identified in Section 5.2.4, and therefore were excluded from future analysis. The other phenotypically normal *Mtrr^{gt/gt}* sample that was excluded had 38 somite pairs. Although this is within the normal range for E10.5 conceptuses, this was higher than the rest of the conceptuses (33 ± 2 somite pairs). The final PCA plot (Figure 5.8D), shows all the samples used to perform differential gene expression analysis (n=6 C57Bl/6 placentas, n=9 phenotypically normal *Mtrr^{gt/gt}* placentas, n=5 growth restricted *Mtrr^{gt/gt}* placentas).

After excluding the outliers mentioned above, MA plots, heatmaps, and the lists of DEGs were created. The cut-off fold change to consider a gene differentially expressed was two ($\log_2\text{foldchange}=1$). Table 5.3 shows the number of DEGs identified when comparing C57Bl/6 and *Mtrr^{gt/gt}* placentas according to their fold change. The new MA plots show a larger number of DEGs when comparing C57Bl/6 placentas to *Mtrr^{gt/gt}* placentas (Figure 5.9A, Table 5.3). This included: 111 downregulated genes and 127 upregulated genes in the placentas of phenotypically normal *Mtrr^{gt/gt}* conceptuses compared to C57Bl/6 placentas (Figure 5.9A, Table 5.3) and 153 downregulated genes and 126 upregulated genes in the placentas of growth restricted *Mtrr^{gt/gt}* conceptuses compared to the C57Bl/6 placentas (Figure 5.9B, Table 5.3). Furthermore, we were more successful in identifying DEGs (23 down-regulated genes, 21 up-regulated genes) when comparing the placentas of growth restricted *Mtrr^{gt/gt}* conceptuses, to those of the phenotypically normal *Mtrr^{gt/gt}* conceptuses

(Figure 5.9C, Table 5.3). The dendrograms above the heatmaps show a clear separation of the C57Bl/6 and phenotypically normal *Mtrr^{gt/gt}* placentas (Figure 5.9D), and between the C57Bl/6 and growth restricted *Mtrr^{gt/gt}* placentas (Figure 5.9E). However, the placentas of

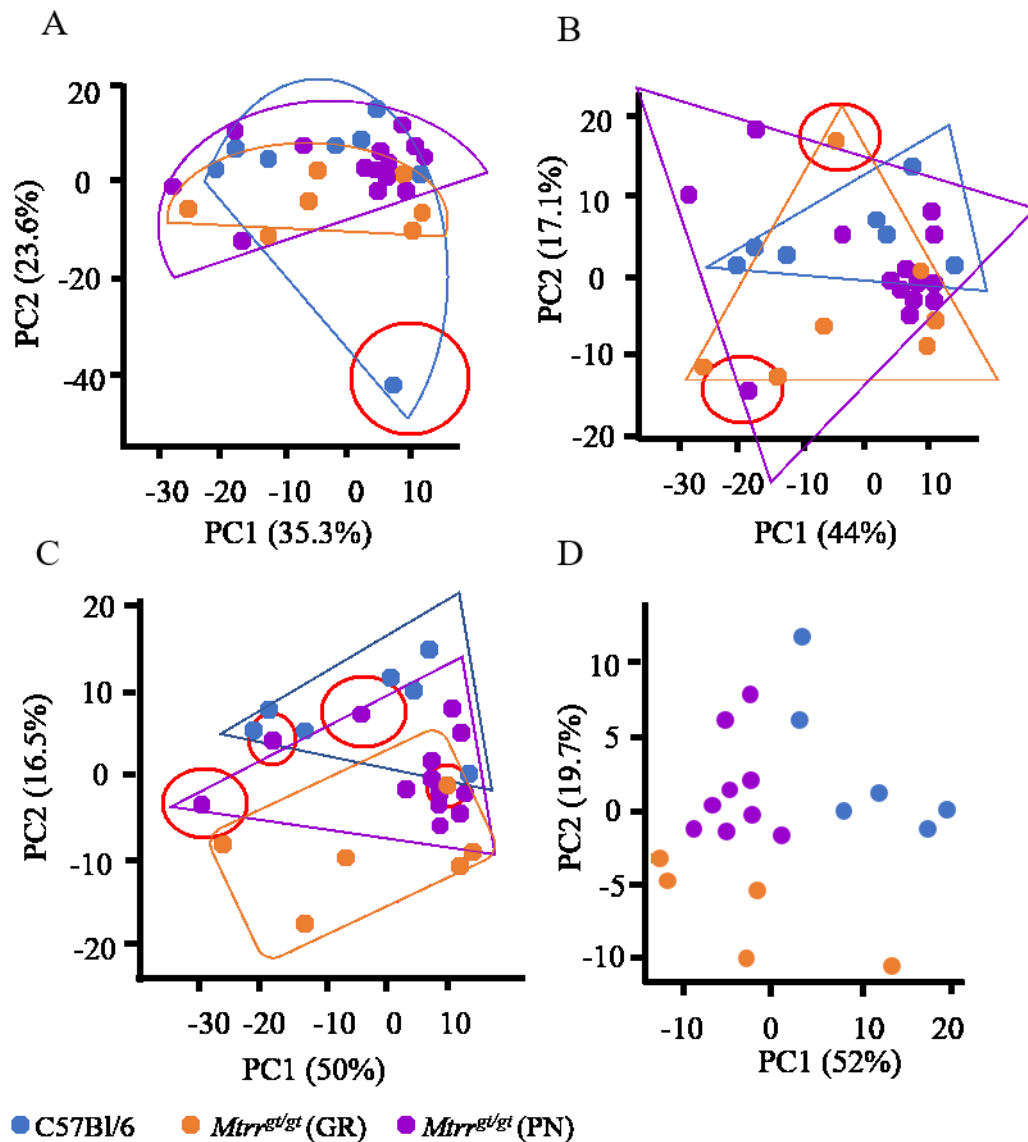
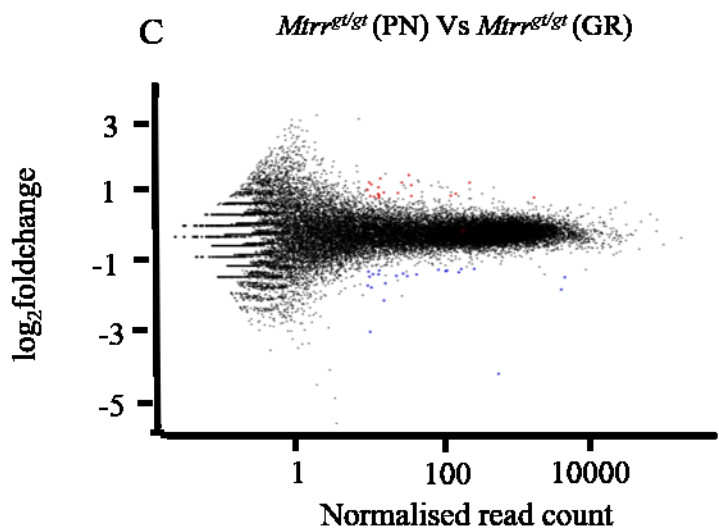
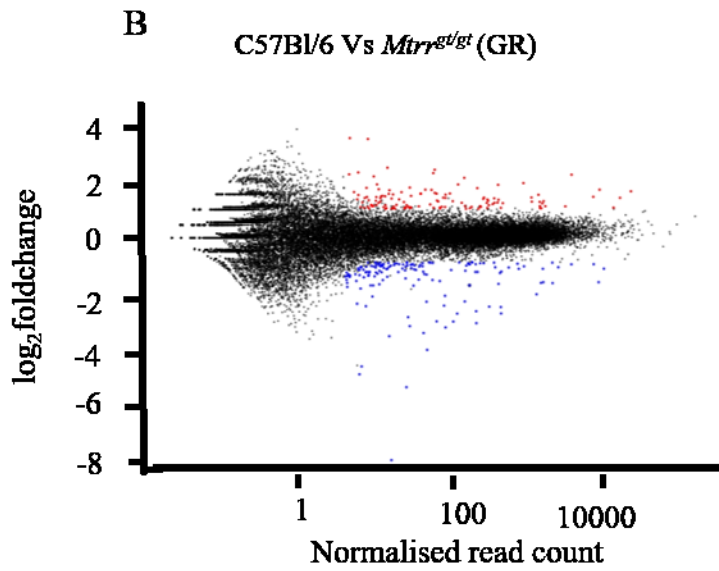
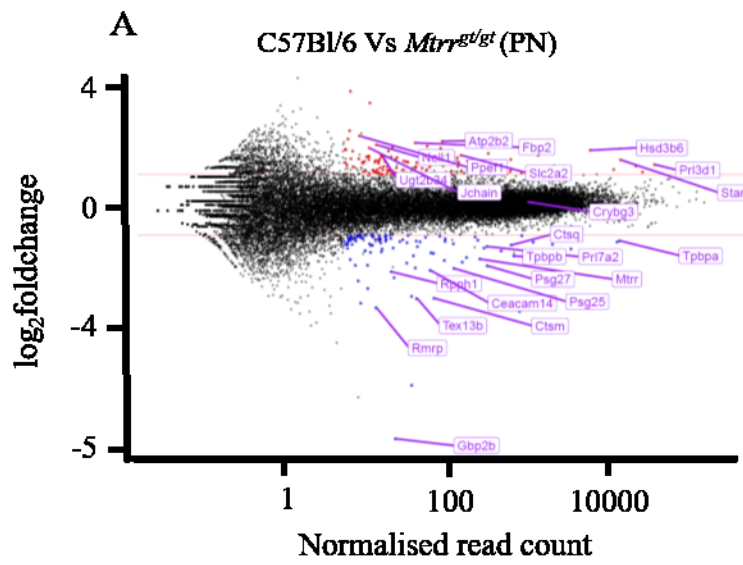


Figure 5.8 Principal component analysis plots used to exclude outliers.

(A) PCA plot based on the 500 most variable genes showing all the C57Bl/6 and *Mtrr^{gt/gt}* samples sequenced in two experiments. (B-D) Further PCA plots generated after removing outlier samples. Red lines indicate the samples removed; blue circles: C57Bl/6 placentas, purple circles: phenotypically normal (PN) *Mtrr^{gt/gt}* placentas; orange circles: growth restricted (GR) *Mtrr^{gt/gt}* placentas.



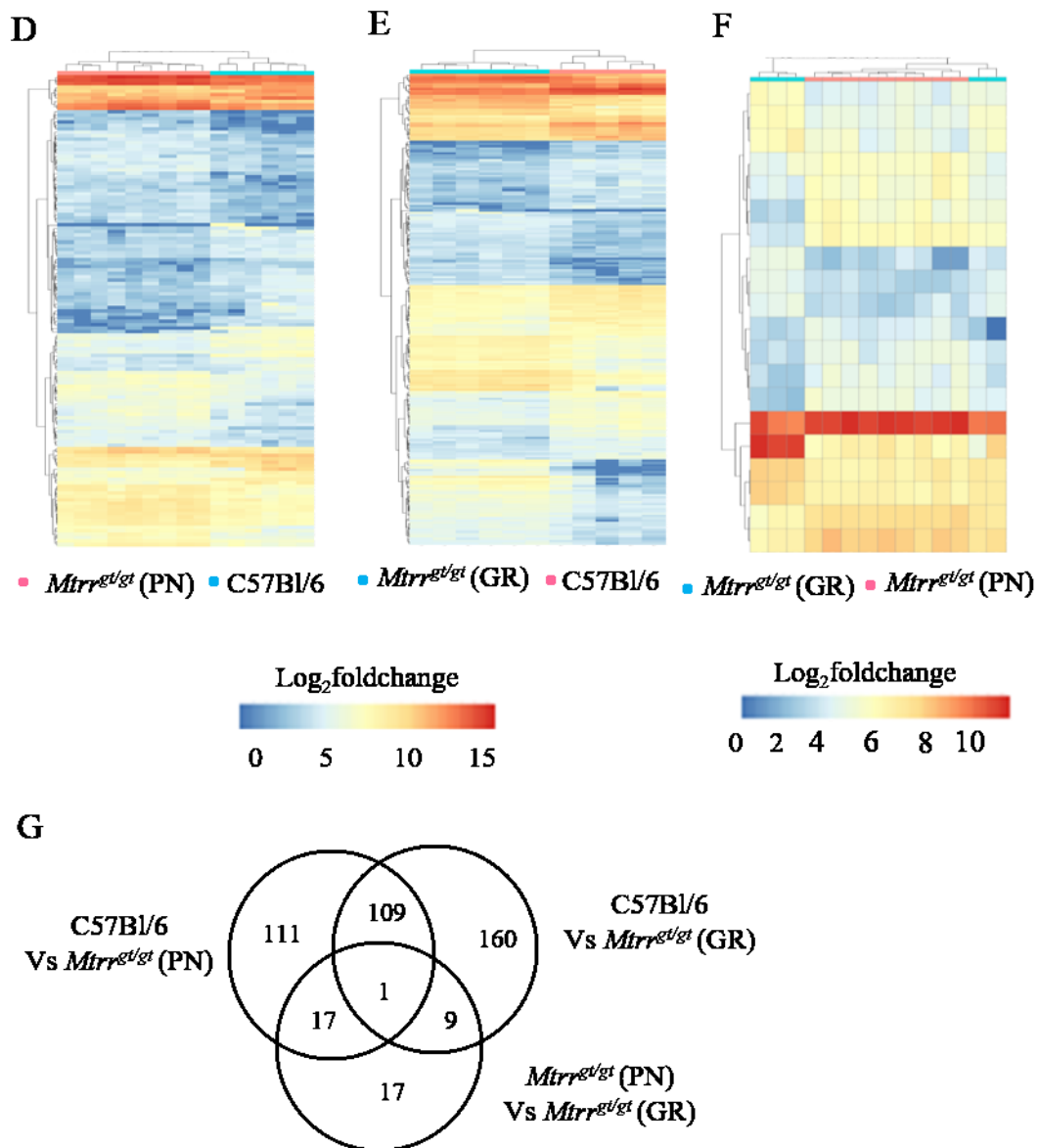


Figure 5.9 Bioinformatic analysis of the RNA sequencing data from placentas of C57Bl/6, and phenotypically normal (PN) and growth restricted (GR) *Mtrr^{gt/gt}* conceptuses.

(A-C) MA plots showing differential gene expression between placentas of (A) C57Bl/6 and phenotypically normal *Mtrr^{gt/gt}* conceptuses, (B) C57Bl/6 and growth restricted *Mtrr^{gt/gt}* conceptuses and (C) phenotypically normal and growth restricted *Mtrr^{gt/gt}* conceptuses. (D-F) Heatmaps showing DEGs between placentas of (D) C57Bl/6 (light blue) and phenotypically normal *Mtrr^{gt/gt}* (pink) conceptuses, (E) C57Bl/6 (pink) and growth restricted *Mtrr^{gt/gt}* (light blue) conceptuses and (F) phenotypically normal (pink) and growth restricted (light blue) *Mtrr^{gt/gt}* conceptuses. Each column represents an individual placenta. Each row represents one gene. (G) Venn diagram comparing the DEG between the three comparisons.

phenotypically normal *Mtrr^{gt/gt}* conceptuses cluster with the *Mtrr^{gt/gt}* placentas of growth restricted conceptuses (dendrogram above, Figure 5.9F). This, together with the fact that only 44 DEGs were identified suggest that there is only a minor difference between the placental transcriptomes of the two growth phenotypes.

Altogether, 109 DEGs were common between phenotypically normal and growth restricted *Mtrr^{gt/gt}* when compared to C57Bl/6 placentas. This suggests that these genes are disrupted due to *Mtrr* deficiency and are not likely associated with a growth phenotype. In addition, one gene (*Prl7a2*) was common in all three comparisons (Figure 5.9G).

Table 5.3 Number of DEGs in *Mtrr^{gt/gt}* placentas at E10.5 per *Mtrr* genotype and phenotype.

Comparison	C57Bl/6 vs <i>Mtrr^{gt/gt}</i> (PN)		C57Bl/6 vs <i>Mtrr^{gt/gt}</i> (GR)		<i>Mtrr^{gt/gt}</i> (PN) vs <i>Mtrr^{gt/gt}</i> (GR)	
	Down in <i>Mtrr^{gt/gt}</i> (PN)	Up in <i>Mtrr^{gt/gt}</i> (PN)	Down in <i>Mtrr^{gt/gt}</i> (GR)	Up in <i>Mtrr^{gt/gt}</i> (GR)	Down in <i>Mtrr^{gt/gt}</i> (GR)	Up in <i>Mtrr^{gt/gt}</i> (GR)
2<fc<3	80	98	107	100	19	20
3<fc<4	12	22	20	16	2	1
4<fc<12	17	6	19	8	1	0
fc>12	2	1	7	2	1	0
Total	111	127	153	126	23	21

PN: phenotypically normal, GR: growth restricted, FC: fold-change

RT-qPCR was performed for validation of the new RNA-seq experiment. The list of DEGs identified in phenotypically normal *Mtrr^{gt/gt}* placentas when compared to C57Bl/6 placentas was used for validation. Genes were selected for validation based on the fold change, and the specificity of the designed primers. Samples that were sequenced and new samples were used. The differential expression of eleven out of the 14 genes that were downregulated in the *Mtrr^{gt/gt}* placentas and analysed, reached statistical significance ($p < 0.05$; Figure 5.10), giving a rate of 78.6%. In contrast, the differential expression of none of the 10 genes that were upregulated in the *Mtrr^{gt/gt}* placentas reached statistical significance ($p > 0.05$; Figure 5.11). Some variability in gene expression was observed in placentas of both the C57Bl/6 and the *Mtrr^{gt/gt}* conceptuses. Even so, the results from the RNA-sequencing experiment were deemed to be robust and reliable, following validation. Next, we performed gene expression

correlation analysis between the RNA sequencing data and the qPCR results (Figure 5.12). We observed a weak positive linear relationship between the expression of downregulated genes in the RNA-seq and qPCR experiments ($r^2=0.2543$, $p=0.0659$; Figure 5.12A), and no relationship between the expression of upregulated genes ($r^2=0.0729$, $p=0.4506$; Figure 5.12B). It is important to note that the higher the read counts, the lower the variance. As a result, any differences in the expression of genes with higher read counts between C57Bl/6 and *Mtrr*^{gt/gt} placentas can be more reliably quantified. This suggests that the higher the read counts, the more reliable the RNA-seq data are. The genes used for validation are shown on the MA plot in Figure 5.9A. One possible reason that the differential expression of *Rmrp* and *Tex13b* did not reach statistical significance via qPCR is that low read counts of these genes were detected via RNA-seq.

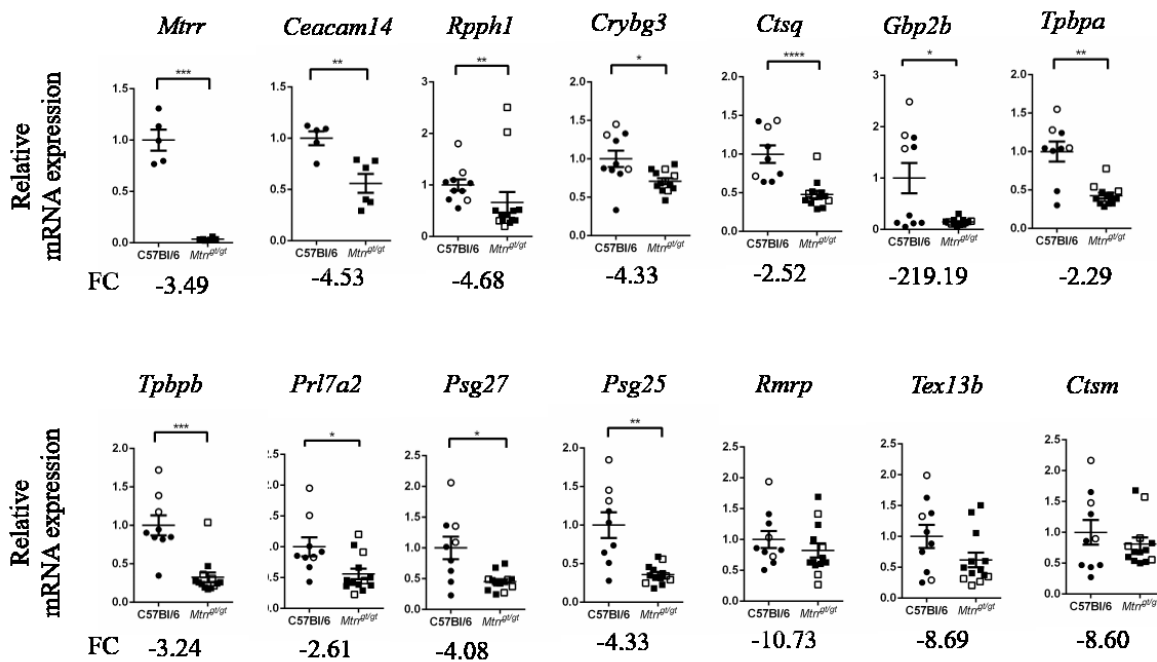


Figure 5.10 Validation by RT-qPCR analysis of downregulated genes identified by RNA-seq.

Graphs show transcripts that were downregulated in the phenotypically normal *Mtrr*^{gt/gt} placentas (squares) compared to the C57Bl/6 (circles). Sequenced (hollow shapes) and biologically independent (full shapes) samples were used. Data are presented as fold change (mean \pm SEM) compared to controls (normalised to 1). N=5-12 placental samples per genotype. The number below each graph represents the fold change (FC) observed in the RNA-seq experiment. Unpaired t tests with Welch correction or Mann-Whitney tests where appropriate were performed to independently compare placentas of C57Bl/6 and *Mtrr*^{gt/gt} conceptuses. * $P<0.05$, ** $P<0.01$, *** $P<0.001$, **** $P<0.0001$.

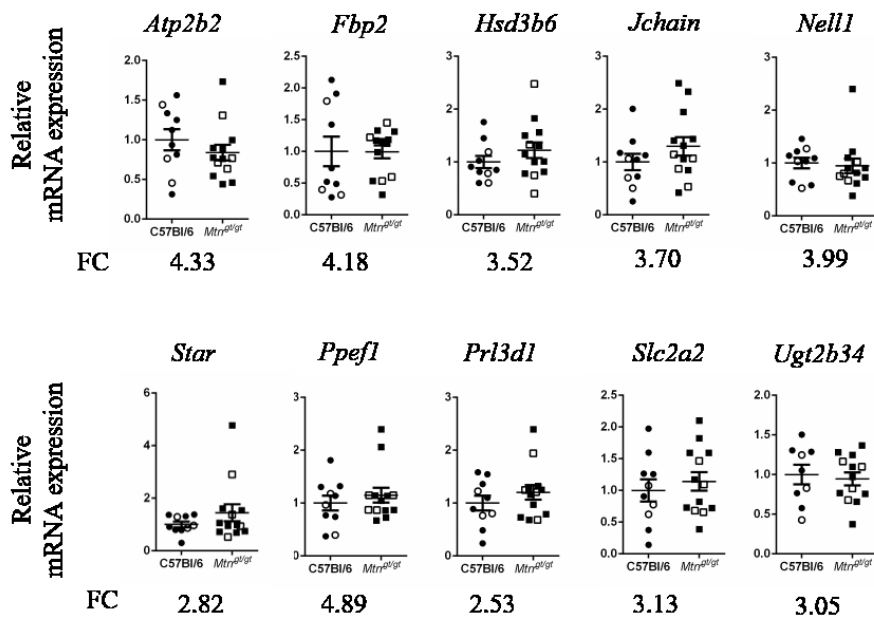


Figure 5.11 Validation by RT-qPCR analysis of up-regulated genes identified by RNA-sequencing.

Graphs show transcripts that were upregulated in the phenotypically normal *Mtrr^{g/g^t}* placentas (squares) compared to the C57Bl/6 (circles). Sequenced (hollow shapes) and biologically independent (full shapes) samples were used. Data are presented as fold change (mean \pm SEM) compared to controls (normalised to 1). N=10-14 placental samples per genotype. The number below each graph represents the fold change (FC) observed in the RNA-sequencing experiment. Unpaired t tests with Welch correction or Mann-Whitney tests where appropriate were performed to independently compare placentas of C57Bl/6 and *Mtrr^{g/g^t}* conceptuses.

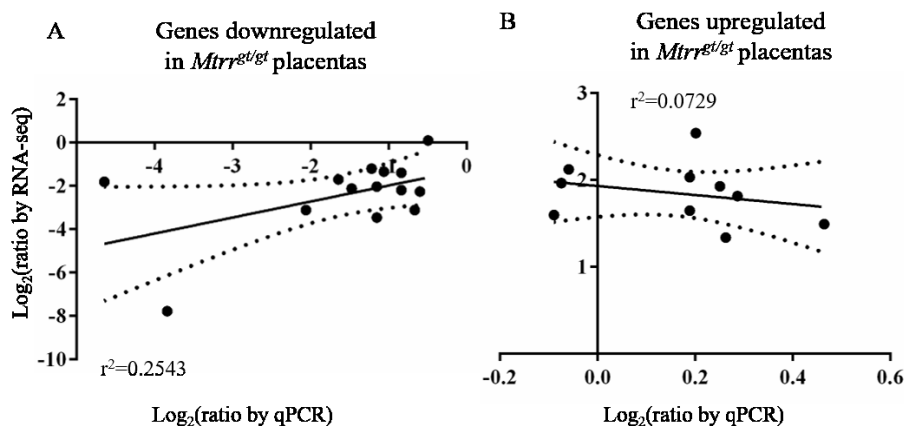


Figure 5.12 Gene expression correlation between the RNA-sequencing data and the qPCR results.

Graphs show the correlation of expression between the RNA sequencing and qPCR data of genes that were (A) downregulated and (B) upregulated in *Mtrr^{g/g^t}* placentas compared to C57Bl/6 placentas and used for qPCR validation. Linear regression and correlation analyses were performed, and the Pearson correlation coefficient was calculated.

5.2.6 The DEGs in the *Mtrr* locus

The *Mtrr*^{gt} mouse model was originally generated in a 129/P2 genetic background, and then backcrossed with C57Bl/6 mice for at least eight generations (Padmanabhan et al. 2013). However, using whole genome sequencing, the Watson lab identified a 20Mb region of 129/P2 genetic sequence (chr13:60162000:70162000) around the *Mtrr* gene when the gene-trap is present (G. Blake, X. Zhao, R. Hamilton, E. Watson, unpublished). Ten of the DEGs identified in *Mtrr*^{gt/gt} placentas were found in this 20 Mb region: *Zfp429*, *Ctsm*, *Tpbpb*, *Ctsq*, *4930525G20Rik*, *Tpbpa*, *Zfp456*, *Cts3*, *Gm16907*, and *Zfp457*. Among these genes, *Ctsm*, *Tpbpb*, *Ctsq*, *Tpbpa*, and *Cts3* have known expression in trophoblast cells. It is unclear whether the differences in genetic sequence around the *Mtrr* gene in *Mtrr*^{gt/gt} conceptuses compared to C57Bl/6 controls affect gene regulation, or whether these genes are misexpressed because of a placental phenotype caused by *Mtrr* deficiency. None of the DEGs identified when comparing phenotypically normal and growth restricted *Mtrr*^{gt/gt} conceptuses were within the *Mtrr* locus. It is unclear whether this is because of the similar genetic sequence around the *Mtrr* gene, or whether similar placental phenotypes caused by the *Mtrr* deficiency occur in both phenotypically normal and growth restricted *Mtrr*^{gt/gt} conceptuses compared to C57Bl/6 conceptuses.

5.2.7 Gene ontology analysis of the DEGs

We performed gene ontology analysis of the DEGs to identify potential enriched biological processes, molecular functions, or mammalian phenotypes that are disrupted or arise in *Mtrr*^{gt/gt} placentas. First, we performed gene ontology on the DEGs between placentas of C57Bl/6 and phenotypically normal *Mtrr*^{gt/gt} conceptuses. Interestingly, not many pathways were identified. This might be due to the variability in gene expression between the *Mtrr*^{gt/gt} placentas. In the *Mtrr*^{gt} model, the availability of methyl groups for cellular methylation is limited. We hypothesise that DNA methylation changes occur stochastically in each individual, and therefore, the genes that are misexpressed vary. This interindividual variability might prevent gene expression from being statistically significant.

Interestingly, enriched biological processes included transport function such as vitamin transport ($p=0.0002$) and fructose metabolism ($p=0.003$). Indeed, an important placental function necessary for proper embryo development, is nutrient transport (Bell & Ehrhardt

2002). We identified 16 genes that encode proteins with transport function in placentas of phenotypically normal *Mtrr^{gt/gt}* conceptuses compared to C57Bl/6 (Table 5.4). Since many of these genes were upregulated, it is possible that the *Mtrr^{gt/gt}* placenta is compensating to maintain fetal growth. We have previously showed that the embryo and placenta weights of phenotypically normal *Mtrr^{gt/gt}* conceptuses are proportionally decreased at E10.5 compared to C57Bl/6 (Padmanabhan et al. 2017). Placental transport assays are required to further assess active placental transport in the *Mtrr^{gt}* model. Additionally, there were no enriched terms related to placenta function or embryo growth. Finally, analysis of DEGs in phenotypically normal *Mtrr^{gt/gt}* placentas suggested a cardiovascular system phenotype (p=0.046, *Scarb1*, *Slc2a2*) and abnormal vitamin homeostasis (p=0.035, *Mtrr*). Interestingly, the genes associated with the cardiovascular system phenotype are *Scarb1* and *Slc2a2*, which also have transport activity.

Table 5.4 DEGs with transport function in phenotypically normal *Mtrr^{gt/gt}* compared to C57Bl/6 placentas at E10.5.

Gene	FC	Function
<i>Rhd</i>	-2.34	Cation transmembrane transport
<i>Afm</i>	-2.31	Vitamin transport
<i>Nanos1</i>	2.01	Regulation of Ca ²⁺ transport
<i>Tnfaip8l3</i>	2.02	Phospholipid transport
<i>Scn7a</i>	2.03	Cation transmembrane transport
<i>Slc23a1</i>	2.04	Carboxylic acid transport
<i>Slc16a5</i>	2.25	Carboxylic acid transport
<i>Scarb1</i>	2.26	Phospholipid transport
<i>Mt-tp</i>	2.4	Phospholipid transport
<i>Mt3</i>	2.53	Cation transmembrane transport
<i>Tpa</i>	2.66	Vitamin transport
<i>Slc5a9</i>	2.9	Hexose transport
<i>Slc2a2</i>	3.13	Hexose transport
<i>Hrc</i>	3.27	Regulation of Ca ²⁺ transport
<i>Atp2b2</i>	4.33	Cation transmembrane transport
<i>Trmp2</i>	8.24	Cation transmembrane transport

Next, we identified enriched gene ontology terms related to the DEGs in growth restricted *Mtrr^{gt/gt}* placentas at E10.5 compared to C57Bl/6 controls. Enriched biological processes include cAMP biosynthesis (p=0.001, *Adcy3*, *Adcy2*, *Adcy5*), regulation of VEGFR signalling (p=0.014, *Flt1*, *Mt3*), cholesterol metabolism (p=0.016, *Cyp11a1*, *Fdx1*, *Dhcr7*, *Mt3*), and

gluconeogenesis (p=0.02, *Pkc1, Fbp1, Fbp2*). Abnormal VEGFR signalling can affect decidual angiogenesis and vascular development of the placenta, leading to growth restriction (Douglas et al. 2014; Li et al. 2015). Interestingly, we identified enriched molecular function terms, such as BMP signalling (p=0.01, *Bmp2, Bmp6*), glucose transport (p=0.03, *Ppbp, Slc2a5*), and WNT-activated receptor activity (p=0.04, *Sfrp4, Fzd3*). BMP signalling is involved in decidualisation, and abnormal expression of *Bmp2* and BMP signalling can lead to abnormal decidualisation and growth restriction (Lee et al. 2007). As mentioned in a previous chapter, we identified decreased expression of *Bmp2* mRNA in implantation sites of *Mtrr^{gt/gt}* females compared to C57Bl/6 controls at GD6.5. We also identified 16 genes that were misexpressed in placentas of growth restricted *Mtrr^{gt/gt}* compared to C57Bl/6 conceptuses (Table 5.5). In contrast to the placentas of phenotypically normal *Mtrr^{gt/gt}* conceptuses, an equal number of these misexpressed transporter genes were up- and down-regulated in the placentas of growth restricted *Mtrr^{gt/gt}* conceptuses, which does not indicate functional compensation.

Table 5.5 DEGs with transport function in growth restricted *Mtrr^{gt/gt}* compared to C57Bl/6 placentas at E10.5.

Gene	FC	Function
<i>Trpm1</i>	-2.73	Calcium transport
<i>Slc1a1</i>	-2.41	Dicarboxylic acid and amidic amino acid transport
<i>Slc26a7</i>	-2.33	Dicarboxylic acid transport
<i>Afm</i>	-2.19	Vitamin transport
<i>Ppbp</i>	-2.17	Glucose transmembrane transport
<i>Trpc3</i>	-2.13	Ion transport
<i>Kcnh2</i>	-2.04	Regulation of cation transport
<i>Kcnj5</i>	-2.02	Regulation of ion transport
<i>Slco2a1</i>	2.14	Fatty acid transport
<i>Slc2a5</i>	2.2	Glucose transmembrane transport
<i>Scarb1</i>	2.74	Vitamin transport
<i>Slc16a5</i>	2.97	Carboxylic acid transport
<i>Mt3</i>	3.03	Ion transport
<i>Hrc</i>	3.43	Regulation of cation transport
<i>Trpm5</i>	3.78	Calcium transport
<i>Atp2b2</i>	5.53	Calcium transport

Finally, enriched mammalian phenotypes include delayed heart development (p=0.018, *Bmp2, Actc1*), abnormal chorion morphology (p=0.03, *Bmp2, Dnmt3l*), and increased trophoblast apoptosis (p=0.04, *Cdx2*). These phenotypes might suggest abnormal

placental development and function, leading to growth restriction, and delayed organ development.

5.2.8 DEGs that are involved in placental function and embryo growth

We identified enriched gene ontology terms based on the DEGs between phenotypically normal and growth restricted *Mtrr^{gt/gt}* conceptuses. Both sample groups have abnormal folate metabolism, therefore this analysis would highlight genes that are responsible for growth. Enriched biological function terms included purine metabolism (p=0.015, *Nudt10*), mRNA stabilisation (p=0.038, *Dazl*), and transport (p=0.02, *Trpc3*). Finally, an enriched mammalian phenotype was small allantois (p=0.02, *Zic3*). Given that we previously reported defects in chorioallantoic attachment in *Mtrr^{gt/gt}* conceptuses (Padmanabhan et al. 2013), *Zic3* will be a gene to explore in the future. Altogether, these data suggest that placentas of growth restricted *Mtrr^{gt/gt}* conceptuses might have altered placental development compared to the placentas of phenotypically normal *Mtrr^{gt/gt}* conceptuses.

Comparing placentas of phenotypically normal *Mtrr^{gt/gt}* conceptuses to C57Bl/6 placentas also revealed a few upregulated genes important for growth (*Fosl1*, *Ctsl*, *Htral*, *Rbp4*, *Ptx3*; Table 5.6). For instance, *Ctsl* mRNA was upregulated in placentas of phenotypically normal *Mtrr^{gt/gt}* conceptuses. *Ctsl* is expressed in trophoblast and endometrial glands, and as a lysosomal cysteine protease, it is thought to play an important role in implantation and placentation (Krueger et al. 2001; Song, Bazer & Spencer 2007; Varanou et al. 2006). Since *Htral* mutants are growth restricted as a result of aberrant vascularisation of the labyrinth (Hasan et al. 2015), it is possible that *Mtrr^{gt/gt}* placentas attempt to increase *Htral* expression to prevent growth restriction. In humans, *RBP4* is required for trophoblast cell proliferation and invasion (Li et al. 2018), while *PTX3* expression is altered in pregnancies complicated with FGR (Cozzi et al. 2012). Altogether, this suggests that the placentas of phenotypically normal *Mtrr^{gt/gt}* conceptuses compensate by upregulating the expression of genes that are important for growth to prevent FGR.

Table 5.6 DEGs in phenotypically normal *Mtrr^{gt/gt}* compared to C57Bl/6 placentas related to placental function.

Gene (FC)	Function	Characteristics related to developmental phenotypes	Reference
<i>Fos11</i> (2.07)	Responsible for the development of trophoblast lineages and establishment of the maternal-fetal interface	Knockdown of <i>Fos11</i> disrupted the expression of <i>Mmp9</i> , associated with the invasive-vascular remodelling trophoblast phenotype. Inhibition of <i>Fos11</i> expression using shRNA abrogated trophoblast invasion.	(Kent et al. 2011)
<i>Ctsl</i> (2.13)	Lysosomal endopeptidase, involved in the initiation of protein degradation	<i>Ctsl</i> regulates cellular invasiveness by promoting migration and basement membrane degradation, it is important for placental development.	(Krueger et al. 2001; Varanou et al. 2006)
<i>Htra1</i> (2.25)	Serine peptidase	Mutants exhibit FGR and have small placentas due to smaller junctional zone and aberrant vascularisation in the labyrinth at midgestation. SAR is also impaired.	(Hasan et al. 2015)
<i>Rbp4</i> (2.09)	Regulates human trophoblast cell proliferation and invasion	RBP4 knockdown inhibits HTR8/SVneo cell proliferation and invasion and represses the expression of matrix metalloproteinases.	(Li et al. 2018)
<i>Ptx3</i> (2.24)	Regulates inflammation and complement activation, plays a role in angiogenesis and tissue remodelling	Increased expression of PTX3 in pregnancies complicated with FGR indicates altered endothelial function due to excessive maternal inflammatory response to pregnancy.	(Cozzi et al. 2012)

Three of these genes were also differentially expressed between placentas of growth restricted *Mtrr^{gt/gt}* and C57Bl/6 conceptuses: *Fos11* (FC=2.34), *Ctsl* (FC=2.67), and *Htra1* (FC=2.89; Table 5.6). Six additional genes involved in placenta development, such as TGC differentiation and formation of labyrinth and spongiotrophoblast layers (i.e., *Sox15*, *Vash2*, *Dnmt3l*, *Flt1*, *Rbm46*, *Cdx2*) were downregulated in the placentas of growth restricted *Mtrr^{gt/gt}* conceptuses compared to C57Bl/6 (Table 5.7). Altogether, these data suggest the potential for a causative or a compensatory mechanism in the placenta in response to abnormal folate metabolism.

Table 5.7 DEGs in placentas of growth restricted *Mtrr^{gt/gt}* compared to C57Bl/6 related to placental phenotypes.

Gene (FC)	Function	Characteristics related to developmental phenotypes	Reference
<i>Sox15</i> (-2.03)	Enhances TGC differentiation	<i>Sox15</i> mutants that lack the HAND1 binding domain have defective TGC differentiation.	(Yamada et al. 2006)
<i>Dsc3</i> (-2.62)	Cadherin family of cell adhesion receptors	Expressed in placental mesenchymal stem cells. Placental phenotype unknown. <i>Dsc3^{-/-}</i> have preimplantation lethality.	(Hart et al. 2017)
<i>Vash2</i> (-2.57)	Carboxypeptidase, activator of angiogenesis	<i>Vash2^{-/-}</i> mutants have thinner villi of the labyrinth and larger maternal lacunae and defective syncytiotrophoblast formation at E18.5.	(Suenaga et al. 2014)
<i>Dnmt3l</i> (-2.39)	DNA methyltransferase	Knockout: defective labyrinth formation, reduced spongiotrophoblast layer, excess TGCs, insufficient attachment between the chorion and the EPC.	(Arima et al. 2006)
<i>Flt1</i> (-2.27)	Placental growth factor receptor	Treatment of a trophoblast cell line with an FLT1 inhibitor leads to slow growth, inhibition of cell proliferation, decreased expression of cell cycle progression genes, and attenuated migration of trophoblast cells in vitro. In vivo, decreased number of cytotrophoblast cells were observed in pregnancies complicated with FGR.	(Wu et al. 2017)
<i>Rbm46</i> (-2.06)	RNA-binding protein	Knockdown of <i>Rbm46</i> leads to downregulation of trophoctoderm markers and upregulation of endoderm and mesoderm markers in ESCs. <i>Rbm46</i> stabilises <i>Cdx2</i> mRNA and regulates trophoctoderm specification.	(Wang et al. 2015)
<i>Cdx2</i> (-2.0)	Transcription factor	<i>Cdx2</i> is required for proper cell fate specification and differentiation of trophoctoderm. Overexpression of <i>Cdx2</i> in human TS cells enhanced cell invasion by increasing MMP9 and decreasing its inhibitor, TIMP1 expression. Also, gain of <i>Cdx2</i> function in ES cells induces differentiation into cells with trophoblast cell characteristics.	(Jia et al. 2014; Strumpf et al. 2005; Tolkunova et al. 2006)
<i>Bmp2</i> (2.15)	Decidualisation marker	<i>Bmp2</i> mutant females have defective decidualisation.	(Lee et al. 2007; Li et al. 2007)

Interestingly, we did not identify any genes involved in developmental phenotypes that were differentially expressed between phenotypically normal and growth restricted *Mtrr^{gt/gt}*, even though these two sample groups have different growth phenotypes. This suggests that the phenotypically normal *Mtrr^{gt/gt}* conceptuses could potentially become growth restricted later during gestation. Overall, these data suggest that abnormal folate metabolism alters the expression of genes involved in trophoblast development and decidualisation. There are more DEGs associated with developmental phenotypes between growth restricted *Mtrr^{gt/gt}* and C57Bl/6 conceptuses than between phenotypically normal *Mtrr^{gt/gt}* and C57Bl/6 conceptuses, which correlates with the severity of the phenotype. The fact that the placentas of phenotypically normal *Mtrr^{gt/gt}* conceptuses are affected, suggests that the associated embryo although phenotypically normal, might be molecularly and metabolically abnormal.

5.2.9 Altered CpG methylation as a predicted mechanism for gene misexpression in *Mtrr^{gt/gt}* placentas

The *Mtrr^{gt}* model is characterised by global DNA hypomethylation in the placentas, and dysregulation of CpG methylation at E10.5 (Padmanabhan et al. 2013). To examine the potential sensitivity of the DEGs to changes in CpG methylation, we evaluated whether the top 50 downregulated genes (FC<-2.34) and top 50 upregulated genes (FC>2.56) in *Mtrr^{gt/gt}* placentas contained CpG repeats that were intragenic or proximal (within 20kb) to the gene (Figure 5.13 A-D). To do this, we used the UCSC Mouse Genome Browser to identify the location of CpG repeats with relation to the DEGs. As a control, 50 randomly selected genes were identified as a proxy of the genome and used in a similar analysis. This analysis did not determine whether the CpG repeats present were methylated, however it highlights the potential for gene dysregulation when methylation patterns are altered.

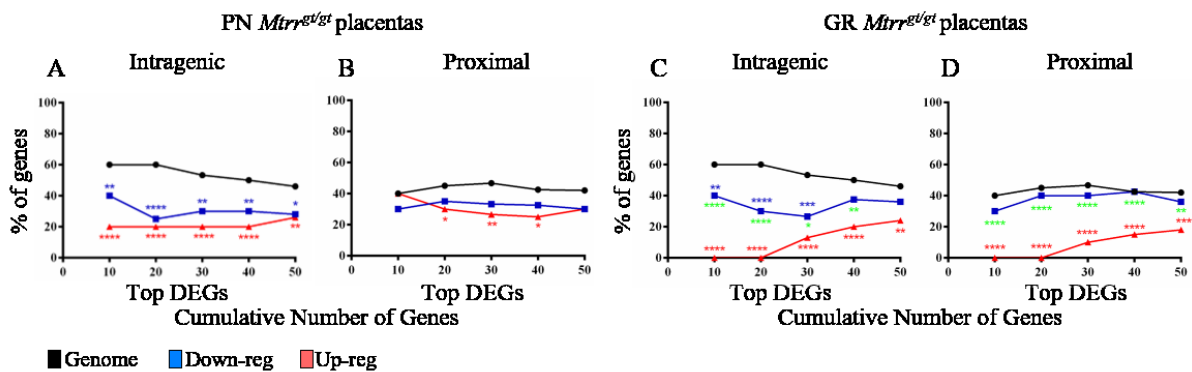


Figure 5.13 The percentage of DEGs in *Mtrr^{gt/gt}* placentas that were associated with CpG repeats.

The percentage of the top 50 down-regulated (blue lines) or up-regulated (pink lines) genes in placentas of (A-B) phenotypically normal *Mtrr^{gt/gt}* conceptuses, or (C-D) growth restricted *Mtrr^{gt/gt}* conceptuses at E10.5 that display CpG repeats localised (A,C) intragenically or (B,D) within 20 kb of the gene. The percentage of 50 randomly selected genes with similar features is indicated as a proxy for the genome (black lines). Data on the x-axis are presented as the cumulative number of differentially expressed genes (DEGs). Statistical analysis: Fisher's exact test. * $p < 0.05$, ** $p < 0.01$, **** $p < 0.001$. Blue asterisks: significance between down-regulated genes and the genome, red asterisks: significance between up-regulated genes and the genome, green asterisks: significance between down-regulated and up-regulated genes.

When the DEGs in placentas of phenotypically normal *Mtrr^{gt/gt}* conceptuses were considered, both up- and down-regulated gene sets were less likely to contain intragenic CpG repeats compared to the rest of the genome (21-30% of DEGs compared of 46% of genes genome-wide; $p < 0.05$, Fisher's exact test; Figure 5.13A). Moreover, upregulated genes were less frequently associated with proximal CpG repeats (30% of DEGs compared to 42% of gene genome wide; $p < 0.05$, Fisher's exact test). Downregulated genes had similar frequencies of proximal CpG repeated (32% of DEG) both to upregulated DEGs and the genome (Figure 5.13B).

Mtrr^{gt/gt} placentas from growth restricted conceptuses displayed a similar frequency of CpG repeats. In this case, both up- and down-regulated gene sets were less likely to contain intragenic CpG repeats (11.4-34% of DEGs compared of 46% of genes genome-wide; $p < 0.05$, Fisher's exact test; Figure 5.13C). Moreover, upregulated genes were less frequently associated with proximal CpG repeats (6.4% of DEGs compared to 42% of gene genome wide; $p < 0.05$, Fisher's exact test) compared to the rest of the genome. The higher the fold change, the less likely it was that the gene is associated with CpG repeats. Downregulated genes had similar frequencies of proximal CpG repeats (37.7% of DEG) to the genome but were less frequently associated with proximal CpG repeats compared to the upregulated genes (Figure 5.13D). Overall, these findings suggest that the DEGs are less likely to be cis regulated by CpG methylation compared to the genome at large. Therefore, it is suggested that epigenetic mechanisms other than CpG methylation, such as histone modification, or RNAi affect the expression of the DEGs. Alternatively, it is possible that CpG methylation of genes that regulate the expression of the DEGs occurs.

The analysis above assumes that the CpG repeats associated with the DEG directly regulate its expression. However, little is known about the functional implications of CpG methylation near specific genes in the genome. We were only able to identify 15 DEGs in *Mtrr^{gt/gt}* placentas whose expression has been directly linked to changes in CpG methylation in other studies (Table 5.8). Based on these studies and our RNA-seq data, we predicted the change of CpG methylation at these locations in the *Mtrr^{gt/gt}* placentas (Table 5.8). Four out of 15 (26.7%) of the DEGs are hypothesised to be associated with hypermethylated CpGs that cause downregulation of gene expression. The remaining 11 DEGs (73.3%) are suspected to display an opposite trend: hypomethylated CpGs that cause upregulation of gene expression. Therefore, we predicted both hypermethylation and hypomethylation of specific CpG sites in response to *Mtrr* deficiency in the placenta. However, locus specific hypomethylation might occur more frequently than hypermethylation.

Table 5.8 DEGs in *Mtrr^{gt/gt}* placentas with known regulation by DNA methylation.

Gene (FC)	Function	DNA methylation characteristics	Predicted CpG methylation	Reference
DEGs in placentas of PN <i>Mtrr^{gt/gt}</i> conceptuses				
<i>Trpm2</i> (-8.23)	Cation channel	DNA methylation of inner CpG island associated with reduced expression	Hyper	(Orfanelli et al. 2008)
<i>Noct</i> (-3.19)	Circadian clock effector, removes poly-A tails from mRNA	IAP promoter demethylation is associated with increased expression	Hyper	(Barbot 2002)
<i>Lrrc2</i> (3.02)	Mediator of mitochondrial and cardiac function	DNA methylation associated with decreased expression	Hypo	(Jin et al. 2016)
<i>Igf1pl1</i> (3.79)	Binds IGFs, either inhibit or stimulate the growth promoting effects of the IGFs	Hypermethylation of intragenic CpG island is associated with decreased expression	Hypo	(Smith et al. 2007)
<i>Nell1</i> (3.98)	Protein kinase C-binding protein	Hypermethylation in promoter or gene body is associated	Hypo	(Tombolan et al. 2017)

		with decreased expression		
<i>Fbp1</i> (10.45)	Gluconeogenesis regulatory enzyme	Promoter hypermethylation is associated with decreased expression	Hypo	(Chen et al. 2011)
<i>Ctsl</i> (2.12)	Lysosomal endopeptidase enzyme which is involved in the initiation of protein degradation	Promoter hypomethylation associated with increased expression	Hypo	(Samaiya et al. 2011)
DEGs in placentas of GR <i>Mtrr</i> ^{g/gt} conceptuses				
<i>Stk33</i> (-3.66)	Serine/threonine kinase	Promoter hypomethylation associated with increased expression	Hyper	(Yin et al. 2018)
<i>Dlx4</i> (-3.17)	Regulates cell growth and differentiation	Demethylation leads to an increase in gene expression	Hyper	(Sakane et al. 2015)
<i>Mt3</i> (3.03)	Metallothionein	Promoter hypermethylation is associated with decreased expression	Hypo	(Peng et al. 2011)
<i>Prl3d1</i> (3.16)	Prolactin hormone family	Placenta-specific DNA hypomethylation of promoter associated with increased expression	Hypo	(Hayakawa et al. 2012)
<i>Star</i> (3.29)	Steroid hormone synthesis enzyme	CpG methylation of Pax6 binding motif in STAR promoter reduces the gene expression	Hypo	(Wang et al. 2011)
<i>Igf1</i> (4.48)	Binds IGFs, either inhibit or stimulate the growth promoting effects of the IGFs	Hypermethylation of intragenic CpG island is associated with decreased expression	Hypo	(Smith et al. 2007)
<i>Nell1</i> (4.66)	Protein kinase C-binding protein	Hypermethylation in promoter or gene body is associated with decreased expression	Hypo	(Tombolan et al. 2017)

<i>Fbp1</i> (12.30)	Gluconeogenesis regulatory enzyme	Promoter hypermethylation is associated with decreased expression	Hypo	(Chen et al. 2011)
------------------------	-----------------------------------	---	------	--------------------

5.2.10 Predicted changes in histone modifications as a mechanism for placental gene misexpression

In general, genes that were upregulated in *Mtrr^{gt/gt}* placentas were less likely to associate with CpG repeats suggesting that their regulation might not depend upon this epigenetic modification. Another epigenetic mechanism of gene regulation is histone modifications. Therefore, we explored histone modifications as a potential mechanism for differential gene expression in *Mtrr^{gt/gt}* placentas. To do this, we used published ChIP-seq data set that shows localised genomic enrichment for H3K4 monomethylation (me1) and H3K27 acetylation (ac) in normal C57Bl/6 mouse placentas at term (Haeussler et al. 2019). High levels of H3K4me1 and H3K27ac are generally associated with transcriptionally active genes (Zhang & Reinberg 2001). To examine the potential sensitivity of the DEGs to changes in histone modifications, we evaluated the top 50 downregulated genes ($FC < -2.79$) and top 50 upregulated genes ($FC > 2.56$). We assessed whether placental intragenic or proximal (within 20 kb) H3K4me1 or H3K27ac enrichment is associated with DEGs under normal circumstances (Figure 5.14). We also assessed 50 randomly selected genes as a proxy of the genome. This analysis did not determine the existence of histone modifications in the *Mtrr^{gt/gt}* placentas, but rather it highlights the potential for gene dysregulation when abnormal histone modification occurs.

When the top 50 up- or down-regulated DEGs in placentas of *Mtrr^{gt/gt}* conceptuses were considered, they were equally as likely to be associated with placental H3K4me1 peaks compared to the genome. This trend was true of intragenic and proximal peaks (Figure 5.14A-B, E-F). Up- and down-regulated gene sets also showed a similar level of association with H3K4me1 enrichment relative to each other (Figure 5.14A-B, E-F).

In contrast, downregulated genes were less likely to be associated with placental H3K27ac peaks compared to upregulated genes and the genome at large ($p < 0.05$; Figure 5.14C-D, G-H). The upregulated genes had similar frequencies of H3K27ac peaks compared to the whole genome at large (Figure 5.14C-D, G-H). Therefore, genes that were downregulated in *Mtrr^{gt/gt}* placentas are unlikely to be controlled in normal conditions by H3K27ac. In contrast, genes that were upregulated are likely similarly sensitive to changes in H3K27ac levels

compared to the rest of the genome. From this, we can speculate that histone acetylation may not be an important mechanism in the context of *Mtrr* deficiency. A ChIP-seq experiment using antibodies against these and other histone modifications in *Mtrr*^{gt/gt} placentas is required to explore this question further.

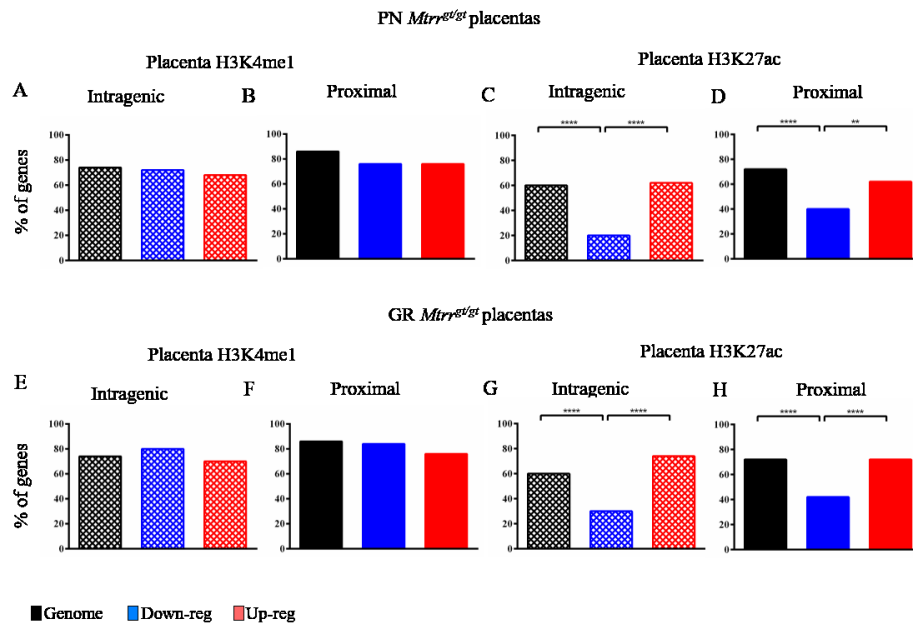


Figure 5.14 Frequency of histone modifications associated with genes that were misexpressed in *Mtrr*^{gt/gt} placentas.

The percentage of the top 50 down-regulated (blue bars) or up-regulated (red bars) genes between placentas of phenotypically normal *Mtrr*^{gt/gt} and C57Bl/6 (A-D), or growth restricted *Mtrr*^{gt/gt} and C57Bl/6 conceptuses (E-H) that display placental H3K4me1 peaks (A-B, E-F) localised (A,E) intragenically or (B,F) within 20 kb of the gene, or placental H3K27ac peaks (C-D, G-H) localised either (C,G) within the gene or (D,H). The percentage of 50 randomly selected genes with similar features is indicated as a proxy for the genome (black bars). Statistical analysis: Fisher's exact test. **p<0.01, ***p<0.001.

5.2.11 Analysis of the placental transcriptome in F2 *Mtrr*^{+/+} conceptuses at E10.5

Since we previously showed that *Mtrr*^{+gt} maternal grandfathers cause gross placental phenotypes in their wildtype grandprogeny (i.e., F2 *Mtrr*^{+/+} conceptuses) at E10.5 (Padmanabhan et al. 2013), we assessed the transcriptome of F2 *Mtrr*^{+/+} placentas at E10.5 and compared the results to similar stage C57Bl/6 control placentas (n=7). The purpose of this experiment was to explore potential molecular pathways affected in the placenta over multiple generations in this context. Additionally, we previously determined that growth

phenotypes were present in the F2 *Mtrr*^{+/+} conceptuses (Padmanabhan et al. 2013, 2017). Therefore, we analysed the placental transcriptomes of phenotypically normal (n=4) and growth enhanced (n=4) F2 *Mtrr*^{+/+} conceptuses to explore how growth is affected by abnormal folate metabolism in the maternal grandfather.

We created a PCA plot to determine the transcriptional relationship of the samples (Figure 5.15A). We observed that there was no clear separation of the samples suggesting that the transcriptomes of the C57Bl/6 and F2 *Mtrr*^{+/+} placentas were similar, regardless of the phenotype. Indeed, there were no genes that were differentially expressed (FC > 2) in placentas of C57Bl/6 and phenotypically normal F2 *Mtrr*^{+/+} conceptuses (Figure 5.15B). When considering genes that were differentially expressed by a fold change greater than 1.5, only one gene was up-regulated (*Gpnmb*, FC= 1.67) in the placentas of phenotypically normal F2 *Mtrr*^{+/+} conceptuses compared to C57Bl/6. In contrast, only one gene was down-regulated (*Gbp2b*, FC= -133.44) in the placentas of growth enhanced F2 *Mtrr*^{+/+} conceptuses compared to C57Bl/6 (Figure 5.15C). *Gbp2b* hydrolyses GTP to GMP and protects against bacterial infection (Kim et al. 2011). Its expression in the placenta or its role in placenta development or function are unknown. A lack of DEGs identified might be due to the small sample size of placentas that were sequenced. Lastly, we compared the placental transcriptome of phenotypically normal and growth enhanced F2 *Mtrr*^{+/+} conceptuses to determine whether specific molecular pathways involved in growth were apparent. Only one gene was upregulated (*Camk2b*, FC= 2.06) in the placentas of phenotypically normal F2 *Mtrr*^{+/+} conceptuses compared to growth enhanced F2 *Mtrr*^{+/+} conceptuses (Figure 5.15D). *De novo* mutations in *Camk2a* and *Camk2b* were shown to cause intellectual disability, intrauterine growth restriction, developmental delay, and placental abnormalities (Küry et al. 2017). These phenotypes were also observed in our model of abnormal folate metabolism (Padmanabhan et al. 2013). Placental expression of *Camk2b* is still unknown. These data suggest that, even though placental phenotypes are present (Padmanabhan et al. 2013), the *Mtrr*^{gl} mutation in the maternal grandfather does not affect the placental transcriptome of the F2 *Mtrr*^{+/+} conceptuses.

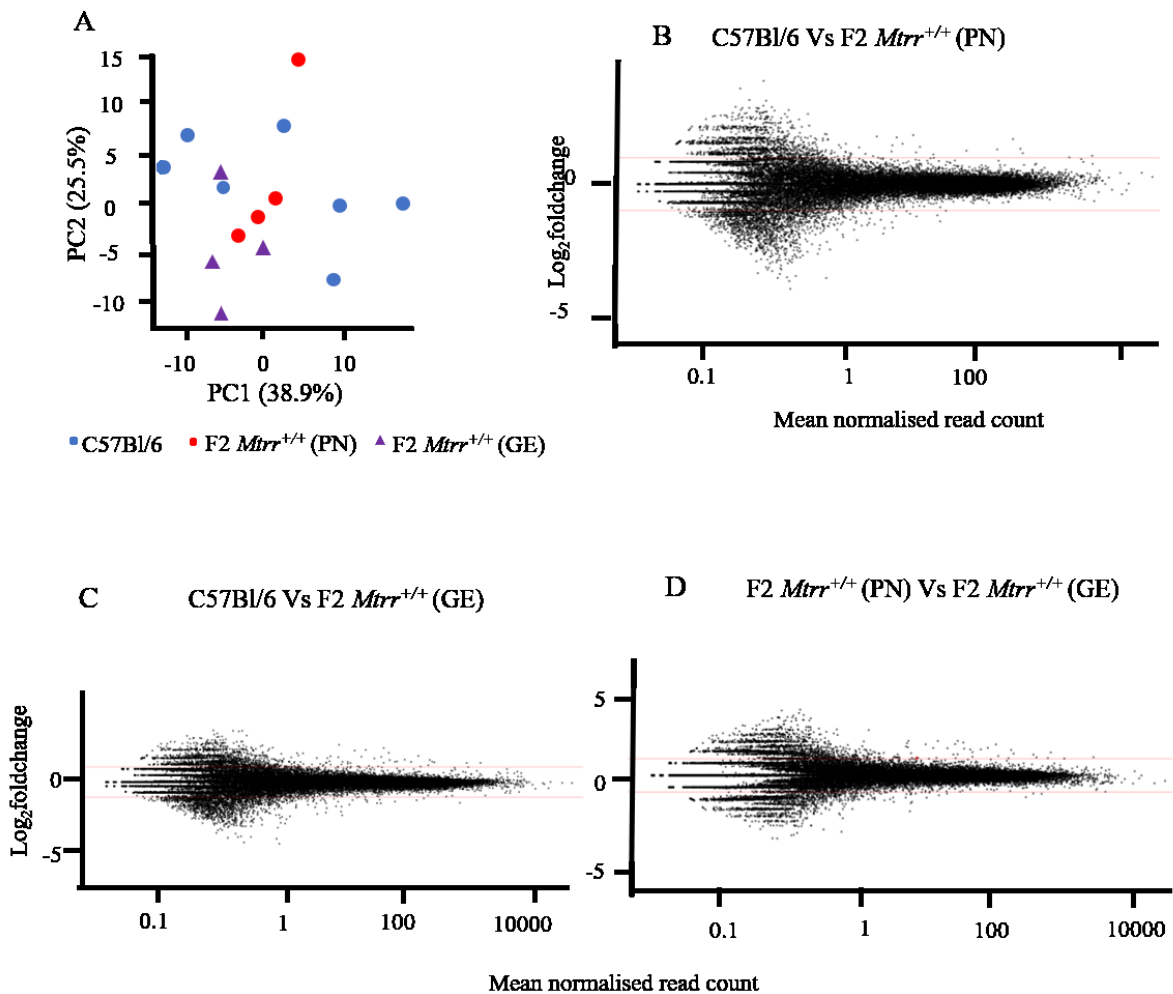


Figure 5.15 Bioinformatic analysis of the RNA sequencing data from placentas of C57Bl/6 and F2 *Mtrr*^{+/+} conceptuses.

(A) PCA plot based on the 500 most variable genes. Blue circles: C57Bl/6, purple triangles: growth enhanced F2 *Mtrr*^{+/+}, red circles: phenotypically normal F2 *Mtrr*^{+/+} (B-D) MA plots showing DEG between placentas of (B) C57Bl/6 and phenotypically normal *Mtrr*^{+/+} conceptuses, (C) C57Bl/6 and growth enhanced *Mtrr*^{+/+} conceptuses and (D) phenotypically normal and growth enhanced *Mtrr*^{+/+} conceptuses. PN: phenotypically normal, GE: growth enhanced.

5.3 Discussion

We have shown that abnormal folate metabolism caused by the *Mtrr*^{gt/gt} mutation in mice results in changes in placental gene expression at E10.5 of gestation in an embryonic phenotype-dependent manner. The placental efficiency of C57Bl/6 and phenotypically

normal *Mtrr^{gt/gt}* conceptuses is similar (Padmanabhan et al. 2017), however, we identified genes involved in placenta development and embryo growth that were differentially expressed in *Mtrr^{gt/gt}* placentas compared to C57Bl/6. In addition, gene ontology analysis of the DEGs in *Mtrr^{gt/gt}* placentas indicated possible altered placental development and function. Human placentas of growth restricted conceptuses have a distinct phenotype, characterised by reduced syncytiotrophoblast area, increased apoptosis, and thicker exchange barrier between the trophoblast and the fetal capillary endothelium (Ishihara et al. 2002; Levy & Nelson 2000; Smith, Baker & Symonds 1997). In addition, these placentas have lower villi vascular density (Chen, Bajoria & Aplin 2002), fewer capillaries in the stroma, and decreased surface area, volume and number of terminal villi (Champlin, Dorr & Gates 1973; Chen, Bajoria & Aplin 2002; Jackson et al. 1995; Krebs et al. 1996; Mayhew et al. 2003; Teasdale 1984). The placental morphology at E10.5 should be analysed in our model, to determine whether the detailed morphology of the placentas of phenotypically normal and growth restricted *Mtrr^{gt/gt}* conceptuses differs compared to the C57Bl/6. Preliminary data on stereological analysis of *Mtrr^{gt/gt}* and C57Bl/6 placentas revealed decreased labyrinth area in the placentas of growth restricted *Mtrr^{gt/gt}* conceptuses compared to the phenotypically normal *Mtrr^{gt/gt}*, or C57Bl/6 conceptuses. In addition, the fetal and maternal blood spaces in placentas of growth restricted *Mtrr^{gt/gt}* conceptuses had also a smaller area compared to the phenotypically normal *Mtrr^{gt/gt}*, or C57Bl/6 conceptuses (data by J.Rakoczy). Decreased labyrinth area in placentas of growth restricted *Mtrr^{gt/gt}* conceptuses compared to C57Bl/6 correlates with our RNA-sequencing data showing decreased expression of *Ctsq*, a marker of sinusoidal TGCs in the labyrinth (Tunster, Creeth & John 2016) in placentas of growth restricted *Mtrr^{gt/gt}* conceptuses compared to C57Bl/6. The parietal-TGC layer area was increased in placentas of growth restricted *Mtrr^{gt/gt}* conceptuses, while the spongiotrophoblast and decidual areas were not affected. *Tpbpa*, an expression marker of the progenitors of spongiotrophoblast, glycogen cells, some P-TGC, spiral artery TGC, and canal TGC (Tunster et al. 2016), was reduced in placentas of both phenotypically normal and growth restricted *Mtrr^{gt/gt}* conceptuses compared to C57Bl/6, but not in placentas of phenotypically normal compared to growth restricted *Mtrr^{gt/gt}* conceptuses. This correlates with unpublished *in situ* hybridisation data by Dr. Nisha Padmanabhan showing that *Tpbpa* mRNA is decreased in *Mtrr^{gt/gt}* placentas compared to C57Bl/6 controls. Considering there are decreased *Tpbpa* mRNA levels, unaffected spongiotrophoblast layer area, and increased parietal-TGC layer area, it is possible that decreased *Tpbpa* expression is due to abnormal differentiation or decreased counts and

increased size of spongiotrophoblast cells and glycogen cells. Abnormal function of spongiotrophoblast cells might lead to abnormal placental endocrine function, i.e. decreased placental prolactin and pregnancy-specific glycoprotein secretion. As mentioned in Chapter 1, these proteins are essential for protecting the developing fetus from being attacked by the maternal immune system, and also to remodel the blood vessels of the placenta and the maternal decidua (Kammerer & Zimmermann 2010; Wu et al. 2008). Abnormal remodelling of placental and decidual blood vessels causes growth restriction (Arroyo & Winn 2008; Barut et al. 2010; Gourvas et al. 2012).

In addition, we identified several genes with transport function that were misexpressed between *Mtrr^{gt/gt}* and C57Bl/6 placentas. Abnormal development of placenta transport systems is a major cause of intrauterine growth restriction in mammals. Placental transport occurs by either passive diffusion, or transporter-mediated transport (Sibley, Glazier & D'Souza 1997). Unpublished data from our lab showed that placental transport mechanisms between phenotypically normal and growth restricted *Mtrr^{gt/gt}* conceptuses vary. Expression of the solute carriers *Slc2a1* (glucose) and *Slc38a4* (amino acids) was decreased in the placentas of growth restricted *Mtrr^{gt/gt}* conceptuses compared to placentas of both phenotypically normal *Mtrr^{gt/gt}* and C57Bl/6 conceptuses. *Slc38a2* was increased in all *Mtrr^{gt/gt}* placentas compared to C57Bl/6 controls. mTORC1 and mTORC2 signalling positively regulates placental amino acid transporters and is inhibited by maternal folate deficiency, leading to decreased expression of amino acid transporters in the trophoblast plasma membrane (Rosario et al. 2017). Studying the uptake of amino acids into plasma membrane vesicles will give us information on amino acid transporter activity (Jansson et al. 2002; Jansson, Scholtbach & Powell 1998; Mahendran et al. 1993; Norberg, Powell & Jansson 1998). More recent techniques of assessing placental activity aim to estimate the time that the nutrients reside at each placental compartment. FGR is associated with dysregulation of placental transporters, such as downregulation of *Slc7a7*, *Slc38a2*, *Slc19a3*, and *Slc22a15*, and upregulation of *Slc38a5*, *Slc2a1*, *Abca1*, and *Slc26a2* (Huang et al. 2018). The expression of these genes was normal in our study, suggesting an alternative mechanism leading to FGR in our model. Analysis of the placental transcriptome of growth restricted F2 *Mtrr^{+/+}* conceptuses could give us more information about misexpression of placental genes that cause growth restriction. More advanced techniques to study placenta transfer mechanisms in humans include confocal laser scanning microscopy, transmission electron microscopy, and tagged tracers (Sölder et al. 2009).

In the *Mtrr^{gt}* model of abnormal folate metabolism, we observed global DNA hypomethylation in the *Mtrr^{gt/gt}* placentas of phenotypically normal and growth restricted conceptuses compared to the C57Bl/6 at E10.5 (Padmanabhan et al. 2013). According to our RNA-seq data, we predicted both hypomethylation and hypermethylation of CpG sites. This correlates with previous findings that global DNA hypomethylation can be associated with locus-specific hypermethylation and hypomethylation in the *Mtrr^{gt/gt}* placentas (Padmanabhan et al. 2013). Further experiments are required to assess the methylation status of the differentially expressed genes that are regulated by DNA methylation by bisulfite pyrosequencing, or to assess the methylation status of the whole genome by MeDIP-seq (Weber et al. 2005).

We have shown that the DEGs in *Mtrr^{gt/gt}* placentas are on average less likely to be associated with CpG repeats than the rest of the genome. Therefore, we considered histone modifications such as methylation and acetylation, as an alternative epigenetic mechanism that regulates gene expression. We showed that the DEGs are equally likely to be associated with H3K4me1 peaks as the rest of the genome, while the downregulated genes are less likely to be associated with H3K27ac peaks than the rest of the genome. We identified two genes, *Mt3* and *Fbp1*, which were upregulated in the placentas of *Mtrr^{gt/gt}* conceptuses compared to the C57Bl/6 and are associated with histone modifications. Increased repressive histone modification (H3K9me2) and decreased active histone modifications (H3K4me2, H3K9ac) are associated with decreased expression of *Mt3* (Peng et al. 2011). Additionally, decreased H3K27Ac in the *Fbp1* enhancer is associated with decreased expression (Yang et al. 2017). Based on our RNA-seq data, we predict decreased H3K9me2 and increased H3K4me2, H3K9ace in *Mt3*, and increased H3K27ac in the *Fbp1* enhancer in the placentas of both phenotypically normal and growth restricted *Mtrr^{gt/gt}* conceptuses. Interestingly, there were no DEGs between phenotypically normal and growth restricted *Mtrr^{gt/gt}* with known regulation by histone modifications. Overall, these data suggest that intrinsic abnormal folate metabolism affects only two genes whose expression is regulated by histone modifications. Chromatin modifications should be assessed via ChIP-seq (Arrigoni et al. 2016; Furey 2012). Interestingly, none of the genes that were upregulated in *Mtrr^{gt/gt}* placentas as determined via RNA-sequencing were validated via RT-qPCR. We observed variation in the expression of the upregulated, but not downregulated genes in the *Mtrr^{gt/gt}* placentas, which could be the reason that the upregulated genes did not validate. A possible explanation is that CpG

methylation in the regulatory regions of these genes is randomly affected in each individual, leading to gene upregulation in some placentas and not others. Finally, differential splicing might explain why some genes do not validate. For instance, according to Ensembl, *Atp2b2*, has eight splice variants, *Hsd3b6* has three, and *Nell1* has five. We performed single-end sequencing, however, paired-end sequencing would detect splice variants during RNA sequencing (Au et al. 2010; Rossell et al. 2014).

Finally, we sequenced the RNA of placentas of phenotypically normal and growth enhanced F2 *Mtrr*^{+/+} conceptuses to assess the effects of maternal grandpaternal *Mtrr*^{gt} mutation on the placental transcriptome. We found that maternal grandpaternal *Mtrr*^{gt} mutation does not affect the placental transcriptome at E10.5. This is interesting since global DNA hypomethylation and dysregulation of locus-specific DNA methylation in imprinted genes were previously observed in the placentas of phenotypically normal F2 *Mtrr*^{+/+} conceptuses at E10.5 (Padmanabhan et al. 2013). It is possible that changes in DNA methylation detected are not directly related to changes in gene expression at E10.5. Additionally, it is possible that changes in DNA methylation at E10.5 affect gene expression later during gestation. Abnormal DNA methylation was more frequently associated with abnormal gene expression in the placentas of growth restricted than phenotypically normal F2 *Mtrr*^{+/+} conceptuses at E10.5 (Padmanabhan et al. 2013). Therefore, a better experiment would be to sequence RNA from placentas of growth restricted F2 *Mtrr*^{+/+} conceptuses at E10.5.

Overall, these data suggest that intrinsic abnormal folate metabolism affects placental transcriptome. We identified DEGs between phenotypically normal or growth restricted *Mtrr*^{gt/gt} and C57Bl/6 placentas that are involved in embryo growth, have transport activity, and regulate gene expression through epigenetic mechanisms. Specific placental phenotypes should be assessed in the future. The RNA-sequencing data will then be used to identify molecular pathways that might cause the identified phenotypes.

Chapter 6: The effects of blastocyst transfer on the placental transcriptome at E10.5

Portions of this chapter are currently submitted for publication.

The embryo transfer experiments were performed by Colleen Geary-Joo and Dr. Erica Watson.

The bioinformatic analysis was performed by Dr. Malwina Prater and Dr. Russell Hamilton.

Bisulfite pyrosequencing was performed by Dr. Gina Blake.

6.1 Introduction

More than seven million babies have been born worldwide using some form of assisted reproduction technology (ART) as a treatment approach to infertility (ESHRE 2018). ART includes a variety of procedures (e.g., superovulation, *in vitro* fertilisation (IVF), intracytoplasmic sperm injection (ICSI), embryo culture, embryo biopsy, gamete and embryo vitrification, and embryo transfer). While ART is generally safe, growing evidence suggests that individuals born using these technologies are at an increased risk of FGR, perinatal complications (Quinn & Fujimoto 2016), and/or developing diseases later in life, such as cardiovascular disease (Guo et al. 2017; Liu et al. 2015; Tararbit et al. 2013; Valenzuela-Alcaraz et al. 2013). Since optimal placental function is required for normal fetal growth and development, it is predicted that placenta pathologies are responsible for some of the adverse pregnancy outcomes associated with ART (Choux et al. 2015; Delle Piane et al. 2010; Thomopoulos et al. 2012). Indeed, ART pregnancies were overrepresented in the highest quartile of placental weight and underrepresented in the highest quartile of birthweight (Haavaldsen, Tanbo & Eskild 2012).

To explore the effects of ART on placental structure and function, animal models (e.g., mouse) have been utilised. As in the human, the mouse placenta is composed of three major layers: i) the outer maternal layer, which includes decidual cells of the uterus, maternal immune cells, and the maternal vasculature that brings blood to and from the implantation site; ii) the metabolic ‘junctional’ region, which attaches the placenta to the uterus through the invasion of trophoblast cells; and iii) an inner layer composed of highly branched villi required for nutrient, gas, and waste exchange between the maternal and fetal circulations (Watson & Cross 2005). Defects in mouse placenta development and/or function have repercussions for fetal growth and health (Perez-Garcia et al. 2018; Watson & Cross 2005). Indeed, IVF and/or superovulation in mice is associated with large placentas with reduced vascular density and altered nutrient transport in villi at late gestation to produce normal sized or growth restricted fetuses (Bloise et al. 2012; Delle Piane et al. 2010; Weinerman et al. 2017). Indeed, the sub-optimally formed placenta might undergo counter-balancing mechanisms that bring about adaptive placental responses (Choux et al. 2015). How and when this dialogue occurs is unclear.

The mechanism through which ART influences placental formation and function is also not well understood. The vast majority of studies have focused on CpG methylation of imprinted

loci in the placenta (Bloise et al. 2012; Choux et al. 2015; Delle Piane et al. 2010; Fauque 2010; Fortier et al. 2008; S Khosla et al. 2001; Mann et al. 2004; Rivera et al. 2008).

Genomic imprinting is an epigenetic phenomenon in mammals whereby a small number of genes are expressed in a parent-of-origin-specific manner, a process that is regulated by DNA methylation. Many imprinted genes are expressed in the placenta and are important for its development and function (Tunster, Jensen & John 2013). Directed analysis of DNA methylation and gene expression at imprinted regions can act as a convenient read-out of functional DNA methylation changes across the genome (Messerschmidt et al. 2012; Padmanabhan et al. 2013). Therefore, studies showing altered DNA methylation at imprinted genes after ART hypothesise that these technologies might influence the establishment of DNA methylation genome-wide with consequences for differentiation of cell lineages, including those required for the placenta (Choux et al. 2015). Dysregulation of other epigenetic mechanisms (e.g., histone methylation or acetylation, non-coding RNA expression) have largely been ignored in the context of ART.

One procedure that all ART have in common is the transfer of the embryo/blastocyst into the uterus of the recipient female. However, the precise impact of this procedure alone on the placenta growth and transcription is not well understood. Here, we show that blastocyst transfer in mice has a stark impact on transcriptional regulation and likely influences placental efficiency even as the placenta matures. Furthermore, our unbiased approach enabled us to determine that changes in DNA methylation not be the primary cause of gene misexpression. Therefore, the study of other epigenetic mechanisms is required.

Here, we hypothesise that blastocyst transfer alters the placental transcriptome at E10.5. To test this hypothesis, we explored the effects of blastocyst transfer on the placental transcriptome at E10.5 in mice by RNA-sequencing. Our study does not involve superovulation, *in vitro* fertilisation, ICSI, or vitrification. Additionally, since growth phenotypes including growth restriction, growth enhancement, and developmental delay in F2 *Mtrr*^{+/+} conceptuses are likely caused by an atypical uterine environment in their wildtype mothers (F1 *Mtrr*^{+/+} females; Padmanabhan et al. 2013), we attempted to determine the effects of blastocyst transfer on the placental transcriptomes of F2 *Mtrr*^{+/+} conceptuses. Specifically, we hypothesise that providing the F2 *Mtrr*^{+/+} conceptuses with a normal uterine environment alters their placental transcriptome, therefore affects their growth. The F2 *Mtrr*^{+/+} conceptuses developed in the abnormal F1 *Mtrr*^{+/+} uteri until E3.0, before being

transferred to the normal uterine environment of a BDF1 female (F1 generation derived from crossing C57Bl/6 females with DBA/2 males; Padmanabhan et al. 2013). Since the F1 *Mtrr*^{+/+} uterine environment is abnormal (Chapters 3 and 4), it is possible that the blastocysts were developmentally programmed such that exposure to a normal uterine environment might alter transcription and developmental trajectory. Ongoing work in the Watson lab is exploring the specific trophoblast phenotypes of F2 *Mtrr*^{+/+} conceptuses, and so the transcriptome analysis presented here will complement this analysis.

6.2 Results

6.2.1 Maternal grandpaternal abnormal folate metabolism affects the placental transcriptome in a growth phenotype-dependent manner

Even though abnormal folate metabolism in the maternal grandfather does not appear to affect the placental transcriptome of F2 *Mtrr*^{+/+} conceptuses (Chapter 5), we wanted to determine whether their epigenomes were metabolically programmed. To do this, the placenta transcriptomes of F2 *Mtrr*^{+/+} conceptuses that had undergone blastocyst transfer were analysed and compared to transferred C57Bl/6 placentas (Figure 6.1A). The RNA from the transferred samples was sequenced in the same sequencing experiment as the RNA from non-transferred samples, as described in Chapter 5. The blastocyst transfer experiment was previously performed and showed that providing a normal uterine environment to the F2 *Mtrr*^{+/+} conceptuses prevented growth restriction and developmental delay (Padmanabhan et al. 2013). However, growth enhancement was more frequently observed compared to C57Bl/6 conceptuses that were transferred (Padmanabhan et al. 2013). First, we compared the placental transcriptome of C57Bl/6 to phenotypically normal and growth enhanced F2 *Mtrr*^{+/+} conceptuses after blastocyst transfer. There were no genes that were differentially expressed when comparing placentas of phenotypically normal F2 *Mtrr*^{+/+} conceptuses to C57Bl/6 or growth enhanced *Mtrr*^{+/+} conceptuses after blastocyst transfer (Figure 6.1B, D). This might be because the sample size was too small. In contrast, we identified six genes (*Prl8a8*, *Prl8a9*, *Psg19*, *Fbln7*, *Zfp964*, *Phldb3*) that are upregulated in the placentas of growth enhanced F2 *Mtrr*^{+/+} conceptuses compared to C57Bl/6 after blastocyst transfer, with at least a two-fold change (Figure 6.1C, E). The placental transcriptomes of phenotypically normal F2 *Mtrr*^{+/+} conceptuses were similar to C57Bl/6, suggesting conceptuses of the

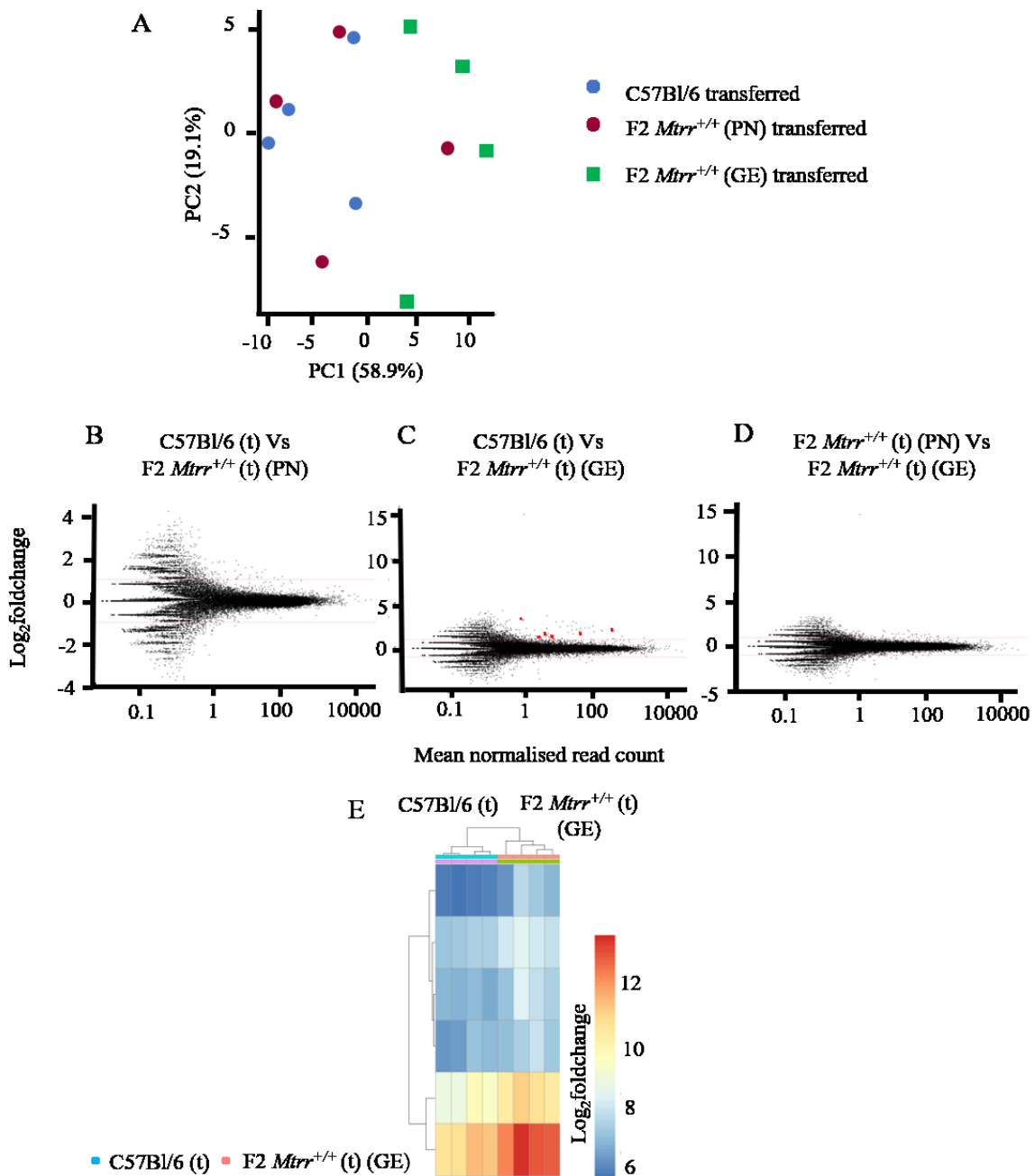


Figure 6.1 Bioinformatic analysis of the RNA sequencing data from C57Bl/6, and placentas of F2 *Mtrr*^{+/+} conceptuses after blastocyst transfer.

(A) PCA plot based on the 500 most variable genes. Blue circles: C57Bl/6 transferred (t), red circles: phenotypically normal *Mtrr*^{+/+} transferred, green squares: growth enhanced (GE) *Mtrr*^{+/+} transferred (B-D) MA plots showing DEG between placentas of (B) C57Bl/6 and phenotypically normal *Mtrr*^{+/+} conceptuses after blastocyst transfer, (C) C57Bl/6 and growth enhanced *Mtrr*^{+/+} conceptuses after blastocyst transfer and (D) phenotypically normal and growth enhanced *Mtrr*^{+/+} conceptuses after blastocyst transfer (E) Heatmap showing the six genes that were differentially expressed between placentas of transferred C57Bl/6 and growth

enhanced *Mtrr*^{+/+} conceptuses. Each column represents an individual placenta. Each row represents one gene.

similar phenotype have similar transcriptome. The chromosomal location and placental expression of these genes are shown in Table 6.1. *Prl8a8* and *Prl8a9* are located on chromosome 13, however they are not within the *Mtrr* locus. *Prl8a8*, *Prl8a9*, *Psg19*, and *Phldb3* are expressed by the trophoblast cells, while the placental expression of *Fbln7* and *Zfp964* is unknown. *Prl8a8* and *Prl8a9* are prolactin family genes and are expressed in the ectoplacental cone lineage and in the maternal decidua (Simmons et al. 2008). *Psg19* is a pregnancy-specific glycoprotein (Wynne et al. 2006) that can bind to CD9 to initiate TGFβ signalling (Ha et al. 2008). *Fbln7* is involved in cell adhesion (Whittington et al. 2018) and might be required for vasculogenesis (de Vega et al. 2016). *Phldb3* plays a role in cell proliferation by regulating p53 degradation (Chao et al. 2016).

Table 6.1 Chromosomal location and placental expression of DEGs.

Gene	Function	Fold-change	Chromosome	Expression in placenta
<i>Prl8a8</i>	Prolactin	9.17	13	TB (SpT)
<i>Prl8a9</i>	Prolactin	3.88	13	TB (parietal TGC)
<i>Psg19</i>	Pregnancy-specific glycoprotein	2.93	7	TB (TGC)
<i>Fbln7</i>	Adhesion molecule	2.8	2	Unknown
<i>Zfp964</i>	Zinc finger protein	2.3	8	Unknown
<i>Phldb3</i>	Oncogene, direct target of p53	2.1	7	TB

TB: trophoblast, SpT: spongiotrophoblast, TGC: trophoblast giant cells, Expression according to Human Protein Atlas

6.2.2 Blastocyst transfer leads to possible increase in placental efficiency at E10.5

Next, we wanted to examine how the uterine environment influences or programmes the placental transcriptome of F2 *Mtrr*^{+/+} conceptuses. To do this, we mated C57Bl/6 donor female mice (n=10) without superovulation to C57Bl/6 male mice (n=10), and F1 *Mtrr*^{+/+} donor female mice (n=11) without superovulation to C57Bl/6 male mice (n=11). Pre-implantation embryos were flushed at E3.25 from oviducts and uteri of donor females and transferred by embryo injection into the oviducts of pseudopregnant B6D2F1 females at the

equivalent of GD2.5. Transferred blastocysts were allowed to implant and were dissected at E10.5 (staged according to the recipient female (Ueda et al. 2003)) for phenotyping. C57Bl/6 and F2 *Mtrr*^{+/+} conceptuses were derived from natural matings, did not undergo the blastocyst transfer procedure, and were dissected at E10.5 for similar analyses.

First, we assessed the blastocyst transfer efficiency in C57Bl/6 conceptuses. Prior to transfer, litter sizes at E3.25 ranged between 8-10 embryos and included compact morula- and blastocyst-staged embryos (Table 6.2). Two litters contained at least one embryo with an abnormal appearance (Table 6.2). However, all embryos were transferred regardless of appearance. Ten pseudopregnant B6D2F1 females received embryos but only eight were pregnant at E10.5 (80% efficiency). The average implantation rate was 47.3% when all transferred litters were considered and 58.9% when only considering transfers that resulted in pregnancy (Table 6.2).

Similarly, we assessed the blastocyst transfer efficiency in F2 *Mtrr*^{+/+} conceptuses. Prior to transfer, litter sizes at E3.25 ranged between 7-11 embryos and included compact morula- and blastocyst-staged embryos (Table 6.3). One litter contained two embryos with an abnormal appearance (Table 6.3) and another litter contained two unfertilised oocytes (Table 6.3). However, all embryos and unfertilised oocytes were transferred regardless of appearance. Eleven pseudopregnant B6D2F1 females received embryos but only nine were pregnant at E10.5 (81.8% efficiency). The average implantation rate was 60% when all transferred litters were considered and 73.2% when only considering transfers that resulted in pregnancy (Table 6.3).

C57Bl/6 litter sizes after transfer were smaller (5.4 ± 0.5 implantation sites per litter; $p < 0.001$) than control C57Bl/6 litters (9.5 ± 0.4 implantation sites per litter; Table 6.4). No congenital malformations were apparent in the control or transferred conceptuses at E10.5 (Table 6.4). However, one litter was developmentally delayed since the number of somite pairs in these embryos ranged between 16-22 pairs (Figure 6.2A) instead of the expected 30-40 somite pairs. At E10.5, 20.9% of the transferred conceptuses were resorbed compared to only 5.3% of control conceptuses (Table 6.4). Although not statistically significant ($p = 0.200$), this result suggests that blastocyst transfer might lead to increased post-implantation lethality before E10.5. A larger data set is required to explore this finding further.

Overall, male and female conceptuses were present in a 1:1 ratio at E10.5 in both control and transferred C57Bl/6 groups (Table 6.4) indicating that sex was not a selective factor on survival after blastocyst transfer. A two-way ANOVA was used to also assess interactions between the two factors assessed (i.e. sex and experimental procedure). The blastocyst transfer ($p=0.5603$), the sex ($p=0.7642$), or the interaction between these two factors ($p=0.3883$) did not have any effect on embryo weight (Figure 6.2B). The blastocyst transfer led to a decreased in the placenta weight ($p<0.0001$) in both sexes, while the sex ($p=0.9531$) had no effect. The interaction between the two factors did not affect placental weight ($p=0.1302$; Figure 6.2C). Indeed, the blastocyst transfer process led to an increase in the embryo:placenta weight ratio in the females ($p=0.0020$), while the sex had no effect on embryo:placenta weight ratio ($p=0.5421$). The interaction between the two factors was not different ($p=0.7052$; Figure 6.2D).

F2 *Mtrr*^{+/+} litter sizes after transfer were similar (6.6 ± 0.6 implantation sites per litter) to control F2 *Mtrr*^{+/+} litters (8.2 ± 0.4 implantation sites per litter; Table 6.5). No growth restriction or developmental delay was observed in the transferred F2 *Mtrr*^{+/+} conceptuses (Table 6.5). Congenital malformations and resorptions were observed in similar frequencies at E10.5 in the non-transferred and transferred F2 *Mtrr*^{+/+} conceptuses (11.0% Vs 75%, and 3.5% Vs 1.9%, respectively; Table 6.5). Overall, male and female conceptuses were present in a 1:1 ratio at E10.5 in both control and transferred groups (Table 6.5) indicating that sex was not a selective factor on survival after blastocyst transfer.

The effects of the blastocyst transfer and the sex on the embryo and placenta weight and embryo:placenta ratio were assessed by a two-way ANOVA. Both the blastocyst transfer ($p<0.0001$) and the sex ($p=0.0099$) led to an increase in embryo weight, however the interaction between these two factors did not affect embryo weight ($p=0.7866$; Figure 6.3B). The blastocyst transfer led to an increase in the placenta weight ($p<0.0001$), while the sex ($p=0.2053$) had no effect. The interaction between the two factors did not affect placenta weights ($p=0.3826$; Figure 6.3C). Indeed, the blastocyst transfer process led to an increase in the embryo:placenta weight ratio in both males and females ($p=0.0001$), while the sex had no effect on embryo:placenta weight ratio ($p=0.0699$). The interaction between the two factors did not affect the embryo:placenta weight ratio ($p=0.9872$; Figure 6.3C).

Table 6.2 Relationship between C57Bl/6 embryos transferred at E3.5 into recipient female and embryonic phenotype at E10.5.

Female ID	Phenotypes of transferred embryos at E3.5				Total No. of conceptuses at E10.5 (Implantation rate [%])	Phenotypes of transferred conceptuses at E10.5*					
	Total No. of embryos transferred	Blastocyst stage	Morula stage	Abnormal appearance		N	GE	GR	DD	CM	R
C57-T1	10	5	4	1	6 (60.0%)	3	1	0	0	0	2
C57-T2	9	6	3	0	0	-	-	-	-	-	-
C57-T3	10	3	7	0	6 (60.0%)	5	0	0	0	0	1
C57-T4	8	4	4	0	4 (50.0%)	0	0	0	4	0	0
C57-T5	10	4	3	3	6 (60.0%)	6	0	0	0	0	0
C57-T6	9	7	2	0	3 (33.3%)	0	1	1	0	0	1
C57-T7	8	7	1	0	5 (62.5%)	3	0	1	0	0	1
C57-T8	9	5	4	0	0	-	-	-	-	-	-
C57-T9	8	7	1	0	7 (87.5%)	5	1	0	0	0	1
C57-T10	10	6	4	0	6 (60.0%)	3	0	0	0	0	3
Total	91	54	33	4	43 (47.3%)	25	3	2	4		9

*N, phenotypically normal; GR, growth restricted; GE, growth enhanced; DD, developmentally delayed; CM, congenital malformation; R, resorption.

Table 6.3 Relationship between F2 *Mtrr*^{+/+} embryos transferred at E3.5 into recipient female and embryonic phenotype at E10.5.

Female ID	Total No. of embryos transferred	Blastocyst stage	Morula stage	Abnormal appearance	Unfertilised oocytes	Total No. of conceptuses at E10.5 (Implantation rate [%])	N	GE	GR	DD	CM	R
F2 <i>Mtrr</i> ^{+/+} - T1	11	9	0	0	2	7 (63.6%)	6	0	0	0	1	0
F2 <i>Mtrr</i> ^{+/+} - T2	8	5	3	0	0	7 (87.5%)	4	2	0	0	1	0
F2 <i>Mtrr</i> ^{+/+} - T3	7	4	3	0	0	0	0	0	0	0	0	0
F2 <i>Mtrr</i> ^{+/+} - T4	10	5	5	0	0	8 (90.0%)	8	0	0	0	1	0
F2 <i>Mtrr</i> ^{+/+} - T5	11	8	3	0	0	8 (72.7%)	5	1	0	0	2	0
F2 <i>Mtrr</i> ^{+/+} - T6	11	6	3	2	0	4 (36.4%)	3	1	0	0	0	0
F2 <i>Mtrr</i> ^{+/+} - T7	11	9	2	0	0	0	0	0	0	0	0	0
F2 <i>Mtrr</i> ^{+/+} - T8	8	4	4	0	0	7 (87.5%)	4	0	0	0	3	0
F2 <i>Mtrr</i> ^{+/+} - T9	7	4	3	0	0	7 (100%)	6	0	0	0	0	1
F2 <i>Mtrr</i> ^{+/+} - T10	7	5	2	0	0	6 (85.7%)	2	4	0	0	0	0
F2 <i>Mtrr</i> ^{+/+} - T11	9	7	2	0	0	5 (55.36%)	3	2	0	0	0	0
Total	100	66	30	2	2	60 (60%)	41	10	0	0	8	1

*N, phenotypically normal; GR, growth restricted; GE, growth enhanced; DD, developmentally delayed; CM, congenital malformation; R, resorption.

Table 6.4 Phenotypic comparison of C57Bl/6 control conceptuses and C57Bl/6 transfer conceptuses at E10.5.

Experimental group		C57Bl/6 control ^a	C57Bl/6 transfer ^a
No. of conceptuses assessed at E10.5			
	Total	95 (10 litters)	43 (8 litters)
	<i>Male</i>	44 ^b	17 ^b
	<i>Female</i>	45 ^b	17 ^b
Average No. of conceptuses/litter [\pmse]			
	Total	9.5 \pm 0.4	5.4 \pm 0.5***
	<i>Male^a</i>	4.4 \pm 0.5 (46.5%) ^b	2.1 \pm 0.5 (39.5%) ^b
	<i>Female^a</i>	4.5 \pm 0.4 (47.4%) ^b	2.1 \pm 0.5 (39.5%) ^b
Phenotypes	Phenotypically normal		
	Total	8.6 \pm 0.5 (90.5%)	3.1 \pm 0.8*** (58.1%)
	<i>Male</i>	4.2 \pm 0.5 (95.5%)	1.3 \pm 0.5*** (58.8%)
	<i>Female</i>	4.1 \pm 0.4 (91.1%)	1.9 \pm 0.5*** (88.2%)
	Growth enhanced		
	Total	0.0	0.4 \pm 0.2^c (7.0%)
	<i>Male</i>	0.0	0.4 \pm 0.2 ^c (17.6%)
<i>Female</i>	0.0	0.0	
Growth restricted			
Total	0.4 \pm 0.2 (4.2%)	0.3 \pm 0.2 (4.7%)	
<i>Male</i>	0.2 \pm 0.1 (4.5%)	0.1 \pm 0.1 (5.9%)	
<i>Female</i>	0.2 \pm 0.1 (4.4%)	0.1 \pm 0.1 (5.9%)	
Developmental delay			
Total	0.0	0.5 \pm 0.5 (9.3%)	
<i>Male</i>	0.0	0.4 \pm 0.4 (17.6%)	
<i>Female</i>	0.0	0.1 \pm 0.1 (5.9%)	
Congenital malformations			
Total	0.0	0.0	
<i>Male</i>	0.0	0.0	
<i>Female</i>	0.0	0.0	
Resorptions^b			
Total	0.5 \pm 0.3 (5.3%)	1.1 \pm 0.4 (20.9%)	
<i>Male</i>	-	-	
<i>Female</i>	-	-	

^aData presented as average number of conceptuses [\pm se] per litter unless otherwise indicated. Number in brackets indicates the percentage of conceptuses with each phenotype;

^bResorptions could not be genotyped for sex due to maternal tissue contamination; ^cp=0.08

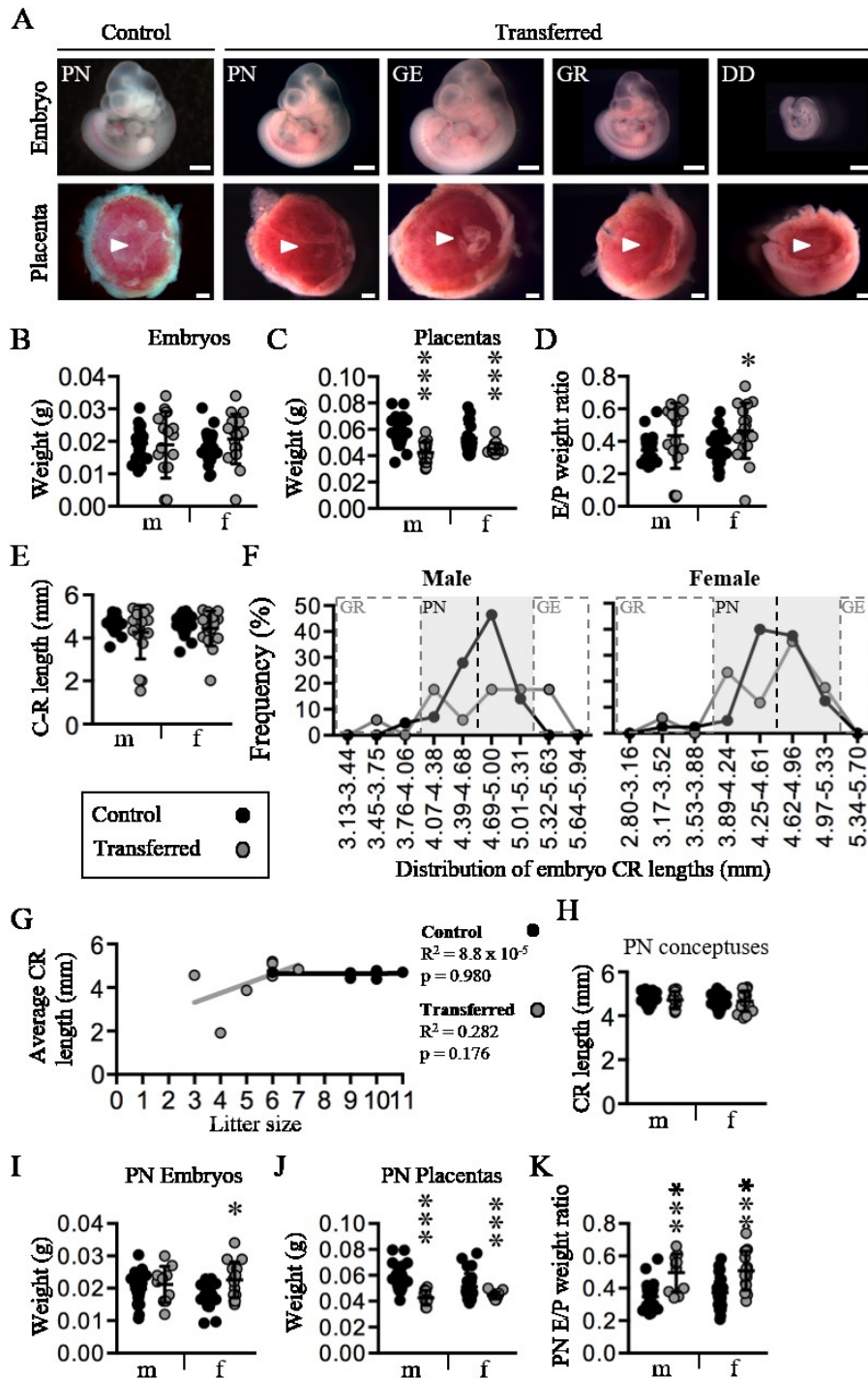


Figure 6.2 Blastocyst transfer results in small placentas with a potential for increased efficiency at E10.5.

(A) Representative images of embryos and placentas from control and transferred conceptuses at E10.5. Phenotypes shown include phenotypically normal (PN), growth enhanced (GE), growth restricted (GR), and developmentally delayed (DD) as determined by crown-rump lengths and somite pair counts. Arrowhead indicates where the allantois (i.e., the umbilical cord) was attached. Scale bars: 500 μ m. (B-E) Graphs showing (B) embryo weights, (C) placenta weights, (D) embryo:placenta (E/P) weight ratios, and (E) embryo

crown-rump (CR) lengths in all control (black) and transferred (grey) conceptuses at E10.5. Values are shown for male (m) and female (f) conceptuses and data are presented as mean \pm standard deviation (SD). (F) Frequency distribution curves of crown-rump (CR) lengths as determined by sex for control (black solid line) and transferred (grey solid line) embryos. The litter that was entirely developmentally delayed was not included in this analysis to ensure that only embryos staged to E10.5 were considered. Black dotted lines indicate the mean crown-rump length for control embryos. Grey shading indicates the lengths of conceptuses that are grossly phenotypically normal (PN). Grey dotted lines indicate crown-rump lengths that are two or more SDs from the control mean. Embryos with lengths that were two SDs below the control mean were considered growth restricted (GR) and two SDs above the mean were considered growth enhanced (GE). (G) Linear regression analysis of litter size versus embryo crown-rump (CR) length in control (black) and transferred (grey) conceptuses. (H-K) Graphs showing parameters for phenotypically normal (PN) conceptuses only including (H) embryo crown-rump (C-R) length, (I) embryo weight, (J) placenta weight, and (K) embryo:placenta (E/P) weight ratios in control (black) and transferred (grey) conceptuses. Data are presented as mean \pm SD and is shown for male (m) and female (f) conceptuses. N=10-43 conceptuses per sex per experiment. Statistical analysis in A-D, G-J: Two-way ANOVA with Sidak's multiple comparison tests were performed to assess the effects of blastocyst transfer and sex on embryo and placenta weights, and embryo:placenta weight ratio. * $p < 0.05$, *** $p < 0.001$.

To further define the growth phenotype of C57Bl/6 conceptuses, crown-rump lengths were measured for each sex. While mean lengths were not different between control and transferred embryos (Figure 6.2E), frequency distribution curves of crown-rump lengths were generated (Figure 6.2F) to detect specific embryos with abnormal growth. Growth restriction and growth enhancement in embryos was defined as crown-rump lengths that were at least two standard deviations below or above the mean crown-rump length of control embryos, respectively. Regardless of sex, a similar frequency of growth restriction was observed in control (4.4 – 4.5% of embryos) and transferred conceptuses at E10.5 (5.9% of embryos, $p = 0.687$; Figure 6.2A, F, Table 6.4). Interestingly, three out of 17 (17.6%) of the transferred male embryos displayed growth enhancement (Figure 6.2A, F, Table 6.4). This frequency was not statistically significant ($p = 0.08$), likely due to the small sample size. No transferred female embryos were growth enhanced (Figure 6.2F, Table 6.4) suggesting that this phenotype might be sexually dimorphic. No correlation between litter size and crown-rump length was observed in control or transferred litters at E10.5 (Figure 6.2G).

When all growth phenotypes (e.g., growth restriction, growth enhancement, developmental delay) and resorptions were grouped together, fewer phenotypically normal (PN) conceptuses

were observed at E10.5 in the transferred group (55.8%; $p < 0.001$) compared to controls (91.6%; Table 6.4). When only PN conceptuses were considered (Figures 6.2A, F), a two-way ANOVA revealed that the blastocyst transfer ($p = 0.0176$) led to an increase in embryo weight, while the sex ($p = 0.9334$) and the interaction between these two factors ($p = 0.2544$) did not have any effect on embryo weight (Figure 6.2I). Similarly, the blastocyst transfer led to a decrease in the placenta weight in both males and females ($p < 0.0001$), while the sex ($p = 0.2780$) had no effect. The interaction between the two factors did not affect placental weight ($p = 0.0597$; Figure 6.2J). Despite that the placentas of transferred conceptuses were smaller than the controls, we observed an increase in the placenta efficiency, as determined by the embryo:placenta weight ratios in PN transferred conceptuses. This reached statistical significance only in the female conceptuses ($p < 0.0001$), while the sex had no effect on embryo:placenta weight ratio ($p = 0.4445$). The interaction between the two factors was not different ($p = 0.8004$; Figure 6.2K). Altogether, these data imply that after blastocyst transfer, the normal growth trajectory of the embryo is reliant upon functional compensation by the placenta, especially in the females.

To further define the growth phenotype of F2 *Mtrr*^{+/+} conceptuses, crown-rump lengths were measured for each sex and frequency distribution curves of crown-rump lengths were generated (Figure 6.3E) to detect specific embryos with abnormal growth. As before, abnormal growth was defined as crown-rump lengths that were at least two standard deviations from the mean length of control embryos. Regardless of sex, growth restriction was rescued after the transfer of the E3.0 blastocyst into the recipient uterus (Padmanabhan et al. 2013; Figure 6.3E). Two out of 26 transferred females (7.7%) and eight out of 26 males (30.8%) were growth enhanced (Figure 6.3E), however this phenotype was not sexually dimorphic ($p = 0.1$), possibly because of the small sample size. This suggests that exposure of the F2 *Mtrr*^{+/+} conceptuses in the abnormal F1 *Mtrr*^{+/+} uterus developmentally programmes them to adjust to a normal environment after blastocyst transfer. This is in contrast to the C57Bl/6 conceptuses, who were never exposed to an abnormal uterine environment, and therefore their placentas possibly undergo less adaptations after transfer into the new maternal environment.

When only PN conceptuses were considered (Figure 6.3A, F), a two-way ANOVA revealed that the blastocyst transfer ($p < 0.0001$), but not the sex ($p = 0.1278$) led to an increase in embryo weight, and the interaction between these two factors also led to an increase in

Table 6.5 Phenotypic comparison of non-transferred F2 *Mtrr*^{+/+} conceptuses and transferred *Mtrr*^{+/+} conceptuses at E10.5.

Experimental group		F2 <i>Mtrr</i> ^{+/+} control ^a	F2 <i>Mtrr</i> ^{+/+} transfer ^a
No. of conceptuses assessed at E10.5			
	Total	172 (21 litters)	53 (8 litters)
	<i>Male</i>	80 ^b	26 ^b
	<i>Female</i>	80 ^b	26 ^b
Average No. of conceptuses/litter [±se]			
	Total	8.2 ± 0.4	6.6 ± 0.6
	<i>Male</i> ^a	3.81 ± 0.4 (46.5%) ^b	3.2 ± 0.3 (49.1%) ^b
	<i>Female</i> ^a	3.9 ± 0.4 (47.1%) ^b	3.2 ± 0.6 (49.1%) ^b
Phenotypes	Phenotypically normal		
	Total	5.6 ± 0.6 (68.6%)	4.8 ± 0.7 (71.7%)
	<i>Male</i>	2.9 ± 0.4 (51.7%)	2.1 ± 0.4 (44.7%)
	<i>Female</i>	2.7 ± 0.4 (48.3%)	2.6 ± 0.6 (55.3%)
	Growth enhanced		
	Total	0.3 ± 0.1 (3.49%)	1.3 ± 0.5 (18.9%)
	<i>Male</i>	0.2 ± 0.1 (3.39%)	1 ± 0.4 (21.1%)
<i>Female</i>	0.1 ± 0.1 (1.7%)	0.3 ± 0.2 (5.3%)	
Growth restricted			
Total	0.1 ± 0.1 (1.7%)	0	
<i>Male</i>	0.1 ± 0.1 (2.5%)	0	
<i>Female</i>	0.4 ± 0.2 (7.6%)	0*	
Developmental delay			
Total	0.3 ± 0.2 (3.5%)	0	
<i>Male</i>	0.1 ± 0.1 (1.7%)	0	
<i>Female</i>	0.2 ± 0.2 (3.4%)	0	
Congenital malformations			
Total	0.9 ± 0.2 (11.0%)	0.5 ± 0.3 (7.5%)	
<i>Male</i>	0.5 ± 0.2 (8.5%)	0.2 ± 0.1 (2.6%)	
<i>Female</i>	0.4 ± 0.1 (7.6%)	0.4 ± 0.3 (7.9%)	
Resorptions^b			
Total	0.3 ± 0.1 (3.5%)	0.1 ± 0.1 (1.9%)	
<i>Male</i>	-	-	
<i>Female</i>	-	-	

^aData presented as average number of conceptuses [± se] per litter unless otherwise indicated. Number in brackets indicates the percentage of conceptuses with each phenotype;

^bResorptions could not be genotyped for sex due to maternal tissue contamination**p*<0.05

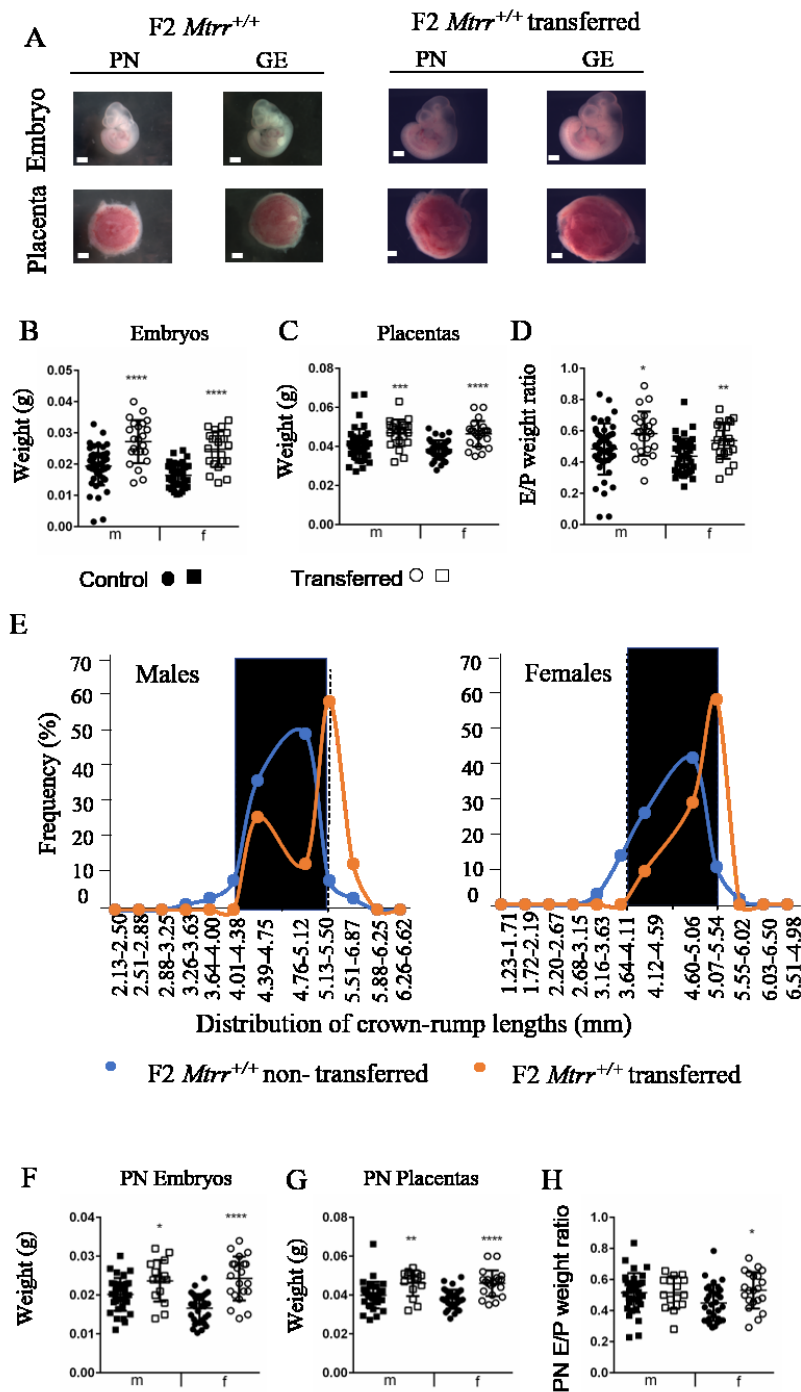


Figure 6.3 Blastocyst transfer into the normal BDF1 environment results in bigger embryos and placentas with a potential for increased efficiency at E10.5.

(A) Representative images of embryos and placentas from non-transferred and transferred F2 *Mtrr*^{+/+} conceptuses at E10.5. Phenotypes shown include phenotypically normal (PN) and growth enhanced (GE) as determined by crown-rump lengths and somite pair counts. Scale bars: 100 μ m. (B-D) Graphs showing (B) embryo weights, (C) placenta weights, and (D) embryo:placenta (E/P) weight ratios, in all non-transferred (full circle) and transferred (hollow circle) F2 *Mtrr*^{+/+} conceptuses at E10.5. Values are shown for male (m) and female (f) conceptuses and data are presented as mean \pm standard deviation (SD). (E) Frequency

distribution curves of crown-rump (CR) lengths as determined by sex for non-transferred (blue solid line) and transferred (orange solid line) F2 *Mtrr*^{+/+} embryos. Black dotted lines indicate the mean crown-rump length for non-transferred embryos. Grey shading indicates the lengths of conceptuses that are grossly phenotypically normal (PN). Grey dotted lines indicate crown-rump lengths that are two or more SDs from the control mean. Embryos with lengths that were two SDs below the control mean were considered growth restricted (GR) and two SDs above the mean were considered growth enhanced (GE). (F-H) Graphs showing parameters for phenotypically normal (PN) conceptuses only including (F) embryo weight, (G) placenta weight, and (H) embryo:placenta (E/P) weight ratios in non-transferred (full circle) and transferred (hollow circle) F2 *Mtrr*^{+/+} conceptuses at E10.. Data are presented as mean \pm SD and is shown for male (m) and female (f) conceptuses. Statistical analysis in A-D, G-J: Two-way ANOVA with Sidak's multiple comparison tests were performed to assess the effects of blastocyst transfer and sex on embryo and placenta weights, and embryo:placenta weight ratio. * $p < 0.05$, ** $p < 0.01$, *** $p < 0.001$, **** $p < 0.0001$.

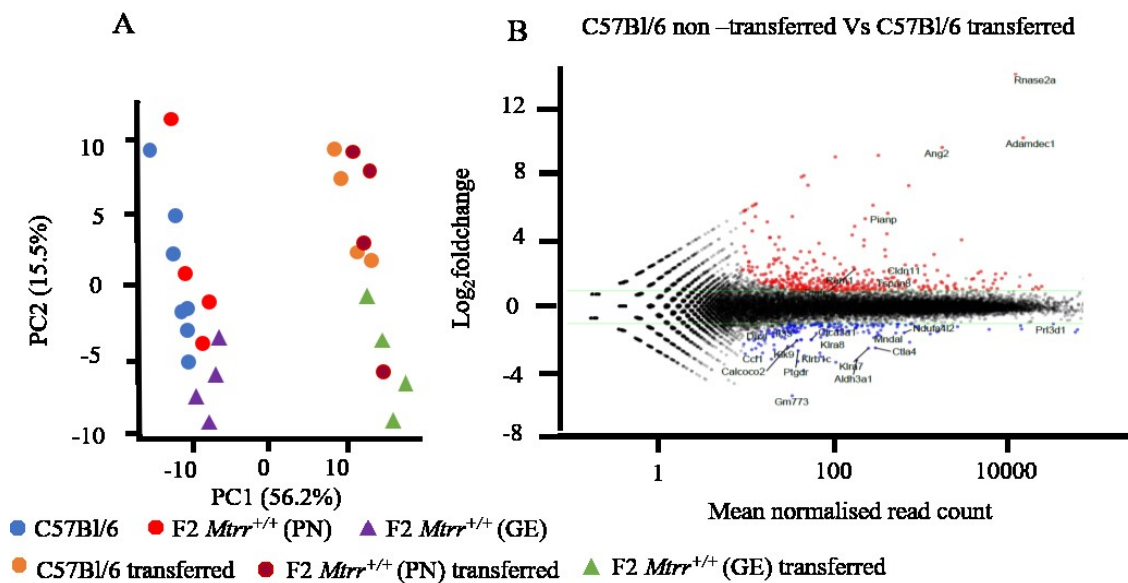
embryo weight ($p = 0.0314$; Figure 6.3F). Similarly, the blastocyst transfer led to decreased placenta weight ($p < 0.0001$), while the sex ($p = 0.4038$) had no effect, suggesting that the placentas of transferred conceptuses, though small, were more efficient. The interaction between the two factors had no effect ($p = 0.4418$; Figure 6.3G). However, neither the blastocyst transfer process ($p = 0.1017$) nor the sex affected the embryo:placenta weight ratio ($p = 0.2938$). Similarly, the interaction between the two factors had no effects on embryo:placenta weight ratio ($p = 0.1009$). However, Sidak's multiple comparisons test revealed an increased embryo:placenta weight ratio in the transferred compared to non-transferred females ($p < 0.05$; Figure 6.3H), reinforcing the hypothesis that placentas of transferred conceptuses are more efficient. Altogether, these data imply that after blastocyst transfer, the normal growth trajectory of the embryo is reliant upon functional compensation by the placenta.

6.2.3 Transferred conceptuses have a different placental transcriptome than non-transferred

To examine how the uterine environment influences or programmes the placental transcriptome of F2 *Mtrr*^{+/+} conceptuses, we assessed the placental transcriptome of non-transferred and transferred placentas via RNA-sequencing. As mentioned in Chapter 5, we observed substantial transcriptional differences between non-transferred and transferred placentas. Similar to our previous analysis (Figure 5.3), we created a PCA plot comparing

non-transferred and transferred C57Bl/6 and F2 *Mtrr*^{+/+} conceptuses (Figure 6.4A), which showed that the samples clustered based on the experimental design: i.e. placentas of non-transferred conceptuses cluster on the left-hand side of the PCA plot, while placentas of transferred conceptuses cluster on the right-hand side.

Firstly, we wanted to determine whether the blastocyst transfer process itself affects placental gene expression. Differential gene expression was determined as a gene that had at least two-fold change in expression. We identified 189 and 355 genes that were downregulated and upregulated, respectively, in the placentas of transferred C57Bl/6 conceptuses compared to the non-transferred C57Bl/6 conceptuses. This suggests that the blastocyst transfer process itself affects placental gene expression (Figure 6.4B, E, Table 6.6). Next, we compared the placental transcriptome of non-transferred and transferred F2 *Mtrr*^{+/+} conceptuses in a phenotype-dependent manner. When comparing transferred to non-transferred conceptuses, we identified 179 and 201 genes that were downregulated and upregulated, respectively, in the placentas of phenotypically normal conceptuses (Figure 6.4C, F, Table 6.6). Additionally, we identified a further 188 and 174 genes that were downregulated and upregulated, respectively, in the placentas of growth enhanced conceptuses that were transferred or non-transferred (Figure 6.4D, G, Table 6.6).



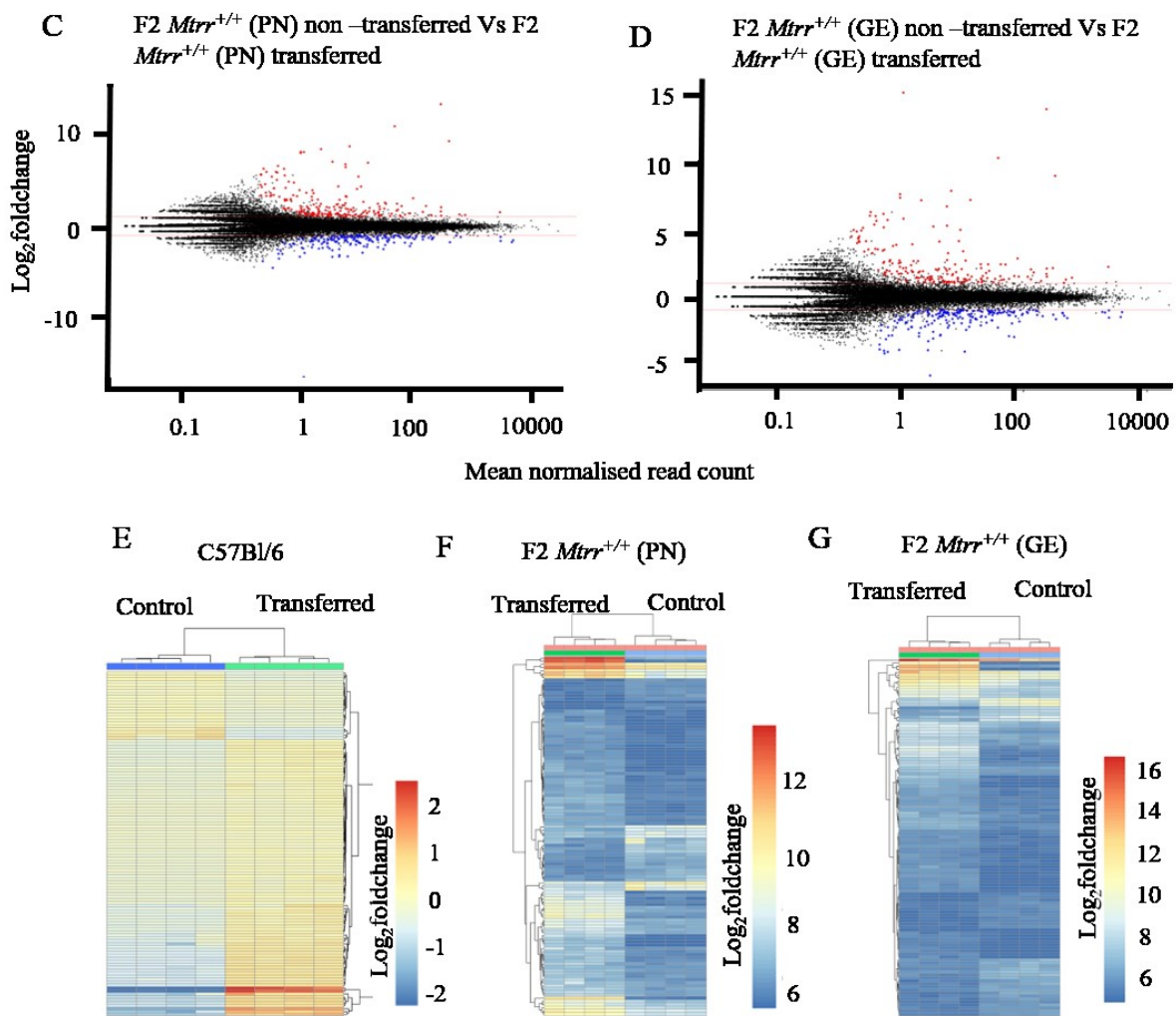


Figure 6.4 Bioinformatic analysis of the RNA sequencing data to compare placental transcriptome of non-transferred and transferred conceptuses.

(A) PCA plot based on the 500 most variable genes. Blue circles: C57Bl/6, red circles: phenotypically normal *Mtrr*^{+/+}, purple triangles: growth enhanced *Mtrr*^{+/+}, orange circles: C57Bl/6 transferred, brown circles: phenotypically normal *Mtrr*^{+/+} transferred, green triangles: growth enhanced *Mtrr*^{+/+} transferred (B-D) MA plots showing DEG between placentas of (B) non-transferred and transferred C57Bl/6 conceptuses (C) non-transferred and transferred phenotypically normal *Mtrr*^{+/+} conceptuses (D) non-transferred and transferred growth enhanced *Mtrr*^{+/+} conceptuses (E-G) Heatmaps showing DEG between placentas of (E) non-transferred and transferred C57Bl/6 (F) non-transferred and transferred phenotypically normal *Mtrr*^{+/+} conceptuses and (G) non-transferred and transferred and growth enhanced *Mtrr*^{+/+} conceptuses. Each column represents an individual placenta. Each row represents one gene.

Table 6.6 Number of DEGs in transferred placentas per genotype and phenotype.

Comparison	C57Bl/6 vs C57Bl/6 transferred		F2 <i>Mtrr</i> ^{+/+} PN vs F2 <i>Mtrr</i> ^{+/+} PN transferred		F2 <i>Mtrr</i> ^{+/+} GE vs F2 <i>Mtrr</i> ^{+/+} GE transferred	
	Down in transferred	Up in transferred	Down in transferred	Up in transferred	Down in transferred	Up in transferred
2<fc<3	131	189	111	86	120	66
3<fc<4	27	64	37	31	29	28
4<fc<10	28	62	27	44	29	34
fc>10	3	40	4	40	10	46
Total	189	355	179	201	188	174

PN: phenotypically normal, GE: growth enhanced, FC: fold-change

Next, we validated the RNA-sequencing experiment using cDNA from C57Bl/6 placentas of non-transferred and transferred conceptuses. We analysed 17 genes that were downregulated in placentas of transferred conceptuses, out of which 11 validated, giving us a validation rate of 64.7% (Figure 6.5). In addition, we analysed eight genes that were upregulated in placentas of transferred conceptuses, out of which five validated, giving us a validation rate of 62.5% (Figure 6.6A). Additionally, we confirmed the expression of two genes, *Med12* and *Serf2*, that was shown to be similar in the placentas of non-transferred and transferred C57Bl/6 conceptuses (Figure 6.6B). Table A.1 shows that all placental cell types are represented by the proteins encoded by the DEGs, as will also be discussed in Section 6.2.5.1. Therefore, the use of whole placentas for qPCR analysis was essential. Finally, we performed gene expression correlation analysis between the RNA sequencing data and the qPCR results (Figure 6.7). We observed no relationship in the expression of downregulated genes between the RNA-seq and qPCR experiments ($r^2=0.02289$, $p=0.5621$; Figure 6.7A). In contrast, we observed a strong positive correlation in the expression of upregulated genes ($r^2=0.9308$, $p=0.0001$ Figure 6.7B). As mentioned in Chapter 5, the reliability of the RNA-seq data increases with higher read counts. The relatively low read counts in combination with the low fold change in the expression of *Tspan8* and *Rem1* compared to the other upregulated genes, might suggest a reason why these two genes did not validate. The genes used for validation are shown on the MA plot in Figure 6.4B. The specific effects of the embryo transfer process itself on the placental transcriptome will be discussed below, by analysing the function of the DEGs between placentas of non-transferred and transferred C57Bl/6 conceptuses.

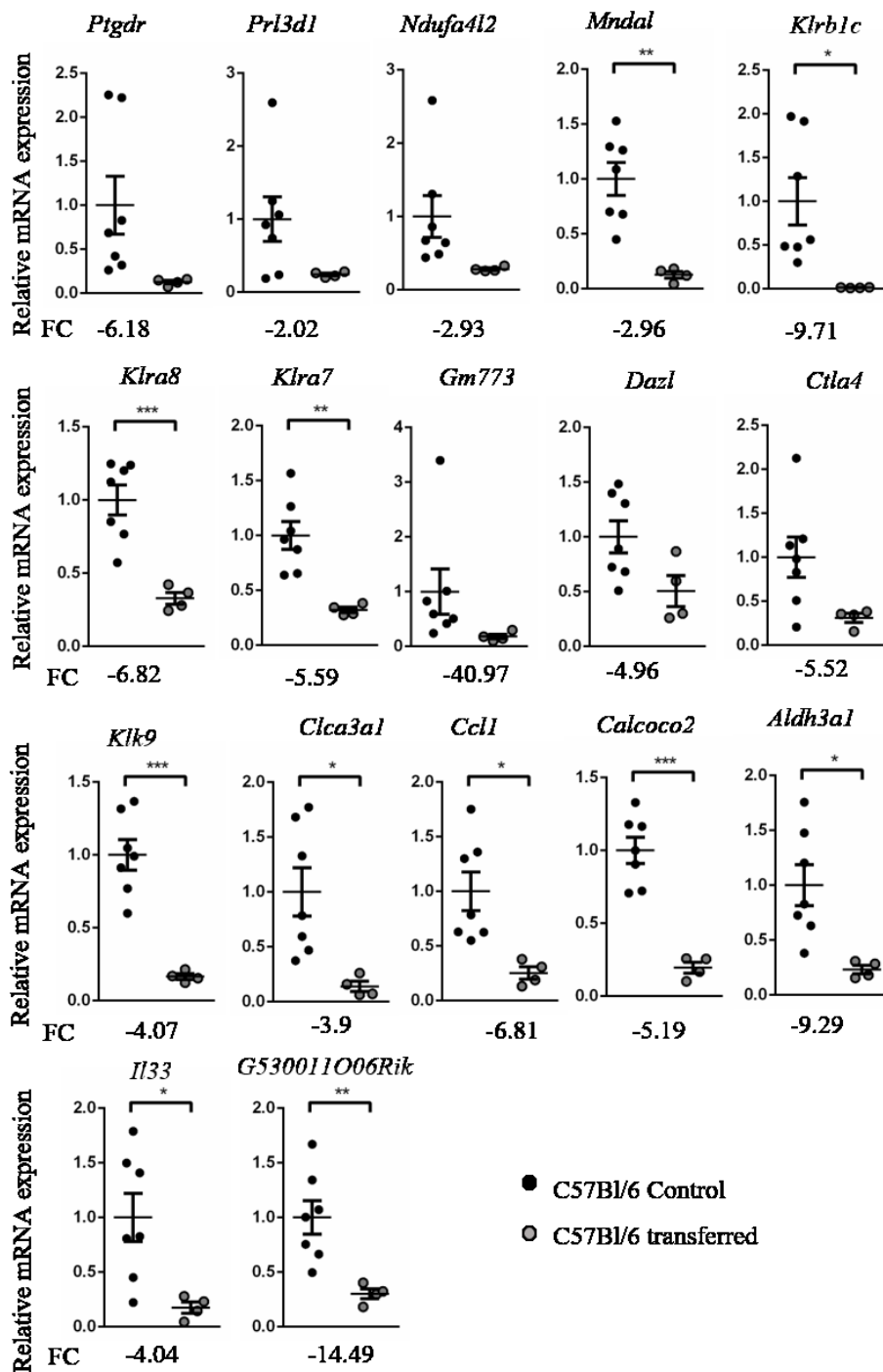


Figure 6.5 Validation of RNA-sequencing data by RT-qPCR analysis of downregulated genes.

Graphs show transcripts that were downregulated in placentas of transferred (grey circles) compared to non-transferred (black circles) C57Bl/6 conceptuses. Data are presented as fold change compared to controls (normalised to 1). N=4-7 placental samples per group. The number below each graph represents the fold change (FC) observed in the RNA-sequencing experiment. Mann-Whitney tests were performed to independently compare transferred

placentas to control placentas, since the sample size was too small to perform a normality test or assume normal Gaussian distribution. *P<0.05, **P<0.01, ***P<0.001.

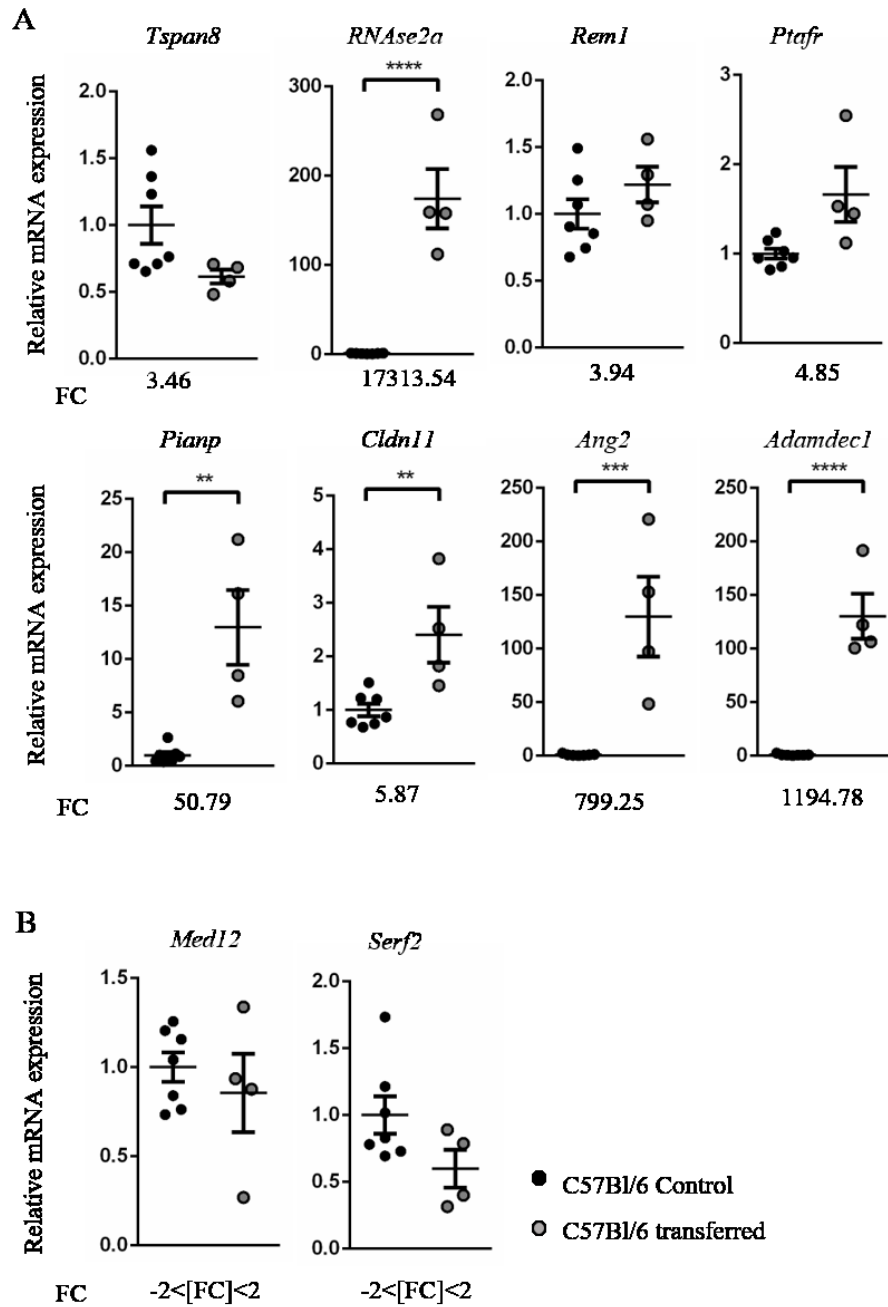


Figure 6.6 Validation of RNA-sequencing data by RT-qPCR analysis of upregulated and non-differentially expressed genes.

Graphs show transcripts that were upregulated in placentas of transferred (grey circles) compared to non-transferred (black circles) C57Bl/6 conceptuses. Data are presented as fold change compared to controls (normalised to 1). N=4-7 placental samples per group. The number below each graph represents the fold change (FC) observed in the RNA-sequencing experiment. Mann-Whitney tests were performed to independently compare transferred placentas to control placentas, since the sample size was too small to perform a normality test or assume normal Gaussian distribution. *P<0.05, **P<0.01, ***P<0.001.

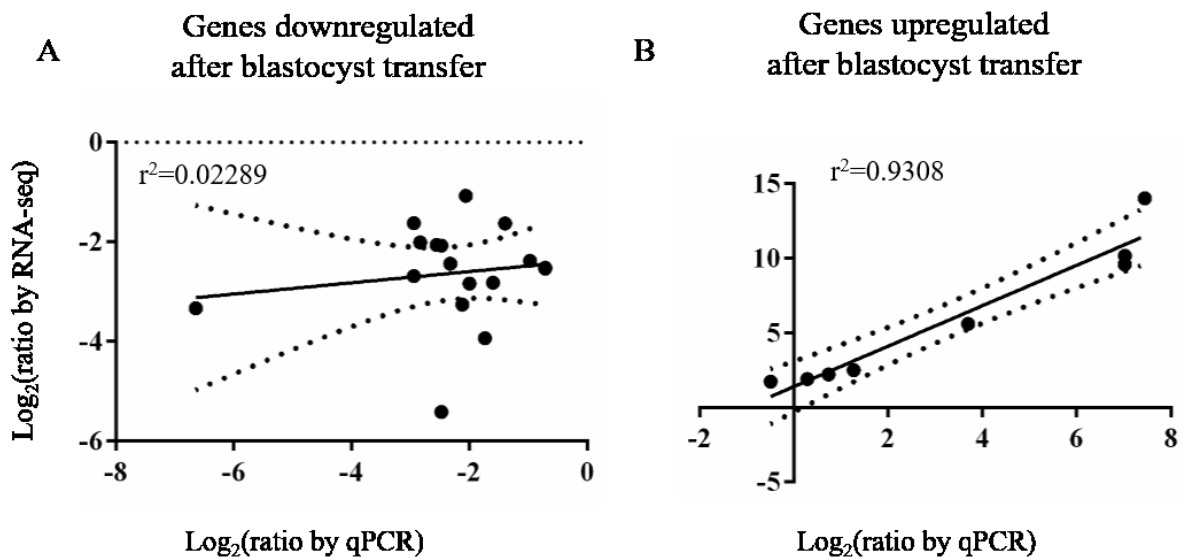


Figure 6.7 Gene expression correlation between the RNA-sequencing data and the qPCR results.

Graphs show the correlation of expression between the RNA sequencing and qPCR data of genes that were (A) downregulated and (B) upregulated in C57Bl/6 placentas after embryo transfer and used for qPCR validation. Linear regression and correlation analyses were performed, and the Pearson correlation coefficient was calculated.

6.2.4 Comparison of DEGs between placentas of non-transferred and transferred conceptuses at E10.5

Considering that there were many DEGs identified when comparing placentas of C57Bl/6 non-transferred and transferred conceptuses, it is likely that a large proportion of DEGs identified in the F2 *Mtrr*^{+/+} placenta comparisons was the result of the blastocyst transfer process. Therefore, we compared the DEGs identified when comparing non-transferred and transferred C57Bl/6 placentas to the DEG lists generated when comparing non-transferred and transferred F2 *Mtrr*^{+/+} conceptuses. Phenotypic comparisons were also kept separate (e.g., placentas from phenotypically normal conceptuses; placentas from growth enhanced conceptuses). Interestingly, there were 271 genes that were differentially expressed between non-transferred and transferred C57Bl/6 placentas only (Figure 6.8). Next, we identified 175 genes that were common between placentas of (a) non-transferred and transferred C57Bl/6 conceptuses, (b) non-transferred and transferred phenotypically normal F2 *Mtrr*^{+/+} conceptuses and (c) non-transferred and transferred growth enhanced F2 *Mtrr*^{+/+} conceptuses

(Figure 6.8). Another 52 and 46 DEGs from F2 *Mtrr*^{+/+} phenotypically normal and growth enhanced, respectively, also overlapped with the C57Bl/6 DEG list. Altogether, these genes were most likely differentially expressed due to the blastocyst transfer procedure and their function will be discussed in Section 6.2.5. Once we removed these genes from the DEG lists, we still identified 153 and 141 misexpressed genes in phenotypically normal and growth enhanced F2 *Mtrr*^{+/+} placentas that underwent blastocyst transfer, respectively, compared to non-transferred F2 *Mtrr*^{+/+} placentas (Figure 6.8). Of these, 50 genes overlapped between phenotypic groups (Figure 6.8), which are likely the result of developmental programming of the conceptus that occurred either during oocyte development or during the first three days of embryo development in the reproductive tract of their F1 *Mtrr*^{+/+} biological mothers.

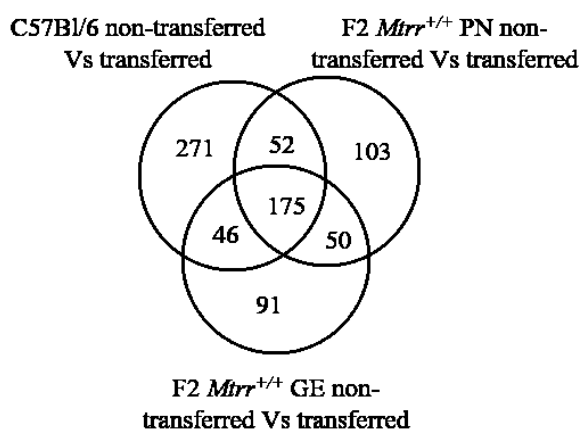


Figure 6.8 Comparisons between the DEGs of controls and transferred conceptuses. Venn diagram comparing the number of DEGs between placentas of non-transferred and transferred conceptuses. PN: phenotypically normal; GE: growth enhanced.

6.2.5 DEGs caused by the embryo transfer protocol

We observed a large number of DEGs in transferred C57Bl/6 conceptuses, therefore we wanted to assess further the effects of the blastocyst transfer process on the placental transcriptome at E10.5. To do this, we performed gene ontology analysis on the DEGs.

6.2.5.1 All major placental cell types are represented by DEGs in transferred C57Bl/6 placentas

To determine whether blastocyst transfer affected gene expression in specific cell types, we performed an extensive literature/database search to resolve the spatial expression of the DEGs in the placenta. Expression was classified in terms of major placental cell types (i.e., trophoblast, fetal vascular endothelium, and decidua) and was largely based on homolog expression in the human placenta due to the availability of data (Uhlen et al. 2015). Of the 544 DEGs identified, the placental expression of 211 genes is currently unknown in mouse and human, and 123 genes are detected in the placenta without information about cell type specificity (i.e., general expression; Figure 6.9A, Table A.1). The spatial expression of the remaining 210 genes was characterised (Figure 6.9A, Table A.1). In many cases, gene expression overlapped in more than one major placental cell populations (Figure 6.9A) indicating that blastocyst transfer is unlikely to affect a single placental cell lineage. A similar proportion of DEGs were detected in trophoblast cells (50.4%) and decidua layer cells (48.6%), though fewer DEGs (27.9%) were detected in the fetal vascular endothelium (27.9%; Figure 6.9A). When distinguished as up- or down-regulated, there was a proportional representation by each gene set in trophoblast cells, decidual layer cells, and fetal vascular endothelial cells (Figure 6.9B). Only a small number of DEGs were exclusively detected in a single major cell population: 1.5% (5/333) of genes in fetal vascular endothelium (e.g., *Cftr*, *Otoa*), 8.1% (27/333) of genes in the decidual layer (e.g., *Klrb1c*, *Cdo1*), and 7.5% (25/333) of genes in trophoblast cells (e.g., *Prl2c2*, *Prl3d1*, *Prl7a1*, and *Prl8a1*; Figure 6.9A, Table A.1). Overall, this result suggests that blastocyst transfer causes broad transcriptional changes throughout the mouse placenta even when the embryo was considered phenotypically normal.

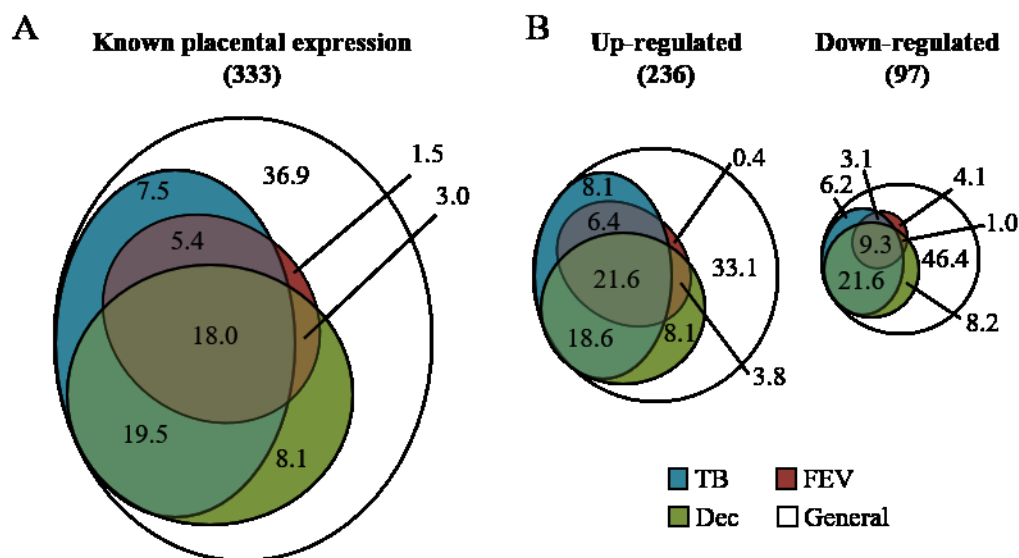


Figure 6.9 Spatial analysis of differentially expressed genes identified in placentas of transferred conceptuses.

(A-B) Venn diagrams showing the percentage of differentially expressed genes with general (white) or known cell-specific expression in the placenta. Trophoblast (TB, blue); fetal endothelial vascular cells (FEV, orange); decidua (Dec, light green). The spatial expression pattern of (A) all differentially expressed genes combined and (B) up-regulated or down-regulated genes separately.

6.2.5.2 *DEG are involved in placental development and function*

The primary annotation terms enriched in whole placentas from transferred conceptuses at E10.5 included genes important for placental development and function (Figure 6.10). Enrichment groups included genes associated with specific mammalian phenotypes (e.g., decreased vascular permeability, abnormal visceral yolk sac, abnormal lipid and glucose homeostasis, and decreased circulating IGF1 and insulin levels), and genes required for specific biological processes (e.g., cell adhesion, response to decreased oxygen levels, and negative regulation of cell proliferation and growth; Figure 6.10). At least 13 DEGs identified are important for placental labyrinth development and/or function as evidenced by gene knockout and over-expression studies (Table 6.7). Furthermore, 31 DEGs encoding for proteins with transporter activity were identified (Table 6.8). The majority of these genes (24/31 genes, 77.4%) were upregulated, which supports the hypothesis that blastocyst transfer results in functional compensation by the placenta to improve transport capacity and maintain embryo growth.

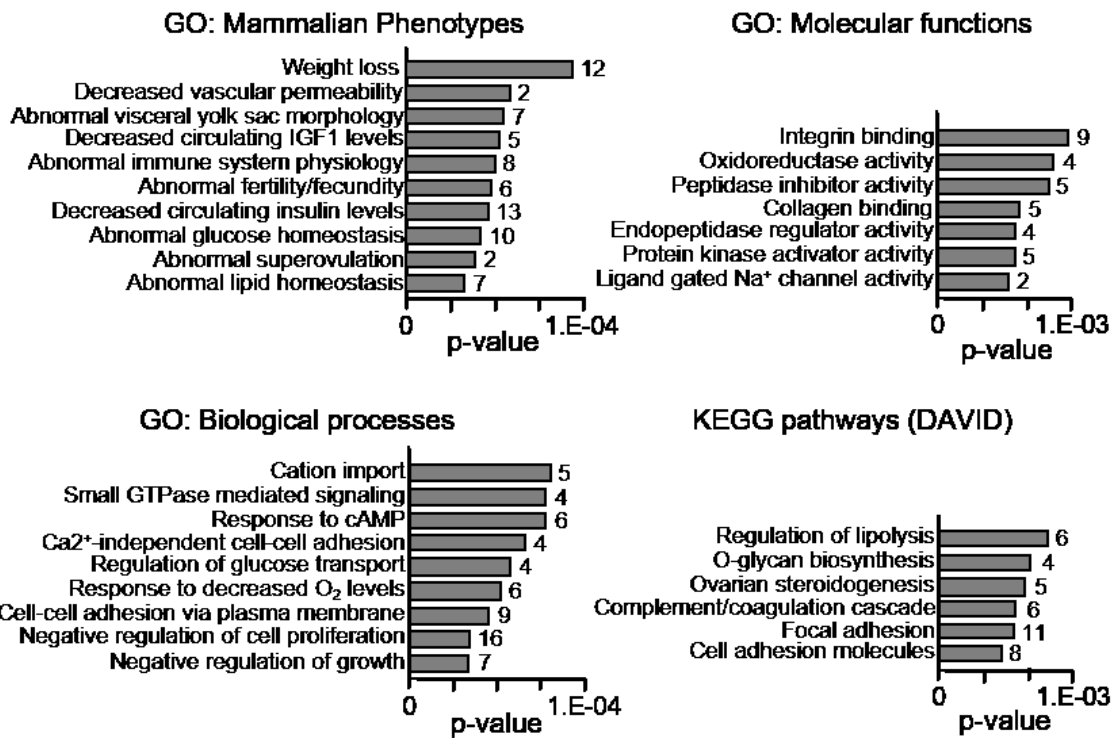


Figure 6.10 Functional analysis of differentially expressed genes identified in placentas of transferred conceptuses.

Gene ontology term enrichment analysis for differentially expressed genes in placentas of transferred conceptuses. The numbers of genes in each term are also given.

Table 6.7 DEGs implicated in growth, placental phenotypes, and/or embryonic lethality at midgestation.

Gene	Gene function	Mouse knockout phenotype or clinical characteristics	Reference	FC
<i>Genetic knockout or decreased expression: defective labyrinth, placental insufficiency and/or growth restriction</i>				
<i>Cubn</i>	Receptor mediated endocytosis	Defects in chorioallantoic attachment [E10.5]	(Smith et al. 2006)	2.9
<i>Enpp2</i>	Angiogenesis	Defective chorioallantoic attachment [E10.5]	(Fotopoulou et al. 2010)	2.5
<i>Zfp361l</i>	RNA binding protein	Failure of chorioallantoic attachment [†] , reduced branching morphogenesis in labyrinth layer, small spongiotrophoblast layer [E10.5 [†]]	(Bell et al. 2006; Stumpo et al. 2004)	2.1
<i>F2</i>	Maintenance of vascular integrity	Reduced or absent branching morphogenesis in labyrinth layer [E10.5 [†]]	(Sun et al. 1998; Xue et al. 1998)	3.4
<i>Rpgrip1</i>	Regulator of ciliary protein traffic	Abnormal vasculature in labyrinth at E14.5 [‘Pre-weaning’ lethality]	DMDD**	-2.0
<i>Slpi</i>	Serine protease inhibitor	Down-regulated expression in rat model of placental insufficiency [ND]	(Goyal et al. 2010)	2.5
<i>Igf1</i>	Insulin-like growth factor	Severely growth restricted; unknown placental phenotype [Perinatal]	(Liu & LeRoith 1999)	2.2
<i>Increased gene expression: trophoblast phenotypes, placental insufficiency, preeclampsia, or FGR</i>				
<i>Aldh3a1</i>	Aldehyde dehydrogenase	OE in mouse TS cells prevents differentiation into <i>Tpbpa</i> ⁺ cells (EPC lineage) [ND]	(Nishiyama et al. 2015)	-9.3
<i>Il33</i>	Interleukin	Inhibits trophoblast invasion and adhesion in vitro [ND]	(Fang et al. 2017)	-4.0
<i>Tac2</i>	Disintegrin and metalloproteinase	Fetal growth restriction in humans associated with increased placental expression [ND]	(Ozler et al. 2016)	-3.1
<i>Crabp2</i>	Retinoic acid signalling pathway	OE in endometrial cell line causes decreased proliferation of trophoblast spheroids [ND]	(Lee, Oh & Cho 2011)	2.3
<i>Cp</i>	Iron peroxidase	Increased placental expression associated with pre-eclampsia in humans [ND]	(Guller et al. 2008)	2.6
<i>Slc9a2</i>	Sodium/hydrogen exchanger	Up-regulated in rat model of placental insufficiency; unknown placental phenotype [Possible embryonic lethality [†]]	(Goyal et al. 2010)	2.9

<i>Genetic knockout: embryonic lethality between E10.5-E11.5 suggesting placental phenotype</i>				
<i>Adamts5</i>	Transcriptional co-activator of SRF	Developmental delay, cardiovascular insufficiency; unknown placental phenotype [E10.5]	(Li et al. 2003)	2.8
<i>Myl7</i>	Myoglobin	Abnormal heart development, growth restriction and developmental delay; unknown placental phenotype [E10.5 [†]]	(Meeson et al. 2001)	-3.7
<i>Myocd</i>	Junctional membrane complex	Abnormal cardiomyocyte development; unknown placental phenotype [E10.5]	(Takeshima et al. 2000)	3.6
<i>Mb</i>	Lipoprotein metabolism	Pale yolk sac, impaired erythropoiesis, neural tube closure defect; unknown placental phenotype [E10.5]	(Raabe et al. 1998)	-2.8
<i>Jph2</i>	Potassium channel	Unknown placental phenotype [E10.5]	(Stieber et al. 2003)	2.4
<i>Mttp</i>	Lipoprotein metabolism	Pale yolk sac, impaired erythropoiesis, neural tube closure defect; unknown placental phenotype [E10.5]	(Raabe et al. 1998)	2.3
<i>Hcn4</i>	Potassium channel	Unknown placental phenotype [E10.5]	(Stieber et al. 2003)	2.6

FC, fold change in RNA-sequencing experiment; KO, knockout; OE, overexpression; E, embryonic day; ND, not determined; *Timing of embryonic lethality; [†]Incomplete penetrance; **Deciphering the Mechanisms of Developmental Disorders (<https://dmdd.org.uk>)

Table 6.8 DEGs encoding proteins with transporter activity.

Gene	FC	Gene Function	Expression in placenta
Down-regulated genes			
<i>Trpm2</i>	-10.11	Calcium channel	TB, Dec
<i>Slc28a2l (Gm14085)</i>	-5.15	Purine nucleoside transporter	General
<i>Clca3a1</i>	-3.90	Calcium-activated chloride channel	Dec
<i>Slc17a8</i>	-3.00	L-glutamate transporter	Unknown
<i>Ndufa4l2</i>	-2.93	NADH dehydrogenase [ubiquinone], mitochondria	General
<i>Slc28a2</i>	-2.03	Sodium-coupled purine nucleoside transporter	Dec

<i>Kcnab2</i>	-2.03	Voltage-gated potassium channel, NADH oxidation	Unknown
Up-regulated genes			
<i>Kcnd2</i>	5.13	Voltage-gated potassium channel	Unknown
<i>Kcne3</i>	3.91	Voltage-gated potassium channel	TB, FVE
<i>Kcnj12</i>	3.07	ATP-sensitive inward rectifier potassium channel	General
<i>Atp6v1c2</i>	2.89	Proton-exporting ATPase, phosphorylative mechanism	TB, FVE, Dec
<i>Slc9a2</i>	2.87	Sodium/hydrogen exchanger	TB, FVE, Dec
<i>Slc13a5</i>	2.87	Sodium-dependent citrate transporter	Dec
<i>Gjb1</i>	2.84	Gap junction protein	TB
<i>Slc7a9</i>	2.72	Sodium-independent L-cystine transporter	General
<i>Abcc6</i>	2.68	ATP-binding cassette transporter	General
<i>Cftr</i>	2.62	ATP-gated chloride channel	FVE
<i>Slc27a2</i>	2.60	Fatty acid transporter	TB
<i>Hcn4</i>	2.58	Cyclic nucleotide-gated potassium channel	Unknown
<i>Slc7a11</i>	2.57	Cysteine/glutamine transporter	General
<i>Cacna1b</i>	2.56	Voltage-gated calcium channel	Unknown
<i>Jph2</i>	2.42	Calcium channel	TB, Dec
<i>Slc39a8</i>	2.31	Zinc ion transporter	TB, Dec
<i>Trpm3</i>	2.31	Cation channel	Unknown
<i>Mtp</i>	2.30	Microsomal triglyceride transfer protein	TB
<i>Kcnk2</i>	2.21	Potassium channel	Unknown
<i>Asic2</i>	2.14	Voltage-gated sodium channel	TB
<i>Apom</i>	2.09	Lipid transport	TB, FE, Dec
<i>Scnn1g</i>	2.07	Amiloride-sensitive sodium channel	General
<i>Amn</i>	2.04	Cobalamin and lipid transport	TB
<i>Slc4a1</i>	2.03	Chloride/bicarbonate exchanger	FBCs

TB, trophoblast; FC, fetal capillaries; FBCs, fetal blood cells; Dec, maternal decidua; General, expression determined by Mouse ENCODE project via RNA-seq of mouse placentas; human placenta expression determined via Human Protein atlas.

6.2.5.3 Dysregulation of DNA methylation by blastocyst transfer is unlikely to be the primary mechanism of transcriptional disruption

Studies have shown the effects of ART procedures, such as superovulation, *in vitro* fertilisation, and embryo culture on the expression of imprinted genes in the placenta (Fortier et al. 2008; Sanjeev Khosla et al. 2001; Mann et al. 2004), a process which is regulated by DNA methylation. The mechanism by which blastocyst transfer alters gene expression is not well understood, though epigenetic dysregulation has been implicated (Canovas et al. 2017; Choux et al. 2015). For instance, embryo transfer alters the expression of imprinted genes in the mouse placenta at E9.5. Monoallelic expression of *H19*, *Snrpn*, *Igf2*, *Kcnq1ot1*, *Cdkn1c*, *Kcnq1*, *Mknr3*, *Ascl2*, *Zim1*, *Peg3* was observed in the unmanipulated conceptuses, while aberrant expression of these genes was observed in placentas and yolk sacs of transferred conceptuses. Placentas and yolk sacs derived from embryos that were cultured *in vitro* prior to embryo transfer, showed an even higher degree of aberrant gene expression. *IgfII* and *Ascl2* levels in placentas of both manipulated groups (i.e. embryo transfer and *in vitro* culture) were downregulated and upregulated respectively, compared to the unmanipulated ones (Rivera et al. 2008). This suggests that embryo transfer might affect DNA methylation, leading to misexpression of imprinted genes. To examine the potential sensitivity of the DEGs to changes in CpG methylation, we evaluated whether the top 50 down-regulated genes (FC>3.1) and top 50 up-regulated genes (FC>6.7) contained intragenic or proximal CpG repeats within 20 kb of the gene (Figure 6.11A). This result was compared to 50 randomly selected genes as a proxy for the genome. While this analysis did not determine whether the CpG repeats present were methylated or directly regulate gene expression, it highlights the potential for gene dysregulation when methylation patterns are altered. Compared to the rest of the genome, both up- and down-regulated gene sets were less likely to contain intragenic CpG repeats (24-30% of DEGs compared of 46% of genes genome-wide; $p<0.05$, Fisher's exact test; Figure 6.11A). Moreover, down-regulated DEGs were less frequently associated with proximal CpG repeats (26% of DEGs; $p<0.05$) than both the up-regulated gene set (40% of DEGs) and the genome (42% of genes; Figure 6.11A). Overall, these findings suggest that genes that were differentially expressed after blastocyst transfer are less likely to be cis regulated by CpG methylation compared to the genome at large.

We identified 15 DEGs whose regulation has been directly linked to CpG methylation at specific genomic locations in other studies (Table 6.9). Based on the published data and our RNA-seq data, we predicted that seven of these DEGs should be associated with CpG

hypomethylation and eight DEGs with CpG hypermethylation (Table 6.9). Next, we sought to validate CpG methylation in two of these 14 loci (i.e., *Prl3dl* and *Rasgrfl*) via bisulfite pyrosequencing (in collaboration with Dr. G. Blake; Figure 6.11B). Whole placentas from transferred conceptuses were compared to non-transferred controls (n=5 female placentas per group). RT-qPCR analysis revealed a 4.1-fold and 2.3-fold decrease in *Prl3dl* mRNA expression in male and female transferred placentas, respectively, compared to controls (Figure 6.11C). Thus, CpG hypermethylation in the *Prl3dl* promoter was expected (Hayakawa et al. 2012). Nevertheless, analysis of five CpG sites across the *Prl3dl* promoter revealed similar levels of methylation in each placenta group (Figure 6.11D). Likewise, we assessed CpG methylation in the differentially methylated region (DMR) associated with the *Rasgrfl* gene. Since RNA-sequencing determined a 2.7-fold decrease in *Rasgrfl* mRNA in transferred placentas, hypomethylation of the *Rasgrfl* DMR was expected (Yoon et al. 2005). However, four out of five CpGs assessed showed consistent levels of methylation in transferred and control placentas (Figure 6.11E). CpG-5 was hypomethylated in transferred placentas ($20.7 \pm 4.1\%$ methylated compared to $38.6 \pm 4.0\%$ in controls; $p < 0.0001$; Figure 6.11E), but hypomethylation of a single CpG among many is unlikely to be responsible for decreased *Rasgrfl* mRNA expression. Altogether, these data suggest that disruption of CpG methylation by blastocyst transfer is unlikely to be a primary mechanism driving transcriptional changes in the mouse placenta at E10.5.

Table 6.9 DEG with known regulation by DNA methylation.

Gene name	Function	Known characteristics of epigenetically regulated expression	Fold change	Predicted CpG methylation*	Ref.
DEGs that were downregulated in the placenta (E10.5) after blastocyst transfer					
<i>Trpm2</i>	Cation channel	Methylation of inner CpG island associated with gene repression	-10.11	Hyper	(Orfanelli et al. 2008)
<i>Klra4</i>	Killer cell lectin-like receptor; cell adhesion	Promoter hypomethylation associated with gene activation	-8.83	Hyper	(Rouhi et al. 2009)
<i>Dazl</i>	RNA binding protein	Promoter methylation is associated with gene repression	-4.96	Hyper	(Hackett et al. 2012)
<i>Prl8a1</i>	Prolactin hormone family	Placenta-specific DNA hypomethylation associated with gene activation	-2.89	Hyper	(Hayakawa et al. 2012)
<i>Prl7a1</i>	Prolactin hormone family	Placenta-specific DNA hypomethylation associated with gene activation	-2.85	Hyper	(Hayakawa et al. 2012)
<i>Rasgrfl</i>	Guanine nucleotide-releasing factor	Paternally-methylated (imprinted) and expressed, methylation leads to gene activation	-2.70	Hypo	(Yoon et al. 2005)
<i>Kazald1</i>	Insulin growth factor binding protein family	Promoter hypomethylation associated gene activation	-2.25	Hyper	(Wang et al. 2013)
<i>Prl3d1</i>	Prolactin hormone family	Placenta-specific DNA hypomethylation of promoter associated with gene activation	-2.02	Hyper	(Hayakawa et al. 2012)

DEGs that were upregulated in the placenta (E10.5) after blastocyst transfer					
<i>Edn2</i>	Angiogenesis	Hypomethylation of intragenic region associated with gene activation	7.15	Hypo	(Wang et al. 2013)
<i>Cldn11</i>	Gap junction protein	Promoter hypermethylation associated with gene repression	5.87	Hypo	(Agarwal et al. 2009)
<i>Eno2</i>	Glycolysis	Promoter hypermethylation associated with gene repression	5.65	Hypo	(Wang et al. 2014)
<i>Inhba</i>	TGF β signaling pathway	Promoter hypermethylation in human placenta associated with gene repression	4.42	Hypo	(Wilson et al. 2015)
<i>Cfb</i>	Complement factor	Promoter hypermethylation associated with gene repression; in human placenta, becomes hypomethylated upon CytoT to SynT differentiation	4.40	Hypo	(Yuen et al. 2013)
<i>Tfpi2</i>	Polycomb repressive complex	Promoter hypomethylation associated with gene repression	3.1	Hypo	(Hu et al. 2017; Ribarska et al. 2010)
<i>Cobl</i>	Actin interacting protein	Tissue-specific parentally-biased expression (<i>Grb10</i> imprinted DMR); maternal methylation at <i>Grb10</i> DMR in yolk sac results in maternal <i>Cobl</i> expression	2.61	Hyper	(Shiura et al. 2009)

*Predicted change in CpG methylation based on differential expression observed in RNA-sequencing experiment; DEG, differentially expressed gene

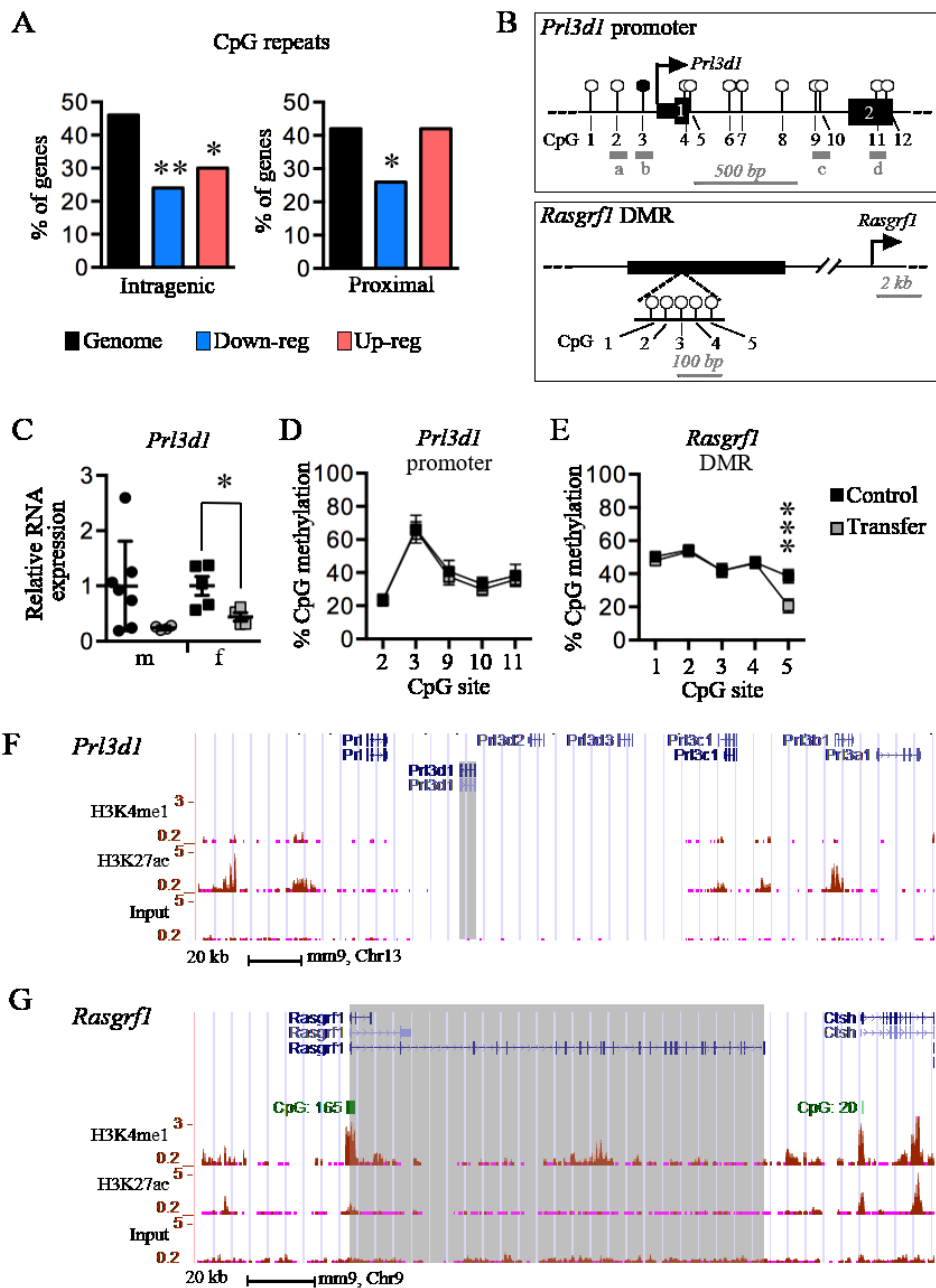


Figure 6.11 Unlikely that blastocyst transfer directly alters placental gene expression via CpG methylation.

(A) The percentage of the top 50 down-regulated (blue bars, FC > 3.1) or up-regulated (pink bars, FC > 6.7) DEGs after blastocyst transfer that associate with CpG repeats localised intragenically or proximally (within 20 kb). The percentage of 50 randomly selected genes is indicated as a proxy for the genome (black bars). Statistical analysis: Fisher's exact test. *p<0.05, **p<0.01. (B) Schematic drawings of the *Prl3dl* promoter and the *Rasgrfl* DMR. Open circles represent unmethylated CpG sites and closed circles indicate methylated CpG sites in placental tissue. a-d represent regions assessed by bisulfite pyrosequencing in *Prl3dl* promoter. (C) RT-qPCR analysis of *Prl3dl* transcripts in male (m) and female (f) placentas

of control (black dots) and transferred (grey dots) conceptuses at E10.5. Data are presented as fold change compared to controls (normalised to 1; mean \pm sd). N = 4-7 placentas per group. Statistical analysis: independent t test. * $p < 0.05$. (D-E) CpG site-specific methylation (mean \pm se) in (D) the promoter region of the *Prl3dl* gene and (E) the *Rasgrfl* DMR as determined via bisulfite pyrosequencing of DNA from control (black) and transferred (grey) female placentas at E10.5. N=5 placentas per gene locus. Statistical analysis: independent t test. *** $p < 0.001$. (F-G) Screen shots of genomic regions of (F) *Prl3dl* and (G) *Rasgrfl* as determined by UCSC mouse genome browser (<http://genome.ucsc.edu>) gene tracks using NCBI37/mm9 genome assembly. The location of the genes, CpG repeats (green), and ChIP-seq data from normal mouse placentas at term showing enrichment of H3K4me1 and H3K27ac histone modifications (from Bing Ren's laboratory) are shown. Shaded regions indicate gene of interest.

6.2.5.4 Some DEGs cluster in the genome implying common transcriptional regulation

Next, we determined the chromosomal location of DEGs ($FC > 3$) including 155 up-regulated and 60 down-regulated genes (Figure 6.11A). While the DEGs were distributed throughout the genome, we identified 18 genomic regions (< 335 kb) with two or more DEGs (Figure 6.12A). This was unlikely to occur by chance since gene clusters were not identified in a group of 60 randomly selected genes (data not shown). This result suggested that clustered genes might share common regulatory mechanisms. Therefore, we assessed whether these genomic regions included CpG repeats and histone modifications using University of California Santa Cruz (UCSC) Mouse Genome Browser (Haeussler et al. 2019; Kent et al. 2002) and a published ChIP-seq data set that displayed genomic enrichment for H3K4 monomethylation (me1) and H3K27 acetylation (ac) in normal C57Bl/6 mouse placentas at term (Stamatoyannopoulos et al. 2012). High levels of H3K4me1 and H3K27ac at enhancers and/or promoters are generally associated with transcriptionally active genes (Zhang & Reinberg 2001). While some regions (5/18 regions, 27.8%) lacked CpG repeats and enrichment of placental H3K4me1 or H3K27ac peaks (eg. Chr1: *Ifi208*, *Mndal*, *Ifi202b*; Figure 6.12D), the majority (13/18 regions, 72.2%) showed potential for a shared regulatory region (Figure 6.12B-C). For example, *Edn2* and *Foxo6* ($FC > 5.3$) are located within a region on chromosome 4 that is enriched in CpG repeats and placental H3K4me1 (Figure 6.12B). Additionally, *Klk8* and *Klk9* genes ($FC > 3.2$) on chromosome 7 share three placental H3K4me1 peaks and a CpG repeat region (Figure 6.12C). Furthermore, *Prl3dl* and *Rasgrfl* genes, which did not show DNA methylation changes after blastocyst transfer (Figure 6.11D-

E), are proximal to histone modification peaks in the placenta (Figure 6.12E-F). Altogether, these data support the hypothesis that, after blastocyst transfer, epigenetic marks including histone modifications might be dysregulated to alter placenta development and/or function.

Interestingly, five DEGs (*AU022751*, *Myocd*, *L3mbtl2*, *Chd5*, and *Pygo1*) are involved in the regulation of histone modifications including methylation and acetylation (Cao et al. 2005; Fiedler et al. 2008; Kloet et al. 2016; Maier et al. 2015; Potts et al. 2011; Trojer et al. 2011; Zhuang et al. 2014). Indeed, the dysregulation of proteins involved in chromatin remodelling has large implications for widespread transcriptional dysregulation. To explore histone modifications as a potential mechanism for transcriptional change after blastocyst transfer, we used the same published ChIP-seq data set as above (Haeussler et al. 2019). The top 50 up-regulated genes (FC >6.7) and top 50 down-regulated genes (FC > 3.1) were assessed for normal intragenic and proximal placental H3K4me1 and H3K27ac peaks. The frequency of association was compared with 50 randomly selected genes representing the genome. DEGs showed a similar association to intragenic placental H3K4me1 (62-70% of DEGs; p=0.1764, Fisher's exact test) compared to the genome (74% of genes; Figure 6.11E). Compared to 86% of upregulated DEGs and genes in the genome, 68% of down-regulated DEGs were associated with proximal placental H3K4me1 (p<0.0001; Figure 6.12E). However, these data suggest that the majority of DEGs might be sensitive to changes in histone methylation, particularly H3K4me1. Alternatively, the top DEGs were less likely to associate with placental H3K27ac peaks under normal conditions compared to the rest of the genome (intragenic: 20-26% of DEGs versus 60% of genes in genome, p<0.0001; proximal: 54-56% of DEGs versus 72% of genes in genome, p=0.0169; Figure 6.12F). While regulation of some DEGs in the placenta might require histone acetylation, it is less likely that this group of genes requires it for their regulation under normal conditions. From this, we hypothesise that the DEGs might be more sensitive to changes in histone methylation than histone acetylation. A ChIP-seq experiment using antibodies against these and other histone modifications in transferred placentas is required to explore this question further.

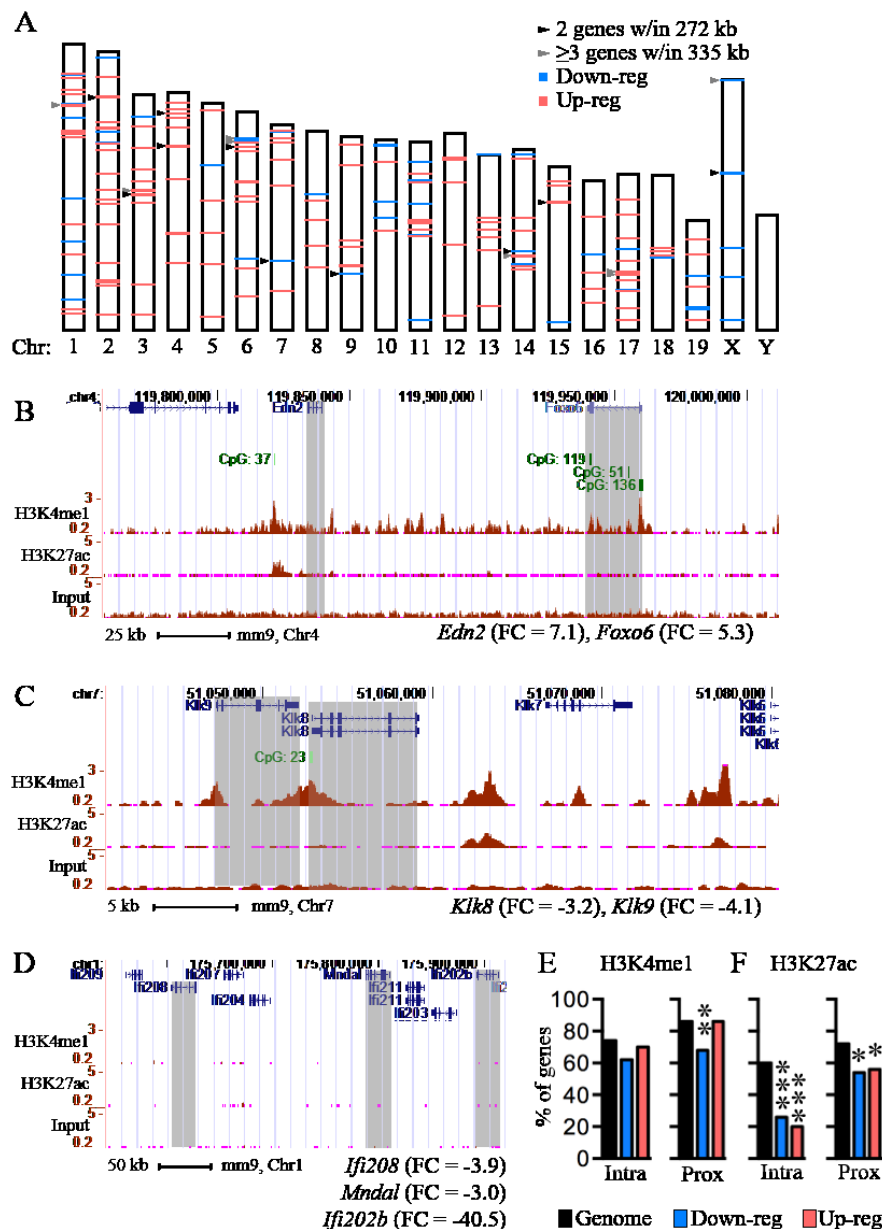


Figure 6.12 Clustering of differentially expressed genes in the genome suggests shared regulatory regions.

(A) Schematic representation of mouse chromosomes 1-19 and X indicating the location of differentially expressed genes (FC > 3) in whole placentas after embryo transfer as determined via RNA-sequencing. Pink lines, up-regulated genes; blue lines, down-regulated genes. Arrowheads indicate gene clusters: black arrowhead, two genes within a 75 kb window; grey arrowhead, three or more genes that are within a 335 kb window. (B-D) Screen shots of examples of clustered gene regions as shown by UCSC genome browser (<http://genome.ucsc.edu>) gene tracks that indicate location of the genes, CpG repeats (green), and ChIP-seq data from mouse placentas at term showing enrichment of H3K4me1 and H3K27ac histone modifications (from Bing Ren's laboratory) are shown. Shaded regions indicate genes of interest. FC, fold-change determined in the RNA-sequencing experiment.

(E-F) The percentage of the top 50 down-regulated (blue bars, FC > 3.1) or up-regulated (pink bars, FC > 6.7) DEGs after blastocyst transfer that display (E) placental H3K4me1 peaks, or (F) placental H3K27ac peaks localised intragenically (Intra) or proximally (Prox; within 20 kb). The percentage of 50 randomly selected genes is indicated as a proxy for the genome (black bars). Statistical analysis: Fisher's exact test. *p<0.05, **p<0.01, ***p<0.001.

6.2.6 DEGs as a result of developmental programming of F2 *Mtrr*^{+/+} conceptuses

Gene ontology analysis of all the genes that were differentially expressed due to the blastocyst transfer process was described in the previous section. Next, we wanted to see whether the F2 *Mtrr*^{+/+} conceptuses respond differently to the blastocyst transfer into the BDF1 uterus compared to the C57Bl/6 conceptuses. Therefore, we performed gene ontology analysis on the DEGs in transferred F2 *Mtrr*^{+/+} placentas.

6.2.6.1 F2 *Mtrr*^{+/+} conceptuses respond differently to the blastocyst transfer into a BDF1 uterus at E3.0 compared to C57Bl/6 conceptuses

First, we performed gene ontology analysis on the 271 genes that were differentially expressed only in the transferred C57Bl/6 placentas. These genes were not differentially expressed in transferred F2 *Mtrr*^{+/+} placentas. Enriched biological processes were involved in metabolism, such as glucose homeostasis (*Prkaa2*, *Hnf4a*, *Hkdc1*, *Igf1*, p=0.02) and regulation of glycogen metabolism (*Igf1*, *Sorbs1*, p=0.02). Other enriched biological processes were involved in embryo development, such as somite development (*Sfrp2*, *Meox1*, p=0.01), cellular response to decreased oxygen levels (*Mt3*, *Hipk2*, *Aqp1*, *Zfp3611*, p=0.01), and regulation of cell growth (*Sfrp2*, *Hnf4a*, *Slit3*, *Inhba*, *Mt3*, p=0.02). Finally, regulation of angiogenesis (*Sfrp2*, *Cntn1*, *Thbs1*, *Pgf*, *Hipk2*, *Aqp1*, p=0.003) and regulation of BMP signalling (*Lrp2*, *Fbn1*, *Hipk2*, p=0.009) were also enriched (Figure 6.13A). Enriched molecular function terms included integrin binding (*Sfrp2*, *Igf1*, *Thbs1*, *Fbn1*, p=0.04), collagen binding (*Clqtnf1*, *Thbs1*, *Antxr1*, p=0.03), insulin receptor binding (*Igf1*, *Sorbs1*, p=0.03), and ion channel activity (*Scnn1g*, *Trpm2*, *Trpv6*, *Cacna1b*, *Trpm3*, p=0.009; Figure 6.13B). Finally, enriched mammalian phenotypes included absent amnion (*Cubn*, *Amn*, *Hnf4a*, p=0.002), weight loss (*Galc*, *Scnn1g*, *Chrm3*, *Sftpd*, *Cntn1*, *Slc4a1*, *Ctsf*, *Cftr*, p=0.002), cardiac hypertrophy (*Gucy2c*, *Amn*, *Fxyd1*, *Slc4a1*, *Trim55*, *Fbn1*, p=0.002),

abnormal circulating insulin levels (*Klb*, *Glp1r*, *Sorbs1*, $p=0.002$), and decreased IGF levels (*Galc*, *Rasgrfl*, *Foxl2*, *Igf1*, $p=0.003$; Figure 6.13C).

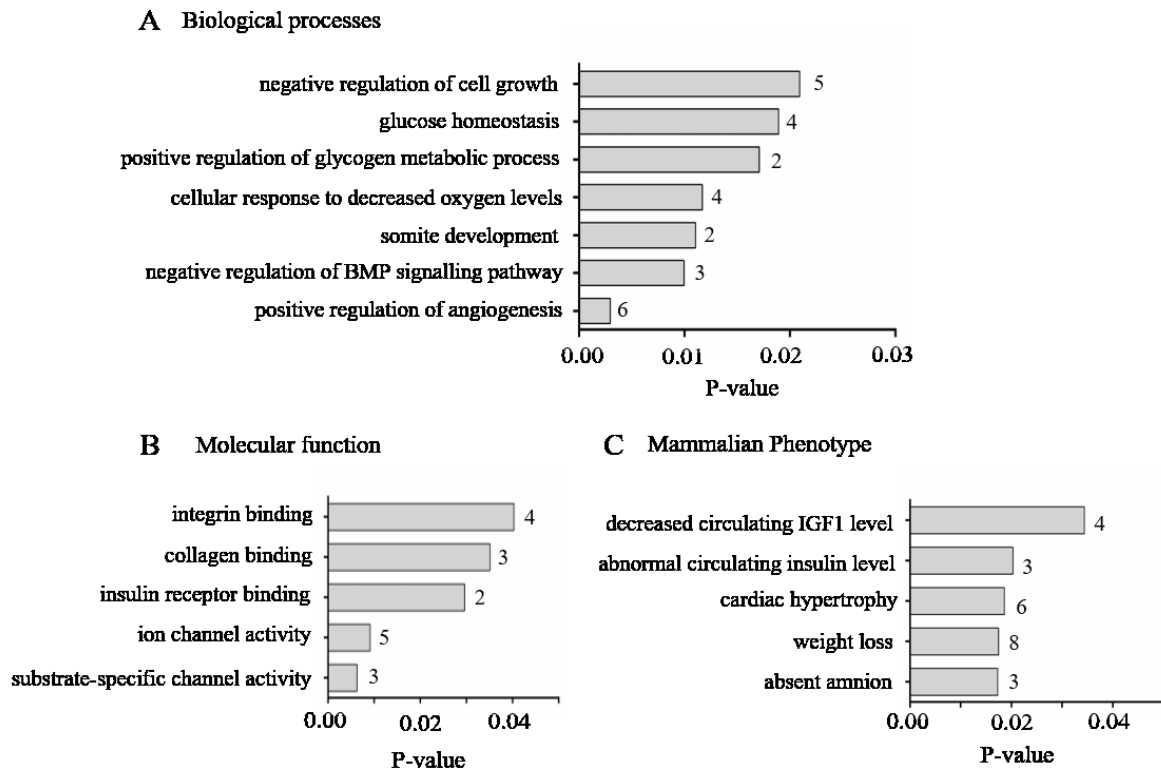


Figure 6.13 Gene ontology analysis of the DEGs in transferred C57Bl/6 but not F2 *Mtrr*^{+/+} placentas.

(A) Biological processes, (B) Molecular function, (C) Mammalian phenotypes that are enriched according to Enrichr. The number next to each bar shows the number of DEGs that fall under that term.

Next, we wanted to see whether similar biological processes and molecular functions are affected in the F2 *Mtrr*^{+/+} conceptuses after blastocyst transfer. The F2 *Mtrr*^{+/+} conceptuses had global DNA hypomethylation (Padmanabhan et al. 2013). Additionally, we showed that F1 *Mtrr*^{+/+} uteri have abnormal structure at estrus, such as increased myometrial thickness, increased invaginations in the lumen epithelium, and decreased *Pgr* mRNA and protein expression at estrus (Chapter 3). Implantation sites of F1 *Mtrr*^{+/+} females also had decreased *Bmp2* levels at E6.5 (Chapter 4). Altogether, these data evidence that the uterine environment of F1 *Mtrr*^{+/+} females is abnormal. The F2 *Mtrr*^{+/+} conceptuses developed in the abnormal F1 *Mtrr*^{+/+} uteri until E3.0, before being transferred to the normal uterine environment of a BDF1 female (Padmanabhan et al. 2013). The F2 *Mtrr*^{+/+} conceptuses were initially

developmentally adapted in the environment of the F1 *Mtrr*^{+/+} uteri, and after E3.0 they were exposed to a different uterine environment. This environmental mismatch (Bateson et al. 2004) is probably responsible for the rescue of growth restriction and developmental delay and increased frequency of growth enhancement of F2 *Mtrr*^{+/+} conceptuses after embryo transfer (Padmanabhan et al. 2013). Therefore, we performed gene ontology analysis on the 244 DEGs in transferred F2 *Mtrr*^{+/+} placentas.

Enriched biological processes include vasoconstriction (*Ednra*, *Htr2b*, *Adra1b*, p=0.0005), regulation of blood vessel diameter (*Ednra*, *Htr2b*, p=0.009), G-protein coupled receptor signalling (*Htr6*, *Vipr1*, *Htr2b*, *Adra1b*, *Rxfp1*, p=0.019), regulation of MAPK cascade (*Bmp2*, *Ccl22*, *Insrr*, *Htr2b*, *Ptpn22*, *Tnfrsf1a1*, *Adra1b*, *Ephb1*, p=0.02), regulation of *ErbB* signalling (*Mmp9*, *Art4*, p=0.03), and regulation of EGF receptor signalling (*Mmp9*, *Sh3gl2*, *Art4*, p=0.03; Figure 6.14A). Enriched molecular function terms include G-protein coupled receptor activity (*Htr6*, *Vipr1*, *Gpr34*, *Ptger2*, *Gpr171*, *Htr2b*, *Gpr75*, *Rxfp1*, *Adgrl3*, p=0.006), BMP binding (*Grem1*, *Gdf5*, p=0.006), CoA hydrolase activity (*Acot11*, *Acot12*, p=0.02), and ribonuclease activity (*Endou*, *Slfn14*, *Samhd1*, p=0.02; Figure 6.14B). Finally, enriched mammalian phenotypes include abnormal heart orientation (*Bmp2*, *Pdlim3*, p=0.02), abnormal body weight (*Pyy*, *Serpine1*, p=0.03), increased angiogenesis (*Serpine1*, *Mmp9*, p=0.03), abnormal embryo implantation (*Dnah11*, p=0.03), and delayed allantois development (*Bmp2*, p=0.04; Figure 6.14C).

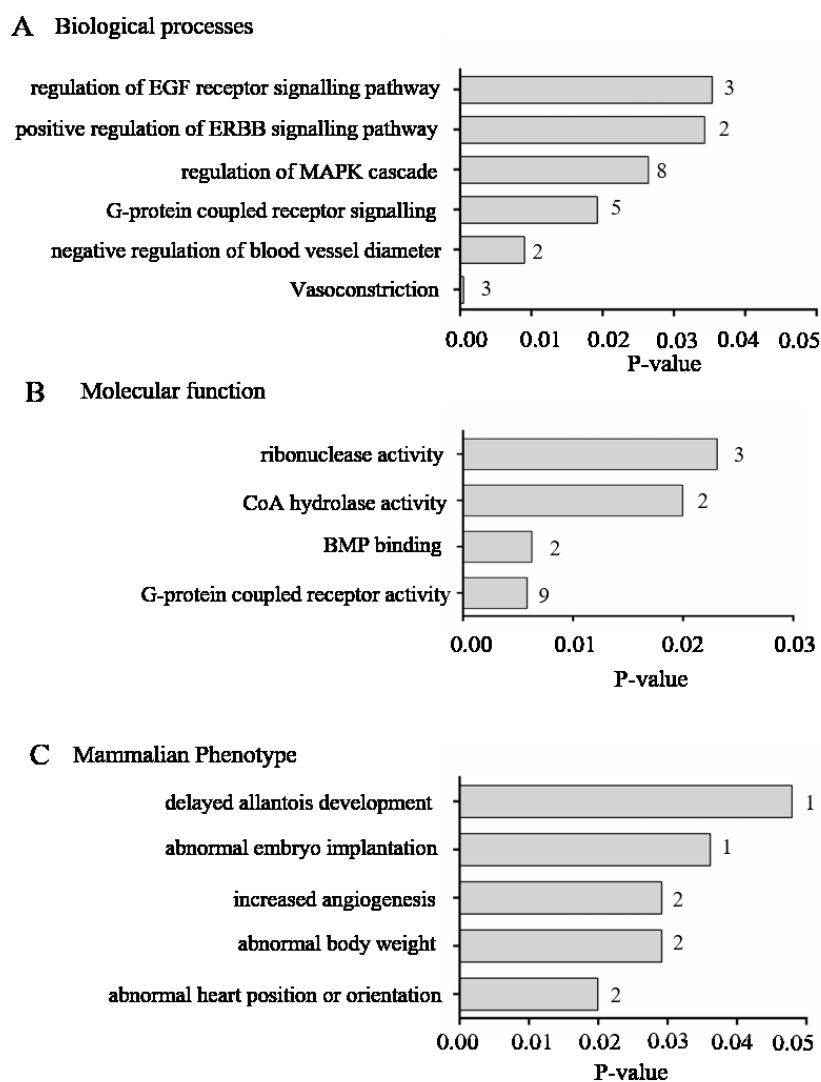


Figure 6.14 Gene ontology analysis of the DEGs in transferred F2 *Mtrr*^{+/+} placentas. (A) Biological processes, (B) Molecular function, and (C) Mammalian phenotypes that are enriched according to Enrichr. The number next to each bar shows the number of DEGs that fall under that term.

We observed that different biological processes, molecular functions, and mammalian phenotypes are affected after blastocyst transfer of F2 *Mtrr*^{+/+} conceptuses when compared to the C57Bl/6 conceptuses. For instance, BMP binding was an enriched molecular function in the F2 *Mtrr*^{+/+}, but not C57Bl/6 conceptuses. This suggests that the placenta might compensate in the new uterine environment by improving the decidualisation reaction. Additionally, enriched biological processes in the transferred F2 *Mtrr*^{+/+} conceptuses suggest changes in the signalling pathways in the placenta, while enriched biological processes in the transferred C57Bl/6 conceptuses are mostly involved in cell growth and metabolism.

Altogether, these data suggest that developmental programming of the F2 *Mtrr*^{+/+} conceptuses occurred in the F1 *Mtrr*^{+/+} uterus during the first three days of development. After blastocyst transfer, the F2 *Mtrr*^{+/+} conceptuses were exposed to a different environment, leading to transcriptional changes in the placenta in order to increase placenta efficiency and maintain growth. In contrast, C57Bl/6 conceptuses were exposed to a normal uterine environment prior and after the embryo transfer, and therefore they responded differently after the blastocyst transfer compared to the F2 *Mtrr*^{+/+} conceptuses.

6.2.6.2 Genes involved in transport are misexpressed after transfer of blastocysts into the recipient uterine environment

Enriched gene ontologies such as increased angiogenesis and regulation of blood vessel diameter, suggest that the uteroplacental flow might be altered in transferred F2 *Mtrr*^{+/+} conceptuses. This might affect placental efficiency, considering abnormal body weight was an enriched mammalian phenotype. Earlier in this chapter, we showed that E:P weight ratio of F2 *Mtrr*^{+/+} conceptuses was increased after blastocyst transfer, implying increased placental efficiency. Therefore, we investigated whether DEGs with transport activity were present (Table 6.10).

We identified two and nine genes with transport-related activity that were upregulated and downregulated respectively in the placentas of transferred compared to non-transferred phenotypically normal F2 *Mtrr*^{+/+} conceptuses. Only two and five transport-related genes were upregulated and downregulated in placentas of transferred compared to non-transferred growth enhanced F2 *Mtrr*^{+/+} conceptuses, respectively. *Slc44a4*, which is downregulated in placentas of phenotypically normal F2 *Mtrr*^{+/+} conceptuses, is known to be expressed both in the trophoblast and the decidua. *Chrna4*, is also expressed by both the trophoblast and the decidua, *Ednra* is expressed by the decidua, and *Slc9b2* is expressed by the trophoblast. These three genes were differentially expressed in placentas of transferred growth enhanced F2 *Mtrr*^{+/+} conceptuses compared to non-transferred ones. The expression of the rest of the genes in Table 6.10 has not yet been identified in the placenta. These data suggest that the provision of a normal uterine environment affects the expression of genes involved in placental transport function.

Table 6.10 DEGs with transport activity in placentas of transferred compared to non-transferred F2 *Mtrr*^{+/+} conceptuses.

Transport activity		
Gene	FC	Function
<i>DEGs in placentas of transferred PN F2 Mtrr</i> ^{+/+} <i> conceptuses</i>		
<i>Abca13</i>	2.92	ATP-binding cassette (ABC) transporter
<i>Atp13a4</i>	-3.55	Calcium-transporting ATPase activity
<i>Atp1a2</i>	-2.2	Sodium/potassium-transporting ATPase activity
<i>Atp6v0a4</i>	-2.25	Proton-transporting ATPase activity
<i>Pacsin1</i>	-3.97	Vesicle mediated transport
<i>Pkd1l2</i>	-2.35	Calcium ion transport
<i>Slc17a8</i>	-3.63	Amino acid transmembrane transporter
<i>Slc44a4</i>	-2.1	Organic cation transport
<i>Slc4a8</i>	-2.05	Bicarbonate transmembrane transport
<i>Slc8a1</i>	2.33	Solute carrier, calcium ion transport
<i>Thrsp</i>	-3.36	Fatty acid transmembrane transport
<i>DEGs in placentas of transferred GE F2 Mtrr</i> ^{+/+} <i> conceptuses</i>		
<i>Abcg5</i>	4.11	Cholesterol transport
<i>Atp1a2</i>	-2.33	Sodium/potassium-transporting ATPase activity
<i>Atp6v0a4</i>	-2.02	Proton-transporting ATPase activity
<i>Chrna4</i>	-2.32	Ion transmembrane transport
<i>Ednra</i>	2.11	Glucose transmembrane transport
<i>Slc9b2</i>	-2.25	Ion transporter activity
<i>Thrsp</i>	-4.39	Fatty acid transmembrane transport

FC: fold-change, PN: phenotypically normal, GE: growth enhanced

6.2.6.3 The uterine environment of the recipient female might cause changes in epigenetic regulation of gene expression

The uteri of *Mtrr*^{+/+} females derived from *Mtrr*^{+/*gt*} intercrosses, and placentas of phenotypically normal F2 *Mtrr*^{+/+} conceptuses at E10.5 had global DNA hypomethylation compared to C57Bl/6 (Padmanabhan et al. 2013). Although global DNA methylation levels have not yet been assessed in F1 *Mtrr*^{+/+} uteri derived from one *Mtrr*^{+/*gt*} parent, we showed that F1 *Mtrr*^{+/+} females had normal homocysteine levels (Padmanabhan et al. 2018). This suggests that they have normal folate metabolism and normal availability of methyl groups. It is however possible that the uteri of F1 *Mtrr*^{+/+} females have altered epigenetic regulation of gene expression, that influences the growth and development of F2 *Mtrr*^{+/+} conceptuses.

We identified *Prdm16*, which is differentially expressed between placentas of non-transferred and transferred phenotypically normal F2 *Mtrr*^{+/+} conceptuses (FC= -3.0), to be involved in histone modifications. More specifically, *Prdm16* has H3K9me1 methyltransferase activity and is required for mammalian heterochromatin integrity (Pinheiro et al. 2012). There were no genes that were differentially expressed after embryo transfer in growth enhanced F2 *Mtrr*^{+/+} placentas that regulate gene expression by epigenetic modifications. Next, we identified DEGs after embryo transfer in F2 *Mtrr*^{+/+} placentas whose expression is directly regulated by CpG methylation as identified in other studies (Table 6.11).

Table 6.11 Genes whose expression is epigenetically regulated by DNA methylation and were differentially expressed in F2 *Mtrr*^{+/+} but not C57Bl/6 conceptuses at E10.5 after blastocyst transfer.

Gene name (FC in PN, FC in GE)	Gene function	Known characteristics of epigenetically regulated expression	Predicted CpG methylation	Reference
<i>Asb18</i> (-9.7, -15.9)	Substrate of E3 ubiquitin-protein ligase complex	Exon hypermethylation leads to decreased gene expression	Hyper	(Fang et al. 2017)
<i>Gjc2</i> (-3.6, -3.1)	Gap junction protein	Hypermethylation associated with decreased gene expression	Hyper	(Sirnes et al. 2011)
<i>Tnxb</i> (-3.5, -4.0)	Extracellular matrix glycoprotein	Hypermethylation associated with decreased gene expression	Hyper	(Men et al. 2017)
<i>Adralb</i> (-3.1, -4.8)	Adrenoreceptor	Increased promoter methylation is associated with decreased expression	Hyper	(Noda et al. 2007)

<i>Bmp2</i> (-2.7, -2.6)	Bone morphogenic protein	Hypermethylation associated with decreased gene expression	Hyper	(Fu et al. 2013)
<i>Tnfrsf11a</i> (-2.6, -2.5)	TNF receptor	Hypomethylation associated with increased gene expression	Hyper	(von dem Knesebeck et al. 2012)
<i>Foxq1</i> (2.2, 2.1)	Nuclear factor	Hypomethylation of super-enhancer associated with increased expression	Hypo	(Heyn et al. 2016)
<i>Grem1</i> (22.1, 35.1)	Angiogenesis-modulator	Hypomethylation associated with increased gene expression	Hypo	(van Vlodrop et al. 2010)
<i>Scara5</i> (-2, -2.3)	Scavenger receptor	Promoter hypermethylation associated with decreased expression	Hyper	(Ulker et al. 2018)

FC: Fold change; PN: phenotypically normal; GE: growth enhanced

We identified nine genes (Table 6.11) whose expression is directly regulated by DNA methylation and were misexpressed between placentas of non-transferred and transferred F2 *Mtrr*^{+/+} conceptuses. Based on the gene expression according to our RNA-seq data, we predicted that seven out of the nine genes have increased methylation at the CpG repeats. Altogether, these data suggest that the uterine environment of the recipient females might cause changes in the epigenetic regulation of placental gene expression.

6.2.6.4 The abnormal uterine environment affects genes implicated in growth, placental phenotypes, and/or embryonic lethality at midgestation

Altered placental gene expression might have adverse effects on fetoplacental development. We therefore wanted to identify the DEGs with a role in placenta development and embryo

growth. First, we identified two genes, *Tfpi* and *Htr2b*, whose expression was altered between placentas of non-transferred and transferred F2 *Mtrr*^{+/+} conceptuses (Table 6.12). *Tfpi* mutant embryos have abnormal vascularisation in the placenta leading to growth restriction (Huang et al. 1997). *Htr2b* mutant embryos are growth restricted by midgestation and have abnormal heart development (Nebigil et al. 2000). Since growth restriction and heart defects are associated with abnormal placental function (Barry, Rozance & Anthony 2008; Grivell, Dodd & Robinson 2009; Perez-Garcia et al. 2018; Roberts & Post 2008), it is possible that *Htr2b* mutants have altered placental development and function. In addition, *Esrrb*, which is downregulated in placentas of phenotypically normal, but not growth enhanced F2 *Mtrr*^{+/+}, is required for chorion development. *Esrrb* mutants have abnormal chorion development, overabundant TGCs, and severe deficiency of diploid trophoblast, leading to embryonic lethality at E10.5 (Luo et al. 1997). Abnormal folate metabolism in mice alters the uterine structure and function of their wildtype daughters (Chapters 3 and 4), possibly leading to developmental programming of their wildtype grandprogeny. Differential expression of genes involved in placental development might be due to the programming of the embryo in the abnormal uterine F1 *Mtrr*^{+/+} environment, before providing it with a normal uterine environment at E3.0.

Altogether, these data suggest that the F2 *Mtrr*^{+/+} conceptuses react differently to the blastocyst transfer into a BDF1 uterus compared to the C57Bl/6 conceptuses, based on the DEGs identified. It is possible that developmental programming of the F2 *Mtrr*^{+/+} conceptuses occurs in the abnormal F1 *Mtrr*^{+/+} uterus. Alternatively, it is possible that the *Mtrr*^{gt} mutation affects not only the uterine environment, but also the environment of other parts of the reproductive system. For instance, the intraovarian or intrafallopian tube environments of the F1 *Mtrr*^{+/+} females might be altered. Therefore, exposure of the oocytes to the adverse intraovarian conditions, or exposure of the zygote to the adverse intrafallopian tube environment could also lead to developmental programming of the F2 *Mtrr*^{+/+} oocytes or zygotes. As a result, once these embryos are transferred into a normal BDF1 uterus, the placental transcriptome is altered to compensate for the different intrauterine environment. In contrast, C57Bl/6 conceptuses were never exposed to an abnormal uterine environment, and therefore their placentas possibly undergo less adaptations after transfer into the normal BDF1 uterus.

Table 6.12 DEGs implicated in growth, placental phenotypes, and/or embryonic lethality at midgestation in placentas of transferred F2 *Mtrr*^{+/+} conceptuses.

Gene (FC in PN, FC in GE)	Gene function	Mouse knockout (KO) phenotype or clinical characteristics	Reference
<i>Tfpi</i> (-2.8, -2.2)	Regulator of tissue factor-dependent pathway of blood coagulation	Placenta vascular abnormalities lead to progressive growth retardation and neonatal lethality	(Huang et al. 1997)
<i>Htr2b</i> (2.1, 2.3)	Serotonin receptor	Growth retardation at E9.5 and E10.5, abnormal heart development	(Nebigil et al. 2000)
<i>Esrrb</i> (-2, N/A)	Transcription factor, important for placental development	Abnormal chorion development, overabundance of trophoblast giant cells, severe deficiency of diploid trophoblast, embryonic lethality at E10.5	(Luo et al. 1997)

FC: fold change, PN: phenotypically normal, GE: growth enhanced

6.3 Discussion

In the third trimester of uncomplicated human pregnancy, the methylation demands increase, as shown by an increase in the transmethylation rate (Dasarathy et al. 2010). Abnormal folate metabolism affects the transfer of methyl groups by decreasing the rate of homocysteine methylation (Cuskelly et al. 2001). In our model of abnormal folate metabolism leading to global DNA hypomethylation (Padmanabhan et al. 2013), the placental epigenome is altered, possibly affecting placental development and function and ultimately leading to growth restriction and developmental delay.

Here, we assessed the placental transcriptome of the conceptuses that have been transferred at the blastocyst stage into a normal BDF1 uterus. First, we assessed the effects of maternal grandpaternal *Mtrr*^{gt} mutation on the placental transcriptome after F2 *Mtrr*^{+/+} conceptuses were provided with a normal uterine environment. Maternal grandpaternal *Mtrr*^{gt} mutation minimally affects the placental transcriptome at E10.5 after blastocyst transfer, since we identified only six genes that were upregulated in growth enhanced F2 *Mtrr*^{+/+} compared to C57Bl/6 transferred conceptuses. The misexpression of these genes suggests minimal alterations in the placental development and function and reinforces the conclusion that

maternal grandpaternal abnormal folate metabolism minimally affects the placental transcriptome of their wildtype grandprogeny.

Evidence suggests that ART might influence pregnancy outcome in an adverse manner, yet the mechanism is not well understood. Here, we found that the blastocyst transfer process affects the placental transcriptome at E10.5. We therefore focused on the blastocyst transfer, as part of routine human ART procedures. Evidence suggests that ART might influence pregnancy outcome in an adverse manner, yet the mechanism is not well understood. Here we show that blastocyst transfer after natural mating of healthy mice is sufficient to restrict placental growth at midgestation, even though the associated embryos were larger on average. This phenotype corresponds with a placental transcriptome that was enriched for genes implicated in labyrinth formation, growth, vascular development, and transport function, and implies compensation by the placenta to increase its functional efficiency. Therefore, even minimal embryo manipulation has developmental implications for the placenta and embryo. Mechanistically, we showed that blastocyst transfer procedure is unlikely to alter CpG methylation in a meaningful way. Consequently, efforts should focus on other epigenetic mechanisms including dysregulation of histone modifications.

Fetal growth is contingent upon the placenta since it is the interface between the maternal and fetal circulations, facilitating gas and metabolic exchange and hormone production (Watson & Cross 2005). After blastocyst transfer, we observed placentas that were small at E10.5 suggesting delayed development and/or reduced placental growth. Since the associated embryos were of normal developmental stage and size, the placentas may have adjusted their functional performance to protect the embryo growth trajectory. To achieve this, the placenta might respond to fetal requirements by altering its structure and/or nutrient transport capacity.

In the mouse, the labyrinth layer is the exchange barrier composed of a complex network of trophoblastic villi that separate the fetal capillaries from the maternal blood circulation (Watson & Cross 2005). We observed several genes associated with labyrinth formation that were upregulated after blastocyst transfer including those involved in branching morphogenesis and vascularisation as determined by genetic knockout mice (Bell et al. 2006; Fotopoulou et al. 2010; Goyal et al. 2010; Liu & LeRoith 1999; Perez-Garcia et al. 2018; Smith et al. 2006; Stumpo et al. 2004; Sun et al. 1998; Xue et al. 1998). These transcriptional changes might promote branching of additional villi and/or an increase in vascular density of existing villi (Wu et al. 2003) to improve the surface area for exchange. In support of this

hypothesis, increased placental vascular density is apparent after IVF (and embryo transfer) in bovine and ovine conceptuses (Grazul-Bilska et al. 2014; Miles et al. 2005). IVF followed by blastocyst transfer in mice might lead to increased branching morphogenesis since an initially small placenta at E12.5 develops into a large placenta by late gestation (Bloise et al. 2012; Delle Piane et al. 2010). To fully understand the effects of blastocyst transfer alone on mouse placental villus structure, a morphological analysis is required.

Alternatively, placentas are capable of stimulating nutrient transport to compensate for poor placental growth (Constância et al. 2002). Similar to IVF in mice (Bloise et al. 2012), we observed many upregulated genes in transferred placentas that encode for transport proteins (e.g., *Gjb1*, gap junction protein; *Slc7a9*, L-cystine transport; *Slc27a2*, fatty acid transport; *Slc7a11*, cysteine/glutamine transport; *Apom*, lipid transport, etc.). This implies functional compensation by a small placenta in response to fetal requirements (Constância et al. 2002). Placental transfer assays will be required to more fully understand the degree to which transcriptional upregulation leads to a functional increase in nutrient transport across the placenta. Furthermore, whether the placenta is able to continue to compensate in later stages of gestation as the demands of the fetus increase remains to be determined.

Other placental regions (e.g., the junctional zone or decidua) might also be reduced after blastocyst transfer. We identified four placenta prolactin cluster genes (i.e., *Prl2c2*, *Prl3d1*, *Prl7a1*, and *Prl8a1*), which are normally expressed in spongiotrophoblast cells and trophoblast giant cell (TGC) subtypes (Simmons et al. 2008) and were downregulated in transferred placentas. *Prl3d1* (also known as *PLI*) is a gene regulated by promoter CpG methylation (Hayakawa et al. 2012) and its expression is often used as marker to quantify parietal-TGCs (Simmons et al. 2008). Since *Prl3d1* promoter methylation was normal, reduced *Prl3d1* mRNA expression might instead indicate that fewer *Prl3d1*⁺ parietal-TGCs are present in transferred placentas. Similarly, reduced *Prl2c2*, *Prl7a1*, and *Prl8a1* mRNA expression might indicate the presence of fewer spongiotrophoblast cells. In support of this, *Aldh3a1* and *Il33* genes that regulate the differentiation and function of the progenitor cells of the junctional zone (i.e., the ectoplacental cone; Fang et al. 2017; Nishiyama et al. 2015) were downregulated in transferred placentas. Together, these data suggest that the blastocyst transfer procedure might reduce this progenitor pool. This potential morphological change has implications for placenta metabolism and hormone production (Woods, Perez-Garcia &

Hemberger 2018). Single cell RNA-sequencing would help assess the effects of the blastocyst transfer on the transcriptomes of the different cell types present in the placenta.

Many researchers studying the epigenetic effects of ART have performed directed analysis of imprinted regions as a read-out of functional changes in global DNA methylation (Choux et al. 2015; Messerschmidt et al. 2012; Padmanabhan et al. 2013). We performed an unbiased approach to assess the placental transcriptome and identified only two DEGs associated with imprinted control regions (i.e., *Rasgrf*, *Cobl*; Shiura et al. 2009; Yoon et al. 2005). Therefore, unlike more invasive ART procedures, such as superovulation, IVF, or pronuclear transfer, blastocyst transfer might not alter DNA methylation to a great extent. Beyond imprinted genes and in support of this hypothesis, fewer misexpressed genes in transferred placentas were associated with CpG repeats than the rest of the genome. This result implies that these genes do not require cis regulation by DNA methylation. We showed that even DEGs with known regulation by CpG methylation (i.e., *Prl3dl* and *Rasgrfl*; Hayakawa et al. 2012; Yoon et al. 2005) displayed normal DNA methylation patterns in transferred placentas.

Alternatively, dysregulation of DNA methylation at the regulatory regions of a few ‘master regulator’ genes (e.g., transcription factors) might secondarily cause extensive transcriptional changes in placentas after blastocyst transfer. A whole methylome analysis (e.g., whole genome bisulfite sequencing) will better address whether blastocyst transfer alters DNA methylation to cause the widespread transcriptional changes observed in transferred placentas.

Instead of DNA methylation, blastocyst transfer might disrupt alternative epigenetic mechanisms, such as histone modifications. The effects of ART on histone modifications are little studied and not well understood. Increased histone acetylation (H3K9ac, H3K14ac) in mouse zygotes is associated with superovulation (Huffman, Pak & Rivera 2015). Whether these changes are maintained by placenta cell lineages during development to affect gene expression is unclear. While we did not assess the effects of blastocyst transfer on histone modifications directly, we found that the majority of DEGs in transferred placentas associate with placental H3K4me1 peaks but not H3K27ac peaks under normal circumstances. As a result, these genes might be sensitive to changes in histone methylation or histone acetylation at key stages of development. Further analysis through ChIP-seq experiments is required to explore the effects of blastocyst transfer on the regulation of histone modifications.

How blastocyst transfer causes placental gene misexpression is still unclear. Since the establishment of epigenetic marks is initiated at the blastocyst stage (Hanna, Demond & Kelsey 2018) it is possible that the stress of a brief culture period, embryo handling, and/or placement into a new uterine environment during this key epigenetic milestone is sufficient to alter epigenetic marks and subsequent gene expression required for cells to differentiate. Since all technologies associated with ART require blastocyst transfer, it will be important to tease apart the transcriptional and developmental effects of the transfer process from the other more invasive techniques. Furthermore, the ART field will benefit from unbiased high throughput epigenetic analyses of placentas derived from these technologies with the aim of stepping away from directed studies on imprinted genes. This will allow for a holistic picture of the epigenetic framework that gives rise to transcriptional and functional changes in the placenta after ART, and thus the immediate and long-term effects on the fetus.

Given that some DEGs clustered together in the genome, it is possible that a shared epigenetic mechanism is disrupted upon blastocyst transfer as discussed above. However, minor differences in the genetic background between the control and transferred placentas might also contribute to differential gene expression. For instance, the placentas from control conceptuses were entirely of C57Bl/6 genetic background. In contrast, the transferred placentas were chimeric since they contained trophoblast and fetal endothelial cells that were C57Bl/6 genetic background and maternally-contributed cells (e.g., decidua cells, uNK cells, and circulating maternal blood) that were B6D2F1 background (i.e., 50% C57Bl/6 and 50% DBA2). F1 hybrids, such as B6D2F1 mice, are often used as recipient females to increase blastocyst transfer efficiency (Wakayama, Mizutani & Wakayama 2010). Since whole placentas were analysed in the RNA sequencing and validation experiments, maternal cells were present. However, only 8.1% of all DEGs were solely expressed within the decidual region that comprise a number of different molecular pathways. Whether this sufficiently represents a confounding effect of genetic background is unclear. Certainly, there is cross talk between maternal decidual and immune cells, and the trophoblast (Pollheimer et al. 2018). Given that a mother's genome is usually only 50% similar to that of her fetus, our study is illustrative of human populations.

In order to eliminate any possible confounding effect of the genetic background on the placental transcriptome, there are two experiments that could be done, all with important limitations. First, we could mate a BDF1 female with a C57Bl/6 male and collect the

embryos at E10.5. We would then compare the expression of decidua-related genes between the placentas of these conceptuses, with the placentas of the conceptuses derived from natural matings between C57Bl/6 males and females and transferred into a BDF1 female at E3.0. In both cases, the maternal environment will be that of a BDF1 female. However, the embryos derived from a C57Bl/6 x C57Bl/6 crossing will be 100% C57Bl/6, while the embryos derived from a C57Bl/6 (male) x BDF1 (female) will have a 75% C57Bl/6 background, and 25% DBA genetic background. This genetic heterogeneity of the embryos might affect expression of placental genes, not only those expressed by the trophoblast, but possibly those expressed by the decidua as well. Alternatively, we would mate C57Bl/6 males and females and transfer the blastocysts to a C57Bl/6 recipient. The placental gene expression of the E10.5 conceptuses would then be compared to that of the conceptuses transferred into a BDF1 female. The genetic background of all the transferred embryos will be identical (100% C57Bl/6), and this experiment will account for the different genetic background of the recipient female. The limitation of this experiment, however, is that C57Bl/6 females are known to be poor recipients, and that is the reason BDF1 females were used as recipients initially (Wakayama, Mizutani & Wakayama 2010). Therefore, this experiment will have a low success rate, and will be very time and resource consuming. If, however, this could be done, any DEGs identified, would be exclusively due to the minimal embryo culture and blastocyst transfer process itself, that includes anaesthesia of the recipient female.

Limitations of these experiments are that the blastocyst transfer procedure is a highly skilled one. Previous blastocyst transfers were performed in the laboratory in the University of Calgary, by Coleen Gary-Goo, and Dr. Erica Watson. Repeating the experiment in Cambridge would mean that different scientists perform the procedure, and the mice will have a different after care. This could cause alterations in the methylome of the placentas of the developing conceptuses, and therefore alter gene expression. Another limitation is that while the blastocyst transfer experiments were performed at the University of Calgary in Canada, using C57Bl/6 mice ordered from Canada, the rest of the dissections were performed at the University of Cambridge, UK, using C57Bl/6 mice ordered from the Jackson Lab, US. The different animal housing conditions and different animal handling might affect gene expression.

Next, we focused on the placental transcriptome of transferred F2 *Mtrr*^{+/+} conceptuses to assess how exposure to the abnormal uterine environment of F1 *Mtrr*^{+/+} females during the

first three days of development affects developmental programming of the F2 generation. We found that the placental transcriptome of F2 *Mtrr*^{+/+} conceptuses is altered after blastocyst transfer. We identified a total of 244 genes that were differentially expressed between placentas of non-transferred and transferred F2 *Mtrr*^{+/+} conceptuses independent of the transfer protocol. This suggests that the placentas of F2 *Mtrr*^{+/+} conceptuses respond differently than the C57Bl/6 placentas after transfer into the recipient uterus. The identified enriched biological processes such as vasoconstriction and regulation of blood vessel diameter, might affect uteroplacental flow and placental transport, and ultimately alter embryo growth. This correlates with the observation that no growth restriction is observed after blastocyst transfer, but rather an increase in growth enhancement (Padmanabhan et al. 2013). Other enriched biological processes such as regulation of *Erbb* signalling, MAPK cascade, and EGF receptor signalling, suggest that signalling pathways have been affected. Enriched mammalian phenotypes such as increased angiogenesis could be the result of a compensatory mechanism to increase fetal growth, once the F2 *Mtrr*^{+/+} conceptuses are transferred in a normal uterine environment. Alterations in body weight were also expected, since we showed an increase in embryo weight and growth enhancement, and absence of growth restriction after blastocyst transfer (Padmanabhan et al. 2013). Finally, placental defects have been associated with heart defects (Perez-Garcia et al. 2018), and therefore the abnormal heart orientation as an enriched mammalian phenotype could be a result of abnormal placenta development or function.

Additionally, we found nine genes whose expression is epigenetically regulated by DNA methylation. The differential expression of these genes suggests that the exposure of the F2 *Mtrr*^{+/+} conceptuses in the abnormal F1 *Mtrr*^{+/+} uterus during the first three days of development alters the epigenetic regulation of gene expression. This might be due to environmental mismatch, since the donor female had an abnormal uterine environment, while the recipient uterus was normal. Further analysis is required to examine the potential sensitivity of the DEGs to changes in DNA methylation, by assessing the whole genome methylome via MeDIP-seq, or whole genome bisulfite pyrosequencing.

Two of the genes whose expression is regulated by DNA methylation are *Bmp2* and *Grem1*. *Bmp2* is involved in decidualisation (Lee et al. 2007) and its expression is decreased in placentas of both phenotypically normal and growth enhanced F2 *Mtrr*^{+/+} conceptuses after blastocyst transfer. Even though *Bmp2* is known to be a decidua-related gene, end-point RT-

PCR analysis revealed that *Bmp2* is expressed in the peri-implantation bovine conceptuses and also the bovine trophectoderm cell line CT1 (Pennington & Ealy 2012). *Bmp2* hypermethylation is associated with decreased gene expression (Fu et al. 2013), suggesting that *Bmp2* promoter is hypermethylated after blastocyst transfer, leading to downregulation of gene expression. However, this is unlikely to have an adverse effect on the decidualisation reaction, since the growth restriction and developmental delay are rescued after blastocyst transfer, and the frequency of growth enhanced conceptuses is increased (Padmanabhan et al. 2013). In Chapter 4 we showed that there is abnormal expression of decidual response markers, such as *Bmp2*, in implantation sites of F1 *Mtrr*^{+/+} females derived from a *Mtrr*^{+/gt} father and mated with a C57Bl/6 male at GD6.5. Abnormal decidualisation at GD6.5 could lead to decreased placental efficiency at E10.5. However, we observed increased placental efficiency in transferred female F2 *Mtrr*^{+/+} conceptuses, suggesting a compensatory mechanism to maintain growth in the new, normal uterine environment. Additionally, we observed upregulation of *Grem1*, which is expressed in the placental labyrinth and is involved in branching morphogenesis (O'Connell et al. 2013). Upregulation of *Grem1* could suggest a role in increased blood vessel formation and ultimately increased placental efficiency.

In summary, we first showed that the blastocyst transfer process affects the placental transcriptome at midgestation. This might have important implications in humans, since embryo transfer is routinely used as part of ART. Next, we observed that some genes are differentially expressed in transferred F2 *Mtrr*^{+/+} placentas, and others are differentially expressed in transferred C57Bl/6 placentas. One important difference between transferred C57Bl/6 and transferred F2 *Mtrr*^{+/+} conceptuses, is that the C57Bl/6 have never been exposed in an adverse uterine environment. In contrast, the F2 *Mtrr*^{+/+} conceptuses were exposed to the abnormal uterus of the F1 *Mtrr*^{+/+} females before being transferred into the normal uterus of a BDF1 female at E3.0 (Padmanabhan et al. 2013). This environmental mismatch experienced by the F2 *Mtrr*^{+/+} conceptuses has possibly developmentally programmed the conceptuses to adjust to the different environment after the blastocyst transfer. Altogether, these data suggest that the maternal grandpaternal *Mtrr*^{gt} mutation minimally affects the placental transcriptome of F2 *Mtrr*^{+/+} conceptuses. However, the F1 *Mtrr*^{+/+} uterus developmentally programmes the F2 *Mtrr*^{+/+} conceptuses during the first three days of development, and their placental transcriptome is altered when they are provided with a normal uterine environment.

Chapter 7: Discussion and future directions

7.1 Summary

The environment we are exposed to during development has a profound effect on our health, but also on the health of our descendants. For instance, folate deficiency in the mother is associated with neural tube defects in the fetus. These effects are sometimes sexually dimorphic (Liu et al. 2018; Seller 1987). However, the mechanism by which abnormal folate metabolism affects embryo growth and development remains unclear. A mouse model with a gene trap mutation in the *Mtrr* gene (*Mtrr^{gt}*), which is necessary for the activation of methionine synthase and the progression of folate and methionine cycles, was created to examine the multigenerational effects of abnormal folate metabolism (Elmore et al. 2007). Previous embryo transfer experiments revealed that the abnormal uterine environment of F1 *Mtrr^{+/+}* females causes growth restriction and developmental delay in the F2 *Mtrr^{+/+}* conceptuses (Padmanabhan et al. 2013).

However, little is known about how folate affects the uterine structure and function. Therefore, in this thesis, we first investigated the effects of *Mtrr^{gt}* mutation on the uterine environment. To do this, we assessed the uterine histological structure and function of estrus-stage females derived from either *Mtrr^{+/gt}* intercrosses, or the F1 generation derived from an *Mtrr^{+/gt}* father and a C57Bl/6 mother. We found that a parental *Mtrr^{gt}* allele is sufficient to alter the cell structure of the lumen epithelium and myometrium (Chapter 3). We then mated these females with C57Bl/6 males and assessed the decidual histology and gene expression of the resulting implantation sites at GD6.5. The implantation sites were histologically normal, however the expression of decidual markers was abnormal (Chapter 4). This suggests that intrinsic or paternal *Mtrr* deficiency might alter the decidualisation reaction. Next, to assess how *Mtrr^{gt/gt}* mutation affects the placental transcriptome, we assessed the placental transcriptome of *Mtrr^{gt/gt}* conceptuses at E10.5 and compared it to the transcriptome of C57Bl/6 placentas via RNA sequencing. We found that *Mtrr^{gt/gt}* mutation affects the placental transcriptome in a phenotype-dependent manner. We identified DEGs that were involved in embryo growth and placental development and function (Chapter 5). To assess the effects of maternal grandpaternal *Mtrr^{gt}* mutation on the placental transcriptome of F2 *Mtrr^{+/+}* conceptuses, we assessed placentas of phenotypically normal and growth enhanced F2 *Mtrr^{+/+}* and compared them to the transcriptome of C57Bl/6 placentas. We found that placentas of phenotypically normal and growth enhanced conceptuses F2 *Mtrr^{+/+}* are transcriptionally similar to C57Bl/6 placentas, suggesting that abnormal uterine structure and function of F1 *Mtrr^{+/+}* has minimal consequences on placental transcriptome of F2 at

midgestation (Chapter 5). Simultaneously, RNA from placentas of F2 *Mtrr*^{+/+} conceptuses after blastocyst transfer was sequenced to determine whether the abnormal maternal environment of F1 developmentally programmes the F2 and if this programming becomes apparent after the F2 offspring is provided with a normal maternal environment (Chapter 6). RNA from placentas of transferred C57Bl/6 conceptuses was used as control. One remarkable finding was that the blastocyst transfer procedure, itself, affected placental gene expression and development, indicating a potential influence of blastocyst transfer, as part of assisted reproductive technology procedures in humans, on fetoplacental growth (Chapter 6). Placentas of transferred F2 *Mtrr*^{+/+} and C57Bl/6 conceptuses were transcriptionally similar, with only six genes (*Prl8a8*, *Prl8a9*, *Psg19*, *Fbln7*, *Zfp964*, *Phldb30*) upregulated in placentas of transferred growth enhanced, but not phenotypically normal conceptuses. Overall, our results indicate that while a parental *Mtrr*^{gt} mutation is sufficient to impair uterine structure and function in their wildtype daughters, this does not substantially alter the placental transcriptome of their wildtype grandprogeny. However, *Mtrr*^{gt/gt} mutation in the placenta cells themselves alters the transcriptome. In summary, abnormal folate metabolism caused by the *Mtrr*^{gt} mutation affects the uterine environment and the placental transcriptome at midgestation. Normal folate metabolism is required to establish a normal maternal-fetal interface. If disrupted, the effects might persist for multiple generations.

7.2 Developmental programming in the *Mtrr*^{gt} model

The intrauterine environment where a mammalian fetus develops is important for its health later in life, as it regulates the function of its physiological systems (Fowden, Giussani & Forhead 2006). Fetal programming occurs when the fetus is exposed to an insult *in utero* that impairs its normal pattern of development (Kwon & Kim 2017; Myatt 2006). Nutrients and oxygen are vital for proper embryonic growth and development (Harding & Johnston 1995), and studies have shown the effects of nutrient and oxygen deficiencies on fetal programming (Brenseke et al. 2013; Wu et al. 2004). For instance, maternal undernutrition during critical periods of fetal development can lead to the development of metabolic syndrome later in life (Correia-Branco, Keating & Martel 2015; Lopez-Jaramillo et al. 2015). In addition, epigenetics influence developmental programming. For instance *Rxra* promoter methylation at birth is associated with increased child's adiposity (Godfrey et al. 2011) and decreased bone mineral content (Harvey et al. 2014). Folate is a methyl donor, and therefore abnormal

folate metabolism is also linked to decreased availability of methyl groups necessary for cellular methylation (Crider et al. 2012; Niculescu & Zeisel 2002). In our *Mtrr^{gt}* model of abnormal folate metabolism, we observed global DNA hypomethylation in the adult uterine tissues, even in *Mtrr^{+/+}* females, and in placentas but not embryos at E10.5 (Padmanabhan et al. 2013), which correlates with the decreased availability of methyl groups in folate deficiency (Crider et al. 2012).

In our study, we used the appropriate controls. For instance, we compared the uterine structure and function of F1 *Mtrr^{+/+}* females and placental transcriptome of F2 *Mtrr^{+/+}* male conceptuses to C57Bl/6 sex-matched controls. This is because the *Mtrr^{gt}* model is a model of transgenerational epigenetic inheritance (Padmanabhan et al. 2013), and therefore the most suitable controls would be those who have never been exposed to *Mtrr* deficiency, such as C57Bl/6 mice. We also compared the structure and function of *Mtrr^{+/gt}* and *Mtrr^{gt/gt}* uteri and implantation sites to the C57Bl/6 control uteri and implantation sites. This is in contrast to other studies, which assessed the effects of *Mtrr^{gt}* mutation on the metabolic phenotype in mice by comparing *Mtrr^{gt/gt}* or *Mtrr^{+/gt}* conceptuses to *Mtrr^{+/+}* littermates instead of C57Bl/6 controls (Elmore et al. 2007). Others assessed the effects of *Mthfr* mutation on metabolism and embryo development by comparing *Mthfr^{-/-}* and *Mthfr^{+/-}* samples to *Mthfr^{+/+}* littermates, instead of C57Bl/6 controls (Chen et al. 2001). In addition, others assessed the effects of folic acid supplementation and *Mthfd1*-synthetase deficiency in mice by comparing *Mthfd1S^{-/-}* and *Mthfd1S^{+/+}* conceptuses to their *Mthfd1s^{+/+}* littermates, instead of C57Bl/6 controls (Christensen et al. 2016). However, according to our study, *Mtrr^{+/+}* uteri are also abnormal, and therefore the use of C57Bl/6 samples as controls is required.

7.2.1 Abnormal uterine morphology and function in *Mtrr^{gt/gt}* and F1 *Mtrr^{+/+}* mice

Previously, little was known about the effects of abnormal folate metabolism on the uterine structure and function. For instance, folate deficiency in monkeys causes decreased cell proliferation of the uterine lumen epithelium (Mohanty & Das 1982). Since most of the studies in mice focused on the role of folate during pregnancy, we first wanted to assess the effects of *Mtrr^{gt/gt}* mutation on the uterine structure at estrus. Additionally, growth defects such as growth restriction, developmental delay, and growth enhancement are observed in F2 *Mtrr^{+/+}* conceptuses derived from an *Mtrr^{+/gt}* maternal grandparent. Transfer of F2 blastocysts

into a normal maternal environment increases the frequency of growth enhancement, while it rescues the growth restriction and developmental delay, suggesting a programming effect of the F1 environment on the F2 conceptuses. F1 *Mtrr*^{+/+} females had normal homocysteine levels (Padmanabhan et al. 2018), suggesting that they have normal folate metabolism and normal availability of methyl groups. Global DNA methylation levels are yet to be assessed in the uteri of these females. However, the epigenetic regulation of gene expression in the F1 *Mtrr*^{+/+} females might have been altered. This can induce a permanent response in the developing fetus resulting in diseases later in life, particularly abnormal growth patterns (Smith & Ryckman 2015). Therefore, we also assessed the effects of paternal *Mtrr*^{+/*gt*} mutation on the uterine structure of F1 *Mtrr*^{+/+} females at estrus (Chapter 3). We found that both *Mtrr*^{*gt/gt*} mutation and paternal *Mtrr*^{+/*gt*} mutation lead to increased myometrial thickness and abnormal cell polarity of the lumen epithelium at estrus. This suggests that abnormal folate metabolism might affect cell polarity, a hypothesis that is reinforced by the identification of DEGs in *Mtrr*^{*gt/gt*} placentas involved in cell adhesion and cytoskeleton organisation (see Section 7.5). Abnormal cell polarity in the lumen epithelium might affect cell-cell signalling and subsequent uterine function, such as decidualisation. In addition, we observed decreased *Pgr* mRNA and PGR protein levels, which suggests that intrinsic or paternal abnormal folate metabolism affects progesterone signalling. It is possible that abnormal cell polarity is associated with improper presentation of PGR on the uterine lumen epithelium. In our model, abnormal folate metabolism and subsequent alterations in the cell polarity of the uterine lumen epithelium does not affect endometrial receptivity, since C57Bl/6, *Mtrr*^{*gt/gt*}, and F1 *Mtrr*^{+/+} mice have similar litter sizes (Padmanabhan *et al.*, 2013 and Chapter 4). This correlates with the finding that embryo implantation is unaffected by folate deficiency (Gao et al. 2012b).

PGR signalling regulates endometrial decidualisation (Large & DeMayo 2012). Studies assessing the effects of folate on the decidualisation reaction, use models of dietary folate deficiency (Gao et al. 2012a; Geng et al. 2015; Liao et al. 2015). However, in our study, we use a model of abnormal folate metabolism, where both control and study groups are fed the same diet. It was shown that folate deficiency causes a decrease in DNA methylation of *Esr1* promoter but does not change the methylation levels of *Pgr* or *Cdh1* promoters at GD4.5 (Gao et al. 2012a). Methylation levels of these genes are yet to be assessed in our model. In contrast to our study, that showed that *Mtrr* deficiency does not affect *Esr1* mRNA levels at estrus (Chapter 3), folate deficiency was shown to decrease *Esr1* levels in the peri-

implantation uteri at E4.5 (Gao et al. 2012a). This discrepancy might be because we assessed estrus-staged uteri, while they assessed peri-implantation sites at GD4.5. Treatment of GD4.5 pregnant uteri with a PGR antagonist led to downregulation of *Bmp2*, which induces stromal cell differentiation (Li et al. 2007). We also observed decreased *Bmp2* mRNA levels in the implantation sites at GD6.5 (Chapter 4), which correlate with the abnormal PGR signalling in the uterine tissues and implantation sites at GD6.5 (Chapters 3, 4). Our data also correlate with other studies that show decreased *Bmp2* levels in folate-deficient mouse uteri that have undergone artificial decidualisation through sesame oil infusion (Geng et al. 2015).

Decreased *Bmp2* mRNA levels suggest that the decidualisation reaction might be affected. *Bmp2* mRNA is expressed in the bovine trophectoderm prior to blastocyst attachment (Pennington & Ealy 2012). This suggests that the *Mtrr^{gt}* mutation and disruption of PGR and BMP2 signalling pathways might not only have a local effect in the uterus, but it is possible to affect placental physiology. This hypothesis is supported by the observation that *Bmp2* mRNA levels were decreased in the implantation sites of *Mtrr^{gt/gt}* and F1 *Mtrr^{+/+}* females derived from an *Mtrr^{+/gt}* father at GD6.5 (Chapter 4) and increased in the placentas of growth restricted *Mtrr^{gt/gt}* conceptuses (Chapter 5).

Altogether, we found that intrinsic or paternal *Mtrr^{gt}* mutation affects the uterine structure and function at estrus, and the decidualisation reaction at GD6.5. The hormonal changes during the estrous cycles should be assessed in the future by performing ELISA on blood samples collected during the different stages of the estrous cycle. In addition, uterine tissues should be collected during proestrus, metestrus, and diestrus, to correlate the changes in the uterine structure to the changes in blood hormone levels during the estrous cycle, similar to Woods *et al.* (2007). Folate deficiency was previously shown to decrease apoptosis of the decidual cells (Liao et al. 2015). Decidual cell apoptosis is essential for decidualisation, as it is involved in decidual regression that occurs to provide space for the developing embryo (Gu et al. 1994). Flow cytometry and TUNEL assay can be used to assess whether *Mtrr* deficiency in either parent can affect the apoptosis of endometrial decidual cells in the F1 *Mtrr^{+/+}* uteri. In addition, *in vitro* experiments are required to assess the decidualisation reaction. For instance, treatment of cultured endometrial stroma cells with PGR agonists could possibly increase *Bmp2* levels and improve the decidualisation reaction.

7.2.2 Abnormal placental transcriptome in *Mtrr^{gt/gt}* and F2 *Mtrr^{+/+}* mice

Placentas but not embryos of phenotypically normal and growth restricted *Mtrr^{gt/gt}* and F2 *Mtrr^{+/+}* conceptuses exhibited global DNA hypomethylation at E10.5, and locus-specific dysregulation of DNA methylation compared to C57Bl/6 (Padmanabhan et al. 2013). Therefore, we sequenced RNA from placentas of phenotypically normal and growth restricted *Mtrr^{gt/gt}* conceptuses and phenotypically normal and growth enhanced F2 *Mtrr^{+/+}* conceptuses. First, we showed that the transcriptome of *Mtrr^{gt/gt}* placentas was dependent on their phenotype and we identified DEGs between placentas of phenotypically normal or growth restricted *Mtrr^{gt/gt}* conceptuses and C57Bl/6 placentas (Chapter 5). More specifically, we showed that transport-related genes are misexpressed in the *Mtrr^{gt/gt}* placentas, most of which were upregulated. This suggests that the placentas of *Mtrr^{gt/gt}* conceptuses adapt to the abnormal uterine environment by regulating the expression of channels, solute carriers, and transport proteins. Other DEGs are involved in embryonic or post-natal growth, suggesting that the *Mtrr^{gt/gt}* mutation affects the expression of genes that regulate growth. These adaptations in placenta transport ensure to meet fetal growth demand and change the fetal composition, and might lead to life-long programming (Fowden et al. 2006; Sandovici et al. 2012; Sibley et al. 2010).

Our RNA sequencing revealed that DEGs whose expression is regulated by DNA methylation are both upregulated and downregulated in *Mtrr^{gt/gt}* placentas, suggesting both hypermethylation and hypomethylation of DNA in our model, confirming the previous results (Padmanabhan et al. 2013). By assessing the frequency of the presence of CpG repeats in the DEGs, we found that they are less likely to contain intragenic or proximal CpG repeats compared to the rest of the genome. This suggests that an epigenetic mechanism other than DNA methylation might be involved. Further analysis of locus-specific DNA methylation of these DEGs using bisulfite pyrosequencing is required to confirm this hypothesis.

Mass spectrometry experiments have shown that mice fed a folate deficient diet have increased H3K4me2 levels in their livers, compared to mice fed the same diet supplemented with 1mg of folic acid per kg of diet (Garcia et al. 2016). Methylation of Lysine 4 is often associated with transcriptional activation (Schneider et al. 2004). Indeed, decreased H3K4me2 is associated with decreased expression of *Mt3* (Peng et al. 2011). *Mt3* was upregulated in *Mtrr^{gt/gt}* placentas, suggesting that H3K4me2 was increased in these placentas (Chapter 5). This correlates with increased H3K4me2 levels in the livers of folate-deficient

mice (Garcia et al. 2016), suggesting that folate deficiency and abnormal folate metabolism might have similar effects on histone modifications. To assess whether histone modification changes occur in the *Mtrr^{gt/gt}* placentas, ChIP-sequencing using antibodies against specific histone modifications would be performed (Lin & Garcia 2012).

Next, we found that the placental transcriptomes of C57Bl/6 and phenotypically normal F2 *Mtrr^{+/+}* conceptuses were similar (Chapter 5). This suggests that placentas of conceptuses with the same genotype and phenotype have similar transcriptomes. A future direction is to assess the placental transcriptome of growth restricted F2 *Mtrr^{+/+}* conceptuses and compare it to the placental transcriptome of either phenotypically normal F2 *Mtrr^{+/+}* or C57Bl/6 conceptuses. This would give us information about the changes in gene expression that cause growth restriction. For instance, it is possible that abnormal vascular changes, such as abnormal spiral artery remodelling, and inadequate angiogenesis occurs (Plaisier 2011). These changes will impair uteroplacental flow and lead to growth defects.

Overall, these data suggest that *Mtrr^{gt/gt}* mutation affects fetoplacental development at E10.5. This might have an implication in human embryo development. For instance, pregnant women with dietary folate deficiency, or those who have genetic mutations in genes involved in folate metabolism, might have abnormal uterus structure during the menstrual cycle and carry fetuses that are growth restricted or have decreased birth weight. Such a phenotype is yet to be assessed.

Abnormal fetoplacental development can lead to uteroplacental insufficiency and FGR (Krishna & Bhalerao 2011). Cases of FGR in humans with unknown aetiology might be due to abnormal folate metabolism or dietary folate deficiency in their maternal grandparents. Although there might be no effects on their placental transcriptome, exposure to a uterine environment with altered epigenetic marks might developmentally programme the embryos and increase the risk of disease later in life. This highlights the importance of folate supplementation in pregnant women or women who are thinking of becoming pregnant, independently of their folate status, since folate deficiency in their parents can also cause FGR in their children. In addition, since it was shown that paternal *Mtrr^{gt}* mutation also affects the uterine structure and function of their wildtype daughters (Chapter 3), folate supplementation in men might also be beneficial for the growth of their grandchildren. However, folate supplementation should be controlled, since studies have shown that high folate levels during pregnancy were associated with insulin resistance and adiposity in

children at 5 years of age (Krishnaveni et al. 2014). Additionally, moderate folic acid supplementation and *Mthfd1S* deficiency resulted in congenital abnormalities, developmental delay and abnormal placental development, such as abnormal labyrinth formation (Christensen et al. 2016). However, a limitation of this study is that they used *Mthfd1S*^{+/+}, instead of C57Bl/6 as controls.

7.2.3 Associations between abnormal uterine and placental phenotypes

Altogether, we have shown that *Mtrr*^{gt/gt} and F1 *Mtrr*^{+/+} mice have abnormal uterine structure and function at estrus, and abnormal expression of decidual markers at GD6.5 (Chapter 3 and 4). In addition, *Mtrr*^{gt/gt} conceptuses have abnormal placental transcriptome at midgestation (Chapter 5). It is possible that the abnormal uterine environment of *Mtrr*^{gt/gt} females leads to poor placenta development of *Mtrr*^{gt/gt} conceptuses. In contrast, the placental transcriptome of F2 *Mtrr*^{+/+} conceptuses was minimally affected at E10.5 compared to C57Bl/6 controls. However, the lack of DEGs might be because we have sequenced phenotypically normal F2 *Mtrr*^{+/+} conceptuses. It is possible that the placenta transcriptome of growth restricted F2 *Mtrr*^{+/+} conceptuses has been altered due to the abnormal uterine structure and function of F1 *Mtrr*^{+/+} females. Additionally, the observation that the F2 *Mtrr*^{+/+} samples are scattered on the PCA plot (Figure 5.14A), after being in an *Mtrr*^{+/+} uterine environment, might suggest that these conceptuses are able to adapt to an abnormal uterine environment in different ways. This makes it difficult to detect subtle changes in their transcriptome that are, for instance, due to epigenetic factors.

Studies have shown that abnormal uterine gene expression can impair placenta development. For instance, a conditional knockout of *Alk5* in the mouse uterus leads to implantation defects, such as defective lumen closure and increased lumen epithelial folding at E4.5, as a result of increased uterine E2 response, as indicated by increased *Esr1* mRNA levels, and increased epithelial cell proliferation (Peng et al. 2015). In our *Mtrr*^{gt} model, we observed increased lumen epithelial folding in non-pregnant, estrus-staged uteri, but normal *Esr1* receptor expression and normal epithelial cell proliferation (Chapter 3). The increased lumen epithelial folding in our model possibly results from the abnormal apicobasal polarity. This hypothesis is supported by a theoretical model proposing that epithelial folding is driven by apical and baso-lateral modulation (Wen, Wang & Shibata 2017). We observed normal

morphology of implantation sites at GD6.5 (Chapter 4) which correlates with the *Alk5* uterine conditional knockout model (Peng et al. 2015). Despite normal morphology at GD6.5, abnormal placenta development was observed in both models. Placenta defects such as off-centred chorioallantoic attachment and placenta haemorrhage were observed at E10.5 in the *Mtrr^{gt}* model (Padmanabhan et al. 2013). Similarly, the *Alk5* uterine conditional knockout model is characterised by placenta defects, such as disorganisation of trophoblast cells, decreased uNK cell numbers, and impaired spiral artery remodelling (Peng et al. 2015). Future studies should assess the uNK cells and spiral artery remodelling in our model. Additionally, uterine *Nodal* knockout leads to abnormal trophoblast giant cell layer, and malformation of the decidua basalis due to decreased cell proliferation and increased cell apoptosis at E10.5 (Park et al. 2012). Furthermore, a retrospective study involving singleton ART births revealed that endometrial thickness is directly correlated to placenta praevia (Rombauts et al. 2014). Placenta praevia is a condition where the placenta attaches to the uterine wall in a position that covers partly or fully the cervical opening. This causes bleeding during pregnancy and has implications during birth (Alouini et al. 2019). Therefore, it is possible that abnormal E2 and P4 levels affect the endometrial thickness and ultimately lead to placenta praevia during gestation. Finally, deletion of the PI3K antagonist *Pten* leads to decreased decidual cell apoptosis and ultimately an increase in the decidual thickness. As a result, trophoblast invasion and spiral artery remodelling are impaired (Lague et al. 2010). Altogether, these studies show how abnormalities in the uterus can affect placenta development and function.

Alternatively, it is possible that abnormal placenta function of *Mtrr^{gt/gt}* conceptuses, as indicated by abnormal gene expression, can affect the decidualisation reaction. One of the functions of the trophoblast during pregnancy is to invade the uterine epithelium. During implantation and early placentation, the trophoblast penetrates the uterine decidua and replaces the vascular endothelial cells in the spiral arteries. Absence of trophoblast results in reduced SAR (Whitley & Cartwright 2010). At E13.5, *Tpbpa⁺* glycogen trophoblast cells invade the decidua basalis (Adamson et al. 2002; Cross et al. 2002; Silva & Serakides 2016), a process that requires extracellular matrix degradation (Favaro, Abrahamsohn & Zorn 2014). This is achieved by the secretion of proteases, such as MMPs by the trophoblast (Aplin 2000; Lala & Graham 1990). Expression of tissue inhibitor metalloproteinase (TIMP) 3 by decidual cells prevents excessive extracellular matrix degradation and excessive trophoblast invasion (Moore & Crocker 2012). Abnormal decidual extracellular matrix remodelling can impair

decidualisation (White, Robb & Salamonsen 2004). Finally, extravillous trophoblast secretions such as *Profilin 1* induce human endometrial stromal cell decidualisation, and decidualised human endometrial stromal cell adhesion, proliferation, and migration (Menkhorst et al. 2017). Altogether, these studies suggest that abnormal placental gene expression and trophoblast function in *Mtrr^{gt/gt}* mice can impair decidualisation.

7.2.4 The blastocyst transfer process affects fetoplacental growth, suggesting ART might affect the adult health of ART-born children

RNA sequencing revealed a large number of DEGs between non-transferred and transferred F2 *Mtrr^{+/+}* conceptuses. However, most of the DEGs were also misexpressed between non-transferred and transferred C57Bl/6 conceptuses, suggesting a possible effect of the blastocyst transfer process on fetoplacental growth, rather than a programming effect of F1 *Mtrr^{+/+}* intrauterine environment on F2 *Mtrr^{+/+}* conceptuses.

These results might have significant importance for assisted reproductive technologies. Blastocyst transfer is routinely used in ART. Here, we assessed the effects of blastocyst transfer and surrogacy on mouse placental transcriptome and showed that the blastocyst transfer process alters the expression of genes that are involved in fetoplacental development and function (Chapter 6). As highlighted in Chapter 6, the recipient female, BDF1, has 50% similar genetic background to C57Bl/6, therefore differences in gene expression between transferred and non-transferred conceptuses that are expressed solely by the decidua might be attributed to the different genetic background of the decidual tissue. This shows the effects that surrogacy possibly has on fetoplacental growth. Our study is different from most studies, which also involve superovulation, *in vitro* fertilisation, *in vitro* culture, gamete or embryo freezing, or blastomere biopsy (Chen et al. 2015; Delle Piane et al. 2010; Fortier et al. 2008; Rivera et al. 2008; Yao et al. 2016). In addition, while other studies focus on the effects of ART on the expression of imprinted genes specifically (Fortier et al. 2008; Nelissen et al. 2013; Rivera et al. 2008), we performed an unbiased RNA sequencing analysis to assess the effects of blastocyst transfer on the placental transcriptome.

First, we observed genes with transport function to be differentially expressed after blastocyst transfer. The placental expression of most of the genes is yet to be determined, therefore we cannot speculate whether these genes are due to the different genetic background of the

recipient female, that contributed to the decidua, or due to the blastocyst transfer itself. If these genes are expressed in the trophoblast, their differential expression is most probably due to the blastocyst transfer procedure and not due to the difference in genetic background of the mothers. Additionally, we identified DEGs that regulate gene expression by epigenetic mechanisms including DNA methylation, histone modifications, and RNA-mediated mechanisms. Therefore, misexpression of these genes might alter the epigenome of the placenta, leading to misexpression of genes important for normal fetoplacental growth. We also identified DEGs that when knocked out, developmental phenotypes are observed. Finally, our study highlights the importance of following up the ART-born babies, since we showed that even the simplest ART technique, the blastocyst transfer, affects the placental transcriptome.

Next, we identified DEGs in transferred F2 *Mtrr*^{+/+} placentas and found that F2 *Mtrr*^{+/+} conceptuses respond differently to the blastocyst transfer into a BDF1 uterus at E3.0 compared to C57Bl/6 conceptuses. The adverse intrauterine conditions that the F2 *Mtrr*^{+/+} conceptuses were exposed to during the first three days of development, i.e. the uterus of F1 *Mtrr*^{+/+}, were sufficient to developmentally programme the embryos. This is supported by the fact that growth restriction and developmental delay are rescued after blastocyst transfer, while the frequency of growth enhancement was increased (Padmanabhan et al. 2013). DEGs were involved in transport, or their expression is regulated by DNA methylation. This suggests that the uterine environment of the recipient female might cause changes in the epigenetic regulation of gene expression (Chapter 6).

In summary, while the C57Bl/6 conceptuses were transferred from a normal C57Bl/6 uterine environment to another normal BDF1 uterine environment, the F2 *Mtrr*^{+/+} conceptuses were transferred from an abnormal F1 *Mtrr*^{+/+} uterus into a normal BDF1 uterus. It is therefore possible that the F2 *Mtrr*^{+/+} conceptuses were developmentally programmed during the first three days of development in the abnormal F1 *Mtrr*^{+/+} uterine environment. This hypothesis is reinforced by the number of DEGs which are misexpressed independently of the blastocyst transfer. It is possible that the abnormal uterine environment of F1 *Mtrr*^{+/+} females prevents or alters the establishment of the epigenetic marks in the pre-implantation embryo. Additionally, it is possible that the epigenetic marks established in the F2 *Mtrr*^{+/+} embryos during the first three days of development are important for embryo survival in the abnormal F1 *Mtrr*^{+/+} uterine environment, while different epigenetic marks are required for embryo

survival in the normal BDF1 uterus. Abnormal establishment of epigenetic marks might affect cell differentiation during development and might ultimately influence placenta development. The long-term effects of developmental programming on the F2 *Mtrr*^{+/+} generation are yet to be assessed. A future experiment would be to assess the reproductive function of the adult transferred mice, by performing sperm analysis and fertility checks, to see whether the blastocyst transfer process, or a developmental programming mechanism affects their reproductive function, by assessing C57Bl/6 and F2 *Mtrr*^{+/+} transferred conceptuses respectively, compared to non-transferred conceptuses of the same pedigrees.

7.3 Sexual dimorphism in the *Mtrr*^{gt} model

Sexual dimorphism has previously been observed in placental transcriptomes (Gabory et al. 2013; Gallou-Kabani et al. 2010). For instance, the expression of the placental housekeeping genes *Ubc*, *Top1*, and *Ywhaz* was higher in males than females, suggesting the necessity of comparing the transcriptome between same-sex placentas (Cleal et al. 2010). *In utero* exposures also have a sex-specific impact on the developing fetus (Gallou-Kabani et al. 2010; Kundakovic et al. 2013; Mao et al. 2010; McKay et al. 2011; Rosenfeld 2015; Tarrade et al. 2013), highlighting the importance of studying the effects of *in utero* exposures in both sexes. Sexual dimorphism has been observed in the *Mtrr*^{gt} model. Firstly, the developmental phenotypes observed in our model, only occur through the maternal lineage (Padmanabhan et al. 2013). More specifically, the developmental phenotypes are due to abnormal folate metabolism in either the maternal grandparent. These phenotypes are not observed in the F2 generation of an *Mtrr*^{+/gt} paternal grandparent (Padmanabhan et al. 2013). Additionally, we have previously showed that there is no sexual dimorphism of the developmental phenotypes in the *Mtrr*^{gt} model at E10.5 (Padmanabhan et al. 2017). However, we observed an increase in the placenta efficiency of the female conceptuses in each subsequent generation, up to the F4, when the phenotypically normal *Mtrr*^{+/+} conceptuses derived from an *Mtrr*^{+/gt} maternal grandparent were considered (Padmanabhan et al. 2017). Finally, we showed that abnormal folate metabolism causes sex-specific haematological defects in mice (Appendix B; Padmanabhan et al. 2018).

In this thesis, we sequenced placental RNA from male conceptuses at E10.5. However, considering the sexually dimorphic effects of abnormal folate metabolism observed in the *Mtrr*^{gt} model, analysis of the placental transcriptome of female C57Bl/6, *Mtrr*^{gt/gt}, and F2

Mtrr^{+/+} conceptuses at E10.5 by RNA sequencing is required. This will give us information on how the female placentas adapt differently than the male ones to the abnormal uterine environment caused by intrinsic or ancestral *Mtrr*^{gt} mutation.

7.4 MTRR polymorphisms in the human population

The effects of folate on embryo growth and development have been determined through studies looking at folate deficiency, or polymorphisms in genes involved in folate metabolism. Hyperhomocysteinemia is a clinical indicator of folate deficiency in humans (Mcmullin et al. 2001; Ni et al. 2017). This correlates with the *Mtrr*^{gt} model, where we observed increased plasma homocysteine in *Mtrr*^{gt/gt} mice, and also in the F0 *Mtrr*^{+/gt} male mice (Padmanabhan et al. 2013).

MTRR A66G polymorphism was found to be associated with increased risk of congenital abnormalities, such as neural tube defects (Wang et al. 2015) and heart defects (Cai et al. 2014). These phenotypes were also observed in the *Mtrr*^{gt} mouse model (Padmanabhan et al. 2013), suggesting that the *Mtrr*^{gt} mouse model can be representative of the human population. The *MTR* A2756G and *MTHFR* C677T polymorphisms were also independently associated with increased risk of neural tube defects (Wang et al. 2015; Zhang et al. 2019), but not heart defects (Cai et al. 2014; Zhang et al. 2019).

Folate metabolism has also been shown to affect the embryonic growth trajectory. For instance, the *MTR* A2756G polymorphism in either the fetus or the mother is associated with increased risk of uteroplacental insufficiency (Furness et al. 2008). Additionally, the *MTHFD1* G1958A polymorphism in the mother is associated with increased risk of FGR (Furness et al. 2008). In contrast, the *MTRR* A66G polymorphism is not associated with FGR or uteroplacental insufficiency in humans (Furness et al. 2008). This does not correlate with our *Mtrr*^{gt} model, where FGR is observed. Additionally, the *MTRR* A66G polymorphism, but not the *MTR* A2756G or *MTHFR* C677T polymorphisms, increases the risk of preeclampsia (Seremak-Mrozikiewicz et al. 2017; Zhang et al. 2019). Preeclampsia is often associated with FGR (Milosevic-Stevanovic et al. 2016). The risk of preeclampsia in the *Mtrr*^{gt} model has to be determined by assessing clinical features of preeclampsia, such as elevated systolic blood pressure, proteinuria, and renal glomerular endotheliosis (Sandgren et al. 2018). Altogether,

these studies highlight the effects of abnormal folate metabolism on embryo growth and development in humans.

7.5 Further analysis of placental phenotype and function in the *Mtrr^{gt}* model

The abnormal uterine environment of F1 *Mtrr^{+/+}* females in the *Mtrr^{gt}* model, characterised by abnormal cellular structure of the lumen epithelium and myometrium at estrus (Chapter 3), and abnormal expression of decidual markers at GD6.5 (Chapter 4), may be responsible for the growth phenotypes observed in the F2 *Mtrr^{+/+}* conceptuses (Padmanabhan et al. 2013). Further experiments in our lab (J. Rakoczy, P. Laouris, L. White, K. Tan, N. Padmanabhan, S. Tunster, E.D. Watson, unpublished) aimed to assess the placental phenotype, since abnormal decidualisation might lead to abnormal interaction between the trophoblast and the decidua (Adamson et al. 2002; Aplin 2000), and ultimately abnormal placenta development and function. First, trophoblast populations were altered in *Mtrr^{gt/gt}* conceptuses including absent or disorganised labyrinth progenitor cells in the chorion at E8.5 (J. Rakoczy, K. Tan, E.D. Watson, unpublished), and fewer ectoplacental cone cells at E8.5 associated with fewer glycogen trophoblast cells at E14.5 (P. Laouris, S. Tunster, E.D. Watson, unpublished). In addition, *Prl3d1* mRNA expression was decreased in phenotypically normal and abnormal *Mtrr^{gt/gt}* conceptuses compared to C57Bl/6, suggesting abnormal differentiation of spongiotrophoblast and TGCs. *Mtrr^{gt/gt}* females mated to *Mtrr^{gt/gt}* males were injected with Rhodamine 123 dye to assess placental diffusion in their *Mtrr^{gt/gt}* conceptuses at E10.5 when epigenetic instability was observed associated with large scale transcriptional changes. Placenta diffusion was determined to be reduced in *Mtrr^{gt/gt}* conceptuses and became more severe as the phenotype worsened (J. Rakoczy, unpublished). Misexpression of transporter genes in the placenta, as identified by the RNA sequencing (Chapter 5), suggests that active transport mechanisms are influenced by the *Mtrr^{gt}* mutation. The expression of three solute carriers was assessed via RT-qPCR. As mentioned in Chapter 5, further experiments in our lab showed that the expression of *Slc38a4* mRNA levels were decreased in the growth restricted and abnormal *Mtrr^{gt/gt}* conceptuses compared to C57Bl/6 (N. Padmanabhan, unpublished data). Methylation analysis of *Slc38a4* DMRs revealed no difference in DNA methylation in any of the CpG sites assessed, suggesting the expression of *Slc38a* might be due to abnormal placental development and abnormal differentiation of the cell types that

express this solute carrier. To further assess the active transport capacity of the placentas of *Mtrr^{gt/gt}* and F2 *Mtrr^{+/+}* conceptuses, we could label nutrients, such as amino acids, with a radioactive label and trace their transport through the placenta (Sferruzzi-Perri 2018).

Trophoblast stem (TS) cells cultured in folate-depleted media do not interact properly with each other, appear more rounded, and exhibit abnormal adhesion (J. Rakoczy, unpublished). Additionally, chorions of *Mtrr^{gt/gt}* placentas appear disorganised. Together, these observations suggest that cell adhesion and tissue polarity might be altered. We previously showed abnormal E-Cadherin mRNA and protein expression and defective cell polarity in the uterine tissues of non-pregnant females (Chapter 3). These data suggest a possible mechanism of folate metabolism in regulating the expression of genes important for adhesion and cellular organisation. We identified DEGs with cell adhesion function in placentas of growth restricted *Mtrr^{gt/gt}*, but not phenotypically normal *Mtrr^{gt/gt}* conceptuses (Chapter 5). For instance, *Plxna1* (FC = 2.15) and *Bmp2* (FC = 2.15) are involved in negative regulation of cell adhesion. *Micall2* (FC = 2.26) is involved in substrate adhesion-dependent cell spreading, and *Ceacam5* (FC = -7.6) is involved in the cell adhesion of cells of identical type. Since the cytoskeleton regulates cell adhesion (Fuhrmann & Engler 2015), we also looked for genes involved in cytoskeleton organisation. Three DEGs, *Pacsin1* (FC = 2.43), *Micall2* (FC = 2.26), and *Trpm2* (FC = -8.24 in PN *Mtrr^{gt/gt}* placentas) are involved in cytoskeleton organisation. Altogether, these data suggest that folate metabolism affects the expression of genes involved in cell adhesion and cellular organisation.

Finally, expression of the methylation machinery enzymes was analysed in embryos and placentas. While *Dnmt1*, *Dnmt3a*, and *Dnmt3b* mRNA expression was normal in embryos and placentas of phenotypically normal and growth restricted *Mtrr^{gt/gt}* conceptuses at E10.5, expression of *Tet2* mRNA was upregulated in placentas, but not embryos of *Mtrr^{gt/gt}* conceptuses, independently of the phenotype, compared to C57Bl/6. Interestingly, *Tet2* expression in *Mtrr^{gt/gt}* estrus-staged uteri was similar to C57Bl/6 (Chapter 3), suggesting its misexpression occurs during pregnancy. *Tet2* continues to be upregulated at E14.5 and E18.5, while *Tet1* and *Tet3* mRNA is decreased in *Mtrr^{gt/gt}* placentas at E14.5 only. *Tet2* upregulation in *Mtrr^{gt/gt}* placentas at E10.5 is due to abnormal methylation of *Tet2* proximal promoter (unpublished data). These data suggest that *Tet2* expression might play a role on the epigenetic modification of the DEGs in placentas of *Mtrr^{gt/gt}* and C57Bl/6 conceptuses (Chapter 5).

7.6 Future directions

Overall, we showed the importance of folate metabolism in the establishment of a normal maternal-fetal interface, by assessing the effects of the *Mtrr^{gt}* mutation that causes abnormal folate metabolism, on the uterine structure at estrus, the decidual reaction at GD6.5, and the placental transcriptome at E10.5. The effects of the abnormal uterine environment on the placenta development should be further assessed. A future direction is to derive endometrial organoids from C57Bl/6, *Mtrr^{gt/gt}*, and F1 *Mtrr^{+/+}* endometrial tissues (Boretto et al. 2017; Deane, Cousins & Gargett 2017; Turco et al. 2018), to study the mechanisms underlying uterine function. By deriving *Mtrr^{gt/gt}* trophoblast stem cell lines, and co-culturing them with the uterine organoids, we could study the maternal-fetal interactions during placentation in our model (Turco et al. 2018).

Further blastocyst transfer experiments should be performed in the *Mtrr^{gt/gt}* pedigree, i.e. *Mtrr^{gt/gt}* embryos to be transferred at E3.0 into a E2.5 pseudopregnant BDF1 females. This is to assess the developmental phenotypes of the transferred conceptuses and see whether the growth phenotypes are rescued even when the conceptus has intrinsic abnormal folate metabolism, and it is provided with a normal uterine environment. Additionally, the *Mtrr^{gt/gt}* blastocyst transfer experiment will allow to assess the placental transcriptome of the transferred *Mtrr^{gt/gt}* conceptuses and compare it with both the transcriptome of non-transferred *Mtrr^{gt/gt}* and transferred C57Bl/6 conceptuses. In addition, assessment of the gross placenta phenotype of transferred F2 *Mtrr^{+/+}* and *Mtrr^{gt/gt}* conceptuses via histology and immunohistochemistry would give us information on the decidua and trophoblast structure and function.

Bibliography

- van Abeelen, A.F.M., De Rooij, S.R., Osmond, C., Painter, R.C., Veenendaal, M.V.E., Bossuyt, P.M.M., Elias, S.G., Grobbee, D.E., Van Der Schouw, Y.T., Barker, D.J.P. & Roseboom, T.J. 2011, 'The sex-specific effects of famine on the association between placental size and later hypertension', *Placenta*, vol. 32, no. 9, pp. 694–8.
- Ables, G.P., Perrone, C.E., Orentreich, D. & Orentreich, N. 2012, 'Methionine-restricted C57BL/6J mice are resistant to diet-induced obesity and insulin resistance but have low bone density', *PloS One*, vol. 7, no. 12, p. e51357.
- Abrahamsohn, P.A. & Zorn, T.M. 1993, 'Implantation and decidualization in rodents', *The Journal of Experimental Zoology*, vol. 266, no. 6, pp. 603–28.
- Adamson, S.L., Lu, Y., Whiteley, K.J., Holmyard, D., Hemberger, M., Pfarrer, C. & Cross, J.C. 2002, 'Interactions between trophoblast cells and the maternal and fetal circulation in the mouse placenta', *Developmental Biology*, vol. 250, no. 2, pp. 358–73.
- Afshar, Y., Jeong, J.-W., Roqueiro, D., DeMayo, F., Lydon, J., Radtke, F., Radnor, R., Miele, L. & Fazleabas, A. 2011, 'Notch1 mediates uterine stromal differentiation and is critical for complete decidualization in the mouse', *The FASEB Journal*, vol. 26, no. 1, pp. 282–94.
- Agarwal, R., Mori, Y., Cheng, Y., Jin, Z., Olaru, A. V, Hamilton, J.P., David, S., Selaru, F.M., Yang, J., Abraham, J.M., Montgomery, E., Morin, P.J. & Meltzer, S.J. 2009, 'Silencing of claudin-11 is associated with increased invasiveness of gastric cancer cells.', *PloS One*, vol. 4, no. 11, p. e8002.
- Ahmed, T., Fellus, I., Gaudet, J., Macfarlane, A.J., Fontaine-Bisson, B. & Bainbridge, S.A. 2016, 'Effect of folic acid on human trophoblast health and function in vitro', *Placenta*, vol. 37, pp. 7–15.
- Aiken, C.E., Tarry-Adkins, J.L., Spiroski, A.-M., Nuzzo, A.M., Ashmore, T.J., Rolfo, A., Sutherland, M.J., Camm, E.J., Giussani, D.A. & Ozanne, S.E. 2019, 'Chronic gestational hypoxia accelerates ovarian aging and lowers ovarian reserve in next-generation adult rats', *The FASEB Journal*, p. fj.201802772R.

- Alahakoon, T.I., Zhang, W., Arbuckle, S., Zhang, K. & Lee, V. 2018, 'Reduced angiogenic factor expression in intrauterine fetal growth restriction using semiquantitative immunohistochemistry and digital image analysis', *Journal of Obstetrics and Gynaecology Research*, vol. 44, no. 5, pp. 861–72.
- Alam, K.S.M., Konno, T. & Soares, M.J. 2015, 'Identification of target genes for a prolactin family paralog in mouse decidua', *Reproduction*, vol. 149, no. 6, pp. 625–32.
- Albano, R.M., Arkell, R., Beddington, R.S. & Smith, J.C. 1994, 'Expression of inhibin subunits and follistatin during postimplantation mouse development: decidual expression of activin and expression of follistatin in primitive streak, somites and hindbrain', *Development*, vol. 120, no. 4, pp. 803–13.
- Allen, E. 1922, 'The oestrous cycle in the mouse', *American Journal of Anatomy*, vol. 30, no. 3, pp. 297–371.
- Alouini, S., Megier, P., Fauconnier, A., Huchon, C., Fievet, A., Ramos, A., Megier, C. & Valery, A. 2019, 'Diagnosis and management of placenta previa and low placental implantation', *The journal of Maternal-fetal & Neonatal Medicine*, pp. 1–6.
- Amleh, A. & Dean, J. 2002, 'Mouse genetics provides insight into folliculogenesis, fertilization and early embryonic development.', *Human Reproduction Update*, vol. 8, no. 5, pp. 395–403.
- Andres, R.L. & Day, M.-C. 2000, 'Perinatal complications associated with maternal tobacco use', *Seminars in Neonatology*, vol. 5, no. 3, pp. 231–41.
- Angst, B.D., Marcozzi, C. & Magee, A.I. 2001, 'The cadherin superfamily: diversity in form and function', *Journal of Cell Science*, vol. 114, no. 4, pp. 629–41.
- Anier, K., Malinovskaja, K., Aonurm-Helm, A., Zharkovsky, A. & Kalda, A. 2010, 'DNA methylation regulates cocaine-induced behavioral sensitization in mice', *Neuropsychopharmacology*, vol. 35, p. 2450.
- Anin, S.A., Vince, G. & Quenby, S. 2004, 'Trophoblast invasion', *Human Fertility*, vol. 7, no. 3, pp. 169–74.
- Antoniades, C., Antonopoulos, A.S., Tousoulis, D., Marinou, K. & Stefanadis, C. 2009, 'Homocysteine and coronary atherosclerosis : from folate fortification to the recent

- clinical trials', *European Heart Journal*, vol. 30, pp. 6–15.
- Aplin, J. 2000, 'Maternal influences on placental development', *Seminars in Cell and Developmental Biology*, vol. 11, no. 2, pp. 115–25.
- Aplin, J.D. & Ruane, P.T. 2017, 'Embryo-epithelium interactions during implantation at a glance', *Journal of Cell Science*, vol. 130, no. 1, pp. 15–22.
- Arima, T., Hata, K., Tanaka, S., Kusumi, M., Li, E., Kato, K., Shiota, K., Sasaki, H. & Wake, N. 2006, 'Loss of the maternal imprint in *Dnmt3Lmat*^{-/-} mice leads to a differentiation defect in the extraembryonic tissue', *Developmental Biology*, vol. 297, no. 2, pp. 361–73.
- Arrigoni, L., Richter, A.S., Betancourt, E., Bruder, K., Diehl, S., Manke, T. & Bonisch, U. 2016, 'Standardizing chromatin research: A simple and universal method for CHIP-seq', *Nucleic Acids Research*, vol. 44, no. 7, p. e67.
- Arroyo, J.A. & Winn, V.D. 2008, 'Vasculogenesis and angiogenesis in the IUGR placenta', *Seminars in Perinatology*, vol. 32, no. 3, pp. 172–7.
- Ashley, R.L., Henkes, L.E., Bouma, G.J., Pru, J.K. & Hansen, T.R. 2010, 'Deletion of the *Isg15* gene results in up-regulation of decidual cell survival genes and down-regulation of adhesion genes: Implication for regulation by IL-1', *Endocrinology*, vol. 151, no. 9, pp. 4527–36.
- Ashton, S. V., Whitley, G.S.J., Dash, P.R., Wareing, M., Crocker, I.P., Baker, P.N. & Cartwright, J.E. 2005, 'Uterine spiral artery remodeling involves endothelial apoptosis induced by extravillous trophoblasts through Fas/FasL interactions', *Arteriosclerosis, Thrombosis, and Vascular Biology*, vol. 25, no. 1, pp. 102–8.
- Au, K.F., Jiang, H., Lin, L., Xing, Y. & Wong, W.H. 2010, 'Detection of splice junctions from paired-end RNA-seq data by SpliceMap', *Nucleic Acids Research*, vol. 38, no. 14, pp. 4570–8.
- Bachelot, A. & Binart, N. 2005, 'Corpus luteum development: lessons from genetic models in mice', *Current Topics in Developmental Biology*, vol. 68, pp. 49–84.
- Bachelot, A. & Binart, N. 2007, 'Reproductive role of prolactin', *Reproduction*, vol. 133, no. 2, pp. 361–9.

- Bagley, P.J. & Selhub, J. 1998, 'A common mutation in the methylenetetrahydrofolate reductase gene is associated with an accumulation of formylated tetrahydrofolates in red blood cells.', *Proceedings of the National Academy of Sciences of the United States of America*, vol. 95, no. 22, pp. 13217–20.
- Bailey, L.B., Rampersaud, G.C. & Kauwell, G.P.A. 2003, 'Folic acid supplements and fortification affect the risk for neural tube defects, vascular disease and cancer: evolving science', *The Journal of Nutrition*, vol. 133, no. 6, p. 1961S–1968S.
- Bailey, L.B., Stover, P.J., McNulty, H., Fenech, M.F., Gregory, J.F. 3rd, Mills, J.L., Pfeiffer, C.M., Fazili, Z., Zhang, M., Ueland, P.M., Molloy, A.M., Caudill, M.A., Shane, B., Berry, R.J., Bailey, R.L., Hausman, D.B., Raghavan, R. & Raiten, D.J. 2015, 'Biomarkers of nutrition for development - Folate review', *The Journal of Nutrition*, vol. 145, no. 7, p. 1636S–1680S.
- Baker, B.C. 2015, 'The Effect of Folate Deficiency on Placental Function', University of Manchester.
- Baker, B.C., Mackie, F.L., Lean, S.C., Greenwood, S.L., Heazell, A.E.P., Forbes, K. & Jones, R.L. 2017, 'Placental dysfunction is associated with altered microRNA expression in pregnant women with low folate status', *Molecular Nutrition & Food Research*, vol. 61, no. 8.
- Banning, C. 1946, 'Food shortage and public health, first half of 1945', *The ANNALS of the American Academy of Political and Social Science*, vol. 245, no. 1, pp. 93–110.
- Bar-Peled, L. & Sabatini, D.M. 2014, 'Regulation of mTORC1 by amino acids', *Trends in Cell Biology*, vol. 24, no. 7, 2014/03/31., pp. 400–6.
- Baran, N., Kelly, P.A. & Binart, N. 2003, 'Decysin, a new member of the metalloproteinase family, is regulated by prolactin and steroids during mouse pregnancy.', *Biology of Reproduction*, vol. 68, no. 5, pp. 1787–92.
- Barbot, W. 2002, 'Epigenetic regulation of an IAP retrotransposon in the aging mouse: progressive demethylation and de-silencing of the element by its repetitive induction', *Nucleic Acids Research*, vol. 30, no. 11, pp. 2365–73.
- Barker, D.J., Bull, a R., Osmond, C. & Simmonds, S.J. 1990, 'Fetal and placental size and

- risk of hypertension in adult life', *BMJ*, vol. 301, pp. 259–62.
- Barker, D.J.P. 1997, 'Maternal nutrition, fetal nutrition, and disease in later life', *Nutrition*, vol. 13, no. 9, pp. 807–13.
- Barker, D.J.P., Hales, C.N., Fall, C.H.D., Smond, C.O., Phipps, K. & Clark, P.M.S. 1993, 'Type 2 (non-insulin-dependent) diabetes mellitus, hypertension and hyperlipidaemia (syndrome X): relation to reduced fetal growth', *Diabetologia*, vol. 36, pp. 62–7.
- Barry, J.S., Rozance, P.J. & Anthony, R. V. 2008, 'An animal model of placental insufficiency-induced intrauterine growth restriction', *Seminars in Perinatology*, vol. 32, no. 3, pp. 225–30.
- Barut, F., Barut, A., Gun, B.D., Kandemir, N.O., Harma, M.I. & Harma, M. 2010, 'Intrauterine growth restriction and placental angiogenesis', *Diagnostic Pathology*, vol. 5, no. 24.
- Baschat, A.A. 2014, 'Neurodevelopment after Fetal Growth Restriction', *Fetal Diagnosis and Therapy*, vol. 36, no. 2, pp. 136–42.
- Bashour, N.M. & Wray, S. 2012, 'Progesterone directly and rapidly inhibits GnRH neuronal activity via progesterone receptor membrane component 1', *Endocrinology*, vol. 153, no. 9, pp. 4457–69.
- Basset, G., Quinlivan, E.P., Ziemak, M.J., Diaz De La Garza, R., Fischer, M., Schiffmann, S., Bacher, A., Gregory, J.F. 3rd & Hanson, A.D. 2002, 'Folate synthesis in plants: the first step of the pterin branch is mediated by a unique bimodular GTP cyclohydrolase I', *Proceedings of the National Academy of Sciences of the United States of America*, vol. 99, no. 19, pp. 12489–94.
- Bateson, P., Barker, D., Clutton-Brock, T., Deb, D., D'Udine, B., Foley, R.A., Gluckman, P., Godfrey, K., Kirkwood, T., Lahr, M.M., McNamara, J., Metcalfe, N.B., Monaghan, P., Spencer, H.G. & Sultan, S.E. 2004, 'Developmental plasticity and human health', *Nature*, vol. 430, no. 6998, pp. 419–21.
- Bell, A.W. & Ehrhardt, R.A. 2002, 'Regulation of placental nutrient transport and implications for fetal growth', *Nutrition Research Reviews*, vol. 15, no. 02, p. 211.
- Bell, S.E., Sanchez, M.J., Spasic-boskovic, O., Santalucia, T., Gambardella, L., Burton, G.J.,

- Murphy, J.J., Norton, J.D., Clark, A.R. & Turner, M. 2006, 'The RNA binding protein Zfp3611 is required for normal vascularisation and post-transcriptionally regulates VEGF expression', *Developmental Dynamics*, vol. 235, no. 11, pp. 3144–55.
- Bellofiore, N., Ellery, S.J., Mamrot, J., Walker, D.W., Temple-Smith, P. & Dickinson, H. 2016, 'First evidence of a menstruating rodent: the spiny mouse (*Acomys cahirinus*)', *bioRxiv*, p. 56895.
- Ben-Jonathan, N. & Hnasko, R. 2001, 'Dopamine as a prolactin (PRL) inhibitor', *Endocrine Reviews*, vol. 22, no. 6, pp. 724–63.
- Benson, G. V, Lim, H., Paria, B.C., Satokata, I., Dey, S.K. & Maas, R.L. 1996, 'Mechanisms of reduced fertility in Hoxa-10 mutant mice : uterine homeosis and loss of maternal Hoxa-10 expression', *Development*, vol. 2696, pp. 2687–96.
- Bergen, N.E., Jaddoe, V.W. V, Timmermans, S., Hofman, A., Lindemans, J., Russcher, H., Raat, H., Steegers-Theunissen, R.P.M. & Steegers, E.A.P. 2012, 'Homocysteine and folate concentrations in early pregnancy and the risk of adverse pregnancy outcomes: The generation R study', *BJOG*, vol. 119, no. 6, pp. 739–51.
- Bertolin, K. & Murphy, B.D. 2014, 'Chapter 7 - Reproductive tract changes during the mouse estrous cycle', in B.A. Croy, A.T. Yamada, F.J. DeMayo & S.L.B.T.-T.G. to I. of M.P. Adamson (eds), *The Guide to Investigation of Mouse Pregnancy*, Academic Press, Boston, pp. 85–94.
- Bhasin, K.K.S., van Nas, A., Martin, L.J., Davis, R.C., Devaskar, S.U. & Lusic, A.J. 2009, 'Maternal low-protein diet or hypercholesterolemia reduces circulating essential amino acids and leads to intrauterine growth restriction', *Diabetes*, vol. 58, no. 3, pp. 559–66.
- Bills, N.D., Koury, M.J., Clifford, A.J. & Dessypris, E.N. 1992, 'Ineffective hematopoiesis in folate-deficient mice', *Blood*, vol. 79, no. 9, pp. 2273–80.
- Blendinger, K. 2007, 'Physiology and pathology of the estrous cycle of the bitch', *Proceedings of the SCIVAC Congress*, vol. 1, pp. 73–7.
- Bloise, E., Lin, W., Liu, X., Simbulan, R., Kolahi, K.S., Petraglia, F., Maltepe, E., Donjacour, A. & Rinaudo, P. 2012, 'Impaired placental nutrient transport in mice generated by in vitro fertilization', *Endocrinology*, vol. 153, no. 7, pp. 3457–67.

- Blom, H.J. & Smulders, Y. 2011, 'Overview of homocysteine and folate metabolism. With special references to cardiovascular disease and neural tube defects', *Journal of Inherited Metabolic Disease*, vol. 34, no. 1, pp. 75–81.
- Blount, B.C., Mack, M.M., Wehr, C.M., MacGregor, J.T., Hiatt, R.A., Wang, G., Wickramasinghe, S.N., Everson, R.B. & Ames, B.N. 1997, 'Folate deficiency causes uracil misincorporation into human DNA and chromosome breakage: Implications for cancer and neuronal damage', *Proceedings of the National Academy of Sciences*, vol. 94, no. 7, pp. 3290–5.
- Boehmer, B.H., Limesand, S.W. & Rozance, P.J. 2017, 'The impact of IUGR on pancreatic islet development and beta-cell function.', *The Journal of Endocrinology*, vol. 235, no. 2, pp. R63–76.
- Boretto, M., Cox, B., Noben, M., Hendriks, N., Fassbender, A., Roose, H., Amant, F., Timmerman, D., Tomassetti, C., Vanhie, A., Meuleman, C., Ferrante, M. & Vankelecom, H. 2017, 'Development of organoids from mouse and human endometrium showing endometrial epithelium physiology and long-term expandability', *Development*, vol. 144, no. 10, pp. 1775–86.
- Boushey, C.J., Beresford, S.A., Omenn, G.S. & Motulsky, A.G. 1995, 'A quantitative assessment of plasma homocysteine as a risk factor for vascular disease. Probable benefits of increasing folic acid intakes.', *JAMA*, vol. 274, no. 13, pp. 1049–57.
- Bovolenta, P., Esteve, P., Ruiz, J.M., Cisneros, E. & Lopez-Rios, J. 2008, 'Beyond Wnt inhibition: new functions of secreted Frizzled-related proteins in development and disease', *Journal of Cell Science*, vol. 121, no. 6, pp. 737–46.
- Boxmeer, J.C., Brouns, R.M., Lindemans, J., Steegers, E.A.P., Martini, E., Macklon, N.S. & Steegers-Theunissen, R.P.M. 2008, 'Preconception folic acid treatment affects the microenvironment of the maturing oocyte in humans', *Fertility and Sterility*, vol. 89, no. 6, pp. 1766–70.
- Braga, V.M. & Gendler, S.J. 1993, 'Modulation of Muc-1 mucin expression in the mouse uterus during the estrus cycle, early pregnancy and placentation', *Journal of Cell Science*, vol. 105 (Pt 2, pp. 397–405.
- Brenseke, B., Prater, M.R., Bahamonde, J. & Gutierrez, J.C. 2013, 'Current thoughts on

- maternal nutrition and fetal programming of the metabolic syndrome’, *Journal of Pregnancy*, vol. 2013.
- Brett, K.E., Ferraro, Z.M., Yockell-Lelievre, J., Gruslin, A. & Adamo, K.B. 2014, ‘Maternal–fetal nutrient transport in pregnancy pathologies: The role of the placenta’, *International Journal of Molecular Sciences*, vol. 15, no. 9, pp. 16153–85.
- Brody, J.R. & Cunha, G.R. 1989, ‘Histologic, morphometric, and immunocytochemical analysis of myometrial development in rats and mice: I. Normal development’, *American Journal of Anatomy*, vol. 186, no. 1, pp. 1–20.
- Brody, L.C., Conley, M., Cox, C., Kirke, P.N., McKeever, M.P., Mills, J.L., Molloy, A.M., O’Leary, V.B., Parle-McDermott, A., Scott, J.M. & Swanson, D. a 2002, ‘A polymorphism, R653Q, in the trifunctional enzyme methylenetetrahydrofolate dehydrogenase/methenyltetrahydrofolate cyclohydrolase/formyltetrahydrofolate synthetase is a maternal genetic risk factor for neural tube defects: report of the Birth Defects Res’, *American Journal of Human Genetics*, vol. 71, no. 5, pp. 1207–15.
- Brown, M.A., Hague, W.M., Higgins, J., Lowe, S., McCowan, L., Oats, J., Peek, M.J., Rowan, J.A. & Walters, B.N.J. 2000, ‘The detection, investigation and management of hypertension in pregnancy: Executive summary’, *Australian and New Zealand Journal of Obstetrics and Gynaecology*, vol. 40, no. 2, pp. 133–8.
- Buckland, M.D., Hall, L., Mowlem, A. & Whatley, B.F. 1981, ‘Chapter 11 - The mouse (*Mus musculus*)’, in M.D. Buckland, L. Hall, A. Mowlem & B.F.B.T.-A.G. to L.A.T. Whatley (eds), *A Guide to Laboratory Animal Technology*, Butterworth-Heinemann, pp. 92–7.
- Bult, C.J., Blake, J.A., Smith, C.L., Kadin, J.A. & Richardson, J.E. 2019, ‘Mouse Genome Database (MGD) 2019’, *Nucleic Acids Research*, vol. 47, no. D1, pp. D801–6.
- Burgoon, J.M., Selhub, J., Nadeau, M. & Sadler, T.W. 2002, ‘Investigation of the effects of folate deficiency on embryonic development through the establishment of a folate deficient mouse model’, *Teratology*, vol. 65, no. 5, pp. 219–27.
- Burke, K.A., Jauniaux, E., Burton, G.J. & Cindrova-Davies, T. 2013, ‘Expression and immunolocalisation of the endocytic receptors megalin and cubilin in the human yolk sac and placenta across gestation’, *Placenta*, vol. 34, no. 11, pp. 1105–9.

- Byers, S.L., Wiles, M. V, Dunn, S.L. & Taft, R.A. 2012, 'Mouse estrous cycle identification tool and images', *PloS One*, vol. 7, no. 4, pp. 1–5.
- Cai, B., Zhang, T., Zhong, R., Zou, L., Zhu, B., Chen, W., Shen, N., Ke, J., Lou, J., Wang, Z., Sun, Y., Liu, L. & Song, R. 2014, 'Genetic variant in MTRR, but not MTR, is associated with risk of congenital heart disease: an integrated meta-analysis', *PloS one*, vol. 9, no. 3, p. e89609.
- Caligioni, C.S. 2009, 'Assessing reproductive status/stages in mice', *Current Protocols in Neuroscience*, vol. Appendix 4, p. Appendix-4I.
- Cambuli, F., Murray, A., Dean, W., Dudzinska, D., Krueger, F., Andrews, S., Senner, C.E., Cook, S.J. & Hemberger, M. 2014, 'Epigenetic memory of the first cell fate decision prevents complete ES cell reprogramming into trophoblast', *Nature Communications*, vol. 5.
- Campbell, S., Diaz-Recasens, J., Griffin, D.R., Cohen-Overbeek, T.E., Pearce, J.M., Willson, K. & Teague, M.J. 1983, 'New doppler technique for assessing uteroplacental blood flow', *Lancet*, vol. 1, no. 8326 Pt 1, pp. 675–7.
- Canovas, S., Ross, P.J., Kelsey, G. & Coy, P. 2017, 'DNA methylation in embryo development: epigenetic impact of ART (Assisted Reproductive Technologies)', *BioEssays*, vol. 39, no. 11.
- Cao, D., Wang, Z., Zhang, C.-L., Oh, J., Xing, W., Li, S., Richardson, J.A., Wang, D.-Z. & Olson, E.N. 2005, 'Modulation of smooth muscle gene expression by association of histone acetyltransferases and deacetylases with myocardin.', *Molecular and Cellular Biology*, vol. 25, no. 1, pp. 364–76.
- Cartwright, J.E., Fraser, R., Leslie, K., Wallace, A.E. & James, J.L. 2010, 'Remodelling at the maternal-fetal interface: relevance to human pregnancy disorders.', *Reproduction*, vol. 140, no. 6, pp. 803–13.
- Castellanos-Sinco, H.B., Ramos-Peñafiel, C.O., Santoyo-Sánchez, A., Collazo-Jaloma, J., Martínez-Murillo, C., Montaña-Figueroa, E. & Sinco-Ángeles, A. 2015, 'Megaloblastic anaemia: Folic acid and vitamin B12 metabolism', *Revista Médica Del Hospital General De México*, vol. 78, no. 3, pp. 135–43.

- CDC, C. for D.C. 1991, 'Use of folic acid for prevention of spina bifida and other neural tube defects--1983-1991', *MMWR. Morbidity and Mortality Weekly Report*, vol. 40, no. 30, pp. 513–6.
- Ceesay, S.M., Prentice, A.M., Cole, T.J., Foord, F., Poskitt, E.M.E., Weaver, L.T. & Whitehead, R.G. 1997, 'Effects on birth weight and perinatal mortality of maternal dietary supplements in rural gambia: 5 year randomised controlled trial', *BMJ*, vol. 315, no. 7111, pp. 786–90.
- Cha, J., Bartos, A., Park, C., Sun, X., Li, Y., Cha, S.-W., Ajima, R., Ho, H.-Y.H., Yamaguchi, T.P. & Dey, S.K. 2014, 'Appropriate crypt formation in the uterus for embryo homing and implantation requires Wnt5a-ROR signaling', *Cell Reports*, vol. 8, no. 2, pp. 382–92.
- Cha, J., Sun, X. & Dey, S.K. 2012, 'Mechanisms of implantation: Strategies for successful pregnancy', *Nature Medicine*, vol. 18, no. 12, pp. 1754–67.
- Champlin, A.K., Dorr, D.L. & Gates, A.H. 1973, 'Determining the stage of the estrous cycle in the mouse by the appearance of the vagina', *Biology of Reproduction*, vol. 8, no. 4, pp. 491–4.
- Chan, P.Y.L., Morris, J.M., Leslie, G.I., Kelly, P.J. & Gallery, E.D.M. 2010, 'The long-term effects of prematurity and intrauterine growth restriction on cardiovascular, renal, and metabolic function', *International Journal of Pediatrics*, vol. 2010, 2010/12/14., p. 280402.
- Chan, Y.-M., Bailey, R. & O'Connor, D.L. 2013, 'Folate', *Advances in Nutrition*, vol. 4, no. 1, pp. 123–5.
- Chan, Y.Y., Jayaprakasan, K., Tan, A., Thornton, J.G., Coomarasamy, A. & Raine-Fenning, N.J. 2011, 'Reproductive outcomes in women with congenital uterine anomalies: a systematic review', *Ultrasound in Obstetrics & Gynecology*, vol. 38, no. 4, pp. 371–82.
- Chang, H.J., Shin, H.S., Kim, T.H., Yoo, J., Teasley, E., Zhao, J.J., Ha, U. & Jeong, J. 2018, 'Pik3ca is required for mouse uterine gland development and pregnancy', *PLoS One*, vol. 13, no. 1, p. e0191433.
- Chao, T., Zhou, X., Cao, B., Liao, P., Liu, H., Chen, Y., Park, H.-W., Zeng, S.X. & Lu, H.

- 2016, 'Pleckstrin homology domain-containing protein PHLDB3 supports cancer growth via a negative feedback loop involving p53', *Nature Communications*, vol. 7, p. 13755.
- Charalambous, F., Elia, A. & Georgiades, P. 2012, 'Decidual spiral artery remodeling during early post-implantation period in mice: Investigation of associations with decidual uNK cells and invasive trophoblast', *Biochemical and Biophysical Research Communications*, vol. 417, no. 2, pp. 847–52.
- Charles, M.A., Johnson, I.T. & Belshaw, N.J. 2012, 'Supra-physiological folic acid concentrations induce aberrant DNA methylation in normal human cells in vitro', *Epigenetics*, vol. 7, no. 7, pp. 689–94.
- Chen, C., Bajoria, R. & Aplin, J.D. 2002, 'Decreased vascularization and cell proliferation in placentas of intrauterine growth – restricted fetuses with abnormal umbilical artery flow velocity waveforms', *American Journal of Obstetrics & Gynecology*, vol. 187, no. 3, pp. 764–9.
- Chen, E.Y., Tan, C.M., Kou, Y., Duan, Q., Wang, Z., Meirelles, G.V., Clark, N.R. & Ma'ayan, A. 2013, 'Enrichr: interactive and collaborative HTML5 gene list enrichment analysis tool', *BMC Bioinformatics*, vol. 14, no. 1, p. 128.
- Chen, L.-M., Wang, R.-S., Lee, Y.-F., Liu, N.-C., Chang, Y.-J., Wu, C.-C., Xie, S., Hung, Y.-C. & Chang, C. 2008, 'Subfertility with defective folliculogenesis in female mice lacking testicular orphan nuclear receptor 4', *Molecular Endocrinology*, vol. 22, no. 4, pp. 858–67.
- Chen, L., Xu, B., Liu, L., Luo, Y., Zhou, H., Chen, W., Shen, T., Han, X., Kontos, C.D. & Huang, S. 2011, 'Cadmium induction of reactive oxygen species activates the mTOR pathway, leading to neuronal cell death', *Free Radical Biology and Medicine*, vol. 50, no. 5, pp. 624–32.
- Chen, M., Zhang, J., Li, N., Qian, Z., Zhu, M., Li, Q., Zheng, J., Wang, X. & Shi, G. 2011, 'Promoter hypermethylation mediated downregulation of FBP1 in human hepatocellular carcinoma and colon cancer', *PLoS One*, vol. 6, no. 10.
- Chen, Q., Zhang, Y., Elad, D., Jaffa, A.J., Cao, Y., Ye, X. & Duan, E. 2013, 'Navigating the site for embryo implantation: biomechanical and molecular regulation of intrauterine

- embryo distribution', *Molecular Aspects of Medicine*, vol. 34, no. 5, pp. 1024–42.
- Chen, Q., Zhang, Y., Peng, H., Lei, L., Kuang, H., Zhang, L., Ning, L., Cao, Y. & Duan, E. 2011, 'Transient β 2-adrenoceptor activation confers pregnancy loss by disrupting embryo spacing at implantation', *The Journal of Biological Chemistry*, vol. 286, no. 6, pp. 4349–56.
- Chen, S., Sun, F., Huang, X., Wang, X., Tang, N., Zhu, B. & Li, B. 2015, 'Assisted reproduction causes placental maldevelopment and dysfunction linked to reduced fetal weight in mice', *Scientific Reports*, vol. 5, p. 10596.
- Chen, Z., Karaplis, A.C., Ackerman, S.L., Pogribny, I.P., Melnyk, S., Lussier-Cacan, S., Chen, M.F., Pai, A., John, S.W., Smith, R.S., Bottiglieri, T., Bagley, P., Selhub, J., Rudnicki, M.A., James, S.J. & Rozen, R. 2001, 'Mice deficient in methylenetetrahydrofolate reductase exhibit hyperhomocysteinemia and decreased methylation capacity, with neuropathology and aortic lipid deposition', *Human Molecular Genetics*, vol. 10, no. 5, pp. 433–43.
- Chen, Z., Zhang, J., Hatta, K., Lima, P.D.A., Yadi, H., Colucci, F., Yamada, A.T. & Croy, B.A. 2012, 'DBA-lectin reactivity defines mouse uterine natural killer cell subsets with biased gene expression', *Biology of Reproduction*, vol. 87, no. 4, p. 81.
- Chern, S.-R., Li, S.-H., Lu, C.-H. & Chen, E.I.T. 2010, 'Spatiotemporal expression of the serine protease inhibitor, SERPINE2, in the mouse placenta and uterus during the estrous cycle, pregnancy, and lactation.', *Reproductive Biology and Endocrinology*, vol. 8, p. 127.
- Cho, Y.H.E.E., Yazici, H., Wu, H.-C., Terry, M.-B., Gonzalez, K., Qu, M., Dalay, N. & Santella, R.M. 2010, 'Aberrant promoter hypermethylation and genomic hypomethylation in tumor, adjacent normal tissues and blood from breast cancer patients', *Anticancer Research*, vol. 30, no. 7, pp. 2489–96.
- Choux, C., Carmignac, V., Bruno, C., Sagot, P., Vaiman, D. & Fauque, P. 2015, 'The placenta: phenotypic and epigenetic modifications induced by Assisted Reproductive Technologies throughout pregnancy', *Clinical Epigenetics*, vol. 7, p. 87.
- Chow, W.N., Lee, Y.L., Wong, P.C., Chung, M.K., Lee, K.F. & Yeung, W.S.B. 2009, 'Complement 3 deficiency impairs early pregnancy in mice', *Molecular Reproduction*

and Development, vol. 76, no. 7, pp. 647–55.

- Christensen, K.E., Hou, W., Bahous, R.H., Deng, L., Malysheva, O. V., Arning, E., Bottiglieri, T., Caudill, M.A., Jerome-Majewska, L.A. & Rozen, R. 2016, ‘Moderate folic acid supplementation and MTHFD1-synthetase deficiency in mice, a model for the R653Q variant, result in embryonic defects and abnormal placental development^{1,2}’, *American Journal of Clinical Nutrition*, vol. 104, no. 5, pp. 1459–69.
- Christian, P. 2003, ‘Effects of alternative maternal micronutrient supplements on low birth weight in rural Nepal: double blind randomised community trial’, *BMJ*, vol. 326, no. 7389, pp. 571–571.
- Chuma, S. & Nakatsuji, N. 2001, ‘Autonomous transition into meiosis of mouse fetal germ cells in vitro and its inhibition by gp130-mediated signaling.’, *Developmental Biology*, vol. 229, no. 2, pp. 468–79.
- Clarke, C.L. & Sutherland, R.L. 1990, ‘Progesterin regulation of cellular proliferation’, *Endocrine Reviews*, vol. 11, no. 2, pp. 266–301.
- Cleal, J.K., Day, P.L., Hanson, M.A. & Lewis, R.M. 2010, ‘Sex differences in the mRNA levels of housekeeping genes in human placenta’, *Placenta*, vol. 31, no. 6, pp. 556–7.
- Clercq, K. De, Hennes, A. & Vriens, J. 2017, ‘Isolation of mouse endometrial epithelial and stromal cells for in vitro decidualization’, *Journal of Visualized Experiments*, vol. 2, no. 121.
- Clifton, V.L. 2010, ‘Sex and the human placenta: mediating differential strategies of fetal growth and survival’, *Placenta*, vol. 31, pp. S33–9.
- Coan, P.M., Conroy, N. & Burton, G.J. 2006, ‘Origin and characteristics of glycogen cells in the developing murine placenta’, *Developmental Dynamics*, vol. 235, no. 12, pp. 3280–94.
- Coe, B.L., Kirkpatrick, J.R., Taylor, J.A. & Vom Saal, F.S. 2008, ‘A new “crowded uterine horn” mouse model for examining the relationship between foetal growth and adult obesity’, *Basic and Clinical Pharmacology and Toxicology*, vol. 102, no. 2, pp. 162–7.
- Cohen, M., Meisser, A. & Bischof, P. 2006, ‘Metalloproteinases and human placental invasiveness’, *Placenta*, vol. 27, no. 8, pp. 783–93.

- Conesa, A., Madrigal, P., Tarazona, S., Gomez-Cabrero, D., Cervera, A., McPherson, A., Szcześniak, M.W., Gaffney, D.J., Elo, L.L., Zhang, X. & Mortazavi, A. 2016, 'A survey of best practices for RNA-seq data analysis', *Genome Biology*, vol. 17, no. 1, p. 13.
- Constância, M., Hemberger, M., Hughes, J., Dean, W., Ferguson-Smith, A., Fundele, R., Stewart, F., Kelsey, G., Fowden, A., Sibley, C. & Reik, W. 2002, 'Placental-specific IGF-II is a major modulator of placental and fetal growth.', *Nature*, vol. 417, no. 6892, pp. 945–8.
- Conway, J.R., Lex, A. & Gehlenborg, N. 2017, 'UpSetR: An R package for the visualization of intersecting sets and their properties', *Bioinformatics*, vol. 33, no. 18, pp. 2938–40.
- Copp, A.J., Brook, F.A. & Roberts, H.J. 1988, 'A cell-type-specific abnormality of cell proliferation in mutant (curly tail) mouse embryos developing spinal neural tube defects', *Development*, vol. 104, no. 2, p. 285 LP-295.
- Correia-Branco, A., Keating, E. & Martel, F. 2015, 'Maternal undernutrition and fetal developmental programming of obesity: the glucocorticoid connection', *Reproductive Sciences*, vol. 22, no. 2, pp. 138–45.
- Courtemanche, C., Elson-Schwab, I., Mashiyama, S.T., Kerry, N. & Ames, B.N. 2004, 'Folate deficiency inhibits the proliferation of primary human CD8⁺ T lymphocytes in vitro.', *Journal of Immunology*, vol. 173, no. 5, pp. 3186–92.
- Cowden Dahl, K.D., Fryer, B.H., Mack, F.A., Compennolle, V., Maltepe, E., Adelman, D.M., Carmeliet, P. & Simon, M.C. 2005, 'Hypoxia-inducible factors 1 α and 2 α regulate trophoblast differentiation', *Molecular and Cellular Biology*, vol. 25, no. 23, p. 10479 LP-10491.
- Cozzi, V., Garlanda, C., Nebuloni, M., Maina, V., Martinelli, A., Calabrese, S. & Cetin, I. 2012, 'PTX3 as a potential endothelial dysfunction biomarker for severity of preeclampsia and IUGR', *Placenta*, vol. 33, no. 12, pp. 1039–44.
- Cramer, O.M., Parker, C.R.J. & Porter, J.C. 1979, 'Estrogen inhibition of dopamine release into hypophysial portal blood', *Endocrinology*, vol. 104, no. 2, pp. 419–22.
- Crider, K.S., Yang, T.P., Berry, R.J. & Bailey, L.B. 2012, 'Folate and DNA methylation: A Review of molecular mechanisms and the evidence for folate's role', *American Society*

for Nutrition, vol. 3, no. 14, pp. 21–38.

Cross, J., Werb, Z. & Fisher, S. 1994, 'Implantation and the placenta: key pieces of the development puzzle', *Science*, vol. 266, no. 5190, pp. 1508–18.

Cross, J.C., Baczyk, D., Dobric, N., Hemberger, M., Hughes, M., Simmons, D.G., Yamamoto, H. & Kingdom, J.C.P. 2003, 'Genes, development and evolution of the placenta', *Placenta*, vol. 24, no. 2–3, pp. 123–30.

Cross, J.C., Hemberger, M., Lu, Y., Nozaki, T., Whiteley, K. & Masutani, M. 2002, 'Trophoblast functions, angiogenesis and remodeling of the maternal vasculature in the placenta', *Molecular and Cellular Endocrinology*, vol. 187, no. 1–2, pp. 207–12.

Cross, J.C., Nakano, H., Natale, D.R.C., Simmons, D.G. & Watson, E.D. 2006, 'Branching morphogenesis during development of placental villi', *Differentiation*, vol. 74, no. 7, pp. 393–401.

Cross, J.C., Simmons, D.G. & Watson, E.D. 2003, 'Chorioallantoic morphogenesis and formation of the placental villous tree', *Annals of the New York Academy of Sciences*, vol. 995, pp. 84–93.

Crume, T.L., Scherzinger, A., Stamm, E., McDuffie, R., Bischoff, K.J., Hamman, R.F. & Dabelea, D. 2014, 'The long-term impact of intrauterine growth restriction in a diverse U.S. cohort of children: the EPOCH study', *Obesity*, vol. 22, no. 2, 2013/09/17., pp. 608–15.

Cui, X.-B., Guo, X. & Chen, S.-Y. 2013, 'Response gene to complement 32 deficiency causes impaired placental angiogenesis in mice', *Cardiovascular Research*, vol. 99, no. 4, pp. 632–9.

Cullinan, E.B., Abbondanzo, S.J., Anderson, P.S., Pollard, J.W., Lessey, B. a & Stewart, C.L. 1996, 'Leukemia inhibitory factor (LIF) and LIF receptor expression in human endometrium suggests a potential autocrine/paracrine function in regulating embryo implantation.', *Proceedings of the National Academy of Sciences of the United States of America*, vol. 93, no. 7, pp. 3115–20.

Currò, M., Gugliandolo, A., Gangemi, C., Risitano, R., Ientile, R. & Caccamo, D. 2014, 'Toxic effects of mildly elevated homocysteine concentrations in neuronal-like cells',

- Neurochemical Research*, vol. 39, no. 8, pp. 1485–95.
- Cuskelly, G.J., Stacpoole, P.W., Williamson, J., Baumgartner, T.G. & Gregory, J.F. 2001, 'Deficiencies of folate and vitamin B6 exert distinct effects on homocysteine, serine, and methionine kinetics', *American Journal of Physiology-Endocrinology and Metabolism*, vol. 281, no. 6, pp. E1182–90.
- Czeizel, A.E. & Dudas, I. 1992, 'Prevention of the first occurrence of neural-tube defects by periconceptional vitamin supplementation.', *The New England Journal of Medicine*, vol. 327, no. 26, pp. 1832–5.
- Czieselsky, K., Prescott, M., Porteous, R., Campos, P., Clarkson, J., Steyn, F.J., Campbell, R.E. & Herbison, A.E. 2016, 'Pulse and surge profiles of luteinizing hormone secretion in the mouse', *Endocrinology*, vol. 157, no. 12, pp. 4794–802.
- Dai, D., Moulton, B.C. & Ogle, T.F. 2000, 'Regression of the decidualized mesometrium and decidual cell apoptosis are associated with a shift in expression of Bcl2 family members', *Biology of Reproduction*, vol. 63, no. 1, pp. 188–95.
- Daikoku, T., Cha, J., Sun, X., Tranguch, S., Xie, H., Fujita, T., Hirota, Y., Lydon, J., DeMayo, F., Maxson, R. & Dey, S.K. 2011, 'Conditional deletion of Msx homeobox genes in the uterus inhibits blastocyst implantation by altering uterine receptivity', *Developmental Cell*, vol. 21, no. 6, pp. 1014–25.
- Dakouane-Giudicelli, M., Duboucher, C., Fortemps, J., Salama, S., Brule, A., Rozenberg, P. & de Mazancourt, P. 2012, 'Identification and localization of netrin-4 and neogenin in human first trimester and term placenta.', *Placenta*, vol. 33, no. 9, pp. 677–81.
- Das, S.K. 2009, 'Cell cycle regulatory control for uterine stromal cell decidualization in implantation', *Reproduction*, vol. 137, no. 6, pp. 889–99.
- Das, S.K. 2010, 'Regional development of uterine decidualization: Molecular signaling by Hoxa-10', *Molecular Reproduction and Development*, vol. 77, no. 5, pp. 387–96.
- Dasarathy, J., Gruca, L.L., Bennett, C., Parimi, P.S., Duenas, C., Marczewski, S., Fierro, J.L. & Kalhan, S.C. 2010, 'Methionine metabolism in human pregnancy', *The American Journal of Clinical Nutrition*, vol. 91, no. 2, pp. 357–65.
- Davis, C.A., Hitz, B.C., Sloan, C.A., Chan, E.T., Davidson, J.M., Gabdank, I., Hilton, J.A.,

- Jain, K., Baymuradov, U.K., Narayanan, A.K., Onate, K.C., Graham, K., Miyasato, S.R., Dreszer, T.R., Strattan, J.S., Jolanki, O., Tanaka, F.Y. & Cherry, J.M. 2018, 'The Encyclopedia of DNA elements (ENCODE): data portal update', *Nucleic Acids Research*, vol. 46, no. D1, pp. D794–801.
- Davis, C.D. & Uthus, E.O. 2003, 'Dietary folate and selenium affect dimethylhydrazine-induced aberrant crypt formation, global DNA methylation and one-carbon metabolism in rats', *The Journal of Nutrition*, vol. 133, no. 9, pp. 2907–14.
- Deane, J.A., Cousins, F.L. & Gargett, C.E. 2017, 'Endometrial organoids: in vitro models for endometrial research and personalized medicine', *Biology of Reproduction*, vol. 97, no. 6, pp. 781–3.
- Deane, J.A., Ong, Y.R., Cain, J.E., Jayasekara, W.S.N., Tiwari, A., Carlone, D.L., Watkins, D.N., Breault, D.T. & Gargett, C.E. 2016, 'The mouse endometrium contains epithelial, endothelial and leucocyte populations expressing the stem cell marker telomerase reverse transcriptase', *Molecular Human Reproduction*, vol. 22, no. 4, pp. 272–84.
- Deb, K., Reese, J. & Paria, B.C. 2006, 'Methodologies to study implantation in mice', *Methods in Molecular Medicine*, vol. 121, pp. 9–34.
- Delle Piane, L., Lin, W., Liu, X., Donjacour, A., Minasi, P., Revelli, A., Maltepe, E. & Rinaudo, P.F. 2010, 'Effect of the method of conception and embryo transfer procedure on mid-gestation placenta and fetal development in an IVF mouse model.', *Human Reproduction*, vol. 25, no. 8, pp. 2039–46.
- Demicheva, E. & Crispi, F. 2014, 'Long-term follow-up of intrauterine growth restriction: Cardiovascular', *Fetal Diagnosis and Therapy*, vol. 36, pp. 143–53.
- Deng, G., Nguyen, A., Tanaka, H., Matsuzaki, K., Bell, I., Mehta, K.R., Terdiman, J.P., Waldman, F.M., Kakar, S., Gum, J., Crawley, S., Sleisenger, M.H. & Kim, Y.S. 2006, 'Regional hypermethylation and global hypomethylation are associated with altered chromatin conformation and histone acetylation in colorectal cancer', *International Journal of Cancer*, vol. 118, no. 12, pp. 2999–3005.
- Deng, L., Elmore, C.L., Lawrance, A.K., Matthews, R.G. & Rozen, R. 2008, 'Methionine synthase reductase deficiency results in adverse reproductive outcomes and congenital heart defects in mice.', *Molecular Genetics and Metabolism*, vol. 94, no. 3, pp. 336–42.

- Desai, R.A., Gao, L., Raghavan, S., Liu, W.F. & Chen, C.S. 2009, 'Cell polarity triggered by cell-cell adhesion via E-cadherin', *Journal of Cell Science*, vol. 122, no. 7, pp. 905–11.
- Desoye, G., Gauster, M. & Wadsack, C. 2011, 'Placental transport in pregnancy pathologies', *American Journal of Clinical Nutrition*, vol. 94, no. 6, pp. 1896–902.
- Detrait, E.R., George, T.M., Etchevers, H.C., Gilbert, J.R., Vekemans, M. & Speer, M.C. 2005, 'Human neural tube defects: Developmental biology, epidemiology, and genetics', *Neurotoxicology and Teratology*, vol. 27, no. 3, pp. 515–24.
- Devenport, D. 2014, 'The cell biology of planar cell polarity', *Journal of Cell Biology*, vol. 207, no. 2, pp. 171–9.
- Dey, S.K., Lim, H., Das, S.K., Reese, J., Paria, B.C., Daikoku, T. & Wang, H. 2004, 'Molecular cues to implantation', *Endocrine Reviews*, vol. 25, no. 3, pp. 341–73.
- Dharmaraj, N., Gendler, S.J. & Carson, D.D. 2009, 'Expression of human MUC1 during early pregnancy in the human MUC1 transgenic mouse model', *Biology of Reproduction*, vol. 81, no. 6, 2009/08/14., pp. 1182–8.
- Ding, Y.B., He, J.L., Liu, X.Q., Chen, X.M., Long, C.L. & Wang, Y.X. 2012, 'Expression of DNA methyltransferases in the mouse uterus during early pregnancy and susceptibility to dietary folate deficiency', *Reproduction*, vol. 144, no. 1, pp. 91–100.
- Dobin, A., Davis, C.A., Schlesinger, F., Drenkow, J., Zaleski, C., Jha, S., Batut, P., Chaisson, M. & Gingeras, T.R. 2013, 'STAR: ultrafast universal RNA-seq aligner', *Bioinformatics*, vol. 29, no. 1, pp. 15–21.
- Dobin, A. & Gingeras, T.R. 2015, 'Mapping RNA-seq Reads with STAR', *Current Protocols in Bioinformatics*, vol. 3, no. 51, pp. 1–19.
- Douglas, N.C., Zimmermann, R.C., Tan, Q.K., Sullivan-Pyke, C.S., Sauer, M. V., Kitajewski, J.K. & Shawber, C.J. 2014, 'VEGFR-1 blockade disrupts peri-implantation decidual angiogenesis and macrophage recruitment', *Vascular Cell*, vol. 6, no. 1, pp. 1–11.
- Dugoff, L., Lynch, A.M., Cioffi-Ragan, D., Hobbins, J.C., Schultz, L.K., Malone, F.D. & D'Alton, M.E. 2005, 'First trimester uterine artery Doppler abnormalities predict subsequent intrauterine growth restriction', *American Journal of Obstetrics and*

Gynecology, vol. 193, no. 3 Pt 2, pp. 1208–12.

- Dunham, I., Kundaje, A., Aldred, S., Collins, P., Davis, C., Doyle, F., Epstein, C., Frietze, S., Harrow, J., Kaul, R., Khatun, J., Lajoie, B., Landt, S., Lee, B., Pauli, F., Rosenbloom, K., Sabo, P., Safi, A., Sanyal, A., Shores, N., Simon, J., Song, L., Trinklein, N., Altshuler, R. & Birne, B.E. 2012, 'An integrated encyclopedia of DNA elements in the human genome', *Nature*, vol. 489, no. 7414, pp. 57–74.
- Dunlap, K.A., Filant, J., Hayashi, K., Rucker, E.B. 3rd, Song, G., Deng, J.M., Behringer, R.R., DeMayo, F.J., Lydon, J., Jeong, J.-W. & Spencer, T.E. 2011, 'Postnatal deletion of *Wnt7a* inhibits uterine gland morphogenesis and compromises adult fertility in mice.', *Biology of Reproduction*, vol. 85, no. 2, pp. 386–96.
- Dupressoir, A., Vernochet, C., Harper, F., Guegan, J., Dessen, P., Pierron, G. & Heidmann, T. 2011, 'A pair of co-opted retroviral envelope syncytin genes is required for formation of the two-layered murine placental syncytiotrophoblast', *Proceedings of the National Academy of Sciences of the United States of America*, vol. 108, no. 46, pp. E1164-73.
- Duthie, S.J. & Hawdon, A. 1998, 'DNA instability (strand breakage, uracil misincorporation, and defective repair) is increased by folic acid depletion in human lymphocytes in vitro', *FASEB Journal*, vol. 12, no. 14, pp. 1491–7.
- Ebisch, I.M.W., Peters, W.H.M., Thomas, C.M.G., Wetzels, A.M.M., Peer, P.G.M. & Steegers-Theunissen, R.P.M. 2006, 'Homocysteine, glutathione and related thiols affect fertility parameters in the (sub)fertile couple', *Human Reproduction*, vol. 21, no. 7, pp. 1725–33.
- Elkin, A.C. & Higham, J. 2000, 'Folic acid supplements are more effective than increased dietary folate intake in elevating serum folate levels.', *BJOG*, vol. 107, no. 2, pp. 285–9.
- Elmore, C.L., Wu, X., Leclerc, D., Watson, E.D., Bottiglieri, T., Krupenko, N.I., Krupenko, S.A., Cross, J.C., Rozen, R., Gravel, R.A. & Matthews, R.G. 2007, 'Metabolic derangement of methionine and folate metabolism in mice deficient in methionine synthase reductase.', *Molecular Genetics and Metabolism*, vol. 91, no. 1, pp. 85–97.
- van den Elzen, H.J., Cohen-Overbeek, T.E., Grobbee, D.E., Quartero, R.W. & Wladimiroff, J.W. 1995, 'Early uterine artery Doppler velocimetry and the outcome of pregnancy in women aged 35 years and older', *Ultrasound in Obstetrics & Gynecology*, vol. 5, no. 5,

pp. 328–33.

Emes, R.D., Goodstadt, L., Winter, E.E. & Ponting, C.P. 2003, ‘Comparison of the genomes of human and mouse lays the foundation of genome zoology’, *Human Molecular Genetics*, vol. 12, no. 7, pp. 701–9.

ESHRE 2018, *ART fact sheet*.

Estève, P., Chin, H.G., Smallwood, A., Feehery, G.R., Gangisetty, O., Karpf, A.R., Carey, M.F. & Pradhan, S. 2006, ‘Direct interaction between DNMT1 and G9a coordinates DNA and histone methylation during replication’, *Genes and Development*, vol. 20, pp. 3089–103.

Ewels, P., Lundin, S. & Max, K. 2016, ‘MultiQC: summarize analysis results for multiple tools and samples in a single report’, *Bioinformatics*, vol. 32, no. 19, pp. 3047–8.

Fang, M., Li, Y., Huang, K., Qi, S., Zhang, J., Zgodzinski, W., Majewski, M., Wallner, G., Gozdz, S., Macek, P., Kowalik, A., Pasiarski, M., Grywalska, E., Vatan, L., Nagarsheth, N., Li, W., Zhao, L., Kryczek, I., Wang, G., Wang, Z., Zou, W. & Wang, L. 2017, ‘IL33 Promotes Colon Cancer Cell Stemness via JNK Activation and Macrophage Recruitment’, *Cancer Research*, vol. 77, no. 10, pp. 2735–46.

Fang, X., Zhao, Z., Yu, H., Li, G., Jiang, P., Yang, Y., Yang, R. & Yu, X. 2017, ‘Comparative genome-wide methylation analysis of longissimus dorsi muscles between Japanese black (Wagyu) and Chinese Red Steppes cattle’, *PLoS One*, vol. 12, no. 8, pp. 1–20.

Fauque, P. 2010, ‘In Vitro Fertilization and Embryo Culture Strongly Impact the Placental Transcriptome in the Mouse Model’, *PLoS One*, vol. 5, no. 2, p. e9218.

Favaro, R., Abrahamsohn, P.A. & Zorn, M.T. 2014, ‘Chapter 11 - Decidualization and Endometrial Extracellular Matrix Remodeling’, in B.A. Croy, A.T. Yamada, F.J. DeMayo & S.L.B.T.-T.G. to I. of M.P. Adamson (eds), *The Guide to Investigation of Mouse Pregnancy Investigation of mouse pregnancy*, Academic Press, Boston, pp. 125–42.

Fiedler, M., Sanchez-Barrena, M.J., Nekrasov, M., Mieszczanek, J., Rybin, V., Muller, J., Evans, P. & Bienz, M. 2008, ‘Decoding of methylated histone H3 tail by the Pygo-

- BCL9 Wnt signaling complex.’, *Molecular Cell*, vol. 30, no. 4, pp. 507–18.
- Figueras, F. & Gardosi, J. 2011, ‘Intrauterine growth restriction: New concepts in antenatal surveillance, diagnosis, and management’, *American Journal of Obstetrics and Gynecology*, vol. 204, no. 4, pp. 288–300.
- Filant, J. & Spencer, T.E. 2013, ‘Endometrial glands are essential for blastocyst implantation and decidualization in the mouse uterus’, *Biology of Reproduction*, vol. 88, no. 4, p. 93.
- Filant, J. & Spencer, T.E. 2014, ‘Uterine glands: biological roles in conceptus implantation, uterine receptivity and decidualization’, *The International Journal of Developmental Biology*, vol. 58, no. 2–4, pp. 107–16.
- Finetti, F., Solito, R., Morbidelli, L., Giachetti, A., Ziche, M. & Donnini, S. 2008, ‘Prostaglandin E2 regulates angiogenesis via activation of fibroblast growth factor receptor-1’, *The Journal of Biological Chemistry*, vol. 283, no. 4, pp. 2139–46.
- Finn, C.A. 1968, ‘Increase in length of the uterus at the time of implantation in the mouse’, *Reproduction*, vol. 17, no. 1, pp. 69–74.
- Fortier, A.L., Lopes, F.L., Darricarre, N. & Trasler, J.M. 2008, ‘Superovulation alters the expression of imprinted genes in the midgestation mouse placenta’, *Human Molecular Genetics*, vol. 17, no. 11, pp. 1653–65.
- Fotopoulou, S., Oikonomou, N., Grigorieva, E., Nikitopoulou, I., Thanassopoulou, A., Zhao, Z., Xu, Y., Kontoyiannis, D.L., Remboutsika, E. & Aidinis, V. 2010, ‘ATX expression and LPA signalling are vital for the development of the nervous system’, *Developmental Biology*, vol. 339, no. 2, pp. 451–64.
- Fowden, A.L. 1995, ‘Endocrine Regulation of Fetal Growth’, *Reproduction Fertility and Development*, vol. 7, no. 3, pp. 351–63.
- Fowden, A.L., Coan, P.M., Angiolini, E., Burton, G.J. & Constancia, M. 2011, ‘Imprinted genes and the epigenetic regulation of placental phenotype’, *Progress in Biophysics and Molecular Biology*, vol. 106, no. 1, pp. 281–8.
- Fowden, A.L., Giussani, D.A. & Forhead, A.J. 2006, ‘Intrauterine programming of physiological systems: causes and consequences’, *Physiology*, vol. 21, pp. 29–37.
- Fowden, A.L., Sibley, C., Reik, W. & Constancia, M. 2006, ‘Imprinted genes, placental

- development and fetal growth', *Hormone Research*, vol. 65 Suppl 3, pp. 50–8.
- Fowden, A.L., Ward, J.W., Wooding, F.P.B., Forhead, A.J. & Constancia, M. 2006, 'Programming placental nutrient transport capacity', *Journal of Physiology*, vol. 572, no. 1, pp. 5–15.
- Fox, N.S., Rebarber, A., Klauser, C.K., Roman, A.S. & Saltzman, D.H. 2011, 'Intrauterine growth restriction in twin pregnancies: Incidence and associated risk factors', *American Journal of Perinatology*, vol. 28, no. 4, pp. 267–72.
- Frank, D., Fortino, W., Clark, L., Musalo, R., Wang, W., Saxena, A., Li, C.-M., Reik, W., Ludwig, T. & Tycko, B. 2002, 'Placental overgrowth in mice lacking the imprinted gene *Ipl*', *Proceedings of the National Academy of Sciences*, vol. 99, no. 11, p. 7490 LP-7495.
- Fraser, R., Whitley, G.S.J., Thilaganathan, B. & Cartwright, J.E. 2015, 'Decidual natural killer cells regulate vessel stability: Implications for impaired spiral artery remodelling', *Journal of Reproductive Immunology*, vol. 110, pp. 54–60.
- Fu, B., Wang, H., Wang, J., Barouhas, I., Liu, W., Shuboy, A., Bushinsky, D.A., Zhou, D. & Favus, M.J. 2013, 'Epigenetic regulation of BMP2 by 1,25-dihydroxyvitamin D3 through DNA methylation and histone modification', *PLoS One*, vol. 8, no. 4, pp. 1–10.
- Fuhrmann, A. & Engler, A.J. 2015, 'The cytoskeleton regulates cell attachment strength', *Biophysical Journal*, vol. 109, no. 1, pp. 57–65.
- Fung, J.N., Mortlock, S., Girling, J.E., Holdsworth-Carson, S.J., Teh, W.T., Zhu, Z., Lukowski, S.W., McKinnon, B.D., McRae, A., Yang, J., Healey, M., Powell, J.E., Rogers, P.A.W. & Montgomery, G.W. 2018, 'Genetic regulation of disease risk and endometrial gene expression highlights potential target genes for endometriosis and polycystic ovarian syndrome', *Scientific Reports*, vol. 8, no. 1, p. 11424.
- Furey, T.S. 2012, 'ChIP-seq and beyond: New and improved methodologies to detect and characterize protein-DNA interactions', *Nature Reviews Genetics*, vol. 13, no. 12, pp. 840–52.
- Furness, D.L.F., Fenech, M.F., Khong, Y.T., Romero, R. & Dekker, G.A. 2008, 'One-carbon metabolism enzyme polymorphisms and uteroplacental insufficiency', *American Journal of Obstetrics and Gynecology*, vol. 199, no. 3, p. 276.e1-8.

- Gabory, A., Attig, L. & Junien, C. 2011, 'Developmental programming and epigenetics', *American Journal of Clinical Nutrition*, vol. 94, pp. 1943–52.
- Gabory, A., Roseboom, T.J., Moore, T., Moore, L.G. & Junien, C. 2013, 'Placental contribution to the origins of sexual dimorphism in health and diseases: sex chromosomes and epigenetics', *Biology of Sex Differences*, vol. 4, no. 5.
- Gallou-Kabani, C., Gabory, A., Tost, J., Karimi, M., Mayeur, S., Lesage, J., Boudadi, E., Gross, M.-S., Taurelle, J., Vige, A., Breton, C., Reusens, B., Remacle, C., Vieau, D., Ekstrom, T.J., Jais, J.-P. & Junien, C. 2010, 'Sex- and diet-specific changes of imprinted gene expression and DNA methylation in mouse placenta under a high-fat diet.', *PLoS One*, vol. 5, no. 12, p. e14398.
- Gao, F., Bian, F., Ma, X., Kalinichenko, V. V. & Das, S.K. 2015, 'Control of regional decidualization in implantation: Role of FoxM1 downstream of Hoxa10 and cyclin D3', *Scientific Reports*, vol. 5, no. 13863, pp. 1–16.
- Gao, F., Ma, X., Rusie, A., Hemingway, J., Ostmann, A.B., Chung, D. & Das, S.K. 2012, 'Epigenetic changes through DNA methylation contribute to uterine stromal cell decidualization', *Endocrinology*, vol. 153, no. 12, pp. 6078–90.
- Gao, R., Ding, Y., Liu, X., Chen, X., Wang, Y., Long, C., Li, S., Guo, L. & He, J. 2012a, 'Effect of folate deficiency on promoter methylation and gene expression of Esr1, Cdh1 and Pgr, and its influence on endometrial receptivity and embryo implantation', *Human Reproduction*, vol. 27, no. 9, pp. 2756–65.
- Gao, R., Ding, Y., Liu, X., Chen, X., Wang, Y., Long, C., Li, S., Guo, L. & He, J. 2012b, 'Effect of folate deficiency on promoter methylation and gene expression of Esr1, Cdh1 and Pgr, and its influence on endometrial receptivity and embryo implantation', *Human Reproduction*, vol. 27, no. 9, pp. 2756–65.
- Gao, Y., Bayless, K.J. & Li, Q. 2014, 'TGFB1 Is Required for Mouse Myometrial Development', *Molecular Endocrinology*, vol. 28, no. 3, pp. 380–94.
- Gao, Y., Duran, S., Lydon, J.P., DeMayo, F.J., Burghardt, R.C., Bayless, K.J., Bartholin, L. & Li, Q. 2015, 'Constitutive activation of transforming growth factor Beta receptor 1 in the mouse uterus impairs uterine morphology and function', *Biology of reproduction*, vol. 92, no. 2, p. 34.

- Gao, Y., Li, S. & Li, Q. 2014, 'Uterine epithelial cell proliferation and endometrial hyperplasia: Evidence from a mouse model', *Molecular Human Reproduction*, vol. 20, no. 8, pp. 776–86.
- Garcia, B.A., Luka, Z., Loukachevitch, L. V, Bhanu, N. V & Wagner, C. 2016, 'Folate deficiency affects histone methylation', *Medical Hypotheses*, vol. 88, pp. 63–7.
- Garcia, E., Bouchard, P., De Brux, J., Berdah, J., Frydman, R., Schaison, G., Milgrom, E. & Perrot-Appianat, M. 1988, 'Use of immunocytochemistry of progesterone and estrogen receptors for endometrial dating', *The Journal of Clinical Endocrinology and Metabolism*, vol. 67, no. 1, pp. 80–7.
- Gardosi, J., Chang, A., Kalyan, B., Sahota, D. & Symonds, E.M. 1992, 'Customised antenatal growth charts', *The Lancet*, vol. 339, no. 8788, pp. 283–7.
- Gardosi, J., Madurasinghe, V., Williams, M. & Malik, A. 2013, 'Maternal and fetal risk factors for stillbirth: population based study', *BMJ (Clinical research ed.)*, vol. 346, p. f108.
- Gaskins, A.J., Mumford, S.L., Chavarro, J.E., Zhang, C., Pollack, A.Z., Wactawski-Wende, J., Perkins, N.J. & Schisterman, E.F. 2012, 'The Impact of Dietary Folate Intake on Reproductive Function in Premenopausal Women: A Prospective Cohort Study', *PLoS One*, vol. 7, no. 9, pp. 1–8.
- Gaynor, L.M. & Colucci, F. 2017, 'Uterine natural killer cells: Functional distinctions and influence on pregnancy in humans and mice', *Frontiers in Immunology*, vol. 8, no. 467.
- Gellersen, B. & Brosens, J.J. 2014, 'Cyclic decidualization of the human endometrium in reproductive health and failure', *Endocrine Reviews*, vol. 35, no. 6, pp. 851–905.
- Geng, Y., Gao, R., Chen, X., Liu, X., Liao, X., Li, Y., Liu, S., Ding, Y., Wang, Y. & He, J. 2015, 'Folate deficiency impairs decidualization and alters methylation patterns of the genome in mice', *Molecular Human Reproduction*, vol. 21, no. 11, pp. 844–56.
- George, J.W., Dille, E.A. & Heckert, L.L. 2011, 'Current concepts of follicle-stimulating hormone receptor gene regulation', *Biology of Reproduction*, vol. 84, no. 1, 2010/08/25., pp. 7–17.
- Geva, E., Ginzinger, D.G., Moore, D.H. 2nd, Ursell, P.C. & Jaffe, R.B. 2005, 'In utero

- angiopoietin-2 gene delivery remodels placental blood vessel phenotype: a murine model for studying placental angiogenesis', *Molecular Human Reproduction*, vol. 11, no. 4, pp. 253–60.
- Ghandour, H., Chen, Z., Selhub, J. & Rozen, R. 2004, 'Mice deficient in methylenetetrahydrofolate reductase exhibit tissue-specific distribution of folates.', *The Journal of Nutrition*, vol. 134, no. 11, pp. 2975–8.
- Ghandour, H., Lin, B., Choi, S., Mason, J.B. & Selhub, J. 2002, 'Folate status and age affect the accumulation of L-isoaspartyl residues in rat liver proteins', *The Journal of Nutrition*, vol. 132, no. 6, pp. 1357–60.
- Gicquel, C., El-Osta, A. & Le Bouc, Y. 2008, 'Epigenetic regulation and fetal programming', *Best Practice & Research Clinical Endocrinology & Metabolism*, vol. 22, no. 1, pp. 1–16.
- Gillich, A., Bao, S., Grabole, N., Hayashi, K., Trotter, M.W.B., Pasque, V., Magnúsdóttir, E. & Surani, M.A. 2012, 'Epiblast stem cell-based system reveals reprogramming synergy of germline factors', *Cell Stem Cell*, vol. 10, no. 4, pp. 425–39.
- Godfrey, K.M., Sheppard, A., Gluckman, P.D., Lillycrop, K.A., Burdge, G.C., McLean, C., Rodford, J., Slater-Jefferies, J.L., Garratt, E., Crozier, S.R., Emerald, B.S., Gale, C.R., Inskip, H.M., Cooper, C. & Hanson, M.A. 2011, 'Epigenetic gene promoter methylation at birth is associated with child's later adiposity.', *Diabetes*, vol. 60, no. 5, pp. 1528–34.
- Goll, M.G., Kirpekar, F., Maggert, K.A., Yoder, J.A., Hsieh, C.-L., Zhang, X., Golic, K.G., Jacobsen, S.E. & Bestor, T.H. 2006, 'Methylation of tRNA^{Asp} by the DNA methyltransferase homolog Dnmt2.', *Science*, vol. 311, no. 5759, pp. 395–8.
- Gonzales, G.F., Steenland, K. & Tapia, V. 2009, 'Maternal hemoglobin level and fetal outcome at low and high altitudes', *American Journal of Physiology*, vol. 297, no. 5, pp. R1477-85.
- Gonzalez, G. 2016, 'Determining the stage of the estrous cycle in female mice by vaginal smear', *Cold Spring Harbor Protocols*, vol. 2016, no. 8, pp. 732–4.
- Gourvas, V., Dalpa, E., Vrachnis, N., Sifakis, S. & Genimatas, G.H.G. 2012, 'Placental angiogenesis and fetal growth restriction', in Dr. Stavros Sifakis (ed.), *From*

preconception to postpartum, InTech, pp. 179–87.

- Goyal, R., Yellon, S.M., Longo, L.D. & Mata-greenwood, E. 2010, 'Placental gene expression in a rat " model " of placental insufficiency', *Placenta*, vol. 31, no. 7, pp. 568–75.
- Goyeneche, A.A., Deis, R.P., Gibori, G. & Telleria, C.M. 2003, 'Progesterone promotes survival of the rat corpus luteum in the absence of cognate receptors', *Biology of Reproduction*, vol. 68, no. 1, pp. 151–8.
- Gradilla, A.C., Sanchez-Hernandez, D., Brunt, L. & Scholpp, S. 2018, 'From top to bottom: Cell polarity in Hedgehog and Wnt trafficking', *BMC Biology*, vol. 16, no. 1, pp. 1–11.
- Graham, I.M., Daly, L.E., Refsum, H.M., Robinson, K., Brattstrom, L.E., Ueland, P.M., Palma-Reis, R.J., Boers, G.H., Sheahan, R.G., Israelsson, B., Uiterwaal, C.S., Meleady, R., McMaster, D., Verhoef, P., Witteman, J., Rubba, P., Bellet, H., Wautrecht, J.C., de Valk, H.W., Sales Luis, A.C., Parrot-Rouland, F.M., Tan, K.S., Higgins, I., Garcon, D. & Andria, G. 1997, 'Plasma homocysteine as a risk factor for vascular disease', *JAMA*, vol. 277, no. 22, pp. 1775–81.
- Granger, J.P., Alexander, B.T., Llinas, M.T., Bennett, W.A. & Khalil, R.A. 2002, 'Pathophysiology of preeclampsia: linking placental ischemia/hypoxia with microvascular dysfunction', *Microcirculation*, vol. 9, no. 3, pp. 147–60.
- Grazul-Bilska, A.T., Johnson, M.L., Borowicz, P.P., Bilski, J.J., Cymbaluk, T., Norberg, S., Redmer, D.A. & Reynolds, L.P. 2014, 'Placental development during early pregnancy in sheep: effects of embryo origin on vascularization', *Reproduction*, vol. 147, no. 5, pp. 639–48.
- Green, E.L. 1966, *Biology of the laboratory mouse*, Blakiston Division, McGraw-Hill, New York.
- Greenwald, G.S. & Rothchild, I. 1968, 'Formation and maintenance of corpora lutea in laboratory animals', *Journal of Animal Science*, vol. 27 Suppl 1, pp. 139–62.
- Grivell, R., Dodd, J. & Robinson, J. 2009, 'The prevention and treatment of intrauterine growth restriction', *Best Practice & Research Clinical Obstetrics & Gynaecology*, vol. 23, no. 6, pp. 795–807.

- Gu, Y., Jow, G.M., Moulton, B.C., Lee, C., Sensibar, J.A., Park-Sarge, O.K., Chen, T.J. & Gibori, G. 1994, 'Apoptosis in decidual tissue regression and reorganization', *Endocrinology*, vol. 135, no. 3, pp. 1272–9.
- Gude, N.M., Roberts, C.T., Kalionis, B. & King, R.G. 2004, 'Growth and function of the normal human placenta', *Thrombosis Research*, vol. 114, no. 5–6, pp. 397–407.
- Guller, S., Buhimschi, C.S., Ma, Y.Y., Huang, S.T.J., Yang, L., Kuczynski, E., Zambrano, E., Lockwood, C.J. & Buhimschi, I.A. 2008, 'Placental expression of ceruloplasmin in pregnancies complicated by severe preeclampsia.', *Laboratory Investigation*, vol. 88, no. 10, pp. 1057–67.
- Guo, X.-Y., Liu, X.-M., Jin, L., Wang, T.-T., Ullah, K., Sheng, J.-Z. & Huang, H.-F. 2017, 'Cardiovascular and metabolic profiles of offspring conceived by assisted reproductive technologies: a systematic review and meta-analysis', *Fertility and Sterility*, vol. 107, no. 3, p. 622–631.e5.
- Ha, C.T., Waterhouse, R., Warren, J., Zimmermann, W. & Dveksler, G.S. 2008, 'N-glycosylation is required for binding of murine pregnancy-specific glycoproteins 17 and 19 to the receptor CD9', *American Journal of Reproductive Immunology*, vol. 59, no. 3, pp. 251–8.
- Haavaldsen, C., Tanbo, T. & Eskild, A. 2012, 'Placental weight in singleton pregnancies with and without assisted reproductive technology: a population study of 536,567 pregnancies', *Human Reproduction*, vol. 27, no. 2, pp. 576–82.
- Hackett, J.A., Reddington, J.P., Nestor, C.E., Dunican, D.S., Branco, M.R., Reichmann, J., Reik, W., Surani, M.A., Adams, I.R. & Meehan, R.R. 2012, 'Promoter DNA methylation couples genome-defence mechanisms to epigenetic reprogramming in the mouse germline', *Development*, vol. 139, no. 19, pp. 3623–32.
- Haeussler, M., Zweig, A.S., Tyner, C., Speir, M.L., Rosenbloom, R., Raney, B.J., Lee, C.M., Lee, B.T., Hinrichs, A.S., Gonzalez, J.N., Gibson, D., Diekhans, M., Clawson, H., Casper, J., Barber, G.P., Haussler, D., Kuhn, R.M., Kent, W.J., Uscs, T. & Browser, G. 2019, 'The UCSC Genome Browser database: 2019 update', *Nucleic Acids Research*, vol. 47, no. D1, pp. D853–D858.
- Haider, B.A. & Bhutta, Z.A. 2017, 'Multiple-micronutrient supplementation for women

- during pregnancy’, *Cochrane Database of Systematic Reviews*, John Wiley & Sons, Ltd.
- Hajkova, P. 2011, ‘Epigenetic reprogramming in the germline: towards the ground state of the epigenome.’, *Philosophical Transactions of the Royal Society of London*, vol. 366, no. 1575, pp. 2266–73.
- Hales, C.N. & Barker, D.J.P. 2001, ‘The thrifty phenotype hypothesis: Type 2 diabetes’, *British Medical Bulletin*, vol. 60, no. 1, pp. 5–20.
- Hales, C.N. & Barker, D.J.P. 2013, ‘Type 2 (non-insulin-dependent) diabetes mellitus: the thrifty phenotype hypothesis’, *International Journal of Epidemiology*, vol. 42, no. 5, pp. 1215–22.
- Hamalainen, H., Hakkarainen, K. & Heinonen, S. 2003, ‘Anaemia in the first but not in the second or third trimester is a risk factor for low birth weight’, *Clinical Nutrition*, vol. 22, no. 3, pp. 271–5.
- Han, X., Wang, R., Zhou, Y., Fei, L., Sun, H., Lai, S., Saadatpour, A., Zhou, Z., Chen, H., Ye, F., Huang, D., Xu, Y., Huang, W., Jiang, M., Jiang, X., Mao, J., Chen, Y., Lu, C., Xie, J., Fang, Q., Wang, Y., Yue, R., Li, T., Huang, H., Orkin, S.H., Yuan, G.-C., Chen, M. & Guo, G. 2018, ‘Mapping the Mouse Cell Atlas by Microwell-Seq’, *Cell*, vol. 173, no. 5, p. 1307.
- Hanna, C.W., Demond, H. & Kelsey, G. 2018, ‘Epigenetic regulation in development: is the mouse a good model for the human?’, *Human Reproduction Update*, vol. 24, no. 5, pp. 556–76.
- Hanson, M. a & Gluckman, P.D. 2014, ‘Early developmental conditioning of later health and disease: physiology or pathophysiology?’, *Physiological Reviews*, vol. 94, no. 4, pp. 1027–76.
- Harding, J.E. & Johnston, B.M. 1995, ‘Nutrition and fetal growth.’, *Reproduction, Fertility and Development*, vol. 7, no. 3, pp. 539–47.
- Harman, R.M., Cowan, R.G., Ren, Y. & Quirk, S.M. 2011, ‘Reduced signaling through the hedgehog pathway in the uterine stroma causes deferred implantation and embryonic loss.’, *Reproduction*, vol. 141, no. 5, pp. 665–74.
- Harmon, R.M., Desai, B. V & Green, K.J. 2009, ‘Regulatory roles of the cadherin

- superfamily', *Biology Reports*, vol. 1, no. 13.
- Harrington, K., Goldfrad, C., Carpenter, R.G. & Campbell, S. 1997, 'Transvaginal uterine and umbilical artery Doppler examination of 12-16 weeks and the subsequent development of pre-eclampsia and intrauterine growth retardation', *Ultrasound in Obstetrics & Gynecology*, vol. 9, no. 2, pp. 94–100.
- Hart, D.J., Finglas, P.M., Wolfe, C. a, Mellon, F., Wright, A.J. a & Southon, S. 2002, 'Determination of 5-methyltetrahydrofolate (13C-labeled and unlabeled) in human plasma and urine by combined liquid chromatography mass spectrometry.', *Analytical Biochemistry*, vol. 305, no. 2, pp. 206–13.
- Hart, M.L., Rusch, E., Kaupp, M., Nieselt, K. & Aicher, W.K. 2017, 'Expression of Desmoglein 2, Desmocollin 3 and Plakophilin 2 in placenta and bone marrow-derived mesenchymal stromal cells', *Stem Cell Reviews*, vol. 13, no. 2, pp. 258–66.
- Hartkopf, J., Schleger, F., Keune, J., Wiechers, C., Pauluschke-froehlich, J., Weiss, M., Conzelmann, A., Brucker, S., Preissl, H., Kiefer-schmidt, I., Miller, S.L. & Welsh, M. 2018, 'Impact of intrauterine growth restriction on cognitive and motor development at 2 years of age', *Frontiers in Physiology*, vol. 9, no. September, p. 1278.
- Harvey, N.C., Sheppard, A., Godfrey, K.M., McLean, C., Garratt, E., Ntani, G., Davies, L., Murray, R., Inskip, H.M., Gluckman, P.D., Hanson, M.A., Lillycrop, K.A. & Cooper, C. 2014, 'Childhood bone mineral content is associated with methylation status of the RXRA promoter at birth.', *Journal of Bone and Mineral Research*, vol. 29, no. 3, pp. 600–7.
- Hasan, M.Z., Ikawati, M., Tocharus, J., Kawaichi, M. & Oka, C. 2015, 'Abnormal development of placenta in HtrA1-deficient mice', *Developmental Biology*, vol. 397, no. 1, pp. 89–102.
- Hashimoto, T., Koizumi, M., Doshida, M., Toya, M., Sagara, E., Oka, N., Nakajo, Y., Aono, N., Igarashi, H. & Kyono, K. 2017, 'Efficacy of the endometrial receptivity array for repeated implantation failure in Japan: A retrospective, two-centers study', *Reproductive Medicine and Biology*, vol. 16, no. 3, pp. 290–6.
- Hata, K., Okano, M., Lei, H. & Li, E. 2002, 'Dnmt3L cooperates with the Dnmt3 family of de novo DNA methyltransferases to establish maternal imprints in mice', *Development*,

vol. 129, pp. 1983–93.

- Haugaard, C.T. & Bauer, M.K. 2001, 'Rodent models of intrauterine growth restriction', *Scandinavian Journal of Laboratory Animal Science*, vol. 28, no. 1, pp. 10–22.
- Hawkins, S.M. & Matzuk, M.M. 2008, 'The menstrual cycle: basic biology', *Annals of the New York Academy of Sciences*, vol. 1135, pp. 10–8.
- Hay, W.W. 2006, 'Placental-fetal glucose exchange and fetal glucose metabolism', *Transactions of the American Clinical and Climatological Association*, vol. 117, pp. 321–40.
- Hayakawa, K., Nakanishi, M.O., Ohgane, J., Tanaka, S., Hirosawa, M., Soares, M.J., Yagi, S. & Shiota, K. 2012, 'Bridging sequence diversity and tissue-specific expression by DNA methylation in genes of the mouse prolactin superfamily.', *Mammalian Genome*, vol. 23, no. 5–6, pp. 336–45.
- Heazell, A.E.P., Sharp, A.N., Baker, P.N. & Crocker, I.P. 2011, 'Intra-uterine growth restriction is associated with increased apoptosis and altered expression of proteins in the p53 pathway in villous trophoblast', *Apoptosis*, vol. 16, no. 2, pp. 135–44.
- Heberle, H., Meirelles, V.G., da Silva, F.R., Telles, G.P. & Minghim, R. 2015, 'InteractiVenn: A web-based tool for the analysis of sets through Venn diagrams', *BMC Bioinformatics*, vol. 16, no. 1, pp. 1–7.
- Helena, C. V, McKee, D.T., Bertram, R., Walker, A.M. & Freeman, M.E. 2009, 'The rhythmic secretion of mating-induced prolactin secretion is controlled by prolactin acting centrally', *Endocrinology*, vol. 150, no. 7, pp. 3245–51.
- Herbison, A.E. 2008, 'Estrogen positive feedback to gonadotropin-releasing hormone (GnRH) neurons in the rodent: the case for the rostral periventricular area of the third ventricle (RP3V)', *Brain Research Reviews*, vol. 57, no. 2, pp. 277–87.
- Heyn, H., Vidal, E., Ferreira, H.J., Vizoso, M., Sayols, S., Gomez, A., Moran, S., Boque-sastre, R., Guil, S., Martinez-cardus, A., Lin, C.Y., Royo, R., Sanchez-mut, J. V, Martinez, R., Gut, M., Torrents, D., Orozco, M. & Gut, I. 2016, 'Epigenomic analysis detects aberrant super-enhancer DNA methylation in human cancer', *Genome Biology*, vol. 17, no. 11.

- Hoffbrand, A.V. 2001, 'Historical Review', *British Journal of Haematology*, vol. 113, pp. 579–89.
- Hogg, B.B., Tamura, T., Johnston, K.E., Dubard, M.B. & Goldenberg, R.L. 2000, 'Second-trimester plasma homocysteine levels and pregnancy-induced hypertension, preeclampsia, and intrauterine growth restriction.', *American Journal of Obstetrics and Gynecology*, vol. 183, no. 4, pp. 805–9.
- Hollick, J.B. 2016, 'Paramutation and related phenomena in diverse species', *Nature Reviews Genetics*, vol. 18, no. 1, pp. 5–23.
- Horne, A.W., White, J.O., Margara, R.A., Williams, R., Winston, R.M. & Lalani, E. 2001, 'MUC 1: a genetic susceptibility to infertility?', *Lancet*, vol. 357, no. 9265, pp. 1336–7.
- Howell, C.Y., Bestor, T.H., Ding, F., Latham, K.E., Mertineit, C., Trasler, J.M. & Chaillet, J.R. 2001, 'Genomic Imprinting Disrupted by a Maternal Effect Mutation in the Dnmt1 Gene', *Cell*, vol. 104, pp. 829–38.
- Hu, D. & Cross, J.C. 2011, 'Ablation of Tpbpa -positive trophoblast precursors leads to defects in maternal spiral artery remodeling in the mouse placenta', *Developmental Biology*, vol. 358, no. 1, pp. 231–9.
- Hu, H., Chen, X., Wang, C., Jiang, Y., Li, J., Ying, X., Yang, Y., Li, B., Zhou, C., Zhong, J., Wu, D., Ying, J. & Duan, S. 2017, 'The role of TFPI2 hypermethylation in the detection of gastric and colorectal cancer', *Oncotarget*, vol. 8, no. 48, pp. 84054–65.
- Huang, D.W., Lempicki, R. a & Sherman, B.T. 2009, 'Systematic and integrative analysis of large gene lists using DAVID bioinformatics resources.', *Nature Protocols*, vol. 4, no. 1, pp. 44–57.
- Huang, D.W., Sherman, B.T. & Lempicki, R.A. 2009, 'Bioinformatics enrichment tools: Paths toward the comprehensive functional analysis of large gene lists', *Nucleic Acids Research*, vol. 37, no. 1, pp. 1–13.
- Huang, X., Anderle, P., Hostettler, L., Baumann, M.U., Surbek, D. V, Ontsouka, E.C. & Albrecht, C. 2018, 'Identification of placental nutrient transporters associated with intrauterine growth restriction and pre-eclampsia', *BMC Genomics*, vol. 19, no. 173.
- Huang, Z.F., Higuchi, D., Lasky, N. & Broze, G.J.J. 1997, 'Tissue factor pathway inhibitor

- gene disruption produces intrauterine lethality in mice.’, *Blood*, vol. 90, no. 3, pp. 944–51.
- Huet-Hudson, Y.M. & Dey, S.K. 1990, ‘Requirement for progesterone priming and its long-term effects on implantation in the mouse’, *Proceedings of the Society for Experimental Biology and Medicine*, vol. 193, no. 4, pp. 259–63.
- Huffman, S.R., Pak, Y. & Rivera, R.M. 2015, ‘Superovulation induces alterations in the epigenome of zygotes, and results in differences in gene expression at the blastocyst stage in mice’, *Molecular Reproduction and Development*, vol. 82, no. 3, pp. 207–17.
- Huh, J.-W., Kim, Y.-H., Lee, S.-R., Kim, H., Kim, D.-S., Kim, H.-S., Kang, H.-S. & Chang, K.-T. 2009, ‘Gain of new exons and promoters by lineage-specific transposable elements-integration and conservation event on CHRM3 gene’, *Molecules and Cells*, vol. 28, no. 2, pp. 111–7.
- Hutter, D., Kingdom, J. & Jaeggi, E. 2010, ‘Causes and mechanisms of intrauterine hypoxia and its impact on the fetal cardiovascular system: a review’, *International Journal of Pediatrics*, vol. 2010, 2010/10/19., p. 401323.
- Huyen, D. V. & Bany, B.M. 2011, ‘Evidence for a conserved function of heart and neural crest derivatives expressed transcript 2 in mouse and human decidualization’, *Reproduction*, vol. 142, no. 2, pp. 353–68.
- Hwang, I.Y., Kwak, S., Lee, S., Kim, H., Lee, S.E., Kim, J.H., Kim, Y.A., Jeon, Y.K., Chung, D.H., Jin, X., Park, S., Jang, H., Cho, E.J. & Youn, H.D. 2016, ‘Psat1-Dependent Fluctuations in α -Ketoglutarate Affect the Timing of ESC Differentiation’, *Cell Metabolism*, vol. 24, no. 3, pp. 494–501.
- IoM, I. of M. 1998, *Dietary Reference Intakes for Thiamin, Riboflavin, Niacin, Vitamin B6, Folate, Vitamin B12, Pantothenic Acid, Biotin, and Choline*, National Academy of Sciences, Washington (DC), USA.
- Ishihara, N., Matsuo, H., Murakoshi, H., Laoag-Fernandez, J.B., Samoto, T. & Maruo, T. 2002, ‘Increased apoptosis in the syncytiotrophoblast in human term placentas complicated by either preeclampsia or intrauterine growth retardation’, *American Journal of Obstetrics & Gynecology*, vol. 186, no. 1, pp. 158–66.

- Ito, N., Ruegg, U.T. & Takeda, S. 2018, 'ATP-induced increase in intracellular calcium levels and subsequent activation of mTOR as regulators of skeletal muscle hypertrophy', *International Journal of Molecular Sciences*, vol. 19, no. 9, p. 2804.
- Jackson, M.R., Walsh, A.J., Morrow, R.J., Muller, B.M., Lye, S.J. & Ritchie, J.W.K. 1995, 'Reduced placental villous tree elaboration in small-for-gestational-age pregnancies: Relationship with umbilical artery Doppler waveforms', *American Journal of Obstetrics & Gynecology*, vol. 172, no. 2, pp. 518–25.
- Jacob, R.A., Gretz, D.M., Taylor, P.C., James, S.J., Pogribny, I.P., Miller, B.J., Henning, S.M. & Swendseid, M.E. 1998, 'Moderate folate depletion increases plasma homocysteine and decreases lymphocyte DNA methylation in postmenopausal women', *The Journal of Nutrition*, vol. 128, no. 7, pp. 1204–12.
- James, S.J., Pogribna, M., Pogribny, I.P., Melnyk, S., Hine, R.J., Gibson, J.B., Yi, P., Tafoya, D.L., Swenson, D.H., Wilson, V.L. & Gaylor, D.W. 1999, 'Abnormal folate metabolism and mutation in the methylenetetrahydrofolate reductase gene may be maternal risk factors for Down syndrome', *American Journal of Clinical Nutrition*, vol. 70, pp. 495–501.
- James, S.J., Pogribny, I.P., Pogribna, M., Miller, B.J., Jernigan, S. & Melnyk, S. 2003, 'Mechanisms of DNA damage, DNA hypomethylation, and tumor progression in the folate/methyl-deficient rat model of hepatocarcinogenesis', *The Journal of Nutrition*, vol. 133, no. 11, p. 3740S–3747S.
- Jansson, T., Ekstrand, Y., Bjorn, C., Wennergren, M. & Powell, T.L. 2002, 'Alterations in the activity of placental amino acid transporters in pregnancies complicated by diabetes.', *Diabetes*, vol. 51, no. 7, pp. 2214–9.
- Jansson, T., Scholtbach, V. & Powell, T.L. 1998, 'Placental transport of leucine and lysine is reduced in intrauterine growth restriction', *Pediatric Research*, vol. 44, no. 4, pp. 532–7.
- Jeong, J., Kwak, I., Lee, K.Y., Kim, T.H., Large, M.J., Stewart, C.L., Kaestner, K.H., Lydon, J.P. & Demayo, F.J. 2010, 'Foxa2 is essential for mouse endometrial gland development and fertility', *Biology of Reproduction*, vol. 83, no. 3, pp. 396–403.
- Jha, R.K., Titus, S., Saxena, D., Kumar, P.G. & Laloraya, M. 2006, 'Profiling of E-cadherin, β -catenin and Ca²⁺ in embryo-uterine interactions at implantation', *FEBS Letters*, vol.

580, no. 24, pp. 5653–60.

- Jhaveri, M.S., Wagner, C. & Trepel, J.B. 2001, 'Impact of extracellular folate levels on global gene expression', *Molecular Pharmacology*, vol. 60, no. 6, p. 1288 LP-1295.
- Jia, R.-Z., Ding, G.-C., Gu, C.-M., Huang, T., Rui, C., Wang, Y.-X. & Lu, Q. 2014, 'CDX2 enhances HTR-8/SVneo trophoblast cell invasion by altering the expression of matrix metalloproteinases', *Cellular Physiology and Biochemistry*, vol. 34, no. 3, pp. 628–36.
- Jiang, H.L., Cao, L.Q. & Chen, H.Y. 2016, 'Blood folic acid, vitamin B12, and homocysteine levels in pregnant women with fetal growth restriction', *Genetics and Molecular Research*, vol. 15, no. 4.
- Jiang, J., Zhang, Y., Wei, L., Sun, Z. & Liu, Z. 2014, 'Association between MTHFD1 G1958A polymorphism and neural tube defects susceptibility: A meta-analysis', *PLoS One*, vol. 9, no. 6, p. e101169.
- Jin, X., Liu, X., Li, X. & Guan, Y. 2016, 'Integrated Analysis of DNA Methylation and mRNA Expression Profiles Data to Identify Key Genes in Lung Adenocarcinoma', *BioMed Research International*, vol. 2016.
- Jindal, U.N. & Jindal, S. 2015, 'Ovulation Induction in Hypogonadotropic Hypogonadism', in S. Ghumman (ed.), *Principles and Practice of Controlled Ovarian Stimulation in ART*, Springer India, New Delhi, pp. 357–68.
- Jirtle, R.L. & Skinner, M.K. 2007, 'Environmental epigenomics and disease susceptibility', *Nature Reviews Genetics*, vol. 8, no. 4, pp. 253–62.
- John, R.M. 2013, 'Epigenetic regulation of placental endocrine lineages and complications of pregnancy', *Biochemical Society Transactions*, vol. 41, no. 3, pp. 701–9.
- Jones, P.A. & Takai, D. 2001, 'The role of DNA methylation in mammalian epigenetics', *Science*, vol. 293, no. 5532, p. 1068 LP-1070.
- Joseph, K.S., Allen, A.C., Dodds, L., Turner, L.A., Scott, H. & Liston, R. 2005, 'The Perinatal Effects of Delayed Childbearing', *Obstetrics & Gynecology*, vol. 105, no. 6, pp. 1410–8.
- Joswig, A., Gabriel, H., Kibschull, M. & Winterhager, E. 2003, 'Apoptosis in uterine epithelium and decidua in response to implantation: evidence for two different

- pathways', *Reproductive Biology and Endocrinology*, vol. 1, no. 44.
- Kammerer, R. & Zimmermann, W. 2010, 'Coevolution of activating and inhibitory receptors within mammalian carcinoembryonic antigen families', *BMC Biology*, vol. 8, no. 12.
- Kang, M.-C., Park, S.J., Kim, H.J., Lee, J., Yu, D.H., Bae, K.B., Ji, Y.R., Park, S.J., Jeong, J., Jang, W.Y., Kim, J.-H., Choi, M.-S., Lee, D.-S., Lee, H.-S., Lee, S., Kim, S.H., Kim, M.O., Park, G., Choo, Y.S., Cho, J.-Y. & Ryoo, Z.Y. 2014, 'Gestational loss and growth restriction by angiogenic defects in placental growth factor transgenic mice', *Arteriosclerosis, Thrombosis, and Vascular Biology*, vol. 34, no. 10, pp. 2276–82.
- Kapitsinou, P.P., Liu, Q., Unger, T.L., Rha, J., Davidoff, O., Keith, B., Epstein, J.A., Moores, S.L., Erickson-Miller, C.L. & Haase, V.H. 2010, 'Hepatic HIF-2 regulates erythropoietic responses to hypoxia in renal anemia', *Blood*, vol. 116, no. 16, p. 3039 LP-3048.
- Kararigas, G., Nguyen, B.T. & Jarry, H. 2014, 'Estrogen modulates cardiac growth through an estrogen receptor alpha-dependent mechanism in healthy ovariectomized mice', *Molecular and Cellular Endocrinology*, vol. 382, no. 2, pp. 909–14.
- Kelleher, A.M., Peng, W., Pru, J.K., Pru, C.A., DeMayo, F.J. & Spencer, T.E. 2017, 'Forkhead box a2 (FOXA2) is essential for uterine function and fertility', *Proceedings of the National Academy of Sciences*, vol. 114, no. 6, pp. E1018–26.
- Kennel, S.J., Lankford, T.K., Foote, L.J., Shinpock, S.G. & Stringer, C. 1993, 'CD44 expression on murine tissues', *Journal of Cell Science*, vol. 104, no. Pt2, pp. 373–82.
- Kent, L.N., Rumi, M.A.K., Kubota, K., Lee, D.-S. & Soares, M.J. 2011, 'FOSL1 is integral to establishing the maternal-fetal interface', *Molecular and Cellular Biology*, vol. 31, no. 23, pp. 4801–13.
- Kent, W.J., Sugnet, C.W., Furey, T.S., Roskin, K.M., Pringle, T.H., Zahler, A.M. & Haussler, D. 2002, 'The human genome browser at UCSC', *Genome Research*, vol. 12, no. 6, pp. 996–1006.
- Khanduri, S., Chhabra, S., Yadav, S., Sabharwal, T., Chaudhary, M., Usmani, T., Goyal, A. & Sharma, H. 2017, 'Role of color Doppler flowmetry in prediction of intrauterine growth retardation in high-risk pregnancy', *Cureus*, vol. 9, no. 11, p. e1827.
- Khanna, K.K. & Jackson, S.P. 2001, 'DNA double-strand breaks: signaling, repair and the

- cancer connection', *Nature Genetics*, vol. 27, p. 247.
- Khosla, S., Dean, W., Brown, D., Reik, W. & Feil, R. 2001, 'Culture of preimplantation mouse embryos affects fetal development and the expression of imprinted genes', *Biology of Reproduction*, vol. 64, pp. 918–26.
- Khosla, S., Dean, W., Reik, W. & Feil, R. 2001, 'Culture of preimplantation embryos and its long-term effects on gene expression and phenotype', *Human Reproduction Update*, vol. 7, no. 4, pp. 419–27.
- Kim, B.-H., Shenoy, A.R., Kumar, P., Das, R., Tiwari, S. & MacMicking, J.D. 2011, 'A Family of IFN- γ -Inducible 65-kD GTPases Protects Against Bacterial Infection', *Science*, vol. 332, no. 6030, p. 717 LP-721.
- Kim, J.H., Jeon, Y.J., Lee, B.E., Kang, H., Shin, J.E., Choi, D.H., Lee, W.S. & Kim, N.K. 2013, 'Association of methionine synthase and thymidylate synthase genetic polymorphisms with idiopathic recurrent pregnancy loss', *Fertility and Sterility*, vol. 99, no. 6, p. 1674–1680.e3.
- Kiserud, T., Piaggio, G., Carroli, G., Widmer, M., Jensen, L.N., Giordano, D., Cecatti, G., Aleem, H.A., Talegawkar, S.A., Benachi, A., Diemert, A., Kitoto, A.T., Thinkhamrop, J., Lumbiganon, P., Tabor, A., Kriplani, A., Perez, R.G., Hecher, K., Hanson, M.A., Gulmezogly, M. & Platt, L.D. 2017, 'The World Health Organization Fetal Growth Charts: A Multinational Longitudinal Study of Ultrasound Biometric Measurements and Estimated Fetal Weight', *PLoS Medicine*, vol. 14, no. 4, p. e1002301.
- Klinger, S., Turgeon, B., Lévesque, K., Wood, G.A., Aagaard-Tillery, K.M. & Meloche, S. 2009, 'Loss of Erk3 function in mice leads to intrauterine growth restriction, pulmonary immaturity, and neonatal lethality', *Proceedings of the National Academy of Sciences*, vol. 106, no. 39, p. 16710 LP-16715.
- Kloet, S.L., Makowski, M.M., Baymaz, H.I., van Voorthuijsen, L., Karemaker, I.D., Santanach, A., Jansen, P.W.T.C., Di Croce, L. & Vermeulen, M. 2016, 'The dynamic interactome and genomic targets of Polycomb complexes during stem-cell differentiation', *Nature Structural and Molecular Biology*, vol. 23, no. 7, pp. 682–90.
- von dem Knesebeck, A., Felsberg, J., Waha, A., Hartmann, W., Scheffler, B., Glas, M., Hammes, J., Mikeska, T., Yan, P.S., Endl, E., Simon, M., Reifenberger, G., Pietsch, T.

- & Waha, A. 2012, 'RANK (TNFRSF11A) is epigenetically inactivated and induces apoptosis in gliomas', *Neoplasia*, vol. 14, no. 6, pp. 526–34.
- Ko, M., Huang, Y., Jankowska, A.M., Pape, U.J., Tahiliani, M., Bandukwala, H.S., An, J., Lamperti, E.D., Koh, K.P., Ganetzky, R., Liu, X.S., Aravind, L., Agarwal, S., Maciejewski, J.P. & Rao, A. 2010, 'Impaired hydroxylation of 5-methylcytosine in myeloid cancers with mutant TET2', *Nature*, vol. 468, no. 7325, pp. 839–43.
- Kooistra, M., Trasler, J.M. & Baltz, J.M. 2013, 'Folate transport in mouse cumulus-oocyte complexes and preimplantation embryos', *Biology of Reproduction*, vol. 89, no. 3, pp. 1–9.
- Koury, M.J., Horne, D.W., Brown, Z.A., Pietenpol, J.A., Blount, B.C., Ames, B.N., Hard, R. & Koury, S.T. 1997, 'Apoptosis of late-stage erythroblasts in megaloblastic anemia: association with DNA damage and macrocyte production', *Blood*, vol. 89, no. 12, pp. 4617–23.
- Koury, M.J. & Ponka, P. 2004, 'New insights into erythropoiesis: the roles of folate, vitamin B12, and iron', *Annual Review of Nutrition*, vol. 24, pp. 105–31.
- Kowluru, R.A., Shan, Y. & Mishra, M. 2016, 'Dynamic DNA methylation of matrix metalloproteinase-9 in the development of diabetic retinopathy', *Laboratory Investigation*, vol. 96, no. 10, pp. 1040–9.
- Kozuki, N., Lee, A.C. & Katz, J. 2012, 'Moderate to severe, but not mild, maternal anemia is associated with increased risk of small-for-gestational-age outcomes', *The Journal of Nutrition*, vol. 142, no. 2, pp. 358–62.
- Kramer, M.S., Goulet, L., Lydon, J., Séguin, L., McNamara, H., Dassa, C., Platt, R.W., Fong Chen, M., Gauthier, H., Genest, J., Kahn, S., Libman, M., Rozen, R., Masse, A., Miner, L., Asselin, G., Benjamin, A., Klein, J. & Koren, G. 2001, 'Socio-economic disparities in preterm birth: causal pathways and mechanisms', *Paediatric and Perinatal Epidemiology*, vol. 15, no. s2, pp. 104–23.
- Kramer, M.S. & Kakuma, R. 2003, 'Energy and protein intake in pregnancy', *Cochrane Database of Systematic Reviews*, no. 4.
- Krebs, C., Macara, L.M., Leiser, R., Bowman, A.W., Greer, I.A. & Kingdom, J.C.P. 1996,

- ‘Intrauterine growth restriction with absent end-diastolic flow velocity in the umbilical artery is associated with maldevelopment of the placental terminal villous tree’, *American Journal of Obstetrics and Gynecology*, vol. 175, no. 6, pp. 1534–42.
- Krishna, U. & Bhalerao, S. 2011, ‘Placental insufficiency and fetal growth restriction’, *Journal of Obstetrics and Gynecology of India*, vol. 61, no. 5, pp. 505–11.
- Krishnaveni, G. V., Veena, S.R., Karat, S.C., Yajnik, C.S. & Fall, C.H.D. 2014, ‘Association between maternal folate concentrations during pregnancy and insulin resistance in Indian children’, *Diabetologia*, vol. 57, no. 1, pp. 110–21.
- Krueger, S., Kellner, U., Buehling, F. & Roessner, A. 2001, ‘Cathepsin L antisense oligonucleotides in a human osteosarcoma cell line: effects on the invasive phenotype’, *Cancer Gene Therapy*, vol. 8, no. 7, pp. 522–8.
- Kuhnel, E., Kleff, V., Stojanovska, V., Kaiser, S., Waldschutz, R., Herse, F., Plosch, T., Winterhager, E. & Gellhaus, A. 2017, ‘Placental-specific overexpression of sFlt-1 alters trophoblast differentiation and nutrient transporter expression in an IUGR mouse model’, *Journal of Cellular Biochemistry*, vol. 118, no. 6, pp. 1316–29.
- Kuleshov, M. V., Jones, M.R., Rouillard, A.D., Fernandez, N.F., Duan, Q., Wang, Z., Koplev, S., Jenkins, S.L., Jagodnik, K.M., Lachmann, A., McDermott, M.G., Monteiro, C.D., Gundersen, G.W. & Ma’ayan, A. 2016, ‘Enrichr: a comprehensive gene set enrichment analysis web server 2016 update’, *Nucleic Acids Research*, vol. 44, no. W1, pp. W90–7.
- Kundakovic, M., Gudsnuk, K., Franks, B., Madrid, J., Miller, R.L. & Perera, F.P. 2013, ‘Sex-specific epigenetic disruption and behavioral changes following low-dose in utero bisphenol A exposure’, *Proceedings of the National Academy of Sciences*, vol. 110, no. 24, pp. 9956–61.
- Kunimoto, H., McKenney, A.S., Meydan, C., Shank, K., Nazir, A., Rapaport, F., Durham, B., Garrett-Bakelman, F.E., Pronier, E., Shih, A.H., Melnick, A., Chaudhuri, J. & Levine, R.L. 2017, ‘Aid is a key regulator of myeloid/erythroid differentiation and DNA methylation in hematopoietic stem/progenitor cells’, *Blood*, vol. 129, no. 13, pp. 1779–90.
- Kurihara, I., Lee, D.K., Petit, F.G., Jeong, J., Lee, K., Lydon, J.P., DeMayo, F.J., Tsai, M.J. & Tsai, S.Y. 2007, ‘COUP-TFII mediates progesterone regulation of uterine

implantation by controlling ER activity’, *PLoS Genetics*, vol. 3, no. 6, pp. 1053–64.

Küry, S., van Woerden, G.M., Besnard, T., Proietti Onori, M., Latypova, X., Towne, M.C., Cho, M.T., Prescott, T.E., Ploeg, M.A., Sanders, S., Stessman, H.A.F., Pujol, A., Distel, B., Robak, L.A., Bernstein, J.A., Denommé-Pichon, A.S., Lesca, G., Sellars, E.A., Berg, J., Carré, W., Busk, Ø.L., van Bon, B.W.M., Waugh, J.L., Deardorff, M., Hoganson, G.E., Bosanko, K.B., Johnson, D.S., Dabir, T., Holla, Ø.L., Sarkar, A., Tveten, K., de Bellescize, J., Braathen, G.J., Terhal, P.A., Grange, D.K., van Haeringen, A., Lam, C., Mirzaa, G., Burton, J., Bhoj, E.J., Douglas, J., Santani, A.B., Nesbitt, A.I., Helbig, K.L., Andrews, M. V., Begtrup, A., Tang, S., van Gassen, K.L.I., Juusola, J., Foss, K., Enns, G.M., Moog, U., Hinderhofer, K., Paramasivam, N., Lincoln, S., Kusako, B.H., Lindenbaum, P., Charpentier, E., Nowak, C.B., Cherot, E., Simonet, T., Ruivenkamp, C.A.L., Hahn, S., Brownstein, C.A., Xia, F., Schmitt, S., Deb, W., Bonneau, D., Nizon, M., Quinquis, D., Chelly, J., Rudolf, G., Sanlaville, D., Parent, P., Gilbert-Dussardier, B., Toutain, A., Sutton, V.R., Thies, J., Peart-Vissers, L.E.L.M., Boisseau, P., Vincent, M., Grabrucker, A.M., Dubourg, C., Tan, W.H., Verbeek, N.E., Granzow, M., Santen, G.W.E., Shendure, J., Isidor, B., Pasquier, L., Redon, R., Yang, Y., State, M.W., Kleefstra, T., Cogné, B., Petrovski, S., Retterer, K., Eichler, E.E., Rosenfeld, J.A., Agrawal, P.B., Bézieau, S., Odent, S., Elgersma, Y. & Mercier, S. 2017, ‘De novo mutations in protein kinase genes CAMK2A and CAMK2B cause intellectual disability’, *American Journal of Human Genetics*, vol. 101, no. 5, pp. 768–88.

Kusinski, L.C., Stanley, J.L., Dilworth, M.R., Hirt, C.J., Andersson, I.J., Renshall, L.J., Baker, B.C., Baker, P.N., Sibley, C.P., Wareing, M. & Glazier, J.D. 2012, ‘eNOS knockout mouse as a model of fetal growth restriction with an impaired uterine artery function and placental transport phenotype’, *American Journal of Physiology*, vol. 303, no. 1, pp. R86-93.

Kwon, E.J. & Kim, Y.J. 2017, ‘What is fetal programming?: a lifetime health is under the control of in utero health’, *Obstetrics & Gynecology Science*, vol. 60, no. 6, pp. 506–19.

Lacko, L.A., Hurtado, R., Hinds, S., Poulos, M.G., Butler, J.M. & Stuhlmann, H. 2017, ‘Altered fetoplacental vascularization, fetoplacental malperfusion and fetal growth restriction in mice with *Egfl7* loss of function’, *Development*, vol. 144, no. 13, pp. 2469–79.

- Lague, M.-N., Detmar, J., Paquet, M., Boyer, A., Richards, J.S., Adamson, S.L. & Boerboom, D. 2010, 'Decidual PTEN expression is required for trophoblast invasion in the mouse', *American Journal of Physiology-Endocrinology and Metabolism*, vol. 299, no. 6, pp. E936-46.
- Lala, P.K. & Graham, C.H. 1990, 'Mechanisms of trophoblast invasiveness and their control: the role of proteases and protease inhibitors', *Cancer Metastasis Reviews*, vol. 9, no. 4, pp. 369-79.
- Lambie, D.G. & Johnson, R.H. 1985, 'Drugs and folate metabolism', *Drugs*, vol. 30, no. 2, pp. 145-55.
- Lanska, D.J. 2010, 'Historical aspects of the major neurological vitamin deficiency disorders: the water-soluble B vitamins.', *Handbook of Clinical Neurology*, vol. 95, Netherlands, pp. 445-76.
- Large, M.J. & DeMayo, F.J. 2012, 'The regulation of embryo implantation and endometrial decidualization by progesterone receptor signaling', *Molecular and Cellular Endocrinology*, vol. 358, no. 2, pp. 155-65.
- Large, M.J., Wetendorf, M., Lanz, R.B., Hartig, S.M., Creighton, C.J., Mancini, M.A., Kovanci, E., Lee, K.-F., Threadgill, D.W., Lydon, J.P., Jeong, J.-W. & DeMayo, F.J. 2014, 'The epidermal growth factor receptor critically regulates endometrial function during early pregnancy', *PLoS Genetics*, vol. 10, no. 6, p. e1004451.
- Laviola, L., Perrini, S., Belsanti, G., Natalicchio, A., Montrone, C., Leonardini, A., Vimercati, A., Scioscia, M., Selvaggi, L., Giorgino, R., Greco, P. & Giorgino, F. 2005, 'Intrauterine growth restriction in humans is associated with abnormalities in placental insulin-like growth factor signaling', *Endocrinology*, vol. 146, no. 3, pp. 1498-505.
- Laws, M.J., Taylor, R.N., Sidell, N., DeMayo, F.J., Lydon, J.P., Gutstein, D.E., Bagchi, M.K. & Bagchi, I.C. 2008, 'Gap junction communication between uterine stromal cells plays a critical role in pregnancy-associated neovascularization and embryo survival', *Development*, vol. 135, no. 15, p. 2659 LP-2668.
- Lee, D.-S., Yanagimoto Ueta, Y., Xuan, X., Igarashi, I., Fujisaki, K., Sugimoto, C., Toyoda, Y. & Suzuki, H. 2005, 'Expression patterns of the implantation-associated genes in the uterus during the estrous cycle in mice', *The Journal of Reproduction and Development*,

vol. 51, no. 6, pp. 787–98.

- Lee, J., Oh, J.S. & Cho, C. 2011, 'Impaired expansion of trophoblast spheroids cocultured with endometrial cells overexpressing cellular retinoic acid-binding protein', *Fertility and Sterility*, vol. 95, no. 8, pp. 2599–601.
- Lee, K., Jeong, J.W., Kwak, I., Yu, C.T., Lanske, B., Soegiarto, D.W., Toftgard, R., Tsai, M.J., Tsai, S., Lydon, J.P. & DeMayo, F.J. 2006, 'Indian hedgehog is a major mediator of progesterone signaling in the mouse uterus', *Nature Genetics*, vol. 38, no. 10, pp. 1204–9.
- Lee, K.Y. & Demayo, F.J. 2004, 'Animal models of implantation', *Reproduction*, vol. 128, no. 6, pp. 679–95.
- Lee, K.Y., Jeong, J.-W., Wang, J., Ma, L., Martin, J.F., Tsai, S.Y., Lydon, J.P. & DeMayo, F.J. 2007, 'Bmp2 is critical for the murine uterine decidual response', *Molecular and Cellular Biology*, vol. 27, no. 15, pp. 5468–78.
- Leeda, M., Riyazi, N., de Vries, J.I., Jakobs, C., van Geijn, H.P. & Dekker, G. a 1998, 'Effects of folic acid and vitamin B6 supplementation on women with hyperhomocysteinemia and a history of preeclampsia or fetal growth restriction', *American Journal of Obstetrics and Gynecology*, vol. 179, no. 1, pp. 135–9.
- Lessey, B.A., Killam, A.P., Metzger, D.A., Haney, A.F., Greene, G.L. & McCarty, K.S.J. 1988, 'Immunohistochemical analysis of human uterine estrogen and progesterone receptors throughout the menstrual cycle', *The Journal of Clinical Endocrinology and Metabolism*, vol. 67, no. 2, pp. 334–40.
- Levy, R. & Nelson, D.M. 2000, 'To be, or not to be, that is the question. Apoptosis in human trophoblast', *Placenta*, vol. 21, no. 1, pp. 1–13.
- Li, E., Bestor, T.H. & Jaenisch, R. 1992, 'Targeted mutation of the DNA methyltransferase gene results in embryonic lethality', *Cell*, vol. 69, pp. 915–26.
- Li, H., Cao, G., Zhang, N., Lou, T., Wang, Q., Zhang, Z. & Liu, C. 2018, 'RBP4 regulates trophoblastic cell proliferation and invasion via the PI3K/AKT signaling pathway', *Molecular Medicine Reports*, vol. 18, no. 3, pp. 2873–9.
- Li, L., Zheng, P. & Dean, J. 2010, 'Maternal control of early mouse development',

Development, vol. 137, no. 6, p. 859 LP-870.

- Li, P., Peng, H., Lu, W.-H., Shuai, H.-L., Zha, Q.-B., Yeung, C.-K., Li, H., Wang, L.-J., Ho Lee, K.K., Zhu, W.-J. & Yang, X. 2015, 'Role of Slit2/Robo1 in trophoblast invasion and vascular remodeling during ectopic tubal pregnancy', *Placenta*, vol. 36, no. 10, pp. 1087–94.
- Li, Q., Kannan, A., Wang, W., DeMayo, F.J., Taylor, R.N., Bagchi, M.K. & Bagchi, I.C. 2007, 'Bone morphogenetic protein 2 functions via a conserved signaling pathway involving Wnt4 to regulate uterine decidualization in the mouse and the human', *Journal of Biological Chemistry*, vol. 282, no. 43, pp. 31725–32.
- Li, R., Wu, J., He, J., Wang, Y., Liu, X., Chen, X., Tong, C., Ding, Y., Su, Y.A.N., Chen, W., Zhang, C. & Gao, R. 2017, 'Mice endometrium receptivity in early pregnancy is impaired by maternal hyperinsulinemia', *Molecular Medicine Reports*, vol. 15, no. 5, pp. 2503–10.
- Li, S., Wang, D.-Z., Wang, Z., Richardson, J.A. & Olson, E.N. 2003, 'The serum response factor coactivator myocardin is required for vascular smooth muscle development', *Proceedings of the National Academy of Sciences of the United States of America*, vol. 100, no. 16, pp. 9366–70.
- Li, Y. & Behringer, R.R. 1998, 'Esx1 is an X-chromosome-imprinted regulator of placental development and fetal growth', *Nature Genetics*, vol. 20, no. 3, pp. 309–11.
- Li, Y., Gao, R., Liu, X., Chen, X., Liao, X., Geng, Y., Ding, Y., Wang, Y. & He, J. 2015, 'Folate deficiency could restrain decidual angiogenesis in pregnant mice', *Nutrients*, vol. 7, no. 8, pp. 6425–45.
- Li, Y., Huang, T., Zheng, Y., Muka, T., Troup, J. & Hu, F.B. 2016, 'Folic acid supplementation and the risk of cardiovascular diseases: A meta-analysis of randomized controlled trials', *Journal of the American Heart Association*, vol. 5, no. 8, p. e003768.
- Liao, X.G., Li, Y.L., Gao, R.F., Geng, Y.Q., Chen, X.M., Liu, X.Q., Ding, Y. Bin, Mu, X.Y., Wang, Y.X. & He, J.L. 2015, 'Folate deficiency decreases apoptosis of endometrium decidual cells in pregnant mice via the mitochondrial pathway', *Nutrients*, vol. 7, no. 3, pp. 1916–32.

- Lim, H., Gupta, R.A., Ma, W., Paria, B.C., Moller, D.E., Morrow, J.D., DuBois, R.N., Trzaskos, J.M. & Dey, S.K. 1999, 'Cyclooxygenase-2-derived prostacyclin mediates embryo implantation in the mouse via PPAR δ ', *Genes & Development*, vol. 13, no. 12, pp. 1561–74.
- Lim, H., Ma, L., Ma, W., Maas, R.L. & Dey, S.K. 1999, 'Hoxa-10 regulates uterine stromal cell responsiveness to progesterone during implantation and decidualization in the mouse', *Molecular Endocrinology*, vol. 13, no. 6, pp. 1005–17.
- Lim, H.J. & Wang, H. 2010, 'Uterine disorders and pregnancy complications : insights from mouse models', *The Journal of Clinical Investigation*, vol. 120, no. 4, pp. 1004–15.
- Lin, S. & Garcia, B.A. 2012, 'Examining histone posttranslational modification patterns by high-resolution mass spectrometry', *Methods in Enzymology*, vol. 512, pp. 3–28.
- Lindblad, B., Zaman, S., Malik, A., Martin, H., Ekstrom, A.M., Amu, S., Holmgren, A. & Norman, M. 2005, 'Folate, vitamin B12, and homocysteine levels in South Asian women with growth-retarded fetuses', *Acta Obstetrica et Gynecologica Scandinavica*, vol. 84, no. 11, pp. 1055–61.
- Lippi, G., Montagnana, M., Targher, G., Salvagno, G.L. & Guidi, G.C. 2008, 'Prevalence of folic acid and vitamin B12 deficiencies in patients with thyroid disorders', *The American Journal of the Medical Sciences*, vol. 336, no. 1, pp. 50–2.
- Liu, H., Zhang, Y., Gu, H.-T., Feng, Q.-L., Liu, J.-Y., Zhou, J. & Yan, F. 2015, 'Association between assisted reproductive technology and cardiac alteration at age 5 years', *JAMA Pediatrics*, vol. 169, no. 6, pp. 603–5.
- Liu, J., Xie, J., Li, Z., Greene, N.D.E. & Ren, A. 2018, 'Sex differences in the prevalence of neural tube defects and preventive effects of folic acid (FA) supplementation among five counties in northern China: results from a population-based birth defect surveillance programme', *BMJ*, vol. 8, no. 11, p. e022565.
- Liu, J.L. & LeRoith, D. 1999, 'Insulin-like growth factor I is essential for postnatal growth in response to growth hormone', *Endocrinology*, vol. 140, no. 11, pp. 5178–84.
- Livak, K.J. & Schmittgen, T.D. 2001, 'Analysis of relative gene expression data using real-time quantitative PCR and the 2- $\Delta\Delta$ CT method', *Methods*, vol. 25, no. 4, pp. 402–8.

- Locasale, J.W. 2013, 'Serine, glycine and one-carbon units: cancer metabolism in full circle', *Nature reviews. Cancer*, vol. 13, no. 8, pp. 572–83.
- Long, C., He, J., Liu, X., Chen, X., Gao, R., Wang, Y. & Ding, Y. 2012, 'Dietary folate deficiency in pseudopregnant mice has no Effect on Homeobox A10 promoter methylation or expression', *Reproductive Sciences*, vol. 19, no. 12, pp. 1268–75.
- Longo, L.D. 1976, 'Carbon monoxide: effects on oxygenation of the fetus in utero', *Science*, vol. 194, no. 4264, pp. 523–5.
- Lopez-Jaramillo, P., Gomez-Arbelaez, D., Sotomayor-Rubio, A., Mantilla-Garcia, D. & Lopez-Lopez, J. 2015, 'Maternal undernutrition and cardiometabolic disease: a Latin American perspective', *BMC Medicine*, vol. 13, p. 41.
- De Luca, L.C., Le, H.T., Mara, D.L. & Beristain, A.G. 2017, 'ADAM28 localizes to HLA-G(+) trophoblasts and promotes column cell outgrowth', *Placenta*, vol. 55, pp. 71–80.
- Luka, Z., Moss, F., Loukachevitch, L. V, Bornhop, D.J. & Wagner, C. 2011, 'Histone Demethylase LSD1 Is a Folate-Binding Protein', *Biochemistry*, vol. 50, no. 21, pp. 4750–6.
- Lumey, L.H. 1992, 'Decreased birthweights in infants after maternal in utero exposure to the Dutch famine of 1944-1945', *Paediatric and Perinatal Epidemiology*, vol. 6, no. 2, pp. 240–53.
- Luo, J., Sladek, R., Bader, J.-A., Matthyssen, A., Rossant, J. & Giguère, V. 1997, 'Placental abnormalities in mouse embryos lacking the orphan nuclear receptor ERR- β ', *Nature*, vol. 388, no. 6644, pp. 778–82.
- Lyall, F., Robson, S.C. & Bulmer, J.N. 2013, 'Spiral artery remodeling and trophoblast invasion in preeclampsia and fetal growth restriction relationship to clinical outcome', *Hypertension*, vol. 62, no. 6, pp. 1046–54.
- Lydon, J.P., Francesco, J.D., Funk, C.R., Mani, S.K. & Angela, R.H. 1995, 'Mice lacking progesterone receptor exhibit pleiotropic reproductive abnormalities', *Genes and Development*, vol. 9, no. 18, pp. 2266–78.
- Ma, N. & Hardy, D.B. 2012, 'The fetal origins of the metabolic syndrome: Can we intervene?', *Journal of Pregnancy*, vol. 2012.

- Ma, S., Charron, J. & Erikson, R.L. 2003, 'Role of Plk2 (Snk) in mouse development and cell proliferation', *Molecular and Cellular Biology*, vol. 23, no. 19, pp. 6936–43.
- Ma, X., Gao, F., Rusie, A., Hemingway, J., Ostmann, A.B., Julie, M., Jegga, A.G. & Das, S.K. 2011, 'Decidual cell polyploidization necessitates mitochondrial activity', *PLoS One*, vol. 6, no. 10, p. e26774.
- Ma, Y., Peng, D., Liu, C., Huang, C. & Luo, J. 2017, 'Serum high concentrations of homocysteine and low levels of folic acid and vitamin B12 are significantly correlated with the categories of coronary artery diseases', *BMC Cardiovascular Disorders*, vol. 17, no. 1, p. 37.
- MacLennan, M., Crichton, J.H., Playfoot, C.J. & Adams, I.R. 2015, 'Oocyte development, meiosis and aneuploidy', *Seminars in Cell & Developmental Biology*, vol. 45, pp. 68–76.
- Macut, D. 2009, 'The role of HPA axis in metabolic derangements in PCOS', *Endocrine Abstracts*, vol. 20, p. S1.3.
- Madzo, J., Liu, H., Rodriguez, A., Vasanthakumar, A., Sundaravel, S., Caces, D.B.D., Looney, T.J., Zhang, L., Lepore, J.B., Macrae, T., Duszynski, R., Shih, A.H., Song, C.-X., Yu, M., Yu, Y., Grossman, R., Raumann, B., Verma, A., He, C., Levine, R.L., Lavelle, D., Lahn, B.T., Wickrema, A. & Godley, L.A. 2014, 'Hydroxymethylation at gene regulatory regions directs stem/early progenitor cell commitment during erythropoiesis', *Cell Reports*, vol. 6, no. 1, 2013/12/27., pp. 231–44.
- Mahendran, D., Donnai, P., Glazier, J.D., D'Souza, S.W., Boyd, R.D. & Sibley, C.P. 1993, 'Amino acid (system A) transporter activity in microvillous membrane vesicles from the placentas of appropriate and small for gestational age babies', *Pediatric Research*, vol. 34, no. 5, pp. 661–5.
- Mahmood, L. 2014, 'The metabolic processes of folic acid and Vitamin B12 deficiency', *Journal of Health Research and Reviews*, vol. 1, no. 1, pp. 5–9.
- Maier, V.K., Feeney, C.M., Taylor, J.E., Creech, A.L., Qiao, J.W., Szanto, A., Das, P.P., Chevrier, N., Cifuentes-Rojas, C., Orkin, S.H., Carr, S.A., Jaffe, J.D., Mertins, P. & Lee, J.T. 2015, 'Functional proteomic analysis of repressive histone methyltransferase complexes reveals ZNF518B as a G9A regulator', *Molecular & Cellular Proteomics*,

vol. 14, no. 6, pp. 1435–46.

- Makkar, A., Mishima, T., Chang, G., Scifres, C. & Sadovsky, Y. 2014, 'Fatty acid binding protein-4 is expressed in the mouse placental labyrinth, yet is dispensable for placental triglyceride accumulation and fetal growth', *Placenta*, vol. 35, no. 10, pp. 802–7.
- Malassiné, A., Frendo, J.L. & Evain-Brion, D. 2003, 'A comparison of placental development and endocrine functions between the human and mouse model', *Human Reproduction Update*, vol. 9, no. 6, pp. 531–9.
- Maltepe, E., Bakardjiev, A.I. & Fisher, S.J. 2010, 'The placenta: transcriptional, epigenetic, and physiological integration during development', *The Journal of Clinical Investigation*, vol. 120, no. 4, pp. 1016–25.
- Mann, M.R.W., Lee, S.S., Doherty, A.S., Verona, R.I., Nolen, L.D., Schultz, R.M. & Bartolomei, M.S. 2004, 'Selective loss of imprinting in the placenta following preimplantation development in culture', *Development*, vol. 131, pp. 3727–35.
- Mao, J., Zhang, X., Sieli, P.T., Falduto, M.T., Torres, K.E. & Rosenfeld, C.S. 2010, 'Contrasting effects of different maternal diets on sexually dimorphic gene expression in the murine placenta', *Proceedings of the National Academy of Sciences*, vol. 107, no. 12, pp. 5557–5562.
- Marcinkevicius, E., Fernandez-Gonzalez, R. & Zallen, J.A. 2009, 'Q&A: Quantitative approaches to planar polarity and tissue organization', *Journal of Biology*, vol. 8, no. 12, p. 103.1-103.5.
- De Marco, P., Merello, E., Calevo, M.G., Mascelli, S., Raso, A., Cama, A. & Capra, V. 2006, 'Evaluation of a methylenetetrahydrofolate-dehydrogenase 1958G>A polymorphism for neural tube defect risk', *Journal of Human Genetics*, vol. 51, no. 2, pp. 98–103.
- Marsal, K. 2002, 'Intrauterine growth restriction', *Current Opinion in Obstetrics & Gynecology*, vol. 14, no. 2, pp. 127–35.
- Martin, A.M., Bindra, R., Curcio, P., Cicero, S. & Nicolaides, K.H. 2001, 'Screening for pre-eclampsia and fetal growth restriction by uterine artery Doppler at 11-14 weeks of gestation', *Ultrasound in Obstetrics & Gynecology*, vol. 18, no. 6, pp. 583–6.
- Martin, L. & Finn, C.A. 1968, 'Hormonal regulation of cell division in epithelial and

- connective tissues of the mouse uterus', *The Journal of Endocrinology*, vol. 41, no. 3, pp. 363–71.
- Matsumoto, H., Ma, W., Daikoku, T., Zhao, X., Paria, B.C., Das, S.K., Trzaskos, J.M. & Dey, S.K. 2002, 'Cyclooxygenase-2 differentially directs uterine angiogenesis during implantation in mice', *Journal of Biological Chemistry*, vol. 277, no. 32, pp. 29260–7.
- Matte, J.J., Girard, C.L. & Tremblay, G.F. 1993, 'Effect of long-term addition of folic acid on folate status, growth performance, puberty attainment, and reproductive capacity of gilts', *Journal of Animal Science*, vol. 71, no. 1, pp. 151–7.
- Mayhew, T.M., Ohadike, C., Baker, P.N., Crocker, I.P., Mitchell, C. & Ong, S.S. 2003, 'Stereological investigation of placental morphology in pregnancies complicated by pre-eclampsia with and without intrauterine growth restriction', *Placenta*, vol. 24, no. 2–3, pp. 219–26.
- McConaha, M.E., Eckstrum, K., An, J., Steinle, J.J. & Bany, B.M. 2011, 'Microarray assessment of the influence of the conceptus on gene expression in the mouse uterus during decidualization', *Reproduction*, vol. 141, no. 4, pp. 511–27.
- McCowan, L.M., Figueras, F. & Anderson, N.H. 2018, 'Evidence-based national guidelines for the management of suspected fetal growth restriction: comparison, consensus, and controversy', *American Journal of Obstetrics & Gynecology*, vol. 218, no. 2, pp. S855–68.
- Mccue, P.M. & Act, D. 1998, 'Review of ovarian abnormalities in the mare', *Proceedings of the Annual Convention of the AAEP*, vol. 44, pp. 125–33.
- Mckay, J.A., Wong, Y.K., Relton, C.L., Ford, D. & Mathers, J.C. 2011, 'Maternal folate supply and sex influence gene-specific DNA methylation in the fetal gut', *Molecular Nutrition and Food Research*, vol. 55, no. 11, pp. 1717–23.
- McLean, A.C., Valenzuela, N., Fai, S. & Bennett, S.A.L. 2012, 'Performing vaginal lavage, crystal violet staining, and vaginal cytological evaluation for mouse estrous cycle staging identification', *Journal of Visualized Experiments*, no. 67, p. e4389.
- Mcmullin, M.F., Young, P.B., Bailie, K.E.M., Savage, G.A., Lappin, T.R.J. & White, R. 2001, 'Homocysteine and methylmalonic acid as indicators of folate and vitamin B12

- deficiency in pregnancy', *Clinical and Laboratory Haematology*, vol. 23, no. 3, pp. 161–5.
- McNulty, H., Pentieva, K., Hoey, L. & Ward, M. 2008, 'Homocysteine, B-vitamins and CVD', *The Proceedings of the Nutrition Society*, vol. 67, no. 2, pp. 232–7.
- Meeson, A.P., Radford, N., Shelton, J.M., Mammen, P.P., DiMaio, J.M., Hutcheson, K., Kong, Y., Elterman, J., Williams, R.S. & Garry, D.J. 2001, 'Adaptive mechanisms that preserve cardiac function in mice without myoglobin', *Circulation Research*, vol. 88, no. 7, pp. 713–20.
- Mehta, F.F., Son, J., Hewitt, S.C., Jang, E., Lydon, J.P., Korach, K.S. & Chung, S. 2016, 'Distinct functions and regulation of epithelial progesterone receptor in the mouse cervix, vagina, and uterus', *Oncotarget*, vol. 7, no. 14, pp. 17455–67.
- Melnyk, S., Pogribna, M., Miller, B.J., Basnakian, A.G., Pogribny, I.P. & James, S.J. 1999, 'Uracil misincorporation, DNA strand breaks, and gene amplification are associated with tumorigenic cell transformation in folate deficient/repleted Chinese hamster ovary cells.', *Cancer Letters*, vol. 146, no. 1, pp. 35–44.
- Men, C., Chai, H., Song, X., Li, Y., Du, H. & Ren, Q. 2017, 'Identification of DNA methylation associated gene signatures in endometrial cancer via integrated analysis of DNA methylation and gene expression systematically', *Journal of Gynecologic Oncology*, vol. 28, no. 6, 2017/09/08., p. e83.
- Menendez-Castro, C., Rascher, W. & Hartner, A. 2018, 'Intrauterine growth restriction - impact on cardiovascular diseases later in life', *Molecular & Cellular Pediatrics*, vol. 5, no. 1.
- Menkhorst, E.M., Van Sinderen, M.L., Rainczuk, K.E., Cuman, C., Winship, A. & Dimitriadis, E. 2017, 'Invasive trophoblast promote stromal fibroblast decidualization via Profilin 1 and ALOX5', *Scientific reports*, vol. 7, no. 1, p. 8690.
- Messerschmidt, D.M., de Vries, W., Ito, M., Solter, D., Ferguson-Smith, A. & Knowles, B.B. 2012, 'Trim28 is required for epigenetic stability during mouse oocyte to embryo transition.', *Science*, vol. 335, no. 6075, pp. 1499–502.
- Mikhael, S., Punjala-Patel, A. & Gavrilova-Jordan, L. 2019, 'Hypothalamic-pituitary-ovarian

- axis disorders impacting female fertility.’, *Biomedicines*, vol. 7, no. 5.
- Miles, J.R., Farin, C.E., Rodriguez, K.F., Alexander, J.E. & Farin, P.W. 2005, ‘Effects of embryo culture on angiogenesis and morphometry of bovine placentas during early gestation’, *Biology of Reproduction*, vol. 73, no. 4, pp. 663–71.
- Miller, A.L. 2008, ‘The methylation, neurotransmitter, and antioxidant connections between folate and depression’, *Alternative Medicine Review*, vol. 13, no. 3, pp. 216–26.
- Miller, B.H. & Takahashi, J.S. 2014, ‘Central circadian control of female reproductive function’, *Frontiers in Endocrinology*, vol. 4, no. 195, pp. 1–8.
- Miller, M.E., Dunn, P.M. & Smith, D.W. 1979, ‘Uterine malformation and fetal deformation’, *The Journal of Pediatrics*, vol. 94, no. 3, pp. 387–90.
- Milman, N. 2012, ‘Intestinal absorption of folic acid - new physiologic & molecular aspects’, *The Indian Journal of Medical Research*, vol. 136, no. 5, pp. 725–8.
- Milosevic-Stevanovic, J., Krstic, M., Radovic-Janosevic, D., Stefanovic, M., Antic, V. & Djordjevic, I. 2016, ‘Preeclampsia with and without intrauterine growth restriction-Two pathogenetically different entities?’, *Hypertension in Pregnancy*, vol. 35, no. 4, pp. 573–82.
- Miniaci, M.C., Dattolo, M.G., Irace, C., Capuozzo, A., Santamaria, R. & Scotto, P. 2015, ‘Glucose deprivation promotes activation of mTOR signaling pathway and protein synthesis in rat skeletal muscle cells’, *European Journal of Physiology*, vol. 467, no. 6, pp. 1357–66.
- Mitchell, H.K., Snell, E.E. & Williams, R.J. 1941, ‘The concentration of “folic acid”’, *Journal of the American Chemical Society*, vol. 63, no. 8, p. 2284.
- MMWR 1992, ‘Recommendations for the use of folic acid to reduce the number of cases of spina bifida and other neural tube defects’, *Morbidity and Mortality Weekly Report*, vol. 41, no. RR-14, pp. 1–7.
- Mohanty, D. & Das, K.C. 1982, ‘Effect of folate deficiency on the reproductive organs of female rhesus monkeys: a cytomorphological and cytokinetic study.’, *The Journal of Nutrition*, vol. 112, no. 8, pp. 1565–76.
- Moore, C.S. & Crocker, S.J. 2012, ‘An alternate perspective on the roles of TIMPs and

- MMPs in pathology', *The American Journal of Pathology*, vol. 180, no. 1, pp. 12–6.
- Mori, M., Bogdan, A., Balassa, T., Csabai, T. & Szekeres-Bartho, J. 2016, 'The decidua—the maternal bed embracing the embryo—maintains the pregnancy', *Seminars in Immunopathology*, vol. 38, no. 6, pp. 635–49.
- Mori, S., Nada, S., Kimura, H., Tajima, S., Takahashi, Y., Kitamura, A., Oneyama, C. & Okada, M. 2014, 'The mTOR pathway controls cell proliferation by regulating the FoxO3a transcription factor via SGK1 kinase', *PLoS One*, vol. 9, no. 2, p. e88891.
- Morris, J.K., Rankin, J., Draper, E.S., Kurinczuk, J.J., Springett, A., Tucker, D., Wellesley, D., Wreyford, B. & Wald, N.J. 2016, 'Prevention of neural tube defects in the UK: a missed opportunity', *Archives of Disease in Childhood*, vol. 101, no. 7, pp. 604–7.
- Morrison, J.L. 2008, 'Sheep models of intrauterine growth restriction: Fetal adaptations', *Clinical and Experimental Pharmacology and Physiology*, vol. 35, no. 7, pp. 730–43.
- MRC, V.S.R.G. 1991, 'Prevention of neural tube defects: Results of the Medical Research Council vitamin study', *The Lancet*, vol. 338, no. 8760, pp. 131–7.
- Mulac-Jericevic, B. & Conneely, O.M. 2004, 'Reproductive tissue selective actions of progesterone receptors', *Reproduction*, vol. 128, no. 2, pp. 139–46.
- Murphy, C.R. 2004, 'Uterine receptivity and the plasma membrane transformation', *Cell Research*, vol. 14, no. 4, pp. 259–67.
- Muthayya, S., Kurpad, A. V, Duggan, C.P., Bosch, R.J., Dwarkanath, P., Mhaskar, A., Mhaskar, R., Thomas, A., Vaz, M., Bhat, S. & Fawzi, W.W. 2006, 'Low maternal vitamin B 12 status is associated with intrauterine growth retardation in urban South Indians', *European Journal of Clinical Nutrition*, vol. 60, no. 6, pp. 791–801.
- Myatt, L. 2006, 'Placental adaptive responses and fetal programming', *The Journal of Physiology*, vol. 572, no. 1, pp. 25–30.
- Nagashima, T., Li, Q., Clementi, C., Lydon, J.P., DeMayo, F.J. & Matzuk, M.M. 2013, 'BMP2 is required for postimplantation uterine function and pregnancy maintenance', *The Journal of Clinical Investigation*, vol. 123, no. 6, 2013/05/08., pp. 2539–50.
- Nagy, A., Vintersten, K. & Behringer, R. 2003, *Manipulating the Mouse Embryo: A Laboratory Manual, 3rd ed.*, CSH Laboratory press.

- Naicker, T., Dorsamy, E., Ramsuran, D., Burton, G.J. & Moodley, J. 2013, 'The role of apoptosis on trophoblast cell invasion in the placental bed of normotensive and preeclamptic pregnancies', *Hypertension in Pregnancy*, vol. 32, no. 3, pp. 245–56.
- Nazki, F.H., Sameer, A.S. & Ganaie, B.A. 2014, 'Folate: metabolism, genes, polymorphisms and the associated diseases', *Gene*, vol. 533, no. 1, pp. 11–20.
- Neagos, D., Cretu, R., Tutulan-Cunita, A., Stoian, V. & Camil Bohiltea, L. 2010, 'Methylenetetrahydrofolate dehydrogenase (MTHFD) enzyme polymorphism as a maternal risk factor for trisomy 21: a clinical study', *Journal of Medicine and Life*, vol. 3, pp. 454–7.
- Nebigil, C.G., Choi, D.-S., Dierich, A., Hickel, P., Le Meur, M., Messaddeq, N., Launay, J.-M. & Maroteaux, L. 2000, 'Serotonin 2B receptor is required for heart development', *Proceedings of the National Academy of Sciences*, vol. 97, no. 17, p. 9508 LP-9513.
- Neitzke, U.T.A., Harder, T. & Plagemann, A. 2011, 'Intrauterine Growth Restriction and Developmental Programming of the Metabolic Syndrome : A Critical Appraisal', *Microcirculation*, vol. 18, no. 4, pp. 304–11.
- Nelissen, E.C.M., Dumoulin, J.C.M., Daunay, A., Evers, J.L.H., Tost, J. & van Montfoort, A.P.A. 2013, 'Placentas from pregnancies conceived by IVF/ICSI have a reduced DNA methylation level at the H19 and MEST differentially methylated regions', *Human Reproduction*, vol. 28, no. 4, pp. 1117–26.
- Ni, J., Zhang, L., Zhou, T., Xu, W.-J., Xue, J.-L., Cao, N. & Wang, X. 2017, 'Association between the MTHFR C677T polymorphism, blood folate and vitamin B12 deficiency, and elevated serum total homocysteine in healthy individuals in Yunnan Province, China', *Journal of the Chinese Medical Association*, vol. 80, no. 3, pp. 147–53.
- Niculescu, M.D. & Zeisel, S.H. 2002, 'Diet, methyl donors and DNA methylation: interactions between dietary folate, methionine and choline', *The Journal of Nutrition*, vol. 132, no. 8 Suppl, p. 2333S–2335S.
- Nishiyama, M., Nita, A., Yumimoto, K. & Nakayama, K.I. 2015, 'FBXL12-Mediated Degradation of ALDH3 is Essential for Trophoblast Differentiation During Placental Development', *Stem Cells*, vol. 33, no. 11, pp. 3327–40.

- Noda, H., Miyaji, Y., Nakanishi, A., Konishi, F. & Miki, Y. 2007, 'Frequent reduced expression of alpha-1B-adrenergic receptor caused by aberrant promoter methylation in gastric cancers', *British Journal of Cancer*, vol. 96, no. 2, pp. 383–90.
- Noguchi, J., Hata, K., Tanaka, H. & Hata, T. 2009, 'Placental vascular sonobiopsy using three-dimensional power doppler ultrasound in normal and growth restricted fetuses', *Placenta*, vol. 30, no. 5, pp. 391–7.
- Nollet, F., Kools, P. & Van Roy, F. 2000, 'Phylogenetic analysis of the cadherin superfamily allows identification of six major subfamilies besides several solitary members', *Journal of Molecular Biology*, vol. 299, no. 3, pp. 551–72.
- Norberg, S., Powell, T.L. & Jansson, T. 1998, 'Intrauterine growth restriction is associated with a reduced activity of placental taurine transporters', *Pediatric research*, vol. 44, no. 2, pp. 233–8.
- Norwitz, E.R., Schust, D.J. & Fisher, S.J. 2001, 'Implantation and the survival of early pregnancy', *The New England Journal of Medicine*, vol. 345, no. 19, pp. 1400–8.
- Novakovic, P., Stempak, J.M., Sohn, K.-J. & Kim, Y.-I. 2006, 'Effects of folate deficiency on gene expression in the apoptosis and cancer pathways in colon cancer cells', *Carcinogenesis*, vol. 27, no. 5, pp. 916–24.
- O'Connell, B.A., Moritz, K.M., Walker, D.W. & Dickinson, H. 2013, 'Synthetic glucocorticoid dexamethasone inhibits branching morphogenesis in the spiny mouse placenta', *Biology of Reproduction*, vol. 88, no. 1, p. 26.
- Odegard, R.A., Vatten, L.J., Nilsen, S.T., Salvesen, K.A. & Austgulen, R. 2000, 'Preeclampsia and fetal growth', *Obstetrics and Gynecology*, vol. 96, no. 6, pp. 950–5.
- Oh-McGinnis, R., Bogutz, A.B. & Lefebvre, L. 2011, 'Partial loss of *Ascl2* function affects all three layers of the mature placenta and causes intrauterine growth restriction', *Developmental Biology*, vol. 351, no. 2, pp. 277–86.
- Okada, H., Tsuzuki, T., Shindoh, H., Nishigaki, A., Yasuda, K. & Kanzaki, H. 2014, 'Regulation of decidualization and angiogenesis in the human endometrium: Mini review', *Journal of Obstetrics and Gynaecology Research*, vol. 40, no. 5, pp. 1180–7.
- Okano, M., Bell, D.W., Haber, D.A. & Li, E. 1999, 'DNA Methyltransferases *Dnmt3a* and

- Dnmt3b are essential for de novo methylation and mammalian development', *Cell*, vol. 99, pp. 247–57.
- Orfanelli, U., Wenke, A., Doglioni, C., Russo, V. & Bosserhoff, A.K. 2008, 'Identification of novel sense and antisense transcription at the TRPM2 locus in cancer', *Cell Research*, vol. 18, no. 11, pp. 1128–40.
- Orwig, K.E., Dai, G., Rasmussen, C.A. & Soares, M.J. 1997, 'Decidual/trophoblast prolactin-related protein: characterization of gene structure and cell-specific expression', *Endocrinology*, vol. 138, no. 6, pp. 2491–500.
- Orwig, K.E., Ishimura, R., Muller, H., Liu, B. & Soares, M.J. 1997, 'Identification and characterization of a mouse homolog for decidual/trophoblast prolactin-related protein', *Endocrinology*, vol. 138, no. 12, pp. 5511–7.
- Orwig, K.E., Rasmussen, C.A. & Soares, M.J. 1997, 'Decidual signals in the establishment of pregnancy: The prolactin family', *Trophoblast Research*, vol. 18, no. Supplement 2, pp. 329–43.
- Osmond, C. & Barker, D.J.P. 2000, 'Fetal, infant, and childhood growth are predictors of coronary heart disease, diabetes, and hypertension in adult men and women', *Environmental Health Perspectives*, vol. 1, no. 3, pp. 8545–53.
- Osol, G. & Mandala, M. 2009, 'Maternal uterine vascular remodeling during pregnancy', *Physiology*, vol. 24, pp. 58–71.
- Ozler, S., Oztas, E., Guler, B.G., Pehlivan, S., Kadioglu, N., Ergin, M., Uygur, D. & Danisman, N. 2016, 'Role of ADAMTS5 in unexplained fetal growth restriction (FGR)', *Fetal and Pediatric Pathology*, vol. 35, no. 4, pp. 220–30.
- Padmanabhan, N., Jia, D., Geary-Joo, C., Wu, X., Ferguson-Smith, A.C., Fung, E., Bieda, M.C., Snyder, F.F., Gravel, R.A., Cross, J.C. & Watson, E.D. 2013, 'Mutation in folate metabolism causes epigenetic instability and transgenerational effects on development', *Cell*, vol. 155, no. 1, pp. 81–93.
- Padmanabhan, N., Menelaou, K., Gao, J., Anderson, A., Blake, G.E.T., Li, T., Daw, B.N. & Watson, E.D. 2018, 'Abnormal folate metabolism causes age-, sex- and parent-of-origin-specific haematological defects in mice', *Journal of Physiology*, vol. 596, no. 18,

pp. 4341–60.

- Padmanabhan, N., Rakoczy, J., Kondratowicz, M., Menelaou, K., Blake, G.E.T. & Watson, E.D. 2017, 'Multigenerational analysis of sex-specific phenotypic differences at midgestation caused by abnormal folate metabolism', *Environmental Epigenetics*, vol. 3, no. 4, pp. 1–11.
- Palmer, A.M., Kamynina, E., Field, M.S. & Stover, P.J. 2017, 'Folate rescues vitamin B12 depletion-induced inhibition of nuclear thymidylate biosynthesis and genome instability', *Proceedings of the National Academy of Sciences of the United States of America*, vol. 114, no. 20, pp. E4095–102.
- Pang, S.C., Janzen-Pang, J., Tse, M.Y., Croy, B.A. & Lima, P.D.A. 2014, 'Chapter 1 - The Cycling and Pregnant Mouse: Gross Anatomy', in B.A. Croy, A.T. Yamada, F.J. DeMayo & S.L.B.T.-T.G. to I. of M.P. Adamson (eds), *The Guide to Investigation of Mouse Pregnancy*, Academic Press, Boston, pp. 3–19.
- Park, C.B., DeMayo, F.J., Lydon, J.P. & Dufort, D. 2012, 'NODAL in the uterus is necessary for proper placental development and maintenance of pregnancy', *Biology of Reproduction*, vol. 86, no. 6, p. 194.
- Parle-McDermott, A., Pangilinan, F., Mills, J.L., Signore, C.C., Molloy, A.M., Cotter, A., Conley, M., Cox, C., Kirke, P.N., Scott, J.M. & Brody, L.C. 2005, 'A polymorphism in the MTHFD1 gene increases a mother's risk of having an unexplained second trimester pregnancy loss', *Molecular Human Reproduction*, vol. 11, no. 7, pp. 477–80.
- Paulson, R.J. 2011, 'Hormonal induction of endometrial receptivity', *Fertility and Sterility*, vol. 96, no. 3, pp. 530–5.
- Pedersen, B., Holscher, T., Sato, Y., Pawlinski, R. & Mackman, N. 2005, 'A balance between tissue factor and tissue factor pathway inhibitor is required for embryonic development and hemostasis in adult mice', *Blood*, vol. 105, no. 7, pp. 2777–82.
- Peng, D.F., Hu, T.L., Jiang, A., Washington, M.K., Moskaluk, C.A., Schneider-Stock, R. & El-Rifai, W. 2011, 'Location-specific epigenetic regulation of the metallothionein 3 gene in esophageal adenocarcinomas', *PLoS One*, vol. 6, no. 7, pp. 1–10.
- Peng, J., Monsivais, D., You, R., Zhong, H., Pangas, S.A. & Matzuk, M.M. 2015, 'Uterine

- activin receptor-like kinase 5 is crucial for blastocyst implantation and placental development', *Proceedings of the National Academy of Sciences of the United States of America*, vol. 112, no. 36, pp. E5098-107.
- Pennington, K.A. & Ealy, A.D. 2012, 'The expression and potential function of bone morphogenetic proteins 2 and 4 in bovine trophectoderm', *Reproductive Biology and Endocrinology*, vol. 10, no. 1, p. 12.
- Perez-Garcia, V., Fineberg, E., Wilson, R., Murray, A., Mazzeo, C.I., Tudor, C., Sienerth, A., White, J.K., Tuck, E., Ryder, E.J., Gleeson, D., Siragher, E., Wardle-Jones, H., Staudt, N., Wali, N., Collins, J., Geyer, S., Busch-Nentwich, E.M., Galli, A., Smith, J.C., Robertson, E., Adams, D.J., Weninger, W.J., Mohun, T. & Hemberger, M. 2018, 'Placentation defects are highly prevalent in embryonic lethal mouse mutants', *Nature*, vol. 555, no. 7697, pp. 463–8.
- Perrin, B.J. & Ervasti, J.M. 2010, 'The actin gene family: Function follows isoform', *Cytoskeleton*, vol. 67, no. 10, pp. 630–4.
- Pickell, L., Li, D., Brown, K., Mikael, L.G., Wang, X.L., Wu, Q., Luo, L., Jerome-Majewska, L. & Rozen, R. 2009, 'Methylenetetrahydrofolate reductase deficiency and low dietary folate increase embryonic delay and placental abnormalities in mice', *Birth Defects Research Part A - Clinical and Molecular Teratology*, vol. 85, no. 6, pp. 531–41.
- Piedrahita, J.A., Oetama, B., Bennett, G.D., van Waes, J., Kamen, B.A., Richardson, J., Lacey, S.W., Anderson, R.G.W. & Finnell, R.H. 1999, 'Mice lacking the folic acid-binding protein Folbp1 are defective in early embryonic development', *Nature Genetics*, vol. 23, p. 228.
- Pilu, R. 2011, 'Paramutation: just a curiosity or fine tuning of gene expression in the next generation?', *Current Genomics*, vol. 12, no. 4, pp. 298–306.
- Pinheiro, I., Margueron, R., Shukeir, N., Eisold, M., Fritsch, C., Richter, F.M., Mittler, G., Genoud, C., Goyama, S., Kurokawa, M., Son, J., Reinberg, D., Lachner, M. & Jenuwein, T. 2012, 'Prdm3 and Prdm16 are H3K9me1 Methyltransferases Required for Mammalian Heterochromatin Integrity', *Cell*, vol. 150, no. 5, pp. 948–60.
- Piyathilake, C.J., Johanning, G.L., Macaluso, M., Whiteside, M., Oelschlager, D.K., Heimburger, D.C. & Grizzle, W.E. 2000, 'Localized Folate and Vitamin B-12

- Deficiency in Squamous Cell Lung Cancer Is Associated With Global DNA Hypomethylation', *Nutrition and Cancer*, vol. 37, no. 1, pp. 99–107.
- Plaisier, M. 2011, 'Decidualisation and angiogenesis', *Best Practice & Research Clinical Obstetrics & Gynaecology*, vol. 25, no. 3, pp. 259–71.
- Plaks, V., Rinkenberger, J., Dai, J., Flannery, M., Sund, M., Kanasaki, K., Ni, W., Kalluri, R. & Werb, Z. 2013, 'Matrix metalloproteinase-9 deficiency phenocopies features of preeclampsia and intrauterine growth restriction', *Proceedings of the National Academy of Sciences of the United States of America*, vol. 110, no. 27, pp. 11109–14.
- Pogribny, I.P., Basnakian, A.G., Miller, B.J., Pogribny, I.P., Basnakian, A.G., Miller, B.J., Lopatina, N.G., Poirier, L.A. & James, S.J. 1995, 'Breaks in genomic DNA and within the p53 gene are associated with hypomethylation in livers of folate/methyl-deficient rats', *Cancer Research*, vol. 55, no. 9, pp. 1894–901.
- Poletini, M.O., Kennett, J.E., McKee, D.T. & Freeman, M.E. 2010, 'Central clock regulates the cervically stimulated prolactin surges by modulation of dopamine and vasoactive intestinal polypeptide release in ovariectomized rats', *Neuroendocrinology*, vol. 91, no. 2, pp. 179–88.
- Pollheimer, J., Vondra, S., Baltayeva, J., Beristain, A.G. & Knofler, M. 2018, 'Regulation of placental extravillous trophoblasts by the maternal uterine environment', *Frontiers in Immunology*, vol. 9, p. 2597.
- Port, C.B., Bowen, J.M., Keyes, P.L. & Townson, D.H. 2000, 'Effects of a 3beta-hydroxysteroid dehydrogenase inhibitor on monocyte-macrophage infiltration into rat corpus luteum and on apoptosis: relationship to the luteolytic action of prolactin', *Journal of Reproduction and Fertility*, vol. 119, no. 1, pp. 93–9.
- Potts, R.C., Zhang, P., Wurster, A.L., Precht, P., Mughal, M.R., Wood, W.H. 3rd, Zhang, Y., Becker, K.G., Mattson, M.P. & Pazin, M.J. 2011, 'CHD5, a brain-specific paralog of Mi2 chromatin remodeling enzymes, regulates expression of neuronal genes', *PLoS One*, vol. 6, no. 9, p. e24515.
- Quinn, M. & Fujimoto, V. 2016, 'Racial and ethnic disparities in assisted reproductive technology access and outcomes', *Fertility and Sterility*, vol. 105, no. 5, pp. 1119–23.

- Raabe, M., Flynn, L.M., Zlot, C.H., Wong, J.S., Véniant, M.M., Hamilton, R.L. & Young, S.G. 1998, 'Knockout of the abetalipoproteinemia gene in mice: Reduced lipoprotein secretion in heterozygotes and embryonic lethality in homozygotes', *Proceedings of the National Academy of Sciences*, vol. 95, no. 15, p. 8686 LP-8691.
- Raheem, K.A. 2018, 'Cytokines, growth factors and macromolecules as mediators of implantation in mammalian species', *International Journal of Veterinary Science and Medicine*, vol. 6, pp. S6–14.
- Rahima, A. & Soderwall, A.L. 1977, 'Uterine collagen content in young and senescent pregnant golden hamsters', *Journal of Reproduction and Fertility*, vol. 49, no. 1, pp. 161–2.
- Rai, A. & Cross, J.C. 2014, 'Development of the hemochorial maternal vascular spaces in the placenta through endothelial and vasculogenic mimicry', *Developmental Biology*, vol. 387, no. 2, pp. 131–41.
- Rajaraman, G., Murthi, P., Pathirage, N., Brennecke, S.P. & Kalionis, B. 2010, 'Downstream targets of homeobox gene HLX show altered expression in human idiopathic fetal growth restriction', *The American Journal of Pathology*, vol. 176, no. 1, pp. 278–87.
- Rakoczy, J., Lee, S., Weerasekera, S.J., Simmons, D.G. & Dawson, P.A. 2015, 'Placental and fetal cysteine dioxygenase gene expression in mouse gestation', *Placenta*, vol. 36, no. 8, pp. 956–9.
- Rakoczy, J., Padmanabhan, N., Krzak, A.M., Kieckbusch, J., Cindrova-Davies, T. & Watson, E.D. 2017, 'Dynamic expression of TET1, TET2, and TET3 dioxygenases in mouse and human placentas throughout gestation', *Placenta*, vol. 59, pp. 46–56.
- Ramathal, C.Y., Bagchi, I.C., Taylor, R.N. & Bagchi, M.K. 2010, 'Endometrial decidualization: of mice and men', *Seminars in Reproductive Medicine*, vol. 28, no. 1, pp. 17–26.
- Rameix-Welti, M.A., Le Goffic, R., Hervé, P.L., Sourimant, J., Rémot, A., Riffault, S., Yu, Q., Galloux, M., Gault, E. & Eléouët, J.F. 2014, 'Visualizing the replication of respiratory syncytial virus in cells and in living mice', *Nature Communications*, vol. 5, no. 5104.

- Rasmussen, C.A., Hashizume, K., Orwig, K.E., Xu, L. & Soares, M.J. 1996, 'Decidual prolactin-related protein: heterologous expression and characterization', *Endocrinology*, vol. 137, no. 12, pp. 5558–66.
- Rasmussen, C.A., Orwig, K.E., Vellucci, S. & Soares, M.J. 1997, 'Dual expression of prolactin-related protein in decidua and trophoblast tissues during pregnancy in rats', *Biology of Reproduction*, vol. 56, no. 3, pp. 647–54.
- Ravelli, A.C., van Der Meulen, J.H., Osmond, C., Barker, D.J. & Bleker, O.P. 1999, 'Obesity at the age of 50 y in men and women exposed to famine prenatally', *The American Journal of Clinical Nutrition*, vol. 70, no. 5, pp. 811–6.
- Ray, J.G. & Laskin, C.A. 1999, 'Folic acid and homocyst(e)ine metabolic defects and the risk of placental abruption, pre-eclampsia and spontaneous pregnancy loss: A systematic review', *Placenta*, vol. 20, no. 7, pp. 519–29.
- Reardon, S.N., King, M.L., MacLean, J.A., Mann, J.L., DeMayo, F.J., Lydon, J.P. & Hayashi, K. 2012, 'Cdh1 Is Essential for Endometrial Differentiation, Gland Development, and Adult Function in the Mouse Uterus', *Biology of Reproduction*, vol. 86, no. 5, pp. 1–10.
- Redline, R.W. & Pappin, A. 1995, 'Fetal thrombotic vasculopathy: The clinical significance of extensive avascular villi', *Human Pathology*, vol. 26, no. 1, pp. 80–5.
- Reidy, J.A. 1988, 'Role of deoxyuridine incorporation and DNA repair in the expression of human chromosomal fragile sites.', *Mutation Research*, vol. 200, no. 1–2, pp. 215–20.
- Reisman, L.E. 1970, 'Chromosome abnormalities and intrauterine growth retardation', *Pediatric clinics of North America*, vol. 17, no. 1, pp. 101–10.
- Relton, C.L., Wilding, C.S., Laffling, A.J., Jonas, P.A., Burgess, T., Binks, K., Tawn, E.J. & Burn, J. 2004, 'Low erythrocyte folate status and polymorphic variation in folate-related genes are associated with risk of neural tube defect pregnancy', *Molecular Genetics and Metabolism*, vol. 81, no. 4, pp. 273–81.
- Relton, C.L., Wilding, C.S., Pearce, M.S., Laffling, A.J., Jonas, P.A., Lynch, S.A., Tawn, E.J. & Burn, J. 2004, 'Gene-gene interaction in folate-related genes and risk of neural tube defects in a UK population', *Journal of Medical Genetics*, vol. 41, no. 4, pp. 256–60.

- Ren, A., Wang, J., Ye, R.W., Li, S., Liu, J.M. & Li, Z. 2007, 'Low first-trimester hemoglobin and low birth weight, preterm birth and small for gestational age newborns', *International Journal of Gynaecology and Obstetrics*, vol. 98, no. 2, pp. 124–8.
- Rendi, M.H., Muehlenbachs, A., Garcia, R.L. & Boyd, K.L. 2012, 'Chapter 17 - Female Reproductive System', in P.M. Treuting & S.M.B.T.-C.A. and H. Dintzis (eds), *Comparative Anatomy and Histology*, Academic Press, San Diego, pp. 253–84.
- Rennie, M.Y., Rahman, A., Whiteley, K.J., Sled, J.G. & Adamson, S.L. 2014, 'Site-Specific Increases in Utero- and Fetoplacental Arterial Vascular Resistance in eNOS-Deficient Mice Due to Impaired Arterial Enlargement', *Biology of Reproduction*, vol. 92, no. 2.
- Ribarska, T., Ingenwerth, M., Goering, W., Engers, R. & Schulz, W. 2010, 'Epigenetic inactivation of the placentally imprinted tumor suppressor gene Tfpi2 in prostate carcinoma', *Cancer Genomics - Proteomics*, vol. 7, no. 2, pp. 51–60.
- Rider, V. 2002, 'Progesterone and the control of uterine cell proliferation and differentiation', *Frontiers in Bioscience*, vol. 7, pp. d1545-55.
- Riesewijk, A. 2003, 'Gene expression profiling of human endometrial receptivity on days LH+2 versus LH+7 by microarray technology', *Molecular Human Reproduction*, vol. 9, no. 5, pp. 253–64.
- Rimon-Dahari, N., Yerushalmi-Heinemann, L., Alyagor, L. & Dekel, N. 2016, 'Chapter 7 - Ovarian Folliculogenesis', in R.P. Piprek (ed.), *Molecular Mechanisms of Cell Differentiation in Gonad Development*, Springer International Publishing, Cham, pp. 167–90.
- Ringnér, M. 2008, 'What is principal component analysis?', *Nature Biotechnology*, vol. 26, no. 3, pp. 303–4.
- Risk, M. & Gibori, G. 2001, 'Mechanism of luteal cell regulation by prolactin', in N.D. Horseman (ed.), *Prolactin*, Springer US, Boston, MA, pp. 265–95.
- Rispoli, L.A. & Nett, T.M. 2005, 'Pituitary gonadotropin-releasing hormone (GnRH) receptor: Structure, distribution and regulation of expression', *Animal Reproduction Science*, vol. 88, no. 1, pp. 57–74.
- Rivera, M., Stein, P., Weaver, J.R., Mager, J. & Á, R.M.S. 2008, 'Manipulations of mouse

- embryos prior to implantation result in aberrant expression of imprinted genes on day 9.5 of development', *Human Molecular Genetics*, vol. 17, no. 1, pp. 1–14.
- Roberts, D.J. & Post, M.D. 2008, 'The placenta in pre-eclampsia and intrauterine growth restriction', *Journal of Clinical Pathology*, vol. 61, no. 12, pp. 1254–60.
- Robinson, J.L., McBreaity, L.E., Randell, E.W., Brunton, J.A. & Bertolo, R.F. 2016, 'Restriction of dietary methyl donors limits methionine availability and affects the partitioning of dietary methionine for creatine and phosphatidylcholine synthesis in the neonatal piglet', *The Journal of Nutritional Biochemistry*, vol. 35, pp. 81–6.
- Roby, K.F., Deb, S., Giboriti, G., Szpirer, C., Tlt, S.C.M.K. & Soaressii, M.J. 1993, 'Decidual prolactin-related protein. Identification, molecular cloning, and characterization', *The Journal of Biological Chemistry*, vol. 268, no. 5, pp. 3136–42.
- Roh, C.-R., Budhreja, V., Kim, H.-S., Nelson, D.M. & Sadovsky, Y. 2005, 'Microarray-based identification of differentially expressed genes in hypoxic term human trophoblasts and in placental villi of pregnancies with growth restricted fetuses.', *Placenta*, vol. 26, no. 4, pp. 319–28.
- Rombauts, L., Motteram, C., Berkowitz, E. & Fernando, S. 2014, 'Risk of placenta praevia is linked to endometrial thickness in a retrospective cohort study of 4537 singleton assisted reproduction technology births', *Human Reproduction*, vol. 29, no. 12, pp. 2787–93.
- de Rooij, S.R., Painter, R.C., Roseboom, T.J., Phillips, D.I.W., Osmond, C., Barker, D.J.P., Tanck, M.W., Michels, R.P.J., Bossuyt, P.M.M. & Bleker, O.P. 2006, 'Glucose tolerance at age 58 and the decline of glucose tolerance in comparison with age 50 in people prenatally exposed to the Dutch famine', *Diabetologia*, vol. 49, no. 4, pp. 637–43.
- Roos, S., Kanai, Y., Prasad, P.D., Powell, T.L. & Jansson, T. 2009, 'Regulation of placental amino acid transporter activity by mammalian target of rapamycin', *American Journal of Physiology. Cell Physiology*, vol. 296, no. 1, pp. C142-50.
- Rosario, F.J., Nathanielsz, P.W., Powell, T.L. & Jansson, T. 2017, 'Maternal folate deficiency causes inhibition of mTOR signaling, down-regulation of placental amino acid transporters and fetal growth restriction in mice', *Scientific Reports*, vol. 7, no. 1, p. 3982.

- Rosario, F.J., Powell, T.L. & Jansson, T. 2017, 'mTOR folate sensing links folate availability to trophoblast cell function', *The Journal of Physiology*, vol. 595, no. 13, pp. 4189–206.
- Rosenberg, A. 2008, 'The IUGR newborn', *Seminars in Perinatology*, vol. 32, no. 3, pp. 219–24.
- Rosenfeld, C.S. 2015, 'Sex-specific placental responses in fetal development', *Endocrinology*, vol. 156, no. 10, pp. 3422–34.
- Rossant, J. & Cross, J.C. 2001, 'Placental development: lessons from mouse mutants', *Nature Reviews Genetics*, vol. 2, no. 7, pp. 538–48.
- Rossell, D., Stephan-Otto Attolini, C., Kroiss, M. & Stocker, A. 2014, 'Quantifying alternative splicing from paired-end RNA-sequencing data', *The Annals of Applied Statistics*, vol. 8, no. 1, pp. 309–30.
- Rouhi, A., Lai, C.B., Cheng, T.P., Takei, F., Yokoyama, W.M. & Mager, D.L. 2009, 'Evidence for high bi-allelic expression of activating Ly49 receptors', *Nucleic Acids Research*, vol. 37, no. 16, pp. 5331–42.
- Ruane, P.T., Berneau, S.C., Koeck, R., Watts, J., Kimber, S.J., Brison, D.R., Westwood, M. & Aplin, J.D. 2017, 'Apposition to endometrial epithelial cells activates mouse blastocysts for implantation', *Molecular Human Reproduction*, vol. 23, no. 9, pp. 617–27.
- Rueda-Clausen, C.F., Davidge, S.T., Lopaschuk, G.D. & Morton, J.S. 2011, 'Long-term effects of intrauterine growth restriction on cardiac metabolism and susceptibility to ischaemia/reperfusion', *Cardiovascular Research*, vol. 90, no. 2, pp. 285–94.
- Sakane, J., Taniyama, K., Miyamoto, K., Saito, A., Kuraoka, K., Nishimura, T., Sentani, K., Oue, N. & Yasui, W. 2015, 'Aberrant DNA methylation of DLX4 and SIM1 is a predictive marker for disease progression of uterine cervical low-grade squamous intraepithelial lesion', *Diagnostic Cytopathology*, vol. 43, no. 6, pp. 462–70.
- Salbaum, J.M., Kruger, C. & Kappen, C. 2013, 'Mutation at the folate receptor 4 locus modulates gene expression profiles in the mouse uterus in response to periconceptual folate supplementation', *Biochimica et Biophysica Acta*, vol. 1832, no. 10, pp. 1653–61.
- Salojin, K. V., Cabrera, R.M., Sun, W., Chang, W.C., Lin, C., Duncan, L., Platt, K.A., Read,

- R., Vogel, P., Liu, Q., Finnell, R.H. & Oravec, T. 2011, 'A mouse model of hereditary folate malabsorption: deletion of the PCFT gene leads to systemic folate deficiency', *Blood*, vol. 117, no. 18, pp. 4895–904.
- Samaiya, M., Bakhshi, S., Shukla, A.A., Kumar, L. & Chauhan, S.S. 2011, 'Epigenetic regulation of cathepsin L expression in chronic myeloid leukaemia', *Journal of Cellular and Molecular Medicine*, vol. 15, no. 10, pp. 2189–99.
- Sandgren, J.A., Deng, G., Linggonegoro, D.W., Scroggins, S.M., Perschbacher, K.J., Nair, A.R., Nishimura, T.E., Zhang, S.Y., Agbor, L.N., Wu, J., Keen, H.L., Naber, M.C., Pearson, N.A., Zimmerman, K.A., Weiss, R.M., Bowdler, N.C., Usachev, Y.M., Santillan, D.A., Potthoff, M.J., Pierce, G.L., Gibson-Corley, K.N., Sigmund, C.D., Santillan, M.K. & Grobe, J.L. 2018, 'Arginine vasopressin infusion is sufficient to model clinical features of preeclampsia in mice', *JCI Insight*, vol. 3, no. 19.
- Sandovici, I., Hoelle, K., Angiolini, E. & Constância, M. 2012, 'Placental adaptations to the maternal-fetal environment: Implications for fetal growth and developmental programming', *Reproductive BioMedicine Online*, vol. 25, no. 1, pp. 68–89.
- Sasaki, M., Knobbe, C.B., Munger, J.C., Lind, E.F., Brenner, D., Brüstle, A., Harris, I.S., Holmes, R., Wakeham, A., Haight, J., You-Ten, A., Li, W.Y., Schalm, S., Su, S.M., Virtanen, C., Reifemberger, G., Ohashi, P.S., Barber, D.L., Figueroa, M.E., Melnick, A., Zúñiga-Pflücker, J.-C. & Mak, T.W. 2012, 'IDH1(R132H) mutation increases murine haematopoietic progenitors and alters epigenetics', *Nature*, vol. 488, no. 7413, pp. 656–9.
- Sato, J., Nasu, M. & Tsuchitani, M. 2016, 'Comparative histopathology of the estrous or menstrual cycle in laboratory animals', *Journal of Toxicologic Pathology*, vol. 29, no. 3, 2016/05/16., pp. 155–62.
- Scanlon, K.S., Yip, R., Schieve, L.A. & Cogswell, M.E. 2000, 'High and low hemoglobin levels during pregnancy: differential risks for preterm birth and small for gestational age', *Obstetrics and Gynecology*, vol. 96, no. 5 Pt 1, pp. 741–8.
- Schieve, L.A., Cohen, B., Nannini, A., Ferre, C., Reynolds, M.A., Zhang, Z., Jeng, G., Macaluso, M. & Wright, V.C. 2007, 'A population-based study of maternal and perinatal outcomes associated with assisted reproductive technology in Massachusetts',

Maternal and Child Health Journal, vol. 11, no. 6, pp. 517–25.

Schneider, C.A., Rasband, W.S. & Eliceiri, K.W. 2012, 'NIH Image to ImageJ: 25 years of image analysis', *Nature Methods*, vol. 9, p. 671.

Schneider, R., Bannister, A.J., Myers, F.A., Thorne, A.W., Crane-Robinson, C. & Kouzarides, T. 2004, 'Histone H3 lysine 4 methylation patterns in higher eukaryotic genes', *Nature Cell Biology*, vol. 6, no. 1, pp. 73–7.

Scifres, C.M. & Nelson, D.M. 2009, 'Intrauterine growth restriction, human placental development and trophoblast cell death', *Journal of Physiology*, vol. 587, no. pt14, pp. 3453–8.

Sehgal, A., Crispi, F. & Boode, W. De 2017, 'Clinician performed ultrasound in fetal growth restriction: fetal, neonatal and pediatric aspects', *Journal of Perinatology*, vol. 37, no. 12, pp. 1251–8.

Seller, M.J. 1987, 'Neural tube defects and sex ratios', *American Journal of Medical Genetics*, vol. 26, no. 3, pp. 699–707.

Seremak-Mrozikiewicz, A., Bogacz, A., Deka-Pawlik, D., Klejewski, A., Wolski, H., Drews, K., Karasiewicz, M. & Czerny, B. 2017, 'The polymorphisms of methionine synthase (MTR) and methionine synthase reductase (MTRR) genes in pathogenesis of preeclampsia', *The Journal of Maternal-fetal & Neonatal Medicine*, vol. 30, no. 20, pp. 2498–504.

Sferruzzi-Perri, A.N. 2018, 'Assessment of placental transport function in studies of disease programming', *Methods in Molecular Biology*, vol. 1735, pp. 239–50.

Sferruzzi-Perri, A.N., Macpherson, A.M., Roberts, C.T. & Robertson, S.A. 2009, 'Csf2 null mutation alters placental gene expression and trophoblast glycogen cell and giant cell abundance in mice', *Biology of Reproduction*, vol. 81, no. 1, pp. 207–21.

Shane, B. & Stokstad, E.L.R. 1985, 'Vitamin B12 - Folate interrelationships', *Annual Review of Nutrition*, vol. 5, pp. 115–41.

Sharma, D., Shastri, S. & Sharma, P. 2016, 'Intrauterine Growth Restriction: Antenatal and Postnatal Aspects', *Clinical Medicine Insights: Pediatrics*, vol. 10, pp. 67–83.

Shi, L. & Wu, J. 2009, 'Epigenetic regulation in mammalian preimplantation embryo

- development', *Reproductive Biology and Endocrinology*, vol. 7, p. 59.
- Shiura, H., Nakamura, K., Hikichi, T., Hino, T., Oda, K., Suzuki-migishima, R., Kohda, T., Kaneko-ishino, T. & Ishino, F. 2009, 'Paternal deletion of Meg1 / Grb10 DMR causes maternalization of the Meg1 / Grb10 cluster in mouse proximal chromosome 11 leading to severe pre- and postnatal growth retardation', *Human Molecular Genetics*, vol. 18, no. 8, pp. 1–2.
- Sibley, C., Glazier, J. & D'Souza, S. 1997, 'Placental transporter activity and expression in relation to fetal growth', *Experimental Physiology*, vol. 82, no. 2, pp. 389–402.
- Sibley, C.P., Brownbill, P., Dilworth, M. & Glazier, J.D. 2010, 'Review: Adaptation in placental nutrient supply to meet fetal growth demand: implications for programming', *Placenta*, vol. 31 Suppl, pp. S70–4.
- Sibley, C.P., Coan, P.M., Ferguson-Smith, A.C., Dean, W., Hughes, J., Smith, P., Reik, W., Burton, G.J., Fowden, A.L. & Constancia, M. 2004, 'Placental-specific insulin-like growth factor 2 (Igf2) regulates the diffusional exchange characteristics of the mouse placenta', *Proceedings of the National Academy of Sciences of the United States of America*, vol. 101, no. 21, pp. 8204–8.
- Silva, J.F. & Serakides, R. 2016, 'Intrauterine trophoblast migration: A comparative view of humans and rodents.', *Cell Adhesion & Migration*, vol. 10, no. 1–2, pp. 88–110.
- da Silva, R.P., Kelly, K.B., Al Rajabi, A. & Jacobs, R.L. 2014, 'Novel insights on interactions between folate and lipid metabolism', *BioFactors*, vol. 40, no. 3, 2013/12/18., pp. 277–83.
- Silver, L.M. 1995, *Mouse genetics: concepts and applications*, *Mouse Genetics: Concepts and Applications*, 1st edn, Oxford University Press, New York.
- Simmons, D.G. & Cross, J.C. 2005, 'Determinants of trophoblast lineage and cell subtype specification in the mouse placenta', *Developmental Biology*, vol. 284, no. 1, pp. 12–24.
- Simmons, D.G., Rawn, S., Davies, A., Hughes, M. & Cross, J.C. 2008, 'Spatial and temporal expression of the 23 murine Prolactin/Placental Lactogen-related genes is not associated with their position in the locus', *BMC Genomics*, vol. 9, no. 352.
- Simmons, R.A., Templeton, L.J. & Gertz, S.J. 2001, 'Intrauterine growth retardation leads to

- the development of type 2 diabetes in the rat.’, *Diabetes*, vol. 50, no. 10, pp. 2279–86.
- Simon, L., Spiewak, K.A., Ekman, G.C., Kim, J., Lydon, J.P., Bagchi, M.K., Bagchi, I.C., DeMayo, F.J. & Cooke, P.S. 2009, ‘Stromal progesterone receptors mediate induction of Indian Hedgehog (IHH) in uterine epithelium and its downstream targets in uterine stroma.’, *Endocrinology*, vol. 150, no. 8, pp. 3871–6.
- Sinclair, K.D., Allegrucci, C., Singh, R., Gardner, D.S., Sebastian, S., Bispham, J., Thurston, A., Huntley, J.F., Rees, W.D., Maloney, C.A., Lea, R.G., Craigon, J., McEvoy, T.G. & Young, L.E. 2007, ‘DNA methylation, insulin resistance, and blood pressure in offspring determined by maternal periconceptional B vitamin and methionine status.’, *Proceedings of the National Academy of Sciences of the United States of America*, vol. 104, no. 49, pp. 19351–6.
- Sirnes, S., Honne, H., Ahmed, D., Danielsen, S.A., Rognum, T.O., Meling, G.I., Leithe, E., Rivedal, E., Lothe, R.A. & Lind, G.E. 2011, ‘DNA methylation analyses of the connexin gene family reveal silencing of GJC1 (Connexin45) by promoter hypermethylation in colorectal cancer’, *Epigenetics*, vol. 6, no. 5, pp. 602–9.
- Sittig, L.J., Herzing, L.B.K., Xie, H., Batra, K.K., Shukla, P.K. & Redei, E.E. 2012, ‘Excess folate during adolescence suppresses thyroid function with permanent deficits in motivation and spatial memory’, *Genes, Brain and Behavior*, vol. 11, no. October 2011, pp. 193–200.
- Smith, B.T., Mussell, J.C., Fleming, P.A., Barth, J.L., Spyropoulos, D.D., Cooley, M.A., Drake, C.J. & Argraves, S. 2006, ‘Targeted disruption of cubilin reveals essential developmental roles in the structure and function of endoderm and in somite formation’, *BMC Developmental Biology*, vol. 6, no. 30.
- Smith, C.J. & Ryckman, K.K. 2015, ‘Epigenetic and developmental influences on the risk of obesity, diabetes, and metabolic syndrome’, *Diabetes, Metabolic Syndrome and Obesity: Targets and Therapy*, vol. 8, pp. 295–302.
- Smith, D., Ordovas, J., Selhub, J., Mason, J.B., Fleet, J.C., Christman, J.K., Cravo, M.L., Salomon, R.N. & Kim, Y.I. 1995, ‘Moderate folate deficiency does not cause global hypomethylation of hepatic and colonic DNA or c-myc-specific hypomethylation of colonic DNA in rats’, *The American Journal of Clinical Nutrition*, vol. 61, no. 5, pp.

1083–90.

- Smith, P., Nicholson, L.J., Syed, N., Payne, A., Hiller, L., Garrone, O., Occelli, M., Gasco, M. & Crook, T. 2007, 'Epigenetic Inactivation Implies Independent Functions for Insulin-like Growth Factor Binding Protein (IGFBP) - Related Protein 1 and the Related IGFBPL1 in Inhibiting Breast Cancer Phenotypes', *Human Cancer Biology*, vol. 13, no. 14, pp. 4061–9.
- Smith, S.C., Baker, P.N. & Symonds, E.M. 1997, 'Increased placental apoptosis in intrauterine growth restriction', *American Journal of Obstetrics & Gynecology*, vol. 177, no. 6, pp. 1395–401.
- Smulders, Y.M., Smith, D.E.C., Kok, R.M., Teerlink, T., Swinkels, D.W., Stehouwer, C.D.A. & Jakobs, C. 2006, 'Cellular folate vitamers distribution during and after correction of vitamin B12 deficiency: A case for the methylfolate trap', *British Journal of Haematology*, vol. 132, no. 5, pp. 623–9.
- Soares, M.J., Chakraborty, D., Kubota, K., Renaud, S.J. & Rumi, M.A.K. 2014, 'Adaptive mechanisms controlling uterine spiral artery remodeling during the establishment of pregnancy', *The International Journal of Developmental Biology*, vol. 58, no. 2–4, pp. 247–59.
- Solano, M.E., Thiele, K., Kowal, M.K. & Arck, P.C. 2016, 'Identification of suitable reference genes in the mouse placenta', *Placenta*, vol. 39, pp. 7–15.
- Söldner, E., Rohr, I., Kremser, C., Hutzler, P. & Debbage, P.L. 2009, 'Imaging of placental transport mechanisms: A review', *European Journal of Obstetrics Gynecology and Reproductive Biology*, vol. 144, no. Suppl 1, pp. 114–20.
- Sonderregger, S., Pollheimer, J. & Knöfler, M. 2010, 'Wnt signalling in implantation, decidualisation and placental differentiation - Review', *Placenta*, vol. 31, no. 10, pp. 839–47.
- Song, G., Bazer, F.W. & Spencer, T.E. 2007, 'Differential expression of cathepsins and cystatin C in ovine uteroplacental tissues', *Placenta*, vol. 28, no. 10, pp. 1091–8.
- Song, H., Han, K. & Lim, H. 2007, 'Progesterone supplementation extends uterine receptivity for blastocyst implantation in mice', *Reproduction*, vol. 133, no. 2, pp. 487–93.

- Song, H. & Lim, H. 2006, 'Evidence for heterodimeric association of leukemia inhibitory factor (LIF) receptor and gp130 in the mouse uterus for LIF signaling during blastocyst implantation', *Reproduction*, vol. 131, no. 2, pp. 341–9.
- Song, H., Lim, H., Paria, B.C., Matsumoto, H., Swift, L.L., Morrow, J., Bonventre, J. V & Dey, S.K. 2002, 'Cytosolic phospholipase A2alpha is crucial [correction of A2alpha deficiency is crucial] for "on-time" embryo implantation that directs subsequent development', *Development*, vol. 129, no. 12, pp. 2879–89.
- Spencer, T.E., Hayashi, K., Hu, J. & Carpenter, K.D.B.T.-C.T. in D.B. 2005, 'Comparative developmental biology of the mammalian uterus', *Current Topics in Developmental Biology*, vol. 68, Academic Press, pp. 85–122.
- Sram, R.J., Binkova, B., Lnenickova, Z., Solansky, I. & Dejmek, J. 2005, 'The impact of plasma folate levels of mothers and newborns on intrauterine growth retardation and birth weight', *Mutation Research*, vol. 591, no. 1–2, pp. 302–10.
- Sroga, J.M., Ma, X. & Das, S.K. 2012, 'Developmental regulation of decidual cell polyploidy at the site of implantation', *Frontiers in Bioscience*, vol. 4, pp. 1475–86.
- Stamatoyannopoulos, J.A., Snyder, M., Hardison, R., Ren, B., Gingeras, T., Gilbert, D.M., Groudine, M., Bender, M., Kaul, R., Canfield, T., Giste, E., Johnson, A., Zhang, M., Balasundaram, G., Byron, R., Roach, V., Sabo, P.J., Sandstrom, R., Stehling, A.S., Thurman, R.E., Weissman, S.M., Cayting, P., Hariharan, M., Lian, J., Cheng, Y., Landt, S.G., Ma, Z., Wold, B.J., Dekker, J., Crawford, G.E., Keller, C.A., Wu, W., Morrissey, C., Kumar, S.A., Mishra, T., Jain, D., Byrsk-Bishop, M., Blankenberg, D., Lajoie, B.R., Jain, G., Sanyal, A., Chen, K.-B., Denas, O., Taylor, J., Blobel, G.A., Weiss, M.J., Pimkin, M., Deng, W., Marinov, G.K., Williams, B.A., Fisher-Aylor, K.I., Desalvo, G., Kiralusha, A., Trout, D., Amrhein, H., Mortazavi, A., Edsall, L., McCleary, D., Kuan, S., Shen, Y., Yue, F., Ye, Z., Davis, C.A., Zaleski, C., Jha, S., Xue, C., Dobin, A., Lin, W., Fastuca, M., Wang, H., Guigo, R., Djebali, S., Lagarde, J., Ryba, T., Sasaki, T., Malladi, V.S., Cline, M.S., Kirkup, V.M., Learned, K., Rosenbloom, K.R., Kent, W.J., Feingold, E.A., Good, P.J., Pazin, M., Lowdon, R.F., Adams, L.B. & Consortium, M.E. 2012, 'An encyclopedia of mouse DNA elements (Mouse ENCODE)', *Genome Biology*, vol. 13, no. 8, p. 418.
- Stegers-Theunissen, R.P., Smith, S.C., Steegers, E.A., Guilbert, L.J. & Baker, P.N. 2000,

- 'Folate affects apoptosis in human trophoblastic cells', *BJOG*, vol. 107, no. 12, pp. 1513–5.
- Stevens, D.U., Al-Nasiry, S., Bulten, J. & Spaanderman, M.E.A. 2012, 'Decidual vasculopathy and adverse perinatal outcome in preeclamptic pregnancy', *Placenta*, vol. 33, no. 8, pp. 630–3.
- Stewart, C.L., Kaspar, P., Brunet, L.J., Bhatt, H., Gadi, I., Kontgen, F. & Abbondanzo, S.J. 1992, 'Blastocyst implantation depends on maternal expression of leukaemia inhibitory factor.', *Nature*, vol. 359, no. 6390, pp. 76–9.
- Stieber, J., Herrmann, S., Feil, S., Loster, J., Feil, R., Biel, M., Hofmann, F. & Ludwig, A. 2003, 'The hyperpolarization-activated channel HCN4 is required for the generation of pacemaker action potentials in the embryonic heart', *Proceedings of the National Academy of Sciences of the United States of America*, vol. 100, no. 25, pp. 15235–40.
- Stocco, C. 2012, 'The long and short of the prolactin receptor: the corpus luteum needs them both!', *Biology of Reproduction*, vol. 86, no. 3, p. 85.
- Stockmann, C. & Fandrey, J. 2006, 'Hypoxia-induced erythropoietin production: a paradigm for oxygen-regulated gene expression', *Clinical and Experimental Pharmacology and Physiology*, vol. 33, no. 10, pp. 968–79.
- Strumpf, D., Mao, C.-A., Yamanaka, Y., Ralston, A., Chawengsaksophak, K., Beck, F. & Rossant, J. 2005, 'Cdx2 is required for correct cell fate specification and differentiation of trophoblast in the mouse blastocyst', *Development*, vol. 132, no. 9, pp. 2093–102.
- Stryjewska, A., Dries, R., Pieters, T., Verstappen, G., Conidi, A., Coddens, K., Francis, A., Umans, L., Van Ijcken, W.F.J., Berx, G., Van Grunsven, L.A., Grosveld, F.G., Goossens, S., Haigh, J.J. & Huylebroeck, D. 2017, 'Zeb2 regulates cell fate at the exit from epiblast state in mouse embryonic stem cells', *Stem Cells*, vol. 35, no. 3, pp. 611–25.
- Stuckenholz, C., Lu, L., Thakur, P.C., Choi, T.Y., Shin, D. & Bahary, N. 2013, 'Sfrp5 Modulates Both Wnt and BMP Signaling and Regulates Gastrointestinal Organogenesis in the Zebrafish, *Danio rerio*', *PLoS One*, vol. 8, no. 4, p. e62470.
- Stumpo, D.J., Byrd, N.A., Phillips, R.S., Ghosh, S., Maronpot, R.R., Castranio, T., Meyers,

- E.N., Mishina, Y. & Blackshear, P.J. 2004, 'Chorioallantoic Fusion Defects and Embryonic Lethality Resulting from Disruption of Zfp36L1, a Gene Encoding a CCCH Tandem Zinc Finger Protein of the Tristetraprolin Family', *Molecular and Cellular Biology*, vol. 24, no. 14, pp. 6445–55.
- Suenaga, K., Kitahara, S., Suzuki, Y., Kobayashi, M., Horie, S., Sugawara, J., Yaegashi, N. & Sato, Y. 2014, 'Role of the vasohibin family in the regulation of fetoplacental vascularization and syncytiotrophoblast formation', *PLoS One*, vol. 9, no. 9, p. e104728.
- Suhag, A. & Berghella, V. 2013, 'Intrauterine Growth Restriction (IUGR): Etiology and Diagnosis', *Current Obstetrics and Gynecology Reports*, vol. 2, no. 2, pp. 102–11.
- Sun, W.Y., Witte, D.P., Degen, J.L., Colbert, M.C., Burkart, M.C., Holmback, K., Xiao, Q., Bugge, T.H. & Degen, S.J. 1998, 'Prothrombin deficiency results in embryonic and neonatal lethality in mice', *Proceedings of the National Academy of Sciences of the United States of America*, vol. 95, no. 13, pp. 7597–602.
- Surveyor, G.A., Gendler, S.J., Pemberton, L., Das, S.K., Chakraborty, I., Julian, J., Pimental, R.A., Wegner, C.C., Dey, S.K. & Carson, D.D. 1995, 'Expression and steroid hormonal control of Muc-1 in the mouse uterus', *Endocrinology*, vol. 136, no. 8, pp. 3639–47.
- Sutter, A., Simmons, L.W., Lindholm, A.K. & Firman, R.C. 2015, 'Function of copulatory plugs in house mice: mating behavior and paternity outcomes of rival males', *Behavioral Ecology*, vol. 27, no. 1, pp. 185–95.
- Swanson, A.M. & David, A.L. 2015, 'Animal models of fetal growth restriction: Considerations for translational medicine', *Placenta*, vol. 36, no. 6, pp. 623–30.
- Swanson, D., Liu, M. & Baker, P. 2001, 'Targeted disruption of the methionine synthase gene in mice', *Molecular and Cellular Biology*, vol. 21, no. 4, pp. 1058–65.
- Szotek, P.P., Chang, H.L., Zhang, L., Preffer, F., Dombkowski, D., Donahoe, P.K. & Teixeira, J. 2007, 'Adult mouse myometrial label-retaining cells divide in response to gonadotropin stimulation', *Stem Cells*, vol. 25, no. 5, pp. 1317–25.
- Szymanski, W. & Kazdepka-Zieminska, A. 2003, 'Effect of homocysteine concentration in follicular fluid on a degree of oocyte maturity', *Ginekologia Polska*, vol. 74, no. 10, pp. 1392–6.

- Tachibana, Y., Nakano, Y., Nagaoka, K., Kikuchi, M., Nambo, Y., Haneda, S., Matsui, M., Miyake, Y.-I. & Imakawa, K. 2013, 'Expression of endometrial immune-related genes possibly functioning during early pregnancy in the mare', *The Journal of Reproduction and Development*, vol. 59, no. 1, pp. 85–91.
- Takamoto, N., Kurihara, I., Lee, K., Demayo, F.J., Tsai, M. & Tsai, S.Y. 2005, 'Haploinsufficiency of Chicken Ovalbumin Upstream Promoter Transcription Factor II in Female Reproduction', *Molecular Endocrinology*, vol. 19, no. 9, pp. 2299–308.
- Takeshima, H., Komazaki, S., Nishi, M., Iino, M. & Kangawa, K. 2000, 'Junctophilins: a novel family of junctional membrane complex proteins', *Molecular Cell*, vol. 6, no. 1, pp. 11–22.
- Takimoto, H., Mito, N., Umegaki, K., Ishiwaki, A., Kusama, K., Abe, S., Yamawaki, M., Fukuoka, H., Ohta, C. & Yoshiike, N. 2007, 'Relationship between dietary folate intakes, maternal plasma total homocysteine and B-vitamins during pregnancy and fetal growth in Japan', *European Journal of Nutrition*, vol. 46, no. 5, pp. 300–6.
- Tan, J., Raja, S., Davis, M.K., Tawfik, O., Dey, S.K. & Das, S.K. 2002, 'Evidence for coordinated interaction of cyclin D3 with p21 and cdk6 in directing the development of uterine stromal cell decidualization and polyploidy during implantation', *Mechanisms of Development*, vol. 111, no. 1–2, pp. 99–113.
- Tan, Y., Li, F., Piao, Y., Sun, X. & Wang, Y. 2003, 'Global gene profiling analysis of mouse uterus during the oestrous cycle', *Reproduction*, vol. 126, no. 2, pp. 171–82.
- Tararbit, K., Lelong, N., Thieulin, A.-C., Houyel, L., Bonnet, D., Goffinet, F. & Khoshnood, B. 2013, 'The risk for four specific congenital heart defects associated with assisted reproductive techniques: a population-based evaluation', *Human Reproduction*, vol. 28, no. 2, pp. 367–74.
- Tarrade, A., Panchenko, P., Junien, C. & Gabory, A. 2015, 'Placental contribution to nutritional programming of health and diseases: epigenetics and sexual dimorphism', *Journal of Experimental Biology*, vol. 218, no. 1, pp. 50–8.
- Tarrade, A., Rousseau-Ralliard, D., Aubriere, M.-C., Peynot, N., Dahirel, M., Bertrand-Michel, J., Aguirre-Lavin, T., Morel, O., Beaujean, N., Duranthon, V. & Chavatte-Palmer, P. 2013, 'Sexual dimorphism of the fetoplacental phenotype in response to a

- high fat and control maternal diets in a rabbit model’, *PLoS One*, vol. 8, no. 12, p. e83458.
- Task, U.S.P.S. 2009, ‘Folic acid for the prevention of neural tube defects: U.S. Preventive Services Task Force recommendation statement’, *Annals of Internal Medicine*, vol. 150, no. 9, pp. 626–31.
- Teasdale, F. 1984, ‘Idiopathic intrauterine growth retardation: histomorphometry of the human placenta’, *Placenta*, vol. 5, no. 1, pp. 83–92.
- Teixeira, J., Rueda, B.R. & Pru, J.K. 2008, ‘Uterine Stem cells’, in P. Donahoe & H. Lin (eds), *StemBook*, The Stem Cell Research Community, StemBook, pp. 1–18.
- Thomopoulos, C., Tsioufis, C., Michalopoulou, H., Makris, T., Papademetriou, V. & Stefanadis, C. 2012, ‘Assisted reproductive technology and pregnancy-related hypertensive complications: a systematic review’, *Journal Of Human Hypertension*, vol. 27, p. 148.
- Tibbetts, T.A., Mendoza-Meneses, M., O’Malley, B.W. & Conneely, O.M. 1998, ‘Mutual and Intercompartmental Regulation of Estrogen Receptor and Progesterone Receptor Expression in the Mouse Uterus’, *Biology of Reproduction*, vol. 59, no. 5, pp. 1143–52.
- Tolkunova, E., Cavaleri, F., Eckardt, S., Reinbold, R., Christenson, L.K., Scholer, H.R. & Tomilin, A. 2006, ‘The caudal-related protein cdx2 promotes trophoblast differentiation of mouse embryonic stem cells’, *Stem Cells*, vol. 24, no. 1, pp. 139–44.
- Tombolan, L., Poli, E., Martini, P., Zin, A., Romualdi, C., Bisogno, G. & Lanfranchi, G. 2017, ‘NELL1, whose high expression correlates with negative outcomes, has different methylation patterns in alveolar and embryonal rhabdomyosarcoma’, *Oncotarget*, vol. 8, no. 20, pp. 33086–99.
- Tong, Z., Xiaowen, Z., Baomin, C., Aihua, L., Yingying, Z., Weiping, T. & Zhongyan, S. 2016, ‘The effect of subclinical maternal thyroid dysfunction and autoimmunity on intrauterine growth restriction: A systematic review and meta-analysis’, *Medicine*, vol. 95, no. 19, pp. e3677–e3677.
- Torrens, C., Brawley, L., Anthony, F.W., Dance, C.S., Dunn, R., Jackson, A.A., Poston, L. & Hanson, M.A. 2006, ‘Folate supplementation during pregnancy improves offspring

- cardiovascular dysfunction induced by protein restriction', *Hypertension*, vol. 47, no. 5, pp. 982–7.
- Tost, J. & Gut, I.G. 2007, 'DNA methylation analysis by pyrosequencing', *Nature Protocols*, vol. 2, no. 9, pp. 2265–75.
- Trojer, P., Cao, A.R., Gao, Z., Li, Y., Zhang, J., Xu, X., Li, G., Losson, R., Erdjument-bromage, H., Tempst, P., Farnham, P.J. & Reinberg, D. 2011, 'Article L3MBTL2 Protein Acts in Concert with PcG Protein-Mediated Monoubiquitination of H2A to Establish a Repressive Chromatin Structure', *Molecular Cell*, vol. 42, no. 4, pp. 438–50.
- Tsutsumi, R. & Webster, N.J.G. 2009, 'GnRH pulsatility, the pituitary response and reproductive dysfunction', *Endocrine Journal*, vol. 56, no. 6, 2009/07/17., pp. 729–37.
- Tunster, S.J. 2017, 'Genetic sex determination of mice by simplex PCR', *Biology of Sex Differences*, vol. 8, no. 1, pp. 6–9.
- Tunster, S.J., Creeth, H.D.J. & John, R.M. 2016, 'The imprinted Phlda2 gene modulates a major endocrine compartment of the placenta to regulate placental demands for maternal resources', *Developmental biology*, vol. 409, no. 1, pp. 251–60.
- Tunster, S.J., Jensen, A.B. & John, R.M. 2013, 'Imprinted genes in mouse placental development and the regulation of fetal energy stores', *Reproduction*, vol. 145, no. 5, pp. R117-37.
- Tunster, S.J., McNamara, G.I., Creeth, H.D.J. & John, R.M. 2016, 'Increased dosage of the imprinted Ascl2 gene restrains two key endocrine lineages of the mouse Placenta', *Developmental Biology*, vol. 418, no. 1, pp. 55–65.
- Tunster, S.J., Tycko, B. & John, R.M. 2010, 'The imprinted Phlda2 gene regulates extraembryonic energy stores', *Molecular and Cellular Biology*, vol. 30, no. 1, pp. 295–306.
- Turco, M.Y., Gardner, L., Kay, R.G., Hamilton, R.S., Prater, M., Hollinshead, M.S., McWhinnie, A., Esposito, L., Fernando, R., Skelton, H., Reimann, F., Gribble, F.M., Sharkey, A., Marsh, S.G.E., O'Rahilly, S., Hemberger, M., Burton, G.J. & Moffett, A. 2018, 'Trophoblast organoids as a model for maternal–fetal interactions during human placentation', *Nature*, vol. 564, no. 7735, pp. 263–7.

- Ueda, O., Yorozu, K., Kamada, N., Jishage, K.-I., Kawase, Y., Toyoda, Y. & Suzuki, H. 2003, 'Possible expansion of "window of implantation" in pseudopregnant mice: time of implantation of embryos at different stages of development transferred into the same recipient.', *Biology of Reproduction*, vol. 69, no. 3, pp. 1085–90.
- Uhlen, M., Fagerberg, L., Hallstrom, B.M., Lindskog, C., Oksvold, P., Mardinoglu, A., Sivertsson, A., Kampf, C., Sjostedt, E., Asplund, A., Olsson, I., Edlund, K., Lundberg, E., Navani, S., Szigartyo, C.A.-K., Odeberg, J., Djureinovic, D., Takanen, J.O., Hober, S., Alm, T., Edqvist, P.-H., Berling, H., Tegel, H., Mulder, J., Rockberg, J., Nilsson, P., Schwenk, J.M., Hamsten, M., von Feilitzen, K., Forsberg, M., Persson, L., Johansson, F., Zwahlen, M., von Heijne, G., Nielsen, J. & Ponten, F. 2015, 'Proteomics. Tissue-based map of the human proteome', *Science*, vol. 347, no. 6220, p. 1260419.
- Ulker, D., Emine, Y., Gucin, Z., Muslumanoglu, M. & Buyru, N. 2018, 'Downregulation of SCARA5 may contribute to breast cancer via promoter hypermethylation', *Gene*, vol. 673, pp. 102–6.
- Uthus, E.O. & Brown-Borg, H.M. 2006, 'Methionine flux to transsulfuration is enhanced in the long living Ames dwarf mouse', *Mechanisms of Ageing and Development*, vol. 127, no. 5, pp. 444–50.
- Valdes, C.T., Schutt, A. & Simon, C. 2017, 'Implantation failure of endometrial origin: it is not pathology, but our failure to synchronize the developing embryo with a receptive endometrium.', *Fertility and Sterility*, vol. 108, no. 1, pp. 15–8.
- Valenzuela-Alcaraz, B., Crispi, F., Bijmens, B., Cruz-Lemini, M., Creus, M., Sitges, M., Bartrons, J., Civico, S., Balasch, J. & Gratacos, E. 2013, 'Assisted reproductive technologies are associated with cardiovascular remodeling in utero that persists postnatally', *Circulation*, vol. 128, no. 13, pp. 1442–50.
- Valsamakis, G., Kanaka-gantenbein, C., Malamitsi-puchner, A. & Mastorakos, G. 2006, 'Causes of Intrauterine Growth Restriction and the Postnatal Development of the Metabolic Syndrome', *Annals of the New York Academy of Sciences*, vol. 1092, pp. 138–47.
- Varanou, A., Withington, S.L., Lakasing, L., Williamson, C., Burton, G.J. & Hemberger, M. 2006, 'The importance of cysteine cathepsin proteases for placental development',

- Journal of Molecular Medicine*, vol. 84, no. 4, pp. 305–17.
- de Vega, S., Hozumi, K., Suzuki, N., Nonaka, R., Seo, E., Takeda, A., Ikeuchi, T., Nomizu, M., Yamada, Y. & Arikawa-Hirasawa, E. 2016, 'Identification of peptides derived from the C-terminal domain of fibulin-7 active for endothelial cell adhesion and tube formation disruption', *Biopolymers*, vol. 106, no. 2, pp. 184–95.
- Verhaar, M.C., Stroes, E. & Rabelink, T.J. 2002, 'Folates and Cardiovascular Disease', *Arteriosclerosis, Thrombosis, and Vascular Biology*, vol. 22, no. 1, pp. 6–13.
- Visentin, M., Diop-Bove, N., Zhao, R. & Goldman, I.D. 2014, 'The intestinal absorption of folates', *Annual Review of Physiology*, vol. 76, pp. 251–74.
- van Vlodrop, I.J.H., Baldewijns, M.M.L., Smits, K.M., Schouten, L.J., van Neste, L., van Criekinge, W., van Poppel, H., Lerut, E., Schuebel, K.E., Ahuja, N., Herman, J.G., de Bruïne, A.P. & van Engeland, M. 2010, 'Prognostic significance of Gremlin1 (GREM1) promoter CpG island hypermethylation in clear cell renal cell carcinoma', *The American Journal of Pathology*, vol. 176, no. 2, pp. 575–84.
- Vuguin, P., Raab, E., Liu, B., Barzilai, N. & Simmons, R. 2004, 'Hepatic insulin resistance precedes the development of diabetes in a model of intrauterine growth retardation.', *Diabetes*, vol. 53, no. 10, pp. 2617–22.
- Waes, J.G. Van, Heller, S., Bauer, L.K., Wilberding, J., Maddox, J.R., Aleman, F., Rosenquist, T.H. & Finnell, R.H. 2008, 'Embryonic development in the reduced folate carrier knockout mouse is modulated by maternal folate supplementation', *Birth Defects Research Part A - Clinical and Molecular Teratology*, vol. 82, no. 7, pp. 494–507.
- Wakayama, S., Mizutani, E. & Wakayama, T. 2010, 'Chapter 9 - Production of Cloned Mice from Somatic Cells, ES Cells, and Frozen Bodies', in P.M. Wassarman & P.M.B.T.-M. in E. Soriano (eds), *Guide to Techniques in Mouse Development, Part A: Mice, Embryos, and Cells, 2nd Edition*, vol. 476, Academic Press, pp. 151–69.
- Wang, C., Chen, Y., Deng, H., Gao, S. & Li, L. 2015, 'Rbm46 regulates trophectoderm differentiation by stabilizing Cdx2 mRNA in early mouse embryos', *Stem Cells and Development*, vol. 24, no. 7, pp. 904–15.
- Wang, H. & Dey, S.K. 2006, 'Roadmap to embryo implantation: clues from mouse models',

- Nature Reviews Genetics*, vol. 7, no. 3, pp. 185–99.
- Wang, H., Feng, Y., Bao, Z. & Jiang, C. 2013, 'Epigenetic silencing of KAZALD1 confers a better prognosis and is associated with malignant transformation / progression in glioma', *Oncology Reports*, vol. 30, no. 5, pp. 2089–96.
- Wang, R., Lohr, C. V, Fischer, K., Dashwood, W.M., Greenwood, J.A., Ho, E., Williams, D.E., Ashktorab, H., Dashwood, M.R. & Dashwood, R.H. 2013, 'Epigenetic inactivation of endothelin-2 and endothelin-3 in colon cancer', *International Journal of Cancer*, vol. 132, no. 5, pp. 1004–12.
- Wang, S., Qiao, F., Feng, L. & Lv, J. 2008, 'Polymorphisms in genes involved in folate metabolism as maternal risk factors for Down syndrome in China', *Journal of Zhejiang University. Science. B*, vol. 9, no. 2, pp. 93–9.
- Wang, T.-C., Song, Y.-S., Wang, H., Zhang, J., Yu, S.-F., Gu, Y.-E., Chen, T., Wang, Y., Shen, H.-Q. & Jia, G. 2012, 'Oxidative DNA damage and global DNA hypomethylation are related to folate deficiency in chromate manufacturing workers', *Journal of Hazardous Materials*, vol. 213–214, pp. 440–6.
- Wang, T., Chen, M., Liu, L., Cheng, H., Yan, Y.-E., Feng, Y.-H. & Wang, H. 2011, 'Nicotine induced CpG methylation of Pax6 binding motif in StAR promoter reduces the gene expression and cortisol production', *Toxicology and Applied Pharmacology*, vol. 257, no. 3, pp. 328–37.
- Wang, Y., Fang, Y., Zhang, F. & Xu, M. 2014, 'Hypermethylation of the enolase gene (ENO2) in autism', *European Journal of Pediatrics*, vol. 173, no. 9, pp. 1233–44.
- Wang, Y., Liu, Y., Ji, W., Qin, H., Wu, H., Xu, D., Tukebai, T. & Wang, Z. 2015, 'Analysis of MTR and MTRR polymorphisms for neural tube defects risk association', *Medicine*, vol. 94, no. 35, p. e1367.
- Wang, Z., Wang, D.-Z., Pipes, G.C.T. & Olson, E.N. 2003, 'Myocardin is a master regulator of smooth muscle gene expression', *Proceedings of the National Academy of Sciences of the United States of America*, vol. 100, no. 12, pp. 7129–34.
- Wanke, M.M., Loza, M.E. & Rebuelto, M. 2006, 'Progestin treatment for infertility in bitches with short interestrus interval', *Theriogenology*, vol. 66, no. 6–7, pp. 1579–82.

- Ward, M. 2001, 'Homocysteine, folate, and cardiovascular disease', *International Journal for Vitamin and Nutrition Research*, vol. 71, no. 3, pp. 173–8.
- Wasson, G.R., McGlynn, A.P., McNulty, H., O'Reilly, S.L., McKelvey-Martin, V.J., McKerr, G., Strain, J.J., Scott, J. & Downes, C.S. 2006, 'Global DNA and p53 region-specific hypomethylation in human colonic cells is induced by folate depletion and reversed by folate supplementation', *The Journal of Nutrition*, vol. 136, no. 11, pp. 2748–53.
- Watson, E.D. & Cross, J.C. 2005, 'Development of structures and transport functions in the mouse placenta', *Physiology*, vol. 20, pp. 180–93.
- Weber, M., Davies, J.J., Wittig, D., Oakeley, E.J., Haase, M., Lam, W.L. & Schübeler, D. 2005, 'Chromosome-wide and promoter-specific analyses identify sites of differential DNA methylation in normal and transformed human cells', *Nature Genetics*, vol. 37, no. 8, pp. 853–62.
- Weinerman, R., Ord, T., Bartolomei, M.S., Coutifaris, C. & Mainigi, M. 2017, 'The superovulated environment, independent of embryo vitrification, results in low birthweight in a mouse model', *Biology of Reproduction*, vol. 97, no. 1, pp. 133–42.
- Wen, F.-L., Wang, Y.-C. & Shibata, T. 2017, 'Epithelial folding driven by apical or basal-lateral modulation: geometric features, mechanical inference, and boundary effects', *Biophysical Journal*, vol. 112, no. 12, 2017/06/20., pp. 2683–95.
- Wen, S.W., Chen, X.-K., Rodger, M., White, R.R., Yang, Q., Smith, G.N., Sigal, R.J., Perkins, S.L. & Walker, M.C. 2008, 'Folic acid supplementation in early second trimester and the risk of preeclampsia', *American Journal of Obstetrics and Gynecology*, vol. 198, no. 1, p. 45.e1-e7.
- Wen, S.W., Zhou, J., Yang, Q., Fraser, W., Olatunbosun, O. & Walker, M. 2008, 'Maternal exposure to folic acid antagonists and placenta-mediated adverse pregnancy outcomes', *CMAJ: Canadian Medical Association journal*, vol. 179, no. 12, pp. 1263–8.
- Wetendorf, M. & DeMayo, F.J. 2012, 'The progesterone receptor regulates implantation, decidualization, and glandular development via a complex paracrine signaling network', *Molecular and Cellular Endocrinology*, vol. 357, no. 1–2, pp. 108–18.

- Wetendorf, M. & DeMayo, F.J. 2014, 'Progesterone receptor signaling in the initiation of pregnancy and preservation of a healthy uterus', *The International Journal of Developmental Biology*, vol. 58, no. 2–4, pp. 95–106.
- Wetendorf, M., Wu, S., Wang, X., Creighton, C.J., Wang, T., Lanz, R.B., Blok, L., Tsai, S.Y., Tsai, M., John, P. & Demayo, F.J. 2017, 'Decreased epithelial progesterone receptor A at the window of receptivity is required for preparation of the endometrium for embryo attachment', *Biology of Reproduction*, vol. 96, no. 2, pp. 313–26.
- White, C.A., Robb, L. & Salamonsen, L.A. 2004, 'Uterine extracellular matrix components are altered during defective decidualization in interleukin-11 receptor α deficient mice', *Reproductive Biology and Endocrinology*, vol. 2, no. 1, p. 76.
- Whitehead, C.L., Walker, S.P., Lappas, M. & Tong, S. 2013, 'Circulating RNA coding genes regulating apoptosis in maternal blood in severe early onset fetal growth restriction and pre-eclampsia.', *Journal of Perinatology*, vol. 33, no. 8, pp. 600–4.
- Whitley, G.S.J. & Cartwright, J.E. 2010, 'Cellular and Molecular Regulation of Spiral Artery Remodelling : Lessons from the Cardiovascular Field', *Placenta*, vol. 31, no. 6, pp. 465–74.
- Whittington, C.M., O'Meally, D., Laird, M.K., Belov, K., Thompson, M.B. & McAllan, B.M. 2018, 'Transcriptomic changes in the pre-implantation uterus highlight histotrophic nutrition of the developing marsupial embryo', *Scientific Reports*, vol. 8, no. 1, p. 2412.
- Wickramasinghe, S.N., Cooper, E.H. & Chalmers, D.G. 1968, 'A study of erythropoiesis by combined morphologic, quantitative cytochemical and autoradiographic methods. Normal human bone marrow, vitamin B12 deficiency and iron deficiency anemia', *Blood*, vol. 31, no. 3, pp. 304–13.
- Wickramasinghe, S.N. & Fida, S. 1993, 'Misincorporation of uracil into the DNA of folate- and B12-deficient HL60 cells', *European Journal of Haematology*, vol. 50, no. 3, pp. 127–32.
- Wilcox, A.J., Baird, D.D. & Weinberg, C.R. 1999, 'Time of implantation of the conceptus and loss of pregnancy', *The New England Journal of Medicine*, vol. 340, no. 23, pp. 1796–9.

- Williams, P.J., Bulmer, J.N., Innes, B.A. & Pipkin, F.B. 2011, 'Possible roles for folic acid in the regulation of trophoblast invasion and placental development in normal early human pregnancy', *Biology of Reproduction*, vol. 84, no. 6, pp. 1148–53.
- Wilson, S.L., Blair, J.D., Hogg, K., Langlois, S., von Dadelszen, P. & Robinson, W.P. 2015, 'Placental DNA methylation at term reflects maternal serum levels of INHA and FN1, but not PAPPa, early in pregnancy', *BMC Medical Genetics*, vol. 16, p. 111.
- Winterhager, E. & Gellhaus, A. 2017, 'Transplacental nutrient transport mechanisms of intrauterine growth restriction in rodent models and humans', *Frontiers in Physiology*, vol. 8, no. 951.
- Winterhager, E., Gellhaus, A., Blois, S.M., Hill, L.A., Barr, K.J. & Kidder, G.M. 2013, 'Decidual Angiogenesis and Placental Orientation Are Altered in Mice Heterozygous for a Dominant Loss-of-Function Gjal (Connexin43) Mutation', *Biology of Reproduction*, vol. 89, no. 5, p. 111 (1-12).
- Wollmann, H.A. 1998, 'Intrauterine Growth Restriction: Definition and aetiology', *Hormone Research*, vol. 49, no. suppl 2, pp. 1–6.
- Wood, G.A., Fata, J.E., Watson, K.L.M. & Khokha, R. 2007, 'Circulating hormones and estrous stage predict cellular and stromal remodeling in murine uterus', *Reproduction*, vol. 133, no. 5, pp. 1035–44.
- Woods, L., Perez-Garcia, V. & Hemberger, M. 2018, 'Regulation of placental development and its impact on fetal growth-New insights from mouse models', *Frontiers in Endocrinology*, vol. 9, p. 570.
- Woods, L., Perez-Garcia, V., Kieckbusch, J., Wang, X., Demayo, F., Colucci, F. & Hemberger, M. 2017, 'Decidualisation and placentation defects are a major cause of age-related reproductive decline', *Nature Communications*, vol. 8, no. 1, p. 352.
- Wu, F., Chen, X., Liu, Y., Liang, B., Xu, H., Li, T.C. & Wang, C.C. 2018, 'Decreased MUC1 in endometrium is an independent receptivity marker in recurrent implantation failure during implantation window', *Reproductive Biology and Endocrinology*, vol. 16, no. 1, p. 60.
- Wu, G., Bazer, F.W., Cudd, T.A., Meininger, C.J. & Spencer, T.E. 2004, 'Maternal Nutrition

- and Fetal Development', *The Journal of Nutrition*, vol. 134, no. 9, pp. 2169–72.
- Wu, J. a, Johnson, B.L., Chen, Y., Ha, C.T. & Dveksler, G.S. 2008, 'Murine pregnancy-specific glycoprotein 23 induces the proangiogenic factors transforming-growth factor beta 1 and vascular endothelial growth factor a in cell types involved in vascular remodeling in pregnancy', *Biology of Reproduction*, vol. 79, no. 6, pp. 1054–61.
- Wu, L., de Bruin, A., Saavedra, H.I., Starovic, M., Trimboli, A., Yang, Y., Opavska, J., Wilson, P., Thompson, J.C., Ostrowski, M.C., Rosol, T.J., Woollett, L.A., Weinstein, M., Cross, J.C., Robinson, M.L. & Leone, G. 2003, 'Extra-embryonic function of Rb is essential for embryonic development and viability', *Nature*, vol. 421, no. 6926, pp. 942–7.
- Wu, W.-B., Xu, Y.-Y., Cheng, W.-W., Yuan, B., Zhao, J.-R., Wang, Y.-L. & Zhang, H.-J. 2017, 'Decreased PGF may contribute to trophoblast dysfunction in fetal growth restriction', *Reproduction*, vol. 154, no. 3, pp. 319–29.
- Wu, Y., Halverson, G., Basir, Z., Strawn, E., Yan, P. & Guo, S.W. 2005, 'Aberrant methylation at HOXA10 may be responsible for its aberrant expression in the endometrium of patients with endometriosis', *American Journal of Obstetrics and Gynecology*, vol. 193, no. 2, pp. 371–80.
- Wynne, F., Ball, M., McLellan, A.S., Dockery, P., Zimmermann, W. & Moore, T. 2006, 'Mouse pregnancy-specific glycoproteins: Tissue-specific expression and evidence of association with maternal vasculature', *Reproduction*, vol. 131, no. 4, pp. 721–32.
- Xu, B., Sun, X., Li, L., Wu, L., Zhang, A. & Feng, Y. 2012, 'Pinopodes, leukemia inhibitory factor, integrin- β 3, and mucin-1 expression in the peri-implantation endometrium of women with unexplained recurrent pregnancy loss', *Fertility and Sterility*, vol. 98, no. 2, pp. 389–95.
- Xu, Y., Ding, J., Ma, X., Ma, Y., Liu, Z. & Lin, N. 2014, 'Treatment with Panax ginseng antagonizes the estrogen decline in ovariectomized mice', *International Journal of Molecular Sciences*, vol. 15, no. 5, pp. 7827–40.
- Xue, J., Wu, Q., Westfield, L.A., Tuley, E.A., Lu, D., Zhang, Q., Shim, K., Zheng, X. & Sadler, J.E. 1998, 'Incomplete embryonic lethality and fatal neonatal hemorrhage caused by prothrombin deficiency in mice', *Proceedings of the National Academy of Sciences*,

vol. 95, no. 13, p. 7603 LP-7607.

- Yamada, K., Gravel, R.A., Toraya, T. & Matthews, R.G. 2006, 'Human methionine synthase reductase is a molecular chaperone for human methionine synthase', *Proceedings of the National Academy of Sciences*, vol. 103, no. 25, p. 9476 LP-9481.
- Yamada, K., Kanda, H., Tanaka, S., Takamatsu, N., Shiba, T. & Ito, M. 2006, 'Sox15 enhances trophoblast giant cell differentiation induced by Hand1 in mouse placenta', *Differentiation*, vol. 74, no. 5, pp. 212–21.
- Yang, H., Ahn, C. & Jeung, E.-B. 2015, 'Differential expression of calcium transport genes caused by COMT inhibition in the duodenum, kidney and placenta of pregnant mice', *Molecular and Cellular Endocrinology*, vol. 401, pp. 45–55.
- Yang, J., Jin, X., Yan, Y., Shao, Y., Pan, Y., Roberts, L.R., Zhang, J., Huang, H. & Jiang, J. 2017, 'Inhibiting histone deacetylases suppresses glucose metabolism and hepatocellular carcinoma growth by restoring FBP1 expression', *Scientific Reports*, vol. 7, no. 43864.
- Yang, Z.-Z., Tschopp, O., Hemmings-Mieszczak, M., Feng, J., Brodbeck, D., Perentes, E. & Hemmings, B.A. 2003, 'Protein kinase B alpha/Akt1 regulates placental development and fetal growth', *The Journal of Biological Chemistry*, vol. 278, no. 34, pp. 32124–31.
- Yao, Q., Chen, L., Liang, Y., Sui, L., Guo, L., Zhou, J., Fan, K. & Jing, J. 2016, 'Blastomere removal from cleavage-stage mouse embryos alters placental function, which is associated with placental oxidative stress and inflammation', *Science Reports*, vol. 6, no. 25023.
- Ye, J., Coulouris, G., Zaretskaya, I., Cutcutache, I., Rozen, S. & Madden, T.L. 2012, 'Primer-BLAST: A tool to design target-specific primers for polymerase chain reaction', *BMC Bioinformatics*, vol. 13, no. 134.
- Ye, X., Hama, K., Contos, J.J.A., Anliker, B., Inoue, A., Skinner, M.K., Suzuki, H., Amano, T., Kennedy, G., Arai, H., Aoki, J. & Chun, J. 2005, 'LPA3-mediated lysophosphatidic acid signalling in embryo implantation and spacing', *Nature*, vol. 435, no. 7038, pp. 104–8.
- Yin, M.-D., Ma, S.-P., Liu, F. & Chen, Y.-Z. 2018, 'Role of serine/threonine kinase 33 methylation in colorectal cancer and its clinical significance', *Oncology letters*, vol. 15,

no. 2, pp. 2153–60.

Yip, K.S., Suvorov, A., Connerney, J., Lodato, N.J. & Waxman, D.J. 2013, ‘Changes in Mouse Uterine Transcriptome in Estrus and Proestrus’, *Biology of Reproduction*, vol. 89 (1), no. 13.

Yoon, B., Herman, H., Hu, B., Park, Y.J., Lindroth, A., Bell, A., West, A.G., Chang, Y., Stablewski, A., Piel, J.C., Loukinov, D.I., Lobanenkova, V. V & Soloway, P.D. 2005, ‘Rasgrfl imprinting is regulated by a CTCF-dependent methylation-sensitive enhancer blocker’, *Molecular and Cellular Biology*, vol. 25, no. 24, pp. 11184–90.

Yoshida, Y., Todo, A., Shirakawa, S., Wakisaka, G. & Uchino, H. 1968, ‘Proliferation of megaloblasts in pernicious anemia as observed from nucleic acid metabolism’, *Blood*, vol. 31, no. 3, pp. 292–303.

Yoshinaga, K. 2013, ‘A sequence of events in the uterus prior to implantation in the mouse’, *Journal of Assisted Reproduction and Genetics*, vol. 30, no. 8, 2013/09/20., pp. 1017–22.

Yue, F., Cheng, Y., Breschi, A., Vierstra, J., Wu, W., Ryba, T., Sandstrom, R., Ma, Z., Davis, C., Pope, B.D., Shen, Y., Pervouchine, D.D., Djebali, S., Thurman, R.E., Kaul, R., Rynes, E., Kirilusha, A., Marinov, G.K., Williams, B.A., Trout, D., Amrhein, H., Fisher-Aylor, K., Antoshechkin, I., DeSalvo, G., See, L.-H., Fastuca, M., Drenkow, J., Zaleski, C., Dobin, A., Prieto, P., Lagarde, J., Bussotti, G., Tanzer, A., Denas, O., Li, K., Bender, M.A., Zhang, M., Byron, R., Groudine, M.T., McCleary, D., Pham, L., Ye, Z., Kuan, S., Edsall, L., Wu, Y.-C., Rasmussen, M.D., Bansal, M.S., Kellis, M., Keller, C.A., Morrissey, C.S., Mishra, T., Jain, D., Dogan, N., Harris, R.S., Cayting, P., Kawli, T., Boyle, A.P., Euskirchen, G., Kundaje, A., Lin, S., Lin, Y., Jansen, C., Malladi, V.S., Cline, M.S., Erickson, D.T., Kirkup, V.M., Learned, K., Sloan, C.A., Rosenbloom, K.R., Lacerda de Sousa, B., Beal, K., Pignatelli, M., Flicek, P., Lian, J., Kahveci, T., Lee, D., Kent, W.J., Ramalho Santos, M., Herrero, J., Notredame, C., Johnson, A., Vong, S., Lee, K., Bates, D., Neri, F., Diegel, M., Canfield, T., Sabo, P.J., Wilken, M.S., Reh, T.A., Giste, E., Shafer, A., Kuttyavin, T., Haugen, E., Dunn, D., Reynolds, A.P., Neph, S., Humbert, R., Hansen, R.S., De Bruijn, M., Selleri, L., Rudensky, A., Josefowicz, S., Samstein, R., Eichler, E.E., Orkin, S.H., Levasseur, D., Papayannopoulou, T., Chang, K.-H., Skoultschi, A., Gosh, S., Disteche, C., Treuting, P., Wang, Y., Weiss, M.J.,

- Blobel, G.A., Cao, X., Zhong, S., Wang, T., Good, P.J., Lowdon, R.F., Adams, L.B., Zhou, X.-Q., Pazin, M.J., Feingold, E.A., Wold, B., Taylor, J., Mortazavi, A., Weissman, S.M., Stamatoyannopoulos, J.A., Snyder, M.P., Guigo, R., Gingeras, T.R., Gilbert, D.M., Hardison, R.C., Beer, M.A. & Ren, B. 2014, 'A comparative encyclopedia of DNA elements in the mouse genome', *Nature*, vol. 515, no. 7527, pp. 355–64.
- Yuen, R.K.C., Chen, B., Blair, J.D., Robinson, W.P. & Nelson, D.M. 2013, 'Hypoxia alters the epigenetic profile in cultured human placental trophoblasts', *Epigenetics*, vol. 8, no. 2, pp. 192–202.
- Zhang, M., Shi, H., Segaloff, D.L. & Van Voorhis, B.J. 2001, 'Expression and localization of luteinizing hormone receptor in the female mouse reproductive tract', *Biology of Reproduction*, vol. 64, no. 1, pp. 179–87.
- Zhang, Y., He, X., Xiong, X., Chuan, J., Zhong, L., Chen, G. & Yu, D. 2019, 'The association between maternal methylenetetrahydrofolate reductase C677T and A1298C polymorphism and birth defects and adverse pregnancy outcomes', *Prenatal Diagnosis*, vol. 39, no. 1, pp. 3–9.
- Zhang, Y. & Reinberg, D. 2001, 'Transcription regulation by histone methylation: interplay between different covalent modifications of the core histone tails', *Genes and Development*, vol. 15, no. 18, pp. 2343–60.
- Zhao, R., Matherly, L.H. & Goldman, I.D. 2009, 'Membrane transporters and folate homeostasis: intestinal absorption and transport into systemic compartments and tissues', *Expert Reviews in Molecular Medicine*, vol. 11, p. e4.
- Zhou, L.M., Yang, W.W., Hua, J.Z., Deng, C.Q., Tao, X. & Stoltzfus, R.J. 1998, 'Relation of hemoglobin measured at different times in pregnancy to preterm birth and low birth weight in Shanghai, China', *American Journal of Epidemiology*, vol. 148, no. 10, pp. 998–1006.
- Zhuang, T., Hess, R.A., Kolla, V., Higashi, M., Raabe, T.D. & Brodeur, G.M. 2014, 'CHD5 is required for spermiogenesis and chromatin condensation', *Mechanisms of Development*, vol. 131, pp. 35–46.
- van der Zwan, A., Bi, K., Norwitz, E.R., Crespo, A.C., Claas, F.H.J., Strominger, J.L. &

Tilburgs, T. 2018, 'Mixed signature of activation and dysfunction allows human decidual CD8(+) T cells to provide both tolerance and immunity', *Proceedings of the National Academy of Sciences of the United States of America*, vol. 115, no. 2, pp. 385–90.

Appendix A

Table A.1 Genes in the placenta at E10.5 after embryo transfer with known expression in trophoblast cells, maternal decidua, or fetal endothelium

Gene name	Fold change	Gene function	Region of known placental expression		Ref.*
			Human homolog	Mouse	
Trophoblast, fetal endothelial vascular cell and decidua expression					
<i>Ang2</i>	799.25	Ribonuclease	SynT, FVE, Dec	S-TGCs, FVE	(Geva et al. 2005)
<i>Adam28</i>	57.59	Metalloprotease disintegrin	SynT, CytoT, EVT, Dec	Unknown	(De Luca et al. 2017)
<i>Actn3</i>	8.40	Actin binding protein	SynT, CytoT, FVE, Dec	Unknown	
<i>Adgrf2</i>	7.79	G-protein coupled receptor activity	SynT, Dec	Unknown	
<i>Tnfsf11</i>	7.78	Cytokine	SynT, Dec	Unknown	
<i>Rnf150</i>	7.53	Ubiquitin protein ligase activity	SynT, CytoT, Dec	General	
<i>Edn2</i>	7.15	Angiogenesis	SynT, Dec	General	
<i>Prokr2</i>	5.32	Angiogenesis	SynT, CytoT, FVE, Dec	Unknown	
<i>Colgalt2</i>	5.27	Extracellular matrix; PPAR γ pathway	SynT, CytoT, FVE, Dec	General	
<i>Ptafr</i>	4.85	G-protein coupled receptor activity	SynT, FVE, Dec	General	
<i>Eno1b</i>	4.73	Glycolysis	(Human ortholog: ENO1) CytoT, FVE, Dec	General	
<i>Csdc2</i>	4.62	RNA-binding factor; histone synthesis	SynT, CytoT, FVE, Dec	General	
<i>C3</i>	4.60	Complement system; ERK1/2 cascade	SynT, FVE, Dec	General	
<i>Adcy2</i>	4.01	Adenylate cyclase	SynT, CytoT, FVE, Dec	General	
<i>Fbln2</i>	3.84	Extracellular matrix	SynT, FVE, Dec	General	
<i>Gldn</i>	-3.77	Extracellular matrix	CytoT, FVE, Dec	Unknown	
<i>Myocd</i>	3.61	Transcriptional co-activator	SynT, CytoT, FVE, Dec	General	
<i>Tspan8</i>	3.46	Integrin binding	SynT, FVE, Dec	General	
<i>F2</i>	3.37	Vascular integrity	SynT, FVE, Dec	General	
<i>Klrb1b</i>	-3.27	Killer cell lectin-like receptor	SynT, CytoT, Dec	General	
<i>Rasl11a</i>	3.25	GTPase	SynT, CytoT, FVE, Dec	Unknown	
<i>Fam189a2</i>	3.20	Unknown	SynT, CytoT, FVE, Dec	General	
<i>Kank4</i>	3.13	Cytoskeleton	SynT, CytoT, FVE, Dec	General	

<i>Fermt1</i>	3.12	Cell adhesion	SynT, CytoT, FVE, Dec	General	
<i>Ptprz1</i>	3.09	FGF binding	SynT, CytoT, FVE, Dec	Unknown	
<i>Gpr176</i>	3.04	G protein coupled receptor activity	SynT, CytoT, FVE, Dec	Unknown	
<i>Unc93a</i>	2.95	Unknown	SynT, CytoT, FVE, Dec	General	
<i>Robo1</i>	2.90	Slit receptor, cell migration	SynT, CytoT, EVT, FVE, Dec	S-TGCs at E13.5 and E15.5	(P. Li et al. 2015)
<i>Atp6v1c2</i>	2.89	Ion transport	SynT, CytoT, FVE, Dec	Unknown	
<i>Rasgrfl</i>	-2.70	Ras protein signal transduction pathway	SynT, CytoT, Dec	General	
<i>Thbs2</i>	2.69	Thrombospondin	SynT, CytoT, FVE, Dec	General	
<i>Wdfyl</i>	2.67	Phosphatidylinositol 3-phosphate binding protein	SynT, FVE, Dec	General	(Sferruzzi-Perri et al. 2009)
<i>Cp</i>	2.63	Iron homeostasis	SynT, FVE, Dec	General	
<i>Il15ra</i>	-2.63	Interleukin	SynT, CytoT, FVE, Dec, uNK	General	
<i>Fam13c</i>	2.60	Unknown	SynT, CytoT, FVE, Dec	Unknown	
<i>Tfpi</i>	-2.57	Tissue factor pathway inhibitor	SynT, CytoT, FVE, Dec	General	(Pedersen et al. 2005)
<i>B3gat2</i>	-2.55	Carbohydrate metabolism	SynT, CytoT, Dec, uNK	General	
<i>Pcdhgal</i>	2.52	Protocadherin	SynT, CytoT, FVE, Dec	General	
<i>Sema3a</i>	2.51	Chemokine	SynT, CytoT, FVE, Dec	Unknown	
<i>Zfp30</i>	2.46	Zinc finger protein	SynT, FVE, Dec	Unknown	
<i>Axin2</i>	2.42	Wnt signaling pathway	SynT, CytoT, FVE, Dec	Unknown	
<i>Jph2</i>	2.42	Junctional membrane complex protein	SynT, FVE, Dec	General	
<i>Draxin</i>	-2.40	Chemokine	SynT, CytoT, FVE, Dec	Unknown	
<i>Fbn1</i>	2.38	Fibrillin	SynT, CytoT, FVE, Dec	General	
<i>Trim55</i>	-2.37	Cytoskeleton	SynT, FE, Dec	General	
<i>Efcab7</i>	2.36	Hedgehog signalling	SynT, CytoT, FVE, Dec	General	
<i>Dpp4</i>	2.32	Adenosine deaminase	CytoT, FVE, Dec	General	
<i>Kng2</i>	2.32	Kininogenin	(Human ortholog: KNG1) SynT, FVE, Dec	General	
<i>Grap2</i>	2.32	GRB2-related adaptor protein	SynT, CytoT, FVE, Dec	General	
<i>Slit3</i>	2.32	Slit/Robo pathway	SynT, FVE, Dec	General	
<i>Sorbs1</i>	2.28	Insulin signalling	SynT, CytoT, FVE, Dec	General	
<i>Fam135b</i>	2.28	Unknown	SynT, CytoT, FVE, Dec	Unknown	
<i>Pde7b</i>	2.26	Phosphodiesterase	SynT, CytoT, FVE, Dec	Unknown	

<i>Tnip3</i>	-2.25	NF-κB inhibitor	SynT, CytoT, FVE, Dec	Unknown	
<i>Hddc3</i>	2.24	Purine metabolism	SynT, CytoT, FVE, Dec	Unknown	
<i>Clqtnfl</i>	2.21	MAPK pathway	SynT, CytoT, FVE, Dec	General	
<i>Hipk2</i>	2.19	Negative regulator of BMP pathway	SynT, CytoT, FVE, Dec	General	
<i>Thbs1</i>	2.15	Thrombospondin	SynT, CytoT, FVE, Dec	General	
<i>Cd53</i>	-2.17	Integrin binding, involved in cell growth	SynT, CytoT, FVE, Dec	General	
<i>Adcy1</i>	2.09	Adenylate cyclase	SynT, CytoT, FVE, Dec	Unknown	
<i>Apom</i>	2.09	Apolipoprotein	SynT, CytoT, FVE, Dec	General	
<i>Ms4a6c</i>	2.09	Membrane protein	(Human ortholog: MS4A6A) SynT, CytoT, FVE, Dec	Unknown	
<i>Ntn4</i>	2.07	ECM protein	SynT, CytoT, FVE, Dec	Unknown	(Dakouane-Giudicelli et al. 2012)
<i>Pygo1</i>	2.06	Wnt signalling pathway	SynT, CytoT, FVE, Dec	Unknown	
<i>Zfp361l</i>	2.06	Zinc finger protein	SynT, CytoT, FVE, Dec	Allantois, chorionic plate, yolk sac	(Deng et al. 2006; Stumpo et al. 2004)
<i>Svip</i>	2.04	Inhibitor of ER-associated degradation	SynT, CytoT, FVE, Dec	Unknown	
<i>Far2</i>	-2.03	fatty-acyl-CoA reductase activity	SynT, CytoT, FVE, Dec	General	
<i>Tcp11l1</i>	2.03	T-complex 11 like 1	CytoT, FVE, Dec	Unknown	
<i>Ctsf</i>	2.02	Cathepsin	SynT, CytoT, FVE, Dec	General	
<i>Trim5</i>	-2.01	E3 ubiquitin-ligase	SynT, CytoT, FVE, Dec	General	
Trophoblast and fetal endothelial vascular cell expression					
<i>Calcoco2</i>	-5.19	Actin cytoskeleton reorganization	SynT, FVE	Unknown	
<i>Cfb</i>	4.40	Cell proliferation	SynT, CytoT, FVE	General	
<i>Kcne3</i>	3.91	Potassium channel activity	SynT, FVE	General	
<i>Chmp4c</i>	3.89	Chromatin modifying protein, mitosis	SynT, CytoT, FVE	General	
<i>P2ry10</i>	-3.55	G-protein coupled receptor	SynT, FVE	General	
<i>Cobl</i>	2.61	Actin nucleator	SynT, CytoT, FVE	Unknown	
<i>Enpp2</i>	2.48	Ectonucleotide pyrophosphatase/ phosphodiesterase	SynT, CytoT, FVE,	General	
<i>Golga7b</i>	2.41	S-palmitoyltransferase	SynT, CytoT, FVE	Unknown	
<i>Mttp</i>	2.30	Lipoprotein assembly	SynT, FVE	General	
<i>Pcdhgb7</i>	2.29	Protocadherin	SynT, CytoT, FVE	General	

<i>Nipa14</i>	2.24	Magnesium ion transmembrane transporter	SynT, FVE	Unknown	
<i>Igfbp11</i>	-2.13	Insulin-like growth factor binding	SynT, FVE	Unknown	
<i>Tmem151a</i>	2.13	Transmembrane protein	SynT, CytoT, FVE	Unknown	
<i>Syt11</i>	2.13	Intracellular protein transport	SynT, CytoT, FVE	Unknown	
<i>Schip1</i>	2.13	Estrogen metabolism	SynT, FVE	General	
Trophoblast and decidua expression					
<i>Adamdec1</i>	1194.78	Metalloprotease	General	GlyT, SpT, Dec	(Baran, Kelly & Binart 2003)
<i>Itmcln1</i>	246.27	Lectin, glucose transport	SynT, CytoT, Dec	Unknown	
<i>Sorcs1</i>	10.26	Growth factor receptor	SynT, CytoT, Dec	Unknown	
<i>Trpm2</i>	-10.10	Cation channel	SynT, Dec	General	
<i>Aldh3a1</i>	-9.29	Aldehyde dehydrogenase	Unknown	TS cells, SpT, Dec	(McConaha et al. 2011; Nishiyama et al. 2015)
<i>Ccl1</i>	-6.81	Chemokine	SynT, Dec, uNK	Unknown	
<i>Kynu</i>	4.64	NAD cofactor biosynthesis	SynT, CytoT, Dec	General	
<i>Duoxa1</i>	4.34	Thyroid hormone synthesis	SynT, Dec	Unknown	
<i>Klb</i>	3.97	FGF signaling pathway	SynT, CytoT, Dec	General	
<i>Dyrk4</i>	-3.93	Protein kinase	SynT, Dec	Unknown	
<i>Gpr183</i>	-3.60	G protein-coupled receptor	SynT, Dec	General	
<i>Cntn1</i>	3.41	Cell adhesion	SynT, Dec	Unknown	
<i>Robo2</i>	3.41	Cell migration	SynT, Dec	General	
<i>Pak7</i>	3.17	Cytoskeleton	SynT, CytoT, Dec	Unknown	
<i>Meox1</i>	3.17	Transcription factor	SynT, CytoT, Dec	Unknown	
<i>Wscd1</i>	3.07	Sulfotransferase activity	SynT, Dec	General	
<i>Gxylt2</i>	3.03	EGF pathway	SynT, Dec	General	
<i>Slc8a1</i>	3.01	Na ⁺ -Ca ²⁺ exchanger	SynT, Dec	General	
<i>Nkd2</i>	3.00	Wnt signaling	SynT, CytoT, Dec	General	
<i>Arsk</i>	3.00	Sulfatase, hormone biosynthesis	SynT, Dec	General	
<i>Galnt2</i>	2.95	Glycosyltransferase	SynT, CytoT, Dec	General	
<i>Mt3</i>	2.93	Metallothionein	SynT, Dec	Unknown	
<i>Slc9a2</i>	2.87	Na ⁺ /H ⁺ transporter	SynT, CytoT, Dec	General	

<i>Gjb1</i>	2.84	Gap junction protein	SynT, CytoT, Dec	General	
<i>Miat</i>	2.78	lncRNA	Cyto, Dec	Unknown	
<i>Klrd1</i>	-2.71	Killer cell lectin-like receptor	SynT, Dec	General	
<i>Lonrf2</i>	2.71	Ubiquitin protein ligase	SynT, Dec	Unknown	
<i>Cd3g</i>	2.71	T-cell receptor-CD3 complex protein	SynT, Dec	General	
<i>Hnf4a</i>	2.66	Transcription factor	SynT, Dec	General	
<i>Tshr</i>	-2.66	Thyroid stimulating hormone receptor	SynT, Dec	Unknown	
<i>Mfsd6l</i>	-2.65	Unknown	SynT, CytoT, Dec	Unknown	
<i>Hkdc1</i>	2.57	Glucose metabolism	SynT, CytoT, Dec	General	
<i>Sytl3</i>	-2.53	Exocytosis	SynT, CytoT, Dec	General	
<i>Aff2</i>	2.51	Transcriptional activator	SynT, Dec	General	
<i>St8sia6</i>	2.40	Sialyltransferase	CytoT, Dec	Unknown	
<i>Pllp</i>	2.37	Ion transport	SynT, Dec	General	
<i>Gucy2c</i>	-2.34	cGMP biosynthesis	SynT, CytoT, Dec	General	
<i>Ntrk1</i>	-2.32	Kinase in MAPK pathway	SynT, Dec	General	
<i>Slc39a8</i>	2.31	Zinc ion transporter	SynT, CytoT, Dec	General	
<i>Fndc1</i>	2.29	Fibronectin	SynT, Dec	Unknown	
<i>Mid1</i>	-2.27	Cytoskeleton	SynT, Dec	General	(Sferruzzi-Perri et al. 2009)
<i>Enox1</i>	2.26	Electron transport	SynT, CytoT, Dec	Unknown	
<i>Kazald1</i>	-2.25	Insulin-like growth factor binding	SynT, CytoT, Dec	General	
<i>Ptgs2</i>	-2.25	Prostaglandin synthesis	SynT, Dec	General	
<i>Galc</i>	2.24	Galactosylceramidase	SynT, CytoT, Dec	Unknown	
<i>Galnt17</i>	2.23	Mucin type O-glycan biosynthesis	SynT, Dec	Unknown	
<i>Aldh1l2</i>	-2.21	One-carbon metabolism (mitochondria)	SynT, Dec	General	
<i>Krt23</i>	2.19	Intermediate filament	SynT, CytoT, Dec	General	
<i>Apbb1ip</i>	-2.13	Ras signaling pathway	SynT, Dec	General	
<i>Fam20a</i>	2.13	Unknown	SynT, CytoT, Dec	General	
<i>Stom</i>	2.12	Membrane protein	SynT, CytoT, Dec	General	
<i>Fam84a</i>	2.09	Unknown	SynT, CytoT, Dec	Unknown	
<i>Rps23</i>	-2.06	Ribosomal protein	SynT, CytoT, Dec	General	
<i>Cdh13</i>	2.03	Cadherin	CytoT, Dec	Unknown	
<i>Tgm6</i>	2.02	Transglutaminase	SynT, CytoT, Dec	Unknown	
<i>Atp1a3</i>	2.02	Potassium ion transport	SynT, Dec	Unknown	

<i>Cmc4</i>	-2.00	Mitochondrial protein import	SynT, Dec	General	
Fetal endothelial vascular and decidual expression					
<i>Pianp</i>	50.79	Cell adhesion	FVE, villus stroma, Dec	General	
<i>Il33</i>	4.04	Interleukin	FVE, Dec	General	
<i>Rem1</i>	3.94	Ras-like GTPase	FVE, Dec	Unknown	
<i>Trpv6</i>	3.68	Calcium transport	FVE, Dec	S-TGCs, GlyT at E17.5	(Yang, Ahn & Jeung 2015)
<i>Chrm3</i>	2.85	Cholinergic receptor	FVE, Dec	Unknown	(Huh et al. 2009)
<i>Adamts5</i>	2.76	Disintegrin and metalloproteinase	FVE, Dec	General	
<i>Gpr19</i>	2.46	G protein coupled receptor	FVE, Dec	General	
<i>Arhgef26</i>	2.37	Rho-guanine nucleotide exchange factor	FVE, Dec	General	
<i>Rasgef1a</i>	2.21	Ras guanyl-nucleotide exchange factor activity	FVE, Dec	Unknown	
<i>Fabp4</i>	2.15	Fatty acid binding protein	FVE, Dec	FVE, Dec	(Makkar et al. 2014)
Trophoblast expression					
<i>Fmo3</i>	21.47	Flavin-containing monooxygenase	SynT	Unknown	
<i>A2ml1</i>	6.63	Peptidase inhibitor	SynT	General	
<i>Pigr</i>	5.93	EGF pathway	SynT	General	
<i>Cldn11</i>	5.87	Tight junction	SynT, CytoT	General	
<i>Inhba</i>	4.42	TGF β signaling pathway	General	EPC, P-TGCs at E7.5	(Albano et al. 1994)
<i>Fam196a</i>	3.89	Unknown	SynT, CytoT	General	
<i>Cldn1</i>	3.30	Tight junction	SynT	General	
<i>Serpina3m</i>	3.09	Peptidase inhibitor	(Human ortholog: SERPINA3) SynT	Unknown	
<i>Cubn</i>	2.89	Receptor mediating endocytosis	SynT, CytoT	General	(Burke et al. 2013)
<i>Prl8a1</i>	-2.89	Prolactin cluster	No orthologs	EPC, SpT, P-TGCs	(Simmons et al. 2008)
<i>mt-Tp</i>	2.87	Mitochondrially encoded tRNA proline	SynT	Unknown	
<i>Prl7a1</i>	-2.85	Prolactin cluster	No orthologs	EPC, SpT, P-TGCs	(Simmons et al. 2008)

<i>Hsd17b1</i>	-2.85	17 β -hydroxysteroid dehydrogenase	SynT	Unknown	
<i>Slc27a2</i>	2.60	Fatty acid transport	CytoT	General	
<i>Spon1</i>	2.39	Cell adhesion	CytoT	General	
<i>Crabp2</i>	2.32	Retinoic acid signaling pathway	CytoT	General	
<i>Prl2c2</i>	-2.27	Prolactin cluster (proliferin)	No orthologs	EPC, SpT, P-TGCs	(Simmons et al. 2008)
<i>Chst10</i>	2.27	Sulfotransferase	SynT, CytoT	Unknown	
<i>Rcan2</i>	2.27	Serine/threonine phosphatase regulator	SynT	Unknown	
<i>Enpep</i>	2.20	Aminopeptidase	CytoT	General	
<i>Naip6</i>	-2.17	Apoptosis inhibitory protein	(Human ortholog: NAIP) SynT, CytoT	General	
<i>Asic2</i>	2.14	Cation channel	SynT, CytoT	Unknown	
<i>Foxs1</i>	2.05	Transcription factor	SynT	Unknown	
<i>Amn</i>	2.04	Cobalamin transport	CytoT	General	
<i>Prl3d1</i>	-2.02	Prolactin cluster	No orthologs	P-TGCs	(Simmons et al. 2008)
Fetal endothelial vascular cell expression					
<i>Otoa</i>	-2.63	Predicted adhesion protein	FVE	General	
<i>Cfir</i>	2.62	Chloride channel	FVE	Unknown	
<i>Napsa</i>	-2.36	Aspartic protease	FVE	General	
<i>Zfand4</i>	-2.19	Zinc finger protein	FVE	General	
<i>Ifi205</i>	-2.15	Transcription factor	FVE	General	
Decidua expression					
<i>Hspb7</i>	16.67	Chaperone	Dec	General	
<i>Pdgfrl</i>	14.46	PDGF receptor-like protein	General	Dec at E7.5, unknown in trophoblast	(Ashley et al. 2010)
<i>Klrb1c</i>	-9.71	Killer cell lectin-like receptor	Dec, uNK	uNK	
<i>Fcgbp</i>	9.67	Fc fragment of IgG binding protein	General	Dec at E7.5, unknown in trophoblast	(McConaha et al. 2011)
<i>Klra4</i>	-8.83	Killer cell lectin-like receptor	Dec, uNK	General	
<i>Clip4</i>	6.38	Microtubule associating protein	Dec	Unknown	

<i>Ctla4</i>	-5.52	Cytotoxic T-lymphocyte-associated protein	Dec, CD8+ T cells	General	(van der Zwan et al. 2018)
<i>Guca2b</i>	4.67	cGMP biosynthesis	Unknown	Dec at E7.5, unknown in trophoblast	(McConaha et al. 2011)
<i>Cldn10</i>	4.16	Tight junction protein	Dec	Unknown	
<i>Cdo1</i>	4.08	SHH co-receptor	Unknown	Dec at E10.5	(Rakoczy et al. 2015)
<i>Clca3a1</i>	-3.90	Calcium-activated chloride channel	Dec	General	
<i>Prap1</i>	3.35	Proline rich acidic protein	Dec	General	
<i>Lcn2</i>	3.34	Lipocalin 2	Unknown	Dec at E7.5	(McConaha et al. 2011)
<i>Erv3</i>	3.27	Endogenous retroviral sequence	Unknown	Dec at E7.5	(McConaha et al. 2011)
<i>Fbp2</i>	3.25	Fructose biphosphatase	Dec	General	
<i>Hdg</i>	3.16	Amino acid catabolism	Dec	Unknown	
<i>Ear2</i>	3.04	Ribonuclease	General	Dec at E7.5	(McConaha et al. 2011)
<i>Btg3</i>	-2.86	Transcription factor binding protein	Dec	General	
<i>Slc13a5</i>	2.86	Sodium-dependent citrate transporter	Dec	Unknown	
<i>Duox1</i>	2.56	NADPH oxidase family	Dec	Unknown	
<i>Slpi</i>	2.47	Serine protease inhibitor	Dec	General	
<i>Ltf</i>	2.28	Lactotransferrin	General	Dec at E7.5	(McConaha et al. 2011)
<i>Styk1</i>	-2.19	Serine-threonine kinase	Dec	Unknown	
<i>Gzmb</i>	-2.18	Hydrolase	Dec	uNK cells	(Tachibana et al. 2013)
<i>Arhgef40</i>	2.13	Rho guanine nucleotide exchange factor	Dec	Unknown	
<i>Slc28a2</i>	-2.03	Sodium-coupled purine nucleoside transporter	Dec	General	

*Human protein expression data was obtained from the Human Protein Atlas (Uhlen et al. 2015). Mouse protein expression data obtained from Mouse Encode (Yue et al. 2014) and Mouse Cell Atlas (Han et al. 2018) transcriptomic data. Further references were provided if specific expression data are published. SynT, syncytiotrophoblast; CytoT, cytotrophoblast; FVE, fetal vascular endothelium; Dec, maternal decidua; uNK, uterine natural killer; EVT, extravillous trophoblast; EPC, ectoplacental cone; SpT, spongiotrophoblast cells; P-TGCs, parietal trophoblast giant cells.

Appendix B

The data included in this appendix have been published in Padmanabhan et al. (2018).

B1 Abnormal maternal physiology caused by the *Mtrr^{gt}* mutation

B1.1 Introduction

Dietary folate deficiency in humans is associated with megaloblastic anaemia (Castellanos-Sinco et al. 2015). Megaloblastic anaemia is a type of macrocytic anaemia characterised by fewer in number but enlarged erythrocytes (red blood cells, RBC), fewer reticulocytes, and fewer platelets (thrombocytopenia) (Koury & Ponka 2004). Folate metabolism is required for the synthesis of purines and pyrimidines, therefore is important for DNA replication (Palmer et al. 2017). Erythropoiesis is characterised by high proliferation rates, and therefore folate deficiency or abnormal folate metabolism can making erythrocyte progenitors (reticulocytes) susceptible to genomic instability during erythropoiesis (Wickramasinghe, Cooper & Chalmers 1968; Yoshida et al. 1968). Additionally, folate is essential for the release of methyl groups essential for the methylation of cellular substances (Ghandour et al. 2002; Jacob et al. 1998). Hematopoietic stem cell commitment and differentiation into the erythroid lineage is characterised by dynamic changes in DNA methylation patterns (Madzo et al. 2014). For instance, the binding sites of transcription factors that regulate erythroid differentiation, such as GATA2 and RUNX1, gain 5-hydroxymethylcytosine during differentiation (Madzo et al. 2014). Abnormal regulation of DNA methylation in mice has been associated with blood phenotypes (Ko et al. 2010; Kunimoto et al. 2017; Sasaki et al. 2012). For instance, a loss of function mutation of *Aid*, which is an enzyme that regulates active DNA demethylation, leads to DNA hypermethylation, expansion of myeloid cells, decreased erythroid progenitors, and ultimately, anaemia (Kunimoto et al. 2017). Epigenetic instability caused by global DNA hypomethylation in the *Mtrr^{gt}* mouse model of abnormal folate metabolism (Padmanabhan et al. 2013) could possibly lead to misexpression of genes essential for erythropoiesis. *Mtrr* deficiency can also possibly cause abnormal DNA methylation in the erythroid lineage affecting its differentiation, maturation, and/ or potential for survival.

We identified an age- and sex- dependent hematopoietic phenotype in *Mtrr^{gt/gt}* mice (Padmanabhan et al. 2018). Specifically, we showed that *Mtrr^{gt/gt}* female mice at 5 months of age display macrocytic anaemia, since they have decreased RBC numbers compared to

C57Bl/6 age-matched females (Padmanabhan et al. 2018). We also analysed females at 7 weeks of age, and found that they have normal RBC counts, suggesting that anaemia emerged with age (Padmanabhan et al. 2018). In contrast, *Mtrr^{gt/gt}* male mice of either age group were not anaemic. Sex-specific lymphopenia was also observed, since *Mtrr^{gt/gt}* females had normal lymphocyte and white blood cell numbers compared to C57Bl/6 controls. *Mtrr^{gt/gt}* males and females had normal levels of basophils, eosinophils, and monocytes, which come from the myeloid lineage (Padmanabhan et al. 2018). Erythrocytic macrocytosis and lymphopenia was observed in *Mtrr^{gt/gt}* males at 5 months of age, but not at 7 weeks of age, suggesting that these haematological effects emerged with age (Padmanabhan et al. 2018). Altogether these data showed that the haematological phenotypes not only emerged with age, but also in a sex-specific manner.

We have previously shown that abnormal phenotypes in the *Mtrr^{gt}* model occur in several wildtype generations later and that these multigenerational effects occur through the maternal lineage (Padmanabhan et al. 2013). Therefore, we analysed the blood profile of F1 *Mtrr^{+/+}* females derived from an *Mtrr^{+/gt}* to assess any generational effects of *Mtrr^{gt}* mutation in haematopoiesis. F1 *Mtrr^{+/+}* females have normal folate metabolism, as indicated by normal homocysteine levels. F1 females derived from *Mtrr^{+/gt}* mothers exhibited anaemia, as indicated by reduced RBC counts and haematocrit. In contrast, F1 females derived from *Mtrr^{+/gt}* fathers had normal RBC counts, and therefore were not anaemic, suggesting a parent-of-origin specific effect (Padmanabhan et al. 2018).

Next, we wanted to identify the mechanism behind the macrocytic anaemia observed in aged *Mtrr^{gt/gt}* females and F1 *Mtrr^{+/+}* females. Haemolysis was ruled out, since there was no difference in iron deposition in spleens of male and female *Mtrr^{gt/gt}* mice compared to C57Bl/6. In addition, *Ftl1* mRNA, which mediates iron uptake, and *Hamp1* mRNA, a hormone that regulates iron storage expression was similar in *Mtrr^{gt/gt}* and C57Bl/6 mice (Padmanabhan et al. 2018). These results excluded the hypothesis that anaemia is due to haemolysis of RBCs. Then, we explored the hypothesis that defective differentiation of erythroid precursor occurs (Padmanabhan et al. 2018), by assessing *Epo* mRNA levels in kidneys of adult *Mtrr^{gt/gt}* and F1 *Mtrr^{+/+}* females. Increased *Epo* mRNA levels would suggest induction of erythrocyte formation as a response to anaemia.

B1.2 Methods

Kidneys were collected from two age groups of *Mtrr^{gt/gt}* mice: females and male mice at 7 weeks of age, and female and male mice at 5 months of age (n=3-5 per sex per age group). Kidneys were also collected from the same age groups of female and male *Mtrr^{+/+}* mice derived from either an *Mtrr^{+/gt}* father and a C57Bl/6 mother (paternal), or an *Mtrr^{+/gt}* mother and a C57Bl/6 father (maternal). Kidney samples were homogenised at 6000x for 20 sec for RNA extraction, as described in Section 2.8.

Epo mRNA expression in kidneys was analysed via RT-qPCR as described in Section 2.12, with the following primers: *Epo* F: TCTGCGACAGTCGAGTTCTG, *Epo* R: CTTCTGCACAACCCATCGT, *Hprt* F: TCCTCCTCAGACCGCTTTT, *Hprt* R: CCTGGTTCATCATCGCTAATC at a concentration of 150nM. *Epo* probe #16 (4686896001, Roche) and *Hprt* probe #45 (4692128001, Roche) were also used.

The following modified RT-qPCR reaction was used: FastStart TaqMan Probe master mix (4673409001, Roche) was used under the following protocol: The enzyme was activated at 95°C for 15 minutes and the cDNA was amplified for 40 cycles under the following conditions: denaturation at 95°C for 30 seconds, annealing at 59.8°C for 30 seconds, and extension at 72°C for 30 seconds.

Statistical analysis was performed using GraphPad Prism 6 software. Data were analysed using independent t-tests or ordinary one-way ANOVA with Tukey multiple comparison tests. P values less than 0.05 were considered significant.

B1.3 Results

To assess whether there is increased differentiation of hematopoietic stem cells into erythrocytes, as a response to anaemia, we assessed the levels of *Epo* (Erythropoietin) mRNA expression in adult kidneys. *Epo* is a hormone that regulates erythropoiesis. It is synthesised in the kidneys and stimulates differentiation of erythroid precursors in the bone marrow into red blood cells. Increased *Epo* levels are associated with anaemia (Koury & Ponka 2004). As expected, since male mice were not anaemic, both young and aged *Mtrr^{gt/gt}* male mice showed normal *Epo* mRNA expression compared to C57Bl/6 age-matched males (Figure B1A). In contrast, we observed a 3.0- and an 8.3-fold increase in *Epo* mRNA expression in kidneys of young and old *Mtrr^{gt/gt}* females, respectively, compared to C57Bl/6 age-matched

females ($p < 0.001$, Figure B1A). The increase of *Epo* mRNA expression in kidneys of young *Mtrr^{gt/gt}* female mice in the absence of anaemia, could suggest an early, symptom-free anaemia that progresses with age.

Remarkably, haematological defects were also observed in F1 *Mtrr^{+/+}* females derived from an *Mtrr^{+/gt}* parent (F0). These defects were parent-of-origin-specific, since *Mtrr^{+/+}* females derived from an *Mtrr^{+/gt}* mother displayed normocytic anaemia, while *Mtrr^{+/+}* females derived from an *Mtrr^{+/gt}* father displayed erythrocytic microcytosis not associated with anaemia (Padmanabhan et al. 2018). However, reticulocyte counts, and reticulocyte production indices were normal in both cases. As before, we wanted to assess whether anaemia observed in the F1 *Mtrr^{+/+}* females derived from an *Mtrr^{+/gt}* mother was due to abnormal haematopoiesis. Renal *Epo* mRNA expression was increased in *Mtrr^{+/+}* females derived from an either *Mtrr^{+/gt}* mother or father (3.0-fold increase caused by *Mtrr^{+/gt}* mother, $p = 0.066$, 4.4-fold increase caused by *Mtrr^{+/gt}* father, $p = 0.033$; Figure B1B), although only the latter was statistically significant (Padmanabhan et al. 2018). These data suggest that the erythroid precursors of F1 females are more sensitive to a maternal, rather than a paternal *Mtrr^{gt}* allele. Transcriptional compensation of *Epo* was sufficient to prevent anemia in F1 *Mtrr^{+/+}* females derived from an *Mtrr^{+/gt}* father, but not F1 *Mtrr^{+/+}* females derived from an *Mtrr^{+/gt}* mother.

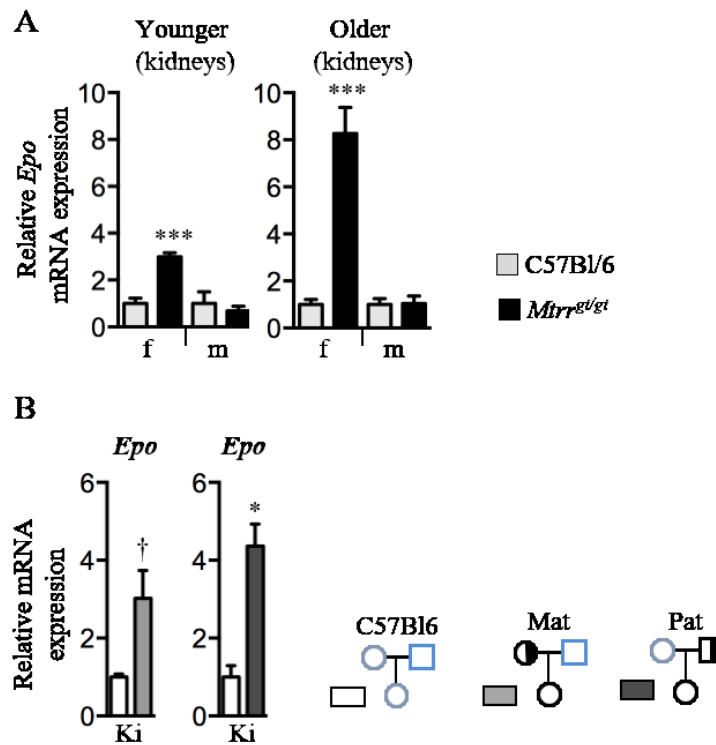


Figure B1 Abnormal erythroid differentiation, not haemolysis is likely the cause of anaemia in mice.

(A) RT-qPCR analysis of *Epo* mRNA expression in kidneys of 7-week old (younger) and 5-month old (older) female (f) and male (m) C57Bl/6 (grey) and *Mtrr^{gt/gt}* (black) mice. n = 3-5 mice were analysed per group. Data are presented as fold change compared to same sex C57Bl/6 controls (normalised to 1) (B) RT-qPCR analysis of *Epo* mRNA expression in kidneys. n = 3-5 mice were analysed per group. Data are presented as fold change compared to C57Bl/6 controls (normalised to 1).

B1.4 Discussion

Megaloblastic anaemia is associated with dietary folate deficiency and defective folate uptake in humans. Abnormal folate metabolism due to the *Mtrr^{gt}* mutation results in an age- and sex-dependent hematopoietic phenotype in *Mtrr^{gt/gt}* mice. More specifically, both young and aged *Mtrr^{gt/gt}* male mice were not anaemic and had normal *Epo* mRNA expression compared to C57Bl/6 age-matched males. In contrast, only aged, but not young *Mtrr^{gt/gt}* females displayed anaemia, although both age groups have increased *Epo* mRNA expression in kidneys compared to C57Bl/6 age-matched females. The increase of *Epo* mRNA expression in kidneys of young *Mtrr^{gt/gt}* female mice in the absence of anaemia, could suggest an early, symptom-free anaemia that progresses with age. Increased *Epo* in our model correlates with

other models of folate deficiency or defective folate uptake (Bills et al. 1992; Koury et al. 1997; Salojin et al. 2011). Anaemia in the *Mtrr^{gt}* model is due to a potential erythrocyte precursor differentiation defect, as indicated by increased *Epo* levels. Normal *Ftl1* and *Hamp1* expression indicated that haemolysis is unlikely to happen. This is in contrast to *Slc46a1* mutants where anaemia is likely to be associated with increased haemolysis of the differentiating erythrocytes (Koury et al. 1997; Salojin et al. 2011).

F1 *Mtrr^{+/+}* females derived from *Mtrr^{+gt}* mothers were anaemic with normal levels of *Epo* mRNA, while F1 *Mtrr^{+/+}* females derived from *Mtrr^{+gt}* fathers were not anaemic, but increased *Epo* mRNA levels. In both instances, this suggests an abnormal maternal environment. In our *Mtrr^{gt}* model of abnormal folate metabolism, the growth phenotypes observed, such as growth restriction and developmental delay, are due to an abnormal maternal environment. A systematic review of the literature and meta-analysis concluded that moderate to severe, but not mild, anaemia in the mother increases the risk of small for gestational age outcomes (Kozuki, Lee & Katz 2012). In these studies, anaemia was defined as low levels of haemoglobin in the blood, associated with reduced quality or quantity of erythrocytes. The cause of anaemia in the studies included in this review is either not stated (Gonzales, Steenland & Tapia 2009; Scanlon et al. 2000), or iron deficiency (Hamalainen, Hakkarainen & Heinonen 2003; Ren et al. 2007; Zhou et al. 1998). This is in contrast to our model, where anaemia is likely due to erythrocyte precursor differentiation defect. Altogether, these data suggest that the *Mtrr^{gt}* heterozygosity of the parent is sufficient to cause an abnormal environment in their *Mtrr^{+/+}* daughter, characterised by anaemia or abnormal *Epo* levels.

The abnormal maternal environment of F1 *Mtrr^{+/+}* females, characterised by anaemia or abnormal *Epo* levels, can be responsible for the growth defects observed in F2 generation. Although FGR is a multifactorial condition, in most cases, fetal growth is constrained by hypoxia and impaired nutrient transport (Hutter, Kingdom & Jaeggi 2010; Marsal 2002). Hypoxia can be caused by anaemia. Even though the levels of haemoglobin, which carries oxygen to the cells, were normal in F1 *Mtrr^{+/+}* females (Padmanabhan et al. 2018), it is possible that the haemoglobin has decreased affinity to oxygen, and therefore lead to hypoxia. Hypoxia leads to increased *Epo* expression (Stockmann & Fandrey 2006). Increased *Epo* levels in F1 *Mtrr^{+/+}* females could suggest that their environment might be hypoxic. This can impair oxygen transport to the placenta or the fetus and impair fetal growth.

Erythropoietic responses to hypoxia, such as increased *Epo* production, are regulated by HIF (Kapitsinou et al. 2010; Stockmann & Fandrey 2006). HIF is a heterodimer, composed of HIF α and HIF β (ARNT) subunits. Defective placental vascularisation was observed in placentas from *Arnt*^{-/-} and *Hif1 α* ^{-/-} *Hif2 α* ^{-/-} conceptuses. In addition, trophoblast stem cells lacking *Hif α* and *Arnt* are unable to differentiate into trophoblast giant cells, or spongiotrophoblast, and differentiate into labyrinth trophoblast instead, suggesting placental development is regulated by hypoxia (Cowden Dahl et al. 2005). Altogether, these studies suggest that the F1 *Mtrr*^{+/+} females might have a hypoxic environment, which might lead to abnormal placental development and function, and ultimately FGR.

Appendix C

Table C.1 DEGs in placentas of phenotypically normal *Mtrr^{gt/gt}* conceptuses compared to C57Bl/6 at E10.5.

C57Bl/6 Vs <i>Mtrr^{gt/gt}</i> PN			
Gene ID	Fold change	Gene abbreviation	Gene name
ENSMUSG00000040264	-219.19	<i>Gbp2b</i>	guanylate binding protein 2b
ENSMUSG00000078994	-63.96	<i>Zfp429</i>	zinc finger protein 429
ENSMUSG00000065922	-11.67	<i>n-R5-8s1</i>	nuclear encoded rRNA 5.8S 1
ENSMUSG00000088088	-10.73	<i>Rmrp</i>	RNA component of mitochondrial RNAase P
ENSMUSG00000073177	-9.64	<i>Gm773</i>	predicted gene 773
ENSMUSG00000042386	-8.69	<i>Tex13b</i>	testis expressed 13B
ENSMUSG00000074871	-8.60	<i>Ctsm</i>	cathepsin M
ENSMUSG00000009292	-8.24	<i>Trpm2</i>	Transient receptor potential cation channel subfamily M member 2
ENSMUSG000000091273	-6.88	<i>Gm6673</i>	predicted gene 6673
ENSMUSG00000067750	-5.78	<i>Khdc1a</i>	KH homology domain-containing protein 1A
ENSMUSG000000100865	-5.36	<i>Gm9320</i>	predicted gene 9320
ENSMUSG000000092837	-4.68	<i>Rpph1</i>	ribonuclease P RNA component H1
ENSMUSG000000023185	-4.53	<i>Ceacam14</i>	carcinoembryonic antigen-related cell adhesion molecule 14
ENSMUSG000000091562	-4.33	<i>Crybg3</i>	beta-gamma crystallin domain containing 3
ENSMUSG000000070798	-4.33	<i>Psg25</i>	pregnancy-specific glycoprotein 25
ENSMUSG000000074359	-4.29	<i>Psg23</i>	pregnancy-specific glycoprotein 23
ENSMUSG000000070797	-4.08	<i>Psg27</i>	pregnancy-specific glycoprotein 27
ENSMUSG000000086695	-4.03	<i>Gm15247</i>	predicted gene 15247
ENSMUSG000000044285	-4.02	<i>Gm1821</i>	predicted gene 1821
ENSMUSG000000065037	-3.83	<i>Rn7sk</i>	RNA, 7SK, nuclear
ENSMUSG000000078793	-3.75	<i>Gm5155</i>	predicted gene 5155

ENSMUSG00000070796	-3.60	<i>Psg21</i>	pregnancy-specific glycoprotein 21
ENSMUSG00000045928	-3.53	<i>4933440M02Rik</i>	RIKEN cDNA 4933440M02 gene
ENSMUSG00000034617	-3.49	<i>Mtrr</i>	5-methyltetrahydrofolate-homocysteine methyltransferase reductase
ENSMUSG00000003505	-3.37	<i>Psg18</i>	pregnancy specific glycoprotein 18
ENSMUSG000000062705	-3.24	<i>Tpbpb</i>	trophoblast specific protein beta
ENSMUSG00000030373	-3.23	<i>Psg28</i>	pregnancy-specific glycoprotein 28
ENSMUSG00000023087	-3.19	<i>Noct</i>	Nocturnin
ENSMUSG00000004540	-3.06	<i>Psg17</i>	pregnancy-specific glycoprotein 17
ENSMUSG00000006154	-3.02	<i>Eps8l1</i>	Epidermal growth factor receptor kinase substrate 8-like protein 1
ENSMUSG00000079476	-2.99	<i>1700011M02Rik</i>	RIKEN cDNA 1700011M02 gene
ENSMUSG00000001901	-2.95	<i>Kcnh6</i>	potassium voltage-gated channel, subfamily H (eag-related), member 6
ENSMUSG00000030368	-2.90	<i>Ceacam11</i>	carcinoembryonic antigen-related cell adhesion molecule 11
ENSMUSG00000103034	-2.89	<i>Gm8797</i>	predicted gene, 8797
ENSMUSG00000097971	-2.87	<i>Gm26917</i>	predicted gene, 26917
ENSMUSG00000098973	-2.84	<i>Mir6236</i>	microRNA 6236
ENSMUSG00000066760	-2.77	<i>Psg16</i>	pregnancy-specific glycoprotein 16
ENSMUSG00000086324	-2.76	<i>Gm15564</i>	predicted gene 15564
ENSMUSG00000061684	-2.72	<i>Rpl21-ps8</i>	ribosomal protein L21, pseudogene 8
ENSMUSG00000026358	-2.71	<i>Rgs1</i>	regulator of G-protein signaling 1
ENSMUSG00000060377	-2.70	<i>Rpl36a-ps1</i>	ribosomal protein L36A, pseudogene 1
ENSMUSG00000094334	-2.62	<i>Fabp5l2</i>	fatty acid binding protein 5-like 2
ENSMUSG00000046899	-2.61	<i>Prl7a2</i>	prolactin family 7, subfamily a, member 2
ENSMUSG00000025789	-2.55	<i>St8sia2</i>	Alpha-2,8-sialyltransferase 8B
ENSMUSG00000040013	-2.54	<i>Fkbp6</i>	Inactive peptidyl-prolyl cis-trans isomerase FKBP6
ENSMUSG00000021439	-2.52	<i>Ctsq</i>	cathepsin Q
ENSMUSG00000029437	-2.50	<i>Il31</i>	Interleukin-31
ENSMUSG00000097276	-2.50	<i>4930525G20Rik</i>	RIKEN cDNA 4930525G20 gene
ENSMUSG00000026390	-2.49	<i>Marco</i>	Macrophage receptor MARCO
ENSMUSG00000053228	-2.48	<i>Ceacam3</i>	carcinoembryonic antigen-related cell adhesion molecule 3

ENSMUSG00000073422	-2.47	<i>H2-Ke6</i>	H2-K region expressed gene 6
ENSMUSG00000075245	-2.46	<i>Gm6043</i>	predicted gene 6043
ENSMUSG00000009596	-2.45	<i>Taf7l</i>	Transcription initiation factor TFIID subunit 7-like
ENSMUSG000000091730	-2.40	<i>Gm17230</i>	predicted gene 17230
ENSMUSG000000080811	-2.39	<i>Gm14513</i>	predicted gene 14513
ENSMUSG00000053411	-2.36	<i>Cbx7</i>	Chromobox protein homolog 7
ENSMUSG00000035202	-2.35	<i>Lars2</i>	Probable leucine--tRNA ligase, mitochondrial
ENSMUSG00000028825	-2.34	<i>Rhd</i>	Rh blood group, D antigen
ENSMUSG00000015224	-2.34	<i>Cyp2j9</i>	cytochrome P450, family 2, subfamily j, polypeptide 9
ENSMUSG00000097368	-2.33	<i>Gm10390</i>	predicted gene, 10390
ENSMUSG00000107810	-2.33	<i>Gm18609</i>	predicted gene, 18609
ENSMUSG00000079017	-2.32	<i>Ifi2712a</i>	Interferon alpha-inducible protein 27-like protein 2A
ENSMUSG00000029369	-2.31	<i>Afm</i>	Afamin
ENSMUSG00000092447	-2.31	<i>Gm7696</i>	predicted gene 7696
ENSMUSG00000027794	-2.30	<i>Sohlh2</i>	Spermatosis- and oosis-specific basic helix-loop-helix-containing protein 2
ENSMUSG00000033834	-2.29	<i>Tpbpa</i>	trophoblast specific protein alpha
ENSMUSG00000086740	-2.28	<i>Gm17029</i>	predicted gene 17029
ENSMUSG00000025932	-2.27	<i>Eya1</i>	Eyes absent homolog 1
ENSMUSG00000062480	-2.27	<i>Acat3</i>	acetyl-Coenzyme A acetyltransferase 3
ENSMUSG00000072940	-2.26	<i>Gm10443</i>	predicted pseudogene 10443
ENSMUSG00000086552	-2.23	<i>Dlx4os</i>	distal-less homeobox 4, opposite strand
ENSMUSG00000020871	-2.23	<i>Dlx4</i>	Homeobox protein DLX-4
ENSMUSG00000034645	-2.23	<i>Zyg11a</i>	zyg-11 family member A, cell cycle regulator
ENSMUSG00000031144	-2.22	<i>Syp</i>	Synaptophysin
ENSMUSG00000069939	-2.21	<i>Gm12070</i>	predicted gene 12070
ENSMUSG00000060727	-2.21	<i>Gm12571</i>	predicted gene 12571
ENSMUSG00000004035	-2.21	<i>Gstm7</i>	Glutathione S-transferase Mu 7
ENSMUSG00000108446	-2.20	<i>Gm44997</i>	predicted gene 44997
ENSMUSG00000081929	-2.19	<i>Rps11-ps2</i>	ribosomal protein S11, pseudogene 2

ENSMUSG00000031994	-2.17	<i>Adamts8</i>	A disintegrin and metalloproteinase with thrombospondin motifs 8 isoform 2
ENSMUSG00000020279	-2.16	<i>Il9r</i>	Interleukin-9 receptor
ENSMUSG00000085465	-2.15	<i>Gm15347</i>	predicted gene 15347
ENSMUSG00000108207	-2.15	<i>1810059H22Rik</i>	RIKEN cDNA 1810059H22 gene
ENSMUSG00000097536	-2.15	<i>2610037D02Rik</i>	RIKEN cDNA 2610037D02 gene
ENSMUSG00000018486	-2.14	<i>Wnt9b</i>	wingless-type MMTV integration site family, member 9B
ENSMUSG00000104443	-2.13	<i>4932442E05Rik</i>	RIKEN cDNA 4932442E05 gene
ENSMUSG00000028137	-2.12	<i>Celf3</i>	CUGBP, Elav-like family member 3
ENSMUSG00000072721	-2.12	<i>Klra14-ps</i>	killer cell lectin-like receptor subfamily A, member 14, pseudogene
ENSMUSG00000031849	-2.11	<i>Comp</i>	Cartilage oligomeric matrix protein
ENSMUSG00000081087	-2.10	<i>Rps15a-ps7</i>	ribosomal protein S15A, pseudogene 7
ENSMUSG00000081231	-2.10	<i>Tcp1-ps1</i>	t-complex protein 1, pseudogene 1
ENSMUSG00000104781	-2.09	<i>Gm43303</i>	predicted gene 43303
ENSMUSG00000097242	-2.07	<i>Gm16907</i>	predicted gene, 16907
ENSMUSG00000095419	-2.07	<i>Gm14328</i>	predicted gene 14328
ENSMUSG00000039079	-2.06	<i>Trhr2</i>	thyrotropin releasing hormone receptor 2
ENSMUSG00000058152	-2.06	<i>Chsy3</i>	Chondroitin sulfate synthase 3
ENSMUSG00000083305	-2.05	<i>Gm13315</i>	predicted gene 13315
ENSMUSG00000086631	-2.05	<i>Gm12784</i>	predicted gene 12784
ENSMUSG00000073530	-2.05	<i>Pappa2</i>	pappalysin 2
ENSMUSG00000105632	-2.04	<i>Gm43272</i>	predicted gene 43272
ENSMUSG00000026919	-2.04	<i>Lcn4</i>	lipocalin 4
ENSMUSG00000104864	-2.04	<i>Gm43655</i>	predicted gene 43655
ENSMUSG00000108402	-2.04	<i>9430064I24Rik</i>	RIKEN cDNA 9430064I24 gene
ENSMUSG00000060938	-2.04	<i>Rpl26</i>	60S ribosomal protein L26
ENSMUSG00000085415	-2.03	<i>Selenok-ps1</i>	selenoprotein K, pseudogene 1
ENSMUSG00000084790	-2.03	<i>Gm15879</i>	predicted gene 15879
ENSMUSG00000026443	-2.02	<i>Lrrn2</i>	leucine rich repeat protein 2, neuronal
ENSMUSG00000086331	-2.02	<i>Gm16310</i>	predicted gene 16310

ENSMUSG00000107428	-2.02	<i>Gm44154</i>	predicted gene, 44154
ENSMUSG00000028730	-2.01	<i>Cfap57</i>	Cilia- and flagella-associated protein 57
ENSMUSG00000097399	-2.01	<i>Gm26555</i>	predicted gene, 26555
ENSMUSG00000040065	2.01	<i>Pfpl</i>	pore forming protein-like
ENSMUSG00000042684	2.01	<i>Npl</i>	N-acetylneuraminate lyase
ENSMUSG00000089704	2.01	<i>Galnt2</i>	Polypeptide N-acetylgalactosaminyltransferase 2 soluble form
ENSMUSG00000000560	2.01	<i>Gabra2</i>	Gamma-aminobutyric acid receptor subunit alpha-2
ENSMUSG00000072437	2.01	<i>Nanos1</i>	Nanos homolog 1
ENSMUSG00000074345	2.02	<i>Tnfaip8l3</i>	Tumor necrosis factor alpha-induced protein 8-like protein 3
ENSMUSG00000054069	2.02	<i>6030452D12Rik</i>	RIKEN cDNA 6030452D12 gene
ENSMUSG00000028158	2.03	<i>Mtp</i>	Microsomal triglyceride transfer protein large subunit
ENSMUSG00000034810	2.03	<i>Scn7a</i>	sodium voltage-gated channel alpha subunit 7
ENSMUSG00000038732	2.04	<i>Mboat1</i>	membrane bound O-acyltransferase domain containing 1
ENSMUSG00000022468	2.04	<i>Endou</i>	Poly(U)-specific endoribonuclease
ENSMUSG00000024354	2.04	<i>Slc23a1</i>	Solute carrier family 23 member 1
ENSMUSG00000062310	2.04	<i>Glrp1</i>	glutamine repeat protein 1
ENSMUSG00000020953	2.04	<i>Coch</i>	Cochlin
ENSMUSG00000026227	2.05	<i>2810459M11Rik</i>	Uncharacterized
ENSMUSG00000046167	2.06	<i>Gldn</i>	Gliomedin Gliomedin shedded ectodomain
ENSMUSG00000026870	2.06	<i>Cutal</i>	cutA divalent cation tolerance homolog-like
ENSMUSG00000029055	2.06	<i>Plch2</i>	1-phosphatidylinositol 4,5-bisphosphate phosphodiesterase eta-2
ENSMUSG00000006221	2.07	<i>Hspb7</i>	Heat shock protein beta-7
ENSMUSG00000024912	2.07	<i>Fosl1</i>	Fos-related antigen 1
ENSMUSG00000098021	2.08	<i>Gm9522</i>	predicted gene 9522
ENSMUSG00000020193	2.08	<i>Zpbp</i>	zona pellucida binding protein
ENSMUSG00000024990	2.09	<i>Rbp4</i>	Retinol-binding protein 4
ENSMUSG00000022755	2.09	<i>Adgrg7</i>	Adhesion G-protein coupled receptor G7
ENSMUSG00000049999	2.09	<i>Ppp1r3d</i>	protein phosphatase 1 regulatory subunit 3D
ENSMUSG00000029380	2.10	<i>Cxcl1</i>	Growth-regulated alpha protein KC(5-72)

ENSMUSG00000045915	2.10	<i>Ccdc42</i>	Coiled-coil domain-containing protein 42
ENSMUSG00000026204	2.11	<i>Ptprn</i>	protein tyrosine phosphatase, receptor type, N
ENSMUSG00000040276	2.12	<i>Pacsin1</i>	Protein kinase C and casein kinase substrate in neurons protein 1
ENSMUSG00000029154	2.13	<i>Cwh43</i>	PGAP2-interacting protein
ENSMUSG00000021477	2.13	<i>Ctsl</i>	cathepsin L
ENSMUSG00000043448	2.14	<i>Gjc2</i>	gap junction protein, gamma 2
ENSMUSG00000059040	2.14	<i>Eno1b</i>	enolase 1B, retrotransposed
ENSMUSG00000103427	2.15	<i>Gm37534</i>	predicted gene, 37534
ENSMUSG00000076612	2.15	<i>Ighg2c</i>	immunoglobulin heavy constant gamma 2C
ENSMUSG00000042734	2.16	<i>Ttc9</i>	tetratricopeptide repeat domain 9
ENSMUSG00000031952	2.16	<i>Chst5</i>	Carbohydrate sulfotransferase 5
ENSMUSG00000026304	2.17	<i>Rab17</i>	Ras-related protein Rab-17
ENSMUSG00000041193	2.18	<i>Pla2g5</i>	phospholipase A2, group V
ENSMUSG00000039313	2.20	<i>AF529169</i>	UPF0258 protein KIAA1024
ENSMUSG00000047797	2.21	<i>Gjb1</i>	gap junction protein, beta 1
ENSMUSG00000040891	2.21	<i>Foxa3</i>	Hepatocyte nuclear factor 3-gamma
ENSMUSG00000108367	2.24	<i>Gm4881</i>	predicted gene, 4881
ENSMUSG00000102189	2.24	<i>Gm37194</i>	predicted gene, 37194
ENSMUSG00000027832	2.24	<i>Ptx3</i>	Pentraxin-related protein PTX3
ENSMUSG00000041577	2.24	<i>Prelp</i>	proline arginine-rich end leucine-rich repeat
ENSMUSG00000045775	2.25	<i>Slc16a5</i>	solute carrier family 16 (monocarboxylic acid transporters), member 5
ENSMUSG00000027376	2.25	<i>Prom2</i>	Prominin-2
ENSMUSG00000052143	2.25	<i>Gm9869</i>	predicted gene, 9869
ENSMUSG00000006205	2.25	<i>Htra1</i>	Serine protease HTRA1
ENSMUSG00000037936	2.26	<i>Scarb1</i>	Scavenger receptor class B member 1
ENSMUSG00000019756	2.28	<i>Prl8a1</i>	prolactin family 8, subfamily a, member 1
ENSMUSG00000031936	2.29	<i>Heph1l</i>	Hephaestin-like protein 1
ENSMUSG00000027249	2.31	<i>F2</i>	coagulation factor II
ENSMUSG00000033102	2.33	<i>Cdc14b</i>	Dual specificity protein phosphatase CDC14B

ENSMUSG00000032496	2.34	<i>Ltf</i>	Lactotransferrin
ENSMUSG00000021364	2.35	<i>Elovl2</i>	Elongation of very long chain fatty acids protein 2
ENSMUSG00000073293	2.36	<i>Nudt10</i>	Diphosphoinositol polyphosphate phosphohydrolase 3-alpha
ENSMUSG00000027870	2.40	<i>Hao2</i>	Hydroxyacid oxidase 2
ENSMUSG00000064372	2.40	<i>mt-Tp</i>	mitochondrially encoded tRNA proline
ENSMUSG00000097017	2.41	<i>Gm26707</i>	predicted gene, 26707
ENSMUSG00000032023	2.42	<i>Jhy</i>	junctional cadherin complex regulator
ENSMUSG00000022949	2.42	<i>Clic6</i>	Chloride intracellular channel protein 6
ENSMUSG00000072978	2.43	<i>Gm5830</i>	predicted pseudogene 5830
ENSMUSG00000056457	2.44	<i>Prl2c3</i>	Mus musculus prolactin family 2, subfamily c, member 4 (Prl2c4), mRNA.
ENSMUSG00000087362	2.49	<i>Gm13710</i>	predicted gene 13710
ENSMUSG00000031760	2.53	<i>Mt3</i>	Metallothionein-3
ENSMUSG00000057170	2.53	<i>Prl3d1</i>	prolactin family 3, subfamily d, member 1
ENSMUSG00000033082	2.53	<i>Clec1a</i>	C-type lectin domain family 1 member A
ENSMUSG00000040600	2.61	<i>Eps8l3</i>	Epidermal growth factor receptor kinase substrate 8-like protein 3
ENSMUSG00000057228	2.61	<i>Aadat</i>	aminoadipate aminotransferase
ENSMUSG00000021850	2.63	<i>1700011H14Rik</i>	RIKEN cDNA 1700011H14 gene
ENSMUSG00000060985	2.65	<i>Tdrd5</i>	Tudor domain-containing protein 5
ENSMUSG00000058626	2.66	<i>Capn11</i>	Calpain-11
ENSMUSG00000073988	2.66	<i>Ttpa</i>	tocopherol (alpha) transfer protein
ENSMUSG00000049556	2.66	<i>Lingol</i>	Leucine-rich repeat and immunoglobulin-like domain-containing nogo receptor-interacting protein 1
ENSMUSG00000028989	2.67	<i>Angptl7</i>	Angiopoietin-related protein 7
ENSMUSG00000035699	2.68	<i>Slc51a</i>	solute carrier family 51, alpha subunit
ENSMUSG00000072849	2.70	<i>Serpina1e</i>	serine (or cysteine) peptidase inhibitor, clade A, member 1E
ENSMUSG00000032257	2.70	<i>Ankk1</i>	Ankyrin repeat and protein kinase domain-containing protein 1
ENSMUSG00000021536	2.70	<i>Adcy2</i>	adenylate cyclase 2
ENSMUSG00000050097	2.72	<i>Ces2b</i>	carboxyesterase 2B
ENSMUSG00000065418	2.72	<i>Mir322</i>	microRNA 322

ENSMUSG00000078995	2.74	<i>Zfp456</i>	zinc finger protein 456
ENSMUSG00000009246	2.75	<i>Trpm5</i>	Transient receptor potential cation channel subfamily M member 5
ENSMUSG00000039037	2.78	<i>St6galnac5</i>	ST6 (alpha-N-acetyl-neuraminyl-2,3-beta-galactosyl-1,3)-N-acetylgalactosaminide alpha-2,6-sialyltransferase 5
ENSMUSG00000031574	2.82	<i>Star</i>	Steroidogenic acute regulatory protein, mitochondrial
ENSMUSG00000076140	2.84	<i>Mir542</i>	microRNA 542
ENSMUSG00000053930	2.84	<i>Shisa6</i>	shisa family member 6
ENSMUSG00000062201	2.84	<i>Prl3d3</i>	prolactin family 3, subfamily d, member 3
ENSMUSG00000019359	2.86	<i>Gdpd2</i>	glycerophosphodiester phosphodiesterase domain containing 2, transcript variant 3
ENSMUSG00000052981	2.89	<i>Ube2ql1</i>	ubiquitin-conjugating enzyme E2Q family-like 1
ENSMUSG00000028544	2.90	<i>Slc5a9</i>	Sodium/glucose cotransporter 4
ENSMUSG00000067081	2.91	<i>Asb18</i>	Ankyrin repeat and SOCS box protein 18
ENSMUSG00000046844	2.93	<i>Vat1l</i>	vesicle amine transport protein 1 like
ENSMUSG00000031883	2.96	<i>Car7</i>	Carbonic anhydrase 7
ENSMUSG00000046203	2.98	<i>Sprr2g</i>	Small proline-rich protein 2G
ENSMUSG00000035226	2.98	<i>Rims4</i>	Regulating synaptic membrane exocytosis protein 4
ENSMUSG00000105703	3.02	<i>Gm43305</i>	predicted gene 43305
ENSMUSG00000032495	3.02	<i>Lrrc2</i>	leucine rich repeat containing 2
ENSMUSG00000029260	3.05	<i>Ugt2b34</i>	UDP glucuronosyltransferase 2 family, polypeptide B34
ENSMUSG00000020226	3.06	<i>Slc5a4b</i>	solute carrier family 5 (neutral amino acid transporters, system A), member 4b
ENSMUSG00000094590	3.06	<i>Gm10251</i>	predicted gene 10251
ENSMUSG00000021795	3.07	<i>Sftpd</i>	Pulmonary surfactant-associated protein D
ENSMUSG00000029273	3.12	<i>Sult1d1</i>	Sulfotransferase 1 family member D1
ENSMUSG00000062737	3.13	<i>Prl3d2</i>	prolactin family 3, subfamily d, member 1
ENSMUSG00000027690	3.13	<i>Slc2a2</i>	solute carrier family 2 (facilitated glucose transporter), member 2
ENSMUSG00000038239	3.27	<i>Hrc</i>	histidine rich calcium binding protein
ENSMUSG00000065503	3.31	<i>Mir351</i>	microRNA 351
ENSMUSG00000049799	3.45	<i>Lrrc19</i>	Leucine-rich repeat-containing protein 19
ENSMUSG00000047990	3.45	<i>C2cd4a</i>	C2 calcium-dependent domain containing 4A

ENSMUSG00000027869	3.52	<i>Hsd3b6</i>	hydroxy-delta-5-steroid dehydrogenase, 3 beta- and steroid delta-isomerase 6
ENSMUSG00000055341	3.55	<i>Zfp457</i>	zinc finger protein 457
ENSMUSG00000011632	3.60	<i>Pinlyp</i>	phospholipase A2 inhibitor and LY6/PLAUR domain containing
ENSMUSG00000101026	3.68	<i>D730001G18Rik</i>	lymphocyte antigen 6 complex, locus G6G (Ly6g6g)
ENSMUSG00000067149	3.70	<i>Jchain</i>	Immunoglobulin J chain
ENSMUSG00000058147	3.76	<i>Xlr3c</i>	X-linked lymphocyte-regulated 3C
ENSMUSG00000035551	3.79	<i>Igfbpl1</i>	Insulin-like growth factor-binding protein-like 1
ENSMUSG00000095079	3.86	<i>Igha</i>	immunoglobulin heavy constant alpha
ENSMUSG00000055409	3.99	<i>Nell1</i>	Protein kinase C-binding protein NELL1
ENSMUSG00000021456	4.18	<i>Fbp2</i>	Fructose-1,6-bisphosphatase isozyme 2
ENSMUSG00000030302	4.33	<i>Atp2b2</i>	Plasma membrane calcium-transporting ATPase 2
ENSMUSG00000105155	4.55	<i>Gm42910</i>	predicted gene 42910
ENSMUSG00000062168	4.89	<i>Ppefl</i>	Serine/threonine-protein phosphatase with EF-hands 1
ENSMUSG00000037334	5.52	<i>H2-M1</i>	histocompatibility 2, M region locus 1
ENSMUSG00000069805	10.46	<i>Fbp1</i>	Fructose-1,6-bisphosphatase 1
ENSMUSG00000031620	13.69	<i>Iqcm</i>	IQ motif containing M

Table C.2 DEGs in placentas of growth restricted *Mtrr^{gt/gt}* conceptuses compared to C57Bl/6 at E10.5.

C57Bl/6 Vs <i>Mtrr^{gt/gt}</i> GR			
Gene ID	Fold change	Gene abbreviation	Gene name
ENSMUSG00000040264	-341.28	<i>Gbp2b</i>	guanylate binding protein 2b
ENSMUSG00000078994	-51.38	<i>Zfp429</i>	zinc finger protein 429
ENSMUSG00000073177	-36.76	<i>Gm773</i>	predicted gene 773
ENSMUSG00000108558	-29.98	<i>Psg-ps1</i>	pregnancy specific glycoprotein, pseudogene 1
ENSMUSG00000074871	-19.49	<i>Ctsm</i>	cathepsin M
ENSMUSG00000030366	-13.64	<i>Ceacam12</i>	carcinoembryonic antigen-related cell adhesion molecule 12
ENSMUSG00000023185	-12.57	<i>Ceacam14</i>	carcinoembryonic antigen-related cell adhesion molecule 14

ENSMUSG00000070798	-10.89	<i>Psg25</i>	pregnancy-specific glycoprotein 25
ENSMUSG00000074359	-10.52	<i>Psg23</i>	pregnancy-specific glycoprotein 23
ENSMUSG00000070797	-9.74	<i>Psg27</i>	pregnancy-specific glycoprotein 27
ENSMUSG00000078793	-9.33	<i>Gm5155</i>	predicted gene 5155
ENSMUSG00000070796	-9.28	<i>Psg21</i>	pregnancy-specific glycoprotein 21
ENSMUSG00000030373	-8.34	<i>Psg28</i>	pregnancy-specific glycoprotein 28
ENSMUSG00000003505	-7.60	<i>Psg18</i>	pregnancy specific glycoprotein 18
ENSMUSG00000008789	-7.55	<i>Ceacam5</i>	Carcinoembryonic antigen-related cell adhesion molecule 5
ENSMUSG00000046899	-7.13	<i>Prl7a2</i>	prolactin family 7, subfamily a, member 2
ENSMUSG00000062705	-6.42	<i>Tpbpb</i>	trophoblast specific protein beta
ENSMUSG00000030368	-6.34	<i>Ceacam11</i>	carcinoembryonic antigen-related cell adhesion molecule 11
ENSMUSG00000091273	-6.26	<i>Gm6673</i>	predicted gene 6673
ENSMUSG00000057195	-6.18	<i>Ceacam13</i>	carcinoembryonic antigen-related cell adhesion molecule 13
ENSMUSG00000067750	-5.88	<i>Khdc1a</i>	KH homology domain-containing protein 1A
ENSMUSG00000004540	-5.57	<i>Psg17</i>	pregnancy specific glycoprotein 17
ENSMUSG00000074870	-5.54	<i>Cts3</i>	cathepsin 3
ENSMUSG00000021345	-4.88	<i>Prl8a6</i>	prolactin family 8, subfamily a, member 6
ENSMUSG00000009596	-4.79	<i>Taf7l</i>	Transcription initiation factor TFIID subunit 7-like
ENSMUSG00000053228	-4.60	<i>Ceacam3</i>	carcinoembryonic antigen-related cell adhesion molecule 3
ENSMUSG00000102700	-3.97	<i>Gm38312</i>	predicted gene, 38312
ENSMUSG00000086050	-3.80	<i>Gm16045</i>	predicted gene 16045
ENSMUSG00000109116	-3.67	<i>Sycp1-ps1</i>	synaptonemal complex protein 1, pseudogene 1
ENSMUSG00000074206	-3.66	<i>Adh6b</i>	alcohol dehydrogenase 6B (class V)
ENSMUSG00000031027	-3.66	<i>Stk33</i>	Serine/threonine-protein kinase 33
ENSMUSG00000034617	-3.64	<i>Mtrr</i>	5-methyltetrahydrofolate-homocysteine methyltransferase reductase
ENSMUSG00000066760	-3.55	<i>Psg16</i>	pregnancy specific glycoprotein 16
ENSMUSG00000021439	-3.51	<i>Ctsq</i>	cathepsin Q
ENSMUSG00000073530	-3.44	<i>Pappa2</i>	pappalysin 2
ENSMUSG00000092624	-3.43	<i>Gm3654</i>	predicted gene 3654

ENSMUSG00000047661	-3.42	<i>1600012P17Rik</i>	RIKEN cDNA 1600012P17 gene
ENSMUSG00000033834	-3.36	<i>Tpbpa</i>	trophoblast specific protein alpha
ENSMUSG00000023087	-3.36	<i>Noct</i>	Nocturnin
ENSMUSG00000019775	-3.26	<i>Rgs17</i>	regulator of G-protein signaling 17
ENSMUSG00000097203	-3.25	<i>4732419C18Rik</i>	RIKEN cDNA 4732419C18 gene
ENSMUSG00000020871	-3.17	<i>Dlx4</i>	Homeobox protein DLX-4
ENSMUSG00000058152	-3.17	<i>Chsy3</i>	Chondroitin sulfate synthase 3
ENSMUSG00000035694	-3.16	<i>Caps2</i>	Calcyphosin-2
ENSMUSG00000058022	-3.14	<i>Adtrp</i>	Androgen-dependent TFPI-regulating protein
ENSMUSG00000034690	-3.04	<i>Nlrp4c</i>	NACHT, LRR and PYD domains-containing protein 4C
ENSMUSG00000027560	-2.96	<i>Dok5</i>	Docking protein 5
ENSMUSG00000045928	-2.92	<i>4933440M02Rik</i>	RIKEN cDNA 4933440M02 gene
ENSMUSG00000031994	-2.92	<i>Adamts8</i>	A disintegrin and metalloproteinase with thrombospondin motifs 8 isoform 2
ENSMUSG00000097276	-2.89	<i>4930525G20Rik</i>	RIKEN cDNA 4930525G20 gene
ENSMUSG00000099812	-2.88	<i>Gm28515</i>	predicted gene 28515
ENSMUSG00000041523	-2.87	<i>Upk2</i>	uroplakin 2
ENSMUSG00000079476	-2.84	<i>1700011M02Rik</i>	RIKEN cDNA 1700011M02 gene
ENSMUSG00000072721	-2.82	<i>Klra14-ps</i>	killer cell lectin-like receptor subfamily A, member 14, pseudogene
ENSMUSG00000073722	-2.80	<i>4931408C20Rik</i>	RIKEN cDNA 4931408C20 gene
ENSMUSG00000000861	-2.80	<i>Bcl11a</i>	B-cell lymphoma/leukemia 11A
ENSMUSG00000025789	-2.79	<i>St8sia2</i>	Alpha-2,8-sialyltransferase 8B
ENSMUSG00000103050	-2.75	<i>Gm38273</i>	predicted gene, 38273
ENSMUSG00000020698	-2.74	<i>Cct6b</i>	chaperonin containing Tcp1, subunit 6b (zeta)
ENSMUSG00000030523	-2.73	<i>Trpm1</i>	Transient receptor potential cation channel subfamily M member 1
ENSMUSG00000006154	-2.72	<i>Eps8ll</i>	Epidermal growth factor receptor kinase substrate 8-like protein 1
ENSMUSG00000034645	-2.69	<i>Zyg11a</i>	zyg-11 family member A, cell cycle regulator
ENSMUSG00000030657	-2.64	<i>Xylt1</i>	xylosyltransferase 1
ENSMUSG00000059898	-2.62	<i>Dsc3</i>	Desmocollin-3
ENSMUSG00000041794	-2.61	<i>Myrip</i>	Rab effector MyRIP

ENSMUSG00000072419	-2.60	<i>Dppa2</i>	Developmental pluripotency-associated protein 2
ENSMUSG00000031972	-2.59	<i>Acta1</i>	Actin, alpha skeletal muscle
ENSMUSG00000067860	-2.59	<i>Zic3</i>	zinc finger protein of the cerebellum 3
ENSMUSG00000086552	-2.58	<i>Dlx4os</i>	distal-less homeobox 4, opposite strand
ENSMUSG00000033453	-2.57	<i>Adamts15</i>	A disintegrin and metalloproteinase with thrombospondin motifs 15
ENSMUSG00000037568	-2.57	<i>Vash2</i>	vasohibin 2
ENSMUSG00000103840	-2.57	<i>1700040K01Rik</i>	RIKEN cDNA 1700040K01 gene
ENSMUSG00000030607	-2.56	<i>Acan</i>	Aggrecan core protein
ENSMUSG00000092225	-2.55	<i>Gm2381</i>	predicted gene 2381
ENSMUSG00000073012	-2.55	<i>Fnd3c2</i>	fibronectin type III domain containing 3C2
ENSMUSG00000022053	-2.50	<i>Ebf2</i>	early B cell factor 2
ENSMUSG00000034450	-2.49	<i>Gulo</i>	gulonolactone (L-) oxidase
ENSMUSG00000024134	-2.47	<i>Six2</i>	Homeobox protein SIX2
ENSMUSG00000022900	-2.44	<i>Ildr1</i>	Immunoglobulin-like domain-containing receptor 1
ENSMUSG00000086631	-2.44	<i>Gm12784</i>	predicted gene 12784
ENSMUSG00000029878	-2.44	<i>Dbpht2</i>	DNA binding protein with his-thr domain
ENSMUSG00000056300	-2.43	<i>Zfp981</i>	zinc finger protein 981
ENSMUSG00000097747	-2.43	<i>Gm26534</i>	predicted gene, 26534
ENSMUSG00000024935	-2.41	<i>Slc1a1</i>	solute carrier family 1 (neuronal/epithelial high affinity glutamate transporter, system Xag), member 1
ENSMUSG00000000730	-2.39	<i>Dnmt3l</i>	DNA (cytosine-5)-methyltransferase 3-like
ENSMUSG00000053411	-2.37	<i>Cbx7</i>	Chromobox protein homolog 7
ENSMUSG00000021347	-2.37	<i>Prl7b1</i>	Prolactin-7B1
ENSMUSG00000021348	-2.36	<i>Prl7d1</i>	prolactin family 7, subfamily d, member 1
ENSMUSG00000036168	-2.36	<i>Ccdc38</i>	Coiled-coil domain-containing protein 38
ENSMUSG00000028354	-2.35	<i>Fmn2</i>	Formin-2
ENSMUSG00000039079	-2.34	<i>Trhr2</i>	thyrotropin releasing hormone receptor 2
ENSMUSG00000040569	-2.33	<i>Slc26a7</i>	Anion exchange transporter
ENSMUSG00000000794	-2.32	<i>Kcnn3</i>	Small conductance calcium-activated potassium channel protein 3

ENSMUSG00000022483	-2.29	<i>Col2a1</i>	Collagen alpha-1(II) chain Collagen alpha-1(II) chain Chondrocalcin
ENSMUSG00000020701	-2.29	<i>Tmem132e</i>	transmembrane protein 132E
ENSMUSG00000005947	-2.28	<i>Itgae</i>	integrin alpha E, epithelial-associated
ENSMUSG000000087651	-2.28	<i>1500009L16Rik</i>	RIKEN cDNA 1500009L16 gene
ENSMUSG00000029648	-2.28	<i>Flt1</i>	fms related tyrosine kinase 1
ENSMUSG00000001661	-2.26	<i>Hoxc6</i>	Homeobox protein Hox-C6
ENSMUSG000000042340	-2.25	<i>Ctfl</i>	Cardiotrophin-1
ENSMUSG00000026357	-2.25	<i>Rgs18</i>	regulator of G-protein signaling 18
ENSMUSG000000068614	-2.24	<i>Actc1</i>	Actin, alpha cardiac muscle 1
ENSMUSG000000031849	-2.24	<i>Comp</i>	Cartilage oligomeric matrix protein
ENSMUSG000000103685	-2.23	<i>Gm37074</i>	predicted gene, 37074
ENSMUSG000000069259	-2.22	<i>Prl6a1</i>	prolactin family 6, subfamily a, member 1
ENSMUSG000000047115	-2.22	<i>Fam221a</i>	Protein FAM221A
ENSMUSG000000030402	-2.21	<i>Ppm1n</i>	Probable protein phosphatase 1N
ENSMUSG000000032224	-2.21	<i>Fam81a</i>	Protein FAM81A
ENSMUSG000000060402	-2.21	<i>Chst8</i>	Carbohydrate sulfotransferase 8
ENSMUSG000000029369	-2.19	<i>Afm</i>	Afamin
ENSMUSG000000025081	-2.19	<i>Tdrd1</i>	Tudor domain-containing protein 1
ENSMUSG000000032908	-2.18	<i>Sgpp2</i>	Sphingosine-1-phosphate phosphatase 2
ENSMUSG000000064194	-2.17	<i>Zfp936</i>	zinc finger protein 936
ENSMUSG000000029372	-2.17	<i>Ppbb</i>	pro-platelet basic protein
ENSMUSG000000064294	-2.17	<i>Aox3</i>	Aldehyde oxidase 3
ENSMUSG000000046854	-2.15	<i>Pip5k1l</i>	Phosphatidylinositol 4-phosphate 5-kinase-like protein 1
ENSMUSG000000028519	-2.15	<i>Dabl</i>	Disabled homolog 1
ENSMUSG000000102555	-2.15	<i>6430511E19Rik</i>	RIKEN cDNA 6430511E19 gene
ENSMUSG000000070331	-2.14	<i>Qrich2</i>	glutamine rich 2
ENSMUSG000000092335	-2.13	<i>Zfp977</i>	zinc finger protein 977
ENSMUSG000000027716	-2.13	<i>Trpc3</i>	transient receptor potential cation channel, subfamily C, member 3
ENSMUSG000000026443	-2.12	<i>Lrrn2</i>	leucine rich repeat protein 2, neuronal

ENSMUSG00000070719	-2.12	<i>Pla2g4d</i>	cytosolic phospholipase A2 delta
ENSMUSG00000069258	-2.11	<i>Prl2b1</i>	prolactin family 2, subfamily b, member 1
ENSMUSG00000027562	-2.10	<i>Car2</i>	Mus musculus carbonic anhydrase 2 (Car2), transcript variant 2, mRNA.
ENSMUSG00000019876	-2.10	<i>Pkib</i>	cAMP-dependent protein kinase inhibitor beta
ENSMUSG00000043549	-2.10	<i>Fam90a1b</i>	family with sequence similarity 90, member A1B
ENSMUSG00000066607	-2.10	<i>6030419C18Rik</i>	UPF0583
ENSMUSG00000086924	-2.10	<i>Gm11766</i>	predicted gene 11766
ENSMUSG00000032015	-2.09	<i>Pou2f3</i>	POU domain, class 2, transcription factor 3
ENSMUSG00000031790	-2.08	<i>Mmp15</i>	matrix metalloproteinase-15
ENSMUSG00000062444	-2.07	<i>Ap3b2</i>	AP-3 complex subunit beta-2
ENSMUSG00000033590	-2.07	<i>Myo5c</i>	myosin VC
ENSMUSG00000033882	-2.07	<i>Rbm46</i>	probable RNA-binding protein 46
ENSMUSG00000031144	-2.05	<i>Syp</i>	Synaptophysin
ENSMUSG00000056972	-2.05	<i>Magel2</i>	MAGE-like protein 2
ENSMUSG00000035104	-2.05	<i>Eva1a</i>	eva1 homolog A
ENSMUSG00000043924	-2.05	<i>Ncmap</i>	noncompact myelin-associated protein
ENSMUSG00000038319	-2.04	<i>Kcnh2</i>	potassium voltage-gated channel subfamily H member 2
ENSMUSG00000021363	-2.04	<i>Mak</i>	serine/threonine-protein kinase MAK
ENSMUSG00000041287	-2.03	<i>Sox15</i>	SRY (sex determining region Y)-box 15
ENSMUSG00000020908	-2.03	<i>Myh3</i>	myosin-3
ENSMUSG00000007989	-2.02	<i>Fzd3</i>	frizzled-3
ENSMUSG00000032034	-2.02	<i>Kcnj5</i>	G protein-activated inward rectifier potassium channel 4
ENSMUSG00000055679	-2.02	<i>Ctsr</i>	cathepsin R
ENSMUSG00000002266	-2.02	<i>Zim1</i>	zinc finger, imprinted 1
ENSMUSG00000029452	-2.02	<i>Tmem116</i>	transmembrane protein 116
ENSMUSG00000045004	-2.01	<i>Spata21</i>	spermatogenesis-associated protein 21
ENSMUSG00000007594	-2.01	<i>Hapln4</i>	hyaluronan and proteoglycan link protein 4
ENSMUSG00000028626	-2.01	<i>Col9a2</i>	collagen type IX alpha 2 chain
ENSMUSG00000027765	-2.01	<i>P2ry1</i>	purinergic receptor P2Y, G-protein coupled 1

ENSMUSG00000004542	-2.01	<i>Psg19</i>	pregnancy specific glycoprotein 19
ENSMUSG00000029646	-2.00	<i>Cdx2</i>	Homeobox protein CDX-2
ENSMUSG00000021482	2.00	<i>Aaed1</i>	AhpC/TSA antioxidant enzyme domain containing 1
ENSMUSG000000087168	2.00	<i>Gm15983</i>	predicted gene 15983
ENSMUSG00000040065	2.01	<i>Pfpl</i>	pore forming protein-like
ENSMUSG00000074575	2.01	<i>Kcng1</i>	potassium voltage-gated channel subfamily G member 1
ENSMUSG00000053930	2.02	<i>Shisa6</i>	shisa family member 6
ENSMUSG00000063704	2.02	<i>Mapk15</i>	mitogen-activated protein kinase 15
ENSMUSG00000039004	2.03	<i>Bmp6</i>	bone morphogenetic protein 6
ENSMUSG00000079598	2.03	<i>Clec2l</i>	C-type lectin domain family 2 member L
ENSMUSG00000109446	2.04	<i>Gm9195</i>	predicted gene 9195
ENSMUSG00000058454	2.04	<i>Dhcr7</i>	7-dehydrocholesterol reductase
ENSMUSG00000049999	2.04	<i>Ppp1r3d</i>	protein phosphatase 1 regulatory subunit 3D
ENSMUSG00000031952	2.04	<i>Chst5</i>	carbohydrate sulfotransferase 5
ENSMUSG00000021319	2.05	<i>Sfrp4</i>	secreted frizzled-related protein 4
ENSMUSG00000041577	2.06	<i>Prelp</i>	proline arginine-rich end leucine-rich repeat
ENSMUSG00000002885	2.06	<i>Adgre5</i>	adhesion G protein-coupled receptor E5
ENSMUSG00000034570	2.06	<i>Inpp5j</i>	phosphatidylinositol 4,5-bisphosphate 5-phosphatase A
ENSMUSG00000055629	2.06	<i>B4galnt4</i>	N-acetyl-beta-glucosaminyl-glycoprotein 4-beta-N-acetylgalactosaminyltransferase 1
ENSMUSG00000022840	2.06	<i>Adcy5</i>	adenylate cyclase type 5
ENSMUSG00000035916	2.07	<i>Ptprq</i>	phosphatidylinositol phosphatase PTPRQ
ENSMUSG00000032323	2.07	<i>Cyp11al</i>	cholesterol side-chain cleavage enzyme, mitochondrial
ENSMUSG00000034159	2.07	<i>2310007B03Rik</i>	Uncharacterized
ENSMUSG00000044748	2.07	<i>Defbl</i>	beta-defensin 1
ENSMUSG00000071984	2.08	<i>Fndc1</i>	fibronectin type III domain containing 1
ENSMUSG00000032023	2.09	<i>Jhy</i>	junctional cadherin complex regulator
ENSMUSG00000036560	2.10	<i>Lgi4</i>	leucine-rich repeat LGI family member 4
ENSMUSG000000087033	2.10	<i>Gm14155</i>	predicted gene 14155
ENSMUSG00000026259	2.11	<i>Ngef</i>	ephexin-1

ENSMUSG00000033595	2.11	<i>Lgi3</i>	leucine-rich repeat LGI family member 3
ENSMUSG00000020654	2.11	<i>Adcy3</i>	adenylate cyclase type 3
ENSMUSG00000004558	2.11	<i>Ndrp2</i>	protein NDRG2 Protein NDRG2, N-terminally processed
ENSMUSG00000034652	2.11	<i>Cd300a</i>	Mus musculus CD300A molecule (Cd300a), transcript variant 2, mRNA
ENSMUSG00000046623	2.11	<i>Gjb4</i>	gap junction protein, beta 4
ENSMUSG00000079012	2.13	<i>Serpina3m</i>	serine protease inhibitor A3M
ENSMUSG00000035735	2.14	<i>Dagla</i>	Sn1-specific diacylglycerol lipase alpha
ENSMUSG00000032548	2.14	<i>Slco2a1</i>	solute carrier organic anion transporter family, member 2a1
ENSMUSG00000030084	2.15	<i>Plxna1</i>	plexin-A1
ENSMUSG00000020017	2.15	<i>Hal</i>	histidine ammonia-lyase
ENSMUSG00000027358	2.15	<i>Bmp2</i>	bone morphotic protein 2
ENSMUSG00000027513	2.15	<i>Pck1</i>	phosphoenolpyruvate carboxykinase, cytosolic [GTP]
ENSMUSG00000020953	2.16	<i>Coch</i>	cochlin
ENSMUSG00000039037	2.16	<i>St6galnac5</i>	ST6 (alpha-N-acetyl-neuraminyl-2,3-beta-galactosyl-1,3)-N-acetylgalactosaminide alpha-2,6-sialyltransferase 5
ENSMUSG00000043448	2.18	<i>Gjc2</i>	gap junction protein, gamma 2
ENSMUSG00000099429	2.18	<i>1600019K03Rik</i>	RIKEN cDNA 1600019K03 gene
ENSMUSG00000028976	2.20	<i>Slc2a5</i>	solute carrier family 2 (facilitated glucose transporter), member 5
ENSMUSG00000062310	2.21	<i>Glrp1</i>	glutamine repeat protein 1
ENSMUSG00000019756	2.21	<i>Prl8a1</i>	prolactin family 8, subfamily a, member 1
ENSMUSG00000056073	2.22	<i>Grik2</i>	glutamate receptor ionotropic, kainate 2
ENSMUSG00000044177	2.22	<i>Wfikkn2</i>	WAP, follistatin/kazal, immunoglobulin, kunitz and netrin domain containing 2
ENSMUSG00000076613	2.22	<i>Ighg2b</i>	immunoglobulin heavy constant gamma 2B
ENSMUSG00000015451	2.25	<i>C4a</i>	complement component 4A (Rodgers blood group)
ENSMUSG00000036718	2.26	<i>Micall2</i>	MICAL-like protein 2
ENSMUSG00000018819	2.31	<i>Lsp1</i>	lymphocyte-specific protein 1
ENSMUSG00000051243	2.32	<i>Islr2</i>	immunoglobulin superfamily containing leucine-rich repeat protein 2
ENSMUSG00000029055	2.34	<i>Plch2</i>	1-phosphatidylinositol 4,5-bisphosphate phosphodiesterase eta-2
ENSMUSG00000024912	2.34	<i>Fosl1</i>	Fos-related antigen 1

ENSMUSG00000027978	2.34	<i>Prss12</i>	protease, serine 12 neurotrypsin (motopsin)
ENSMUSG00000054069	2.35	<i>6030452D12Rik</i>	RIKEN cDNA 6030452D12 gene
ENSMUSG00000042734	2.36	<i>Ttc9</i>	tetratricopeptide repeat domain 9
ENSMUSG00000026420	2.38	<i>Il24</i>	interleukin 24
ENSMUSG00000090291	2.39	<i>Lrrc10b</i>	leucine rich repeat containing 10B
ENSMUSG00000023885	2.40	<i>Thbs2</i>	thrombospondin-2
ENSMUSG00000032051	2.41	<i>Fdx1</i>	ferredoxin 1
ENSMUSG00000040276	2.43	<i>Pacsin1</i>	protein kinase C and casein kinase substrate in neurons protein 1
ENSMUSG00000090588	2.43	<i>Gm9573</i>	predicted gene 9573
ENSMUSG00000072601	2.45	<i>Ear1</i>	eosinophil cationic protein 1
ENSMUSG00000079092	2.45	<i>Prl2c2</i>	prolactin-2C2
ENSMUSG00000033102	2.47	<i>Cdc14b</i>	dual specificity protein phosphatase CDC14B
ENSMUSG00000050635	2.47	<i>Sprr2f</i>	small proline-rich protein 2F
ENSMUSG00000033765	2.48	<i>Calm4</i>	calmodulin-4
ENSMUSG00000025475	2.51	<i>Adgral</i>	adhesion G protein-coupled receptor A1
ENSMUSG00000031936	2.54	<i>Heph1l</i>	hephaestin-like protein 1
ENSMUSG00000026204	2.55	<i>Ptprn</i>	protein tyrosine phosphatase, receptor type, N
ENSMUSG00000078995	2.56	<i>Zfp456</i>	zinc finger protein 456
ENSMUSG00000061540	2.57	<i>Orm2</i>	orosomuroid 2
ENSMUSG00000033082	2.60	<i>Clec1a</i>	C-type lectin domain family 1 member A
ENSMUSG00000098021	2.62	<i>Gm9522</i>	predicted gene 9522
ENSMUSG00000022468	2.63	<i>Endou</i>	Poly(U)-specific endoribonuclease
ENSMUSG00000097017	2.64	<i>Gm26707</i>	predicted gene, 26707
ENSMUSG00000032495	2.66	<i>Lrrc2</i>	leucine rich repeat containing 2
ENSMUSG00000058755	2.67	<i>Osm</i>	oncostatin-M
ENSMUSG00000021477	2.67	<i>Ctsl</i>	cathepsin L
ENSMUSG00000041193	2.68	<i>Pla2g5</i>	phospholipase A2, group V
ENSMUSG00000068536	2.68	<i>Doxl2</i>	diamine oxidase-like protein 2
ENSMUSG00000027376	2.69	<i>Prom2</i>	prominin-2

ENSMUSG00000045915	2.72	<i>Ccdc42</i>	coiled-coil domain-containing protein 42
ENSMUSG00000094590	2.73	<i>Gm10251</i>	predicted gene 10251
ENSMUSG00000037936	2.74	<i>Scarb1</i>	scavenger receptor class B member 1
ENSMUSG00000067081	2.76	<i>Asb18</i>	ankyrin repeat and SOCS box protein 18
ENSMUSG00000108367	2.78	<i>Gm4881</i>	predicted gene 4881
ENSMUSG00000060985	2.81	<i>Tdrd5</i>	tudor domain-containing protein 5
ENSMUSG00000027603	2.81	<i>Ggt7</i>	glutathione hydrolase 7
ENSMUSG00000085651	2.87	<i>Gm11695</i>	predicted gene 11695
ENSMUSG00000006205	2.89	<i>Htra1</i>	serine protease HTRA1
ENSMUSG00000026241	2.90	<i>Nppc</i>	natriuretic peptide type C
ENSMUSG00000046203	2.92	<i>Sprr2g</i>	small proline-rich protein 2G
ENSMUSG00000058147	2.95	<i>Xlr3c</i>	X-linked lymphocyte-regulated 3C
ENSMUSG00000095079	2.97	<i>Igha</i>	immunoglobulin heavy constant alpha
ENSMUSG00000045775	2.97	<i>Slc16a5</i>	solute carrier family 16 (monocarboxylic acid transporters), member 5
ENSMUSG00000021536	2.98	<i>Adcy2</i>	adenylate cyclase 2
ENSMUSG00000049556	2.99	<i>Lingo1</i>	leucine-rich repeat and immunoglobulin-like domain-containing nogo receptor-interacting protein 1
ENSMUSG00000031760	3.03	<i>Mt3</i>	metallothionein-3
ENSMUSG00000032257	3.09	<i>Ankk1</i>	ankyrin repeat and protein kinase domain-containing protein 1
ENSMUSG00000000049	3.10	<i>ApoH</i>	beta-2-glycoprotein 1
ENSMUSG00000057170	3.16	<i>Prl3d1</i>	prolactin family 3, subfamily d, member 1
ENSMUSG00000076612	3.25	<i>Ighg2c</i>	immunoglobulin heavy constant gamma 2C
ENSMUSG00000035226	3.28	<i>Rims4</i>	regulating synaptic membrane exocytosis protein 4
ENSMUSG00000031574	3.30	<i>Star</i>	steroidogenic acute regulatory protein, mitochondrial
ENSMUSG00000046844	3.30	<i>Vat1l</i>	vesicle amine transport protein 1 like
ENSMUSG00000021795	3.33	<i>Sftpd</i>	pulmonary surfactant-associated protein D
ENSMUSG00000038239	3.43	<i>Hrc</i>	histidine rich calcium binding protein
ENSMUSG00000020226	3.46	<i>Slc5a4b</i>	solute carrier family 5 (neutral amino acid transporters, system A), member 4b
ENSMUSG00000021456	3.49	<i>Fbp2</i>	fructose-1,6-bisphosphatase isozyme 2

ENSMUSG00000062201	3.74	<i>Prl3d3</i>	prolactin family 3, subfamily d, member 3
ENSMUSG00000009246	3.78	<i>Trpm5</i>	transient receptor potential cation channel subfamily M member 5
ENSMUSG00000019359	3.79	<i>Gdpd2</i>	glycerophosphodiester phosphodiesterase domain containing 2, transcript variant 3
ENSMUSG00000062737	3.91	<i>Prl3d2</i>	prolactin family 3, subfamily d, member 1
ENSMUSG00000035551	4.48	<i>Igfbpl1</i>	insulin-like growth factor-binding protein-like 1
ENSMUSG00000055409	4.66	<i>Nell1</i>	protein kinase C-binding protein NELL1
ENSMUSG00000027869	4.87	<i>Hsd3b6</i>	hydroxy-delta-5-steroid dehydrogenase, 3 beta- and steroid delta-isomerase 6
ENSMUSG00000037334	4.91	<i>H2-M1</i>	histocompatibility 2, M region locus 1
ENSMUSG00000101026	5.07	<i>D730001G18Rik</i>	lymphocyte antigen 6 complex, locus G6G (Ly6g6g)
ENSMUSG00000062168	5.16	<i>Ppefl</i>	serine/threonine-protein phosphatase with EF-hands 1
ENSMUSG00000030302	5.53	<i>Atp2b2</i>	plasma membrane calcium-transporting ATPase 2
ENSMUSG00000105703	5.83	<i>Gm43305</i>	predicted gene 43305
ENSMUSG00000069805	12.30	<i>Fbp1</i>	fructose-1,6-bisphosphatase 1
ENSMUSG00000031620	12.59	<i>Iqcm</i>	IQ motif containing M

Table C.3 DEGs in placentas of phenotypically normal *Mtrr^{gt/gt}* conceptuses compared to growth restricted *Mtrr^{gt/gt}* conceptuses at E10.5.

<i>Mtrr^{gt/gt}</i> PN Vs <i>Mtrr^{gt/gt}</i> GR			
Gene ID	Fold change	Gene abbreviation	Gene name
ENSMUSG00000065922	-16.62	<i>n-R5-8s1</i>	nuclear encoded rRNA 5.8S 1
ENSMUSG00000088088	-7.19	<i>Rmrp</i>	RNA component of mitochondrial RNAase P
ENSMUSG00000092837	-3.85	<i>Rpph1</i>	ribonuclease P RNA component H1
ENSMUSG00000097971	-3.09	<i>Gm26917</i>	predicted gene, 26917
ENSMUSG00000069939	-2.97	<i>Gm12070</i>	predicted gene 12070
ENSMUSG00000085415	-2.86	<i>Selenok-ps1</i>	selenoprotein K, pseudogene 1
ENSMUSG00000091562	-2.73	<i>Crybg3</i>	beta-gamma crystallin domain containing 3
ENSMUSG00000098973	-2.42	<i>Mir6236</i>	microRNA 6236

ENSMUSG00000060727	-2.39	<i>Gm12571</i>	predicted gene 12571
ENSMUSG00000094334	-2.36	<i>Fabp512</i>	fatty acid binding protein 5-like 2
ENSMUSG00000082566	-2.35	<i>Gm11485</i>	predicted gene 11485
ENSMUSG00000003477	-2.29	<i>Inmt</i>	indolethylamine N-methyltransferase
ENSMUSG00000026919	-2.28	<i>Lcn4</i>	lipocalin 4
ENSMUSG00000095419	-2.27	<i>Gm14328</i>	predicted gene 14328
ENSMUSG00000072612	-2.25	<i>Gm10382</i>	predicted gene 10382
ENSMUSG00000081087	-2.19	<i>Rps15a-ps7</i>	ribosomal protein S15A, pseudogene 7
ENSMUSG00000109408	-2.16	<i>A930037H05Rik</i>	RIKEN cDNA A930037H05 gene
ENSMUSG00000101567	-2.14	<i>Txn-ps1</i>	thioredoxin, pseudogene 1
ENSMUSG00000092116	-2.12	<i>Gm10320</i>	predicted gene 10320
ENSMUSG00000104864	-2.11	<i>Gm43655</i>	predicted gene 43655
ENSMUSG00000020018	-2.08	<i>Snrpf</i>	small nuclear ribonucleoprotein polypeptide F
ENSMUSG00000072940	-2.05	<i>Gm10443</i>	predicted pseudogene 10443
ENSMUSG00000106926	-2.05	<i>Rpl7-ps7</i>	ribosomal protein L7, pseudogene 7
ENSMUSG00000027716	2.00	<i>Trpc3</i>	transient receptor potential cation channel, subfamily C, member 3
ENSMUSG00000021347	2.03	<i>Prl7b1</i>	prolactin-7B1
ENSMUSG00000073293	2.06	<i>Nudt10</i>	diphosphoinositol polyphosphate phosphohydrolase 3-alpha
ENSMUSG00000001657	2.08	<i>Hoxc8</i>	homeobox protein Hox-C8
ENSMUSG00000074817	2.09	<i>Papolb</i>	poly(A) polymerase beta
ENSMUSG00000029878	2.09	<i>Dbpht2</i>	DNA binding protein with his-thr domain
ENSMUSG00000100826	2.10	<i>Snhg14</i>	small nucleolar RNA host gene 14
ENSMUSG00000010592	2.15	<i>Dazl</i>	deleted in azoospermia-like
ENSMUSG00000067860	2.18	<i>Zic3</i>	zinc finger protein of the cerebellum 3
ENSMUSG00000091955	2.19	<i>Gm9844</i>	predicted pseudogene 9844
ENSMUSG00000096929	2.22	<i>A330023F24Rik</i>	RIKEN cDNA A330023F24 gene
ENSMUSG00000036168	2.24	<i>Ccdc38</i>	coiled-coil domain-containing protein 38
ENSMUSG00000031027	2.36	<i>Stk33</i>	serine/threonine-protein kinase 33
ENSMUSG00000075324	2.49	<i>Fign</i>	fidgetin
ENSMUSG00000040167	2.60	<i>Ikzf5</i>	zinc finger protein Pegasus

ENSMUSG00000099812	2.64	<i>Gm28515</i>	predicted gene 28515
ENSMUSG00000046899	2.73	<i>Pr17a2</i>	prolactin family 7, subfamily a, member 2
ENSMUSG00000046942	2.74	<i>Mageb16</i>	melanoma-associated antigen B16
ENSMUSG00000021345	2.75	<i>Pr18a6</i>	prolactin family 8, subfamily a, member 6
ENSMUSG00000072978	2.96	<i>Gm5830</i>	predicted pseudogene 5830
ENSMUSG00000109116	3.17	<i>Sycp1-ps1</i>	synaptonemal complex protein 1, pseudogene 1

Table C.4 DEGs in placentas of growth enhanced F2 *Mtrr*^{+/+} conceptuses compared to C57Bl/6 placentas at E10.5.

C57Bl/6 Vs F2 <i>Mtrr</i>^{+/+} GE			
Gene ID	Fold change	Gene abbreviation	Gene name
ENSMUSG00000040264	-7.06	<i>Gbp2b</i>	guanylate binding protein 2b

Table C.5 DEGs in placentas of growth enhanced F2 *Mtrr*^{+/+} conceptuses compared to placentas of phenotypically normal F2 *Mtrr*^{+/+} conceptuses E10.5.

F2 <i>Mtrr</i>^{+/+} PN Vs F2 <i>Mtrr</i>^{+/+} GE			
Gene ID	Fold change	Gene abbreviation	Gene name
ENSMUSG00000057897	2.06	<i>Camk2b</i>	calcium/calmodulin-dependent protein kinase II, beta

Table C.6 DEGs in placentas of growth enhanced F2 *Mtrr*^{+/+} conceptuses compared to C57Bl/6 placentas at E10.5 after embryo transfer.

C57Bl/6 transferred Vs F2 <i>Mtrr</i>^{+/+} GE transferred			
Gene ID	Fold change	Gene abbreviation	Gene name
ENSMUSG00000021346	9.17	<i>Pr18a8</i>	prolactin family 8, subfamily a, member 81
ENSMUSG00000006490	3.88	<i>Pr18a9</i>	prolactin family8, subfamily a, member 9
ENSMUSG00000004542	2.93	<i>Psg19</i>	pregnancy specific glycoprotein 19
ENSMUSG00000027386	2.80	<i>Fbln7</i>	fibulin 7

ENSMUSG00000091764	2.30	<i>Zfp964</i>	zinc finger protein 964
ENSMUSG00000074277	2.10	<i>Phldb3</i>	pleckstrin homology like domain, family B, member 3

Table C.7 DEGs in placentas of C57Bl/6 conceptuses at E10.5 after embryo transfer.

C57Bl/6 Vs C57Bl/6 transferred			
Gene ID	Fold change	Gene abbreviation	Gene name
ENSMUSG00000073177	-40.97	<i>Gm773</i>	predicted gene 773
ENSMUSG00000072844	-14.49	<i>G530011O06Rik</i>	RIKEN cDNA G530011O06 gene
ENSMUSG00000009292	-10.10	<i>Trpm2</i>	transient receptor potential cation channel, subfamily M, member 2
ENSMUSG00000030325	-9.71	<i>Klrblc</i>	killer cell lectin-like receptor subfamily B member 1C
ENSMUSG00000019102	-9.29	<i>Aldh3a1</i>	aldehyde dehydrogenase family 3, subfamily A1
ENSMUSG00000090015	-9.00	<i>Gm15446</i>	predicted gene 15446
ENSMUSG00000079852	-8.83	<i>Klra4</i>	killer cell lectin-like receptor, subfamily A, member 4
ENSMUSG00000072721	-8.07	<i>Klra14-ps</i>	killer cell lectin-like receptor subfamily A, member 14, pseudogene
ENSMUSG00000090710	-7.90	<i>Gm9513</i>	predicted gene 9513
ENSMUSG00000023093	-7.67	<i>Gm7257</i>	predicted gene 7257
ENSMUSG00000062310	-7.40	<i>Glrp1</i>	glutamine repeat protein 1
ENSMUSG00000090709	-7.09	<i>Gm17173</i>	predicted gene 17173
ENSMUSG00000089727	-6.82	<i>Klra8</i>	killer cell lectin-like receptor, subfamily A, member 8
ENSMUSG00000020702	-6.81	<i>Ccl1</i>	chemokine (C-C motif) ligand 1
ENSMUSG00000071489	-6.18	<i>Ptgdr</i>	prostaglandin D receptor
ENSMUSG00000067750	-5.97	<i>Khdc1a</i>	KH domain containing 1A
ENSMUSG00000085391	-5.95	<i>Gm16150</i>	predicted gene 16150
ENSMUSG00000073294	-5.63	<i>AU022751</i>	expressed sequence AU022751
ENSMUSG00000067599	-5.59	<i>Klra7</i>	killer cell lectin-like receptor, subfamily A, member 7
ENSMUSG00000026011	-5.52	<i>Ctla4</i>	cytotoxic T-lymphocyte-associated protein 4
ENSMUSG00000006056	-5.19	<i>Calcoco2</i>	calcium binding and coiled-coil domain 2

ENSMUSG00000079071	-5.15	<i>Gm14085</i>	predicted gene 14085
ENSMUSG00000010592	-4.96	<i>Dazl</i>	deleted in azoospermia-like
ENSMUSG00000087263	-4.86	<i>Gm15726</i>	predicted gene 15726
ENSMUSG00000073010	-4.69	<i>Gm5127</i>	predicted gene 5127
ENSMUSG00000086695	-4.63	<i>Gm15247</i>	predicted gene 15247
ENSMUSG00000026358	-4.34	<i>Rgs1</i>	regulator of G-protein signalling 1
ENSMUSG00000079105	-4.09	<i>C7</i>	complement component 7
ENSMUSG00000024155	-4.07	<i>Meiob</i>	meiosis specific with OB domains
ENSMUSG00000047884	-4.07	<i>Klk9</i>	kallikrein related-peptidase 9
ENSMUSG00000024810	-4.04	<i>Il33</i>	interleukin 33
ENSMUSG00000031654	-3.95	<i>Cbln1</i>	cerebellin 1 precursor protein
ENSMUSG00000066677	-3.95	<i>Ifi208</i>	interferon activated gene 208
ENSMUSG00000030345	-3.93	<i>Dyrk4</i>	dual-specificity tyrosine-(Y)-phosphorylation regulated kinase 4
ENSMUSG00000042816	-3.90	<i>Gpr151</i>	G protein-coupled receptor 151
ENSMUSG00000056025	-3.90	<i>Clca3a1</i>	chloride channel accessory 3A1
ENSMUSG00000046167	-3.77	<i>Gldn</i>	gliomedin
ENSMUSG00000020469	-3.71	<i>Myl7</i>	myosin, light polypeptide 7, regulatory
ENSMUSG00000056290	-3.71	<i>Ms4a4b</i>	membrane-spanning 4-domains, subfamily A, member 4B
ENSMUSG00000051212	-3.60	<i>Gpr183</i>	G protein-coupled receptor 183
ENSMUSG00000068536	-3.59	<i>Doxl2</i>	diamine oxidase-like protein 2
ENSMUSG00000050921	-3.55	<i>P2ry10</i>	purinergic receptor P2Y, G-protein coupled 10
ENSMUSG00000087066	-3.52	<i>Gm15518</i>	predicted gene 15518
ENSMUSG00000040950	-3.49	<i>Mgl2</i>	macrophage galactose N-acetyl-galactosamine specific lectin 2
ENSMUSG00000107985	-3.33	<i>Gm35037</i>	predicted gene, 35037
ENSMUSG00000041309	-3.29	<i>Nkx6-2</i>	NK6 homeobox 2
ENSMUSG00000079298	-3.27	<i>Klrblb</i>	killer cell lectin-like receptor subfamily B member 1B
ENSMUSG00000064023	-3.25	<i>Klk8</i>	kallikrein related-peptidase 8
ENSMUSG00000103899	-3.22	<i>Gm37940</i>	predicted gene, 37940
ENSMUSG00000042671	-3.10	<i>Rgs8</i>	regulator of G-protein signalling 8

ENSMUSG00000025400	-3.09	<i>Tac2</i>	tachykinin 2
ENSMUSG00000093446	-3.07	<i>Gm20694</i>	predicted gene 20694
ENSMUSG00000084826	-3.05	<i>AI847159</i>	expressed sequence AI847159
ENSMUSG00000030365	-3.02	<i>Clec2i</i>	C-type lectin domain family 2, member i
ENSMUSG00000020599	-3.01	<i>Rgs9</i>	regulator of G-protein signalling 9
ENSMUSG00000074635	-3.01	<i>3110070M22Rik</i>	RIKEN cDNA 3110070M22 gene
ENSMUSG00000060445	-3.00	<i>Sycp2</i>	synaptonemal complex protein 2
ENSMUSG00000019935	-3.00	<i>Slc17a8</i>	solute carrier family 17 (sodium-dependent inorganic phosphate cotransporter), member 8
ENSMUSG00000064137	-2.97	<i>Rhox8</i>	reproductive homeobox 8
ENSMUSG00000076867	-2.96	<i>Trdv4</i>	T cell receptor delta variable 4
ENSMUSG00000090272	-2.96	<i>Mndal</i>	myeloid nuclear differentiation antigen like
ENSMUSG00000040065	-2.95	<i>Pfpl</i>	pore forming protein-like
ENSMUSG00000040280	-2.93	<i>Ndufa4l2</i>	NADH dehydrogenase (ubiquinone) 1 alpha subcomplex, 4-like 2
ENSMUSG00000019756	-2.89	<i>Prl8a1</i>	prolactin family 8, subfamily a, member 1
ENSMUSG00000080783	-2.89	<i>Gm8250</i>	predicted gene 8250
ENSMUSG00000030178	-2.87	<i>Klra13-ps</i>	killer cell lectin-like receptor subfamily A, member 13, pseudogene
ENSMUSG00000070063	-2.87	<i>Snora33</i>	small nucleolar RNA, H/ACA box 33
ENSMUSG00000022863	-2.86	<i>Btg3</i>	B cell translocation gene 3
ENSMUSG00000006488	-2.85	<i>Prl7a1</i>	prolactin family 7, subfamily a, member 1
ENSMUSG00000010796	-2.85	<i>Asz1</i>	ankyrin repeat, SAM and basic leucine zipper domain containing 1
ENSMUSG00000019301	-2.85	<i>Hsd17b1</i>	hydroxysteroid (17-beta) dehydrogenase 1
ENSMUSG00000025491	-2.83	<i>Ifitm1</i>	interferon induced transmembrane protein 1
ENSMUSG00000032021	-2.83	<i>Crtam</i>	cytotoxic and regulatory T cell molecule
ENSMUSG00000103175	-2.83	<i>Gm37169</i>	predicted gene, 37169
ENSMUSG00000044117	-2.82	<i>2900011O08Rik</i>	RIKEN cDNA 2900011O08 gene
ENSMUSG00000070111	-2.81	<i>Gm10286</i>	predicted gene 10286
ENSMUSG00000109293	-2.81	<i>Dcst2</i>	DC-STAMP domain containing 2
ENSMUSG00000107385	-2.80	<i>C330024D21Rik</i>	RIKEN cDNA C330024D21 gene

ENSMUSG00000054951	-2.76	<i>9130008F23Rik</i>	RIKEN cDNA 9130008F23 gene
ENSMUSG00000018893	-2.75	<i>Mb</i>	myoglobin
ENSMUSG00000024032	-2.75	<i>Tff1</i>	trefoil factor 1
ENSMUSG00000020279	-2.73	<i>Il9r</i>	interleukin 9 receptor
ENSMUSG00000046908	-2.71	<i>Ltb4r1</i>	leukotriene B4 receptor 1
ENSMUSG00000079355	-2.71	<i>Ackr4</i>	atypical chemokine receptor 4
ENSMUSG00000030165	-2.71	<i>Klrd1</i>	killer cell lectin-like receptor, subfamily D, member 1
ENSMUSG00000032356	-2.70	<i>Rasgrf1</i>	RAS protein-specific guanine nucleotide-releasing factor 1
ENSMUSG00000103731	-2.70	<i>Gm17530</i>	predicted gene, 17530
ENSMUSG00000073491	-2.70	<i>Ifi213</i>	interferon activated gene 213
ENSMUSG00000020963	-2.66	<i>Tshr</i>	thyroid stimulating hormone receptor
ENSMUSG00000048329	-2.65	<i>Mfsd6l</i>	major facilitator superfamily domain containing 6-like
ENSMUSG00000079652	-2.65	<i>Fam71f2</i>	family with sequence similarity 71, member F2
ENSMUSG00000034990	-2.63	<i>Otoa</i>	otoancorin
ENSMUSG00000050241	-2.63	<i>Klre1</i>	killer cell lectin-like receptor family E member 1
ENSMUSG00000005045	-2.63	<i>Chd5</i>	chromodomain helicase DNA binding protein 5
ENSMUSG00000023206	-2.63	<i>Il15ra</i>	interleukin 15 receptor, alpha chain
ENSMUSG00000015476	-2.62	<i>Prrt1</i>	proline-rich transmembrane protein 1
ENSMUSG00000075042	-2.59	<i>4930431P03Rik</i>	RIKEN cDNA 4930431P03 gene
ENSMUSG00000027082	-2.57	<i>Tfpi</i>	tissue factor pathway inhibitor
ENSMUSG00000002500	-2.57	<i>Rpl3l</i>	ribosomal protein L3-like
ENSMUSG00000026156	-2.55	<i>B3gat2</i>	beta-1,3-glucuronyltransferase 2 (glucuronosyltransferase S)
ENSMUSG00000031845	-2.55	<i>Bco1</i>	beta-carotene oxygenase 1
ENSMUSG00000026919	-2.54	<i>Lcn4</i>	lipocalin 4
ENSMUSG00000041831	-2.53	<i>Syt13</i>	synaptotagmin-like 3
ENSMUSG00000021594	-2.52	<i>Srd5a1</i>	steroid 5 alpha-reductase 1
ENSMUSG00000063458	-2.45	<i>Lrmda</i>	leucine rich melanocyte differentiation associated
ENSMUSG00000066684	-2.45	<i>Pilrb1</i>	paired immunoglobulin-like type 2 receptor beta 1
ENSMUSG00000035105	-2.45	<i>Egln3</i>	egl-9 family hypoxia-inducible factor 3

ENSMUSG00000077734	-2.43	<i>Snord83b</i>	small nucleolar RNA, C/D box 83B
ENSMUSG00000005883	-2.42	<i>Spo11</i>	SPO11 meiotic protein covalently bound to DSB
ENSMUSG00000029005	-2.40	<i>Draxin</i>	dorsal inhibitory axon guidance protein
ENSMUSG00000078795	-2.39	<i>Ceacam15</i>	carcinoembryonic antigen-related cell adhesion molecule 15
ENSMUSG00000060913	-2.37	<i>Trim55</i>	tripartite motif-containing 55
ENSMUSG00000002204	-2.36	<i>Napsa</i>	napsin A aspartic peptidase
ENSMUSG00000097433	-2.36	<i>Gm26781</i>	predicted gene, 26781
ENSMUSG00000103034	-2.36	<i>Gm8797</i>	predicted pseudogene 8797
ENSMUSG00000042638	-2.34	<i>Gucy2c</i>	guanylate cyclase 2c
ENSMUSG00000028072	-2.32	<i>Ntrk1</i>	neurotrophic tyrosine kinase, receptor, type 1
ENSMUSG00000044285	-2.31	<i>Gm1821</i>	predicted gene 1821
ENSMUSG00000001520	-2.31	<i>Nrip2</i>	nuclear receptor interacting protein 2
ENSMUSG00000087259	-2.30	<i>2610035D17Rik</i>	RIKEN cDNA 2610035D17 gene
ENSMUSG000000051499	-2.30	<i>Zfp786</i>	zinc finger protein 786
ENSMUSG000000022818	-2.30	<i>Cyp2ab1</i>	cytochrome P450, family 2, subfamily ab, polypeptide 1
ENSMUSG000000039492	-2.29	<i>Ccdc27</i>	coiled-coil domain containing 27
ENSMUSG000000027238	-2.28	<i>Frmd5</i>	FERM domain containing 5
ENSMUSG000000053101	-2.27	<i>Gpr141</i>	G protein-coupled receptor 141
ENSMUSG000000035299	-2.27	<i>Mid1</i>	midline 1
ENSMUSG00000079092	-2.27	<i>Prl2c2</i>	prolactin family 2, subfamily c, member 2
ENSMUSG00000010021	-2.25	<i>Kif19a</i>	kinesin family member 19A
ENSMUSG000000044162	-2.25	<i>Tnip3</i>	TNFAIP3 interacting protein 3
ENSMUSG000000025213	-2.25	<i>Kazald1</i>	Kazal-type serine peptidase inhibitor domain 1
ENSMUSG000000032487	-2.25	<i>Ptgs2</i>	prostaglandin-endoperoxide synthase 2
ENSMUSG00000015443	-2.23	<i>Gzmn</i>	granzyme N
ENSMUSG000000020256	-2.21	<i>Aldh1l2</i>	aldehyde dehydrogenase 1 family, member L2
ENSMUSG000000092187	-2.21	<i>Gm20457</i>	predicted gene 20457
ENSMUSG000000098024	-2.21	<i>Gm27003</i>	predicted gene, 27003
ENSMUSG00000107458	-2.20	<i>Gm44040</i>	predicted gene, 44040

ENSMUSG00000054003	-2.19	<i>Tdrd9</i>	tudor domain containing 9
ENSMUSG00000032899	-2.19	<i>Styk1</i>	serine/threonine/tyrosine kinase 1
ENSMUSG00000020310	-2.19	<i>Madcam1</i>	mucosal vascular addressin cell adhesion molecule 1
ENSMUSG00000042213	-2.19	<i>Zfand4</i>	zinc finger, AN1-type domain 4
ENSMUSG00000015437	-2.18	<i>Gzmb</i>	granzyme B
ENSMUSG00000078942	-2.17	<i>Naip6</i>	NLR family, apoptosis inhibitory protein 6
ENSMUSG00000040747	-2.17	<i>Cd53</i>	CD53 antigen
ENSMUSG00000086938	-2.16	<i>4930481A15Rik</i>	RIKEN cDNA 4930481A15 gene
ENSMUSG00000086652	-2.15	<i>Gm14029</i>	predicted gene 14029
ENSMUSG00000054203	-2.15	<i>Ifi205</i>	interferon activated gene 205
ENSMUSG00000066258	-2.14	<i>Trim12a</i>	tripartite motif-containing 12A
ENSMUSG00000107227	-2.14	<i>Gm42559</i>	predicted gene 42559
ENSMUSG00000030156	-2.13	<i>Cd69</i>	CD69 antigen
ENSMUSG00000026786	-2.13	<i>Apbb1ip</i>	amyloid beta (A4) precursor protein-binding, family B, member 1 interacting protein
ENSMUSG00000035551	-2.13	<i>Igfbp1l</i>	insulin-like growth factor binding protein-like 1
ENSMUSG00000079056	-2.11	<i>Kcnip3</i>	Kv channel interacting protein 3, calsenilin
ENSMUSG00000074264	-2.11	<i>Amy1</i>	amylase 1, salivary
ENSMUSG00000054293	-2.10	<i>A630033H20Rik</i>	RIKEN cDNA A630033H20 gene
ENSMUSG00000000223	-2.10	<i>Drp2</i>	dystrophin related protein 2
ENSMUSG00000083226	-2.10	<i>Gm7831</i>	predicted gene 7831
ENSMUSG00000094845	-2.10	<i>Tmem95</i>	transmembrane protein 95
ENSMUSG00000086474	-2.10	<i>9130204K15Rik</i>	RIKEN cDNA 9130204K15 gene
ENSMUSG00000102609	-2.10	<i>Gm18432</i>	predicted gene, 18432
ENSMUSG00000029026	-2.09	<i>Trp73</i>	transformation related protein 73
ENSMUSG00000091575	-2.07	<i>2010016I18Rik</i>	RIKEN cDNA 2010016I18 gene
ENSMUSG00000049517	-2.06	<i>Rps23</i>	ribosomal protein S23
ENSMUSG00000086264	-2.06	<i>Gm15850</i>	predicted gene 15850
ENSMUSG00000071716	-2.05	<i>Apol7e</i>	apolipoprotein L 7e
ENSMUSG0000007216	-2.05	<i>Zfp775</i>	zinc finger protein 775

ENSMUSG00000105814	-2.05	<i>Mir703</i>	microRNA 703
ENSMUSG00000076434	-2.05	<i>Wfdc3</i>	WAP four-disulfide core domain 3
ENSMUSG00000057596	-2.04	<i>Trim30d</i>	tripartite motif-containing 30D
ENSMUSG00000004707	-2.04	<i>Ly9</i>	lymphocyte antigen 9
ENSMUSG00000058755	-2.04	<i>Osm</i>	oncostatin M
ENSMUSG00000030098	-2.04	<i>Grip2</i>	glutamate receptor interacting protein 2
ENSMUSG00000057132	-2.04	<i>Rpgrip1</i>	retinitis pigmentosa GTPase regulator interacting protein 1
ENSMUSG00000075334	-2.03	<i>Rprm</i>	reprimo, TP53 dependent G2 arrest mediator candidate
ENSMUSG00000030303	-2.03	<i>Far2</i>	fatty acyl CoA reductase 2
ENSMUSG00000027219	-2.03	<i>Slc28a2</i>	solute carrier family 28 (sodium-coupled nucleoside transporter), member 2
ENSMUSG00000101970	-2.03	<i>1810026B05Rik</i>	RIKEN cDNA 1810026B05 gene
ENSMUSG00000029055	-2.03	<i>Plch2</i>	phospholipase C, eta 2
ENSMUSG00000027794	-2.03	<i>Sohlh2</i>	spermatogenesis and oogenesis specific basic helix-loop-helix 2
ENSMUSG00000028931	-2.02	<i>Kcnab2</i>	potassium voltage-gated channel, shaker-related subfamily, beta member 2
ENSMUSG00000057170	-2.02	<i>Prl3d1</i>	prolactin family 3, subfamily d, member 1
ENSMUSG00000004791	-2.02	<i>Pgf</i>	placental growth factor
ENSMUSG00000063383	-2.02	<i>Zfp947</i>	zinc finger protein 947
ENSMUSG00000036570	-2.02	<i>Fxyd1</i>	FXVD domain-containing ion transport regulator 1
ENSMUSG00000084899	-2.02	<i>Gm15344</i>	predicted gene 15344
ENSMUSG00000042345	-2.01	<i>Ubash3a</i>	ubiquitin associated and SH3 domain containing, A
ENSMUSG00000038094	-2.01	<i>Atp13a4</i>	ATPase type 13A4
ENSMUSG00000060441	-2.01	<i>Trim5</i>	tripartite motif-containing 5
ENSMUSG00000090110	-2.00	<i>Cmc4</i>	C-x(9)-C motif containing 4
ENSMUSG00000076490	-2.00	<i>Trbc1</i>	T cell receptor beta, constant region 1
ENSMUSG00000043518	2.00	<i>Rai2</i>	retinoic acid induced 2
ENSMUSG00000028518	2.00	<i>Prkaa2</i>	protein kinase, AMP-activated, alpha 2 catalytic subunit
ENSMUSG00000042115	2.00	<i>Klhdc8a</i>	kelch domain containing 8A
ENSMUSG00000056133	2.00	<i>Gm9992</i>	predicted gene 9992
ENSMUSG00000023000	2.00	<i>Dhh</i>	desert hedgehog

ENSMUSG00000022949	2.00	<i>Clic6</i>	chloride intracellular channel 6
ENSMUSG00000069814	2.01	<i>Ccdc92b</i>	coiled-coil domain containing 92B
ENSMUSG00000030020	2.01	<i>Prickle2</i>	prickle planar cell polarity protein 2
ENSMUSG00000040907	2.02	<i>Atp1a3</i>	ATPase, Na ⁺ /K ⁺ transporting, alpha 3 polypeptide
ENSMUSG00000083282	2.02	<i>Ctsf</i>	cathepsin F
ENSMUSG00000091269	2.02	<i>Gm6682</i>	predicted gene 6682
ENSMUSG00000027403	2.02	<i>Tgm6</i>	transglutaminase 6
ENSMUSG00000031841	2.03	<i>Cdh13</i>	cadherin 13
ENSMUSG00000006574	2.03	<i>Slc4a1</i>	solute carrier family 4 (anion exchanger), member 1
ENSMUSG00000033207	2.03	<i>Mamdc2</i>	MAM domain containing 2
ENSMUSG00000004730	2.03	<i>Adgre1</i>	adhesion G protein-coupled receptor E1
ENSMUSG00000027175	2.03	<i>Tcp111l</i>	t-complex 11 like 1
ENSMUSG00000021278	2.04	<i>Amn</i>	amnionless
ENSMUSG00000074093	2.04	<i>Svip</i>	small VCP/p97-interacting protein
ENSMUSG00000084304	2.05	<i>Gm6142</i>	predicted pseudogene 6142
ENSMUSG00000074676	2.05	<i>Foxs1</i>	forkhead box S1
ENSMUSG00000107810	2.05	<i>Gm18609</i>	predicted gene, 18609
ENSMUSG00000046844	2.06	<i>Vat1l</i>	vesicle amine transport protein 1 like
ENSMUSG00000021127	2.06	<i>Zfp361l</i>	zinc finger protein 36, C3H type-like 1
ENSMUSG00000034910	2.06	<i>Pygol</i>	pygopus 1
ENSMUSG00000055413	2.06	<i>H2-Q5</i>	histocompatibility 2, Q region locus 5
ENSMUSG00000020019	2.07	<i>Ntn4</i>	netrin 4
ENSMUSG00000105461	2.07	<i>Gm4742</i>	predicted gene 4742
ENSMUSG00000033420	2.07	<i>Antxr1</i>	anthrax toxin receptor 1
ENSMUSG00000000216	2.08	<i>Scnn1g</i>	sodium channel, nonvoltage-gated 1 gamma
ENSMUSG00000107317	2.08	<i>Gm19719</i>	predicted gene, 19719
ENSMUSG00000072941	2.08	<i>Sod3</i>	superoxide dismutase 3, extracellular
ENSMUSG00000079419	2.09	<i>Ms4a6c</i>	membrane-spanning 4-domains, subfamily A, member 6C
ENSMUSG00000073412	2.09	<i>Lst1</i>	leukocyte specific transcript 1

ENSMUSG00000024391	2.09	<i>Apom</i>	apolipoprotein M
ENSMUSG00000020431	2.09	<i>Adcy1</i>	adenylate cyclase 1
ENSMUSG00000090622	2.09	<i>A930033H14Rik</i>	RIKEN cDNA A930033H14 gene
ENSMUSG00000020607	2.09	<i>Fam84a</i>	family with sequence similarity 84, member A
ENSMUSG00000082292	2.10	<i>Gm12250</i>	predicted gene 12250
ENSMUSG00000076258	2.11	<i>Gm23935</i>	predicted gene, 23935
ENSMUSG00000012428	2.11	<i>Steap4</i>	STEAP family member 4
ENSMUSG00000028834	2.11	<i>Trim63</i>	tripartite motif-containing 63
ENSMUSG00000099375	2.12	<i>Gm28187</i>	predicted gene 28187
ENSMUSG00000036040	2.12	<i>Adamtsl2</i>	ADAMTS-like 2
ENSMUSG00000026880	2.12	<i>Stom</i>	stomatin
ENSMUSG0000004562	2.13	<i>Arhgef40</i>	Rho guanine nucleotide exchange factor (GEF) 40
ENSMUSG00000027777	2.13	<i>Schip1</i>	schwannomin interacting protein 1
ENSMUSG00000028860	2.13	<i>Sytl1</i>	synaptotagmin-like 1
ENSMUSG00000062588	2.13	<i>Gm6104</i>	predicted gene 6104
ENSMUSG00000061451	2.13	<i>Tmem151a</i>	transmembrane protein 151A
ENSMUSG00000020614	2.13	<i>Fam20a</i>	family with sequence similarity 20, member A
ENSMUSG00000020704	2.14	<i>Asic2</i>	acid-sensing (proton-gated) ion channel 2
ENSMUSG00000023064	2.14	<i>Sncg</i>	synuclein, gamma
ENSMUSG00000022763	2.14	<i>Aifm3</i>	apoptosis-inducing factor, mitochondrion-associated 3
ENSMUSG00000062515	2.15	<i>Fabp4</i>	fatty acid binding protein 4, adipocyte
ENSMUSG00000040152	2.15	<i>Thbs1</i>	thrombospondin 1
ENSMUSG00000063727	2.17	<i>Tnfrsf11b</i>	tumor necrosis factor receptor superfamily, member 11b (osteoprotegerin)
ENSMUSG00000027908	2.18	<i>Tchhl1</i>	trichohyalin-like 1
ENSMUSG00000074071	2.18	<i>Fam169b</i>	family with sequence similarity 169, member B
ENSMUSG00000061436	2.19	<i>Hipk2</i>	homeodomain interacting protein kinase 2
ENSMUSG00000028825	2.19	<i>Rhd</i>	Rh blood group, D antigen
ENSMUSG00000006777	2.19	<i>Krt23</i>	keratin 23
ENSMUSG00000096780	2.19	<i>Tmem181b-ps</i>	transmembrane protein 181B, pseudogene

ENSMUSG00000003273	2.20	<i>Car11</i>	carbonic anhydrase 11
ENSMUSG000000028024	2.20	<i>Enpep</i>	glutamyl aminopeptidase
ENSMUSG000000030208	2.20	<i>Emp1</i>	epithelial membrane protein 1
ENSMUSG000000037624	2.21	<i>Kcnk2</i>	potassium channel, subfamily K, member 2
ENSMUSG000000072115	2.21	<i>Ang</i>	angiogenin, ribonuclease, RNase A family, 5
ENSMUSG000000030134	2.21	<i>Rasgefla</i>	RasGEF domain family, member 1A
ENSMUSG000000025867	2.21	<i>Cplx2</i>	complexin 2
ENSMUSG000000017446	2.21	<i>Clqtnfl</i>	C1q and tumor necrosis factor related protein 1
ENSMUSG000000020053	2.23	<i>Igfl</i>	insulin-like growth factor 1
ENSMUSG000000034040	2.23	<i>Galnt17</i>	polypeptide N-acetylgalactosaminyltransferase 17
ENSMUSG000000030532	2.24	<i>Hddc3</i>	HD domain containing 3
ENSMUSG000000020411	2.24	<i>Nipal4</i>	NIPA-like domain containing 4
ENSMUSG000000021003	2.24	<i>Galc</i>	galactosylceramidase
ENSMUSG000000019990	2.26	<i>Pde7b</i>	phosphodiesterase 7B
ENSMUSG000000022012	2.26	<i>Enox1</i>	ecto-NOX disulfide-thiol exchanger 1
ENSMUSG000000063696	2.26	<i>Gm8730</i>	predicted pseudogene 8730
ENSMUSG000000039601	2.27	<i>Rcan2</i>	regulator of calcineurin 2
ENSMUSG000000026080	2.27	<i>Chst10</i>	carbohydrate sulfotransferase 10
ENSMUSG000000032496	2.28	<i>Ltf</i>	lactotransferrin
ENSMUSG000000050397	2.28	<i>Foxl2</i>	forkhead box L2
ENSMUSG000000036800	2.28	<i>Fam135b</i>	family with sequence similarity 135, member B
ENSMUSG000000025006	2.28	<i>Sorbs1</i>	sorbin and SH3 domain containing 1
ENSMUSG000000029123	2.28	<i>Stk32b</i>	serine/threonine kinase 32B
ENSMUSG000000071984	2.29	<i>Fndc1</i>	fibronectin type III domain containing 1
ENSMUSG000000047230	2.29	<i>Cldn2</i>	claudin 2
ENSMUSG0000000104063	2.29	<i>Pcdhgb7</i>	protocadherin gamma subfamily B, 7
ENSMUSG000000026676	2.29	<i>Ccdc3</i>	coiled-coil domain containing 3
ENSMUSG000000028158	2.30	<i>Mtp</i>	microsomal triglyceride transfer protein
ENSMUSG000000052387	2.31	<i>Trpm3</i>	transient receptor potential cation channel, subfamily M, member 3

ENSMUSG00000031530	2.31	<i>Dusp4</i>	dual specificity phosphatase 4
ENSMUSG00000053897	2.31	<i>Slc39a8</i>	solute carrier family 39 (metal ion transporter), member 8
ENSMUSG00000074217	2.31	<i>2210011C24Rik</i>	RIKEN cDNA 2210011C24 gene
ENSMUSG00000056427	2.32	<i>Slit3</i>	slit homolog 3 (Drosophila)
ENSMUSG00000004655	2.32	<i>Aqp1</i>	aquaporin 1
ENSMUSG00000004885	2.32	<i>Crabp2</i>	cellular retinoic acid binding protein II
ENSMUSG00000060459	2.32	<i>Kng2</i>	kininogen 2
ENSMUSG00000042351	2.32	<i>Grap2</i>	GRB2-related adaptor protein 2
ENSMUSG00000035000	2.32	<i>Dpp4</i>	dipeptidylpeptidase 4
ENSMUSG00000001281	2.34	<i>Itgb7</i>	integrin beta 7
ENSMUSG00000014602	2.34	<i>Kif1a</i>	kinesin family member 1A
ENSMUSG00000032262	2.34	<i>Elovl4</i>	elongation of very long chain fatty acids (FEN1/Elo2, SUR4/Elo3, yeast)-like 4
ENSMUSG000000081126	2.36	<i>Gm15784</i>	predicted gene 15784
ENSMUSG00000073791	2.36	<i>Efcab7</i>	EF-hand calcium binding domain 7
ENSMUSG000000087150	2.37	<i>BC064078</i>	cDNA sequence BC064078
ENSMUSG00000031775	2.37	<i>Pllp</i>	plasma membrane proteolipid
ENSMUSG00000036885	2.37	<i>Arhgef26</i>	Rho guanine nucleotide exchange factor (GEF) 26
ENSMUSG00000027204	2.38	<i>Fbn1</i>	fibrillin 1
ENSMUSG00000038156	2.39	<i>Spon1</i>	spondin 1, (f-spondin) extracellular matrix protein
ENSMUSG00000003418	2.40	<i>St8sia6</i>	ST8 alpha-N-acetyl-neuraminide alpha-2,8-sialyltransferase 6
ENSMUSG00000042532	2.41	<i>Golga7b</i>	golgi autoantigen, golgin subfamily a, 7B
ENSMUSG00000017817	2.42	<i>Jph2</i>	junctophilin 2
ENSMUSG00000000142	2.43	<i>Axin2</i>	axin 2
ENSMUSG00000066553	2.43	<i>Gm6969</i>	predicted pseudogene 6969
ENSMUSG00000053957	2.44	<i>Gm12474</i>	predicted gene 12474
ENSMUSG00000036446	2.45	<i>Lum</i>	lumican
ENSMUSG00000047473	2.46	<i>Zfp30</i>	zinc finger protein 30
ENSMUSG00000032641	2.46	<i>Gpr19</i>	G protein-coupled receptor 19
ENSMUSG00000017002	2.47	<i>Slpi</i>	secretory leukocyte peptidase inhibitor

ENSMUSG00000022425	2.48	<i>Enpp2</i>	ectonucleotide pyrophosphatase/phosphodiesterase 2
ENSMUSG00000003477	2.48	<i>Inmt</i>	indolethylamine N-methyltransferase
ENSMUSG00000072571	2.48	<i>Tmem253</i>	transmembrane protein 253
ENSMUSG00000056771	2.48	<i>Gm10010</i>	predicted gene 10010
ENSMUSG00000106664	2.49	<i>Gm17936</i>	predicted gene, 17936
ENSMUSG00000052504	2.49	<i>Epha3</i>	Eph receptor A3
ENSMUSG00000082566	2.49	<i>Gm11485</i>	predicted gene 11485
ENSMUSG00000032889	2.50	<i>Gm6685</i>	predicted pseudogene 6685
ENSMUSG00000031189	2.51	<i>Aff2</i>	AF4/FMR2 family, member 2
ENSMUSG00000028883	2.51	<i>Sema3a</i>	sema domain, immunoglobulin domain (Ig), short basic domain, secreted, (semaphorin) 3A
ENSMUSG00000078605	2.52	<i>E030025P04Rik</i>	RIKEN cDNA E030025P04 gene
ENSMUSG00000103144	2.52	<i>Pcdhgal</i>	protocadherin gamma subfamily A, 1
ENSMUSG00000097993	2.53	<i>Ptprv</i>	protein tyrosine phosphatase, receptor type, V
ENSMUSG00000065503	2.55	<i>Mir351</i>	microRNA 351
ENSMUSG00000004113	2.56	<i>Cacna1b</i>	calcium channel, voltage-dependent, N type, alpha 1B subunit
ENSMUSG00000033268	2.56	<i>Duox1</i>	dual oxidase 1
ENSMUSG00000027737	2.57	<i>Slc7a11</i>	solute carrier family 7 (cationic amino acid transporter, y+ system), member 11
ENSMUSG00000020080	2.57	<i>Hkdc1</i>	hexokinase domain containing 1
ENSMUSG00000040613	2.58	<i>Apobec1</i>	apolipoprotein B mRNA editing enzyme, catalytic polypeptide 1
ENSMUSG00000032338	2.58	<i>Hcn4</i>	hyperpolarization-activated, cyclic nucleotide-gated K+ 4
ENSMUSG00000090394	2.59	<i>4930523C07Rik</i>	RIKEN cDNA 4930523C07 gene
ENSMUSG00000043259	2.60	<i>Fam13c</i>	family with sequence similarity 13, member C
ENSMUSG00000015957	2.60	<i>Wnt11</i>	wingless-type MMTV integration site family, member 11
ENSMUSG00000027359	2.60	<i>Slc27a2</i>	solute carrier family 27 (fatty acid transporter), member 2
ENSMUSG00000020173	2.61	<i>Cobl</i>	cordons-bleu WH2 repeat
ENSMUSG00000041301	2.62	<i>Cftr</i>	cystic fibrosis transmembrane conductance regulator
ENSMUSG00000003617	2.63	<i>Cp</i>	ceruloplasmin
ENSMUSG00000083186	2.65	<i>Gm11805</i>	predicted gene 11805

ENSMUSG00000032425	2.65	<i>Zfp949</i>	zinc finger protein 949
ENSMUSG00000017950	2.66	<i>Hnf4a</i>	hepatic nuclear factor 4, alpha
ENSMUSG00000085666	2.67	<i>Gm9855</i>	predicted pseudogene 9855
ENSMUSG00000073643	2.67	<i>Wdfyl</i>	WD repeat and FYVE domain containing 1
ENSMUSG00000030834	2.68	<i>Abcc6</i>	ATP-binding cassette, sub-family C (CFTR/MRP), member 6
ENSMUSG00000023885	2.69	<i>Thbs2</i>	thrombospondin 2
ENSMUSG00000053835	2.69	<i>H2-T24</i>	histocompatibility 2, T region locus 24
ENSMUSG0000002033	2.71	<i>Cd3g</i>	CD3 antigen, gamma polypeptide
ENSMUSG00000048814	2.71	<i>Lonrf2</i>	LON peptidase N-terminal domain and ring finger 2
ENSMUSG00000030492	2.72	<i>Slc7a9</i>	solute carrier family 7 (cationic amino acid transporter, y+ system), member 9
ENSMUSG00000057228	2.73	<i>Aadat</i>	aminoadipate aminotransferase
ENSMUSG00000044748	2.74	<i>Defb1</i>	defensin beta 1
ENSMUSG00000086043	2.74	<i>Gm12473</i>	predicted gene 12473
ENSMUSG00000055926	2.75	<i>Gm14137</i>	predicted gene 14137
ENSMUSG00000043556	2.76	<i>Fbxl7</i>	F-box and leucine-rich repeat protein 7
ENSMUSG00000022894	2.76	<i>Adamts5</i>	a disintegrin-like and metallopeptidase (reprolysin type) with thrombospondin type 1 motif, 5 (aggrecanase-2)
ENSMUSG00000052353	2.77	<i>Cemip</i>	cell migration inducing protein, hyaluronan binding
ENSMUSG00000097767	2.78	<i>Miat</i>	myocardial infarction associated transcript (non-protein coding)
ENSMUSG00000103428	2.80	<i>Gm20754</i>	predicted gene, 20754
ENSMUSG00000105331	2.81	<i>Gm29865</i>	predicted gene, 29865
ENSMUSG00000086108	2.83	<i>Gm5602</i>	predicted gene 5602
ENSMUSG00000027996	2.84	<i>Sfrp2</i>	secreted frizzled-related protein 2
ENSMUSG00000037362	2.84	<i>Nov</i>	nephroblastoma overexpressed gene
ENSMUSG00000090124	2.84	<i>Ugt1a7c</i>	UDP glucuronosyltransferase 1 family, polypeptide A7C
ENSMUSG00000047797	2.84	<i>Gjb1</i>	gap junction protein, beta 1
ENSMUSG00000046159	2.85	<i>Chrm3</i>	cholinergic receptor, muscarinic 3, cardiac
ENSMUSG00000080811	2.85	<i>Gm14513</i>	predicted gene 14513
ENSMUSG00000020805	2.87	<i>Slc13a5</i>	solute carrier family 13 (sodium-dependent citrate transporter), member 5

ENSMUSG00000064372	2.87	<i>mt-Tp</i>	mitochondrially encoded tRNA proline
ENSMUSG00000026062	2.87	<i>Slc9a2</i>	solute carrier family 9 (sodium/hydrogen exchanger), member 2
ENSMUSG00000060068	2.87	<i>Gm12222</i>	predicted gene 12222
ENSMUSG00000020566	2.89	<i>Atp6v1c2</i>	ATPase, H ⁺ transporting, lysosomal V1 subunit C2
ENSMUSG00000019359	2.89	<i>Gdpd2</i>	glycerophosphodiester phosphodiesterase domain containing 2
ENSMUSG00000026726	2.89	<i>Cubn</i>	cubilin (intrinsic factor-cobalamin receptor)
ENSMUSG00000022883	2.90	<i>Robo1</i>	roundabout guidance receptor 1
ENSMUSG00000046372	2.92	<i>Gm5590</i>	predicted gene 5590
ENSMUSG00000031760	2.93	<i>Mt3</i>	metallothionein 3
ENSMUSG00000089704	2.95	<i>Galnt2</i>	polypeptide N-acetylgalactosaminyltransferase 2
ENSMUSG00000067049	2.95	<i>Unc93a</i>	unc-93 homolog A (<i>C. elegans</i>)
ENSMUSG00000091345	2.97	<i>Col6a5</i>	collagen, type VI, alpha 5
ENSMUSG00000050010	3.00	<i>Shisa3</i>	shisa family member 3
ENSMUSG00000021592	3.00	<i>Arsk</i>	arylsulfatase K
ENSMUSG00000021567	3.00	<i>Nkd2</i>	naked cuticle 2 homolog (<i>Drosophila</i>)
ENSMUSG00000054640	3.01	<i>Slc8a1</i>	solute carrier family 8 (sodium/calcium exchanger), member 1
ENSMUSG00000030074	3.03	<i>Gxylt2</i>	glucoside xylosyltransferase 2
ENSMUSG00000032023	3.04	<i>Jhy</i>	junctional cadherin complex regulator
ENSMUSG00000044468	3.04	<i>Fam46c</i>	family with sequence similarity 46, member C
ENSMUSG00000040133	3.04	<i>Gpr176</i>	G protein-coupled receptor 176
ENSMUSG00000072596	3.05	<i>Ear2</i>	eosinophil-associated, ribonuclease A family, member 2
ENSMUSG00000039518	3.06	<i>Cdsn</i>	corneodesmosin
ENSMUSG00000042529	3.07	<i>Kcnj12</i>	potassium inwardly-rectifying channel, subfamily J, member 12
ENSMUSG00000022766	3.07	<i>Serpind1</i>	serine (or cysteine) peptidase inhibitor, clade D, member 1
ENSMUSG00000020811	3.07	<i>Wscd1</i>	WSC domain containing 1
ENSMUSG00000068748	3.09	<i>Ptprz1</i>	protein tyrosine phosphatase, receptor type Z, polypeptide 1
ENSMUSG00000079012	3.09	<i>Serpina3m</i>	serine (or cysteine) peptidase inhibitor, clade A, member 3M
ENSMUSG00000099342	3.11	<i>Gm18180</i>	predicted gene, 18180
ENSMUSG00000063296	3.11	<i>Tmem117</i>	transmembrane protein 117

ENSMUSG00000029664	3.12	<i>Tfpi2</i>	tissue factor pathway inhibitor 2
ENSMUSG00000027356	3.12	<i>Fermt1</i>	fermitin family member 1
ENSMUSG00000075217	3.12	<i>4833423E24Rik</i>	RIKEN cDNA 4833423E24 gene
ENSMUSG00000005628	3.13	<i>Tmod4</i>	tropomodulin 4
ENSMUSG00000035407	3.13	<i>Kank4</i>	KN motif and ankyrin repeat domains 4
ENSMUSG00000022821	3.16	<i>Hgd</i>	homogentisate 1, 2-dioxygenase
ENSMUSG00000001493	3.17	<i>Meox1</i>	mesenchyme homeobox 1
ENSMUSG00000057715	3.19	<i>A830018L16Rik</i>	RIKEN cDNA A830018L16 gene
ENSMUSG00000039913	3.19	<i>Pak7</i>	p21 protein (Cdc42/Rac)-activated kinase 7
ENSMUSG00000060044	3.20	<i>Tmem26</i>	transmembrane protein 26
ENSMUSG00000071604	3.20	<i>Fam189a2</i>	family with sequence similarity 189, member A2
ENSMUSG00000041577	3.24	<i>Prelp</i>	proline arginine-rich end leucine-rich repeat
ENSMUSG00000029641	3.25	<i>Rasl11a</i>	RAS-like, family 11, member A
ENSMUSG00000021456	3.25	<i>Fbp2</i>	fructose bisphosphatase 2
ENSMUSG00000054150	3.26	<i>Syne3</i>	spectrin repeat containing, nuclear envelope family member 3
ENSMUSG00000037482	3.27	<i>Erv3</i>	endogenous retroviral sequence 3
ENSMUSG00000022512	3.30	<i>Cldn1</i>	claudin 1
ENSMUSG00000042429	3.30	<i>Adora1</i>	adenosine A1 receptor
ENSMUSG00000081434	3.30	<i>Gm14165</i>	predicted gene 14165
ENSMUSG00000007682	3.30	<i>Dio2</i>	deiodinase, iodothyronine, type II
ENSMUSG00000026185	3.33	<i>Igfbp5</i>	insulin-like growth factor binding protein 5
ENSMUSG00000026822	3.34	<i>Lcn2</i>	lipocalin 2
ENSMUSG00000025467	3.35	<i>Prap1</i>	proline-rich acidic protein 1
ENSMUSG00000027249	3.37	<i>F2</i>	coagulation factor II
ENSMUSG00000052516	3.41	<i>Robo2</i>	roundabout guidance receptor 2
ENSMUSG00000055022	3.41	<i>Cntn1</i>	contactin 1
ENSMUSG00000027070	3.43	<i>Lrp2</i>	low density lipoprotein receptor-related protein 2
ENSMUSG00000034127	3.46	<i>Tspan8</i>	tetraspanin 8
ENSMUSG00000078183	3.56	<i>Gm15610</i>	predicted gene 15610

ENSMUSG00000020542	3.61	<i>Myocd</i>	myocardin
ENSMUSG00000045322	3.67	<i>Tlr9</i>	toll-like receptor 9
ENSMUSG00000029868	3.68	<i>Trpv6</i>	transient receptor potential cation channel, subfamily V, member 6
ENSMUSG00000070866	3.69	<i>Zfp804a</i>	zinc finger protein 804A
ENSMUSG00000020609	3.74	<i>Apob</i>	apolipoprotein B
ENSMUSG00000050860	3.76	<i>Phospho1</i>	phosphatase, orphan 1
ENSMUSG00000041986	3.82	<i>Elmod1</i>	ELMO/CED-12 domain containing 1
ENSMUSG00000064080	3.84	<i>Fbln2</i>	fibulin 2
ENSMUSG00000028116	3.87	<i>Myoz2</i>	myozenin 2
ENSMUSG00000027536	3.89	<i>Chmp4c</i>	charged multivesicular body protein 4C
ENSMUSG00000073805	3.89	<i>Fam196a</i>	family with sequence similarity 196, member A
ENSMUSG00000021795	3.91	<i>Sftpd</i>	surfactant associated protein D
ENSMUSG00000027188	3.91	<i>Pamr1</i>	peptidase domain containing associated with muscle regeneration 1
ENSMUSG00000035165	3.91	<i>Kcne3</i>	potassium voltage-gated channel, Isk-related subfamily, gene 3
ENSMUSG00000000359	3.94	<i>Rem1</i>	rad and gem related GTP binding protein 1
ENSMUSG00000029195	3.97	<i>Klb</i>	klotho beta
ENSMUSG00000028989	3.99	<i>Angptl7</i>	angiopoietin-like 7
ENSMUSG00000006205	3.99	<i>Htra1</i>	HtrA serine peptidase 1
ENSMUSG00000044320	4.01	<i>1700001O22Rik</i>	RIKEN cDNA 1700001O22 gene
ENSMUSG00000028356	4.01	<i>Ambp</i>	alpha 1 microglobulin/bikunin
ENSMUSG00000021536	4.01	<i>Adcy2</i>	adenylate cyclase 2
ENSMUSG00000034918	4.01	<i>Cdhr2</i>	cadherin-related family member 2
ENSMUSG00000037254	4.03	<i>Itih2</i>	inter-alpha trypsin inhibitor, heavy chain 2
ENSMUSG00000033022	4.08	<i>Cdo1</i>	cysteine dioxygenase 1, cytosolic
ENSMUSG00000050635	4.09	<i>Sprr2f</i>	small proline-rich protein 2F
ENSMUSG00000031517	4.09	<i>Gpm6a</i>	glycoprotein m6a
ENSMUSG00000018822	4.15	<i>Sfrp5</i>	secreted frizzled-related sequence protein 5
ENSMUSG00000026725	4.15	<i>Tnn</i>	tenascin N
ENSMUSG00000022132	4.16	<i>Cldn10</i>	claudin 10

ENSMUSG00000107349	4.18	<i>Gm6655</i>	predicted gene 6655
ENSMUSG00000040412	4.28	<i>5330417C22Rik</i>	RIKEN cDNA 5330417C22 gene
ENSMUSG00000027224	4.34	<i>Duoxal</i>	dual oxidase maturation factor 1
ENSMUSG00000030935	4.34	<i>Acsm3</i>	acyl-CoA synthetase medium-chain family member 3
ENSMUSG00000090231	4.40	<i>Cfb</i>	complement factor B
ENSMUSG00000041324	4.42	<i>Inhba</i>	inhibin beta-A
ENSMUSG00000021876	4.43	<i>Rnase4</i>	ribonuclease, RNase A family 4
ENSMUSG00000105233	4.46	<i>Gm20568</i>	predicted gene, 20568
ENSMUSG00000028359	4.55	<i>Orm3</i>	orosomuroid 3
ENSMUSG00000024164	4.60	<i>C3</i>	complement component 3
ENSMUSG00000042109	4.62	<i>Csdc2</i>	cold shock domain containing C2, RNA binding
ENSMUSG00000026866	4.64	<i>Kynu</i>	kynureninase (L-kynurenine hydrolase)
ENSMUSG00000074280	4.65	<i>Gm6166</i>	predicted gene 6166
ENSMUSG00000032978	4.67	<i>Guca2b</i>	guanylate cyclase activator 2b (retina)
ENSMUSG00000029260	4.71	<i>Ugt2b34</i>	UDP glucuronosyltransferase 2 family, polypeptide B34
ENSMUSG00000059040	4.73	<i>Eno1b</i>	enolase 1B, retrotransposed
ENSMUSG00000102189	4.73	<i>Gm37194</i>	predicted gene, 37194
ENSMUSG00000024027	4.81	<i>Glp1r</i>	glucagon-like peptide 1 receptor
ENSMUSG00000056529	4.85	<i>Ptafr</i>	platelet-activating factor receptor
ENSMUSG00000060882	5.13	<i>Kcnd2</i>	potassium voltage-gated channel, Shal-related family, member 2
ENSMUSG00000082809	5.15	<i>Gm14150</i>	predicted gene 14150
ENSMUSG00000046203	5.19	<i>Sprr2g</i>	small proline-rich protein 2G
ENSMUSG00000032649	5.27	<i>Colgalt2</i>	collagen beta(1-O)galactosyltransferase 2
ENSMUSG00000050558	5.32	<i>Prokr2</i>	prokineticin receptor 2
ENSMUSG00000052135	5.33	<i>Foxo6</i>	forkhead box O6
ENSMUSG00000024114	5.36	<i>Prss41</i>	protease, serine 41
ENSMUSG00000097929	5.55	<i>Tunar</i>	Tcl1 upstream neural differentiation associated RNA
ENSMUSG00000010651	5.56	<i>Acaal1b</i>	acetyl-Coenzyme A acyltransferase 1B
ENSMUSG00000004267	5.65	<i>Eno2</i>	enolase 2, gamma neuronal

ENSMUSG00000042751	5.68	<i>Nmnat2</i>	nicotinamide nucleotide adenylyltransferase 2
ENSMUSG00000037625	5.87	<i>Cldn11</i>	claudin 11
ENSMUSG00000026417	5.93	<i>Pigr</i>	polymeric immunoglobulin receptor
ENSMUSG00000036377	6.08	<i>C530008M17Rik</i>	RIKEN cDNA C530008M17 gene
ENSMUSG00000041750	6.10	<i>Cd1d2</i>	CD1d2 antigen
ENSMUSG00000097554	6.25	<i>Gm26825</i>	predicted gene, 26825
ENSMUSG00000024059	6.38	<i>Clip4</i>	CAP-GLY domain containing linker protein family, member 4
ENSMUSG00000047228	6.63	<i>A2ml1</i>	alpha-2-macroglobulin like 1
ENSMUSG00000074206	6.70	<i>Adh6b</i>	alcohol dehydrogenase 6B (class V)
ENSMUSG00000040627	6.72	<i>Aicda</i>	activation-induced cytidine deaminase
ENSMUSG00000105300	6.97	<i>Gm30613</i>	predicted gene, 30613
ENSMUSG00000028635	7.15	<i>Edn2</i>	endothelin 2
ENSMUSG00000070533	7.34	<i>Wfdc8</i>	WAP four-disulfide core domain 8
ENSMUSG00000047747	7.53	<i>Rnf150</i>	ring finger protein 150
ENSMUSG00000081329	7.55	<i>Gm12492</i>	predicted gene 12492
ENSMUSG00000022015	7.78	<i>Tnfsf11</i>	tumor necrosis factor (ligand) superfamily, member 11
ENSMUSG00000057899	7.79	<i>Adgrf2</i>	adhesion G protein-coupled receptor F2
ENSMUSG00000102474	7.90	<i>2610012C04Rik</i>	RIKEN cDNA 2610012C04 gene
ENSMUSG00000006457	8.40	<i>Actn3</i>	actinin alpha 3
ENSMUSG00000020953	9.07	<i>Coch</i>	cochlin
ENSMUSG00000004552	9.27	<i>Ctse</i>	cathepsin E
ENSMUSG00000047730	9.67	<i>Fcgbp</i>	Fc fragment of IgG binding protein
ENSMUSG00000025930	10.02	<i>Msc</i>	musculin
ENSMUSG00000043531	10.26	<i>Sorcs1</i>	sortilin-related VPS10 domain containing receptor 1
ENSMUSG00000018451	11.02	<i>6330403K07Rik</i>	RIKEN cDNA 6330403K07 gene
ENSMUSG00000081355	11.02	<i>Gm15264</i>	predicted gene 15264
ENSMUSG00000068877	11.23	<i>Selenbp2</i>	selenium binding protein 2
ENSMUSG00000095026	12.64	<i>Gm3336</i>	predicted gene 3336
ENSMUSG00000067235	13.01	<i>H2-Q10</i>	histocompatibility 2, Q region locus 10

ENSMUSG00000076757	13.82	<i>Tcrg-C4</i>	T cell receptor gamma, constant 4
ENSMUSG00000031595	14.46	<i>Pdgfrl</i>	platelet-derived growth factor receptor-like
ENSMUSG00000079507	16.56	<i>H2-Q1</i>	histocompatibility 2, Q region locus 1
ENSMUSG00000006221	16.67	<i>Hspb7</i>	heat shock protein family, member 7 (cardiovascular)
ENSMUSG00000100837	18.33	<i>I700063D05Rik</i>	RIKEN cDNA 1700063D05 gene
ENSMUSG00000097644	18.44	<i>Gm26862</i>	predicted gene, 26862
ENSMUSG00000020890	18.70	<i>Gucy2e</i>	guanylate cyclase 2e
ENSMUSG00000084403	20.49	<i>Rps15a-ps8</i>	ribosomal protein S15A, pseudogene 8
ENSMUSG00000026691	21.47	<i>Fmo3</i>	flavin containing monooxygenase 3
ENSMUSG00000033182	24.30	<i>Kbtbd12</i>	kelch repeat and BTB (POZ) domain containing 12
ENSMUSG00000091705	29.40	<i>H2-Q2</i>	histocompatibility 2, Q region locus 2
ENSMUSG00000093880	33.35	<i>Tmem181c-ps</i>	transmembrane protein 181C, pseudogene
ENSMUSG00000108608	35.38	<i>Gm6916</i>	predicted pseudogene 6916
ENSMUSG00000026535	40.50	<i>Ifi202b</i>	interferon activated gene 202B
ENSMUSG00000026535	40.50	<i>Ifi202b</i>	interferon activated gene 202B
ENSMUSG00000059565	44.17	<i>Gm5292</i>	predicted gene 5292
ENSMUSG00000070661	44.32	<i>Rnf186</i>	ring finger protein 186
ENSMUSG00000030329	50.79	<i>Pianp</i>	PILR alpha associated neural protein
ENSMUSG00000097891	55.21	<i>Gm3650</i>	predicted gene 3650
ENSMUSG00000041735	57.50	<i>Gm13178</i>	predicted gene 13178
ENSMUSG00000014725	57.59	<i>Adam28</i>	a disintegrin and metallopeptidase domain 28
ENSMUSG00000101639	68.84	<i>Gm8597</i>	predicted gene 8597
ENSMUSG00000073402	70.98	<i>Gm8909</i>	predicted gene 8909
ENSMUSG00000072324	72.56	<i>Gm8420</i>	predicted gene 8420
ENSMUSG00000006216	75.48	<i>Clnkb</i>	chloride channel, voltage-sensitive Kb
ENSMUSG00000083773	161.82	<i>Gm13394</i>	predicted gene 13394
ENSMUSG00000079492	164.59	<i>Gm11127</i>	predicted gene 11127
ENSMUSG00000036322	231.87	<i>H2-Ea-ps</i>	histocompatibility 2, class II antigen E alpha, pseudogene
ENSMUSG00000038209	246.27	<i>Itln1</i>	intelectin 1 (galactofuranose binding)

ENSMUSG00000091373	537.65	<i>Gm8810</i>	predicted gene 8810
ENSMUSG00000073403	573.81	<i>Gm10499</i>	predicted gene 10499
ENSMUSG00000047894	799.25	<i>Ang2</i>	angiogenin, ribonuclease A family, member 2
ENSMUSG00000022057	1194.78	<i>Adamdec1</i>	ADAM-like, decysin 1
ENSMUSG00000047222	17313.54	<i>Rnase2a</i>	ribonuclease, RNase A family, 2A (liver, eosinophil-derived neurotoxin)

Table C.8 DEGs in placentas of phenotypically normal F2 *Mtrr*^{+/+} conceptuses, but not C57Bl/6 at E10.5 after embryo transfer.

F2 <i>Mtrr</i>^{+/+} PN Vs F2 <i>Mtrr</i>^{+/+} PN transferred			
Gene ID	Fold change	Gene abbreviation	Gene name
ENSMUSG00000066362	-69933.60	<i>Rps13-ps1</i>	ribosomal protein S13, pseudogene 1
ENSMUSG00000089229	-21.97	<i>Gm25043</i>	predicted gene, 25043
ENSMUSG00000060416	-13.41	<i>Gm839</i>	predicted gene 839
ENSMUSG00000105440	-11.11	<i>Gm31693</i>	predicted gene, 31693
ENSMUSG00000067081	-9.67	<i>Asb18</i>	ankyrin repeat and SOCS box-containing 18
ENSMUSG00000031738	-7.88	<i>Irx6</i>	Iroquois homeobox 6
ENSMUSG00000086164	-7.76	<i>Gm13029</i>	predicted gene 13029
ENSMUSG00000049571	-7.29	<i>Cfap46</i>	cilia and flagella associated protein 46
ENSMUSG00000095079	-5.99	<i>Igha</i>	immunoglobulin heavy constant alpha
ENSMUSG00000061633	-5.96	<i>1700029P11Rik</i>	RIKEN cDNA 1700029P11 gene
ENSMUSG00000109485	-5.58	<i>Gm45016</i>	predicted gene 45016
ENSMUSG00000060985	-4.65	<i>Tdrd5</i>	tudor domain containing 5
ENSMUSG00000029597	-4.64	<i>Sds</i>	serine dehydratase
ENSMUSG00000040276	-3.97	<i>Pacsin1</i>	protein kinase C and casein kinase substrate in neurons 1
ENSMUSG00000079853	-3.89	<i>Klral</i>	killer cell lectin-like receptor, subfamily A, member 1
ENSMUSG00000002769	-3.79	<i>Gnmt</i>	glycine N-methyltransferase
ENSMUSG00000028362	-3.66	<i>Tnfsf8</i>	tumor necrosis factor (ligand) superfamily, member 8
ENSMUSG00000043448	-3.61	<i>Gjc2</i>	gap junction protein, gamma 2

ENSMUSG00000033327	-3.45	<i>Tnxb</i>	tenascin XB
ENSMUSG00000044294	-3.42	<i>Krt84</i>	keratin 84
ENSMUSG00000022468	-3.39	<i>Endou</i>	endonuclease, polyU-specific
ENSMUSG00000035686	-3.36	<i>Thrsp</i>	thyroid hormone responsive
ENSMUSG00000049556	-3.33	<i>Lingol</i>	leucine rich repeat and Ig domain containing 1
ENSMUSG00000039209	-3.16	<i>Rpl39l</i>	ribosomal protein L39-like
ENSMUSG00000096035	-3.16	<i>Odaph</i>	odontogenesis associated phosphoprotein
ENSMUSG00000050541	-3.10	<i>Adra1b</i>	adrenergic receptor, alpha 1b
ENSMUSG00000070880	-3.03	<i>Gad1</i>	glutamate decarboxylase 1
ENSMUSG00000079357	-3.00	<i>Gm11100</i>	predicted gene 11100
ENSMUSG00000039410	-2.96	<i>Prdm16</i>	PR domain containing 16
ENSMUSG00000027978	-2.76	<i>Prss12</i>	protease, serine 12 neurotrypsin (motopsin)
ENSMUSG00000028747	-2.76	<i>Htr6</i>	5-hydroxytryptamine (serotonin) receptor 6
ENSMUSG00000026204	-2.74	<i>Ptprn</i>	protein tyrosine phosphatase, receptor type, N
ENSMUSG00000004558	-2.74	<i>Ndr2</i>	N-myc downstream regulated gene 2
ENSMUSG00000005640	-2.73	<i>Insrr</i>	insulin receptor-related receptor
ENSMUSG00000027376	-2.69	<i>Prom2</i>	prominin 2
ENSMUSG00000029369	-2.69	<i>Afm</i>	afamin
ENSMUSG00000027358	-2.65	<i>Bmp2</i>	bone morphogenetic protein 2
ENSMUSG00000025776	-2.64	<i>Crispld1</i>	cysteine-rich secretory protein LCCL domain containing 1
ENSMUSG00000049719	-2.63	<i>Prss46</i>	protease, serine 46
ENSMUSG00000026321	-2.59	<i>Tnfrsf11a</i>	tumor necrosis factor receptor superfamily, member 11a, NFkB activator
ENSMUSG00000046807	-2.57	<i>Lrrc75b</i>	leucine rich repeat containing 75B
ENSMUSG00000046731	-2.49	<i>Kctd11</i>	potassium channel tetramerisation domain containing 11
ENSMUSG00000090273	-2.49	<i>Prr22</i>	proline rich 22
ENSMUSG00000071047	-2.45	<i>Ces1a</i>	carboxylesterase 1A
ENSMUSG00000018581	-2.44	<i>Dnah11</i>	dynein, axonemal, heavy chain 11
ENSMUSG00000042414	-2.43	<i>Prdm14</i>	PR domain containing 14
ENSMUSG00000031958	-2.42	<i>Ldhd</i>	lactate dehydrogenase D

ENSMUSG00000028573	-2.41	<i>Fggy</i>	FGGY carbohydrate kinase domain containing
ENSMUSG00000018819	-2.40	<i>Lsp1</i>	lymphocyte specific 1
ENSMUSG00000030732	-2.39	<i>Chrdl2</i>	chordin-like 2
ENSMUSG00000025265	-2.39	<i>Fgd1</i>	FYVE, RhoGEF and PH domain containing 1
ENSMUSG00000053963	-2.37	<i>Stum</i>	mechanosensory transduction mediator
ENSMUSG00000027636	-2.37	<i>Sla2</i>	Src-like-adaptor 2
ENSMUSG00000038179	-2.36	<i>Slamf7</i>	SLAM family member 7
ENSMUSG00000034416	-2.35	<i>Pkd1l2</i>	polycystic kidney disease 1 like 2
ENSMUSG00000041479	-2.35	<i>Syt15</i>	synaptotagmin XV
ENSMUSG00000012819	-2.26	<i>Cdh23</i>	cadherin 23 (otocadherin)
ENSMUSG00000046999	-2.26	<i>1110032F04Rik</i>	RIKEN cDNA 1110032F04 gene
ENSMUSG00000038600	-2.25	<i>Atp6v0a4</i>	ATPase, H ⁺ transporting, lysosomal V0 subunit A4
ENSMUSG00000085683	-2.25	<i>Tmem238l</i>	transmembrane protein 238 like
ENSMUSG00000076617	-2.24	<i>Ighm</i>	immunoglobulin heavy constant mu
ENSMUSG00000009633	-2.24	<i>G0s2</i>	G0/G1 switch gene 2
ENSMUSG00000007097	-2.23	<i>Atp1a2</i>	ATPase, Na ⁺ /K ⁺ transporting, alpha 2 polypeptide
ENSMUSG00000037411	-2.23	<i>Serpine1</i>	serine (or cysteine) peptidase inhibitor, clade E, member 1
ENSMUSG00000025064	-2.22	<i>Col17a1</i>	collagen, type XVII, alpha 1
ENSMUSG00000027316	-2.22	<i>Gfra4</i>	glial cell line derived neurotrophic factor family receptor alpha 4
ENSMUSG00000031636	-2.19	<i>Pdlim3</i>	PDZ and LIM domain 3
ENSMUSG00000054065	-2.19	<i>Pkp3</i>	plakophilin 3
ENSMUSG00000107761	-2.19	<i>2010008C14Rik</i>	RIKEN cDNA 2010008C14 gene
ENSMUSG00000003545	-2.18	<i>Fosb</i>	FBJ osteosarcoma oncogene B
ENSMUSG00000031990	-2.16	<i>Jam3</i>	junction adhesion molecule 3
ENSMUSG00000028071	-2.15	<i>Sh2d2a</i>	SH2 domain containing 2A
ENSMUSG00000025017	-2.14	<i>Pik3ap1</i>	phosphoinositide-3-kinase adaptor protein 1
ENSMUSG00000006529	-2.13	<i>Itih1</i>	inter-alpha trypsin inhibitor, heavy chain 1
ENSMUSG00000075604	-2.13	<i>Cyp11b1</i>	cytochrome P450, family 11, subfamily b, polypeptide 1
ENSMUSG00000079547	-2.13	<i>H2-DMb1</i>	histocompatibility 2, class II, locus Mb1

ENSMUSG00000007034	-2.11	<i>Slc44a4</i>	solute carrier family 44, member 4
ENSMUSG00000021200	-2.11	<i>Asb2</i>	ankyrin repeat and SOCS box-containing 2
ENSMUSG00000074006	-2.10	<i>Omp</i>	olfactory marker protein
ENSMUSG00000030217	-2.10	<i>Art4</i>	ADP-ribosyltransferase 4
ENSMUSG00000037940	-2.10	<i>Inpp4b</i>	inositol polyphosphate-4-phosphatase, type II
ENSMUSG00000036718	-2.10	<i>Micall2</i>	MICAL-like 2
ENSMUSG00000046080	-2.10	<i>Clec9a</i>	C-type lectin domain family 9, member a
ENSMUSG00000043789	-2.09	<i>Vwce</i>	von Willebrand factor C and EGF domains
ENSMUSG00000028749	-2.08	<i>Pla2g2f</i>	phospholipase A2, group IIF
ENSMUSG00000027460	-2.08	<i>Angpt4</i>	angiopoietin 4
ENSMUSG00000037469	-2.08	<i>Acp7</i>	acid phosphatase 7, tartrate resistant
ENSMUSG00000073418	-2.06	<i>C4b</i>	complement component 4B (Chido blood group)
ENSMUSG00000023032	-2.05	<i>Slc4a8</i>	solute carrier family 4 (anion exchanger), member 8
ENSMUSG00000045725	-2.05	<i>Prr15</i>	proline rich 15
ENSMUSG00000022032	-2.05	<i>Scara5</i>	scavenger receptor class A, member 5
ENSMUSG00000026259	-2.05	<i>Ngef</i>	neuronal guanine nucleotide exchange factor
ENSMUSG00000034438	-2.04	<i>Gbp8</i>	guanylate-binding protein 8
ENSMUSG00000021322	-2.03	<i>Aoah</i>	acyloxyacyl hydrolase
ENSMUSG00000021255	-2.02	<i>Esrrb</i>	estrogen related receptor, beta
ENSMUSG00000026890	-2.01	<i>Lhx6</i>	LIM homeobox protein 6
ENSMUSG00000028751	-2.01	<i>Pla2g2e</i>	phospholipase A2, group IIE
ENSMUSG00000019876	2.01	<i>Pkib</i>	protein kinase inhibitor beta, cAMP dependent, testis specific
ENSMUSG00000024253	2.02	<i>Dync2li1</i>	dynein cytoplasmic 2 light intermediate chain 1
ENSMUSG00000038354	2.04	<i>Ankrd35</i>	ankyrin repeat domain 35
ENSMUSG00000027254	2.07	<i>Map1a</i>	microtubule-associated protein 1 A
ENSMUSG00000096942	2.08	<i>Rps19-ps6</i>	ribosomal protein S19, pseudogene 6
ENSMUSG00000026228	2.08	<i>Htr2b</i>	5-hydroxytryptamine (serotonin) receptor 2B
ENSMUSG00000096950	2.13	<i>Gm9530</i>	predicted gene 9530
ENSMUSG00000059058	2.13	<i>Tma7-ps</i>	translational machinery associated 7 homolog (S. cerevisiae), pseudogene

ENSMUSG00000038415	2.20	<i>Foxq1</i>	forkhead box Q1
ENSMUSG00000104943	2.21	<i>Gm42868</i>	predicted gene 42868
ENSMUSG00000032226	2.22	<i>Gcnt3</i>	glucosaminyl (N-acetyl) transferase 3, mucin type
ENSMUSG00000037605	2.22	<i>Adgrl3</i>	adhesion G protein-coupled receptor L3
ENSMUSG00000058927	2.23	<i>Gm10053</i>	predicted gene 10053
ENSMUSG00000026579	2.27	<i>F5</i>	coagulation factor V
ENSMUSG00000081975	2.27	<i>Gm12482</i>	predicted gene 12482
ENSMUSG00000090247	2.28	<i>Bloc1s1</i>	biogenesis of lysosomal organelles complex-1, subunit 1
ENSMUSG00000041984	2.33	<i>Rptn</i>	repetin
ENSMUSG00000096557	2.34	<i>Gm7258</i>	predicted gene 7258
ENSMUSG00000086477	2.36	<i>Gm15506</i>	predicted gene 15506
ENSMUSG00000091764	2.36	<i>Zfp964</i>	zinc finger protein 964
ENSMUSG00000094320	2.40	<i>Chchd2-ps</i>	coiled-coil-helix-coiled-coil-helix domain containing 2, pseudogene
ENSMUSG00000064317	2.40	<i>Gm10146</i>	predicted gene 10146
ENSMUSG00000051149	2.48	<i>Adnp</i>	activity-dependent neuroprotective protein
ENSMUSG00000044468	2.49	<i>Tent5c</i>	terminal nucleotidyltransferase 5C
ENSMUSG00000032246	2.49	<i>Calml4</i>	calmodulin-like 4
ENSMUSG00000093483	2.49	<i>AA465934</i>	expressed sequence AA465934
ENSMUSG00000074766	2.55	<i>Ism1</i>	isthmin 1, angiogenesis inhibitor
ENSMUSG00000041794	2.58	<i>Myrip</i>	myosin VIIA and Rab interacting protein
ENSMUSG00000079173	2.59	<i>Zan</i>	zonadhesin
ENSMUSG00000043633	2.59	<i>Fam221b</i>	family with sequence similarity 221, member B
ENSMUSG00000081700	2.67	<i>Atp5k-ps2</i>	ATP synthase, H ⁺ transporting, mitochondrial F1F0 complex, subunit E, pseudogene 2
ENSMUSG00000034009	2.82	<i>Rxfp1</i>	relaxin/insulin-like family peptide receptor 1
ENSMUSG00000057897	2.82	<i>Camk2b</i>	calcium/calmodulin-dependent protein kinase II, beta
ENSMUSG00000078190	2.86	<i>Dnm3os</i>	dynamamin 3, opposite strand
ENSMUSG00000044668	2.92	<i>Abca13</i>	ATP-binding cassette, sub-family A (ABC1), member 13
ENSMUSG00000091955	3.06	<i>Gm9844</i>	predicted pseudogene 9844

ENSMUSG00000090136	3.22	<i>Gm10177</i>	predicted gene 10177
ENSMUSG00000071141	3.35	<i>Rpl36a-ps3</i>	ribosomal protein L36A, pseudogene 3
ENSMUSG00000082456	3.38	<i>Gm11598</i>	predicted gene 11598
ENSMUSG00000104765	3.41	<i>Gm43058</i>	predicted gene 43058
ENSMUSG00000100174	3.78	<i>Gm28719</i>	predicted gene 28719
ENSMUSG00000038259	3.78	<i>Gdf5</i>	growth differentiation factor 5
ENSMUSG00000105703	4.92	<i>Gm43305</i>	predicted gene 43305
ENSMUSG00000063628	6.77	<i>Gm7665</i>	predicted pseudogene 7665
ENSMUSG00000051590	7.10	<i>Map3k19</i>	mitogen-activated protein kinase kinase kinase 19
ENSMUSG00000096878	8.73	<i>Gm21083</i>	predicted gene, 21083
ENSMUSG00000060161	9.21	<i>Klk1b7-ps</i>	kallikrein 1-related peptidase b7, pseudogene
ENSMUSG00000021620	9.65	<i>Acot12</i>	acyl-CoA thioesterase 12
ENSMUSG00000021852	9.72	<i>Slc35f4</i>	solute carrier family 35, member F4
ENSMUSG00000043999	9.89	<i>Gpr75</i>	G protein-coupled receptor 75
ENSMUSG00000109186	11.46	<i>Gm34821</i>	predicted gene, 34821
ENSMUSG00000100744	11.81	<i>Gm17764</i>	predicted gene, 17764
ENSMUSG00000017311	17.82	<i>Pyy</i>	peptide YY
ENSMUSG00000074934	22.09	<i>Grem1</i>	gremlin 1, DAN family BMP antagonist
ENSMUSG00000024747	54.70	<i>Aldh1a7</i>	aldehyde dehydrogenase family 1, subfamily A7

Table C.9 DEGs in placentas of growth enhanced F2 *Mtrr*^{+/+} conceptuses, but not C57Bl/6 at E10.5 after embryo transfer.

F2 <i>Mtrr</i>^{+/+} GE Vs F2 <i>Mtrr</i>^{+/+} GE transferred			
Gene ID	Fold change	Gene abbreviation	Gene name
ENSMUSG00000109482	-19.08	<i>Gm4756</i>	predicted gene 4756
ENSMUSG00000085020	-17.68	<i>2310081O03Rik</i>	RIKEN cDNA 2310081O03 gene
ENSMUSG00000031779	-16.59	<i>Ccl22</i>	chemokine (C-C motif) ligand 22
ENSMUSG00000067081	-15.92	<i>Asb18</i>	ankyrin repeat and SOCS box-containing 18

ENSMUSG00000089757	-15.55	<i>Gm16334</i>	predicted gene 16334
ENSMUSG00000024678	-9.15	<i>Ms4a4d</i>	membrane-spanning 4-domains, subfamily A, member 4D
ENSMUSG00000044294	-7.79	<i>Krt84</i>	keratin 84
ENSMUSG00000079853	-7.60	<i>Klra1</i>	killer cell lectin-like receptor, subfamily A, member 1
ENSMUSG00000028362	-7.52	<i>Tnfsf8</i>	tumor necrosis factor (ligand) superfamily, member 8
ENSMUSG00000095079	-6.24	<i>Igha</i>	immunoglobulin heavy constant alpha
ENSMUSG00000031738	-5.82	<i>Irx6</i>	Iroquois homeobox 6
ENSMUSG00000059213	-5.05	<i>Ddn</i>	dendrin
ENSMUSG00000021440	-4.99	<i>Cts7</i>	cathepsin 7
ENSMUSG00000050541	-4.84	<i>Adra1b</i>	adrenergic receptor, alpha 1b
ENSMUSG00000096035	-4.70	<i>Odaph</i>	odontogenesis associated phosphoprotein
ENSMUSG00000035686	-4.39	<i>Thrsp</i>	thyroid hormone responsive
ENSMUSG00000033327	-3.99	<i>Tnxb</i>	tenascin XB
ENSMUSG00000027875	-3.93	<i>Hmgcs2</i>	3-hydroxy-3-methylglutaryl-Coenzyme A synthase 2
ENSMUSG00000050075	-3.91	<i>Gpr171</i>	G protein-coupled receptor 171
ENSMUSG00000005338	-3.82	<i>Cadm3</i>	cell adhesion molecule 3
ENSMUSG00000028488	-3.64	<i>Sh3gl2</i>	SH3-domain GRB2-like 2
ENSMUSG00000036062	-3.53	<i>Phf24</i>	PHD finger protein 24
ENSMUSG00000030173	-3.41	<i>Klra5</i>	killer cell lectin-like receptor, subfamily A, member 5
ENSMUSG00000074199	-3.26	<i>Krtdap</i>	keratinocyte differentiation associated protein
ENSMUSG00000039313	-3.18	<i>AF529169</i>	cDNA sequence AF529169
ENSMUSG00000043448	-3.11	<i>Gjc2</i>	gap junction protein, gamma 2
ENSMUSG00000040229	-2.93	<i>Gpr34</i>	G protein-coupled receptor 34
ENSMUSG00000027457	-2.91	<i>Snph</i>	syntrophin
ENSMUSG00000057446	-2.89	<i>Cts8</i>	cathepsin 8
ENSMUSG00000073418	-2.87	<i>C4b</i>	complement component 4B (Chido blood group)
ENSMUSG00000046807	-2.86	<i>Lrrc75b</i>	leucine rich repeat containing 75B
ENSMUSG00000032172	-2.81	<i>Olfm2</i>	olfactomedin 2
ENSMUSG00000053963	-2.76	<i>Stum</i>	mechanosensory transduction mediator

ENSMUSG00000047793	-2.76	<i>Sned1</i>	sushi, nidogen and EGF-like domains 1
ENSMUSG00000104802	-2.71	<i>Gm5869</i>	predicted gene 5869
ENSMUSG00000046999	-2.70	<i>1110032F04Rik</i>	RIKEN cDNA 1110032F04 gene
ENSMUSG00000005973	-2.70	<i>Rcn1</i>	reticulocalbin 1
ENSMUSG00000028713	-2.70	<i>Cyp4b1</i>	cytochrome P450, family 4, subfamily b, polypeptide 1
ENSMUSG00000054978	-2.67	<i>Kbtbd13</i>	kelch repeat and BTB (POZ) domain containing 13
ENSMUSG00000029675	-2.66	<i>Eln</i>	elastin
ENSMUSG00000027358	-2.59	<i>Bmp2</i>	bone morphogenetic protein 2
ENSMUSG00000029334	-2.58	<i>Prkg2</i>	protein kinase, cGMP-dependent, type II
ENSMUSG00000041479	-2.58	<i>Syt15</i>	synaptotagmin XV
ENSMUSG00000075707	-2.55	<i>Dio3</i>	deiodinase, iodothyronine type III
ENSMUSG00000026321	-2.53	<i>Tnfrsf11a</i>	tumor necrosis factor receptor superfamily, member 11a, NFkB activator
ENSMUSG00000045725	-2.53	<i>Prr15</i>	proline rich 15
ENSMUSG00000087698	-2.52	<i>Gm13031</i>	predicted gene 13031
ENSMUSG00000104350	-2.52	<i>Gm38244</i>	predicted gene, 38244
ENSMUSG00000005640	-2.52	<i>Insrr</i>	insulin receptor-related receptor
ENSMUSG00000020926	-2.47	<i>Adam11</i>	a disintegrin and metallopeptidase domain 11
ENSMUSG00000026365	-2.44	<i>Cfh</i>	complement component factor h
ENSMUSG00000038179	-2.43	<i>Slamf7</i>	SLAM family member 7
ENSMUSG00000037759	-2.42	<i>Ptger2</i>	prostaglandin E receptor 2 (subtype EP2)
ENSMUSG00000025742	-2.37	<i>Prps2</i>	phosphoribosyl pyrophosphate synthetase 2
ENSMUSG00000032528	-2.35	<i>Vipr1</i>	vasoactive intestinal peptide receptor 1
ENSMUSG00000022468	-2.35	<i>Endou</i>	endonuclease, polyU-specific
ENSMUSG00000027376	-2.34	<i>Prom2</i>	prominin 2
ENSMUSG00000022032	-2.34	<i>Scara5</i>	scavenger receptor class A, member 5
ENSMUSG00000032537	-2.33	<i>Ephb1</i>	Eph receptor B1
ENSMUSG00000007097	-2.33	<i>Atp1a2</i>	ATPase, Na ⁺ /K ⁺ transporting, alpha 2 polypeptide
ENSMUSG00000035948	-2.33	<i>Acss3</i>	acyl-CoA synthetase short-chain family member 3
ENSMUSG00000027577	-2.33	<i>Chrna4</i>	cholinergic receptor, nicotinic, alpha polypeptide 4

ENSMUSG00000002831	-2.30	<i>Plin4</i>	perilipin 4
ENSMUSG000000027639	-2.28	<i>Samhd1</i>	SAM domain and HD domain, 1
ENSMUSG000000017737	-2.27	<i>Mmp9</i>	matrix metalloproteinase 9
ENSMUSG000000031958	-2.26	<i>Ldhd</i>	lactate dehydrogenase D
ENSMUSG000000067220	-2.26	<i>Cngal</i>	cyclic nucleotide gated channel alpha 1
ENSMUSG000000037994	-2.25	<i>Slc9b2</i>	solute carrier family 9, subfamily B (NHA2, cation proton antiporter 2), member 2
ENSMUSG000000027377	-2.24	<i>Mall</i>	mal, T cell differentiation protein-like
ENSMUSG000000028749	-2.24	<i>Pla2g2f</i>	phospholipase A2, group IIF
ENSMUSG000000021508	-2.22	<i>Cxcl14</i>	chemokine (C-X-C motif) ligand 14
ENSMUSG000000037846	-2.22	<i>Rtkn2</i>	rhotekin 2
ENSMUSG000000027848	-2.20	<i>Olfml3</i>	olfactomedin-like 3
ENSMUSG000000034853	-2.20	<i>Acot11</i>	acyl-CoA thioesterase 11
ENSMUSG000000049744	-2.19	<i>Arhgap15</i>	Rho GTPase activating protein 15
ENSMUSG000000079547	-2.18	<i>H2-DMb1</i>	histocompatibility 2, class II, locus Mb1
ENSMUSG000000029082	-2.18	<i>Bst1</i>	bone marrow stromal cell antigen 1
ENSMUSG000000027796	-2.17	<i>Smad9</i>	SMAD family member 9
ENSMUSG000000006642	-2.15	<i>Tcf23</i>	transcription factor 23
ENSMUSG000000006342	-2.15	<i>Susd2</i>	sushi domain containing 2
ENSMUSG000000026204	-2.12	<i>Ptprn</i>	protein tyrosine phosphatase, receptor type, N
ENSMUSG000000046731	-2.10	<i>Kctd11</i>	potassium channel tetramerisation domain containing 11
ENSMUSG000000051431	-2.09	<i>Gpr87</i>	G protein-coupled receptor 87
ENSMUSG000000027460	-2.09	<i>Angpt4</i>	angiopoietin 4
ENSMUSG000000052861	-2.07	<i>Dnah6</i>	dynein, axonemal, heavy chain 6
ENSMUSG000000041608	-2.07	<i>Entpd3</i>	ectonucleoside triphosphate diphosphohydrolase 3
ENSMUSG00000104713	-2.05	<i>Gbp6</i>	guanylate binding protein 6
ENSMUSG000000043789	-2.05	<i>Vwce</i>	von Willebrand factor C and EGF domains
ENSMUSG000000037411	-2.05	<i>Serpine1</i>	serine (or cysteine) peptidase inhibitor, clade E, member 1
ENSMUSG000000027843	-2.04	<i>Ptpn22</i>	protein tyrosine phosphatase, non-receptor type 22 (lymphoid)
ENSMUSG000000026259	-2.04	<i>Ngef</i>	neuronal guanine nucleotide exchange factor

ENSMUSG00000073678	-2.04	<i>Pgap1</i>	post-GPI attachment to proteins 1
ENSMUSG00000020848	-2.03	<i>Doc2b</i>	double C2, beta
ENSMUSG00000038600	-2.02	<i>Atp6v0a4</i>	ATPase, H ⁺ transporting, lysosomal V0 subunit A4
ENSMUSG00000086591	-2.02	<i>Dnah2os</i>	dynein, axonemal, heavy chain 2, opposite strand
ENSMUSG00000024912	-2.02	<i>Fosl1</i>	fos-like antigen 1
ENSMUSG00000021322	-2.02	<i>Aoah</i>	acyloxyacyl hydrolase
ENSMUSG00000031990	-2.01	<i>Jam3</i>	junction adhesion molecule 3
ENSMUSG00000026832	-2.01	<i>Cytip</i>	cytohesin 1 interacting protein
ENSMUSG00000004709	-2.00	<i>Cd244a</i>	CD244 molecule A
ENSMUSG00000057880	-2.00	<i>Abat</i>	4-aminobutyrate aminotransferase
ENSMUSG00000039114	-2.00	<i>Nrn1</i>	neuritin 1
ENSMUSG00000107355	2.05	<i>AI839979</i>	expressed sequence AI839979
ENSMUSG00000031616	2.11	<i>Ednra</i>	endothelin receptor type A
ENSMUSG00000038354	2.12	<i>Ankrd35</i>	ankyrin repeat domain 35
ENSMUSG00000038415	2.12	<i>Foxq1</i>	forkhead box Q1
ENSMUSG00000103472	2.12	<i>Pcdhga7</i>	protocadherin gamma subfamily A, 7
ENSMUSG00000038555	2.18	<i>Reep2</i>	receptor accessory protein 2
ENSMUSG00000067158	2.19	<i>Col4a4</i>	collagen, type IV, alpha 4
ENSMUSG00000026228	2.27	<i>Htr2b</i>	5-hydroxytryptamine (serotonin) receptor 2B
ENSMUSG00000104943	2.32	<i>Gm42868</i>	predicted gene 42868
ENSMUSG00000045555	2.34	<i>Mettl24</i>	methyltransferase like 24
ENSMUSG00000069072	2.42	<i>Slc7a14</i>	solute carrier family 7 (cationic amino acid transporter, y ⁺ system), member 14
ENSMUSG00000041984	2.42	<i>Rptn</i>	repetin
ENSMUSG00000033491	2.46	<i>Prss35</i>	protease, serine 35
ENSMUSG00000040666	2.47	<i>Sh3bgr</i>	SH3-binding domain glutamic acid-rich protein
ENSMUSG00000091764	2.48	<i>Zfp964</i>	zinc finger protein 964
ENSMUSG00000044468	2.52	<i>Tent5c</i>	terminal nucleotidyltransferase 5C
ENSMUSG00000078190	2.64	<i>Dnm3os</i>	dynamamin 3, opposite strand
ENSMUSG00000106554	2.66	<i>Gm33474</i>	predicted gene, 33474

ENSMUSG00000034226	2.67	<i>Rhov</i>	ras homolog family member V
ENSMUSG00000040653	3.05	<i>Ppp1r14c</i>	protein phosphatase 1, regulatory inhibitor subunit 14C
ENSMUSG00000046748	3.25	<i>Tmem45a2</i>	transmembrane protein 45A2
ENSMUSG00000054013	3.29	<i>Tmem179</i>	transmembrane protein 179
ENSMUSG00000097495	3.72	<i>Gm26651</i>	predicted gene, 26651
ENSMUSG00000026023	3.99	<i>Cdk15</i>	cyclin-dependent kinase 15
ENSMUSG00000082101	4.39	<i>Slfn14</i>	schlafen 14
ENSMUSG00000015090	5.13	<i>Ptgds</i>	prostaglandin D2 synthase (brain)
ENSMUSG00000024747	10.44	<i>Aldh1a7</i>	aldehyde dehydrogenase family 1, subfamily A7
ENSMUSG00000096878	11.70	<i>Gm21083</i>	predicted gene, 21083
ENSMUSG00000086820	16.22	<i>Gm11465</i>	predicted gene 11465
ENSMUSG00000040505	17.25	<i>Abcg5</i>	ATP binding cassette subfamily G member 5
ENSMUSG00000046160	17.89	<i>Olig1</i>	oligodendrocyte transcription factor 1
ENSMUSG00000083623	22.86	<i>Gm7224</i>	predicted gene 7224
ENSMUSG00000091553	22.89	<i>Serpina3e-ps</i>	serine (or cysteine) peptidase inhibitor, clade A, member 3E, pseudogene
ENSMUSG00000027209	29.55	<i>Fam227b</i>	family with sequence similarity 227, member B
ENSMUSG00000062148	32.03	<i>Ear6</i>	eosinophil-associated, ribonuclease A family, member 6
ENSMUSG00000074934	35.81	<i>Greml</i>	gremlin 1, DAN family BMP antagonist
ENSMUSG00000101939	81.30	<i>Gm28438</i>	predicted gene 28438
ENSMUSG00000066362	40479.63	<i>Rps13-ps1</i>	ribosomal protein S13, pseudogene 1